

0016 7284
LEVEL II

12

REPORT ON SENSOR TECHNOLOGY FOR BATTLEFIELD AND PHYSICAL SECURITY APPLICATIONS

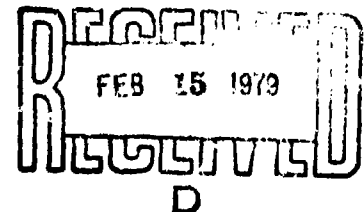
July 1977



**MOBILITY EQUIPMENT
RESEARCH AND DEVELOPMENT COMMAND**

Fort Belvoir, Virginia

DDC



DISTRIBUTION STATEMENT A

Approved for public release;
Distribution Unlimited

79 02 15 027

ADA064670

DDC FILE COPY

568 p. 1 (11) Jul 77

12

LEVEL II

REPORT ON SENSOR TECHNOLOGY FOR BATTLEFIELD AND PHYSICAL SECURITY APPLICATIONS

This report includes technical papers prepared at the invitation of MERADCOM to survey the current requirements for and state-of-the-art of sensors for Battlefield and Physical Security Applications. These papers were presented at Fort Belvoir, Humphreys Hall on 13-15 July 1977. Classified papers are included in a separate addendum to this report.

ACCESSION BY	
DTIC	Write Section <input checked="" type="checkbox"/>
DDI	DDI Section <input type="checkbox"/>
UNAPPROVED	<input type="checkbox"/>
NOTIFICATION	
Per IDC Form 50	
or on file	
DISTRIBUTION/AVAILABILITY CODES	
DECL	AVAIL. and/or SPECIAL
A	

DISTRIBUTION STATEMENT A
Approved for public release;
Distribution Unlimited

DDC
RECEIVED
FEB 15 1979
REGULATED
D

79 02 15 027

403 160 Jm

CONTENTS

Title	Page
Welcoming Address, COL Bernard C. Hughes, Commander, MERADCOM	1
Keynote Address, COL Herbert Dixon, ODDR&E	4
Session I	
The Overview	
Description of the REMBASS ED System, LTC William R. Green, APM, REMBASS.	21
US Army Physical Security Equipment Program, Stuart Kilpatrick, Acting DA Project Officer for Physical Security Equipment.	54
BISS Overview, COL Roger Kozuma, BISS PO	68
The Marine Corps Tactical Remote Sensor System (TRSS), CAPT Earl, MCDEC	88
Combat Area Security Sensor Requirement Study (CASSR), MAJ Pinkerton, US Army Military Police School	90
Air Force Operational Concept for External Physical Security, MAJ John Siedlarz, USAF Security Police	No paper submitted
Sensor Technology in the Army's Non-Mine Barrier Systems, Ben C. Barker, Sensors & Barriers Division, MERADCOM	113
Session II	
State-of-the-Art in Sensor Technology	
Fluidic Sensors for Physical Security Applications, Ted Drzewiecki, Harry Diamond Labs	126
IRCCD Radiometric Fence Sensor, R. Taylor, L. Skolnik, B. Capone, W. Ewing, S. Roosild, F. Shepherd, and A. Yang, Rome Air Development Center, AFSC, Deputy for Electronic Technology	127
Use of the Pyroelectric Vidicon for Installation Security, F. T. Doepel, Night Vision Laboratories	147
Comparison of Magnetic and Stress Response of Magnetic Intrusion Line Sensor (MILES), T. F. Ezell, R. W. Madsen, and F. G. Yost, Sandia Laboratories	155
Active Ultrasonic Tape Perimeter Security System, G. Kirby Miller, GTE Sylvania, Inc.	179
Piezoelectric and Pyroelectric Polymer Sensors, Seymour Edelman, NBS	204
Discussion of Selected New Sensor Transducer Technology, Herbert Reich, MERADCOM	213

Title	Page
Session III	
State-of-the-Art in Signal Processing Technology	
Selective Digital Filtering, Glenn Elliott, Sandia Laboratories.	224
Radar Video Processing with Charge Coupled Devices, W. H. Bailey, W. L. Eversole, L. R. Hite, Texas Instruments, Inc.; and J. A. McCray, USAECOM.	236
PAR Detection Logic for Line Sensors, Raymond J. D'Amore, Dr. Robert J. Dick, Dr. Donald H. Foley, and Dr. Om P. Gupta, PAR Corporation.	252
Detection of Mechanical Waves Generated by Concealed Persons, Francis J. Cook, ENSCO, Inc.	258
On-Site Data Communication in Security Systems, Robert J. Carpenter, NBS.	266
Data Encryption, S. Jeffery and D. K. Branstad, NBS.	281
Session IV	
Target Classification and Position Location	
Experimental Radar - Electro/Optic Hybrid for Multifunctional Engagement System, R. S. Rohde, W. Fishbein, R. G. Buser, and O. Rittenbach, CS&TA Laboratory.	Classified Addendum
Cross Correlation Vehicle Classification, Richard L. Sebastian, ENSCO, Inc.	287
Comparison of Available Target Classification Techniques, Donald W. Keehan, Sensors and Barriers Division, MERADCOM.	297
FAALS Sensor Design, Dr. James W. Follin, Applied Physics Laboratory.	Classified Addendum
Mixed and Multitarget Classification Feasibility Study, Dr. Marvin P. Pastel, TRADOC.	304
Improved Techniques for Seismic and Seismic-Acoustic Passive Ranging from a Single Sensor, Roger L. Barron, Adaptronics, Inc.	312
Seismic/Acoustic Target Ranger, Norman P. Huffnagle and Gwynn M. Reel, Martin Marietta Corporation.	Classified Addendum
Session V	
Physical Security Sensors	
Passive Infrared Motion Sensor (PIMS), Robert A. Brubaker, MERADCOM.	339
Sensor Test System for the FIDS, L. J. Nivert, J. E. Bender, and A. R. Zushin, MERADCOM.	351



Title	Page
Electric Field Sensor Studies, R. D. Griffith, and S. Parks, Sandia Laboratories	365
Installation Security Radar Employing Microprogrammed Signal Processing and Threat Analysis, P. B. McCorison and C. E. Muehe, MIT Lincoln Laboratory	381
Ported Coaxial Cable Sensor, R. K. Harman, Computing Devices Company	393
Personal Attributes Verification, Dr. Mark R. Nelson and Raymond J. Staron, Jr PAR Corporation	414
Waterborne Intruder Detection Sensors, Dr. Alan J. Stratton, Dynatrend, Inc.	420

Session VI
Selected Topics

Test Results of an Acoustic/IR Guidance System, J. A. Alfieri, Northrop.	
Classified Addendum	
Detection of Terrorist Explosives in Luggage and Mail, J. Roland Gonano, MERADCOM	432
High-Resolution Seismic Detection of Shallow Tunnels in Rock, T. E. Owen, and G. T. Darilek, SwRI.	442
Tunnel Detection Surveys Using Earth Resistivity Techniques, L. S. Fountain and F. X. Herzig, SwRI; R. K. Young, MERADCOM.	
Classified Addendum	
Acquisition, Processing, and Analysis of Magnetic Signatures of Vehicles, Joseph M. Iseman, Harry Diamond Laboratories	
No paper submitted	
Terrain Considerations and Data Base Development for Sensors Designed to Detect Intruder-Induced Ground Motion, Daniel H. Cress, WES.	468
The Effects of Artificial Lighting on CCTV Perimeter Alarm Assessment System, B. B. Jancowskis and D. K. Bellinger, NAFL	495
AN/GSS-20, Gerald J. Zdyb, US Air Force Electronic Systems Division, L. G. Hanscom Field	503
Practical Testing and Calibration of Electrodynamic Seismometers (Geophones), Louis Lechenger, Geo Space Corporation	526

WELCOMING ADDRESS
COL BERNARD C. HUGHES, COMMANDER
MERADCOM

I WOULD LIKE TO SINCERELY WELCOME EACH OF YOU TO FORT BELVOIR AND MERADCOM. I AM SURE THAT THIS SEMINAR ON SENSOR TECHNOLOGY FOR BATTLE-FIELD & PHYSICAL SECURITY APPLICATION WILL BE A WORTHWHILE ENDEAVOR FOR YOU ALL. WE CONSIDER THIS A TIMELY AND AN EXTREMELY IMPORTANT TECHNICAL SESSION BECAUSE OF THE SIGNIFICANTLY INCREASED EMPHASIS BEING PLACED ON THE UTILIZATION OF SENSOR TECHNOLOGY TO PROTECT THIS NATION'S CRITICAL ASSETS SUCH AS NUCLEAR AND CHEMICAL WEAPON STORAGE SITES AND SENSITIVE MILITARY INSTALLATIONS AND FOR THE FIELDING OF NEW AND IMPROVED BATTLE-FIELD UNATTENDED SENSOR SYSTEM.

AS NOTED IN THE AGENDA FOR THIS MEETING,  THE SESSIONS DEAL WITH A REVIEW OF ALL OF THE SERVICE SENSOR PROGRAMS TO INCLUDE: THE STATE-OF-THE-ART IN SENSOR TRANSDUCER TECHNOLOGY AND SIGNAL PROCESSING; THE UTILIZATION OF SENSOR TECHNIQUES FOR TARGET DETECTION, CLASSIFICATION AND LOCATION; SENSORS DESIGNED SPECIFICALLY FOR PHYSICAL SECURITY APPLICATION; AND SPECIAL PURPOSE DETECTING SYSTEMS. 

SINCE MANY OF YOU PROBABLY ARE NOT FAMILIAR WITH THE OVERALL MISSION OF MERADCOM, I THOUGHT I'D TAKE A FEW MINUTES TO TELL YOU WHAT WE DO AND HOW WE FIT INTO THE ARMY R&D MANAGEMENT STRUCTURE. I WOULD THEN LIKE TO SPEND A FEW MINUTES DESCRIBING THE SCOPE OF OUR SENSOR DEVELOPMENT PROGRAM.

MERADCOM IS ONE OF EIGHT RESEARCH AND DEVELOPMENT COMMANDS THAT REPORT

TO THE MATERIAL DEVELOPMENT AND READINESS COMMAND, REFERRED TO AS DARCOM.

THE MERADCOM MISSION IS TO ACCOMPLISH RESEARCH, DEVELOPMENT, ENGINEERING AND FIRST-TIME BUYS OF EQUIPMENT IN FOUR AREAS ESSENTIAL TO THE SUPPORT OF A MOBILE ARMY; BARRIER AND COUNTERBARRIER SYSTEMS; COUNTERSURVEILLANCE SYSTEMS; ENERGY AND ENVIRONMENTAL SYSTEMS; AND SUPPLY DISTRIBUTION AND CONSTRUCTION EQUIPMENT SYSTEMS.

TO GET OUR JOB DONE, MERADCOM HAS AN ORGANIZATION CONSISTING OF SEVEN COMMODITY ORIENTED RESEARCH AND DEVELOPMENT LABORATORIES AND A MATERIAL TECHNOLOGY LABORATORY. THE NAMES OF THE LABORATORIES, COUNTERMINE, ENERGY & WATER RESOURCES, COUNTER INTRUSION, ELECTRICAL POWER, ETC., INDICATE WE ARE INDEED INVOLVED IN A DIVERSITY OF TECHNICAL ENDEAVORS. OUR COUNTER INTRUSION LABORATORY HAS RESPONSIBILITY FOR THE MERADCOM SENSOR R&D PROGRAM.

MERADCOM'S EXPERIENCE IN SENSOR TECHNOLOGY DATES BACK MANY YEARS WITH ITS PROGRAM IN MINE DETECTION AND THEN, OF COURSE, ITS HEAVY INVOLVEMENT IN THE TACTICAL SENSOR SYSTEMS FOR SOUTH EAST ASIA AND THE FOLLOW-ON PHYSICAL SECURITY PROGRAM FOR THE DEFENSE SPECIAL PROJECTS GROUP.

OUR PRESENT EFFORTS IN SENSORS CONSIST OF THE FOLLOWING ACTIVITIES.

IN THE TACTICAL SENSOR AREA, SUPPORT IS PROVIDED TO THE PROJECT MANAGER OF THE REMOTELY MONITORED BATTLEFIELD SENSOR SYSTEM (REMBASS) IN THE AREA OF TARGET DETECTION, CLASSIFICATION AND LOCATION.

IN THE PHYSICAL SECURITY AREA, MERADCOM HAS TYPE CLASSIFIED THE JOINT SERVICES INTERIOR INTRUSION DETECTION SYSTEM (J-SIIDS) WHICH CONSISTS OF A FAMILY OF SEVEN SENSORS, PROCESSING LOGIC, A DATA TRANSMISSION SYSTEM, AND READOUT EQUIPMENT. THE FOLLOW-ON DETECTION SYSTEM CONSISTS OF A NUMBER OF DIFFERENT SENSING TECHNIQUES, A HIGH SECURITY DATA TRANSMISSION SYSTEM, AND

A MICROPROCESSOR CONTROLLED COMMAND DISPLAY SYSTEM. THE INTERIM FIDS SYSTEMS IS IN ENGINEERING DEVELOPMENT AT THIS TIME. MERADCOM PROVIDES SUPPORT TO THE NUCLEAR REGULATORY COMMISSION AND THE NAVY PME-121 OFFICE IN THIS AREA.

IN THE AREA OF SPECIAL PURPOSE DETECTORS, A PROGRAM TO DETECT THE PRESENCE OF TUNNELS BY VARIOUS SENSING TECHNIQUES IS BEING PURSUED TO MEET AN URGENT OPERATIONAL REQUIREMENT. ALSO, IN THIS CATEGORY SUPPORT IS PROVIDED TO THE DRUG ENFORCEMENT AGENCY AND THE SINAI SUPPORT MISSION IN THE STATE DEPARTMENT.

WE ARE FORTUNATE TO HAVE WITH US AS OUR KEYNOTE SPEAKER THIS MORNING, COL DIXON, CHAIRMAN OF THE PHYSICAL SECURITY EQUIPMENT ACTION GROUP IN THE OFFICE OF THE DIRECTOR OF DEFENSE RESEARCH AND ENGINEERING. COL DIXON IS AWARE OF SENSOR DEVELOPMENTS IN MANY MISSION AREAS AND I AM CERTAIN HE WILL CHALLENGE US TO CONTINUE EFFORTS SUCH AS THIS SEMINAR, DEDICATED TO THE PURPOSE OF WIDELY DISSEMINATING TECHNICAL INFORMATION CONCERNING SENSOR DEVELOPMENTS IN DOD, OTHER GOVERNMENT AGENCIES AND PRIVATE INDUSTRY. IT IS A GREAT PLEASURE FOR ME TO INTRODUCE TO YOU OUR KEYNOTE SPEAKER, COL HERBERT DIXON.

KEYNOTE ADDRESS

COL HERBERT DIXON, ODDR&E

SLIDE 1 ON

IT IS INDEED A PRIVILEGE AND A PLEASURE FOR ME TO BE WITH YOU ALL TODAY.

AS I LOOK OVER THE GROUP, I SEE MANY OLD FRIENDS, A LOT OF FAMILIAR FACES AND A NUMBER OF RECENT ACQUAINTANCES. THIS SORT OF SETTING MAKES THE SEMINAR ESPECIALLY MEANINGFUL TO ME.

THIS MORNING I WOULD LIKE TO TAKE YOU AWAY FROM THE HIGHLY TECHNICAL AND COMPLEX ARENA OF PHYSICAL SECURITY EQUIPMENTS COMPONENTS, WHICH YOU WILL BE ADDRESSING DURING THE REMAINING THREE DAYS, AND TALK IN BROAD TERMS ABOUT THE TOTAL DOD PHYSICAL SECURITY EQUIPMENT PROGRAMS.

SLIDE 1 OFF

SLIDE 2 ON

I BELIEVE THAT NO MATTER HOW MUCH EACH OF US MAY HAVE LEARNED ABOUT INDIVIDUAL PHYSICAL SECURITY EQUIPMENT END ITEMS, IT SHOULD BE USEFUL IF WE GET A HANDLE ON THE OVERALL MANAGEMENT CONCEPT, THE PROGRAM OBJECTIVES, AND THE ESTIMATED FUNDING LEVELS ASSOCIATED WITH THIS NEW OSD INITIATIVE IN THE PHYSICAL SECURITY EQUIPMENT AREA.

I'M SURE MOST OF YOU ARE AWARE THAT THE SERVICES HAVE HAD STRUCTURED PHYSICAL SECURITY EQUIPMENT PROGRAMS FOR MANY YEARS, BUT THE OSD HAS NOT HAD A RECENT ACTIVE ROLE UNTIL 1 DECEMBER 1976. I SHOULD EMPHASIZE THE WORD "RECENT" BECAUSE I UNDERSTAND THAT THERE WAS A PREVIOUS ATTEMPT IN 1950 BY THE OSD TO BECOME ACTIVELY

INVOLVED THROUGH CLOSE ASSOCIATION WITH THE SERVICES' PHYSICAL SECURITY EQUIPMENT PROGRAMS. AS A MATTER OF FACT, A GROUP CALLED THE PHYSICAL SECURITY EQUIPMENT AGENCY, UNDER THE DIRECTION OF AIR FORCE COLONEL MCCORD, WAS ESTABLISHED AND IT WAS SUBSEQUENTLY ABOLISHED.

IN MANY RESPECTS, HOWEVER, THE PROBLEMS ASSOCIATED WITH THE DEVELOPMENT OF PHYSICAL SECURITY EQUIPMENT THAT EXISTED IN THE 1950'S ARE STILL WITH US TODAY. WE STILL HAVE EXCESSIVE FALSE ALARMS; WE STILL HAVE EXCESSIVE NUISANCE ALARMS. IF YOU WISH TO DISTINGUISH BETWEEN THE TWO, OUR SYSTEMS ARE STILL TOO EXPENSIVE AND THEY HAVE NOT PERMITTED US TO SUBSTANTIALLY REDUCE THE NUMBER OF PERSONNEL REQUIRED TO PERFORM SECURITY DUTIES. AS A POINT OF INTEREST, WE HAVE MORE THAN 20,000 U.S. MILITARY PERSONNEL, WORLDWIDE, PARTICIPATING AS SECURITY GUARDS OR REACTION FORCES IN SUPPORT OF LAND-BASED NUCLEAR WEAPONS STORAGE FACILITIES - THAT FIGURE EXCEEDS THE FOXHOLE STRENGTH OF A FULL INFANTRY DIVISION.

SLIDE 2 OFF

WHEN WE COMBINE THE KNOWN NUMBER OF PERSONNEL CONNECTED WITH NUCLEAR WEAPONS SECURITY AND THE SPECULATED NUMBER ASSOCIATED WITH OTHER SECURITY REQUIREMENTS, THE NEED FOR A NEAR TERM PHYSICAL SECURITY EQUIPMENT SYSTEM, THAT WILL PERMIT A REDUCTION IN THE NUMBER OF DEDICATED SECURITY PERSONNEL, BECOMES RATHER OBVIOUS.

THIS INTRODUCTION LEADS ME INTO THE MAIN PORTION OF MY REMARKS AND I WILL BEGIN LIKE ALL GOOD BUREAUCRATS, WITH AN ORGANIZATION CHART.

SLIDE 3 ON

ON 21 JUNE 1976, AFTER AN EXTENSIVE INVESTIGATION INTO THE PHYSICAL SECURITY EQUIPMENT PROGRAMS OF THE SERVICES, A DOD TASK FORCE RECOMMENDED THAT THE DDR&E TAKE THE LEAD IN OVERSEEING ALL PHYSICAL SECURITY EQUIPMENT EFFORTS AND EFFECT CENTRALIZED COORDINATION.

ON 3 SEPTEMBER 1976, THE DOD PHYSICAL SECURITY EQUIPMENT ACTION GROUP WAS CREATED TO ACCOMPLISH THE DIRECTED COORDINATION.

NOTICE THAT WE HAVE A REPRESENTATIVE FROM EACH SERVICE'S R&D SECRETARIAT AND ONE FROM EACH MILITARY STAFF. (THE NAVY IS PERMITTED TWO REPRESENTATIVES FROM ITS MILITARY STAFF BECAUSE OF A SPECIAL MISSION WHICH I WILL DISCUSS LATER.)

YOU WILL ALSO NOTICE THAT WE HAVE A FULL OR EXECUTIVE GROUP AND A WORKING GROUP. THE FULL GROUP MEETS ON CALL TO ADDRESS MAJOR PROGRAM ISSUES AND THE WORKING GROUP MEETS WEEKLY TO KEEP ABREAST OF THE PROGRESS BEING MADE IN EACH OF OUR SEVEN PROGRAM AREAS.

NOT SHOWN IS A MEMBER FROM THE PM REMBASS OFFICE WHO ALSO ATTENDS OUR WEEKLY MEETINGS. WE RECOGNIZE THE NEED FOR CLOSE COORDINATION BETWEEN THE TACTICAL SENSOR AND PHYSICAL SECURITY SENSOR ORGANIZATIONS. SO, BESIDES THE VARIOUS LETTERS OF AGREEMENT, SHARING OF TECHNOLOGIES AND EVEN SHARING SEMINARS, THE INCLUSION OF A TACTICAL SENSOR REPRESENTATIVE IN OUR WORKING GROUP FURTHERS OUR COOPERATIVE EFFORTS.

THIS ORGANIZATIONAL ARRANGEMENT FACILITATES COORDINATION BY

PROVIDING TWO LEVELS OF DIRECT ENTRY, AND IT ALSO ALLOWS FOR A LITTLE "ARM TWISTING" SHOULD THE NEED ARISE.

AT THIS POINT, I WOULD LIKE TO SPEND A FEW MINUTES DISCUSSING THE ROLE OF THE DEFENSE NUCLEAR AGENCY IN OUR EFFORT. AT THE OUTSET, LET ME EMPHASIZE THAT NUCLEAR SECURITY, WHILE OF PARAMOUNT IMPORTANCE, REPRESENTS A VERY SMALL PORTION OF THE TOTAL COST OF OUR ESTIMATED DOD PROGRAM. NONETHELESS, IT DOES HAVE PRIORITY FOR SYSTEM INSTALLATION.

AS WE DEVELOP PHYSICAL SECURITY EQUIPMENT FOR THE PROTECTION OF NUCLEAR WEAPONS, WE WILL ALSO BE LEARNING ABOUT TECHNOLOGIES WHICH WILL HAVE APPLICATION TO THE OTHER ASPECTS OF PHYSICAL SECURITY EQUIPMENT REQUIREMENTS. AS OUR SYSTEMS ARE ENVISIONED, MANY OF THE SOPHISTICATED FEATURES OF THE SECURITY EQUIPMENT USED AT NUCLEAR SITES WILL NOT NECESSARILY BE DESIGNED INTO SECURITY EQUIPMENT USED FOR OTHER PURPOSES. IN ANY EVENT, THE DEFENSE NUCLEAR AGENCY HAS BEEN ASSIGNED SOME SIGNIFICANT TASKS
BY THE OFFICE OF THE DIRECTOR OF DEFENSE RESEARCH & ENGINEERING IN MATTERS PERTAINING TO PHYSICAL SECURITY EQUIPMENT PROGRAMS.

THE WORKING GROUP MEETS EACH TUESDAY MORNING AT 9 O'CLOCK. WE HAVE A PRACTICE OF INVITING MEMBERS OF THE BUSINESS WORLD TO PRESENT BRIEFINGS ON THE CAPABILITIES OF THEIR FIRMS AND ANY SECURITY EQUIPMENT WHICH THEY MAY HAVE THAT OFFERS NEW AND EXCITING POSSIBILITIES. AT PRESENT WE ARE BOOKED THROUGH AUGUST 9TH, BUT I WOULD LIKE FOR EACH OF YOU TO KNOW THAT THE ACTION GROUP WOULD WELCOME THE OPPORTUNITY TO MEET WITH YOU AND

DISCUSS MATTERS OF MUTUAL INTEREST.

AS AN ASIDE, ALTHOUGH THE ACTION GROUP IS RELATIVELY NEW, IT OCCUPIES A VERY PROMINENT PLACE IN THE CURRENT DOD PHONE BOOK. I CAN ONLY ASSUME THERE MUST HAVE BEEN A COUP IN THE PRINTING ROOM BECAUSE WE ARE ON PAGE 1, COLUMN 1 OF THE YELLOW PAGES WITH A TITLE IN BOLDER PRINT THAN THE TITLE OF THE SECRETARY OF DEFENSE. I SHOULD CAUTION YOU NOT TO LOOK ON PAGE 1 FOR US IN SUBSEQUENT ISSUES, HOWEVER, BECAUSE I WAS ADVISED LAST WEEK THAT WE WILL BE RELEGATED TO THE "MISCELLANECUS SECTION" FOR FUTURE EDITIONS.

SLIDE 3 OFF

IN EARLY 1976, AS THE DOD TASK FORCE WAS ASSESSING THE VARIOUS PHYSICAL SECURITY EQUIPMENT EFFORTS UNDERWAY IN THE SERVICES, IT BECAME CLEAR THAT THE PROGRAMS FELL INTO FOUR GENERAL CATEGORIES. THESE CATEGORIES SERVE AS TITLES TO OUR CURRENT PROGRAM EFFORTS AND ARE LISTED ON THE NEXT SLIDE.

SLIDE 4 ON

WE ARE PRESENTLY ATTEMPTING TO PURCHASE A COMMERCIAL PHYSICAL SECURITY EQUIPMENT SYSTEM FOR USE IN EUROPE. AN RFP WAS RELEASED ON 30 JUNE WHICH PERMITS THE SELECTED CONTRACTOR TO SPECIFY THE COMPONENTS HE WILL USE AT ^{APPROXIMATELY 50} / DIFFERENT LOCATIONS. THE BID IS OPEN TO ALL NATO COUNTRIES WITH THE BRITISH, GERMANS AND AMERICANS SHOWING THE GREATEST INTEREST TO DATE. THE FIRM WHICH RECEIVES THIS CONTRACT COULD HAVE AN ADVANTAGE IN SUBSEQUENT AWARDS WHICH COULD COVER OVER 100 AN ADDITIONAL LOCATIONS. HOWEVER, IF THE WINNER IS PLAGUED WITH SITUATIONS

SIMILAR TO OUR EXPERIENCES. HE MAY NOT WANT ANY SUBSEQUENT CONTRACTS. CONCURRENT WITH OUR EUROPEAN BUY, WE ARE INTENDING TO PURCHASE DOD AND COMMERCIALY DEVELOPED COMPONENTS FOR USE AT OTHER STORAGE FACILITIES.

UNDER "DOD RESEARCH AND DEVELOPMENT," THE ARMY IS DEVELOPING INTERIOR SENSORS AND THE AIR FORCE IS DEVELOPING EXTERIOR SENSORS. WE HAVE ASKED THE DEFENSE NUCLEAR AGENCY TO CONDUCT AN INDEPENDENT ASSESSMENT OF THESE TWO PROGRAMS, IN COOPERATION WITH THE SERVICES, TO DETERMINE IF ANY HARDWARE DUPLICATION EXISTS. THIS STEP IS BEING TAKEN IN THE INTEREST OF GOOD MANAGEMENT, AND THE DATA WILL CERTAINLY BE USEFUL IN PREPARING FUTURE RESPONSES TO THE CONGRESS AND OTHER INTERESTED PARTIES. THE CONGRESS HAS NOT BEEN TOTALLY PLEASED WITH THE DOD PHYSICAL SECURITY EQUIPMENT PROGRAMS. IN FACT, IN 1976 THE CONGRESS SAID IT WAS DISPLEASED WITH THE PROGRESS BEING MADE. UNFORTUNATELY, WE DID NOT HAVE OUR ACT TOGETHER AT THE TIME AND A BAD IMPRESSION APPEARS TO HAVE BEEN FORMED. WE STILL DO NOT HAVE THE ANSWERS TO A LOT OF QUESTIONS, BUT I BELIEVE WE HAVE INITIATED THE EFFORTS WHICH WILL CAUSE THE ANALYSIS TO BE PERFORMED OVER THE NEXT SEVERAL YEARS THAT WILL GIVE US A LOT OF THE ANSWERS. IN THE INTERVENING TIME FRAME, WE EXPECT TO ENTER PRODUCTION WITH LAND-BASED AND SHIPBOARD PHYSICAL SECURITY SYSTEMS FROM OUR CURRENT R&D EFFORTS.

WHEN WE LOOKED AROUND TO SEE WHAT PROGRAMS WERE ONGOING WHICH WOULD HELP US IN THE AREA OF EXPLORATORY DEVELOPMENT FOR PHYSICAL SECURITY EQUIPMENT, WE FOUND THAT THE DEFENSE NUCLEAR AGENCY WAS THE ONLY ORGANIZATION WITH AN IDENTIFIED AND FUNDED

LINE ITEM THAT COULD BE SO CLASSIFIED. CONSEQUENTLY, AND IN KEEPING WITH OUR RESEARCH AND DEVELOPMENT PHILOSOPHY THAT TECHNOLOGIES PERFECTED FOR NUCLEAR SECURITY WILL HAVE APPLICATION TO OTHER ASPECTS OF PHYSICAL SECURITY, THE DEFENSE NUCLEAR AGENCY WAS TASKED TO DEVELOP, IN COOPERATION WITH THE SERVICES, A DOD PHYSICAL SECURITY EQUIPMENT EXPLORATORY DEVELOPMENT PROGRAM. THE DNA HAS MADE SIGNIFICANT PROGRESS AND WE HOPE TO HAVE THE FINAL PROGRAM PROPOSAL IN FEBRUARY 1978.

I BELIEVE THAT IT IS IMPORTANT THAT YOU UNDERSTAND THAT THE DNA IS DEVELOPING THE PROGRAM BASED ON INPUTS FROM THE SERVICES, BUT CONTRACTING AND TRACKING OF THE FUNDS ARE THE SOLE RESPONSIBILITY OF THE DNA. THE DNA BUDGET WILL CONTAIN ALL THE 6.2 MONEY FOR THIS DOD EFFORT, BUT THE MILITARY DEPARTMENTS AND CIVILIAN FIRMS WILL BE USED TO ACCOMPLISH THE TASKS. WE ARE VERY EXCITED ABOUT THE PROSPECTS OF THIS ELEMENT OF THE TOTAL PROGRAM, AND WE ARE HOPEFUL, THAT OF THE MANY ANSWERS WE EXPECT TO GET CONCERNING EQUIPMENT AND HUMAN BEHAVIOR, THAT THE FUNDAMENTAL QUESTION, "SHOULD WE DEVELOP A FOLLOW-ON PHYSICAL SECURITY EQUIPMENT SYSTEM FOR 1990, OR SHOULD WE SIMPLY UPGRADE COMPONENTS OF THE EQUIPMENT SYSTEM PRESENTLY BEING DEFINED," WILL BE ANSWERED.

AS WE LOOK AT THE TOTAL PHYSICAL SECURITY SYSTEM, BOTH EQUIPMENT AND MAN, OR WOMAN AS THE CASE MAY BE, WE BELIEVE THAT THE SYSTEM SHOULD DETER, DETECT, DENY AND DESTROY OR DISABLE, AS WARRANTED BY A GIVEN SITUATION.
/ THE FENCES, LIGHTS, DOGS, AND SENTRIES ARE THE DETERRENCE.
SHOULD THEY FAIL THEN OUR SENTRIES AND SENSORS SHOULD DETECT.
DENIAL, WITHIN THE CAPABILITIES OF THE DESIGNED AND DEPLOYED

SYSTEM, IS ACHIEVED BY GUARDS, LOCKS, REINFORCED STRUCTURES AND SO FORTH. SHOULD ALL THESE FAIL, THE ULTIMATE STEP IN DENIAL IS TO DESTROY ^{IF NECESSARY,} THAT WHICH YOU ARE PROTECTING.

SINCE THE PUEBLO INCIDENT IN 1968, THE NAVY HAS HAD A MODEST PROGRAM AIMED AT DEVELOPING ANTICOMPROMISE EMERGENCY DESTRUCT DEVICES. ON 13 JUNE 1977, THE DDR&E ASKED THE NAVY TO EXPAND ITS EFFORT TO ADDRESS CERTAIN VALIDATED DOD REQUIREMENTS. THE NAVY IS HOSTING A USERS CONVERENCE ON 3 AND 4 AUGUST TO REFINE AND POSSIBLY ADD TO THOSE REQUIREMENTS, WHICH WILL SERVE AS A BASIS FOR STRUCTURING THE NEW ACED PROGRAM.

ASIDE FROM THE "GEE WHIZ" ITEMS SUCH AS SELF DESTRUCTING SAFES AND BRIEFCASES, THE NAVY WILL BE EXPENDING A CONSIDERABLE EFFORT ON ERASABLE ELECTRONICS AND THEIR POTENTIAL USE IN THE PRODUCTION MODELS OF OUR COMBAT SYSTEMS. IN ADDITION, THERE WILL BE SEVERAL OTHER ACED APPLICATIONS BEING INVESTIGATED BUT THEY GO BEYOND THE SECURITY CLASSIFICATION OF THIS SEMINAR. THEREFORE, WHILE THIS AREA IS ONE OF GREAT INTEREST, ITS SENSITIVITY PRECLUDES ADDITIONAL DISCUSSION.

LOOKING BACK OVER THE PROGRAM TITLES, IF YOU WILL CONSIDER THE COMMERCIAL PHYSICAL SECURITY EQUIPMENT SYSTEMS PRESENTLY INSTALLED OR UNDER CONTRACT AS OUR OLD SYSTEM, AND THE CURRENT R&D EFFORT AS NECESSARY TO PROVIDE A REPLACEMENT FOR THAT OLD SYSTEM, AND THE NEW EXPLORATORY DEVELOPMENT INITIATES AS THE LOGICAL PROGRESSION IN PURSUING AN OUT YEAR SYSTEM, THEN ONE COULD ARGUE THAT WE HAVE A STRUCTURED PROGRAM, ALTHOUGH IT WAS DEFINED AFTER THE FACT, WHICH SHOULD SATISFY OUR NEAR AND LONG

TERM PHYSICAL SECURITY EQUIPMENT NEEDS. IN ADDITION, THIS DIVISION PERMITS US TO DO BATTLE WITH THE PROGRAM ANALYZERS IN TERMS THAT HAVE MEANING TO THEM.

SLIDE 4 OFF

NO DOD BRIEFING ON A HARDWARE DEVELOPMENT PROGRAM WOULD BE COMPLETE WITHOUT A LIST OF OBJECTIVES. SO, THE ACTION GROUP HAS DEVELOPED ITS LIST OF OBJECTIVES.

SLIDE 5 ON

I SUPPOSE WE COULD CALL THESE THE BIG ELEVEN OR SOME OTHER CATCHY NAME, BUT WHATEVER, I'M SURE YOU WILL AGREE THAT A LOT OF PEGS MUST FALL INTO THE RIGHT PLACES BEFORE ANY AND ALL OF THESE OBJECTIVES WILL BE MET.

THE DEFINING OF THE LAND-BASED AND SHIPBOARD SYSTEMS IN 1978 IS CRITICAL IF WE ARE TO BE IN PRODUCTION BY THE END OF 1981.

OUR CONCEPT HERE IS THAT THE NAVY IS TO UTILIZE TO THE MAXIMUM EXTENT PRACTICABLE, THE LAND-BASED COMPONENTS DEVELOPED BY THE ARMY AND THE AIR FORCE. TO THAT END, WE WILL BE OUTFITTING A SHIP IN FY 78 TO SERVE AS A TEST BED/LABORATORY FOR THAT PURPOSE. INCIDENTALLY, WE HAVE TESTED A COMMERCIAL LAND-BASED INFRARED SENSOR ABOARD A COUPLE OF SHIPS, AND THE RESULTS ARE VERY ENCOURAGING.

AS I MENTIONED EARLIER, WHILE WE ARE ENTERING INTO PRODUCTION WITH THE DOD SYSTEM, WE DO EXPECT TO AWARD THE LAST CONTRACT IN 1980 FOR THE PURCHASE OF A PURE COMMERCIAL SYSTEM. THAT CONTRACT WILL ROUND OUT A SEGMENT OF OUR TOTAL PHYSICAL SECURITY EQUIPMENT

UPGRADE EFFORT.

JUST YESTERDAY MEMBERS OF THE ACTION GROUP, UNDER SPONSORSHIP OF THE DNA, MET WITH REPRESENTATIVES OF SEVERAL OTHER FEDERAL AGENCIES. OUR TOPIC OF DISCUSSION WAS, "THE NEED FOR A PHYSICAL SECURITY EQUIPMENT INFORMATION AND ANALYSIS CENTER." THE DOD HAS COLLECTED A LARGE AMOUNT OF INFORMATION ABOUT PHYSICAL SECURITY EQUIPMENT AND TECHNIQUES. AS WE PROGRESS INTO OUR FUTURE PROGRAMS, WE EXPECT TO GREATLY INCREASE THE VOLUME OF INFORMATION BEING COLLECTED, ESPECIALLY ABOUT COMMERCIAL SECURITY EQUIPMENT. WE HAVE FUNDS PROGRAMMED IN FY 79 WHICH WILL PERMIT US TO INITIATE A QUALIFIED PRODUCTS LIST TEST PROGRAM TO LEARN MORE ABOUT THE DEVICES THAT WILL BE AVAILABLE ON THE OPEN MARKET. WE WOULD EXPECT SUCH A CENTER TO BE ACCESSABLE BY ALL FEDERAL AGENCIES AND TO STORE DATA ON ALL TESTED PHYSICAL SECURITY EQUIPMENT (DOD AND COMMERCIAL), GOVERNMENT AND INDUSTRY SECURITY EQUIPMENT PERFORMANCE SPECIFICATIONS, AND NON-U.S. SECURITY EQUIPMENT CAPABILITIES. THE SCOPE OF ANALYTICAL CAPABILITY THAT SUCH A CENTER SHOULD POSSESS IS YET TO BE DETERMINED. HOWEVER, I DO BELIEVE IT IS SAFE TO SAY THAT ALL INTERESTED AGENCIES EXPECT SOMETHING MORE THAN A SIMPLE INFORMATION RETRIEVAL SYSTEM.

A RATHER INTERESTING STATISTIC OF WHICH I WAS RECENTLY MADE AWARE IS THAT THE DOD HAS ABOUT 10 MILLION SMALL ARMS STORED IN APPROXIMATELY 12,000 ARMS ROOMS AND WAREHOUSES AND MORE THAN 19,000 CONVENTIONAL AMMUNITION STORAGE IGLOOS ALL WHICH MAY REQUIRE THE INSTALLATION OR UPGRADE OF PHYSICAL SECURITY EQUIPMENT.

THEREFORE, IT IS IMPERATIVE THAT WE STANDARDIZE OUR PHYSICAL SECURITY EQUIPMENT SYSTEM AS MUCH AS POSSIBLE IN THE INTEREST OF MAINTENANCE AND OPERATOR TRAINING IF FOR NO OTHER REASONS.

WE MAY BE FORCED TO REPLACE SOME OF OUR SYSTEMS EARLIER THAN 1985 BECAUSE MANY OF THEM WERE DEPLOYED IN THE EARLY 1970'S AND THEY WERE NOT ALL THAT RELIABLE AT THE TIME.

BUT, IF ALL OF THE ABOVE MEET WITH SUCCESS, WE SHOULD HAVE OUR ULTIMATE SYSTEM, ONE THAT WILL DETER, DETECT, DENY, AND DISABLE OR DESTROY BY 1990.

SLIDE 5 OFF

WELL, I'M SURE YOUR MOST LIKELY THOUGHT AT ABOUT THIS POINT IN TIME IS, "GEE THAT'S GREAT, BUT HOW MUCH WILL IT COST AND HOW MUCH DO YOU HAVE?"

SLIDE 6 ON

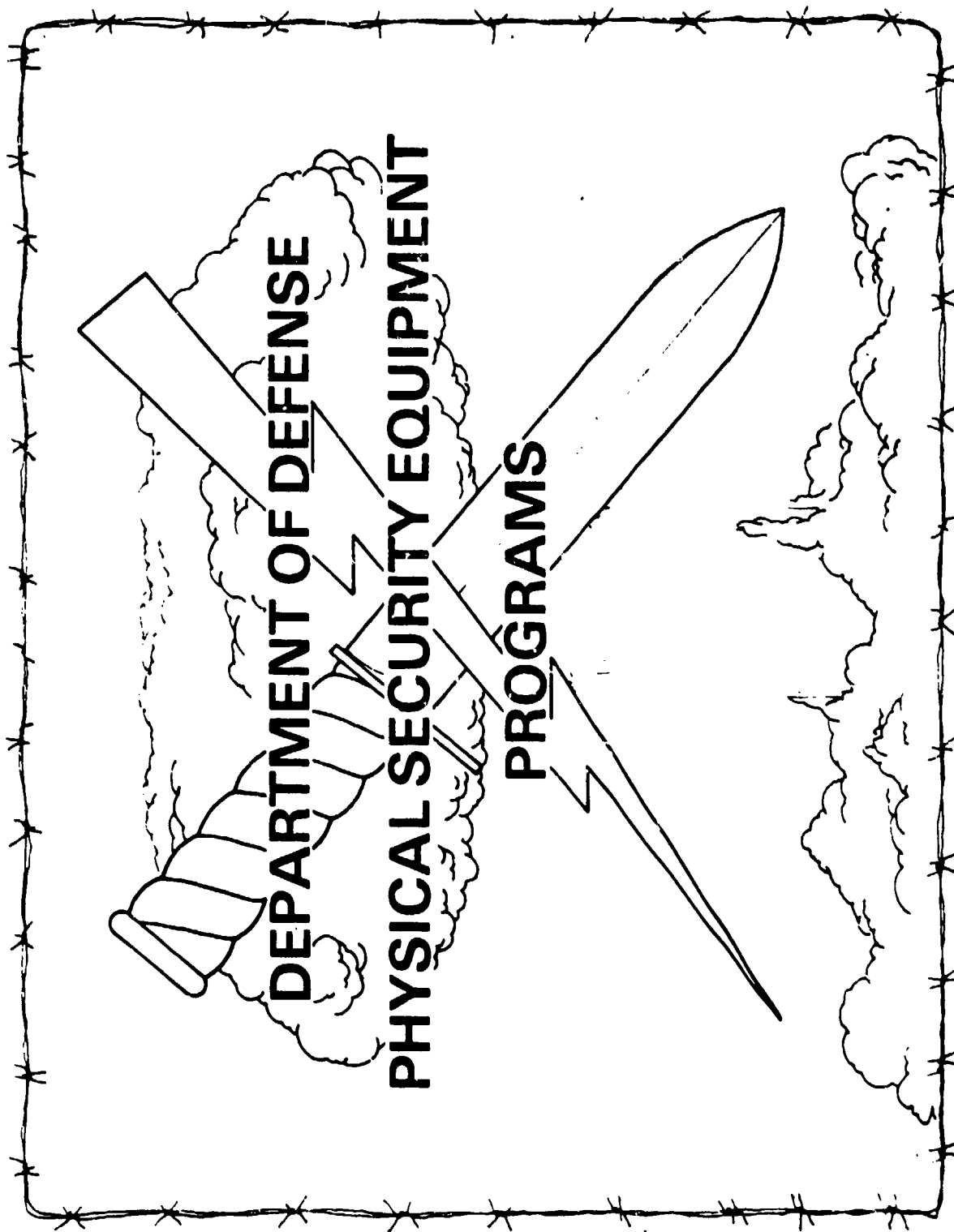
THIS SLIDE SHOWS YOU WHAT WE THINK IT WILL COST US TO GET THROUGH OUR FIRST TEN OBJECTIVES. WE HOPE TO KNOW WHAT NUMBER ELEVEN WILL COST BY THE END OF FY 79.

FOR THOSE OF YOU WHO KNOW THE LEVELS REQUESTED FOR FY 78, YOU WILL RECOGNIZE THAT THERE HAS TO BE A SUBSTANTIAL INCREASE IN SUBSEQUENT YEAR FUNDING TO ARRIVE AT THESE TOTALS. THE R&D TOTALS DO INCLUDE ARMY, NAVY, AIR FORCE AND DNA, AND THE PROCUREMENT TOTALS ARE FOR ALL SERVICES.

I'M SURE I HAVE RAMBLED QUITE A BIT DURING THE PAST TWENTY MINUTES OR SO AND I SUPPOSE THE BOTTOM LINE OF MY PITCH IS:

THE UNITED STATES CANNOT PERMIT ANY OF ITS NUCLEAR OR CERTAIN

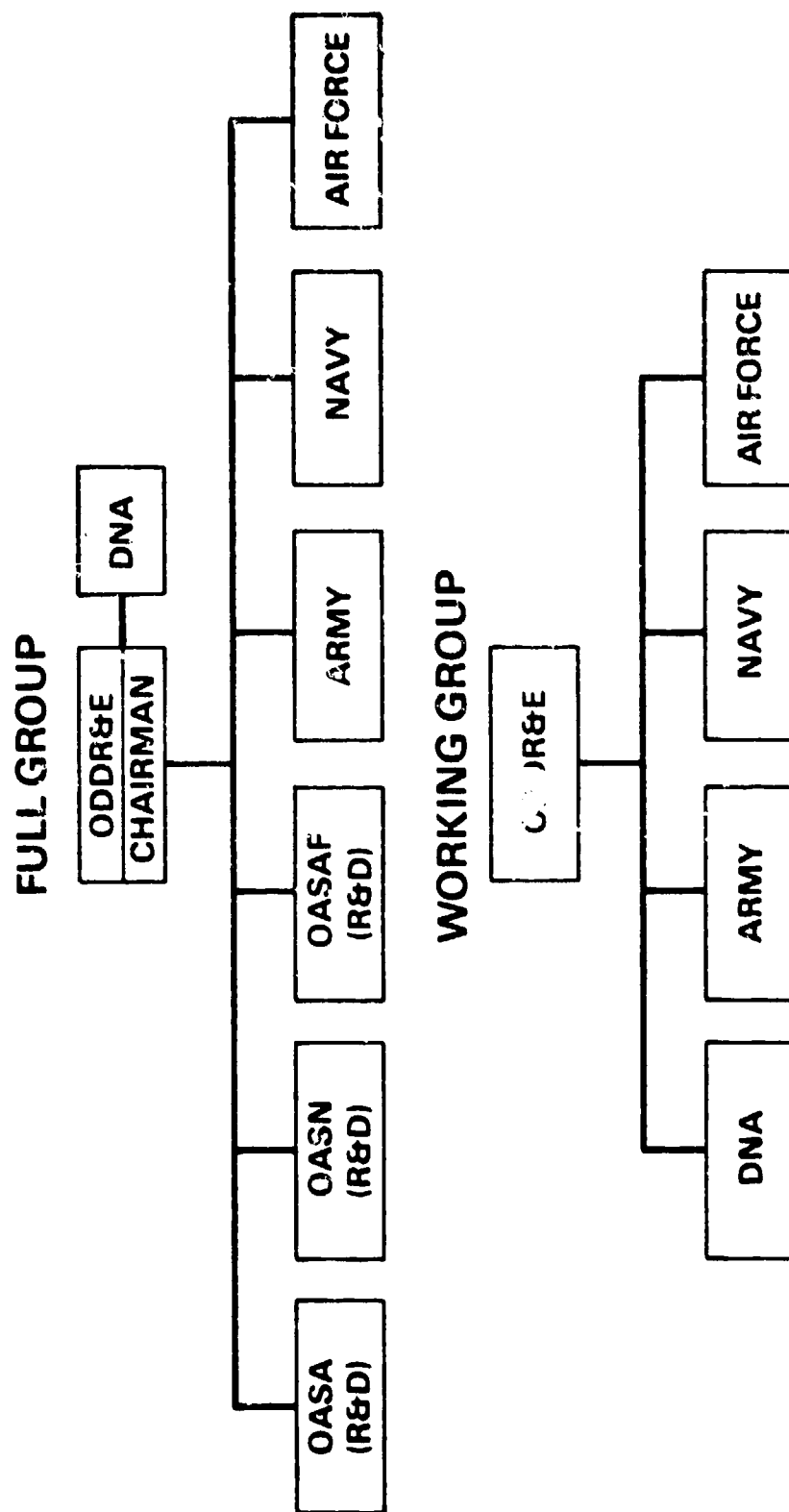
OTHER HIGHLY SENSITIVE WEAPONS TO BE TAKEN ILLEGALLY FROM ITS CUSTODY, NOR CAN IT AFFORD TO LOSE THE CRITICAL SUPPLIES THAT ARE SO VITAL DURING THE EARLY STAGES OF COMBAT. AT PRESENT, WE USE PEOPLE TO GUARANTEE THAT SUCH EVENTS WILL NOT OCCUR. IN THE FUTURE, UTILIZING SOME OF THE CONCEPTS AND DEVICES WHICH YOU WILL BE DISCUSSING AT THIS SEMINAR, PERHAPS WE WILL BE ABLE TO REDUCE THE NUMBER OF SECURITY PERSONNEL REQUIRED FOR THE PROTECTION OF THESE CRITICAL AND SENSITIVE DOD ASSETS. I DO WISH TO RESTATE THE WORDS "REDUCE THE NUMBER OF SECURITY PERSONNEL" AND EMPHASIZE THAT MAN WILL NEVER BE REPLACED IN OUR SECURITY SYSTEM AS LONG AS THE USE OF DEADLY FORCE IS AN OPTION.



PHYSICAL SECURITY EQUIPMENT PROGRAMS

- **PROCUREMENT OF COMMERCIAL
SYSTEMS**
- **DOD RESEARCH AND DEVELOPMENT**
- **DEFINITION OF EXPLORATORY
DEVELOPMENT**
- **ANTICOMPROMISE EMERGENCY
DESTRUCT**

DOD PHYSICAL SECURITY EQUIPMENT ACTION GROUP



PHYSICAL SECURITY EQUIPMENT PROGRAM OBJECTIVES

- **DEFINE A LAND-BASED PSE SYSTEM IN 1978**
- **DEFINE A SHIPBOARD PSE SYSTEM IN 1978**
- **BEGIN EXPLORATORY DEVELOPMENT FOR 1990 SYSTEM IN 1978**
- **INITIATE QUALIFIED PRODUCTS LIST IN 1979**
- **AWARD CONTRACTS FOR 150 SENSITIVE LOCATIONS BY 1980**
- **PLACE DOD LAND-BASED SYSTEM IN PRODUCTION BY 1981**
- **PLACE DOD SHIPBOARD SYSTEM IN PRODUCTION BY 1981**
- **ESTABLISH INFORMATION AND ANALYSIS CENTER IN 1982**
- **COMPLETE UPGRADE OF 30,000 SELECTED STRUCTURES BY 1984**
- **BEGIN REPLACING EARLIER SYSTEMS BY 1985**
- **PLACE FOLLOW-ON LAND-BASED/SHIPBOARD SYSTEMS IN PRODUCTION BY 1990**

PHYSICAL SECURITY EQUIPMENT PROGRAMS
ESTIMATED FUNDING FY 78-83
(DOLLARS IN MILLIONS)

RESEARCH AND DEVELOPMENT	\$ 225
SECURITY UPGRADE (NUCLEAR)	265
SECURITY UPGRADE (CHEMICAL)	10
SECURITY UPGRADE (OTHER SENSITIVES)	<u>1,000</u>
ESTIMATED COST LESS OMA	\$1,500

DESCRIPTION
OF THE
REMOTELY MONITORED BATTLEFIELD SENSOR SYSTEM
(REMBASS)

ENGINEERING DEVELOPMENT (ED) SYSTEM

PRESENTED BY
WILLIAM R. GREEN
LTC, SigC
APM, REMBASS

1.0 INTRODUCTION

1.1 General

This is a description of the Basic Remotely Monitored Battlefield Sensor System (REMBASS), designed in accordance with the REMBASS Materiel Need as approved by the Department of Army on 4 April 1972, and revised on 16 April 1976. The hardware fabrication phase of Engineering Development (ED) began 27 June 1977, when RCA Corporation, Camden, New Jersey, was awarded the design and fabrication contract for the Basic REMBASS. The REMBASS Project Office is also sponsoring Advanced Development (AD) efforts in imaging sensors, battery power units, target classification, data transmission and sensor monitoring. The results of the AD will be applied to extend the basic design to more advanced REMBASS configurations.

1.2 System Composition.

The REMBASS system is a family of sensors, repeaters and displays. The subsystems are (1) Sensor Subsystem; (2) Data Transmission Subsystem; and (3) Monitoring Subsystem. These subsystems and their associated elements are described in terms of functions and characteristics.

2.0 PERFORMANCE

REMBASS is a ground-based battlefield sensor system designed to provide the commander with an all-weather, day-and-night, alerting,* surveillance** and target acquisition*** capability for targets of interest. It is designed to accommodate world-wide terrain and climatic conditions. Further, it complements and supplements other manned and unmanned reconnaissance and surveillance systems such as surveillance radars, RPV's, and night vision thermal imaging devices.

REMBASS is intended to be used in both offensive and defensive roles, and in all intensities of warfare. It will be employed by echelons from battalion to division.

To accommodate the wide range of applications, the REMBASS design concept allows the commander to select various combinations of equipment for a given mission. Sensors may be hand-emplaced, or delivered by artillery or aircraft. Radio repeaters may be hand-emplaced, delivered by aircraft, or mounted on aircraft. Sensors utilizing magnetic, seismic, acoustic, infrared and pressure phenomena will be available for deployment, and different types may be mixed at the same site. Following emplacement, the sensors will operate autonomously, transmitting reports directly or via repeaters to remote readouts for monitoring. The sensor monitoring configuration can include either small portable monitoring sets, or a more elaborate man-portable Sensor Monitoring Set designed to accommodate many sensors.

The following sensor types may transmit reports:

- (1) Detection-only sensors, capable of giving an intrusion alarm, and, if so designed, to indicate direction of travel
- (2) Classifying sensors, designed to report probable target classification (personnel, tracked, or wheeled vehicle)
- (3) Analog audio confirming sensors, designed to pick up and relay audible disturbances generated by intrusions

* "Alerting" means detection of an intrusion by a sensor, and timely transmission of the information to a sensor monitor.

** "Surveillance" means systematic observation of the emplacement site for intelligence-gathering purposes.

*** "Target," as used in this description, means any intruder, whether hostile or not, and refers to one object only (i.e., a target element). "Target acquisition" means determining hostility, probable location, and other relevant information preparatory to hand-over to a fire control system.

Records of sensor reports in time-ordered sequence will be generated at sensor monitor stations. These records, as well as the audible disturbances, will be available for analysis by system operators. The operators will be able to estimate location, speed, direction of travel, convoy size, and class of targets.

REMBASS includes a data link capable of transmitting and relaying sensor reports. The data link will be compatible with other battlefield systems, specifically the Field Artillery Acoustic Locating System (FAALS) and the Air Force Base Installation Security System (BISS), that may operate in the same radio frequency band. Compatibility will ensure that one system does not interfere with another, when in simultaneous operation.

2.1 Illustrative Deployment

Figure 1 illustrates deployment and use of remotely monitored sensors and other REMBASS equipment, as follows:

- (1) A passive magnetic detection sensor emplaced near the road-side
- (2) A strain-sensitive cable sensor emplaced across the road
- (3) A passive infrared sensor set up within line-of-sight of the road
- (4) A seismic/acoustic classifier within the range of road and footpath
- (5) An analog audio sensor emplaced within the range of the road

The functions of these sensors are described in Section 3.1.

Figure 1 also illustrates two methods for transmitting sensor reports to the readout. In one example, the infrared sensor and seismic/acoustic classifier are shown transmitting directly from the sensor to a portable monitoring set. In the second example, an analog audio sensor transmits via a ground emplaced repeater.



REHBASS

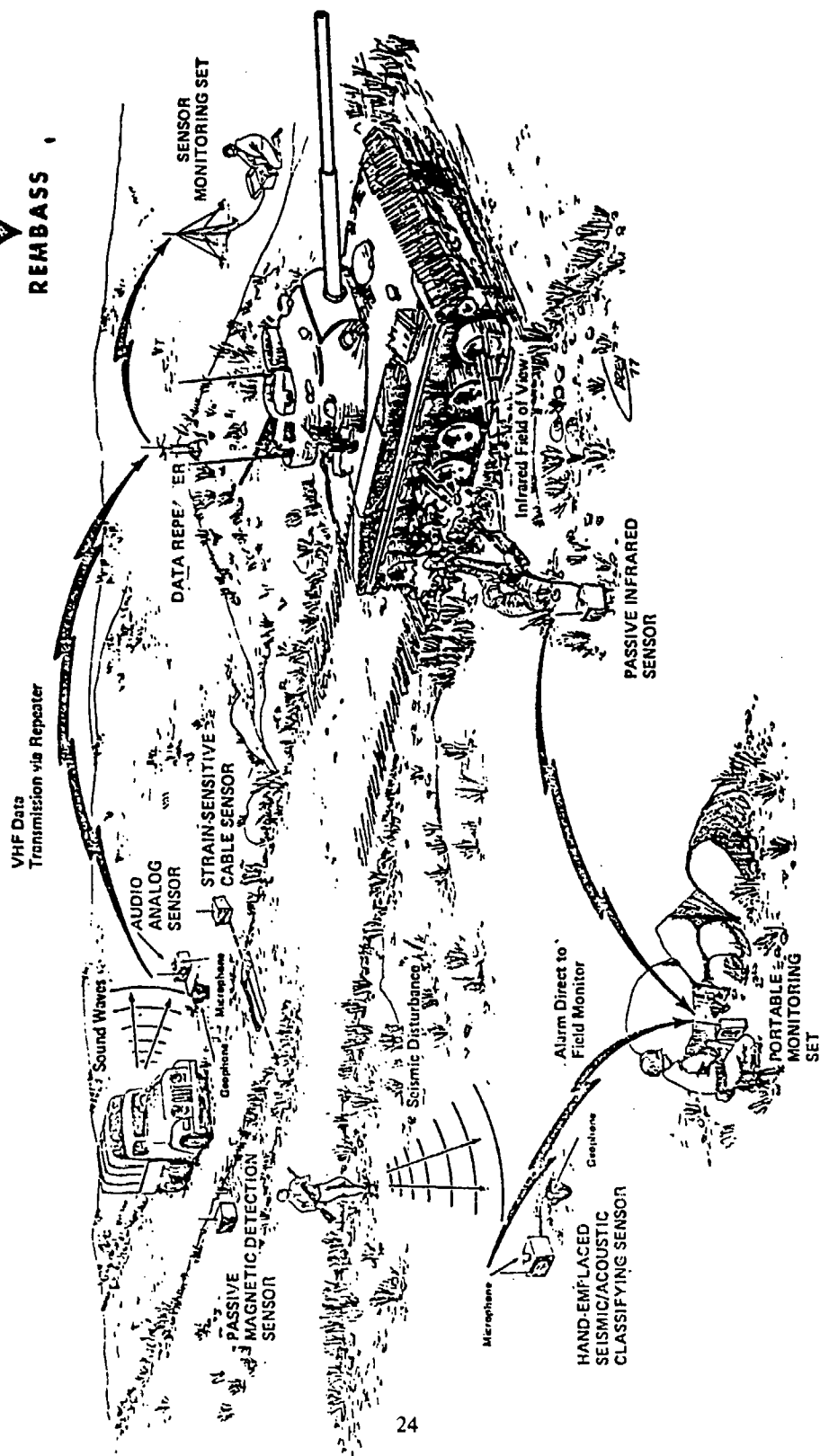


FIGURE 1

ILLUSTRATION OF SENSOR DEPLOYMENT AND USE

3.0 SYSTEM FUNCTIONS

The REMBASS equipments required to meet the performance characteristics described in Section 2.0 have been organized into subsystems as shown in Figure 2. They are (1) Sensor Subsystem; (2) Data Transmission Subsystem; and (3) Monitoring Subsystem. Delivery equipment and methods, and power sources support these subsystems. The following sections describe, in summary, the functions and characteristics of these subsystems and their support.

3.1 Sensor Subsystem

The sensor design philosophy has an important effect on the system characteristics and methods of use. The sensors are designed to function autonomously after emplacement, automatically transmitting reports when intrusions are detected. Sensors of different types are intended to operate at the same emplacement site so as to complement one another. The mix of types varies, and is usually selected to suit the mission.

Each sensor is equipped with (1) transducers; (2) internal sensing and detection and/or classification logic; (3) self-initiated reporting capability; (4) data link transmitter; and (5) battery power supply. The battery supply enables the sensor to operate independently; batteries have adequate capacity to support mission life of 7, 15 or 30 days.

Sensor data transmission outputs conform to a standard REMBASS communications format. Sensors can be employed in large numbers with little risk of interference, since channels and identity codes can be selected for each sensor prior to deployment in the field.

The seven sensor types provided for in the Basic REMBASS are shown in Table 1 and Figure 3. Each type employs detection and/or classification logic suited to the physical disturbance (seismic, acoustic, magnetic, etc.) being monitored. As shown in the table, each type has different operational characteristics with distinctive capabilities and limitations. The distinctive sensor characteristics and limitations, and the applications-oriented factors, are brought out in Sections 3.1.1 - 3.1.5.

The common design goal characteristics are as follows:

Operation in a world-wide environment

Minimum risk of radio interference with other sensor systems
(FAALS and BISS)

High probability of deployment survivability

Camouflage to minimize risk of enemy discovery

REMBASS SUBSYSTEMS

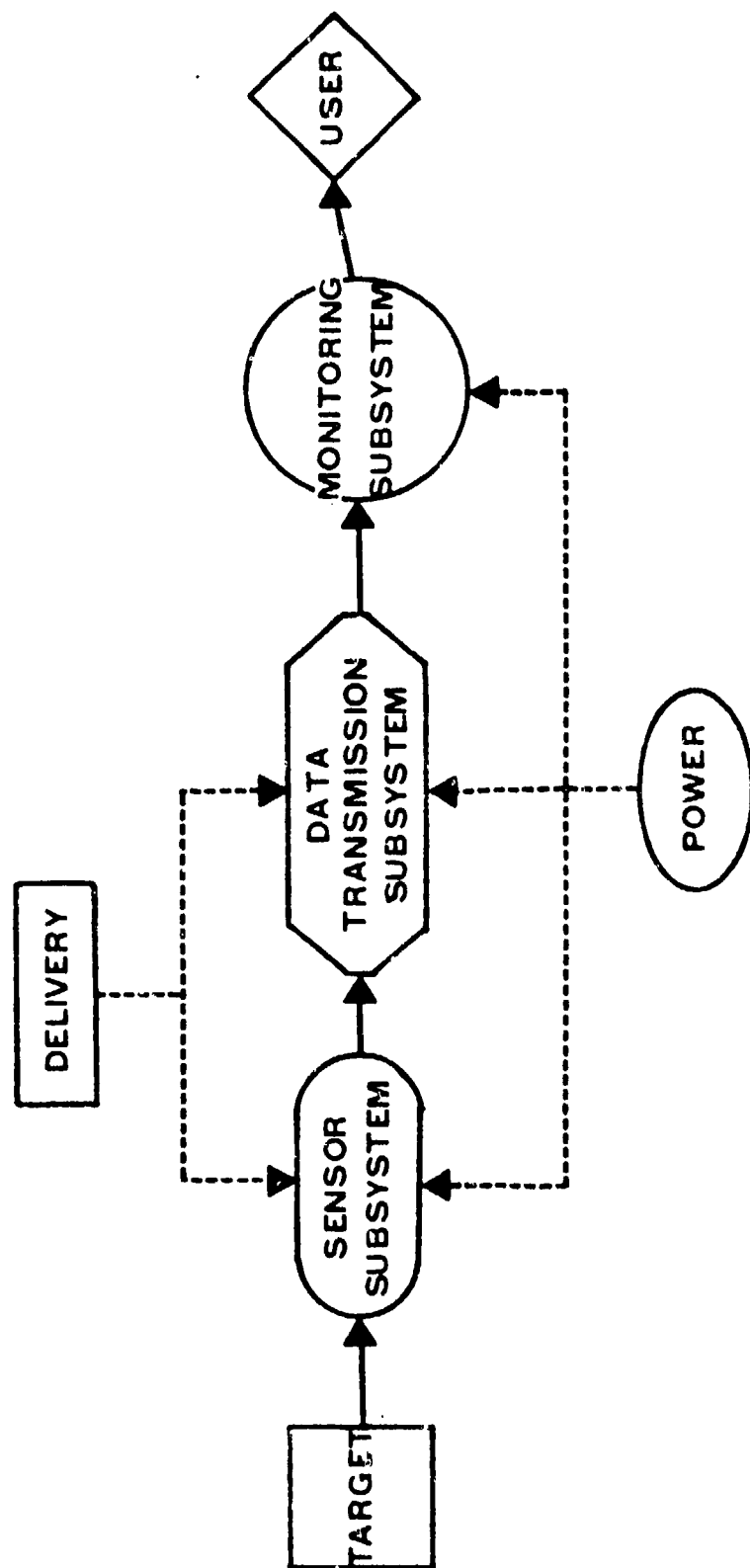


FIGURE 2

Type of Sensor	Designation	Technique	Delivery Method			Class Outputs	Detection (1) Capability	Direction (Sense) Capability	Analog Acoustic Output	Size (in ³)	Weight (lbs)	Selectable Operating Life (Days)
			Delivery Method									
			Hand	Artillery	Aircraft							
Classification	DT-562	Seismic/Acoustic	X			P, W, T				200	8	7, 15, 30 or EOL
	DT-570	Seismic		X		P, W, T	P, W, T			TDV	15	7, or EOL
	DT-567	Seismic			X	P, W, T	P, W, T			SES	20	7, 15, 30, or EOL
Magnetic Detection	DT-561	Passive Magnetic	X				P _A , W, T			200	8	7, 15, 30, or EOL
Infra-red	DT-565	Passive IR	X				P, W, T	X		200	8	7, 15, 30, or EOL
Strain Cable	DT-573	Pressure Sensitive Cable	X			P, W, T	P, W, T			200	8	7, 15, 30 or EOL
Analog	DT-563	Seismic Trigger; Acoustic Data	X				W, T		X	300	12	7, 15 or EOL

KEY: P - Personnel
 A - Armed Personnel
 W - Wheeled Vehicles
 T - Tracked Vehicles
 TDV - Terminal Delivery Vehicle
 SES - Surface Emplaced Sensor
 EOL - End of Battery Life

Note: (1) Detection messages are generated by the classification sensors when their logic determines that a target is present but cannot be classified. For the other sensors, a valid detection message is generated when their logic senses the presence of any of the targets indicated in the detection column for the sensor.

TABLE 1. REMBASS SENSORS (BASIC SYSTEM)

REMBASS SYSTEM SENSORS

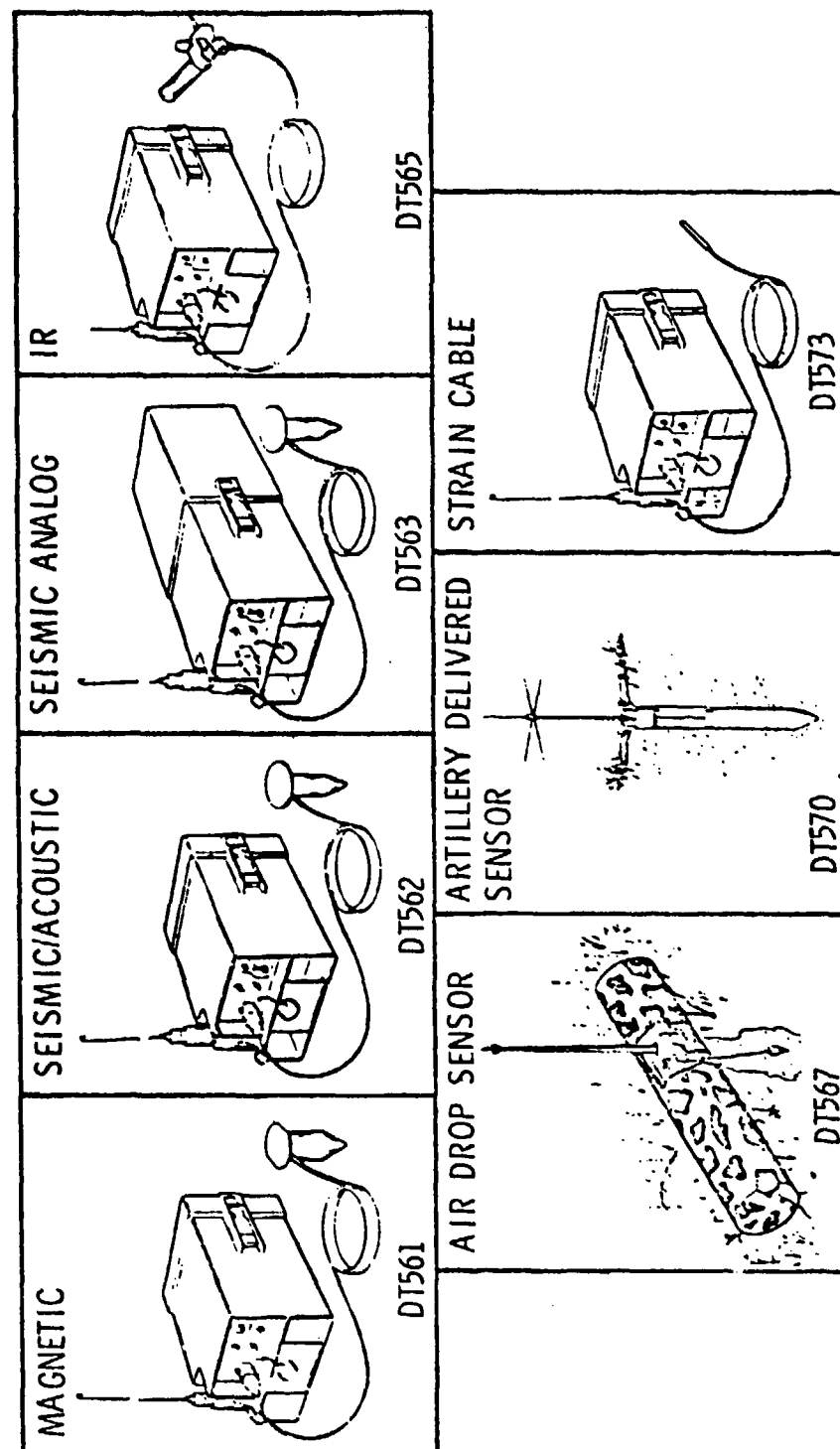


FIGURE 3

High probability of target detection

Low false alarm rates

Conformance to standard data transmission format

Field selection of identity code and frequency channel

Internal disable, triggered by tampering, improper implantation, and battery end-of-life

3.1.1 Classification Sensors

The classification sensors (DT-562, DT-567 and DT-570) detect and automatically discriminate among personnel, wheeled vehicles and tracked vehicles. The result is a target class report, which is transmitted to a monitor set. If the sensor detects a target intrusion but cannot determine class, a "detection only" message is sent.

Classification sensors provide automatic analysis of signature information. The signature analysis process depends on measurement of features (e.g., signal intensity in various frequency bands) by sensor circuitry. Two types of classification sensor are provided in the Basic REMBASS: (1) A seismic classifier that analyzes seismic signals from a geophone; and (2) A seismic/acoustic classifier that analyzes seismic signals from a geophone and also acoustic signals from a microphone.

Figure 4 illustrates the hand-emplacable seismic/acoustic classifier sensor DT-562. Its size is 200 cubic inches, and weight, including battery, is approximately 8 pounds. It features a combined antenna/acoustic pick-up assembly which can be remotely operated at a distance of up to 10 feet from the sensor. The geophone can also be implanted in the ground up to 10 feet from the sensor.

The frequency, sensor identification (ID), gain and life of battery (LOB) controls are located on the front panel. The geophone and microphone with antenna can be stowed under the control panel. The battery is located inside the rear housing cover.

The functional block diagram (Figure 5) shows the major components. The transducers (microphone and/or geophone) feed analog disturbance signals to the detection and classification logic. Reports generated by the logic circuits are encoded by the data transmission circuitry and are transmitted at radio frequencies via the antenna. Identity-code selection settings are used in the data transmission circuits to generate part of the message.

DT-562 SEISMIC/ACOUSTIC CLASSIFIER SENSOR

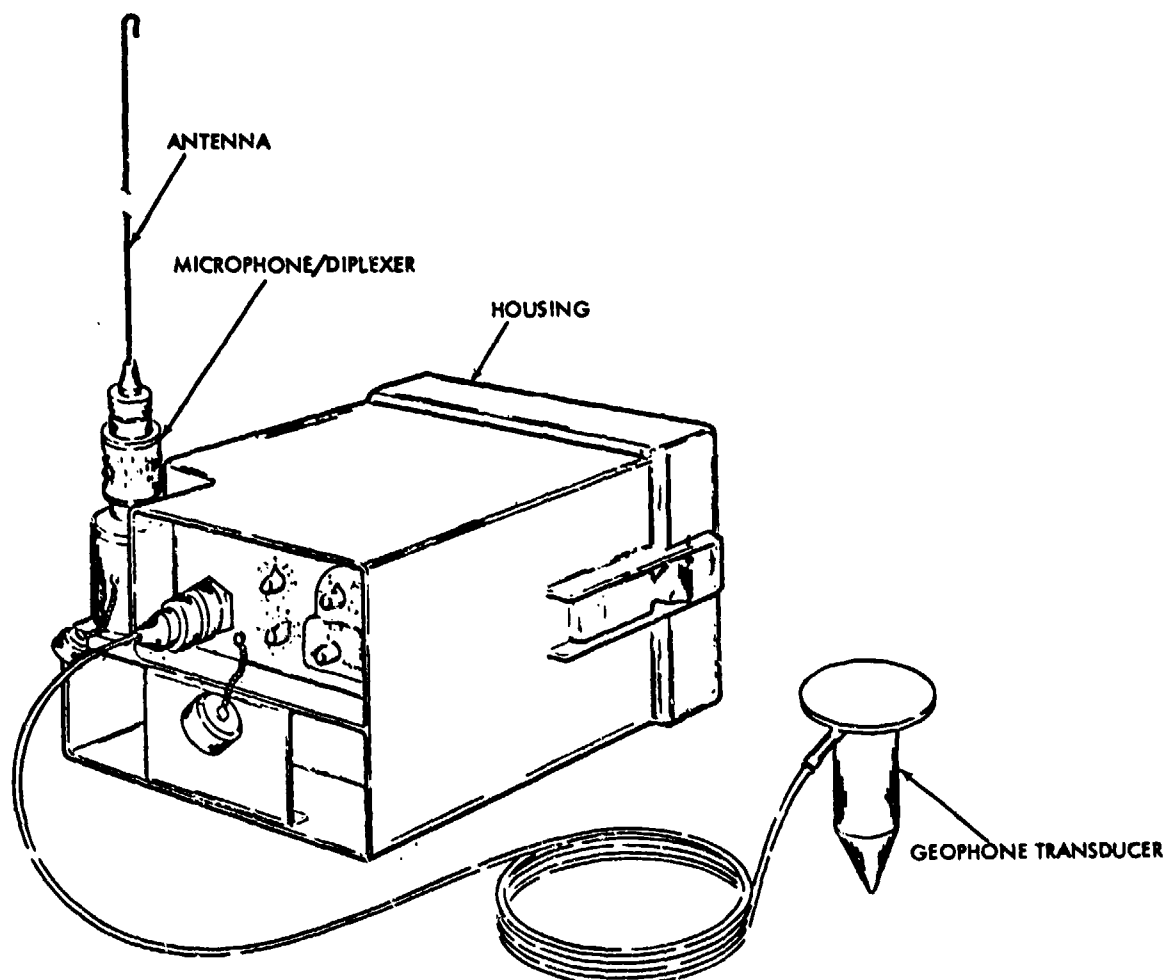


FIGURE 4

CLASSIFICATION SENSOR BLOCK DIAGRAM

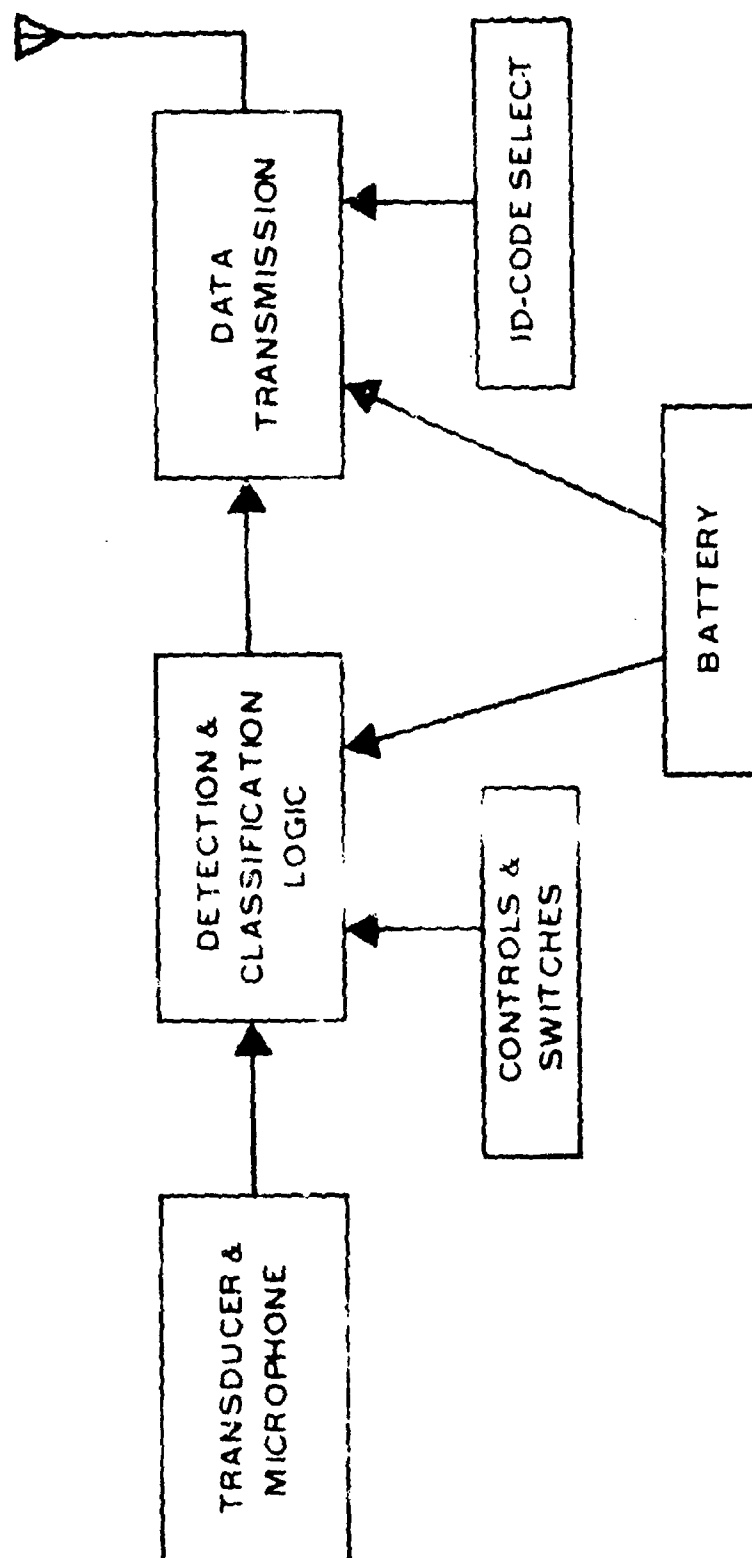


FIGURE 5

3.1.2 Magnetic Detection Sensor

The Magnetic Detection Sensor DT-561 uses a passive magnetic technique to detect targets. The detector is of the magnetometer type. The sensor detects changes in ambient magnetic flux resulting from the motion of a ferromagnetic object in the immediate vicinity. An alarm is registered when a preset number of threshold activations are produced within a given time interval.

The sensor will not provide target classification, but will indicate the presence of an intruder (either vehicle or armed personnel) by sending a "detection only" message. Characteristically, the detection range is short, (5 meters for armed personnel to 25 meters for tracked vehicles), so the sensor must be hand emplaced within close proximity of expected traffic. Since only one target will usually be within the detection range at a given time, the number of targets that have passed the sensor can be estimated by counting the number of alarms.

The physical appearance of the magnetic detector will be identical to the classification sensor (Figure 4), except that the microphone will not be included.

Figure 6 shows the functional block diagram: The magnetometer transducer feeds signals to the detection logic where a threshold can be activated. The logic counts threshold activations and generates intrusion reports. The reports are encoded and reported via the data transmission circuit and antenna.

3.1.3 Infrared Sensor

The DT-565 Infrared (IR) Sensor is a passive IR sensing system designed to detect intrusions and to encode the direction of motion of vehicles and personnel ("right or left") relative to the sensor. A single lens employing side by side detectors provides two fields of view. Personnel or vehicles passing within the field of view, depending on their temperature, add or subtract from the quiescent power. It is this change in power which is detected that is used as a criteria for intrusion detection. Careful siting is required during emplacement to ensure unobstructed line-of-sight.

The IR sensor is a medium-range sensor capable of detecting personnel, tracked or wheeled vehicles. This medium-range capability permits emplacement at a convenient distance from roads or trails. It can be used to count objects passing through its field of view.

MAGNETIC DETECTOR BLOCK DIAGRAM

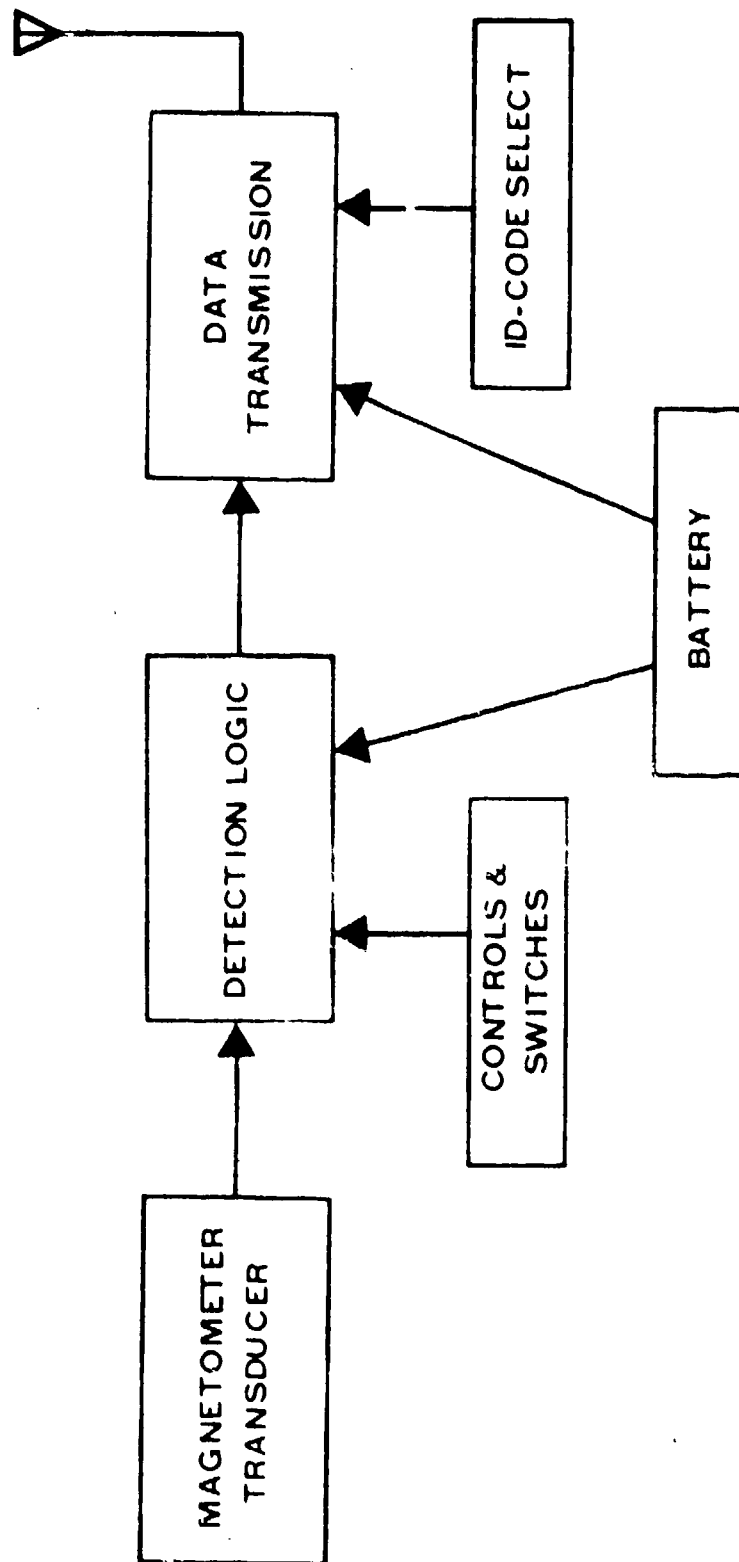


FIGURE 6

The DT-565 IR Sensor is shown in Figure 7 and is identical in physical appearance to the classification and magnetic sensor except for the IR transducer and its tree/post mounting hardware. The IR head has gum-barrel sights provided for base sighting the optics.

The functional block diagram (Figure 8) shows the IR optics (including IR detectors) feeding detection logic. The logic circuits provide detection thresholds which are activated by the IR signals. The sequence of activations determines direction of travel. Detections are encoded and reported by transmission via the data transmission circuits and antenna.

3.1.4 Strain-Cable Sensor

The DT-573 sensor employs a strain-sensitive cable which is buried in a shallow ditch across a road or pathway. The cable generates a small electrical signal when subjected to mechanical pressure on the nearby road surface. The signals from the cable are analyzed by the logic portion of the sensor and the targets are classified as personnel, tracked vehicles or wheeled vehicles. A target must exert pressure very close to the cable to activate the sensor; it therefore provides accurate target location and also permits resolution and classification of closely spaced targets. Because of the short detection range, there is inherently a low nuisance-alarm rate.

Target classification (wheeled vs. tracked vehicles) is accomplished by automatic analysis of the pressure-generated signals. The relative spacing of the signals is indicative of the spacing of the vehicle wheels and is characteristic of the vehicle class.

The DT-573 Strain Cable Sensor is shown in Figure 9. The strain cable transducer is 30 meters in length and can be cut down for field use to a minimum of 2 meters. It will classify personnel, walking or running and wheeled or tracked vehicles.

The functional block diagram (Figure 10) shows strain-cable signals transmitted to the detection and classification logic. Detection and class reports from the logic circuits are encoded and transmitted via the data transmission circuits and antenna.

3.1.5 Audio Analog Sensor

The Audio Analog Sensor DT-563 detects target-generated acoustic signals and transmits them undistorted to the monitoring station. There the signals can be reproduced in analog form and interpreted by an operator. The detector transducer is a microphone. The audio transmission,

lasting approximately 15 seconds, is initiated only when seismic detection logic (which is considered a component of the analog sensor) detects a target. The audio signal is transmitted with reasonably wide bandwidth, of the order of 50 to 2000 Hz, and good fidelity, which aids in interpretation. The signal can be transmitted directly or via repeaters to the Sensor Monitoring Set.

The physical appearance of the DT-563 Analog Sensor is shown in Figure 11. The front of the case is identical to the other hand emplaced units. However, since this sensor operates with a higher duty cycle, additional batteries are required and the rear cover has been extended to except two additional batteries. The microphone at the base of the antenna serves as the audio pick-up. The geophone transducer provides the seismic signal to activate the 15 second audio transmission. The DT-563 has a required mission life of 15 days.

Figure 12 shows the functional block diagram. The pick-up microphone feeds audio signals to the amplifier. The amplified audio is transmitted in analog form by the data transmission circuits and antenna. The seismic transducer feeds seismic disturbances to the detection logic, which automatically activates the audio amplifier and a transmitter when sufficient disturbance is detected.

3.2 Delivery Methods and Equipment

3.2.1 Sensors

Hand emplacement of sensors is preferred when feasible. The transducer emplacement tends to be better than for air or artillery delivered sensors. Also, there is usually more effective placement relative to the target path, and better knowledge of sensor location. These factors contribute to better performance in detecting and locating targets.

Sensor deployment in hostile or inaccessible areas may have to be by air or artillery delivery. The known placement errors of air or artillery must be accepted and allowed for.

3.2.1.1 Hand Emplacement

Hand emplacement may involve digging if suitable concealment is not naturally available. The commonly used infantry digging tools will suffice. In the case of the strain-sensitive cable, a special ditch-digging machine and surface-patching material may be required to emplace the cable across a hard-surfaced road. In all cases, camouflage materials, such as painted tape and wire, should be available.

DT-565 IR SENSOR

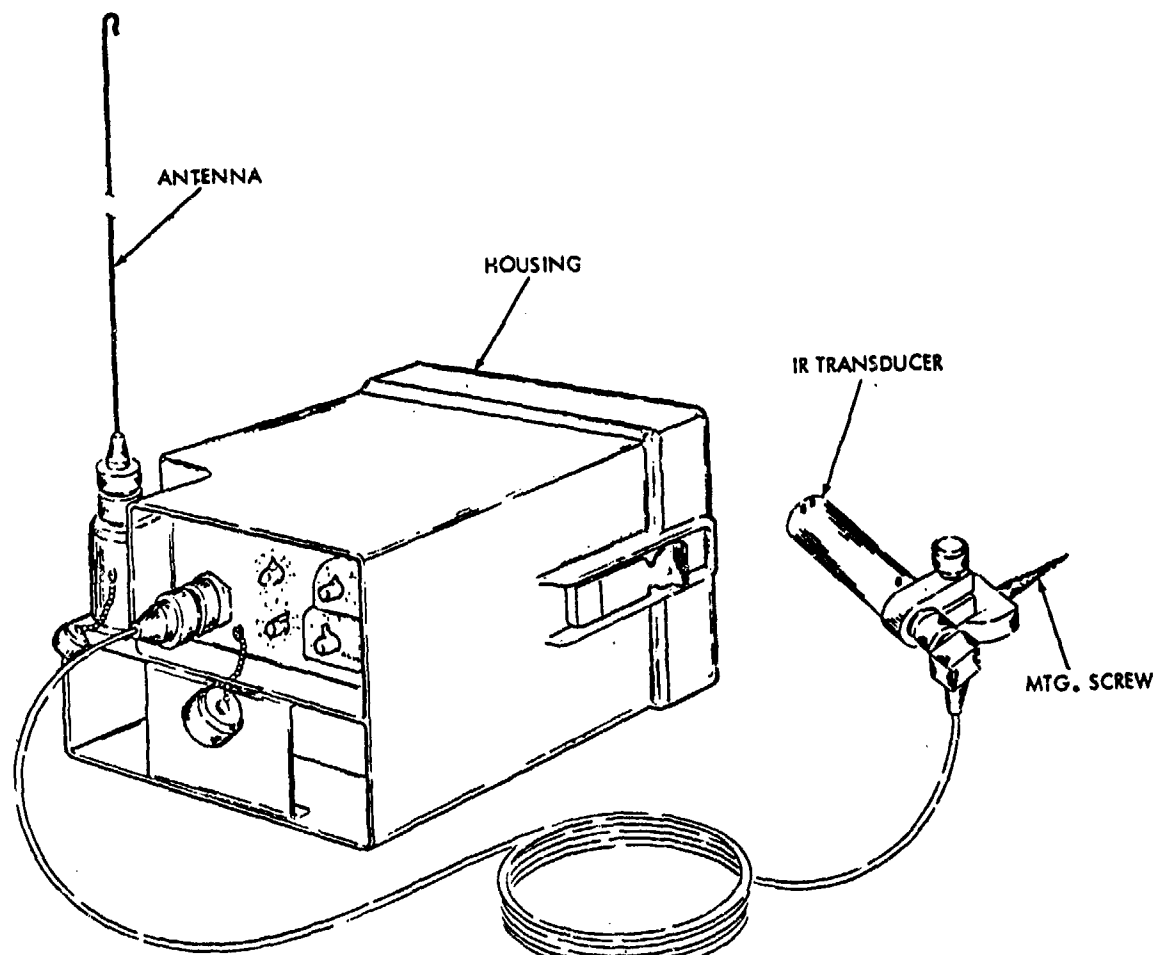


FIGURE 7

INFRARED SENSOR BLOCK DIAGRAM

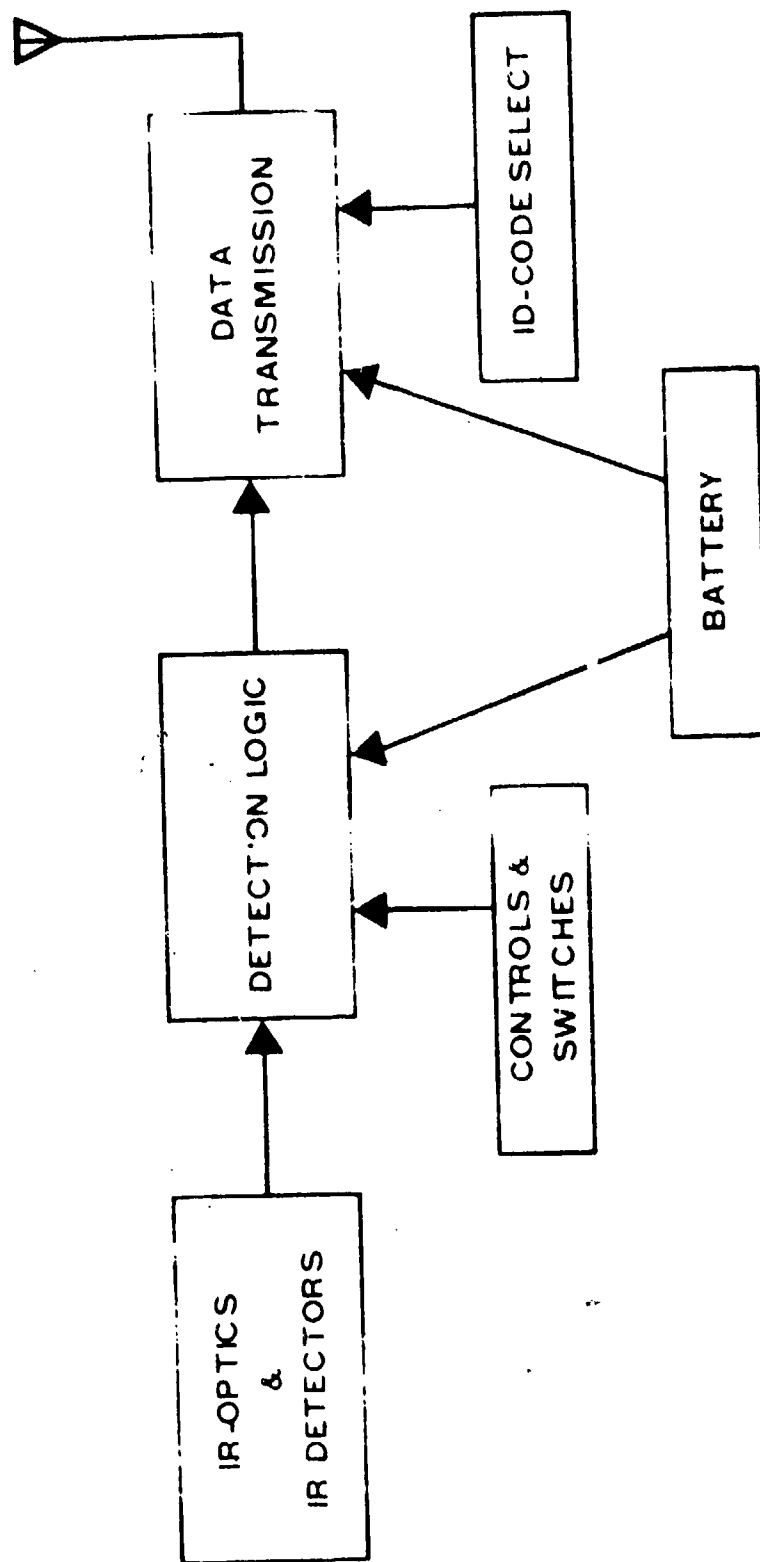


FIGURE 8

DT-573 STRAIN-CABLE SENSOR

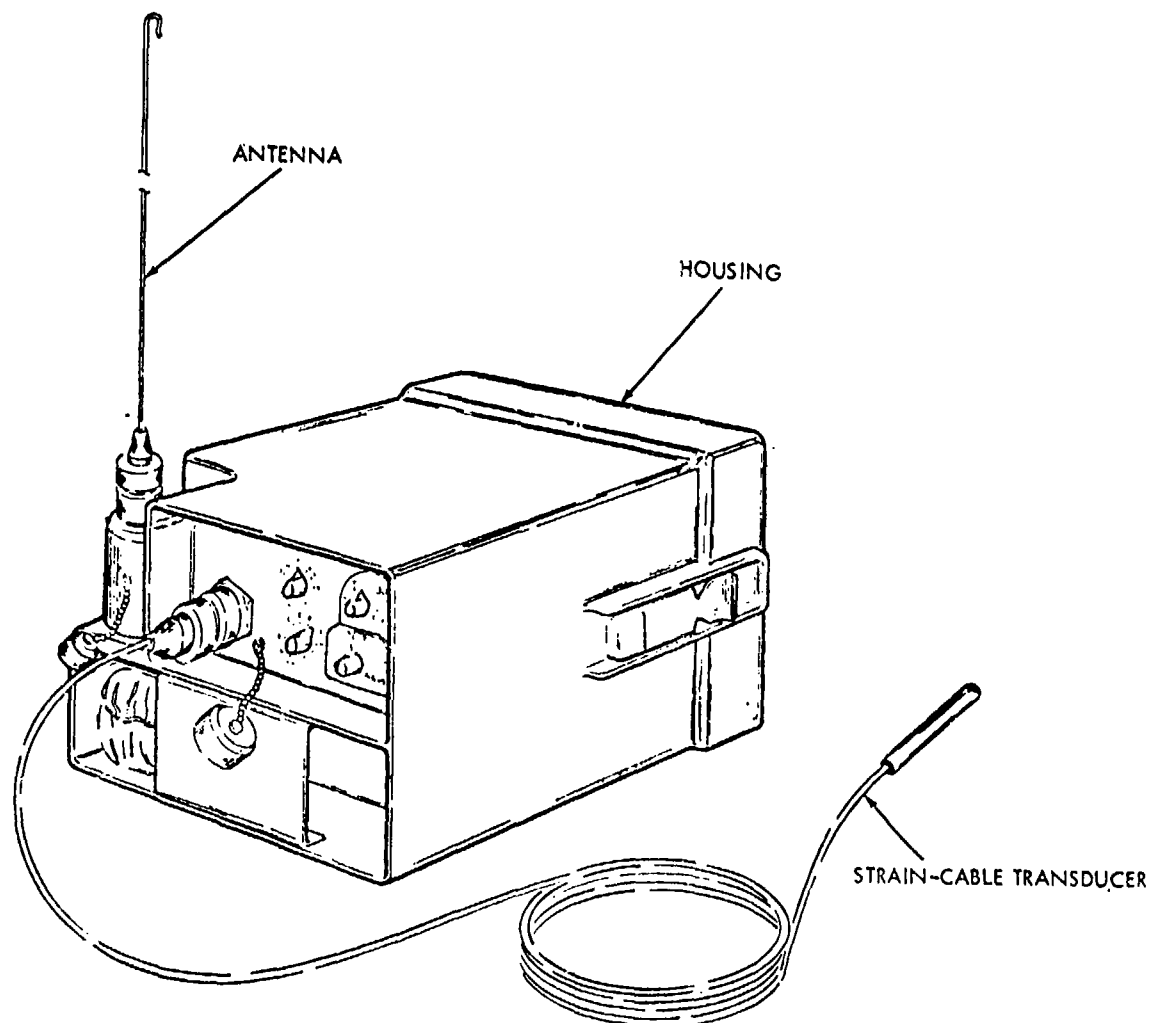


FIGURE 9

STRAIN CABLE SENSOR BLOCK DIAGRAM

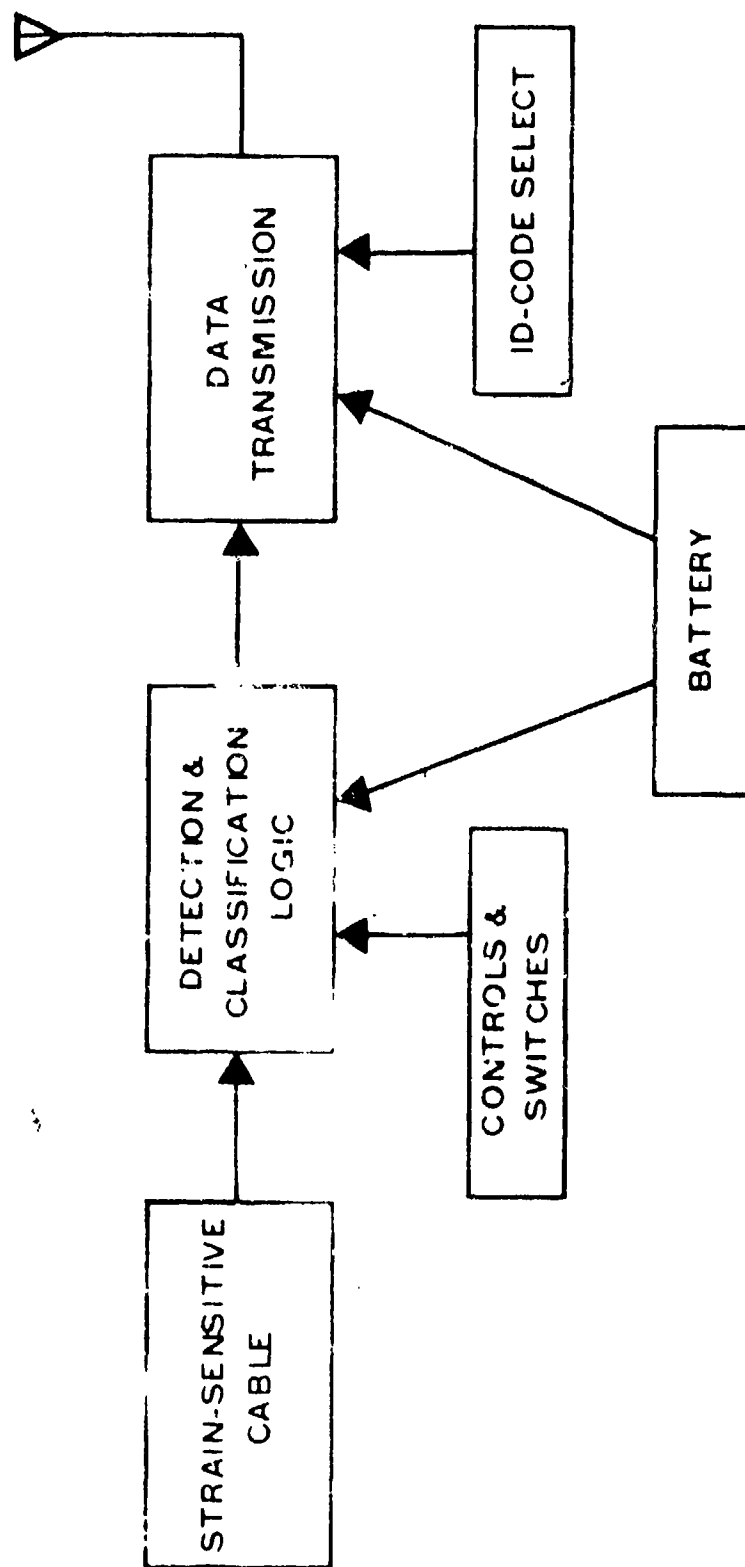


FIGURE 10

DT-563 ANALOG SENSOR

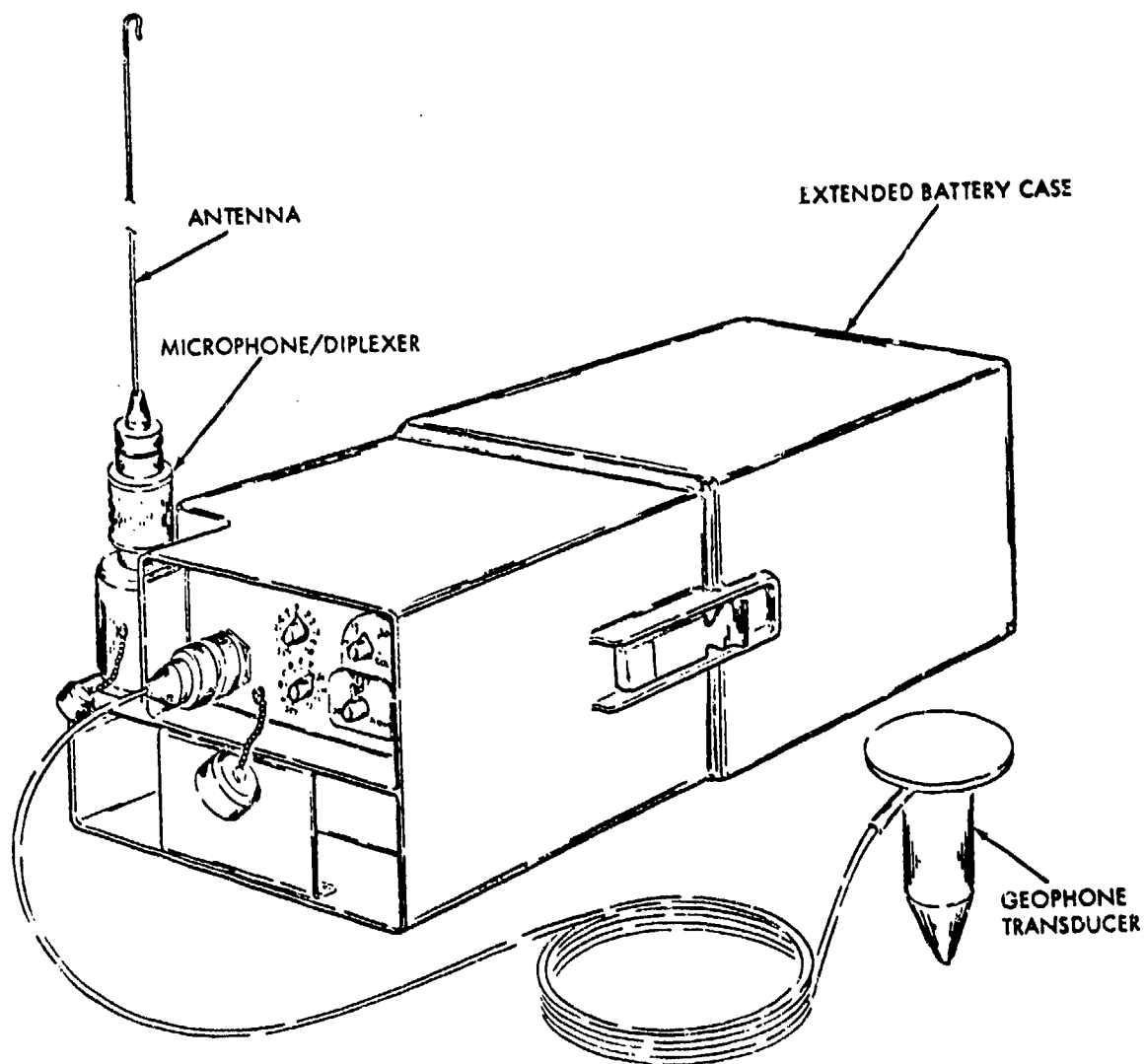


FIGURE 11

AUDIO ANALOG SENSOR BLOCK DIAGRAM

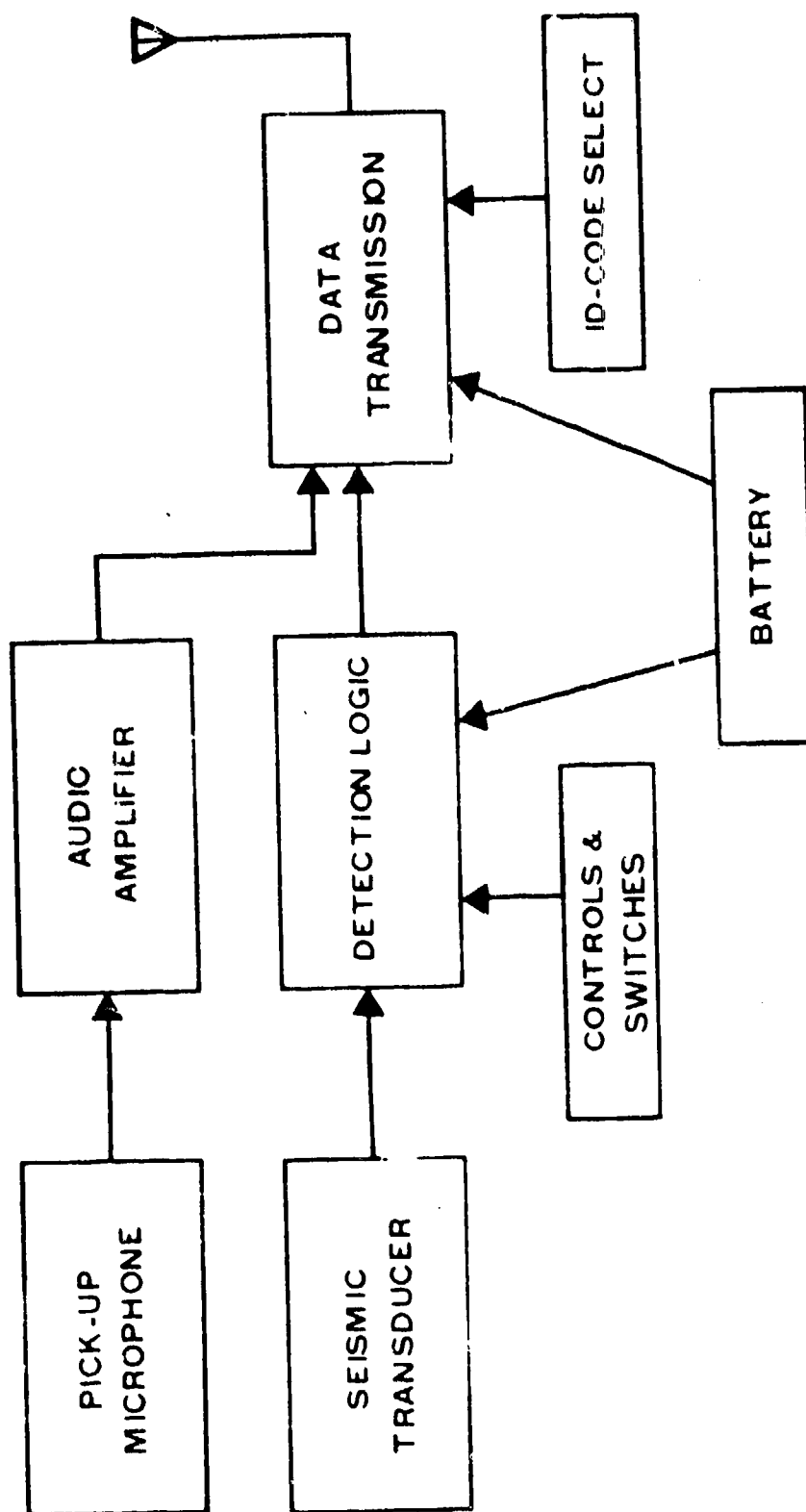


FIGURE 12

3.2.1.2 Artillery Delivery

Artillery delivery requires use of a special shell to house the terminal delivery vehicle (TDV). The TDV separates from the shell housing at a designated point in the trajectory and impacts with sufficient energy to implant. The sensor becomes buried upon implant, except for a detachable "after body" of the TDV carrying the antenna, which remains at the surface. The sensor is automatically activated by the impact and begins to function immediately. The sensor components are designed to withstand the intense shock of firing and impaction. The DT-570 artillery delivered sensor is shown in Figure 13.

3.2.1.3 Air Delivery

For aircraft delivery, the DT-567 Surfaced Emplaced Sensor (SES) can be dispensed from a helicopter dispenser system, or a Practice Multiple Bomb Rack (PMBR) mounted on either an OV-1 Army aircraft or an OV-10 Marine Corps aircraft. The SES uses a cylindrical housing which includes a retardation parachute. The parachute is used in high speed deployment and is cut away prior to impact. After the SES has stopped rolling, a self orienting mechanism positions the geophone for implant and automatically erects the antenna. Figure 14 shows a DT-567 (SES) after deployment.

3.2.2 Repeaters

Repeaters are designed for hand-emplacement and for air delivery. Hand-emplacement is much preferred because it permits the antenna to be properly located and positioned. Antenna siting is considered a critical task. Figure 15 illustrates the Hand-Emplaced RT-1175. The hand-emplacable repeater is also designed to operate from an aircraft in flight, and will conform to airborne equipment specifications.

For air delivery, one of the repeaters, the RT-1201, is fitted with a parachute which is automatically deployed after dropping from an aircraft. The parachute-equipped repeater is designed for canopy hang-up; the parachute aids in the hang-up by snagging tree branches. Figure 16 illustrates the RT-1201 Canopy Repeater deployed.

Another form of air delivery is the implant method. Where terrain permits, the RT-1200 can be used. The repeater can be launched from medium performance aircraft or helicopters using the SUU-42/SUU-25 launchers. After ejection, the folded fins (terra-brakes) pop out and stabilize the flight. Upon ground impact (see Figure 17) the forward section separates from the detachable after-body and can penetrate to a depth up to 140 inches. On impact, the 10 foot antenna/mast is deployed. Canopy hang-up is preferred when feasible, since the greater antenna height is more likely to avoid line-of-sight obstructions.

DT-570 ARTILLERY DELIVERED SENSOR

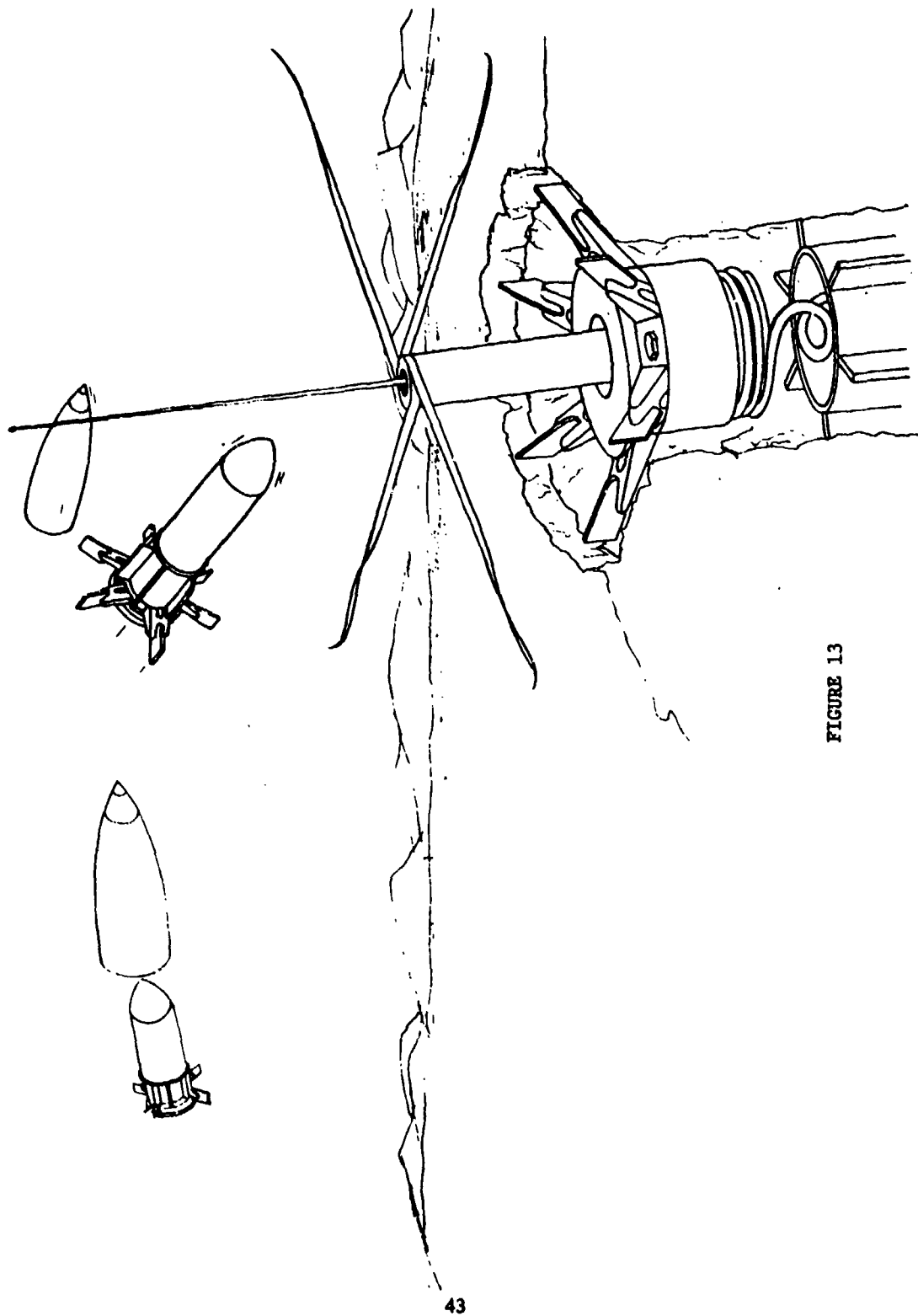
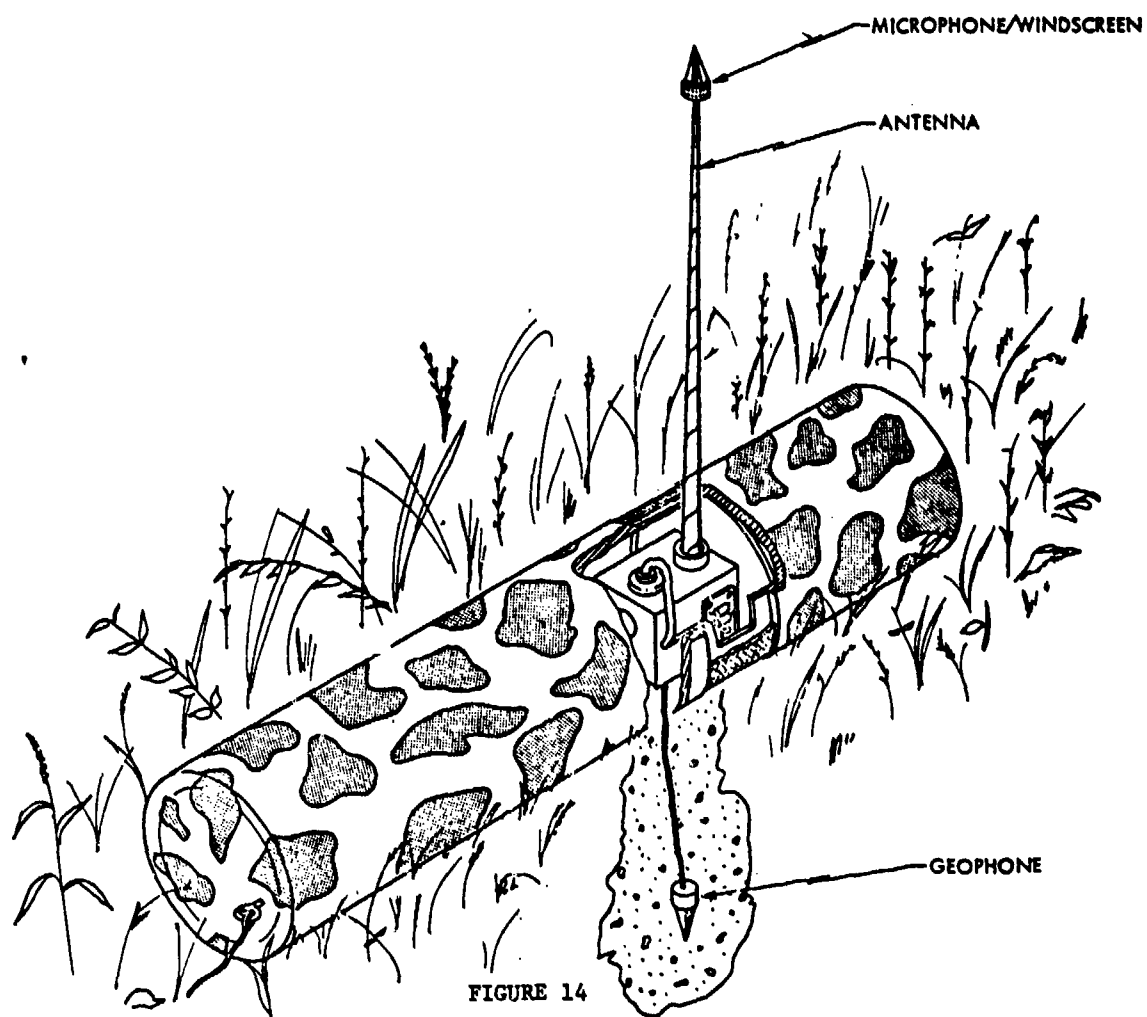
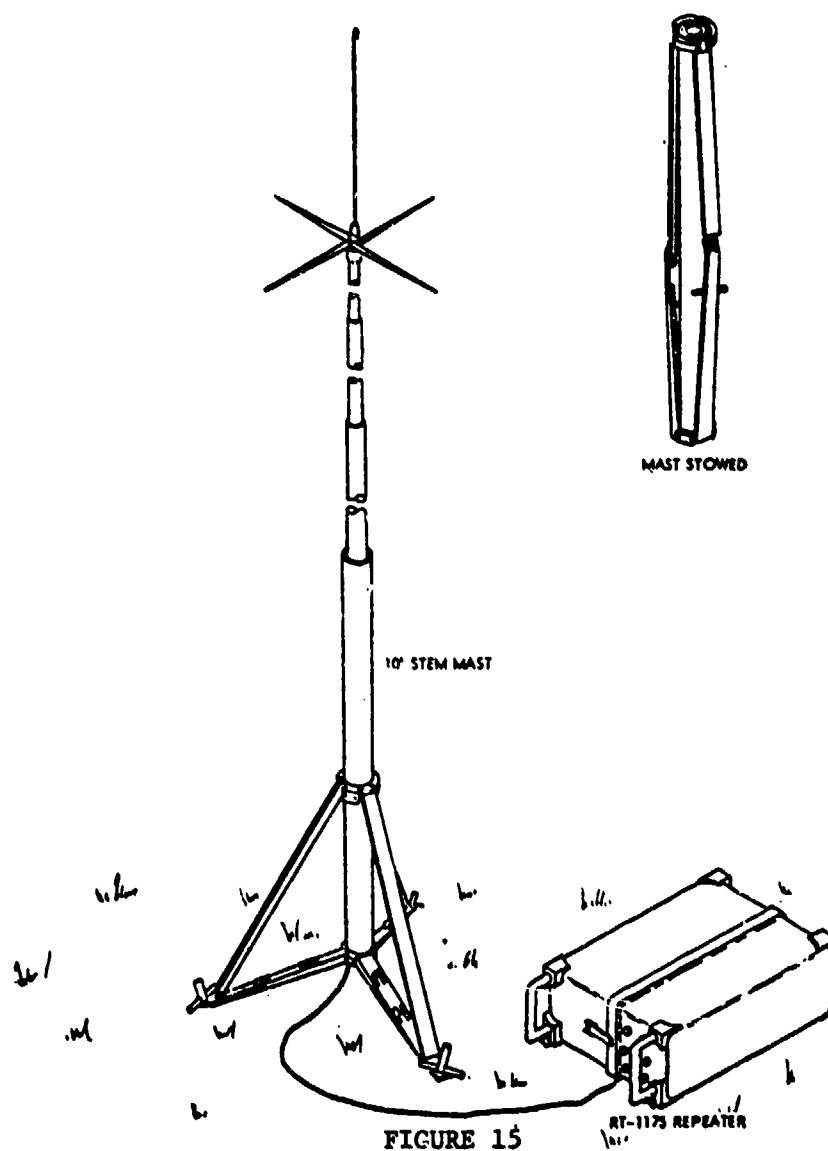


FIGURE 13

DT-567 SURFACE EMPLACED SENSOR



HAND-EMPLACED RT-1175 REPEATER



RT-1201 CANOPY REPEATER DEPLOYED

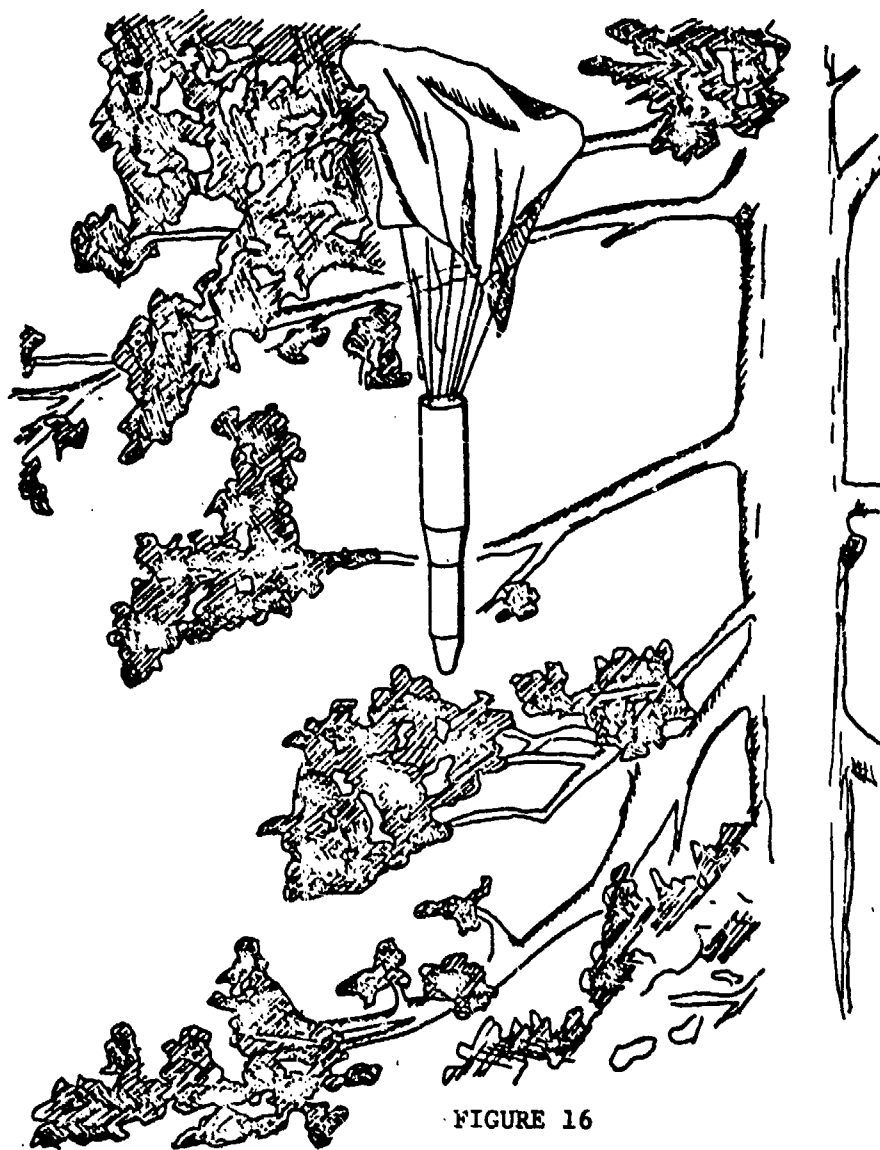


FIGURE 16

RT-1200 REPEATER DEPLOYED

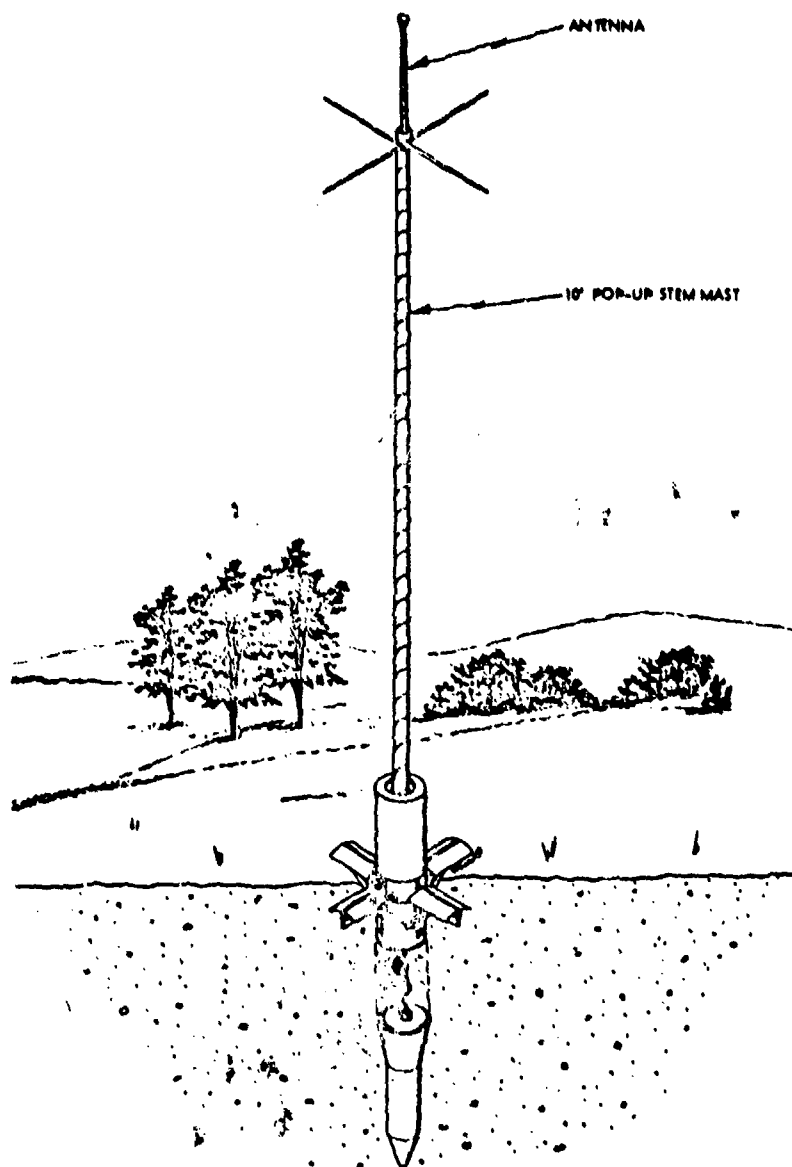


FIGURE 17

3.3 Data Transmission Subsystem

3.3.1 General

The data transmission subsystem provides the VHF transmission link between the sensors and the monitoring stations. Transmission may be direct or via radio repeaters, as required. Repeater are used to increase available transmission range, and to overcome line-of-sight limitations inherent in VHF communications.

All transmissions (except those from the analog sensor) are digitally encoded. An analog transmission mode is used to transmit audio from the analog sensor.

In the design of the data transmission subsystem, consideration was given to frequency band selection, mutual interference of sensor transmissions, relay chain reliability, maintenance factors, operational flexibility and ECM. These considerations resulted in a subsystem design which provides adequate channels in the VHF frequency band. A channel accommodates up to 64 different sensors, each having a different identity code. Digital messages are as short as possible, in order to decrease the chance of interference on a given channel. The channel bandwidth is minimized for power economy, and to maximize the number of channels available in the band.

Each sensor contains a transmitter that operates on all channels. The frequency channel and sensor identity code can be selected in the field before or during emplacement. Field selection facilitates frequency management where many sensors are involved. All hand emplaced sensors have frequency controls on the sensor. The DT-570 and DT-567 frequencies are set prior to a mission by using a hand held External Programming Device (EPD).

The sensor identity code can also be pre-selected by switch adjustments on the sensor exterior for each hand emplaced sensor. This simplifies the problem of distinguishing messages from a number of sensors located at the same site. ID codes for the DT-570 and DT-567 are set with the EPD.

For digital messages, repeaters are designed to relay a single channel only. The frequency channel is pre-selected in the field before or during emplacement. For analog messages two channels must be pre-selected (see Section 3.3.2).

3.3.2 Message Formats

The digital message contains the sensor ID, detection data, classification data, error checking (parity), and communications overhead (synchronization and header information). The repeater uses the store-and-forward (F_1 - F_1) technique to relay digital messages. The message is received by the repeater and momentarily stored in its entirety; it is then checked for parity, and immediately retransmitted if the parity is correct.

The analog signal from an audio analog sensor is transmitted using a format which has 15 seconds of audio preceded by a short digital message identifying the sensor. The message format is called "hybrid" because of the combination of digital and analog. If the message is relayed, the repeater retransmits the hybrid message in the F_1 - F_2 mode. In this mode, a message being received by the repeater on channel frequency F_1 is immediately retransmitted, without temporary storage, on another channel frequency F_2 . The F_1 - F_2 mode is used exclusively to relay the transmissions from the analog sensor DT-563.

3.4 Monitoring Subsystem

The function of the monitoring subsystem is to display the sensor outputs to an operator. The display permits the operator to determine the class, speed, direction of travel, and location of targets.

Monitoring sets are provided for this purpose which include receivers, and data output and display means. Two types of monitoring sets are available: the Sensor Monitoring Set, AN/GSQ-187, and the Portable Monitoring Set, R-2016, as described in the following paragraphs.

3.4.1 Sensor Monitoring Set

The Sensor Monitoring Set has a dual-channel receiver, and a hard copy recorder for recording up to 60 sensors, and for simultaneous comparison of their outputs. There is also an audio output for analog sensor data. See Figure 18 for illustration of the Sensor Monitoring Set.

The hard copy recorder generates a 60-column strip chart. Each column records a selected sensor. This provides a time-ordered history of sensor activations which permits the operator to observe activation patterns as they develop.

Classification sensor reports are recorded with distinctive characters to indicate the classifications determined in the sensor. Direction of target movement and detection-only alarms are also indicated by distinctive characters when transmitted by the sensor. Monitoring capability can be expanded by paralleling Sensor Monitoring Sets.

SENSOR MONITORING SET

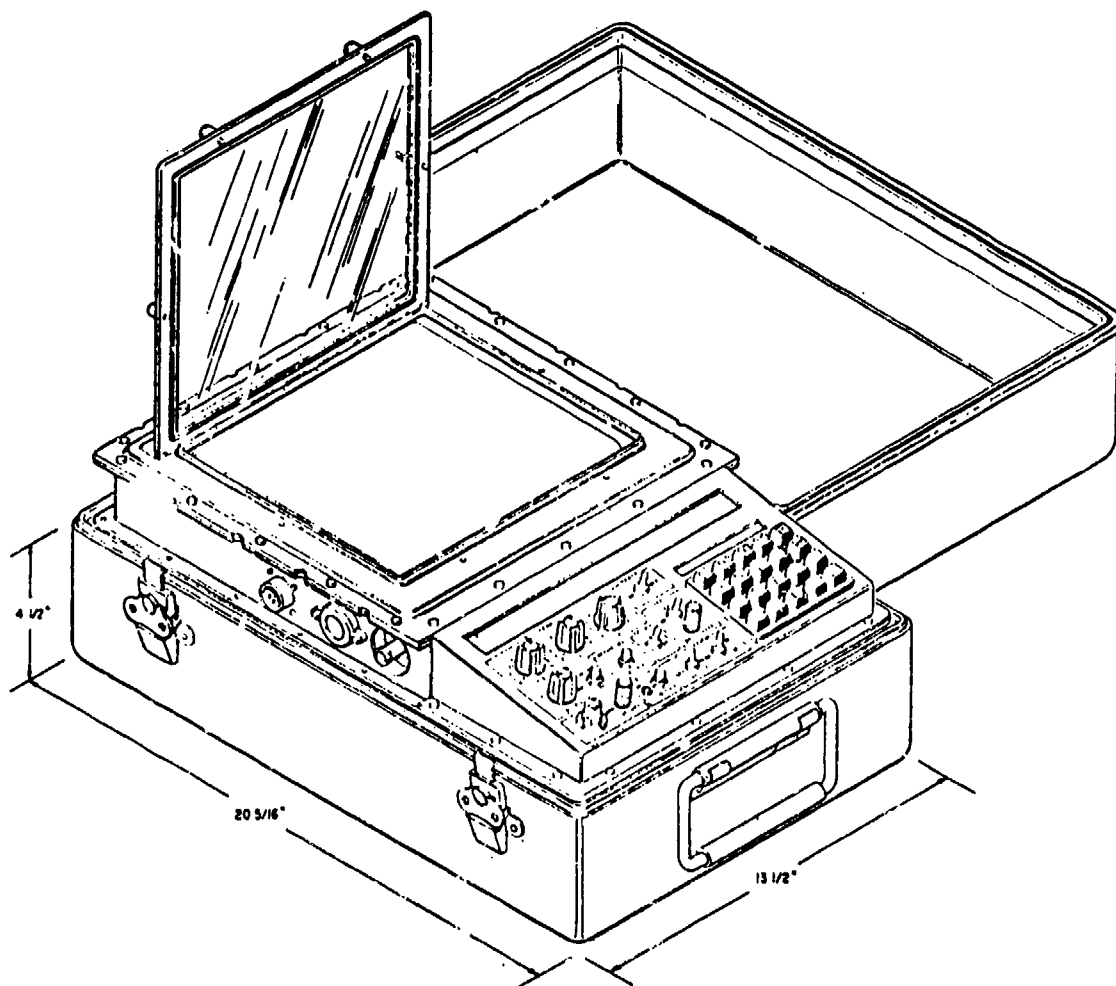


FIGURE 18

The Sensor Monitoring Set is man-portable. It can be battery operated or supplied by power mains. The set is designed to be utilized by operators in the field, in military vehicles, or more permanent quarters.

3.4.2 Portable Monitoring Set

The Portable Monitoring Set is designed to be easier to carry than the Sensor Monitoring Set, and consequently is smaller and has more limited capabilities. The set has a single channel (selectable by operator) receiver and a light display which provides a readout of sensor responses. It can be set to display data from any 10 of the 64 possible codes. In operation, an incoming sensor message activates an audible alarm and the sensor identification and classification data are presented on the light display for a period of three (3) seconds.

The Portable Monitoring Set is approximately 100 cubic inches in volume and weighs less than five pounds. The battery life is at least one week of continuous operation (168 hours or more). See Figure 19 for illustration of the Portable Monitoring Set.

3.5 Power Sources

Power Sources for the REMBASS equipments serve the sensors, repeaters, and monitoring sets. In keeping with the objectives of field use and portability, all REMBASS equipments are designed to operate on battery power. The Sensor Monitoring Set is, in addition, designed for use with externally supplied AC/DC power, if available at the local site.

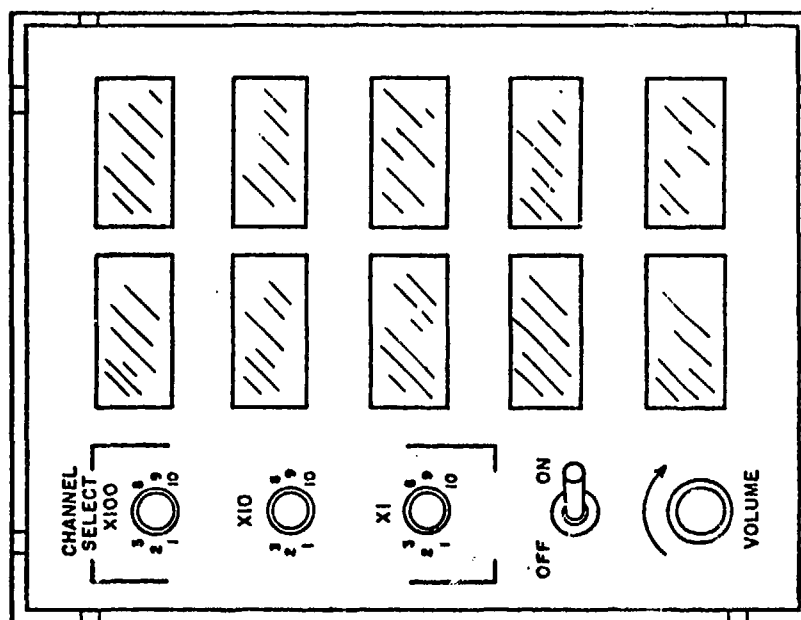
Battery power is standardized, for REMBASS purposes, at a nominal 12 volts. All battery-powered electronics must be capable of operating solely on 12 V primary power, without requiring lower-voltage battery taps.

The following types of batteries are preferred for the REMBASS design:

- (1) For low shock applications (less than 175 g peak), the BA-5590/U Lithium Organic Battery is the standard. This battery is used in a 12 volt configuration, for hand-emplaced sensors and repeaters, and in the Sensor Monitoring Set.
- (2) For high shock applications (equal to or greater than 175 g peak*), a special form of mercury battery may be designed to fit the application. The battery design will be in accordance with MIL-B-55679, except as modified to meet the high shock requirement.

*Specification requirement.

PORTABLE MONITORING SET



FRONT VIEW

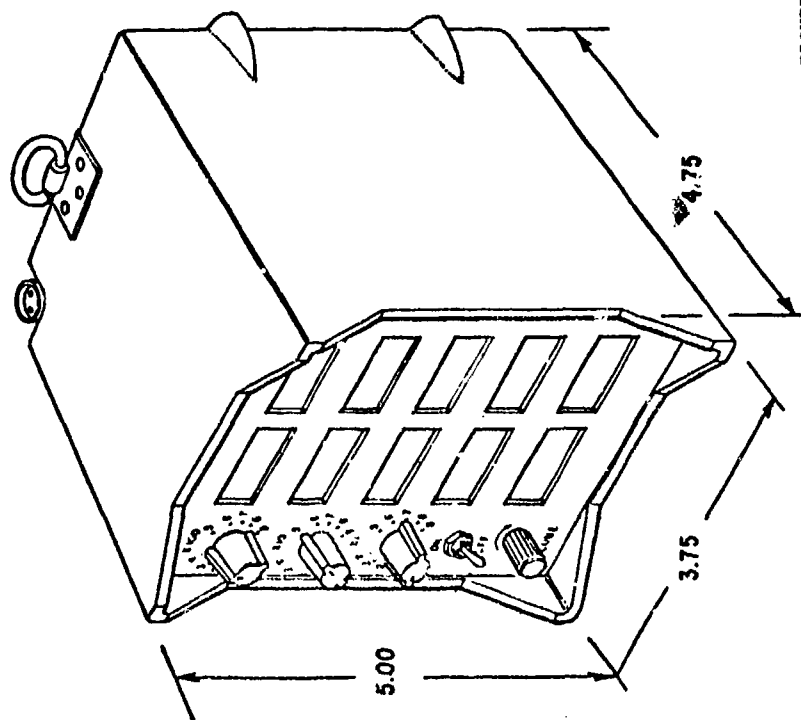


FIGURE 19

- (3) As an alternative possibility for high shock applications, a shock-resistant form of the Lithium Organic Battery will be developed.

The BA-5590/U Lithium Organic Battery has sufficient capacity to power the hand-emplaced digital type of sensor for a least 30 days operational life*. For longer life requirements, two or more such batteries may be needed. For the analog sensor, supplementary batteries (forming a multi-battery pack) will be required to supply the longer-duration analog message. Also, such supplementary batteries may be needed for the repeaters, since the message rate and transmitter power requirements are generally greater than for sensors.

*Specification Requirement

US ARMY PHYSICAL SECURITY EQUIPMENT PROGRAM

Presented by

Mr. Stuart A. Kilpatrick
Acting DA Project Officer
Physical Security Equipment

CHART 1

The Department of the Army Project Office for Physical Security Equipment (PO-PSE) has been established as the Army's response to DOD Directive 3224.3 "Physical Security Equipment: Assignment of Responsibility for Research, Engineering, Procurement, Installation, and Maintenance." US Army Material Development and Readiness Command (DARCOM) was tasked by the Department of the Army staff to establish a single focal point to centralize the management of PSE program throughout its life cycle. DARCOM Regulation 1-1 of 8 Apr 77 formalized PO-PSE at the US Army Mobility Equipment Research and Development Command (MERADCOM).

CHART 2

The PO-PSE was formed on the matrix principle project management structure where the office is an austerity staffed focal point which draws upon the management and support function for the functional organizations with which it works. In this case the PO-PSE is supported by MERADCOM for the research and development function and by USA Troop Support and Aviation Material Readiness Command, (TSARCOM), formerly TROSCOM, for the readiness function. After study of several management structures matrix approach was chosen as being the most efficient and least disruptive to the on-going development and readiness programs. As management of both programs were well established and meeting the Army's requirements within the funding constraints, the establishment of a large management structure was unnecessary and uneconomical.

The mission of the PO-PSE is to serve as the central Army focal point for PSE and be responsible for coordinating and monitoring the management for the development, acquisition, and integrated logistic support assigned PSE systems.

Under DOD Directive 3224.3 the Army is assigned the tri-service responsibility for interior physical security equipment and the barrier and lighting portions of exterior PSE.

I am currently serving as the acting PO-PSE until mid-August when the permanent officer, LTC Van C. Holiday, reports to MERADCOM. LTC Holiday is currently the Executive Officer to the Provost Marshall's Office, HQS USAREUR, Heidelberg, Germany.

In discussion of the Army's PSE program, I will stay primarily with the research and development aspects because of the nature of this seminar.

CHART 3

The 6.2 for base technology effort is divided between two programs, the Army is currently funding physical security research under project AH20 at a very low level for work on a microprocessor controlled "smart" sensor. The other area will be funded under the Defense Nuclear Agency 6.2 program. The Department of Defense has charged the Defense Nuclear Agency to provide the funding and guidance for the DOD base technology program. The level of effort for this program is currently being determined. The Army's area of interest in which we have requested funding are included on the accompanying chart. This includes the efforts of three Army R&D laboratories.

CHART 4

The primary development effort for 6.4 programs is facility intrusion and detection system FIDS in response to a material need of that title. FIDS system provides a completely integrated physical security system through the use of a microprocessor control system alarm display and command system shown in this viewgraph. The Army has developed and fielded a joint service intrusion and detection system J-SIIDS which is now being fielded and utilized by all the services. The J-SIIDS was based upon the 72-72 technologies and provides excellent protection against the intruder.

CHART 5

The FIDS requirements are satisfied by J-SIIDS in the areas listed on this chart. The areas highlighted are in the 6.3 development effort and the remainder is in the 6.4 effort.

CHART 6

The Army's effort is conducted under project DK82 and is subdivided into the listed tasks on this chart. The 6.3 effort was unfunded during FY77 and funds for FY78 have been reprogrammed to the 6.4 effort in order to maintain the FIDS schedule.

The unfunded FY78 effort has been approved by DARCOM and forwarded to the Department of the Army. We expect approval of at least some portion of the effort.

CHART 7

The 6.3 program objectives are listed in this chart. During FY78 we expect to initiate a complete systems analysis of the overall interior

In discussion of the Army's PSE program, I will stay primarily with the research and development aspects because of the nature of this seminar.

CHART 3

The 6.2 for base technology effort is divided between two programs, the Army is currently funding physical security research under project AH20 at a very low level for work on a microprocessor control "smart" sensor. The other area will be funded under the Defense Nuclear Agency 6.2 program. The Department of Defense has charged the Defense Nuclear Agency to provide the funding and guidance for the DOD base technology program. The level of effort for this program is currently being determined. The Army's area of interest in which we have requested funding are included on the accompanying chart. This includes the efforts of three Army R&D laboratories.

CHART 4

The primary development effort 6.3 and 6.4 programs is facility intrusion and detection system FIDS in response to a material need of that title. FIDS system provides a completely integrated physical security system through the use of a microprocessor control system alarm display and command subsystem shown in this viewgraph. The Army has developed and fielded a joint services intrusion and detection system J-SIIDS which is now being procured and installed by all the services. The J-SIIDS was based upon the 1972-1973 technologies and provides excellent protection against the semi-skilled intruder.

CHART 5

The FIDS requirements are not satisfied by J-SIIDS in the areas listed on this chart. The areas highlighted are in the 6.3 development effort and the remainder are in the 6.4 effort.

CHART 6

The Army's 6.3 effort is conducted under project DK82 and is subdivided into the listed tasks on this chart. The 6.3 effort was unfunded during FY77 and the funds for FY78 have been reprogrammed to the 6.4 effort in order to maintain the FIDS schedule.

A large unfunded FY78 effort has been approved by DARCOM and forwarded to Department of the Army. We expect approval of at least some portion of the 6.3 effort.

CHART 7

The 6.3 program objectives are listed in this chart. During FY78 we expect to initiate a complete systems analysis of the overall interior

physical security system as required by the DOD and to develop advance FIDS components to satisfy the advanced FIDS requirements highlighted in the 6.3 area on a previous chart. Significant efforts are the covert duress sensor, a secure RF data link and CRT displays for the command control and display systems. During FY79 we will continue the systems analysis, access the countermeasure and threats as defined by the user requirements and to continue the development of the advanced FIDS components.

CHART 8

The program structure for the 6.4 effort for engineering development under project DL82 is listed on this chart, the tasks are similar to those under the 6.3, but in a later stage of development. Two new tasks are shown at the bottom of the list, barriers and lighting.

CHART 9

This chart shows the 6.4 development objectives for FY78 and FY79. During FY78 in the area of J-SIIDS we will continue the in-house evaluation and initiate the DT/OT II testing of the data transmission system number II, the large area motion system and intrinsically safe components. We expect to complete the integration of the basic FIDS system which includes the integration of J-SIIDS, the FIDS self-test stimuli, the command control and display subsystem and the passive infrared motion sensor. We will procure the DT/OT II hardware of ultrasonic motion sensor, the passive ultrasonic sensor, and capacitance proximity sensor.

We intend to prepare the technical data package drawings of the command control display system and the passive infrared motion sensor which we have procured during FY77. The FY79 objectives listed include the completion of the J-SIIDS DT/OT II with type classification and completion of the technical data packages. DT/OT II FIDS sensors procured will be the large area motion sensor and the vibration sensors. We will complete the productibility engineering and planning effort (PEP) for all the FIDS components and work on the installation guidelines supporting TECOM in the DT/OT II preparation effort. We will initiate two new programs, lighting and barriers, and develop small and large area FIDS monitor subsystems. These are subsystems for the monitoring of less than 32 protecting areas and larger than 96 protected areas.

Let me very briefly cover the readiness program by indicating that we have made basic J-SIIDS buys in FY75 and FY76 and the FY77 procurement package will be on the street within the month and we are currently programing the FY78 and FY79 requirements. The additional add-ons J-SIIDS components recently typed classified will be first procured in FY77 and that package is currently on the street. TROSCOM is currently planning a follow-on FY78 buy. This is a large effort and the current requirement within the Department of the Army is to secure all conventional ammunition storage igloos by FY82. This is an additional 30,00 structures to be protected.

CHART 10

I will close with a listing of those current Army activities receiving management emphasis from the Project Office for Physical Security Equipment. I had originally intended to show a chart of the dollar magnitude of the Army's PSE effort, but we are currently undergoing the R&D budget cycle and the figures seem to change on a daily basis. Any comments to the dollars to be approved is premature. Another area of intense interest is chemical storage site update. In this effort, we will upgrade during FY78 and 79 all of the chemical storage sites in CONUS to the level of security that is now afforded nuclear storage sites. Of course our effort continues with the user in the long range requirements.

This has been a quick overview of the Army Physical Security Equipment Program. The project office is available to answer any questions and discuss new developments.

DEPARTMENT OF ARMY
PROJECT OFFICE
PHYSICAL SECURITY EQUIPMENT

58

CHART 1

DEPARTMENT OF ARMY PHYSICAL SECURITY EQUIPMENT PROGRAM

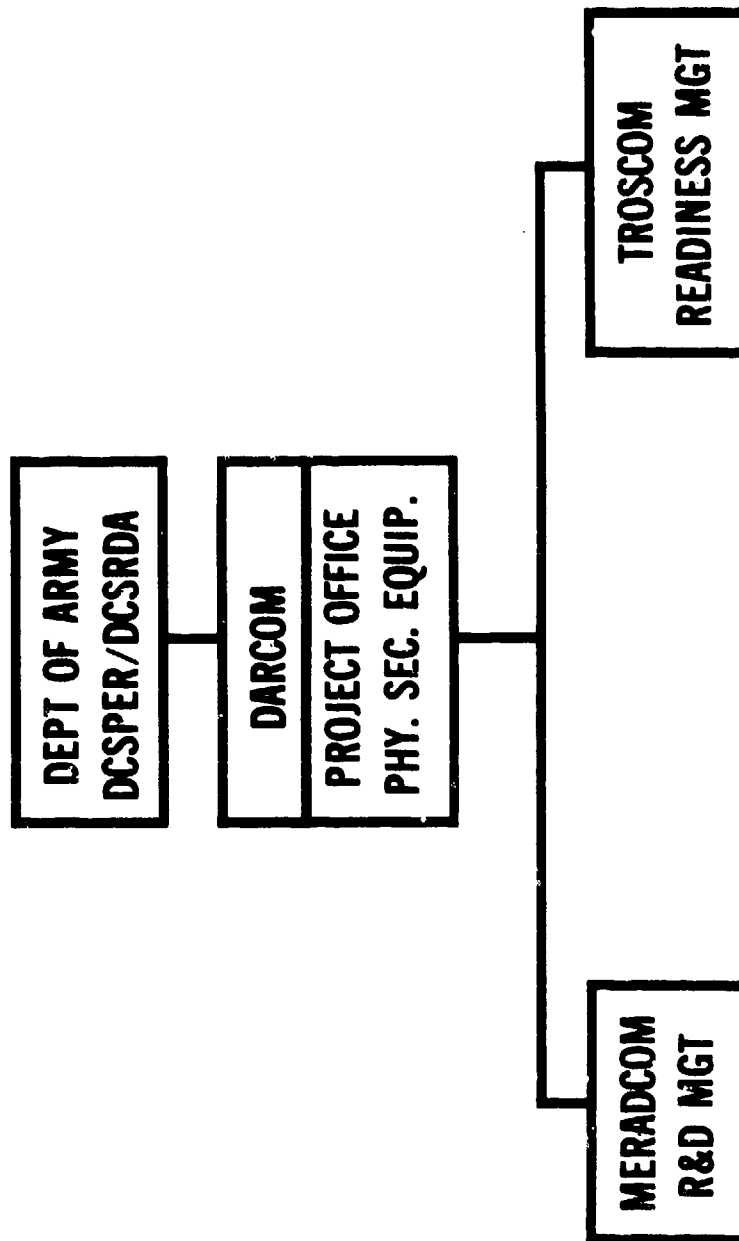


CHART 2

ARMY BASE TECHNOLOGY (6.2) EFFORT

ARMY FUNDED AH20

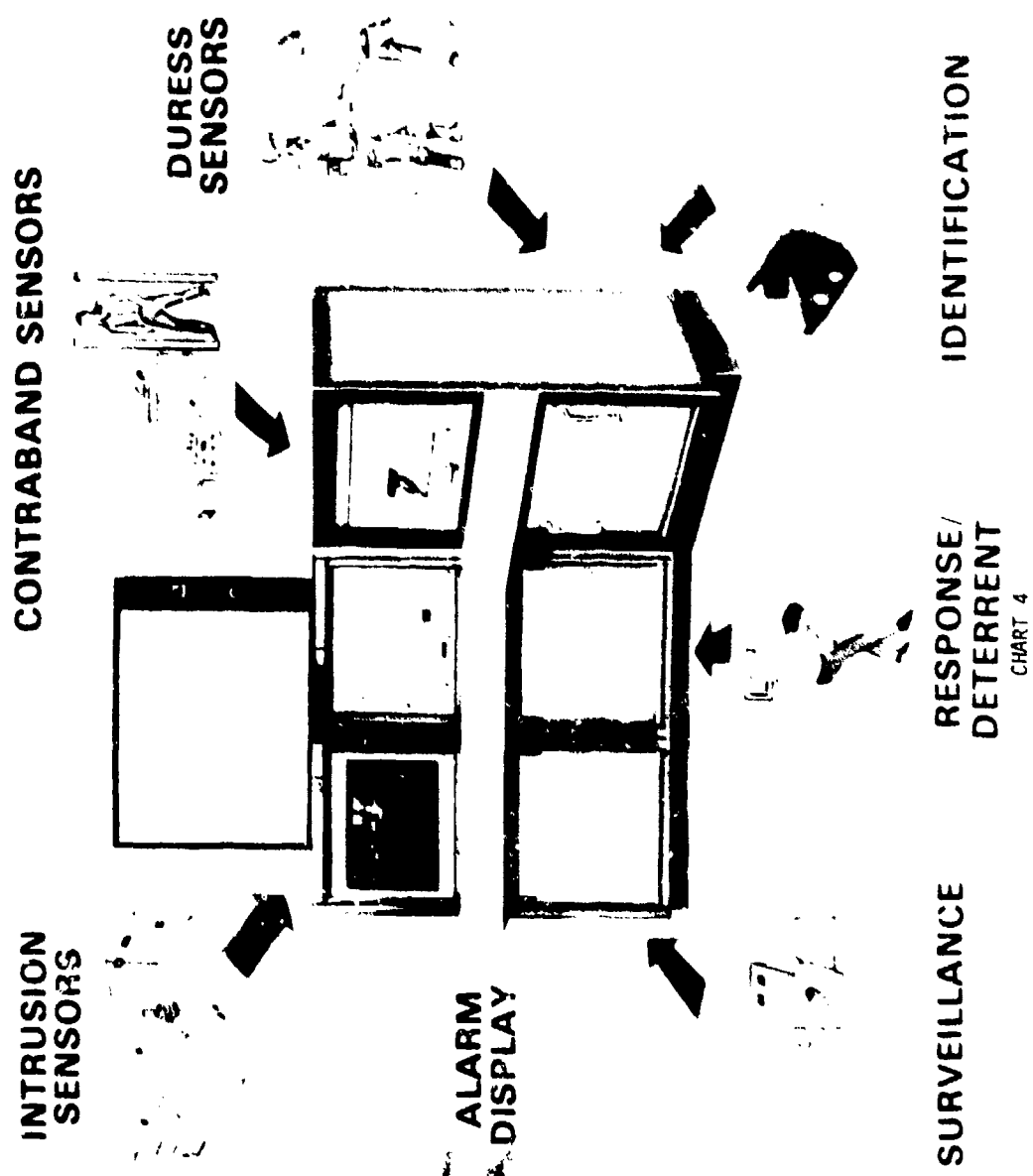
- MICROPROCESSOR CONTROLLED "SMART" SENSOR

DEFENSE NUCLEAR AGENCY (PROPOSED)

- IMPROVED PROCESSING/DECISION FUNCTIONS
- IMPROVED DATA TRANSMISSION SYSTEMS
- LIGHTING FACTORS IN VISUAL DETECTION
- MINIATURE LLL CCD-TV W/SENSOR PACK
- DUAL PURPOSE HARD WIRE DATA TRANSMISSION
- PHYS/PSYC EFFECTS OF BARRIERS/DETERRENTS
- COVERT DURESS SENSORS
- ELECTRO-OPTIC PHYSICAL SECURITY DEVICES
- ULTRASONIC AND CAPACITIVE INTRUSION DETECTION
- MAGNETIC INFLUENCE SENSING SYSTEM

CHART 3

FACILITY INTRUSION DETECTION SYSTEM



FIDS REQUIREMENTS NOT SATISFIED BY J-SIIDS

- **WORLD-WIDE OPERATION**
- **HIGHER DEFEAT RESISTANCE COMPONENTS**
- **ADDITIONAL SENSING CAPABILITIES**
- **COMMAND CAPABILITY**
- **CENTRALIZED PROCESSING AND DISPLAY CAPABILITY**
- **IMPROVED CONTROL UNIT AND MONITOR UNIT**
- **CONTRABAND SENSORS**
- **ENTRY CONTROL**
- **IMPROVED DURESS SENSORS**
- **RESPONSE/DETERRENT SYSTEM**

CHART 5

PHYSICAL SECURITY PROGRAM STRUCTURE

6.3 EFFORT-PROJECT DK82

- 01 SYSTEMS ANALYSIS & CONTROL**
- 02 EXTERIOR SENSORS**
- 03 INTERIOR SENSORS**
- 04 DATA PROCESSING**
- 05 ALARM DISPLAY**
- 06 EQUIPMENT EVALUATION**
- 07 RESPONSE DEVICES**
- 08 CARGO SECURITY**
- 09 LOCKS AND SAFES**

CHART 6

PSE 6.3 PROGRAM OBJECTIVES

PROJECT DK82

- FY78**
- **SYSTEMS ANALYSIS**
 - **DEVELOP ADVANCED FIDS COMPONENTS**
 - CONTRABAND & DURESS SENSORS**
 - RF DATA LINK**
 - CRT REMOTE DISPLAY**
 - PSYCHOLOGICAL RESPONSE DEVICES**
 - IDENTIFICATION ELEMENTS**
 - WEAPONS & KEY CONTAINERS**
- FY79**
- **CONTINUE SYSTEM ANALYSIS**
 - **ASSESS CM & THREATS**
 - **CONTINUE ADVANCED FIDS COMPONENTS**
 - PILFERAGE/TAMPERING SENSORS**
 - INTRINSICALLY SECURE DATA LINKS**
 - LED LIQUID CRYSTAL REMOTE DISPLAYS**
 - SECURE LOCKS & SAFES**
 - AUDIO AND VISUAL SURVEILLANCE**
 - CARGO SECURITY DEVICES**

CHART 7

PHYSICAL SECURITY PROGRAM STRUCTURE

6.4 EFFORT - PROJECT DL82

- 01 EXTERIOR SENSORS**
- 02 INTERIOR SENSORS**
- 03 DATA PROCESSING**
- 04 ALARM DISPLAY**
- 05 J-SIIDS**
- 06 EQUIPMENT APPLICATION**
- 07 RESPONSE DEVICES**
- 09 CARGO SECURITY**
- 10 LOCKS AND SAFES**
- XX BARRIERS**
- XX LIGHTING**

CHART 8

PSE 6.4 PROGRAM OBJECTIVES

PROJECT DL 82

FY78

- CONTINUE JSIID EVALUATION & INITIATE DTII/OTII
- COMPLETE INTEGRATION OF BASIC FIDS
- PROCURE DTII/OTII FIDS SENSORS
- PREPARE TDP DRAWINGS OF FIDS COMPONENTS

FY79

- COMPLETE JSIIDS DTII/OTII, TC AND PREPARE TDP'S
- PROCURE ADDITIONAL FIDS SENSORS FOR DTII OTII
- PEP FOR ALL FIDS COMPONENTS
- DEVELOP APPLICATION & INSTALLATION GUIDELINES
- SUPPORT FIDS DTII/OTII PREPARATION
- INITIATE LIGHTING PROGRAM
- INITIATE BARRIER PROGRAM
- DEVELOP SMALL AND LARGE AREA FIDS MONITOR SUBSYSTEMS

CHART 9

PROJECT OFFICE - PHYSICAL SECURITY EQUIPMENT

CURRENT MANAGEMENT EMPHASIS

- R&D BUDGET CYCLE
- J-SIIDS REQUIREMENTS & PROCUREMENTS
- J-SIIDS ADD ON PROCUREMENT
- CHEMICAL STORAGE SITE UPDATE
- HIGH SECURITY LOCKING DEVICES
- TRANSPORTATION SECURITY
- LONG RANGE REQUIREMENTS
- USER INTERFACE

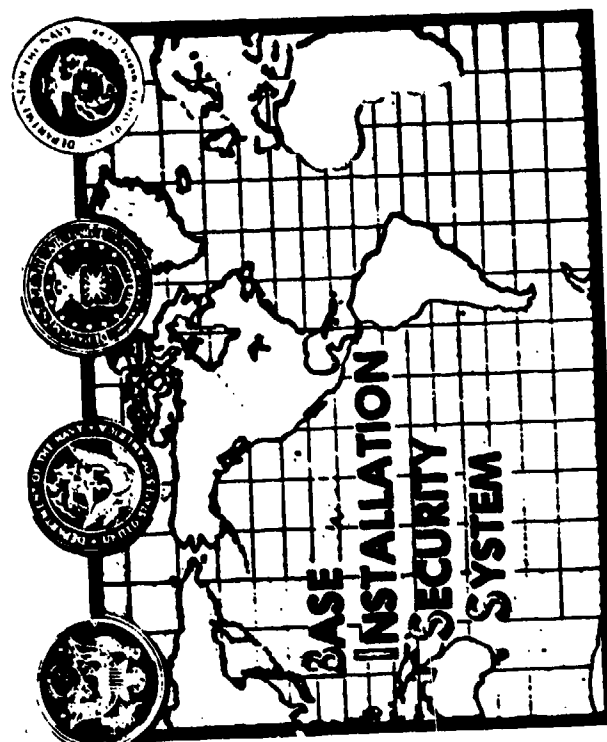
CHART 10

BISS OVERVIEW

The following vugraphs were used by Colonel Roger KOZUMA (BISS PO) to discuss the Air Force SAFE Program and the BISS Program.



USAF "SAFE"
PROGRAMS



PERMANENT INSTALLATION

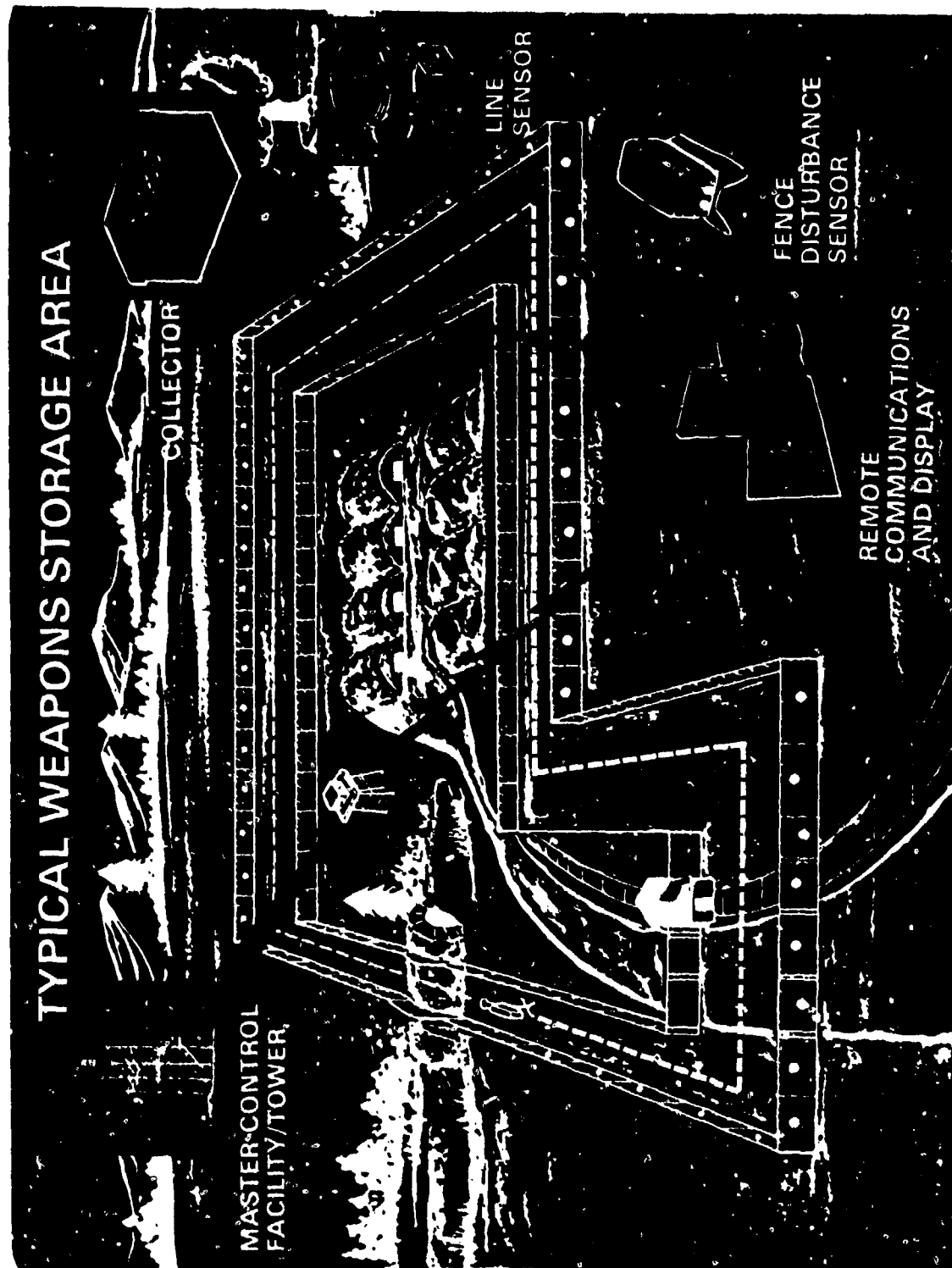


DIRECTED PROGRAM OBJECTIVES

<u>PMD OBJECTIVES</u>	<u>ACQUISITION STAGE</u>	<u>FOC</u>
BOUNDARY DETECTION SEGMENT	DEPLOYMENT	JUL 79
SHELTER (MSCF) HARDENING	IN PROCUREMENT	DEC 79
WEAPONS STORAGE STRUCTURE SENSOR	IN PROCUREMENT	DEC 79
LONG RANGE PERSONNEL/VEHICLE SENSOR	IN PROCUREMENT	DEC 80
ALERT AIRCRAFT SHELTER SENSOR	BISS DEV	JUL 80
INDIVIDUAL RESOURCE PROTECTION SENSOR	BISS DEV	JUL 82
BOUNDARY ALARM ASSESSMENT SEGMENT	BISS DEV	JUL 80
OPEN RAMP BOUNDARY SENSOR	BISS DEV	JUL 81
ENTRY CONTROL SEGMENT	BISS DEV	DEC 81

BOUNDARY DETECTION SEGMENT

<u>COMPONENT</u>	<u>FUNCTION</u>
FENCE DISTURBANCE SENSOR (FDS)	MOTION DETECTOR
MAG INTRUSION LINE SENSOR (MILES)	TRANSDUCER
MAG ANTI INTRUSION DETECTOR (MAID)	SIGNAL PROCESSOR
CODED-MULTIPLEXER SENSOR DATA (CMSD)	COLLECTOR
MASTER SURVEILLANCE CONTROL FACILITY (MSCF)	SHELTER
TOWER	ELEV OBSERVATION
SMALL PERMANENT COMM & DISPLAY SEGMENT (SPCDS)	SENSOR C ³



SAFE PROGRAM ACTIVITY - PAST & PRESENT

<u>PROJECT</u>	<u>LOCATION</u>	<u>APPLICATION</u>	<u>TIME PERIOD</u>
*SAFE LOOK	PACAF	4 BASE DEF SYS (THAILAND) 6 MUNITIONS STORAGE AREAS 4 A/C PARKING AREAS	1969-1974
*SAFE RAMP	AS	27 SAC BOMBER ALERT AREAS	1972-1975
*SAFE NEST	USAF	9 FIGHTER ALERT AREAS 11 WEAPONS STORAGE AREAS(WSA)	1973-1974
PAVE SAFE	AF WIDE	9 SPECIFIED OBJECTIVES 99 SITES - ALERT A/C AREAS - WSA - COMM POST	1973-1981

* COMPLETED AS DIRECTED

SAFE PROGRAMS

EVENTS	PRIOR YEARS												
		CY 77			CY 78			CY 79			CY 80		
		1	2	3	4	1	2	3	4	1	2	3	4
BOUNDARY DETECTION SEG	QTR/YR	1	2	3	4	1	2	3	4	1	2	3	4
EQUIP PROCUREMENT	6/74												
INSTALL & FOC*	4/75												
SHELTER (MSCF)HARDENING													
FABRICATION													
INSTALL & FOC*													
WEAPON STOR STRUCT SEN													
AN/GSS-20 PROCUREMENT	10/75												
INSTALL & FOC*													
LVG RVG PERSYL/VEH SEN													
AN/PPS-15 (MOD)													
PRODUCTION													
DELIVERY & FOC*													

*DIRECTED FOC

SAFE PROGRAMS (CONT)

EVENTS	PRIOR YEARS	CY 77				CY 78				CY 79				CY 80				CY 81				CY 82			
		1	2	3	4	1	2	3	4	1	2	3	4	1	2	3	4	1	2	3	4	1	2	3	4
		DIR/YR																							
ALERT A/C SHELTER SEN																									
MOD AN/GSS-20(BISS DEV)	4/76																								
PRODUCTION																									
INSTALL & FOC*																									
INDIVID RES PROTECT SEN																									
SM AREA RADAR(BISS DEV)	1/75																								
PRODUCTION																									
INSTALL & F																									
BOUND ALARM ASSESS SEG																									
BAAAS (BISS DEV)	12/73																								
PRODUCTION																									
INSTALL & FOC*																									

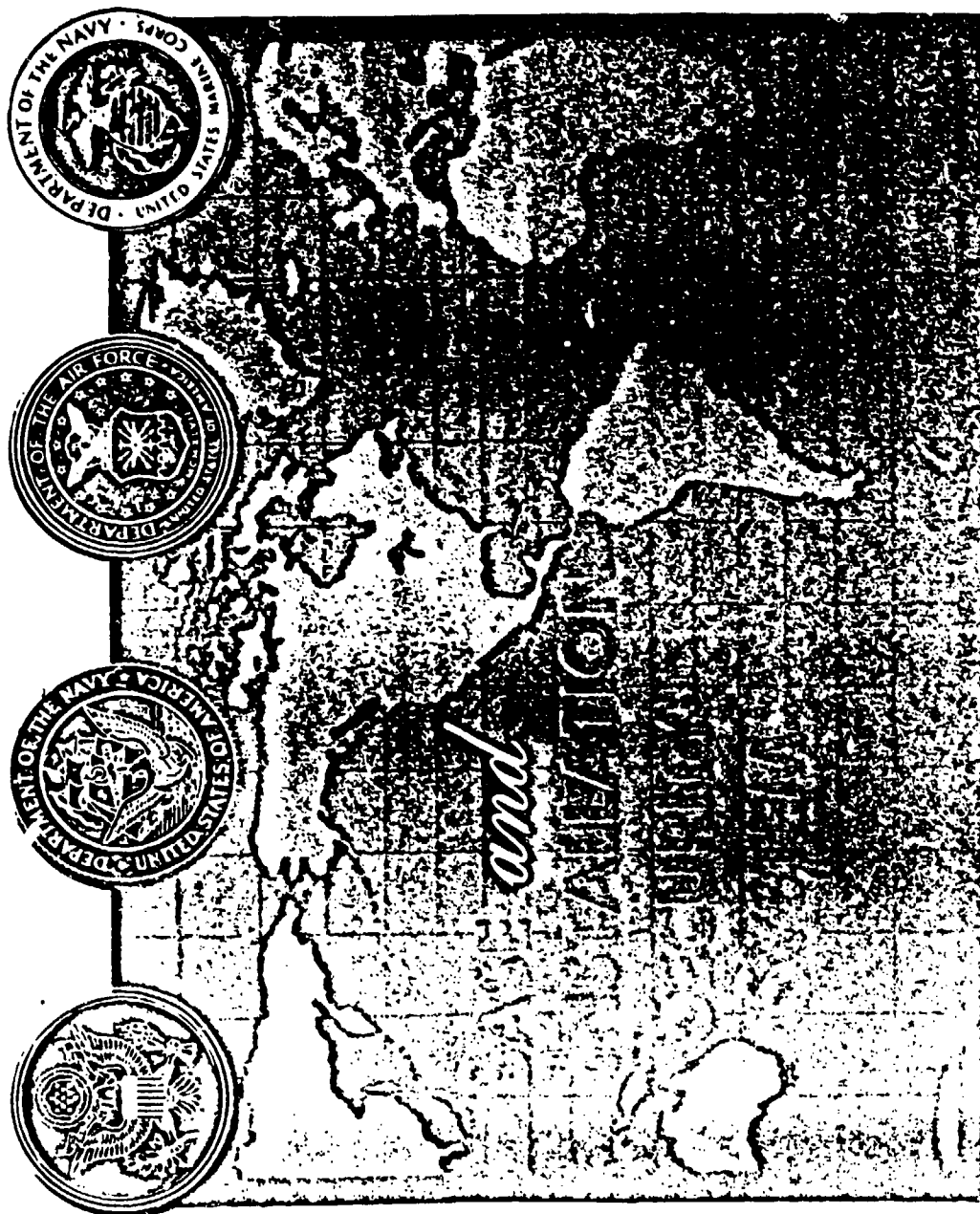
* DIRECTED FOC

SAFE PROGRAMS (CON'T)

EVENTS	PRIOR YEARS	CY 77				CY 78				CY 79				CY 80				CY 81				CY 82			
		QTR/YR																							
		1	2	3	4	1	2	3	4	1	2	3	4	1	2	3	4	1	2	3	4	1	2	3	4
OPEN RAMP BOUNDARY SEN																									
LASER FENCE(BISS DEV)	2/75				◇		↑																		
PILOT PRODUCTION					◇		↑																		
COMPETITIVE PROD																									
INSTALL & FGC*																									
ENTRY CONTROL SEGMENT																									
VOICEPRINT(BISS DEV)	5/74																								
PRODUCTION																									
INSTALL & FGC*																									

*DIRECTED FOC

DEPARTMENT OF DEFENSE



PROGRAM OBJECTIVES

ADVANCED DEVELOPMENT

PROTOTYPES - DESIGN SPECIFICATIONS (TYPE B)

ENGINEERING DEVELOPMENT

PRE-PRODUCTION - FABRICATION SPECIFICATIONS (TYPE C)

ACQUISITION PLANNING FOR ALL DOD COMPONENTS

PROCUREMENT, DEPLOYMENT AND LOGISTICS SUPPORT

(JOINT SERVICES BROAD QUALITATIVE REQUIREMENTS)

GENERAL

- SYSTEM TO FUNCTION IN NON-HOSTILE AND HOSTILE ENVIRONMENTS
- MANY VARIABLES IN MILITARY BASES :
 - FLEXIBILITY AND MODULARITY
 - DESIGN COMPLEX AND COSTLY
- BROAD THREAT SPECTRUM, BOTH INTERNAL AND EXTERNAL
- SYSTEM MUST ACCOMMODATE UPGRADE WITHOUT MAJOR REPLACEMENTS
- SYSTEM MUST BE INTEGRABLE :
 - INTERIOR (STRUCTURE) SYSTEMS
 - EXTERNAL TACTICAL SYSTEMS
 - DISPLAY DATA FROM ALL AS COMMON DISPLAY

(JOINT SERVICES BROAD QUALITATIVE REQUIREMENTS)

SPECIFIC

- REALTIME DETECTION AT PERIMETERS, WITHIN AREAS, REMOTE LOCATIONS
- TRACK MOVEMENT
- SIGNAL DURESS SITUATIONS
- VISUAL AND AUDIBLE INDICATION OF :
 - SENSOR ACTIVATIONS AND LOCATIONS
 - POWER LOSS, LINE TAMPERING, FAIL SAFE
 - SENSOR STATUS (ACCESS OR SECURE)
- REMOTE ASSESSMENT OF SENSOR ACTIVATION
- SECURE TRANSMISSION, BOTH HARDWIRE AND RF
- LONG SERVICE LIFE WITH CONTINUOUS OPERATION WORLDWIDE
- NO EQUIPMENT ALARMS - ONE NUISANCE ALARM / DAY / SYSTEM
- ESSENTIALLY CERTAIN DETECTION
- AUTOMATIC IDENTIFICATION AND CONTROL OF PERSONNEL ENTRY
- RIGID POWER REQUIREMENTS, BOTH PRIMARY AND AUTOMATIC START BACKUP

TECHNOLOGY

DETECTION (SENSORS)

SEISMIC	CAPACITANCE
LASER	ELECTRO-MAGNETIC
MICROWAVE	ACOUSTIC
INFRARED	ELECTRET
RADAR	SONAR

IMAGING

SILICON VIDICON TUBE
SILICON INTENSIFIED TARGET TUBE
SODIUM VAPOR LAMPS
INFRARED

ENTRY CONTROL

VOICE PATTERN RECOGNITION
FINGERPRINT RECOGNITION
HANDWRITING PATTERN RECOGNITION
CODED CARD READERS

COMMAND & CONTROL

ANTI-JAM/ANTI-TAMPER
DIALOG CODING
SIGNAL PROCESSING
COMPUTERIZED COMMAND/CONTROL
PROCESSING

AS OF: 31 MAY 77

[illegible]

***1090 only**

Adv Dev

Eng Dev

Prod

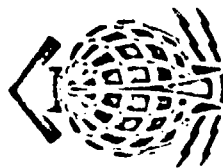
Prod

BISS/SAFE PROGRAMS (CONT'D)

AS OF: 31 MAY 77

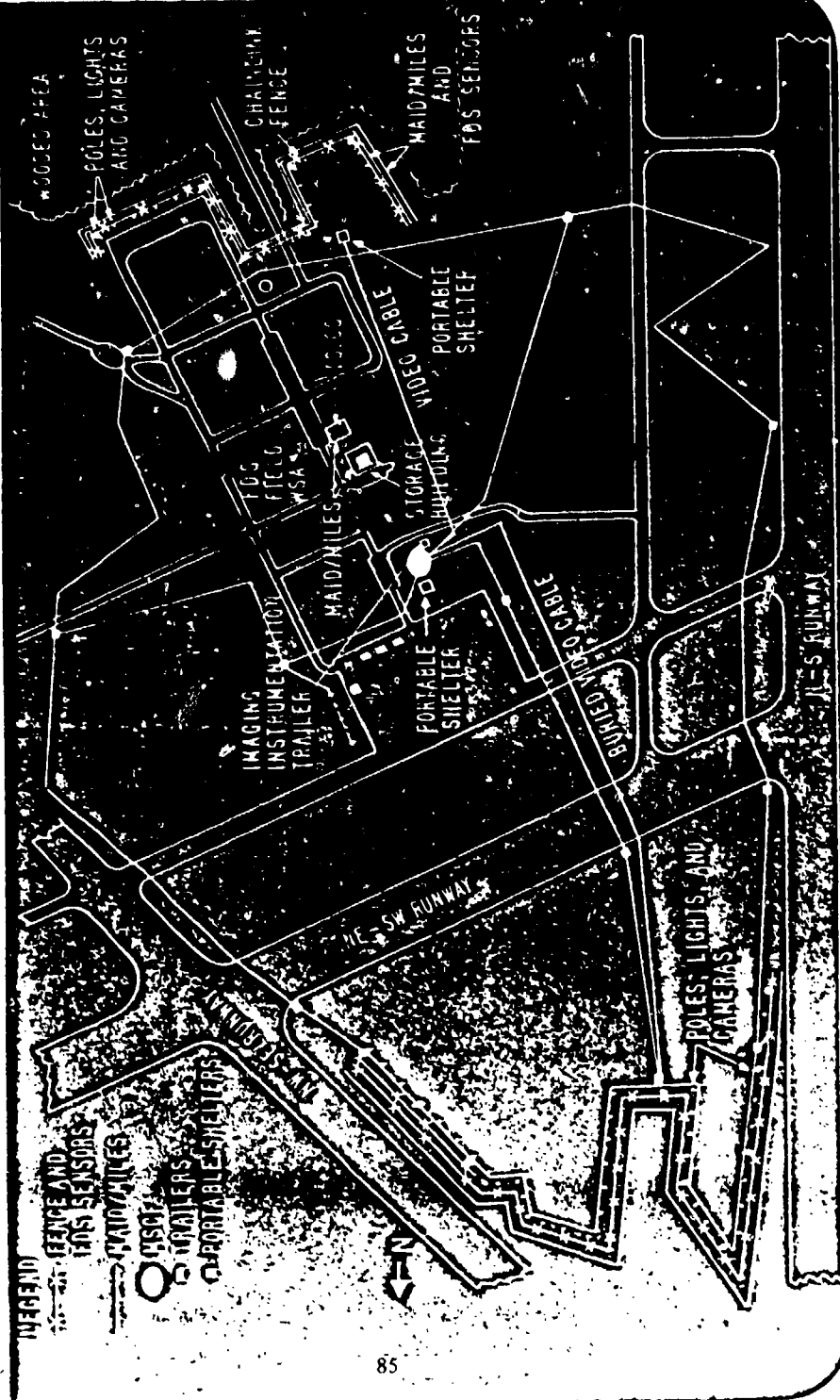
PROJECT	SHORT TITLE	PRIN CRG	TASK NO.	76	77	78	79	80	81	82	83
IMAGING											
BOUNDARY ALARM ASSESS SEC	BAAS	ERDA	76-1								
COAX CABLE MULTIPLEX	CCH	NAFI	77-1								
WIDEBAND RF VIDEO COMM	WVC	NAFI	77-2								
PYROELECTRIC VIDICON	PZV	NVL	77-4								
INDUSTRIAL CAMERA	IC	NAFI	77-2								
VIDEO FRAME STORAGE	VFS	NAFI	77-4								
REMOTE INT IMAGING SENSOR	RAIS	NVL	77-3								
ENTRY CONTROL											
ENTRY CONTROL SEGMENT	ECS/ASV										
VOICE		T.I.									
FINGERPRINT		CALSPAR									
HANDWRITING		VERIPER									
TOTAL VOICE VERIFICATION		RADC	77-8								
REMOTE VERIF IDENT		RADC	77-9								
COMMAND & CONTROL											
TOWERS	T	ELT									
MASTER SURV CONTROL FACILITY	MSCP	B'WICK									
SMALL PERM COMM & DISPLAY SEC	SPCDS	ERDA									
STORAGE STRUCTURE COMM	VCSS	AFCS									
HIGH LEVEL LINE SUPERVISION	HLLS	ERDA	76-10								
RF COLLECTOR	RFC	ERDA	76-9								
ADV SIGNAL PROCESSING		ERDA	76-12								
ADV COMMAND & CONTROL SEC		ERDA	76-13								

Adv Dev Eng Dev Prod

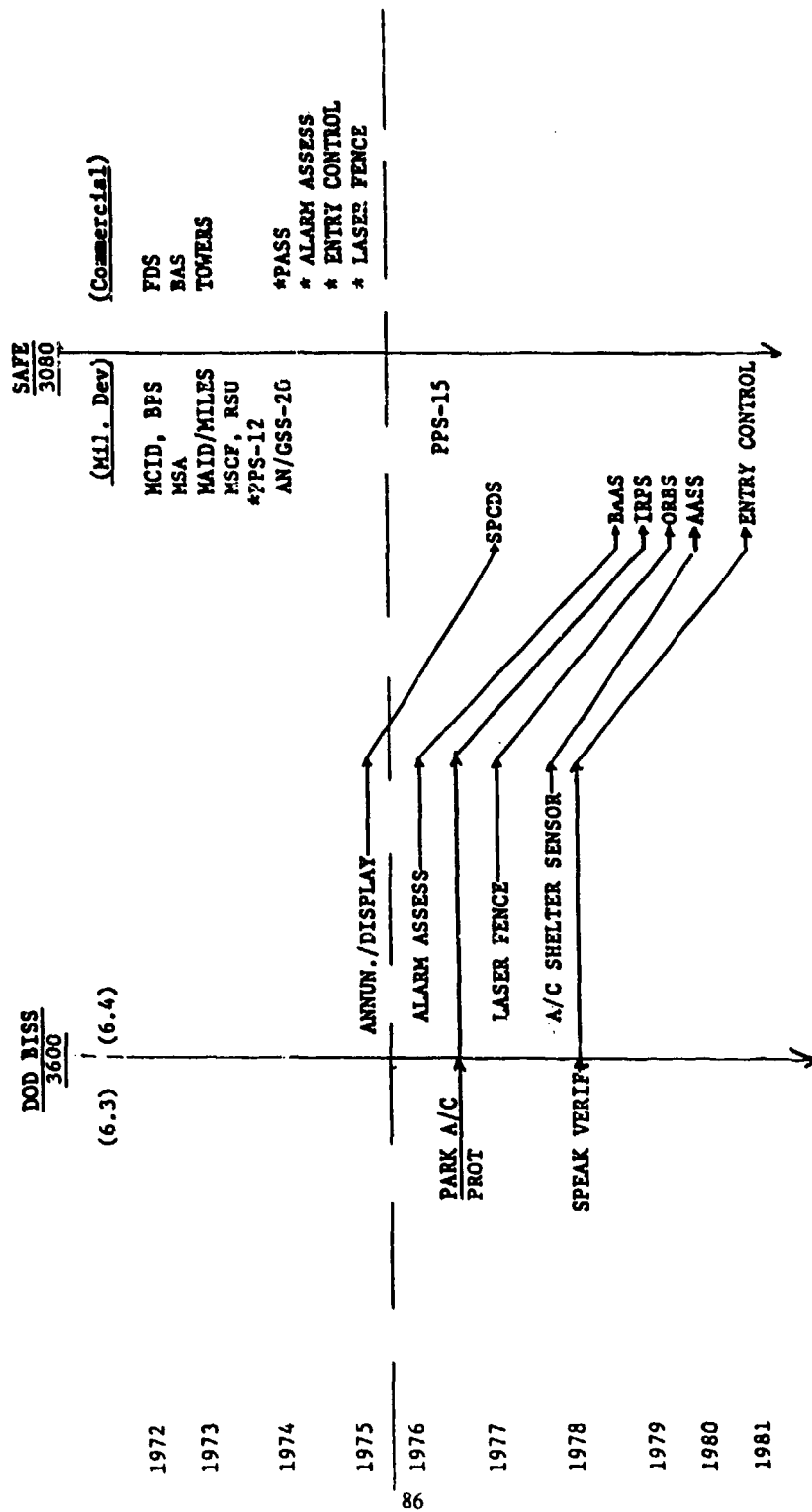


ELECTRONIC
SYSTEMS
DIVISION

BISS TEST SITE - EGLIN AFB



BISS/SAFE COUPLING



*FAILED TO QUALIFY AGAINST RQMT.

SUMMARY

SAFE PROGRAMS

- USAF DEPLOYMENT WORLDWIDE
- 9 SEPARATE OBJECTIVES
- EXTENSIVE SITE ACTIVITY NOW - ACCELERATING
- MANPOWER INTENSIVE - SPO AND PARTICIPATING COMMANDS

DOD BISS

- DEVELOPMENT FOR ALL DOD COMPONENTS
- NEW PMD - PROCURE/LOG SPT ALL DOD COMPONENTS
- MORE TRI-SERVICE COORD - CONCEPTS, ROOMTS, MANNING
- MULTI-PROJECT/MANPOWER INTENSIVE

COUPLING - PROGRAMS ARE MUTUALLY SUPPORTIVE

THE MARINE CORPS TACTICAL REMOTE SENSOR SYSTEM (TRSS)

The requirement exists within the Marine Corps for an advanced, tactical remote sensor system which is capable of continuous, all-weather detection, location determination, and monitoring of enemy activity within an Amphibious Objective Area (AOA). The Marine Corps TRSS ROC signed on 4 January 1977, states this requirement. The Tactical Remote Sensor System (TRSS) consists of remote sensors, relays, display, and sensor activation storage equipment. The remote sensors detect target activity using seismic, magnetic, acoustic, infrared, and electromagnetic energy. Detection is accomplished when a sensor-established field is disturbed or by sensing target-generated energy. A VHF radio link provides communication between the sensors, relays and storage equipment.

The TRSS will be used by:

(1) Commander, Amphibious Task Force (CATF) during the pre-assault phase. Reconnaissance and surveillance information will be obtained by monitoring appropriately placed remote sensors in the AOA. This will aid the commander and naval planners in determining enemy activity and disposition of forces inland.

(2) Commander, Landing Force (CLF) during the post-assault phase. Reconnaissance and surveillance information will be obtained by monitoring appropriately placed remote sensors, as required, throughout the AOA. Remote sensors will enable the commander to monitor enemy activities and be provided with information for planning subsequent operations. Primarily, tactical sensors complement other intelligence information gathering means, but occasionally can provide limited target acquisition information.

The need for timely information of enemy activity is of utmost importance to the commander in an amphibious operation. A serious deficiency exists in reconnaissance and surveillance capabilities during pre-assault operations. Similar difficulties are encountered during some post-assault activities such as displacement of a command post forward in offensive operations. The TRSS is needed to provide the commander with appropriate reconnaissance and surveillance information during these periods in any climate, weather, or terrain conditions.

The most significant improvement in the capability of the TRSS compared to the Phase III or SEAOPSS sensors is the Forward Pass sensor data storage system. The Forward Pass System will provide sensor intelligence without the necessity of continuous, real-time monitoring. The sensors will transmit their data to storage/relay units (SU's) which will re-transmit the data to any aircraft producing the proper command signal. The SU's will be capable of receiving information from a maximum of 62 unattended sensors within line-of-sight, storing a total of approximately 35,000 sensor outputs. The system terminates with the data interrogated from the SU's being transmitted to a naval vessel or to a mobile ground station. The storage unit will receive digital output from a maximum

of 62 sensors (at a rate of 15 activations/hour/day), time tag the data, and store a minimum of 5 days' accumulation of such data. It is of such configuration and strength to withstand the landing impact of high speed air delivery or artillery delivery without damaging the electronic components. Although required by the ROC, artillery delivery is currently considered more of a nice-to-have capability, given the requirement for high speed aerial delivery. The interrogation unit (IU) is to be carried on an operational aircraft or RPV with the electronics contained in an externally mounted pod. The control to the interrogation unit will be located in the cockpit. Manned aircraft must be capable of interrogating the storage unit from a stand-off distance of 100 miles (minimum). The interrogation unit will command the storage unit to release its information in a burst transmission of less than 30 seconds; the data received by the storage unit will also be able to be released in real-time relay. The interrogation unit must be capable of recording data from a minimum of five storage units and must possess a capability for commandable relay of this recorded data to a ground-based or sea-based display unit. The existing threat to operation in a hostile environment requires the use of high-performance aircraft in delivery and interrogation operations; rather than the low performance aircraft of U.S. Army/REMBASS scenarios. Therefore, all air deliverable components of Forward Pass must be compatible with high-performance aircraft operations.

Under the Marine Corps remote sensor development program, a jointly funded engineering development effort with the Navy is currently being pursued which, when completed, should satisfy the requirements delineated to monitor remote sensors in real and non-real time modes and provide the means to evaluate the data received aboard aircraft, amphibious ships, or unit command posts ashore. An IOC of FY-83 is planned.

COMBAT AREA SECURITY SENSOR REQUIREMENT STUDY

(CASSR)

USAMPS SCORES EVALUATION

1. PURPOSE. The purpose of this evaluation is to determine the effectiveness of using sensors in security roles in a Corps area as depicted in TRADOC Standard Scenario, Europe I, Sequence 2A. Three main factors will be considered:

a. Probability of detecting intruders at four high priority targets in the Corps area.

b. Probability associated with various possible outcomes of employing sensors in a security role.

c. Number of sensors necessary to maximize effectiveness.

2. METHODOLOGY. The methodology consisted of a free play wargaming simulation. Basically, two types of data were utilized to design and conduct the simulation.

a. Nonvariable data.

(1) Four high priority targets located in the Corps area were selected as test units. The units were selected from PART I, TROOP LIST, VOL I, TRADOC STANDARD SCENARIO, Europe I, Sequence 2A, with the exception of the pipeline which was simulated. The unit designations and their locations have been deleted in order to avoid classifying this Appendix.

(2) The location of other units in the vicinity of test units were held constant as given in the scenario and influenced the simulation in two ways:

(a) They were "off limits" as an avenue of approach over terrain which they physically occupied.

(b) They provided the Rear Area Security (RAS) reaction forces for the attacked units.

(3) Sensor arrays were plotted in accordance with guidance in Chapter 2, Interpretation and Analysis Text for Unattended Ground Sensors, US Army Intelligence Center and School, Fort Huachuca, AZ, May 1975. The strings were plotted prior to commencement of the simulation and remained constant throughout the exercise.

(4) A reinforced special operations squad, consistent with Soviet Special Operations Doctrine, the SCORES Rear Area Threat Appendix, and Appendix B, CASSR Study, was developed by the USAMPS Threats Officer. The composition of this squad remained constant throughout the exercise.

(5) Detection range of each sensor was held constant at 50 meters.

(6) The assumptions and limitations of the SCORES Scenario were held constant throughout the analysis.

b. Variable data.

(1) The approximately 136 iterations which were conducted during the exercise were almost totally unstructured with respect to employment concepts. The main limiting factors were mission and composition of aggressor forces.

(2) Distance from Reaction Forces to the target varied according to the type of unit involved, but remained constant for all iterations pertaining to any one unit.

c. Procedures.

(1) Selection of the type of units to be evaluated was based upon priorities extracted from threat documents, a survey of CS and CSS units, and the employment concepts from the CASSR Study. While the approximate location of the units could easily be established from the SCORES scenario, the interior configuration of each element was obtained from each proponent service school, again with the exception of the pipeline. The interior configuration was not a significant variable in the simulation; however, it aided personnel conducting the evaluation in visualizing the assets. Annexes I-III contain diagrams of the three unit/installation targets used in the simulation.

(2) The location of each unit was plotted on a 1/50000 scale standard US Army TOPO Map. Photographs were taken of each location and enlarged such that the unit was in the center of a 36 square kilometer area with each grid square measuring 3 1/4 inches. The 36 square kilometer area permitted all possible likely avenues of approach, as well as mortar positions within maximum effective range of enemy mortars, to be covered by sensor arrays. The sensor arrays were drawn to scale (50 meter detection range) on the enlarged photo and divided into three discreet blocks as follows:

<u>COLOR</u>	<u>CATEGORY</u>	<u>AVE OF APPROACH</u>
RED	I	PRIMARY
BLUE	II	SECONDARY
GREEN	III	TERTIARY

Figure 1. Discreet Blocks

The types of sensors within each array were labeled either "Identification" or "Confirming" describing the function of the sensor as opposed to its technology. The sensor arrays were plotted by two officers and one NCO, two of whom have had extensive experience in Special Forces and other small units, and one of whom is familiar with the techniques of implanting sensor arrays. Thus, the sensor arrays were implanted prior to the commencement of the simulation and remained constant throughout. At Annexes IV-VII are reduced photographs depicting the sensor arrays.

(3) Following the placement of the sensor arrays, a threat force and operations order for that force were developed. At Annex VIII is a description of the threat force to include its weapons composition which, including the basic load, averaged approximately 70 pounds per man. The operations order followed the five paragraph field order format and contained, among the routine information, the following critical instructions:

(a) The mission of the threat force was to attack each target and to inflict maximum damage to each friendly unit consistent with personnel, weapons and time constraints.

(b) The threat force was instructed to avoid becoming decisively engaged.

(4) The final preparatory step was to select the participants for the exercise. It was decided that a combination of officers and NCO's, of various branches, representing different elements of USAMPS, would constitute a more representative sample than a completely homogeneous group. Accordingly, officers and NCO's from the various divisions of the Directorate of Combat Developments, the Tactical Operations Group, and the Directorate of Training Developments, were selected to participate as members of the "Red Team." The composition of each team by grade and branch is at Annex IX.

(5) Each participant was individually briefed as to the purpose of the evaluation and the specific situation pertaining to each target. Each participant was provided with an enlarged photograph

of the 36 square kilometer area, a copy of the interior configuration of the targets, a copy of the operations order, a copy of the threat force composition, a copy of the map symbols to be utilized, and overlay paper. The organization and location of reaction forces, as well as other friendly units located in the area, were provided. Participants were advised that friendly units had the capability of using unattended ground sensors as part of their overall defense plan. Unlimited time was provided for reconnaissance. A standard, 1/50000 topo map was available for reference. Then each participant was asked to plan an attack on each of the four targets and to diagram on a separate overlay for each target the following information:

- (a) Grid reference points
- (b) Route to the objective
- (c) Assembly area or attack position
- (d) Location of mortar positions
- (e) Location of the attack (concept)
- (f) Rallying points
- (g) Withdraw route
- (h) Time of attack.

Few constraints were imposed on the participants. The only terrain over which enemy activity was prohibited was that physically occupied by friendly units; the assumption being that such a route would result in certain detection by members of the friendly units. Otherwise the participants were permitted free movements throughout the area.

d. Evaluation.

(1) The first step in the evaluation involved comparing the overlays developed by the Red Team members with the sensor arrays depicted on the enlarged photographs. An analysis of each overlay was conducted in order to obtain the data from which the probabilities associated with detection interception and mission accomplishment could be calculated. Certain predetermined measures were applied to each iteration, and the resulting data recorded on charts for further analysis. Important variables which determined the nature of the recorded data are as follows:

(a) The only reasons for not including the data from any iteration, regardless of how seemingly implausible the plan might appear, would be illegibility or incompleteness. The results of the evaluation were such that 98 of the 100 iterations displaying the routes to the objectives and 97 of the 100 iterations showing the withdrawal routes were usable.

(b) An assumption was made that all sensors were in working condition; no allowance was made for inoperable sensor arrays.

(c) A sensor was determined to have been activated if the route of the enemy squad to or from the objectives, or the assembly area or mortar position, passed within the detection range (50 meters) of a sensor. Since the sensors, including their detection range, had been drawn to scale, if the enemy route or assembly position touched a sensor, an activation was recorded.

(d) False or nuisance alarms were determined to have occurred if only one sensor was activated by the enemy in a line formation. The presumption in such instances was that only one person in the squad would have activated the sensor. Accordingly, the result was recorded as a nondetection. In all other situations, such as when the enemy was in column formation, or when mortar positions were being established, it was determined that numerous activations would have occurred, and a detection was recorded.

(2) The next step was to determine the probability distribution associated with the three types of sensor arrays and the relative frequency of different events. The events were grouped according to where they occurred during the simulation. For instance, one of the objectives was to determine the probability of detecting the enemy before he accomplished his mission. Accordingly, those detections which occurred prior to the enemy physically reaching the objective were divided into one of four possible events:

- Detection along route to objective (Event A)
- Detection at Attack Position (Event B)
- Detection at Mortar Position (Event C)
- Detection during assault (Event D).

Detections which occurred after the enemy reached the objective occurred at two possible points:

- Detection at Rally Points (Event D)
- Detection along withdrawal route (Event E).

It remained to determine which category of sensor detected the presence of the enemy. Since a detection by one category of sensor

would preclude the necessity of detecting the enemy by another category of sensor, which would constitute a duplication of effort and resources, it was determined that the different categories would be mutually exclusive. Therefore, a probability of detection could be computed for each category of sensor or any combination thereof as well as for the total cumulative probability. For simplicity, events A-D were grouped to determine probability of detection before the attack and events D-E grouped to determine the probability of detection after the attack. This technique permitted a more thorough analysis to be conducted and also assisted in determining the approximate number of sensors which would be needed to achieve any of three different levels of detection.

(3) Following determination of the probability distribution for events A-E, the probabilities associated with various possible outcomes of employing sensors in a security role were determined. These were placed in a probability tree format from which the conditional probabilities for all possible outcomes could be determined. The possible outcomes are listed below in the order in which they were developed:

- (a) Detected incoming; not detected: $P(A)$; $P(\bar{A})$
- (b) Intercepted by RAS forces; not intercepted: $P(B)$; $P(\bar{B})$
- (c) Completed mission; not completed: $P(C)$; $P(\bar{C})$
- (d) Detected outgoing; not detected: $P(D)$; $P(\bar{D})$
- (e) Intercepted outgoing; not intercepted: $P(E)$; $P(\bar{E})$
- (f) Escape engagement; not escape: $P(F)$; $P(\bar{F})$.

(4) The probabilities associated with each branch of the above sequence were developed from various data sources. These data were not always readily apparent, and it was necessary to compile the information from among the best available references. The following is an explanation of the probabilities associated with each of the possible outcomes.

(a) $P(A)$, $P(\bar{A})$, $P(D)$, $P(\bar{D})$. These probabilities were determined by analyzing the data developed from the simulation. However, because of the three discreet categories of sensors, there were three possible probabilities associated with each of events A-D and E-F and one associated with the total of all categories. It was decided that the probability of detection for the category which offered the greatest relative effectiveness per sensor would be used for that branch of the tree. The relative effectiveness was computed as follows: IF:

$$\frac{\frac{\text{EFFECTIVENESS CAT I}}{\text{EFFECTIVENESS CAT I}}}{\frac{\text{NUMBER CAT I SENSORS}}{\text{NUMBER CAT I SENSORS}}} = 1$$

THEN: Relative Effectiveness (RE) of the other categories of sensors would be:

$$\frac{\frac{\text{CUMULATIVE EFFECTIVENESS CAT I + CAT II OR III}}{\text{EFFECTIVENESS CAT I}}}{\frac{\text{CUMULATIVE NUMBER SENSORS}}{\text{NUMBER OF CAT I SENSORS}}}$$

at Annex X is a graph showing the RE of each discrete category. RE of CAT I was significantly higher than that of CAT II or CAT III. The RE for each category was almost exactly the same for events A-D as compared to events E-F. Accordingly, the probability of detection for CAT I sensors only was used for both P(A) and P(D) because it provided the greatest RE per sensor. Relative cost (RC) for each discrete category was not a factor because the total number of sensors involved in this scenario would be insufficient to generate cost savings through economics of scale. Therefore, RE would remain proportional even if RC was calculated.

(b) P(B), P(B), P(E), P(E) was determined to be a function of whether reaction forces could assemble and reach the enemy before (events A-D) the enemy could either accomplish the mission or escape (events E-F) from the 36 square kilometer area, which was assumed to be a reasonable limit of the area of influence of the reaction force. Each iteration was evaluated separately to determine if the reaction forces could intercept the enemy. The probability was calculated by the formula: $\frac{\text{Number of successes}}{\text{Number of attempts}}$ separately for events A-D and E-F. (The factors which determined whether an intercept was registered or not are described below.)

1 Platoon size reaction forces were assembled from combat support and combat service support units IAW FM 31-85, Rear Area Protection Operations.

2 Distances between reaction forces and each target were measured and determined to be as follows:

- a TGT 1: .2 KM (organic reaction forces)
- b TGT 2: 5 KM (RAS reaction force)
- c TGT 3: 5 KM (RAS reaction force)
- d TGT 4: 15 KM (RAS reaction force).

3 Determination was made that reaction forces would not be alerted until at least two sensors had been activated. This constraint significantly reduced the number of successful interceptions as opposed to what would have occurred if reaction forces had been alerted upon the activation of one sensor; however, the constraint was necessary to approximate a more realistic sequence of events. Requiring the activation of at least two sensors avoided exhausting reaction forces and aided in determining the enemy objective.

4 Assembly time (AT) for reaction forces was held constant at 15 minutes (Table II-12, SOCREs "Jiffy" War Gaming Methodology (U), USACAC, July, 1975).

5 Movement time (MT) for reaction forces was held constant at 24 K/H for truckmounted troops moving along roads at night in terrain type B. (Table II-13, SCORES "Jiffy".)

6 Reaction time (RT) after arrival by the reaction force was determined by measuring the distance travelled dismounted and computing the time required using an average cross-country rate of .8 KM/HR (Table II-13, "Jiffy").

7 MT1 for the enemy from the location of the second sensor activation to the enemy's assembly area was calculated using an average speed of .8 KM/HR (Table II-13, "Jiffy").

8 AT for the enemy was extrapolated using the data in Table II-12, "Jiffy," and held constant at 7.5 minutes.

9 MT2 for the enemy from its assembly area to the objective was calculated using an average rate of speed of 2.27 m/s (Test Data, Sys Perf + Concept Dir, USA Hum Egr Lab, APG, MD, 1 Apr 76).

10 The total elapsed time (ET) for both the reaction forces and the enemy was calculated for each iteration, and an interception was recorded if ET for reaction forces was less than ET for the enemy. As a formula, this can be expressed as follows: Interception (B) = (RF) ET = AT + 60 $\left(\frac{D}{R_T} + \frac{D}{R_T} \right) < (E) E_T = A_T + 60 \left(\frac{D}{R_{T1}} + \frac{D}{R_{T2}} \right)$

11 To determine the probability of intercepting the enemy following an attack, the ET for the enemy had to be computed differently because if the enemy reached the boundary of the 36 sq KM area an interception would not be recorded. Accordingly, while the ET for reaction forces could be calculated as described above, ET for the enemy was stopped at the boundary. This was accomplished by subtracting the distance from the target at which the enemy was

detected from 3000, the minimum distance from the target which the enemy would have to travel to reach the 36 sq KM boundary. Again, if ET for reaction forces was less than that of the enemy, an interception was recorded.

(c) $P(C)$, $P(\bar{C})$, $P(F)$, $P(\bar{F})$. The probabilities associated with these branches were essentially a function of firepower ratios of the attacker and defender. The firepower ratios were dependent upon the number of personnel who could be committed to the fight and the weapons employed. The threat force weapons potential score was constant because it was assumed that each enemy soldier would be engaged in the fight. The weapons potential for the friendly forces varied according to which branch of the possible outcomes was involved. These were calculated as follows:

1 $P(C/B/A)$; $P(\bar{C}/B/A)$; $P(C/B/\bar{A})$; $P(\bar{C}/B/\bar{A})$; $P(F/E/D/C/B/A)$; $P(\bar{F}/E/D/C/B/A)$; $P(F/D/C/B/\bar{A})$; $P(\bar{F}/D/C/B/\bar{A})$: The key variable for all of these probabilities is interception by reaction forces either prior to the attack or during withdrawal prior to reaching the boundary of the area. To determine the firepower ratio it was determined that the reaction force would normally consist of one military police platoon from a military police company (TOE 19-77H), or a similarly configured unit. Firepower ratios for both friendly and enemy units were computed using the firepower potential scores contained in Table II-1, SCORES "Jiffy" War Gaming Methodology. The ratio of reaction force to enemy was 2.815 to 1. Consulting Table III-B-1, Ground Combat Personnel Casualty Rates, SCORES "Jiffy" under the heading "Meeting Engagement," it can be determined that the enemy will sustain between two and four times as many casualties as the reaction forces. Accordingly, the probability that the reaction force prevents the enemy from accomplishing the mission or escaping intact is very high. Since the reaction force would have the second highest maneuver firepower ratio for which casualty rates are listed, and since the enemy casualty rate is so high, a probability of .9 was assigned to preventing the enemy from accomplishing the mission or escaping, given that the enemy had been intercepted.

2 $P(C/\bar{B}/\bar{A})$; $P(\bar{C}/\bar{B}/\bar{A})$: These probabilities reflect the enemy's undetected and uninterrupted approach to the target. Without prior warning of imminent attack it was determined that friendly forces would have a very low probability of preventing the enemy from accomplishing his basic missions. Therefore, the probability of mission completion given no detection or interception was .9. This could be sensitive to other defensive factors such as improved barrier delay time, use of mines, or artillery support. However, .9 does represent the "worst case" and is useful for evaluating use of sensors in that context.

3 $P(C/B/A)$; $P(C/B/A)$. These probabilities are associated with the chances of preventing the enemy from accomplishing the mission given that he had been detected, but for any one of a number of reasons, not intercepted by friendly reaction forces. This was primarily a function of whether the organic personnel of the unit could react in sufficient time to stop the enemy. Each iteration was analyzed to determine where the sensor activation occurred, what type of force could be assembled, how long it would take to assemble, etc. The probability of preventing the enemy from accomplishing the mission (.27) was then calculated by dividing the number of successes by the total number of iterations.

(5) Sensitivity. Side analyses were conducted to answer certain "what if" questions which became obvious during the analysis. The following is a list of those analyses, the results of which are addressed under "Findings" below:

(a) Would the probability of detection vary significantly if the exercise were performed by a different "Red Team?"

(b) Was the overall probability distribution sensitive to the results of the findings of any one of the target analyses.

(c) How successful were the sensor arrays in detecting the mortar crews.

e. Findings.

(1) At Figure 2 is the probability of detection of events A-D and E-F for each of the three discreet categories of sensors.

CATEGORY	PROBABILITY OF DETECTION	
	EVENTS	
	A-D	E-F
I	.62	.54
II	.15	.12
III	.04	.05
CUMULATIVE	.81	.71

n = A-D: 98; E-F: 97

Figure 2

While the total cumulative probability of detection is quite high, it should be noted that the greatest degree of effectiveness per sensor is obtained with category I sensors only. Given the high cost of sensors and the time associated with implanting sensor arrays, the best course of action in most instances would be to maximize effectiveness by covering only the most likely avenues of approach (i.e., category I). In some instances, such as when there is a very well defined threat, when the assets to be protected are of critical value, or when the asset is fixed for more than a few days, the commander could achieve a significantly improved probability of detection, even with decreased marginal effectiveness, by covering the secondary avenues of approach. In no case could the benefits derived justify using sensors to cover tertiary avenues of approach.

(2) At Figure 3 is the number of sensors by type category emplaced per target.

CATEGORY	NUMBER OF SENSORS PER TGT #					CUM TTL
	1	2	3	4	TTL	
I	56	51	49	45	201	201
II	32	32	35	23	122	323
III	25	18	13	18	74	397
TOTAL	113	101	97	86	397	

Figure 3. Distribution of Sensors

These sensors were implanted along the three types of avenues of approach without constraints as to the number of sensors. The number for each category was not determined until the Blue Team was satisfied that the avenues of approach were covered with sensors where such devices could be utilized. The 397 sensors were apportioned among 79 arrays; the mean number of sensors per array being 5.02. 61 of the 79 arrays (77%) were activated by the enemy at least once with a mean activation of 2.3 sensors per array at a mean distance of 1136.7 meters per sensor. Analysis of the unused sensor arrays reveals that the same probability of detection could have been achieved with a total of 316 sensors by merely eliminating the unused sensors. This is not feasible, however, due to the obvious problem of deciding in advance which of the arrays should be eliminated. If such perfect information could be obtained, there would be no need to use any early warning techniques. A more meaningful analysis of the sensor arrays indicates that one category II array at each of targets 1-3 was activated more than the majority of the category I arrays. This suggests the importance of selecting

primary avenues of approach when planning the sensor arrays. In these instances, the Blue Team had regarded the avenues of approach as secondary while the Red Team perceived them as primary avenues of approach. A switch from Cat II to Cat I of only three sensor arrays with a total of 15 sensors would have significantly improved the Pd for Cat I sensors. Again, this is hindsight and should be used only to emphasize the importance of selecting avenues of approach when resources are limited.

(3) At Annex XI is a graph of the probabilities of detection for each category per target. Significant findings of this information are as follows:

(a) Pd varies significantly among the different targets, with the cumulative Pd for target 4 being the highest. This was the single most surprising result of the entire exercise because the pipeline was widely assumed to be the most difficult asset to protect with sensors due to its length, and because fewer sensors were used for target 4 than any other. It should be noted that when analyzing the iterations to determine the probability of interception by reaction forces given detection, the lowest number of interceptions was achieved with the pipeline. This suggests that improved procedures for intercepting the enemy need to be devised for such extended assets as pipelines as well as critical communications links, electrical power lines, water supplies, and main supply routes.

(b) The Pd for target 2 airfield is the lowest primarily because it was a large facility with more likely avenues of approach than any other target with the possible exception of the pipeline. Because reaction forces were sufficiently close to the asset to respond quickly upon the activation of two or more sensor arrays, the probability of interception increased significantly from .31 for the pipeline to .73 for the airfield, despite the rather large size of target 3.

(c) Pd for target 1, the reduced SASP, was highest of all for category I sensors. In addition, because of its inherent security force, the probability of interception was a virtual certainty. With the reduced signature of the unit, and its inherent security forces, the SASP should be able to utilize sensors in such a manner as to significantly reduce the threat of successful enemy attack.

(d) Target 3, the POL storage/pumping facility was the only asset which received absolutely no marginal utility by adding category III sensors. This particular target also was subject to the most unusual enemy concepts of attack, which were directed at exploiting the vulnerability of the storage tanks to the mortars, RPG, and demolitions. In three instances, where no detection was

as to have been possibly classified as "outliers." To prevent prejudicing the study, and because the concepts were obviously a genuine effort to accomplish the mission, all three iterations were classified as successful attacks.

(4) At Annex XII is a probability tree depicting all reasonable possible outcomes of all iterations. This was calculated in order to depict how using sensors in a security role would interface with existing Rear Area Security (RAS) concepts. The probability of each branch was determined as described in paragraphs 2d(4)(a)-2d(4)(d) above. By following the different branches and summing those outcomes which prevent the enemy from accomplishing the mission or prevent his escape, some expectation of obtaining a favorable outcome of using sensors in conjunction with current RAS capabilities can be determined. Analysis of the entire exercise reveals that given that the enemy enters the 36 sq KM area, there is a .68 probability that he will either not accomplish his mission or will be rendered ineffective prior to exiting the area. This is assuming the use of category I sensors only, because they offered the highest relative effectiveness. Significant improvement in this expectation could be obtained by adding category II sensors. However, the decreasing marginal utility of the CAT II sensors would be an important consideration in any such decision.

(5) A side analysis using a different Red Team was conducted to determine if there was any significant difference between the results of the initial evaluation and that of the side analysis. The Red Team was composed of nine Military Police Officer's Advanced Course students who had completed the Tactical Operations Module (6 weeks) and who were participating in the evaluation in partial fulfillment of course requirements. All data relative to the exercise were held constant. Iterations were conducted and evaluated in the same manner as for the original exercise described above. Figure 4 depicts the results of the side analysis compared with those of the original evaluation:

	PD EVENTS			
	A-D		E-F	
	CA	ORIG EVAL	OA	ORIG EVAL
CAT I	.64	.62	.44	.54
CAT II	.19	.15	.28	.12
CAT III	.03	.04	.06	.05
CUM PD	.86	.81	.78	.71
	n = 36	n = 98	n = 36	n = 97

Figure 4. Comparative PD

Comparison of the results using "Interval Estimation of a Proportion" technique (see pp. 382-383, Statistical Analysis for Decision Making, by Morris Hamburg), revealed that the overall PD for the MPOAC evaluation was within the standard error interval for the original evaluation with a 95% confidence coefficient. Therefore, it is concluded that there is no significant statistical difference between the cumulative probabilities of detection for the two evaluations.

(6) A side analysis was conducted to determine the probability of detecting mortar positions only. This was accomplished by dividing the number of iterations where mortars were detected by the total number of iterations during which mortars were used. Of the 92 iterations in which mortars were used, 37 were detected by sensors for an overall PD of .40. Figure 5 depicts the PD for each target.

	PD	n =
(TGT 1) SASP	.44	25
(TGT 2) Airfield	.41	22
(TGT 3) POL	.59	22
(TGT 4) Pipeline	.17	23
CUM TTL	.40	92

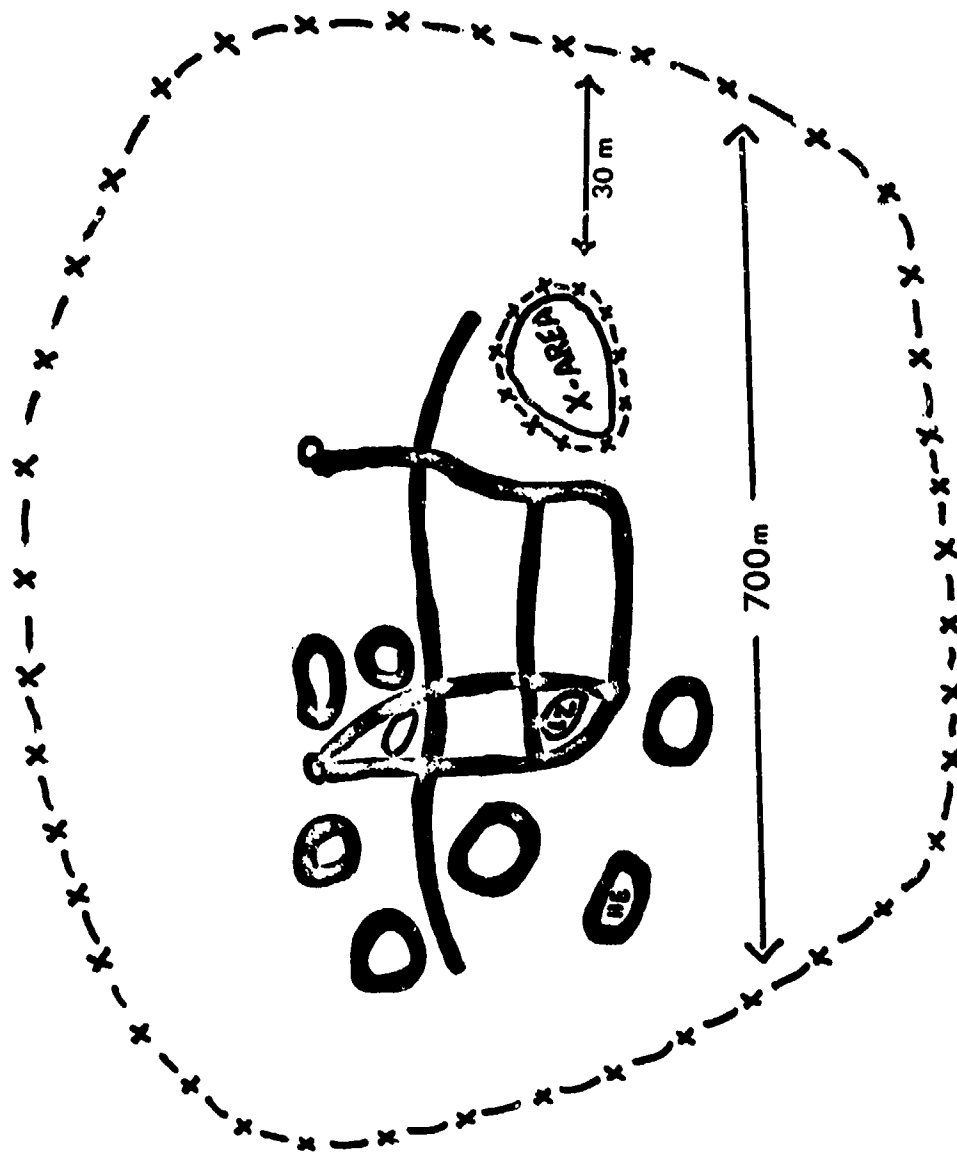
Figure 5. PD for Mortars

As expected, PD mortars for the pipeline was considerably lower than for any other target. However, mortars do not constitute a serious threat to pipelines where demolitions and direct fire weapons are more effective. The concept is to use sensors at the most likely indirect fire positions near high priority assets. It is important, also, for artillery support to be readily available due to the short period of time that the enemy is likely to remain at the mortar position.

3. CONCLUSIONS.

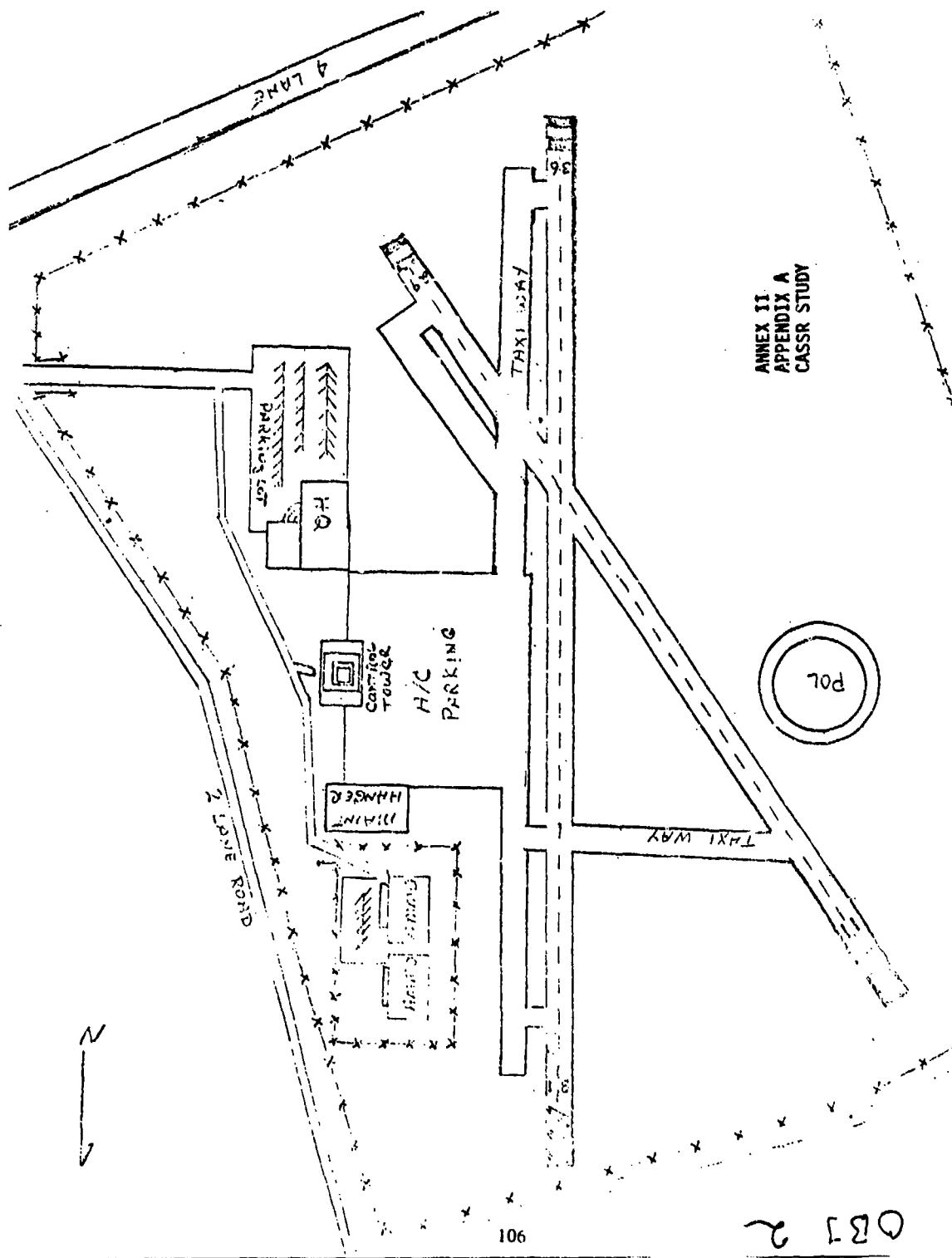
- a. Tactical sensors can be used effectively in a security role in the Corps area.
- b. Because of their cost, and the time required to install, sensors should be used to assist in the protection of high priority assets in the Corps area.
- c. Control of sensor assets within the Corps should be centralized.
- d. Employment of sensors should be decentralized with redundant monitor capability at a centralized location.
- e. Sensors should be made recoverable.
- f. A basis of issue of approximately 50 sensors per asset to be protected should be used. The sensor mix can be the same as that used for the division.
- g. Quick reaction by RAP task forces is the single most important variable in RAP operations.
- h. Avenues of approach to be covered by sensors must be selected carefully.
- i. Sensors can be used to detect the presence of intruders along extended assets such as pipelines. However, methods of intercepting these intrusions must be improved significantly.
- j. Use of sensors to detect the presence of indirect weapons such as rockets or mortars can be incorporated into an overall defense plan for a critical asset. Relatively few sensors can be used to cover the most likely mortar positions in many areas.

ANNEXES IV THROUGH VII HAVE BEEN DELETED FOR CLASSIFICATION REASONS.



$$P = \pi d$$

$$2200 = \frac{22}{7} \cdot 700$$



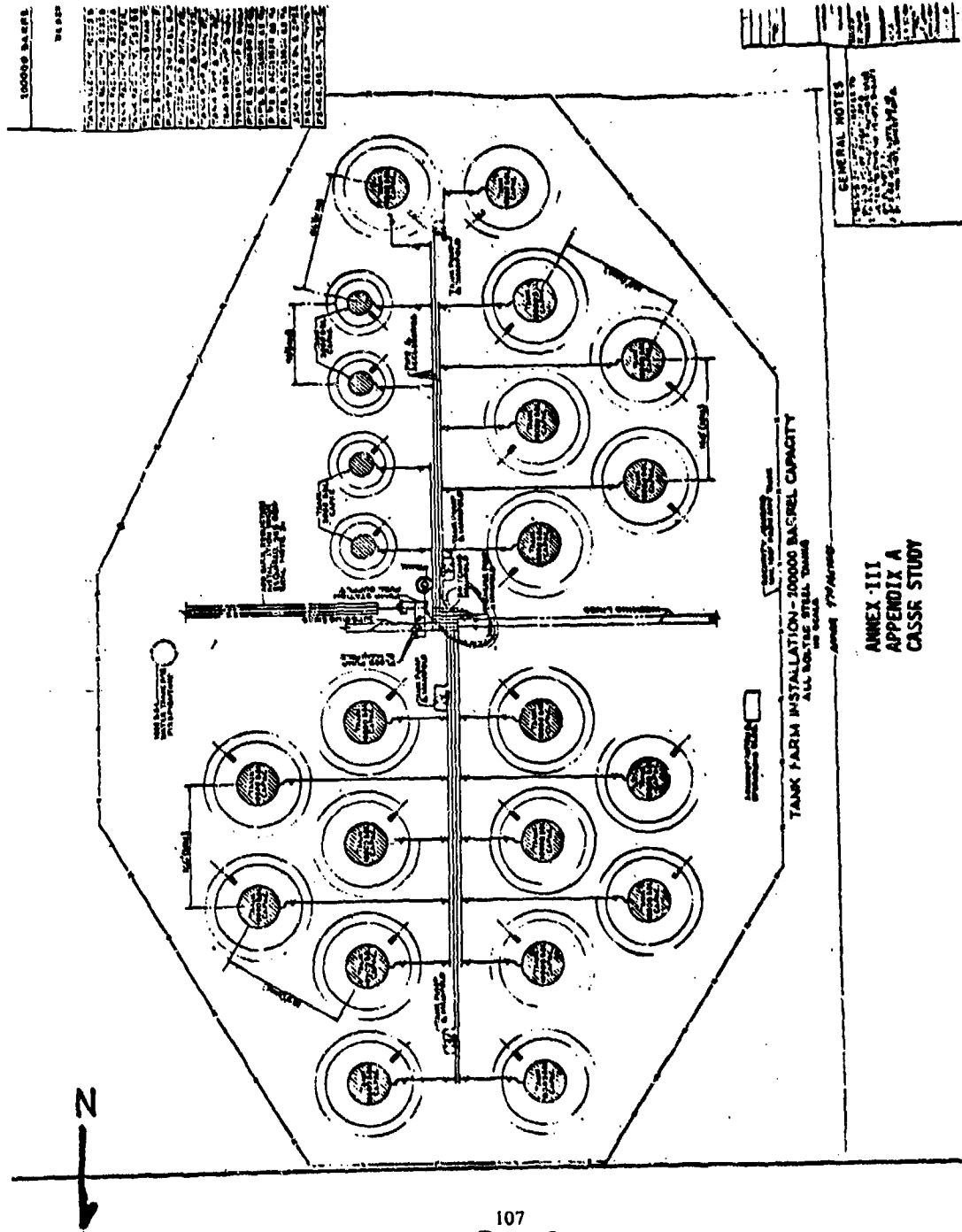
ANNEX II
APPENDIX A
CASSR STUDY

081 2

OBJ 3

107

N



REINFORCED SPECIAL OPERATIONS SQUAD

	7.62	7.62 (MG)	RPG	Demo	82mm
1. Squad Leader: AKM	360 Rds 7.62				2
2. Asst Squad Leader: AKM	360 Rds 7.62				2
3. Machine Gunner: MGPK		750 Rds 7.62 MG			
4. Asst Machine Gunner: AKM	120 Rds 7.62	750 Rds 7.62 MG			
5. AT Grenadier: RPG-7D			4 Rds RPG		
6. Asst Grenadier: AKM	360 Rds 7.62		4 Rds RPG		
7. Sniper: SVD	200 Rds 7.62				4
8. RTD/Rifleman/Demo: AKM	360 Rds 7.62			10 lbs Demo	
9. Rifleman/Demo: AKM	360 Rds 7.62			20 lbs Demo	1
10. Rifleman/Demo: AKM	360 Rds 7.62			20 lbs Demo	1
11. Mortarman: Pistol					2
12. Mortarman: Pistol					2
13. Asst Mortarman: AKM	360 Rds 7.62				1
14. Asst Mortarman: AKM	360 Rds 7.62				1
15. Ammo Bearer: Pistol					4
16. Ammo Bearer: Pistol					4
TOTAL 16 Men	3,200 Rds 7.62	1,500 Rds 7.62MG	8 Rds RPG	50 lbs Demo	24 Rds

TOTAL WEAPONS

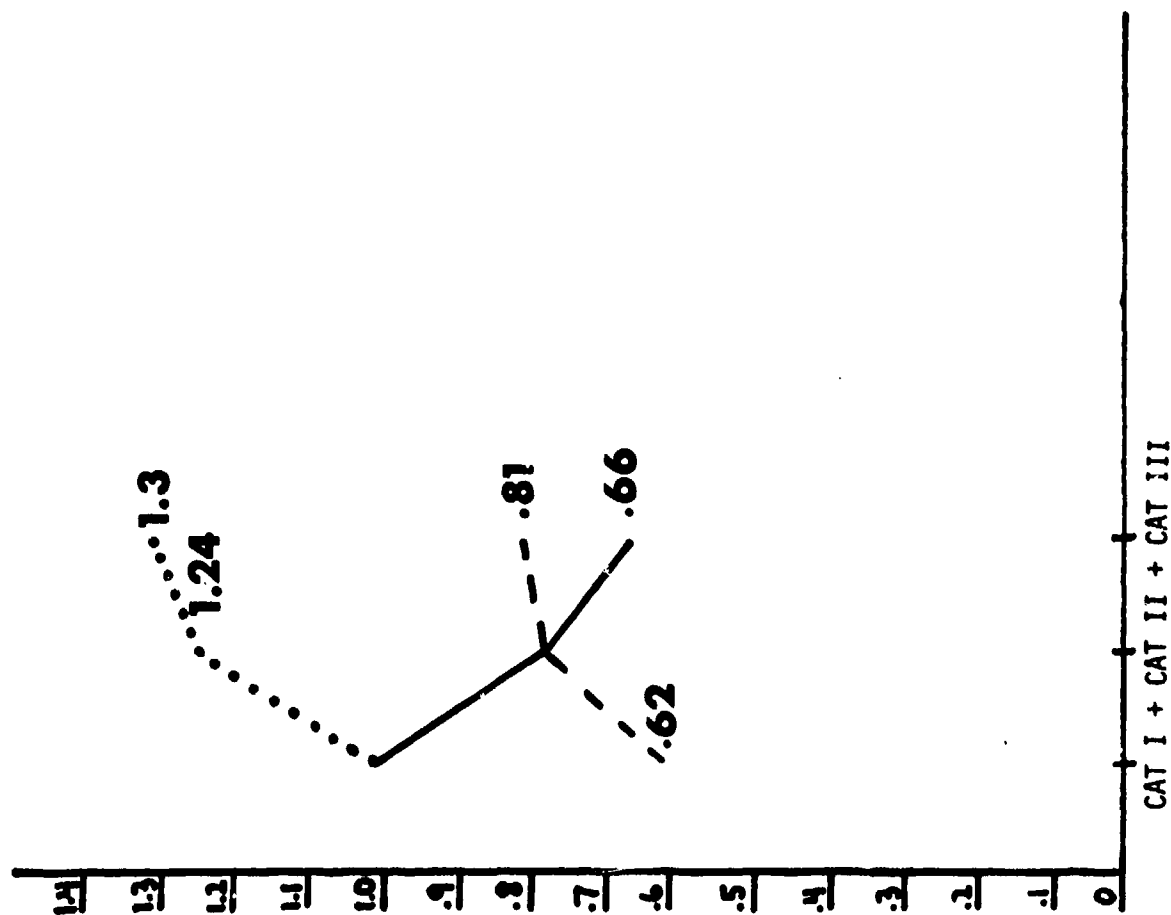
- 9 AKM
- 4 Pistol
- 1 MGPK
- 1 RPG-7D Launcher
- 1 SVD Rifle
- 2 82mm Mortar

ANNEX VIII
APPENDIX A
CASSR STUDY

ANNEX IX
APPENDIX A
USAMPS SCORES EVALUATION
CASSR STUDY

Profile of Participants

	<u>GRADE</u>	<u>NUMBER PERSONNEL</u>	<u>BRANCH</u>
1. Blue Team	CPT	2	MP
	SFC	1	IN
2. Red Team	LTC	1	IN
		1	MP
	MAJ	6	MP
	CPT	5	MP
		2	MP/AVN
		1	QM
		1	IN
	LT	1	ORD
		1	SIG
		1	MI
	SFC	2	IN
		1	MP
	SSG	1	IN
		1	MP



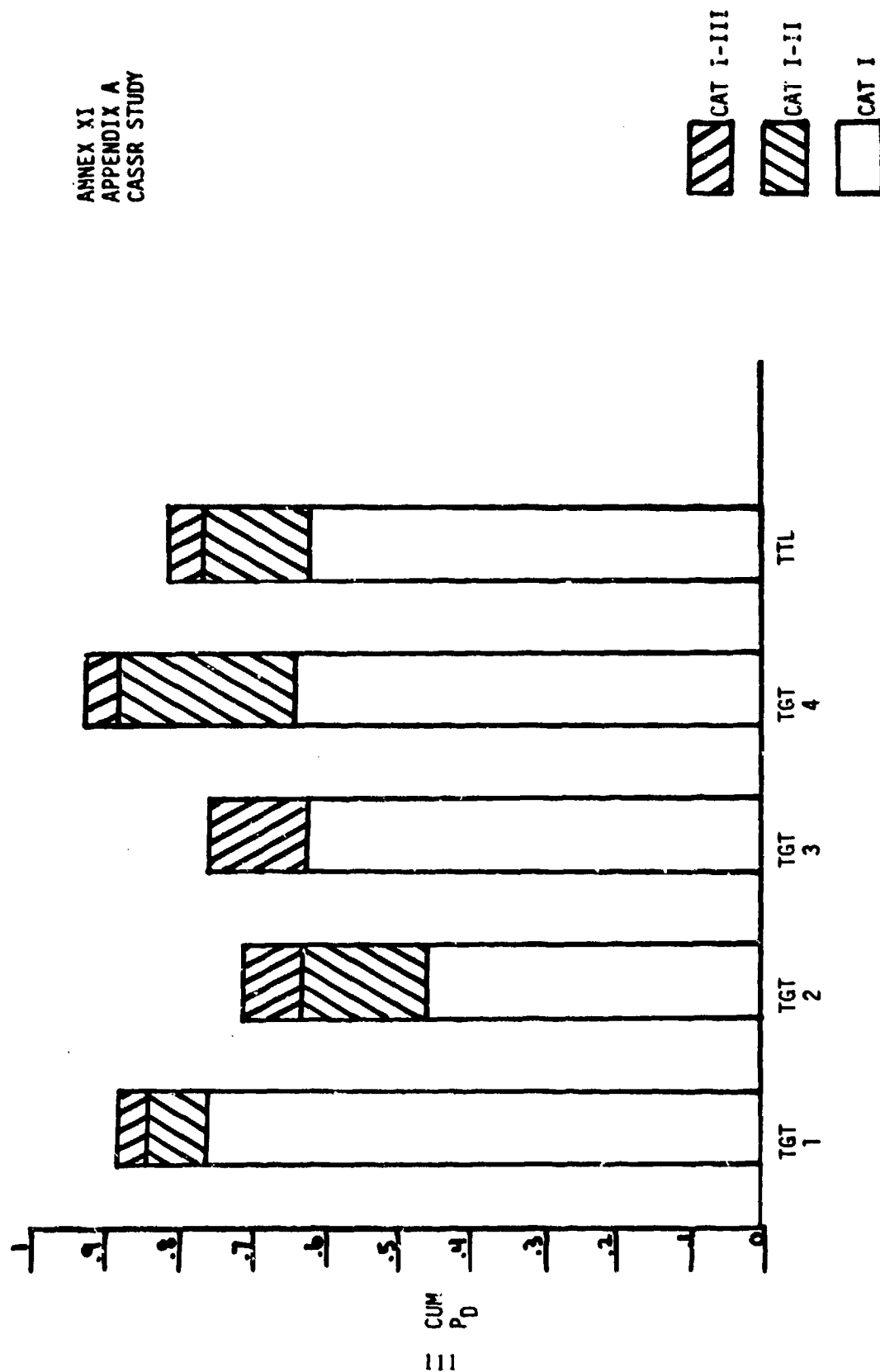
ANNEX X
APPENDIX A
CASSR STUDY

..... CUM EFF/SENSOR

—— RE/SENSOR

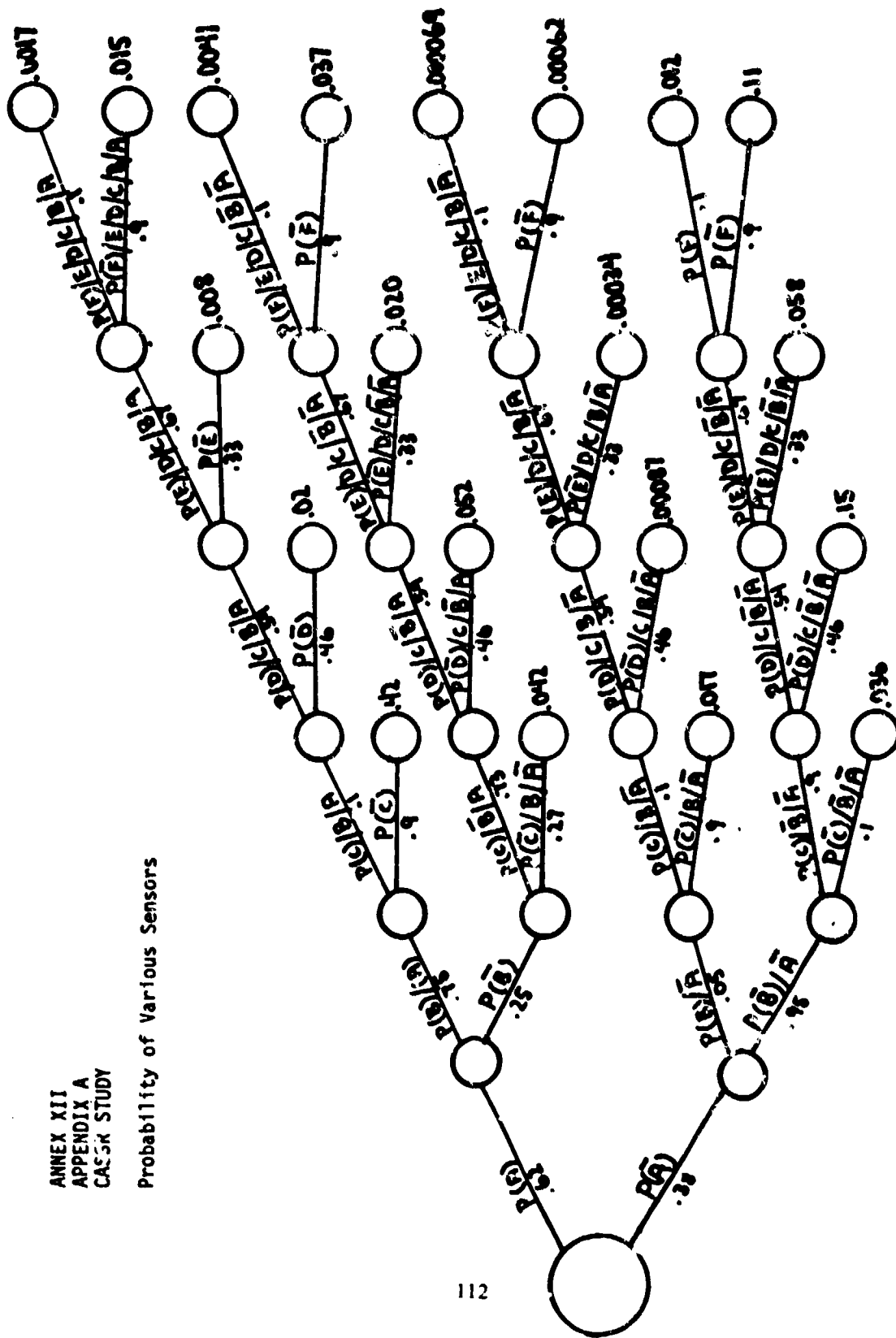
--- P D

ANNEX XI
APPENDIX A
CASSR STUDY



ANNEX XII
APPENDIX A
CASGR STUDY

Probability of Various Sensors



SENSOR TECHNOLOGY IN THE ARMY'S
NON-MINE BARRIER SYSTEMS

By: Ben C. Barker
Mobility Equipment Research and Development Command
Fort Belvoir, Virginia

INTRODUCTION:

The United States Army has an urgent need for barrier systems that require less time and logistical burden for emplacement than existing conventional barriers such as the M-15 mine field. Considerable improvements in logistical burden and emplacement times of mine field barrier systems have been made with the Army's Family of Scatterable Mines (FASCAM); however, the non-mine barrier concepts being investigated by MERADCOM may realize greater improvements and are becoming more important from the standpoint of providing "politically acceptable" barrier systems. "Political" considerations relate to minimizing the lasting effects of the barrier system on the environment, minimizing the danger to the populace from unmarked obstacles (such as mines) remaining after hostilities subside, providing the capability for early deployment of the barrier at the first indication of possible attack by using barriers which do not have the same restrictions on deployment as do mine fields, and providing inexpensive barrier systems which are affordable by the smaller European nations. The purpose of this paper is to describe the non-mine barrier system concepts being investigated by MERADCOM and to show how sensors can provide a valuable function in these systems.

DEFINITIONS -

The Army definition of a "barrier" is "a coordinated series of obstacles designed or employed to canalize, direct, restrict, delay or stop the movement of an opposing force and impose additional losses in personnel, time and equipment." An "obstacle" is defined as "any terrain feature, condition of soil, climate or manmade object other than firepower, that is used to stop, delay or divert enemy movement."

BARRIER EFFECTS -

It should be noted that the primary function of a barrier system is not to "kill the target." A barrier's usefulness is found in its ability to increase the targets exposure to friendly fire. This can be accomplished by affecting the targets mobility, which can result in delaying the target in the field of fire or causing a more favorable target profile. This effect is the greatest tactical benefit of a mine field barrier system, since to cross a mine field requires time for mine clearing or

breaching of the field, thus exposing the target to friendly fire for a longer period of time. Also, if breaching is effected, the resulting canalization of the enemy improves the capability of the friendly force to acquire and fire on the enemy targets. This discussion should make it obvious that a barrier's effectiveness tends to be zero if not covered by friendly fire; no barrier system is impenetrable in and of itself!

A means to degrade the vision of the opposing force can also have a significant barrier effect since the capability of the opposing force to acquire and fire on the friendly force would be degraded. The decrease in suppressive fire received by the friendly force would translate directly to more intense and accurate fire being brought on the opposing force; providing the capability of the friendly force to acquire and fire on targets of the opposing force is not also degraded. To more clearly illustrate this point, a large area smoke screen around an advancing armored force could delay and confuse him, if it persisted for a long enough period; and would definitely degrade his capability to fire on the friendly force. However, a viable barrier effect would not be achieved unless a means is provided to locate and fire on the armored vehicles while they are in the smoke screen.

FUNCTIONS OF SENSORS IN BARRIER SYSTEMS -

Sensors can be used as the control elements in a barrier system and can provide target identification capability for achieving a controllable barrier system. The requirement for a controllable barrier is continually emphasized by the user because of the advantages it would provide in enabling the friendly force to attack or retreat through its barrier field without encountering the barrier effect. Controllability of this type can be achieved by sensing target proximity and activating the barrier effect only if the target identification so indicates. The target identification feature can be provided through recognition of target signatures which are unique to the enemy force; or through "on/off" control of the barrier field.

On/off control can be provided through a command link to each obstacle device and a method to protect the on/off control from tampering by the enemy. Such protection can be provided through unique code words in the command link which are known only to the friendly force. Another method of providing on/off control is to provide the friendly forces with a transponder device which would respond to an active signal transmitted from each obstacle when target proximity is detected. The transponder return signal code would have to be selectable so that it could be different for each mission and would therefore be unknown to the enemy. The obstacle device would then be prevented from activation when this unique transponder signal is received. User comments in this area favor a system which uses a command link to deactivate each obstacle

device and receives a status report in return from each obstacle device indicating that it has been deactivated.

One other method of control which has been used for mine field barrier systems is a time delayed "self destruct" or defusing feature. This technique could also be used for non-mine barrier systems; however, the possibility for continued use of the barrier field is lost.

As previously stated, a sensor's function in a barrier system is to control the effects of the barrier system in a manner which will allow friendly forces to pass through the barrier without suffering the effects of the barrier. In order for a sensor to perform this function effectively, it must be capable of sensing target proximity, identity and position location. The remainder of this paper will be concerned with a description of non-mine barrier concepts being developed by MERADCOM and their interface with various types of sensors.

NON-MINE ANTI-PERSONNEL BARRIER SYSTEMS -

Both anti-personnel and anti-armor barrier systems are required. Anti-personnel barrier systems of the non-mine type presently consist of barbed tape concertina or general purpose barbed tape obstacles. Advanced concepts for energy fields which would significantly delay personnel have been considered by MERADCOM. Personnel classification sensors of the REMBASS type could be used to "turn on" such energy fields when enemy personnel are present. As indicated earlier, complete controllability of such a barrier system would have to be provided through an on/off command from the friendly troops.

Work at MERADCOM on water based foams may be used to enhance the effectiveness of barbed tape obstacles. A triple row of general purpose barbed tape obstacle could be covered with water based foam as shown in figure 1.

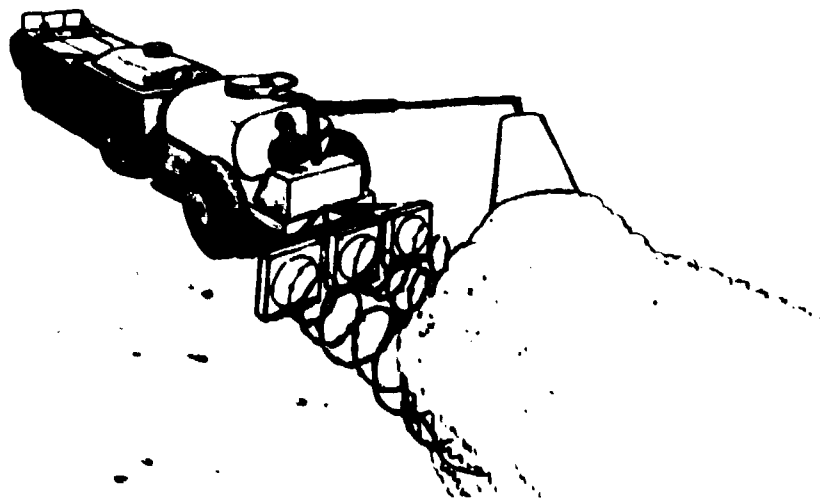


Figure 1 - BARBED TAPE COVERED WITH FOAM

The foam is being developed to have a minimum persistence of 24 hours to one half its original height. The effect of the foam on personnel would be loss of orientation and a significant increase in the time required to traverse the three rows of barbed tape, which could not be seen to avoid its entangling effects. A sensor such as the Fence Tamper Sensor could be attached to the barbed tape in 100 meter sections to detect personnel trying to breach the barrier (see figure 2).



Figure 2 - BARBED TAPE WITH SENSOR CABLE ATTACHED

Air burst artillery shells could then be fired over that section of the barrier to cause enemy casualties.

NON-MINE ANTI-ARMOR BARRIER SYSTEMS -

Anti-armor barrier systems of the non-mine type presently consist of natural and manmade terrain obstacles such as ravines, rivers, ditches, posts, etc. The non-mine anti-armor barrier system concepts being investigated by MERADCOM were based on a systems study that identified the following as critical obstacle/target interactions:

- Mobility Reduction - Hold enemy at favorable stand-off range.

- Firepower Modification - Increase relative firepower advantage.

Many techniques were then considered for achieving these effects and those shown in figure 3 were chosen for further investigation.

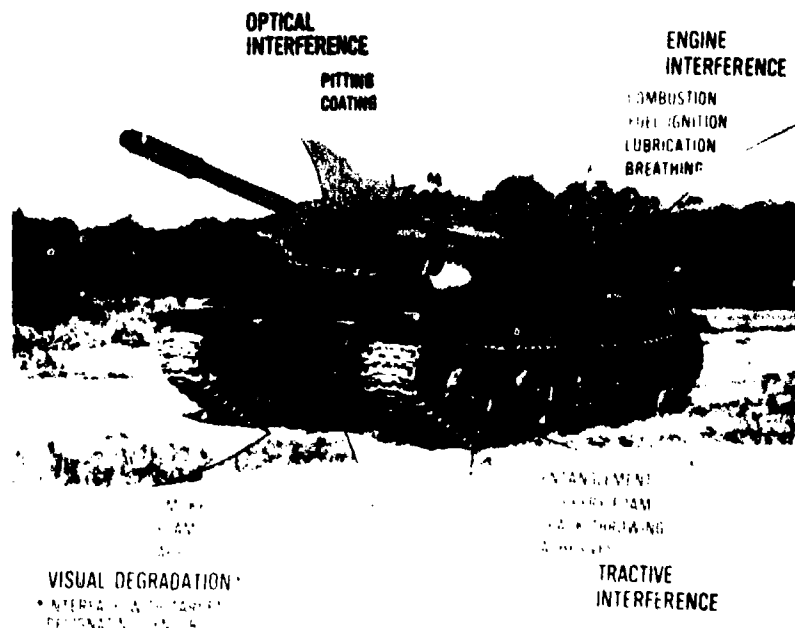
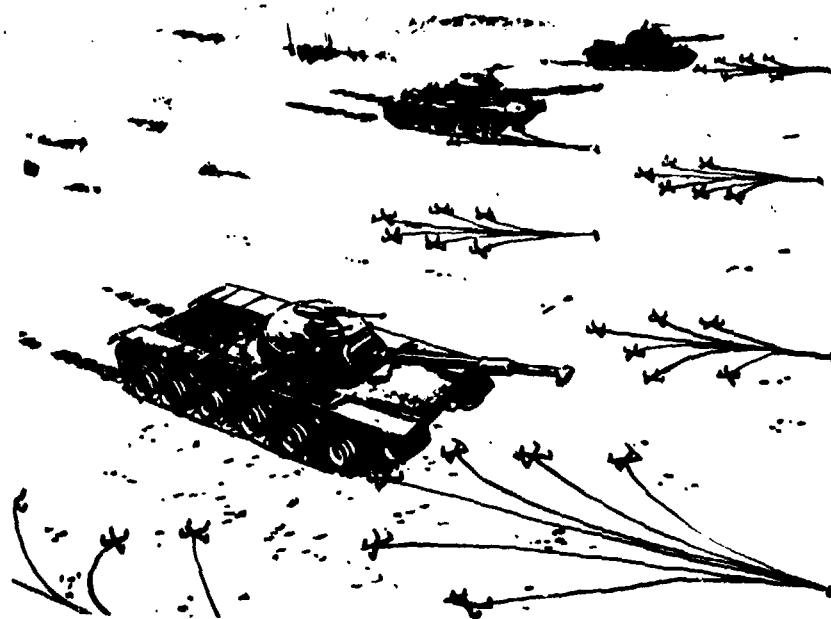


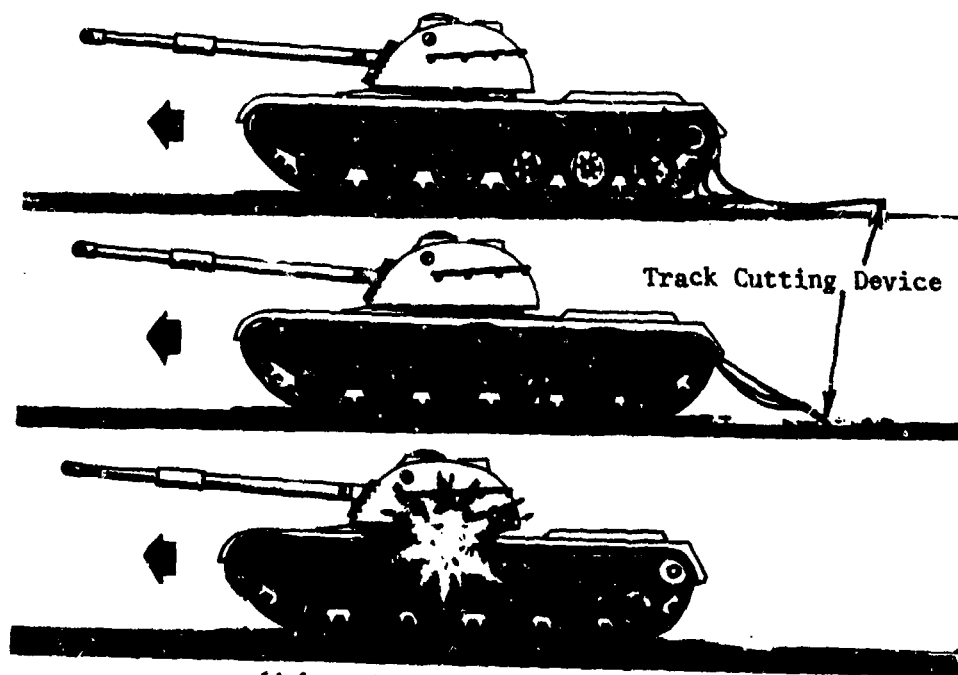
Figure 3 - VEHICLE VULNERABILITIES

MERADCOM is actively pursuing concepts for anti-armor barrier systems which create tractive interference, engine interference and visual degradation effects. Tractive interference concepts which appear promising are slippery agents for MOBA (military operations in built-up areas) and tractive entanglement (see figure 4) for open field environment. Initial investigations in tractive entanglement were pointed towards entangling a mechanical device which would either break or throw the vehicle track. However, the logistics involved in emplacing sufficient numbers and sizes of the mechanical devices in the field has led to the conclusion that an explosive track cutting device is required. An orientation sensor is used in the track cutting device to determine when the track cutting device is in position on top of the track and to initiate the explosive reaction (figure 4.b). Slippery agents can be pre-emplaced or cannisters of the agent, which could be dispensed upon sensor activation, can be emplaced in selected locations. Sensors could recognize foreign vehicle signatures and release the slippery agent to degrade the mobility of the armored and/or wheeled vehicles.

Concepts for engine interference have been based on the effects of



(4.a. - Deployment Concept)



(4.b. - Track Cutting Sequence)

Figure 4 - TRACTIVE ENTANGLEMENT BARRIER SYSTEM

propane gas on combustion in a diesel engine. Tests against a small diesel engine showed loss of power and ultimate stalling of the engine when subjected to 3-5% propane in the engine air intake. Original concepts for free air dispersion of the gas could have been sensor activated, however, dissipation in free air was found to be too great to affect the engine. Subsequent concepts have relied on encapsulation of the propane gas in a water based foam barrier strip (see figure 5).

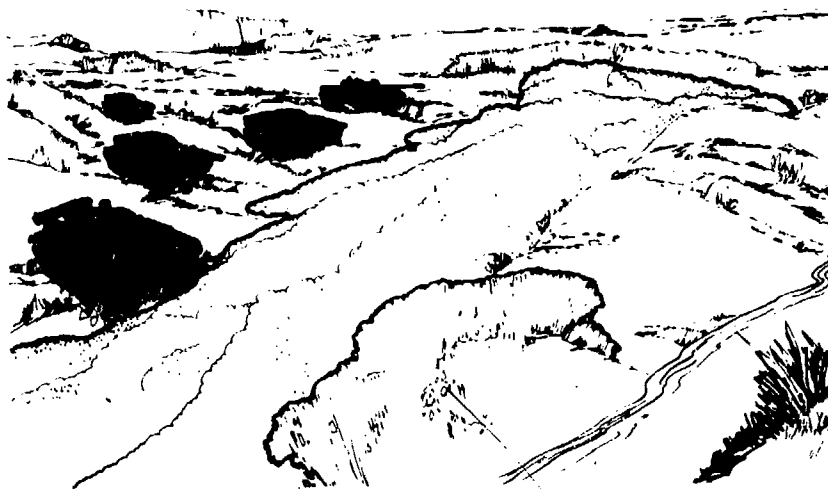


Figure 5 - FOAM BARRIER

Recent tests of the effects of propane on large diesel engines have not produced the anticipated results. Future efforts in this area will concentrate on finding a more effective engine interfering agent for large diesel engines.

Sensors are likely to find their greatest application in anti-armor barrier systems which utilize visual degradation to achieve the barrier effect. Sensors will be used to either detect the enemy targets and cue the deployment of a large area obscurant cloud (see figure 6) or activate devices to coat the firing optics of the armored vehicle (see figure 7). Recent tests at MERADCOM on a directed spray device for coating the vehicle optics indicate that many devices would have to be placed in the field to achieve a high probability of successfully coating the firing



Figure 6 - OBSCURANT CLOUD

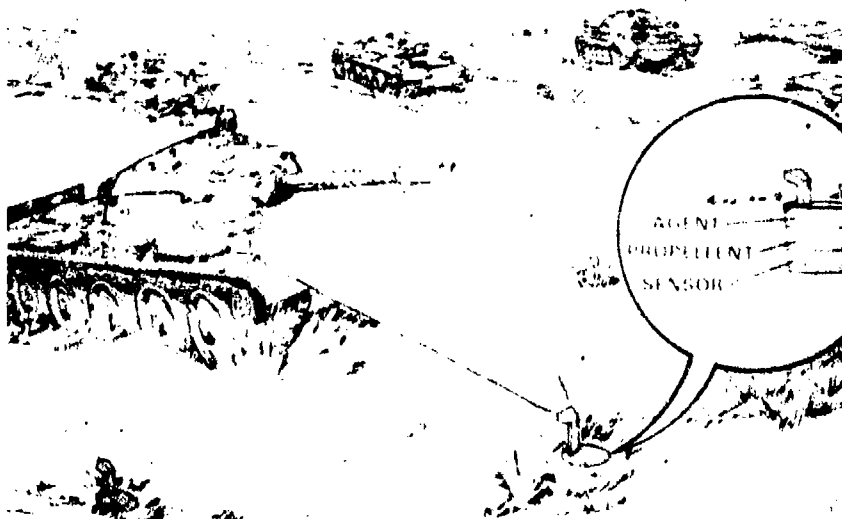


Figure 7 - DIRECTIONAL OPTICAL COATING BARRIER CONCEPT

optics of a Soviet armored vehicle. Future efforts will concentrate on the large area obscurant cloud. In this concept, sensors will also be used to locate the target within the obscurant cloud so that firepower can be brought to bear on the target. The sensors used for location of the target may actually locate the geographical position of the target so that ballistic trajectory projectiles can be fired on the target. However, a more likely approach will be to passively home a guided missile to the target, as shown in figure 8, by sensing a unique target signature such as the infrared or acoustic energy radiated by the vehicle. Use of the acoustic signature, rather than the infrared or other target signature, may be the best approach. This is true since infrared energy radiated by the target, and other active energy sources such as lasers used for illuminating the target for missile homing purposes, are also obscured by any obscurant screen which would keep the target from using sensing devices to "see" while it is in the obscurant cloud.



Figure 8 - HOMING MISSILE ATTACKING TANK THROUGH OBSCURANT CLOUD

In 1972, MERADCOM achieved a feasibility demonstration of acoustic homing technology against a US armored vehicle (see figure 9). This demonstration proved that acoustic homing is certainly feasible; however, a direct hit was not achieved. Test results indicate that improvements in the probability of hitting the target can be made through



Figure 9 - ACOUSTIC HOMING FEASIBILITY TEST

improvements in the guidance system and missile flight characteristics, and by using new developments in digital signal processing technology. The device tested in 1972 was guided by a signal processor which proved adequate to demonstrate feasibility, but which had known limitations in the following areas:

- a. Selecting the highest priority target from a group of different target types (classification).
- b. Selecting one target from a group of closely spaced identical target types.
- c. Homing on the Soviet armored vehicle because of its unique spectral characteristics.

These problems were inherent because the original signal processor design did not extract a sufficiently fine grain power spectra within the analysis band to obtain target separation and classification. By going to a Fast Fourier Transform (FFT) processor, capability in the above areas can be significantly improved.

NEW SENSOR DEVELOPMENT PLANS

MERADCOM intends to pursue development of a two channel microcomputer based FFT signal processor which can be used in many applications including acoustic

target bearing and classification processing. Prototype models of this processor will be constructed and evaluated in-house at MERADCOM. MERADCOM engineers have conceived a preliminary system architecture for this processor and are confident that the required parameters can be achieved with existing micro-electronic circuits at a cost of less than \$2000 in production quantities.

The processing will be based on the Fast Fourier Transform (FFT) of each of two input channels and will function as in figure 10.

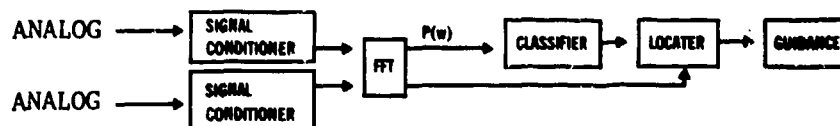


Figure 10 - PROCESSOR FUNCTIONAL DIAGRAM

The analog signal to each channel is conditioned and digitized and then fed into the FFT operation. The FFT produces the power spectra for each channel $P_1(\omega)$, $P_2(\omega)$ and the phase difference between the spectral lines of each spectra $\Delta\theta = \theta_1(\omega) - \theta_2(\omega)$. The power spectra will be transferred to a different portion of the processor for classification, and the appropriate phase information will be used to locate the desired target when the processor is used in applications requiring target bearing information.

The classification algorithms for the barrier system application will be developed by MERADCOM and will be based on the analysis of foreign vehicle acoustic signatures collected for PM REMBASS and on additional signatures recently collected specifically for this purpose. These signatures will be analyzed with the VACIDS (Vehicle Automatic Classification and Identification System) cross correlation processing facility at MERADCOM to determine the greatest number of possible classes into which the acoustic target signatures can be separated and still provide reliable classification in the presence of other battlefield noises.

The FFT section of the processor will be microprocessor (μ PS) controlled, and will use some state-of-the-art LSI (see figure 11 for further detail). μ PS₁ will control the A/D conversion, and will perform rudimentary classification and locating algorithms. These algorithms can be optimized by changing the EPROM. μ PS₂ and the hardware multiply chip will perform the FFT operation with the results stored in RAM. The emphasis of this effort will be on developing an FFT processor. Optimization of classifying and locating algorithms for each processor application will be accomplished as separate efforts and may require the addition of a third μ PS.

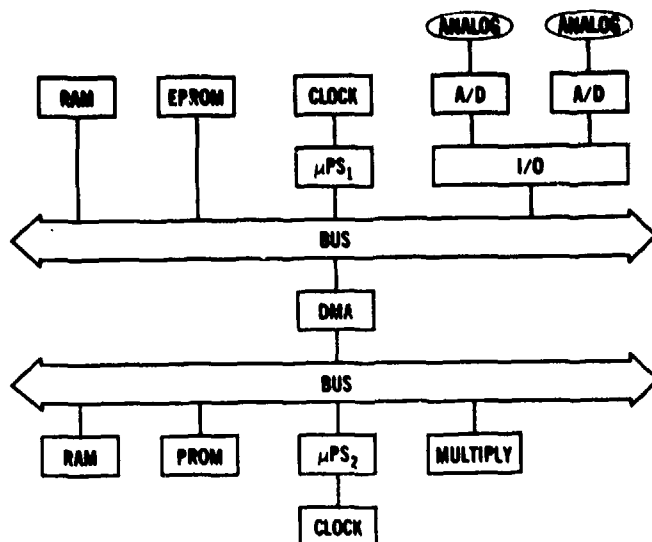


Figure 11 - FFT PROCESSOR HARDWARE DIAGRAM

MERADCOM intends to evaluate the above described signal processor for acoustic homing applications by interfacing it with the target tracker which was previously developed by MERADCOM for evaluation of the original acoustic homing signal processor. The target tracker consists of a bore-sited TV camera on a gimbaled, servo-controlled platform (figure 12) which is provided with the guidance signal from the acoustic homing signal processor. The new signal processor will also be evaluated in an unattended ground sensor (UGS) configuration for the purpose of multiple target classification. The capability of classifying multiple targets in the same vicinity will be required for the barrier system to assess the types of targets attempting to breach the barrier field. Multiple target classification capability is also stated as a desired feature of REMBASS classifying sensors. The processor will also be evaluated for physical security sensor applications.

Since the processing logic of the new processor is software controlled, the processor can be adapted for many other missions by changing only the software program.

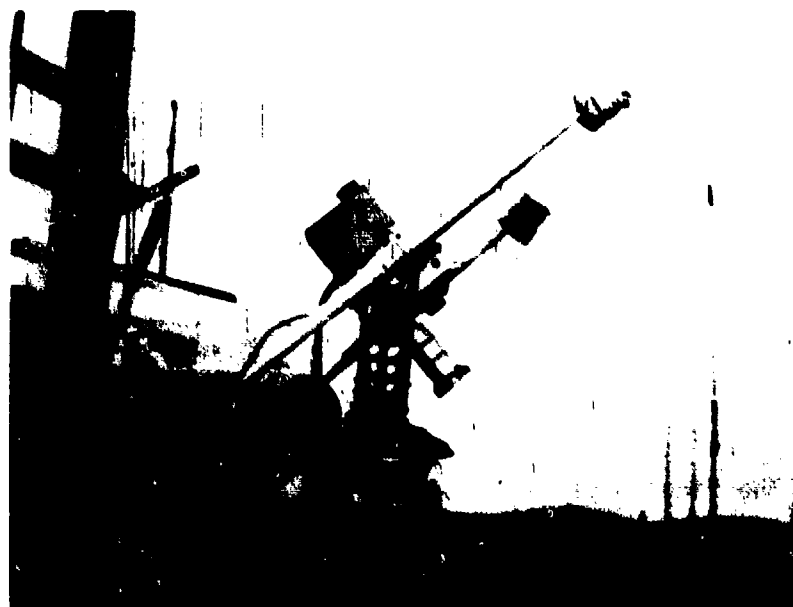


Figure 12 - ACOUSTIC TARGET TRACKER

CONCLUSION

Sensors form a useful part of barrier systems to selectively control the application of the barrier effect. It is hoped that this paper has provided a greater understanding of the relationship of sensors to controllable barrier systems and will serve as a vehicle for making known the interest of the Sensors and Barriers Division at MERADCOM in all types of new sensor concepts and hardware developed by industry or other government laboratories. The assistance of Mr. Les Jacobs (Sensors and Barriers Division) and Mr. Alan Johnson (Intrusion Detection Division) at MERADCOM in developing the parameters of the proposed micro-computer based FFT processor is gratefully acknowledged.

FLUIDIC SENSORS
FOR
PHYSICAL SECURITY APPLICATIONS

The final paper was classified SECRET and
can be obtained directly from HARRY DIAMOND
Laboratory.

IRCCD RADIOMETRIC FENCE SENSOR

by

R. Taylor, L. Skolnik, B. Capone, W. Ewing
S. Roosild, F. Shepherd, and A. Yang
Rome Air Development Center, AFSC
Deputy for Electronic Technology
Hanscom AFB, MA 01731

I. Introduction

The development of a low cost, remote, passive, infrared sensor with automatic target classification capability would greatly enhance current BISS inventory. In particular, the sensor system would provide all weather and night detection capability without the need for active illumination by either visible, IR, or RF radiation. This paper describes the development of a linear 256 element monolithic array of metal silicide Schottky barrier diodes with all solid state charge coupled device (CCD) readout to be used as a focal plane for the BISS IRCCD Radiometric Fence Program. The sensor is in the early stages of a 6.3 effort to construct a covert IR detection system which will include off chip video signal processing for target identification purposes. It is the purpose here to discuss the IR sensor itself; the signal processing study is currently underway and will be reported at a later time.

II. Schottky Barrier IRCCD Technical Background

Schottky IR focal plane operation has been described previously by several authors;⁽¹⁻⁵⁾ however, we present a brief description here for completeness. Figure 1 depicts the basic Schottky photo-response mechanism. The Schottky detector cell is formed by combining platinum and silicon into a platinum silicide (Pt-Si) alloy. This composition yields a Pt-Si Schottky detector which has a long wavelength cut-off near $4.5 \mu\text{m}$. The detector array is back side illuminated through the silicon substrate; wavelengths less than $1.1 \mu\text{m}$ are absorbed in the substrate while longer wavelengths are transmitted to the Schottky Pt-Si diodes. The transmitted IR radiation is absorbed in the silicide and gives rise to internal photo-emission of majority carriers from the silicide alloy to the silicon substrate. The local emission rate from the array is proportional to the local IR scene illumination. At the end of a staring time (i.e. line time) the charge which has accumulated on the electrode array is read out serially by a CCD shift register.

The photo yield, Y for Schottky internal emission photodiodes is given by⁽⁵⁾

$$Y(h\nu, \psi_{ms}) = \frac{C_1 (h\nu - \psi_{ms})^2}{h^2} \left(\frac{\text{electron}}{\text{photon}} \right), \quad (1)$$

where ψ_{ms} is the barrier height, h Planck's constant, ν the photon frequency and C_1 is a factor determined by the geometrical, optical and transport properties of the silicide contact.

The infrared background photoresponse, V_S , of an IRCCD corresponding to the yield of Equation (1) is given by⁽³⁾

$$V_S = \frac{e C_1 t A k^4 C_g}{c^2 h^3 [F^2 (M+1)^2 + \frac{1}{4}]} T_b^{-4} \left(\frac{\psi_{ms}}{kT_b} + 3 \right) \exp \left(-\frac{\psi_{ms}}{kT_b} \right), \quad (\text{volts}) \quad (2)$$

where the parameters are the black body temperature, T_b ; the sensor cell size, A ; the video frame time, t ; the f -number of the optics, F ; and the floating gate capacitance, C_g . In Equation (2), e , k , and c are the electronic charge, Boltzmann's constant, and the speed of light, respectively.

The Schottky barrier-CCD focal plane was fabricated for BISSPO by RCA under contract to RADC/ET. Figure 2 shows a photomicrograph of the 256 Pt-Si/P-Si IRCCD array. Each Pt-Si detector is $15 \mu\text{m}$ wide X $200 \mu\text{m}$ long on $30 \mu\text{m}$ centers. Total chip length is 400 mils. The chip incorporates two buried n -channel two phase CCD shift registers along with output summing and difference sample and hold amplifiers. These two CCD shift registers (transfer inefficiency $\sim 2 \times 10^{-5}$) are driven by common clocks; thus common mode noise can be eliminated by differencing the outputs of the two registers. Also, it is possible to perform on-chip video line subtraction for moving target indication by multiplexing successive IR video lines into each of the shift registers and differencing the CCD outputs.

In staring mode operation, an end of line pulse causes the charge image accumulated on the Schottky diodes to be loaded into the CCD multiplexer. The video line is then clocked out serially into the output video amplifier. Staring time for the 256 element array can be varied from 10 msec to 1 sec; read out (line) frequencies are variable between 1 KHz and 5 MHz. For most measurements, both staring time and line times are kept at 30 msec and 25 msec, respectively (near normal TV rate). For a complete discussion of IRCCD operation (including noise analysis) see papers by Shepherd, et al⁽³⁾ and Kohn, et al.⁽⁴⁾

It should be noted that the Schottky array must be cooled to temperatures between 80 and 100°K so that thermal emission does not degrade IR video signal. For these measurements, cooling was accomplished by an Air Products closed cycle helium refrigerator. The cold stage was operated at temperatures between 80°K and 86°K. Figure 3 shows the laboratory set-up for testing the IRCCD sensor. A black body source is visible in the foreground; the optics (a four element SORL f/1.2 Si/Ge lens) and detector cooling head are shown in the background.

III. Experimental Results

In this section we present laboratory measurements of Pt-Si IRCCD array performance. It should be noted that much of this data is preliminary in that the experimental set-up has not yet been optimized with respect to cold filtering and cold shielding.

The performance characteristics of the Pt-Si IRCCD focal plane which we will consider here include CCD linearity, Schottky photo-response, uniformity, Schottky linearity, resolution, and transfer characteristic.

CCD Linearity

The BISS IRCCD sensor utilizes buried channel technology in order to minimize shading and video signal degradation which arises due to charge transfer inefficiency in surface channel devices. It is therefore necessary that the buried channel CCD multiplexers have sufficient dynamic range to accommodate the large background, low contrast video signal characteristic of infrared scenes. Figure 4 shows a plot of shift register output voltage versus electrical input attenuation to the shift register. In this measurement, the photo-detectors were completely cold blocked and an electrical word (5 volts input to the attenuator) was entered into the CCD multiplexer. Thus the data of Figure 4 represents CCD performance independent of photo-generated carriers. As can be seen from the graph, the shift register is linear over ~50 db input dynamic range. This dynamic range was determined by a noise threshold of 1 mv and CCD well saturation at 400 mv. This CCD dynamic range was the limiting one for the array.

Photoresponse

The photoresponse as a function of black body temperature (Eq. 2) for a previously constructed 64 element surface channel Pt-Si array is shown in Figure 5. Here we plot output signal voltage as a function of target temperature. The solid line is the theoretical curve generated by Equation (2) with the parameters shown in the figure. Generally, excellent agreement is found between the experimental data and the analysis. As can be seen from the graph, the Pt-Si array is

easily capable of detecting human targets against a 300°K background. In fact, if a photoresponse nonuniformity of $<0.4\%$ can be achieved, this array will be capable of detecting a temperature difference of 0.1°K ⁽³⁾ ($\text{NE}\Delta\text{T} = 0.1^{\circ}\text{K}$ with $f/1.2$ optics).

Schottky Uniformity

Photoresponse spatial uniformity is a critical factor in obtaining small resolvable temperature differences with staring infrared imagers.⁽³⁾ State-of-the-art conventional semiconductor IR sensors have failed to meet uniformity requirements for staring mode imaging because variations in substrate doping, minority carrier diffusion lengths, and compensating impurity concentrations are extremely difficult to control to precise tolerance. Since the Schottky barrier detector is a majority carrier device, and since the barrier height (ψ_{ms}) has been shown to be independent of substrate doping variations over several orders of magnitude,^(2,6) a Schottky detector array can be made extremely uniform. (Recall from above that a nonuniformity of $<0.4\%$ is needed to resolve temperature changes of 0.1°K). Figure 6 shows an oscilloscope trace of a 256 Pt-Si array with a 130°C black body source (80% neutral density filter) imaged on the IRCCD. As can be seen from the pictures the peak-to-peak nonuniformity for this array is $\sim 5\%$ (10 mv out of 150 mv). Note that previous arrays fabricated from Pd_2Si had spatial nonuniformities on the order of 0.5% .⁽⁷⁾ In an attempt to determine whether the Pt-Si photoresponse nonuniformity is due to metallurgy or photomask (i.e. detector area) problems, a large area Pt-Si photodiode ($3 \times 10^{-5} \text{ cm}^2$) was fabricated and a spatial photoresponse scan of the diode was made. Figure 7 shows the photoscan taken at 77°K . This data shows diode spatial nonuniformities of less than 0.3% . Hence, the nonuniformity of 5% exhibited by the 256 element array is believed to be processing related (photomask, etching, cleaning) and not a basic Pt-Si metallurgy problem. For example, a diode width variation of $\pm 0.3 \mu\text{m}$ would account for the observed 5% spatial nonuniformity. Further studies are underway to correct the nonuniformity and thus reduce fixed pattern noise. It is emphasized, however, that even this 5% nonuniformity exceeds the best available extrinsic silicon arrays by a factor of 5 to 10.

Resolution

Figure 8 shows a delayed sweep oscillograph of a black body target viewed through a four bar resolution mask. This picture demonstrates resolution at the Nyquist limit (16.4 lp/mm).

Schottky Linearity

Figure 9 shows a series of curves generated by placing neutral density filters in front of the black body source and measuring the

sensor output voltage for a variety of target temperatures. The data shows Schottky linearity until a 130°C target temperature is reached at which point output saturation occurs. This effect is due to saturation of the CCD shift register and not to photodiode saturation (see Figure 4). No blooming is observed under saturation conditions.

Transfer Characteristic

The transfer characteristic of the sensor is a measurement which provides both sensitivity and dynamic range data. Figure 10 plots voltage output of the Pt-Si array versus power incident on the focal plane. In deriving this data all effects of optics, filters and atmosphere are removed. The differential power density on the focal plane is given by

$$H_S = \frac{\Delta H_{\lambda_1 \lambda_2}}{[4F^2 (M+1)^2 + 1]} \tau_o \tau_A \tau_{N.F.} \quad (\text{watts/cm}^2),$$

$$\Delta H_{\lambda_1 \lambda_2} = \int_{\lambda_1}^{\lambda_2} W_{\lambda}(T_S) d\lambda - \int_{\lambda_1}^{\lambda_2} W_{\lambda}(T_A) d\lambda$$

$\Delta H_{\lambda_1 \lambda_2}$ is the differential power density radiated by the black body

$W_{\lambda}(T)$ is the Planck radiation function at temperature T

T_S is the source temperature

T_A is the ambient temperature

λ_1, λ_2 are the lower and upper wavelength limits, respectively

F is the f/no of the optical system (f/1.2)

M is the optics magnification (~1)

τ_o is the transmission of the optics

τ_A is the transmission of the atmosphere

$\tau_{N.F.}$ is the neutral density filter transmission.

From Figure 10 we see that this array has a noise equivalent irradiance (NEI) in the 2.5 - 4.5 μm band of $1.0 \times 10^{-6} \text{ w/cm}^2$ (assuming a 0.5% nonuniformity could be obtained) and a dynamic range of 500. This NEI corresponds to an elemental NEP of $3 \times 10^{-11} \text{ watts}$.

IV. The BISS IRCCD Fence System

Because the video signal from the Schottky detector array is discretely time sampled and multiplexed out by the CCD shift register, it is an extremely attractive device for forming the basis of a covert, automatic detection and target classification system. The proposed BISS IRCCD Fence System concept is shown in Fig. 11. The sensor system is mounted on a tower or building in a downward looking attitude such that each detector in the array views a cell on the ground that is 30 cm wide by 50 m long. The range from the sensor tower to the perimeter is 200 m; each 256 element IRCCD array spans an 80 m fence line (Fig. 12). As shown in Fig. 11, the video output from each cell represents a specific 30 cm resolution element at the fence line. This 30 cm resolution was chosen so that a man would subtend one (or at most two) sensor elements, thus simplifying video signal processing. By observing spatial output amplitude as a function of time, targets at the fence line are covertly detected by their thermal emission and their position to within 30 cm along the perimeter is determined. In addition, off chip video processing provides moving target indication, background suppression, and number of targets present at the fence line. Automatic intruder classification (man, animal, vehicle) is accomplished via individual spatial and spectral infrared signatures which are distinctive of each class of target. Video processing for background removal minimizes false alarms due to sun glint and diurnal cycles.

The entire BISS IRCCD radiometric fence system is conceptually depicted in Fig. 13. It consists of three basic modules: the IRCCD chip, video processing circuit, and cooler-optics. The system is scheduled for advanced development completion by late 1980, and for completion of engineering development in 1982.

V. Summary

We have presented photoresponse uniformity, radiometric, and resolution data on a new monolithic Schottky barrier IRCCD staring sensor being developed for ESD/BISSPO by RADC/ET. Because the sensor focal plane uses standard silicon gate CCD processing technology, it is low cost and extremely reliable. The Schottky IRCCD promises to form the basis for a second generation physical security system which will have covert all weather, and night-time capability. In addition, because of the unique CCD read out, automatic target position, as well as target classification, and false alarm suppression will be provided. The IRCCD Radiometric Fence System will greatly enhance current BISS inventory and add extremely valuable capabilities to the protection of military installations and facilities.

Acknowledgement: The authors are grateful to R. Phipps of RADC/ET for much of the artwork used in this paper.

REFERENCES

1. F. D. Shepherd, Jr. and A. C. Yang, "Silicon Schottky Retinas for Infrared Imaging", 1973 International Electron Devices Meeting, Technical Digest, pp. 310-313.
2. V. E. Vickers, "Model of Schottky Barrier Hot-Electron-Mode Photodetection", Applied Optics, 10, 2190 (1971).
3. F. D. Shepherd, Jr., R. Taylor, S. Roosild, L. Skolnik, B. Cochran, E. Kohn, "Ambient Thermal Response of Monolithic Schottky IRCCD's", Proceedings of IRIS Thermal Imaging Meeting, El Toro, CA., 1977.
4. E. S. Kohn, S. Roosild, F. Shepherd, and A. Yang, "Infrared Imaging with Monolithic, CCD-Addressed Schottky Barrier Detector Arrays: Theoretical and Experimental Results", Proc. 1975 International Conference on the Applications of Charge-Coupled Devices, pp. 59-69, 1975.
5. F. D. Shepherd, Jr., et al, "Silicon Schottky Barrier Monolithic IRTV Focal Planes", Advances in Electronics and Electron Physics, 40B, 981 (1975).
6. R. J. Archer and T. O. Yep, "Dependence of Schottky Barrier Height on Donor Concentration", J. Appl. Phys. 41, 303 (1970).
7. R. Taylor, F. Shepherd, S. Roosild, A. Yang, and E. Kohn, "Schottky IRCCD's", IRIS Detector Specialty Group Meeting, AF Academy, CO, March 1977.

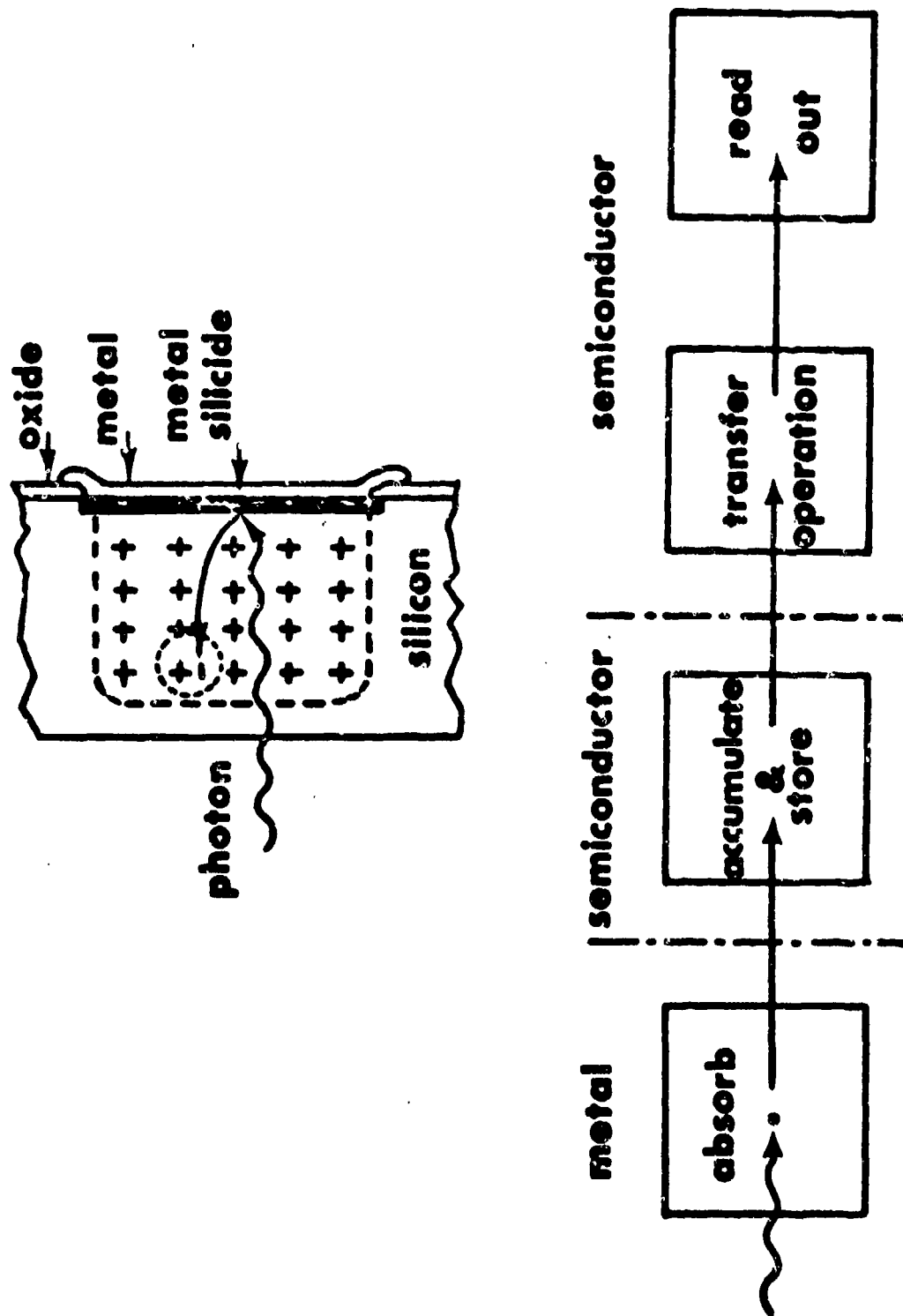


Figure 1. IRCCD Photoresponse Mechanism.

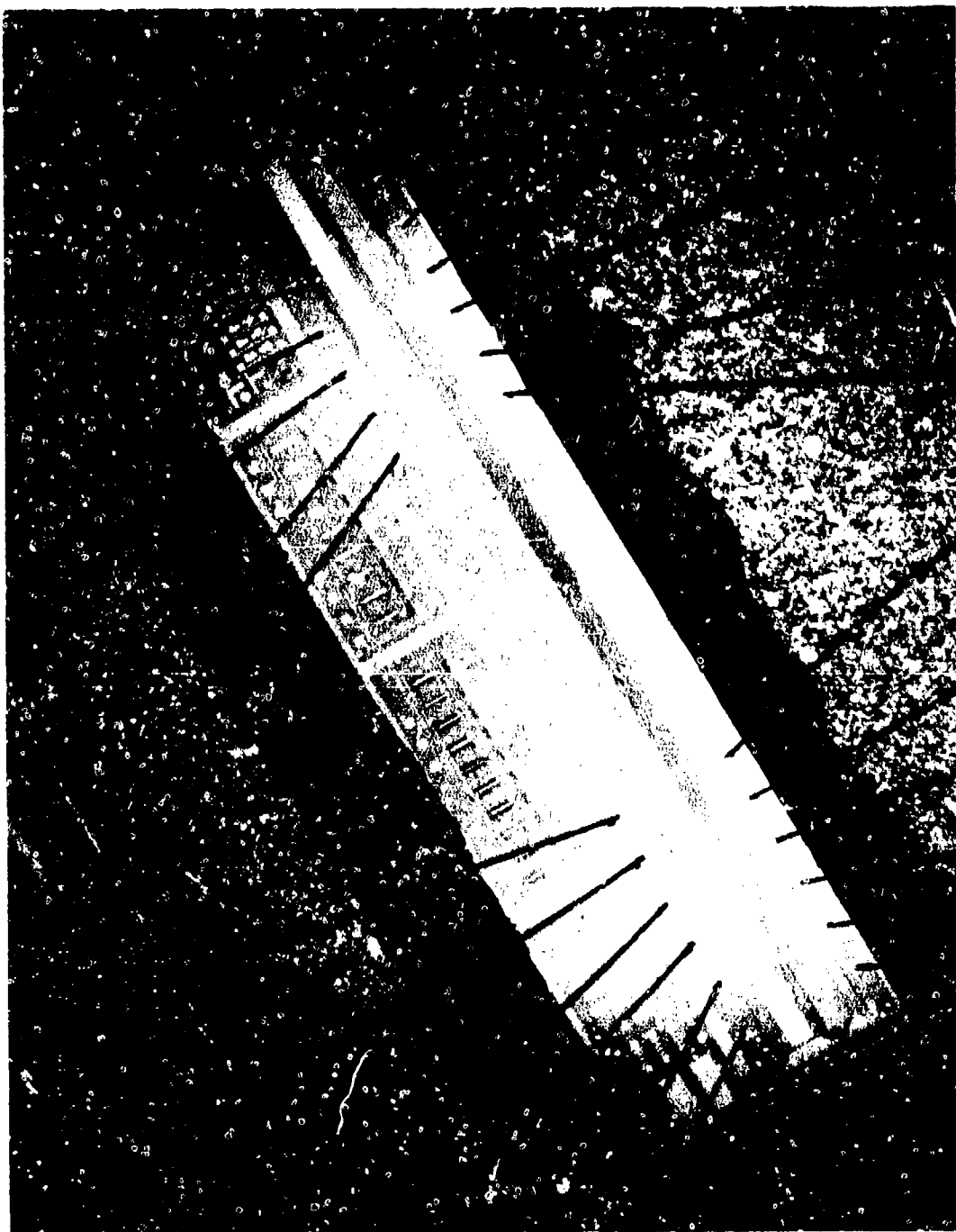


Figure 2. 1X256 element Pt-Si IRCCD array. Total chip length is 0.4".



Figure 3. Laboratory arrangement for measuring IRCCD performance. A black body source is in the foreground; sensor cooling head and f/1.2 IR optics are in the background.

CCD MULTIPLEXER LINEARITY

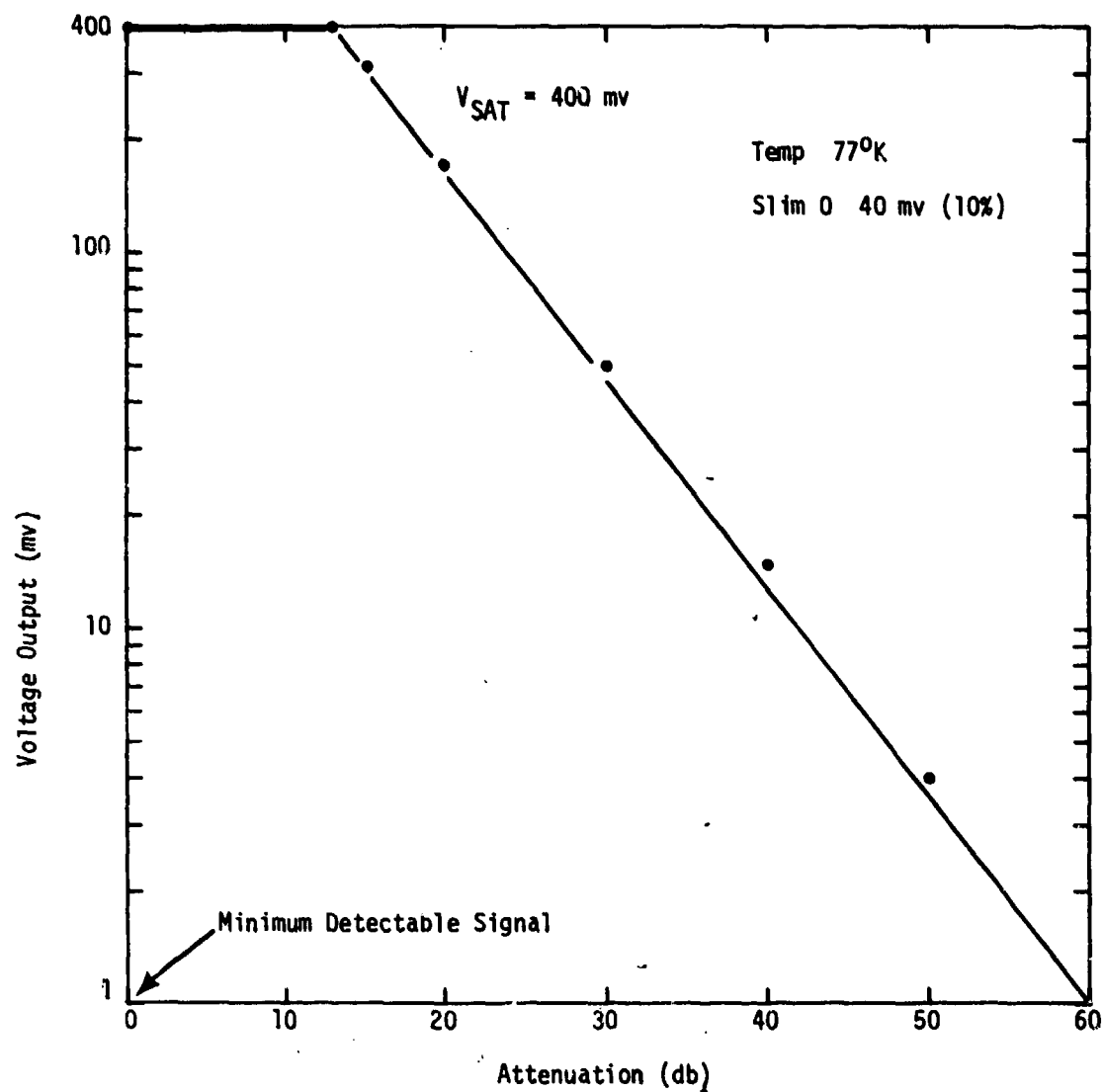


Figure 4. Buried channel CCD multiplexer linearity. Maximum output voltage before saturation is 400 mv. Minimum signal detectable (limited by dark current at 77°K) is 1 mv.

THERMAL TRANSFER RESPONSE OF PT-Si-IRCCD

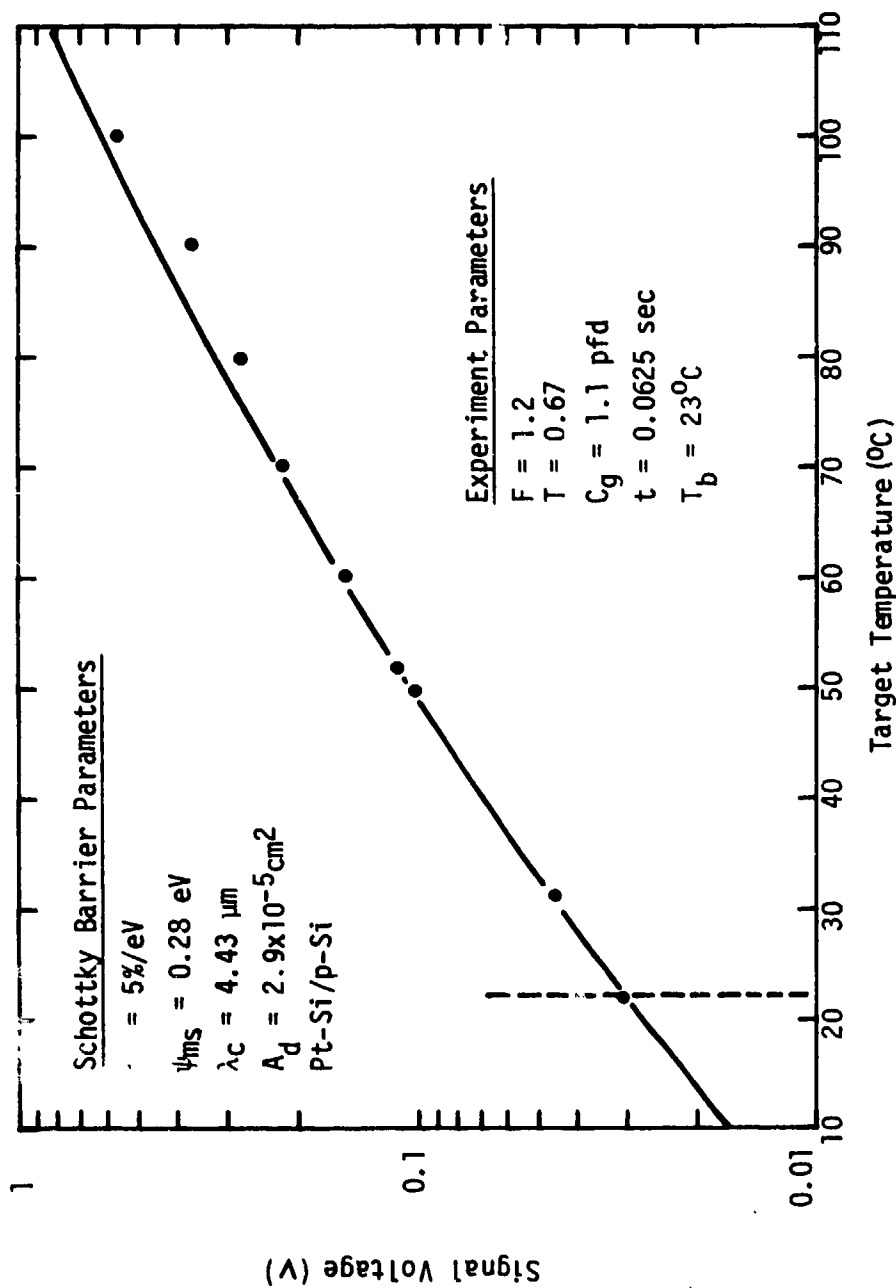


Figure 5. Photoresponse of a 1X64 element Pt-Si IRCCD array.



Figure 6. Oscillograph trace of 256 element Pt-Si array illuminated with a 130°C black body source and 80% neutral density filter. Peak to peak spatial nonuniformity is about 6%.

Pt-Si UNIFORMITY SCAN

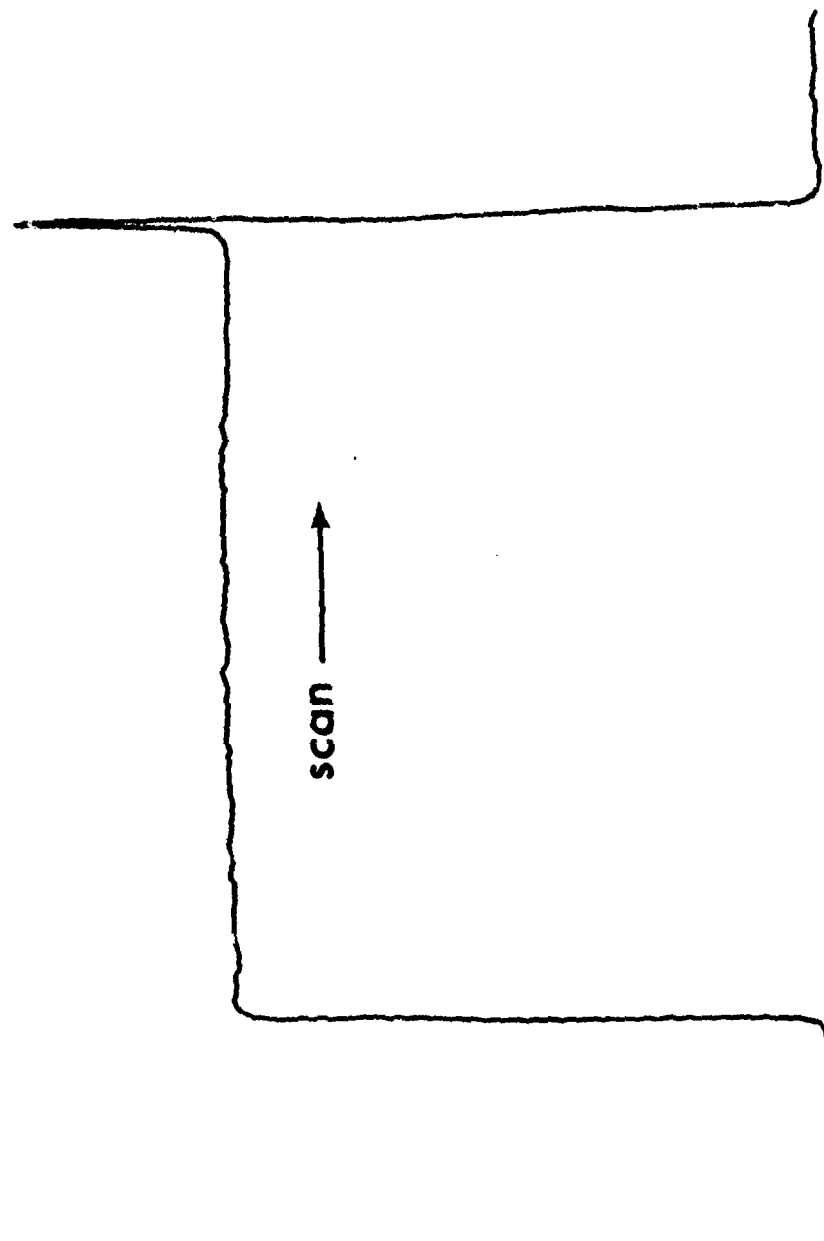


Figure 7. Photoresponse scan of a large area Pt-Si diode showing a peak-to-peak nonuniformity of .3%. The peak is due to metal feathering at the diode's leading edge.



Figure 8. Oscilloscope trace of four bar pattern showing resolution. Each $0.6 \mu\text{m}$ detector is "imaging" one bar.

SCHOTTKY LINEARITY

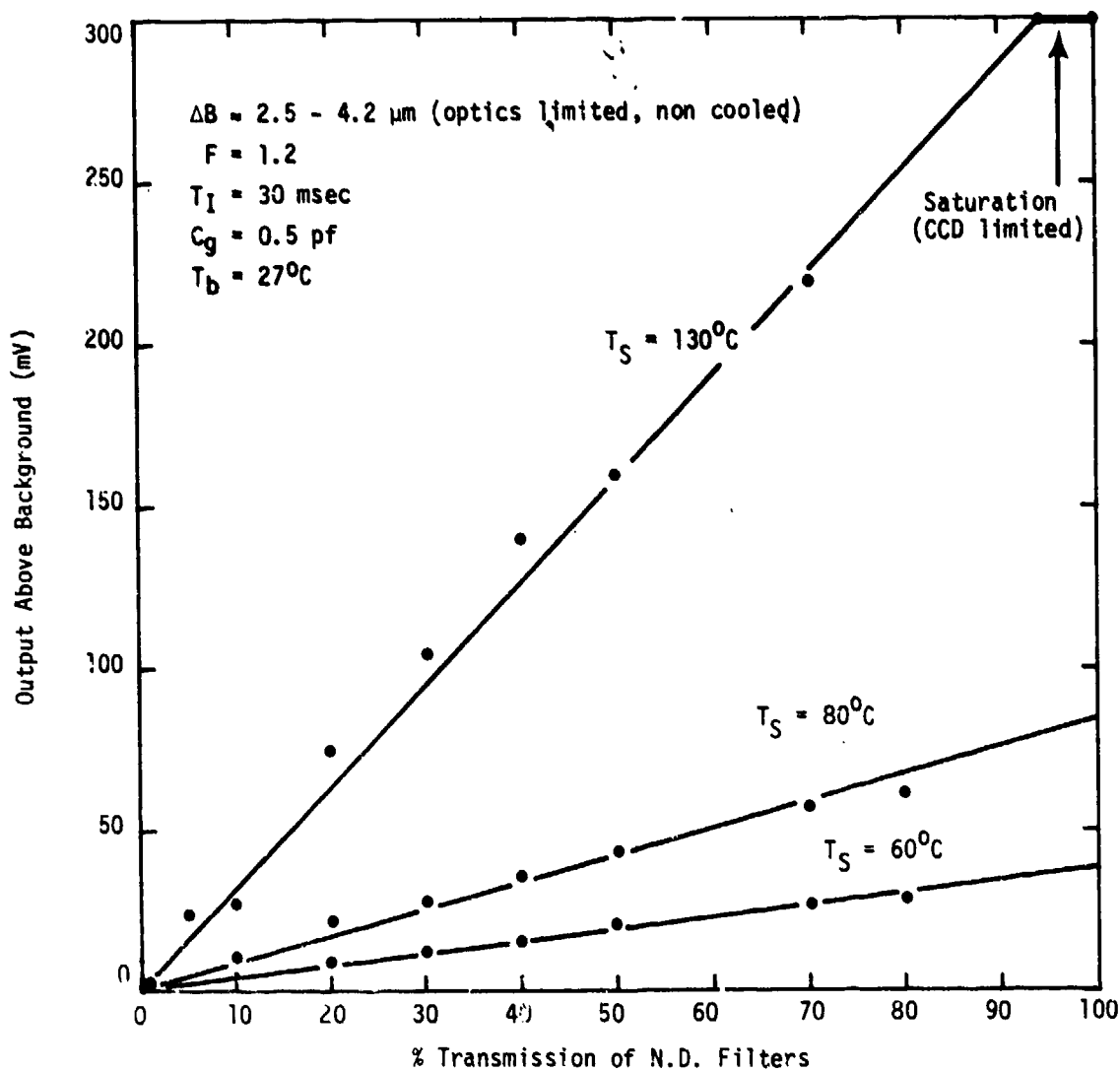


Figure 9. Schottky IRCCD linearity. Saturation at $130^\circ C$ is CCD limited.

TRANSFER CHARACTERISTIC 256 Pt-Si IRCCD

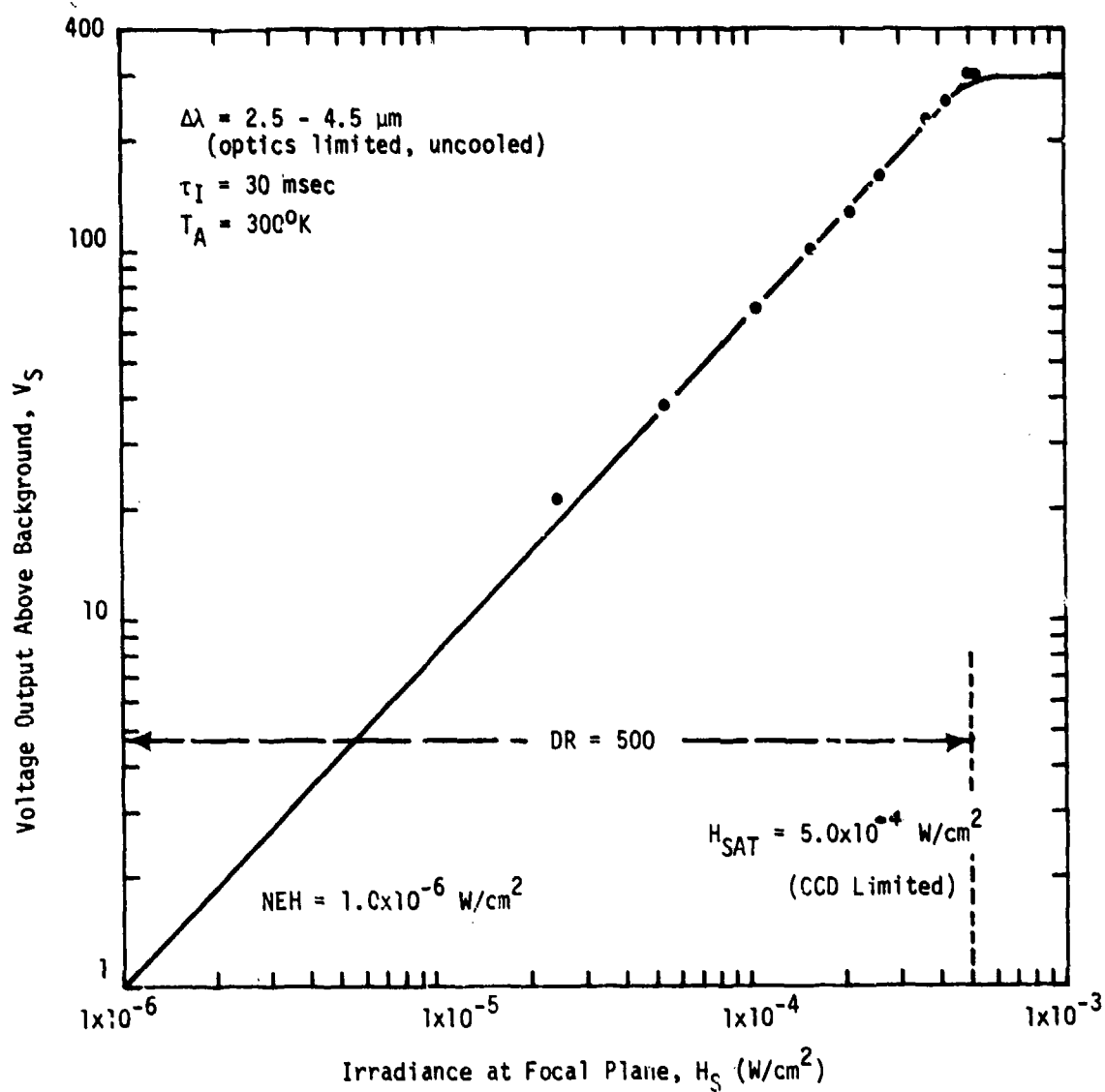


Figure 10. Transfer characteristic for 256 element Pt-Si array. An NEH of better than $1 \times 10^{-6} \text{ w/cm}^2$ is attainable in the $2.5 - 4.5 \mu\text{m}$ band.

IRCCD RADIOMETRIC FENCE CONCEPT

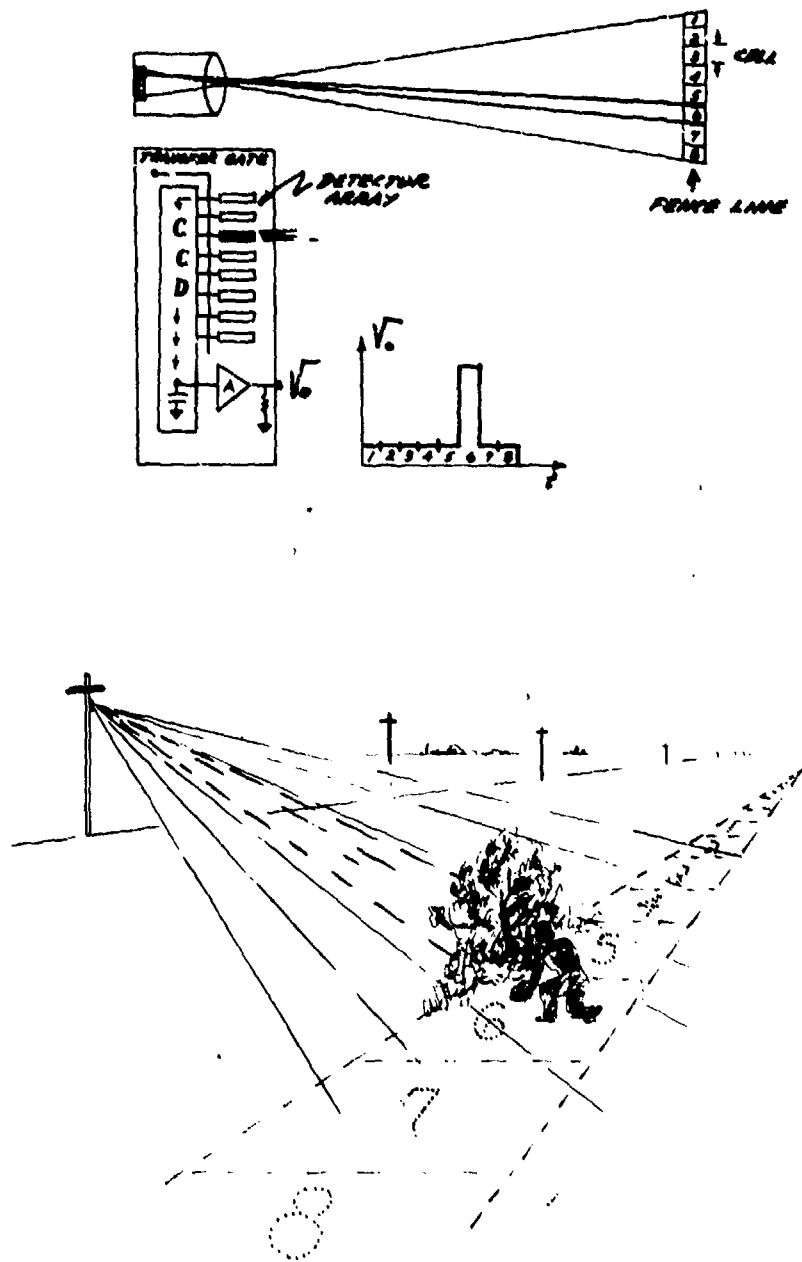


Figure 11. BISS IRCCD Radiometric Fence Concept.

IRCCD RADIOMETRIC FENCE PARAMETERS

FENCE	SIGNAL PROCESSING	
RANGE	100-200 M	BACKGROUND REMOVAL
SPAN	78 M (256 CELLS)	MOVING TARGET INDICATION
CELL WIDTH	30 CM	SENSITIVITY CONTROL
DETECTOR	SENSOR OUTPUTS	
TYPE MONOLITHIC SILICON	A) ALARM SIGNAL	
SCHOTTKY ARRAY	B) TARGET DATA	
SPECTRUM	3.3 - 4.2 μ M	- POSITION
OPERATING T	100°K	- MOTION
FRAME RATE	0.03 - 1 SEC	- SIZE
SENSITIVITY	0.2°K AT 0.03 SEC	- TEMPERATURE

Figure 12. IRCCD Fence Parameters.

BISS IRCCD FENCE

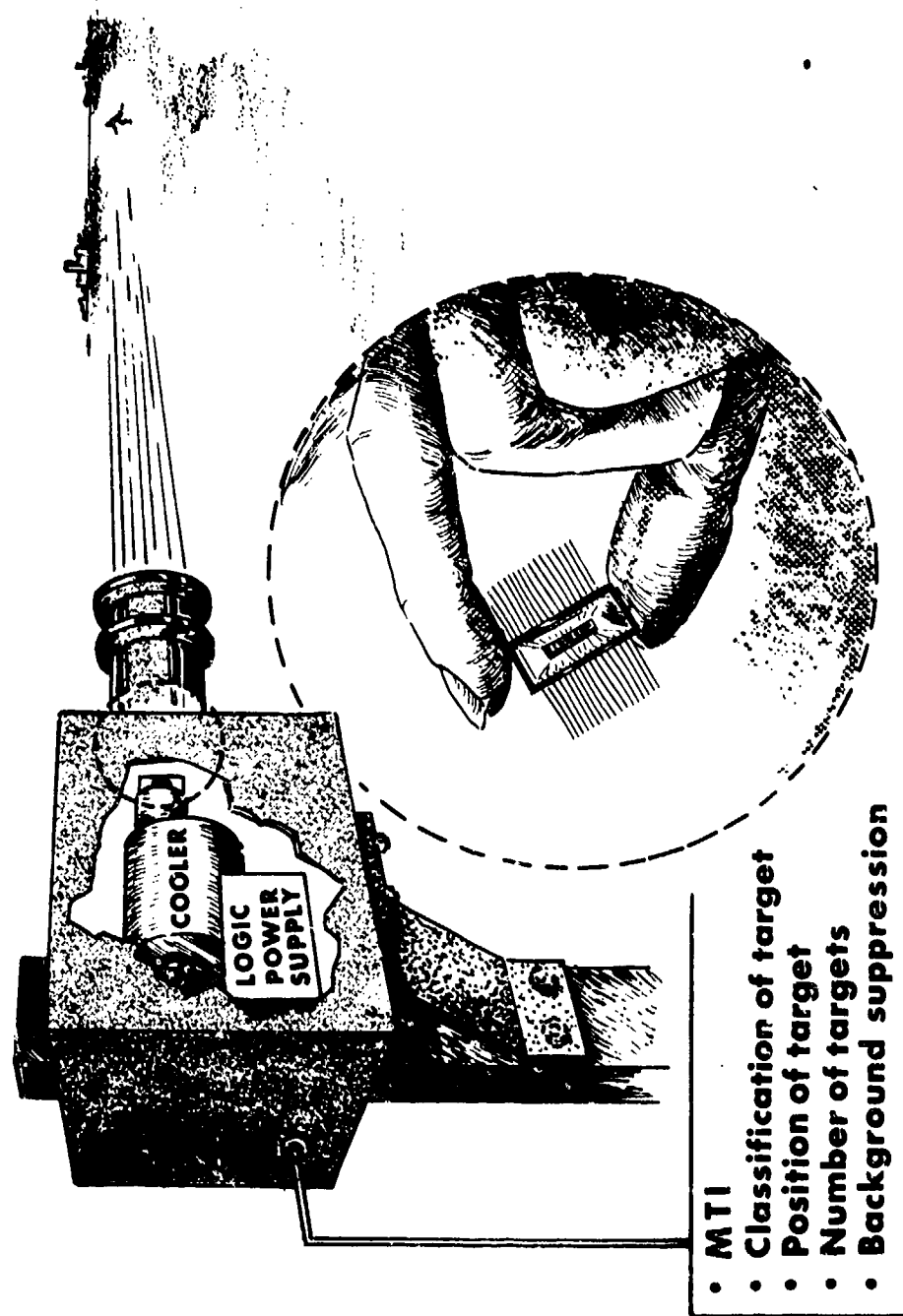


Figure 13. Conceptual drawing of firal BISS IRCCD Fence System.

USE OF THE PYROELECTRIC VIDICON FOR INSTALLATION SECURITY

F. T. DOEPEL
NIGHT VISION LABORATORY

INTRODUCTION

The pyroelectric vidicon (PEV) thermal imager is an uncooled infrared imaging closed circuit television system. The imager operates within the standard television format of 525 lines at 30 frames per second (EIA RS-330). The pyroelectric vidicon system is a passive infrared thermal imager which means that it requires no additional lighting during operation, only the electro-magnetic radiation which is emitted by all objects which are above zero temperature (-273°C). It consists of a 1" diameter pyroelectric camera tube, a television camera, and an infrared optics or lens. The vidicon camera tube is essentially a conventional vidicon with the usual photosensitive target and window replaced by an infrared sensitive pyroelectric target such as TGS (triglycine sulphate) and a 8 - 14 micron wavelength transmitting window. The camera utilizes optimized "off the shelf" video circuitry already developed by the television industry in order to minimize system cost. Recent improvements in this device have increased its performance to the point that it is now able to provide the military with a very favorable cost/performance trade-off when ever moderate performance applications such as day/night perimeter security and surveillance are being considered. The Base Installation Security Systems Program Office¹ sponsored and funded the evaluation of the PEV at Eglin AFB.

RECENT DEVELOPMENTS IN PYROELECTRIC VIDICONS

Operating life in excess of 5,000 hours have been achieved with present tubes without sacrificing performance. Present performance is a Minimum Resolvable Temperature (MRT) of 1°C at 250 television lines/picture height using 30 Hz chopping with eye integration and a MRT approximately 0.5°C at 250 TVL using 30 Hz chopping with memory, panning or staring. The range of operating temperatures for the vidicon are better than that of commercial television equipment due to the introduction of a new pyroelectric target material named deuterated triglycine flurooberylate (DTGFB). The pyroelectric vidicon has a " γ "² of one and its dynamic range is approximately 10,000: 1 from threshold detection to damage overload.

The transition from laboratory prototypes to production models has been completed. The Ampere Corporation, a division

of North American Philips Corporation, has added the pyroelectric vidicon to its camera tube line. In small production quantities of 100 tubes or more, the pyroelectric vidicon has been priced from \$1K to \$1.5K per unit. With a projected total system cost less than \$5K per unit, the infrared thermal imaging option will for the first time be inexpensive relative to mechanical infrared scanners (FLIR type) and not much more expensive than a good visible closed circuit television system.

System reliability should be comparable to a visible imager.

THERMAL VERSUS LOWLIGHT LEVEL AND VISIBLE IMAGERY

As was mentioned above, all bodies above -273°C emit thermal infrared radiation. Then diverse objects within an infrared scene will be at different temperatures providing the necessary contrasts for thermal imaging. This type of imagery is virtually immune to camouflage techniques and able to see into foliage areas. It is independent of visible sight level and penetrates all military "smokes." With reduced sensitivity, it has the ability to image through fog and rain where standard vidicons and low light television cameras such as the Silicon Intensified Target cannot.

AN INFRARED IMAGER FOR PERIMETER SECURITY AND SURVEILLANCE

Because of its ease of operation, ruggedness, relatively low cost, television format, and requires no cooling, the pyroelectric vidicon thermal imager is ideally suited for perimeter security and surveillance. A combination of two of its operating modes will enable this device to perform two functions. In the staring mode, it is able to provide intrusion alarm alerting the security personnel to the presence of a moving target within its field of view. Simultaneous with intrusion detection, the pyroelectric vidicon can automatically switch into chopping mode for imaging confirmation. This requires only some minor additional electronic circuitry and automatically the picture fills in around the intruder location and recognition.

In the following table, a list of specifications for the pyroelectric vidicon thermal imager is given for two optical fields of view.

Field of View:	10° X 10°	20° X 20°
Focal Length:	100mm	50mm
Recognition Range for Personnel Targets:	350M	175M

The field of view selection is left to the user and its obviously dependent on his particular application.

FIELD ASSESSMENT

An evaluation of the PEV was conducted in December 1976 at Eglin AFB. Three laboratory prototype PEV cameras operating in various modes were supplied and supported by the Night Vision Laboratory during the tests. They were:

1. A staring/panning PEV.
2. A chopped PEV using eye integration.
3. A chopped PEV using NAFI signal processor.

PEV cameras #2 and #3 were installed on poles approximately 15 feet off the ground at the extremes of a 410 foot chainlink fence. Camera #1 was installed on a 3 foot tripod underneath camera #2 on the outside of the fence perimeter. It alternately stared or panned. All cameras had their respective video signals routed to the video van and tower for assessment. T/1-100mm infrared optics were utilized on all cameras.

The tests were conducted during the evening hours of 14 and 15 December. On 14 December, ambient temperature varied from 48-52° with a three m.p.h. wind. It was a foggy night with a wet mist. On 15 December, it was a cloudy night with an ambient temperature of 56°F and 5 m.p.h. wind.

Various intrusion scenarios were run and every intrusion was correctly assessed and verified by the PEV.

The results of the PEV field tests are listed below:

1. No supplemental lighting is required for the PEV to perform.
2. The PEV is immune to typical camouflage techniques.
3. The use of the hoods, gloves, or blankets to mask the I.R. signature of intruders has little or no affect.
4. The PEV provides automatic MTI capability when in the staring mode.
5. Intruders hiding within the shadows of the supplemental lighting are easily detected and verified by the PEV.
6. The PEV was 100% effective with extremely short assessment times against all intrusion scenarios run during the test.

CCST EXAMPLE (A CASE FOR THE PEV)

The PEV requires no lighting. However, for the following example, we will assume lighting is required for the visual process, and if an intrusion occurs, it will aid the response

force. This assumption is valid and will include the acquisition and installation costs of a PEV at a typical base.

The cost of electricity presently varies in bulk rate from three to seven cents per kilowatt hour. Assume an installation with a perimeter of 4,000 feet, with poles spaced at an average of 75 feet apart, and lighted for 12 hours a day, year round. For this example, assume 150 watt lamps, or 2 watts per foot, of perimeter. The utility cost of this installation for one year at five cents per kilowatt hour is \$4.32 per year per foot of installation, or \$17,280 per year. Over a ten year period, the cost for one installation is \$172,800 (CY77 dollars), and for 100 installations, the cost exceeds 17 million dollars. This cost excludes inflation, lamp replacement, and maintenance costs which is estimated conservatively at one dollar per foot per year.

Furthermore, if visual augmentation devices are utilized by response forces, (i.e., night vision equipment), then the installation cost of lighting can be eliminated. This cost represents a one time savings of between \$10 to \$30 per foot of perimeter. Thus using the previous example, (choosing \$20 per foot), results are 8 million dollars savings in installation costs. The total lighting costs for ten years is 25 million (CY77 dollars).

Using a rough guideline of one camera per 200 feet of perimeter, and projecting the cost of the PEV to be \$1,000 more per unit than the presently planned camera, the additional costs of the PEV are 2 million.

With this example, approximately \$23,000,000 can be saved. Based on this, the PEV is potentially a very cost effective thermal imaging sensor.

1. The Base and Installation Security System (BISS) Program Office, Air Force Electronic Systems Division, Hanscom AFB, MA, 01731.

2. Vidicon output response to input thermal energy.

APPENDIX A

PEV THEORY OF OPERATION

BACKGROUND HISTORY

The development of the pyroelectric vidicon was initiated in Europe. The approach followed there required the presence of residual gas ions within the camera tube envelope to eliminate electronic charge accumulation on the pyroelectric target. This method created certain undesirable results such as limited sensitivity and a shortened life. The program initiated at the Night Vision Laboratory, however, had as its goal the development of "hard" or non-gassy vacuum vidicons in order to circumvent these problems. By developing a secondary emission pedestal mode (SEPM) which eliminates the need for residual gas within the tube and placing a protective coating of SiO₂ over the pyroelectric target, the pyroelectric vidicon has become a practical thermal imaging device.

OPERATING DETAILS

Because of the nature of pyroelectricity, the pyroelectric vidicon only responds to changes in incident radiation. Thus when imaging a stationary thermal scene, some form of optical modulation, i.e., panning or chopping, is required. Depending upon the particular application, 3 modes of operation are possible and will be described below.

1. Staring: In this mode, the imager is an automatic moving target indicator. Background clutter is automatically subtracted from the video signal without the need for any additional video circuitry. Thus only moving targets appear on the television monitor.

2. Panning: This is the most sensitive mode of operation when viewing stationary scenes. It is easy to implement requiring only an inexpensive pan head. However, there are certain features of panning modulation which adversely affect the quality of images making it unsuitable for some applications. The features include thermal streaking and the loss of low spatial frequency resolution in the panning directions.

3. Chopping: In this mode, a mechanical chopper is positioned between the lens and camera. The chopper can be either a mylar belt consisting of open and closed segments or a rotary chopper blade passing in front of the tube. A pyroelectric vidicon operating in the chopped mode is inherently less sensitive than a panning system by a factor of 2.

a. Chopping with blanking of the negative image.

Another inherent property that affects image quality is that while the chopper is closed, the target produces an image identical, but opposite in polarity, to the image produced while the chopper is open. Without some form of signal processing, these two images will interfere with each other. The simplest type of signal processing which will eliminate the interference between the positive and negative images is to blank the display while the chopper is closed, thereby eliminating the negative image altogether. Although this does remove the negative image, it introduces distracting flicker at chopping frequencies of 15 Hz and below.

b. Chopping with memory.

A better technique for cancelling interference between the positive and negative images is to invert the negative image before it reaches the display. Helmick and Woodworth successfully demonstrated a modification of this approach by synchronously inverting the polarity of the negative image signal, delaying it one frame time and adding it to the succeeding frame before displaying it at the CRT. This technique called "chopping with memory" requires sufficient memory to store a frame and the electronics to add two frames before display. For applications interfacing the video signals with a machine, it offers the best approach. This image processing eliminates thermal streaking and avoids the problems of panning systems such as pan reversal transients and the loss of resolution in the direction perpendicular to the pan velocity. It also has a secondary benefit of recovering part of the factor of the loss of sensitivity inherent in the chopping mode.

c. Chopping with eye integration.

For human observers, the costly electronic memory can be eliminated by synchronously inverting the negative polarity image, displaying it in real time and permitting the eye to perform the integration. The black level of the inverted negative image signal is adjusted to the same level as the positive image to prevent flicker. This approach, called "Chopping with Eye Integration" has been investigated by Night Vision Laboratory. It provides the same result for observer as adding the images in an electronic memory, i.e., improved signal to noise ratio as perceived by the eye and superior overall image quality because of the reduction of thermal streaking and the elimination of other effects associated with panning systems.

COMPARATIVE FEATURES

PYROELECTRIC VIDICON CAMERA

1. Not light level dependent.
2. Senses and alarms on "Hot" targets movement.
3. Gives Image.
4. Has inherent motion detection capability in staring mode can be coupled with motion detection equipment if desired.
5. Can subtract out stationary background showing only what is moving.
6. Has foliage or clutter penetration capability.
7. Technology is new and requires engineering support.
8. Must be cropped or dithered for continuous imagery.

TV CAMERA MOTION DETECTOR

Operation is affected by ambient light level.

Senses reflected radiation will alarm on any movement where sufficient contrast exists, won't alarm on movement if contrast is low i.e., green uniform against foliage background.

Gives Image.

Camera has no staring mode motion detection capability must have motion detection device as auxiliary equipment.

Without considerable storage cannot subtract background.

Has capability.

Standard product, commercially available.

No chopping, panning optional.

9. Optics are expensive, reflective objective lens should be developed to lower costs.

10. No Cooling required.

11. No hardened camera exists.

12. Ultimate production costs will be of the same order as a silicon intensifier camera (Sans optics).

13. Better performance in haze & fog.

14. Not sensitive to specular reflection (glare).

Optics are inexpensive.

No cooling required.

Semi-hardened cameras are available.

Cost of motion detection equipment must be added to camera price (approx. 1K per camera for motion detectors).

Little capability in fog & haze.

Will have problem with specular reflection.

COMPARISON OF MAGNETIC AND STRESS RESPONSE
OF MAGNETIC INTRUSION LINE SENSOR (MILES)*

T. F. Ezell
R. W. Madsen
F. G. Yost
Sandia Laboratories,
Albuquerque, N.M. 87115

INTRODUCTION

The MAID/MILES intrusion sensor detects both stress waves as well as ferrous objects. Stress waves are produced by seismic noise, wind, animals, and other naturally occurring phenomena, as well as by man-made sources, such as vehicles, machinery, people walking, etc. Both modes of detection occur by similar physical mechanisms, but it is not clear that the sensitivities of each mechanism correlate because of soil characteristics and soil coupling and because of magnetic material properties. This paper presents results of both laboratory and field measurements made by Sandia Laboratories on the magnetic and stress properties of MILES cables.

Knowledge that stress and magnetic sensitivities correlate would be helpful in diagnosing problems with installed cables and for quality control in the manufacture of new cables because the magnetic sensitivity can be more easily measured than the stress sensitivity. This paper presents the results of stress-magnetic correlation measurements made at Sandia Laboratories. Rigorous tests indicate little, if any, correlation exists between the stress and magnetic properties even though preliminary walk tests indicated that a correlation might exist.

MAID/MILES System

The MAID/MILES intrusion detection system was designed for the Air Force by Honeywell, Inc., and consists of a buried cable, called MILES (Magnetic Intrusion Line Sensor), and an electronic processor, called MAID (Magnetic Anti-Intrusion Detector). The MILES cable (Figure 1) is a round cable 100 metres long with a sensing coil wound around a stranded

* This work jointly supported by the United States Energy Research and Development Administration and the Base and Installation Security Systems Program.

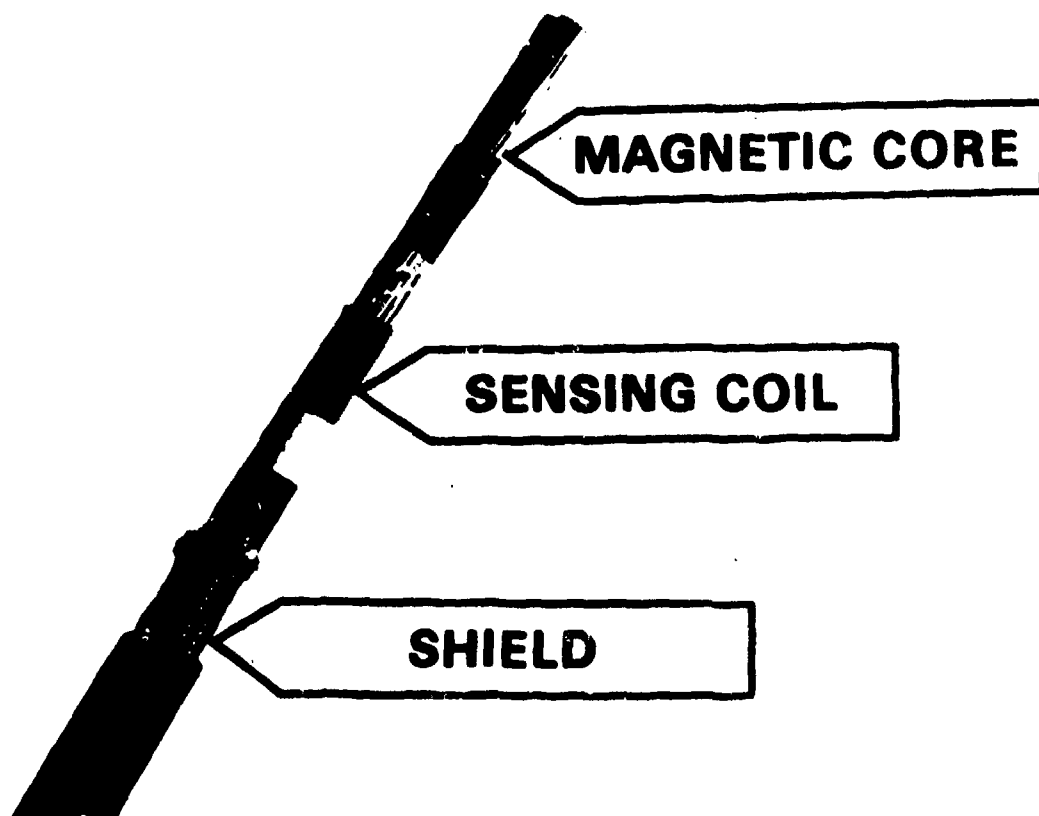


Figure 1. Construction of MILES cable.

magnetic core. The coil is wound 15.7 turns/cm (40 turns/inch). The sense winding reverses every 1.09 metres (43 inches) (this reversal is called a transposition) in order to provide cancellation for signals originating far from the cable. The MAID processor contains active filter-amplifiers which provides amplification within a 0.2 to 4 Hz passband. Output circuitry produces an alarm if response within this passband exceeds ± 1 volt in amplitude for a specified time.

Theory of Operation of Sensor

A voltage is generated in the sensing coil of the MILES when the flux density in the core changes. This flux density change can occur in either of two ways: (1) motion of a ferrous object near the cable causes a change in the ambient flux set up in the core by the earth's magnetic field; (2) stresses transmitted to the cable cause a magnetostrictive change in core permeability which in turn causes a change in flux density in the core. The change in flux density induces a voltage according to $E = \int n(d\phi/dt)dl$. Thus, in both cases the induced signal is determined by the magnetic properties of the core, but not necessarily the same properties.

SIGNAL ENHANCEMENT OF OPERATIONAL MILES BY MAGNETIC TREATMENT

This portion of the paper deals with the magnetic state of the MILES core material and how it affects the sensor operation. The MILES stress response has been found to be variable from cable to cable and sometimes even varies along the length of a given MILES sensor. One way to measure the stress response of a buried MILES is to record analog output while a person repeatedly crosses the cable. A surveyor's tape with markers every 1.09 metres is laid on the ground over the cable and a person carrying no magnetic material crosses the markers.

Our first experience with the effect of the magnetic state of the MILES core on the MILES response was at an operational site in late 1975. Here a very noisy MILES cable which produced almost constant alarming through the MAID was compared with a new MILES cable installed parallel to and 1.25 metres from it. The new cable operated very well with a high detection sensitivity and a low background noise level. Leigh Wold of Honeywell was consulting with us at the time and began experimenting with the old MILES by applying a DC current to it. It was found that the background noise of the old MILES could be adjusted up or down depending on the magnitude,

polarity, and sequence of current applications. The DC current flowing through the MILES sense windings was affecting the magnetic state of the core material and the operation of the MILES cable. The old MILES was left in an operational state of having improved detection and a background noise level low enough to operate with a low nuisance alarm rate.

This work was followed by a contract with Honeywell to investigate the effect of the MILES core characteristics on MILES sensor operation. A summary of the results of this contract to date shows that the current injection technique discussed above sometimes works, but in some cases it can also be harmful to sensor operation. Two improved methods of magnetic treatment have been developed. One method involves passing the MILES through a solenoid carrying DC current before the cable is buried (Figure 2). The high magnetic field in the solenoid saturates the core and leaves it in its proper magnetic state. The second method is for buried MILES and involves dragging a large current carrying coil over the surface of the ground above the MILES. The magnetic field produced by the coil is sufficient to saturate the MILES core material even when the MILES is 0.5 metres underground (Honeywell design criteria was a 5×10^{-4} tesla (5 gauss) field at 5 metres). Figure 3 illustrates the use of the coil. The polarity of both the solenoid and the coil are chosen so that the direction of the final magnetic field is in the same direction as the earth's magnetic field. Figure 4 is a picture of the coil mounted on a sled in use.

Magnetic treatment has been observed to have no effect on a uniformly sensitive MILES cable, but for a very poor cable, a drastic improvement is usually noted. Figure 5 shows analog and alarm outputs for a person carrying no magnetic material crossing every 1.09 metres of a MILES before and after magnetic treatment with the sled. The sensitivity of this MILES was improved enough to restore it to operation.

The mechanism of magnetic treatment of the MILES may be explained by referring to Figure 6 which presents the voltage output of a short section of round MILES cable being subjected to a constant amplitude sinusoidal stress and a varying external magnetic field. In effect, the figure illustrates a measure of stress or seismic sensitivity of a MILES sensor as a function of the magnetic field around the sensor. Further information on how these curves are generated is presented in reference 2.

The sensitivity curve of Figure 6 for a buried MILES cable in the earth's magnetic field, H_E (the component parallel to the MILES is represented by the vertical line marked H_E in



Figure 2. DC solenoid.

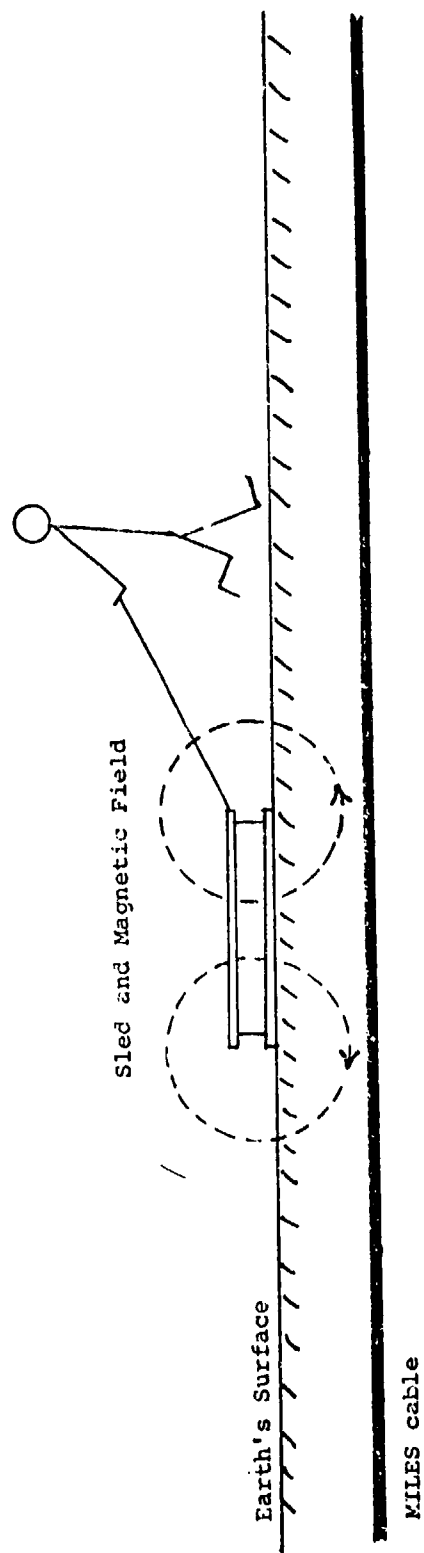


Figure 3. Concept of coil used in magnetic treatment of MILES.



Figure 4. Coil mounted on sled.

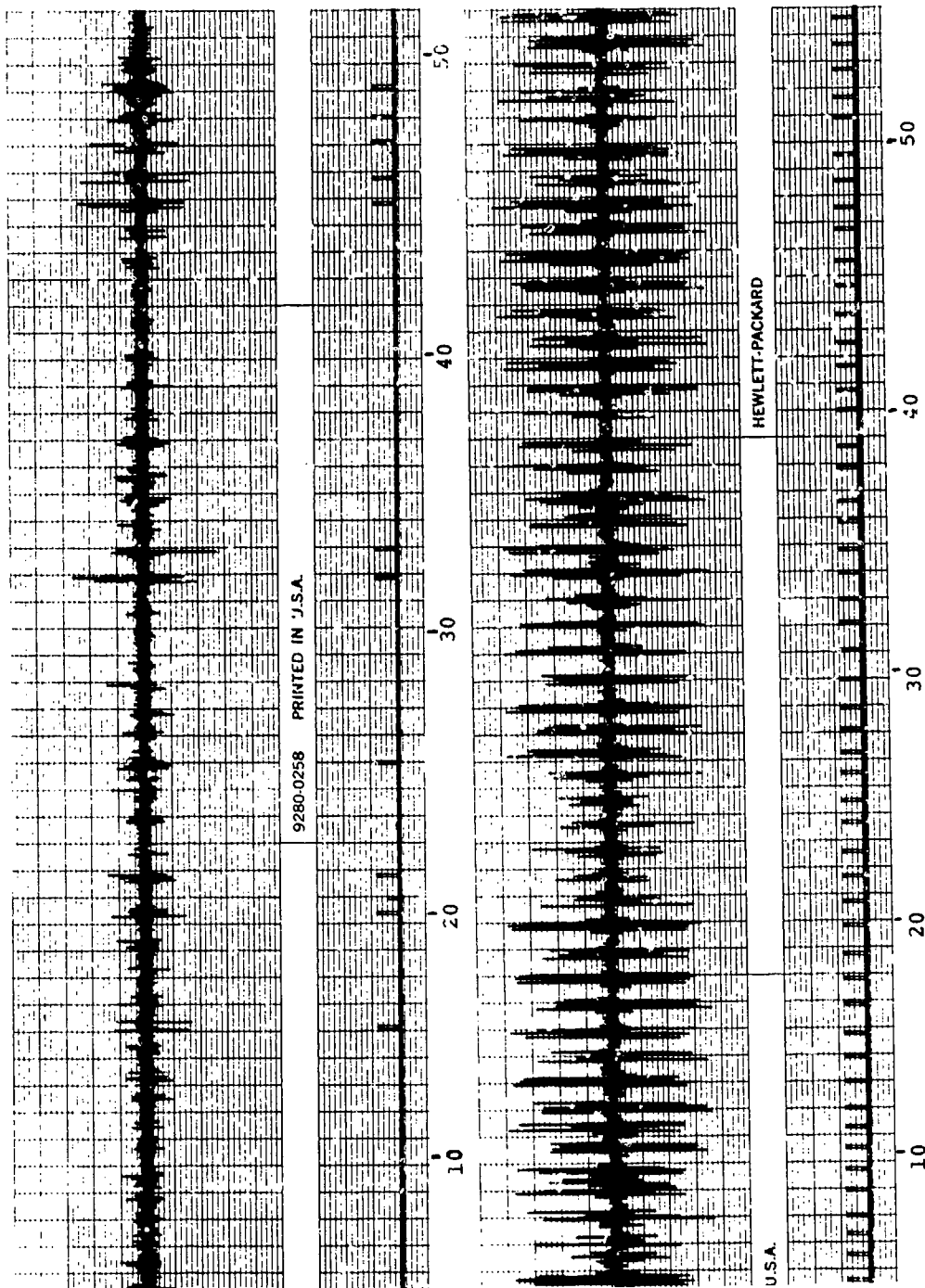


Figure 5. MAID analog signal and alarm output for person crossing cable at every 1.09 metre marking.
 Scale: 200 mv/mm vertical, time 1 mm/sec.
 Top: Before magnetic treatment Bottom: After magnetic treatment

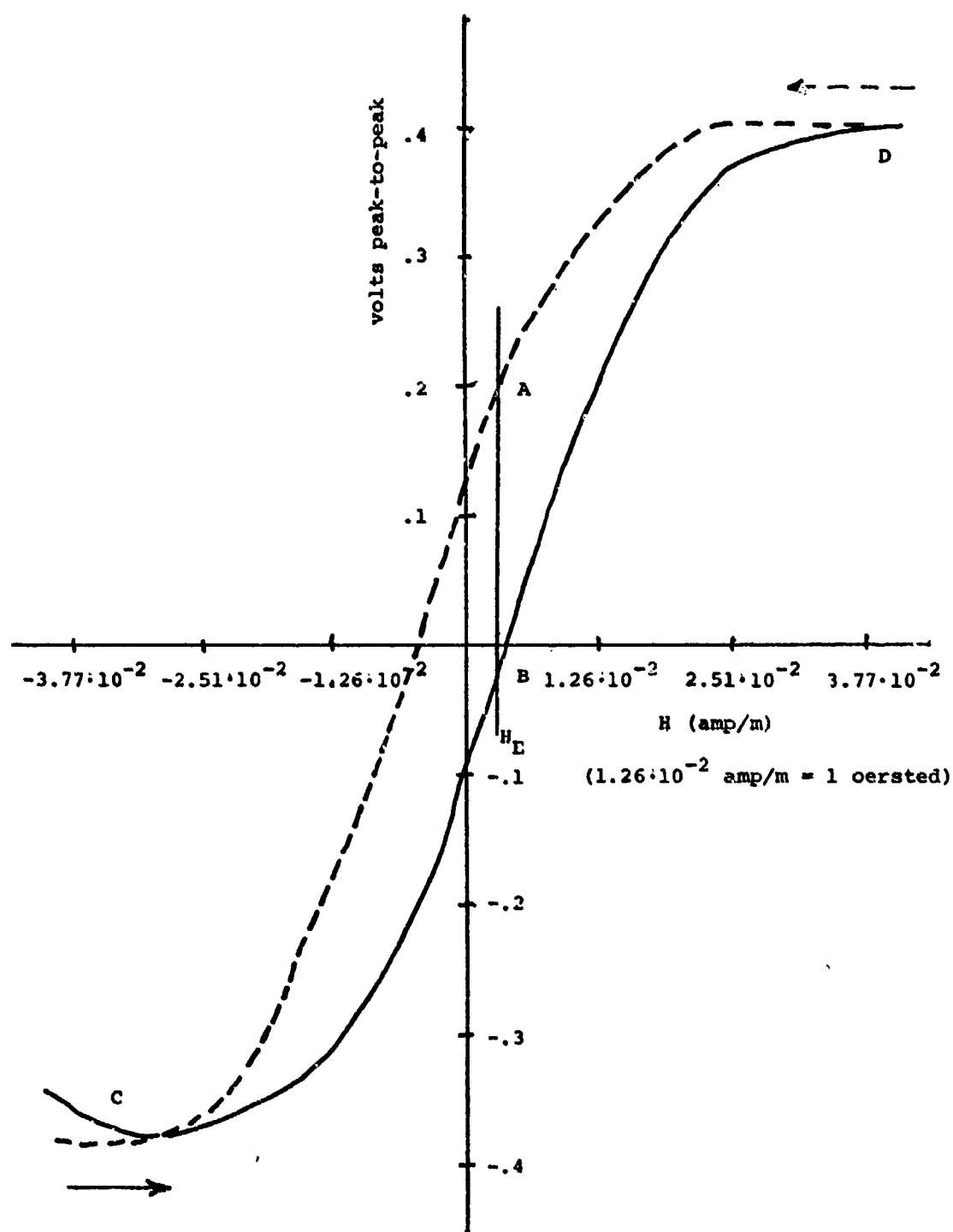


Figure 6. Voltage output for a round MILES as it is subjected to sinusoidal stress and external magnetic field (reproduced from reference 1).

Figure 6.), can be used to explain the effect of the magnetizing coil. The operating point of this MILES then must be along the line H_E somewhere between points A and B. Note that random operating points along the line H_E would produce drastically different outputs. For instance, an operating point near A produces approximately a 0.2 volt peak-to-peak output for this stress input while an operating point near B gives an output near zero. The desirable conditions for uniform sensitivity for a MILES cable are: (1) all portions of the core material must have the same characteristic curve such as that given in Figure 6, and (2) all portions must be at the same operating point on the curve.

The magnetic fields at the ends of the sled are in opposite directions (Figure 3). In use, the field at the rear of the sled is chosen to be in the same direction as the earth's magnetic field, and the field produced by the sled is sufficient to saturate the MILES core. Then as the sled moves over the cable, (1) the field from the sled will drive the MILES operating point in Figure 6 to point C (somewhere in negative saturation); (2) as the sled passes, the operating point will begin to move up the lower curve in Figure 6 to point D (somewhere in positive saturation); and finally, (3) as the sled's field passes away the MILES operating point will shift back along the upper curve to point A. All points of the MILES cable will then be at the same operating point if all of the MILES cable has the same characteristic curve. This curve is of course determined by the core material itself and its past history of heat treatment, cold working, and any other factors that influence magnetic properties. It is important that MILES cables come from the production line with uniform core material and then are handled carefully during shipment, storage, and installation so that portions of the cables are not damaged and their characteristic curves degraded.

Magnetic treatment has not been effective in bringing all portions of all MILES cables up to a uniform sensitivity. The explanation for all the magnetic treatment effects is not totally understood but is being pursued in laboratory and field work. One difficulty with field work is that other variables such as soil coupling, burial depth, and variations in cable crossings enter into the measurements.

LABORATORY EXPERIMENTS ON MAGNETIC PROPERTIES

Mechanical Treatment of Core Material

This section presents the results of work performed to determine the effects of mechanical treatment on the magnetic

properties of the core. To illustrate the extraordinary effects of cold work upon magnetic properties of the MILES core material, we determined the DC normal induction curve and hysteresis loop for a single strand of 0.109 cm diameter MILES core wire 30 cm long. These curves are shown in Figure 7. The coercivity is approximately $6.28 \cdot 10^{-4}$ amps/m (0.05 oersteds), and the maximum and initial permeabilities are approximately 98.7. To contrast this material we obtained well annealed wire of the same alloy 0.150 cm in diameter and drew it down to 0.109 cm in diameter for a 50% cold work. The magnetic properties for this material are shown in Figure 8. Notice that its permeability is drastically reduced and its coercivity has drastically increased. This will reduce the magnetic mode sensitivity of MILES cables. Other related experiments, carried out in our laboratory, involving simple bending of core material have shown actual magnetic mode desensitization.

Laboratory Measurements of Magnetic Properties

The magnetic mode sensitivity of MILES cable is largely determined by the reversible permeability of the core material which, due to localized bending and other core inhomogeneities, can vary significantly over the length of a 100 metre cable. Reversible permeability is defined in Figure 9 as the slope of a minor loop located on the normal induction curve at a field value equal to the tangential component of the earth's magnetic field. As ferrous material moves near the cable, it causes a slight change, ΔH , in the field value at that point. This in turn causes a flux density change, ΔB . The limit of the ratio of these quantities, $\Delta B / \Delta H$, as ΔH approaches zero is defined as the reversible permeability. Although we have not studied the effects of bending on reversible permeability, we shall present data taken in our laboratory on an undamaged, well annealed specimen.

To investigate the effects of remnant magnetization and applied magnetic fields on magnetic cable output we injected current into one winding length (1.09 metres, the length between two transpositions) of MILES cable. The cable was excited by a ferrous object swinging above the cable. After a momentary application of current on the order of milliamps to fractions of an amp, no improvement of cable output was observed. With the continual application of larger and larger current, the cable output decreased. This prompted us to wrap 19 strands of 0.109 cm diameter core wire on a 5.38 cm diameter mandrel to form a toroid whose cross section approximated that of a MILES cable. It was then annealed for four hours at 1150°C in dry hydrogen and then cooled according to the

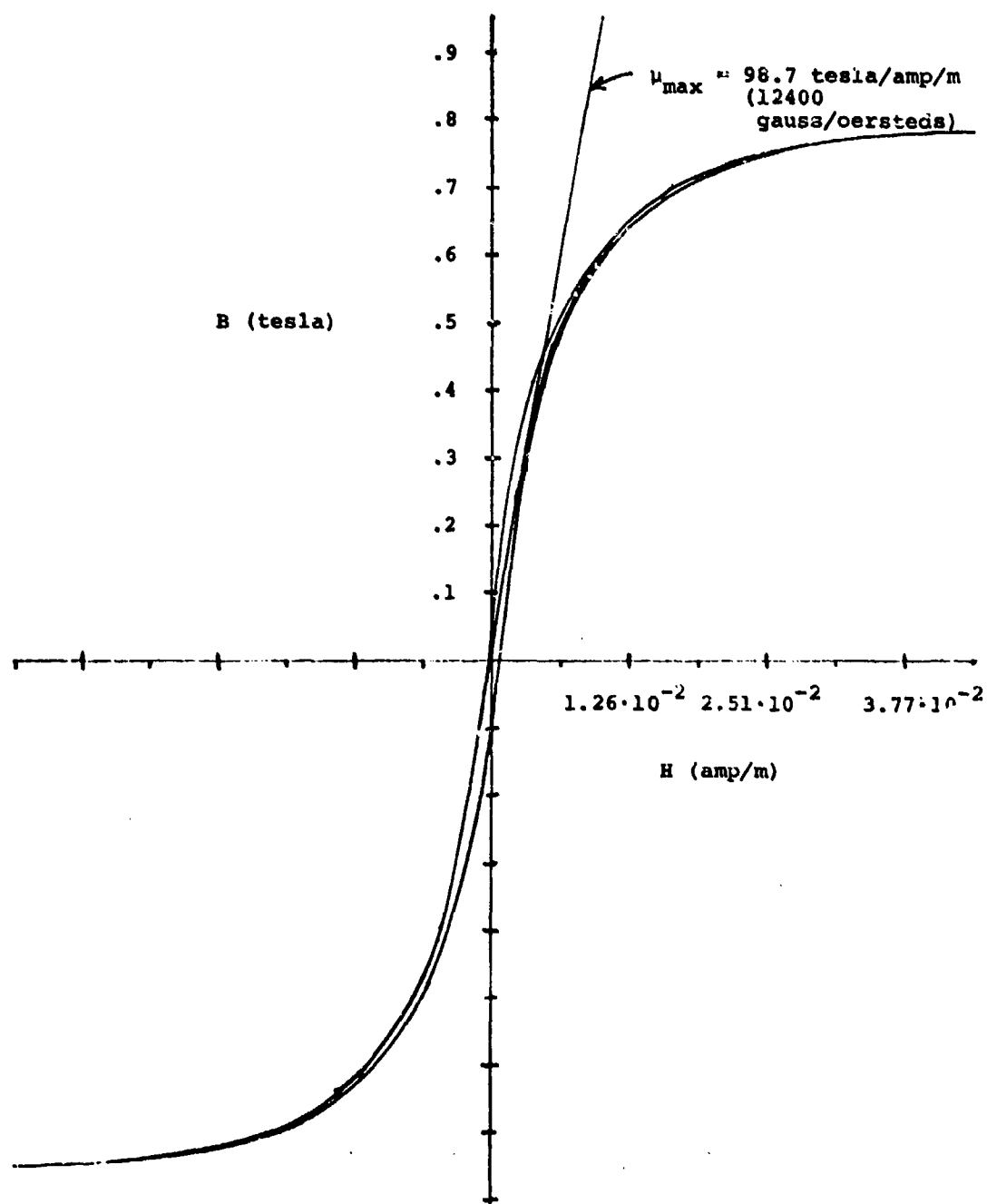


Figure 7. Normal induction curve and hysteresis loop for one strand of MILES core wire.

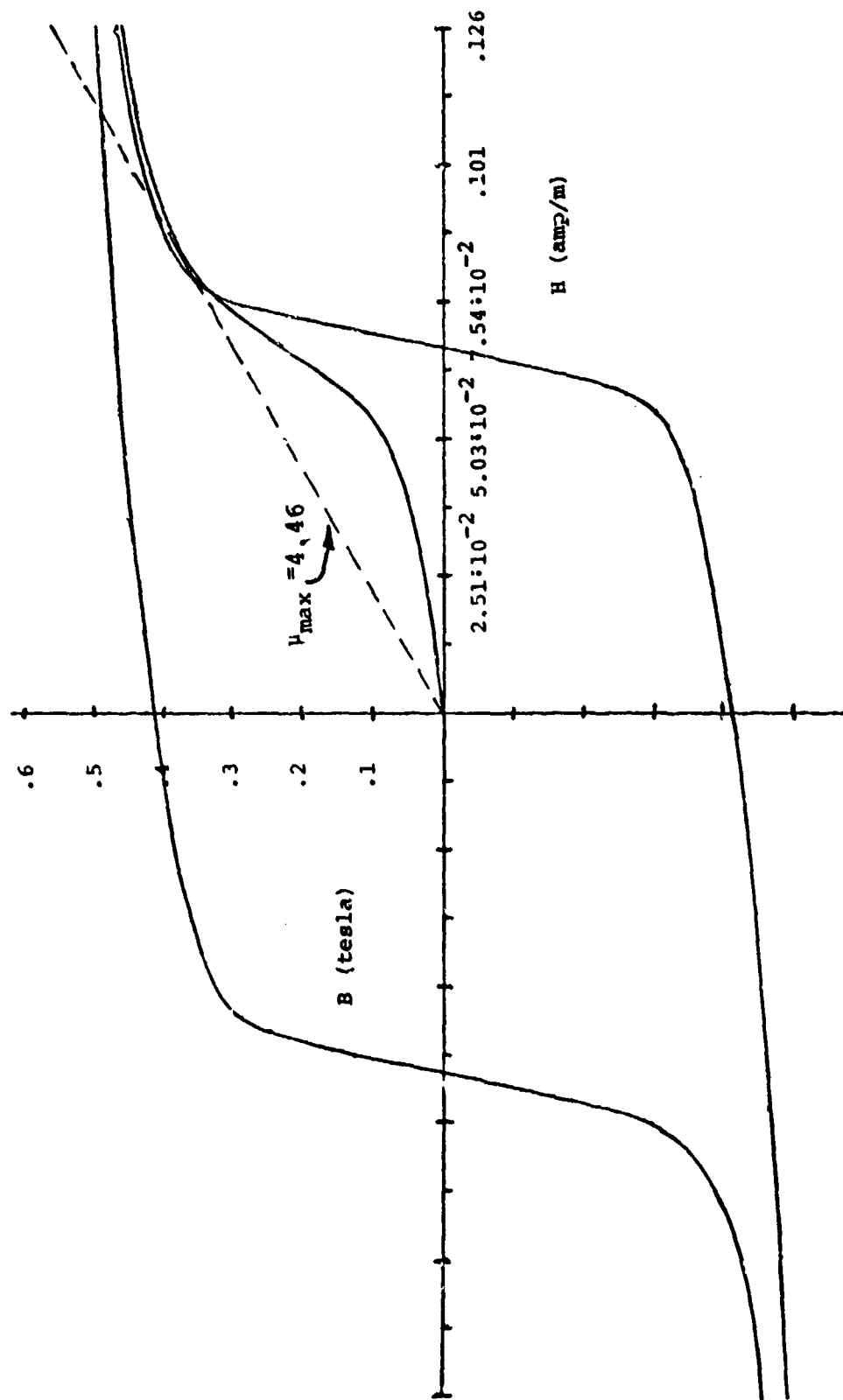


Figure 8. Normal induction curve and hysteresis loop for a strand of wire of the same alloy as used in MILES cables and 50¢ cold worked.

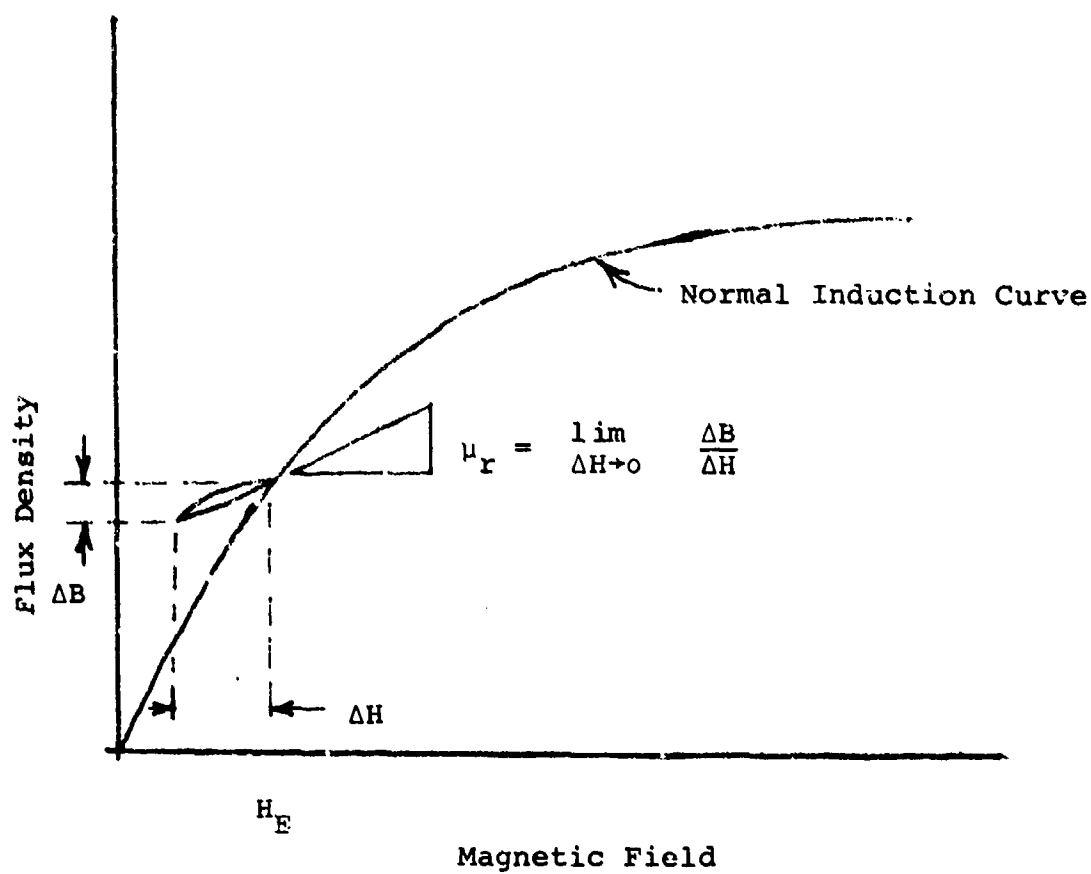


Figure 9. The normal induction curve and the definition of reversible permeability.

recommended heat treatment for supermalloy type materials. The toroid was then wrapped with three 0.644 mm (#22 gauge) copper windings. These windings served as a DC bias field winding, a small 60 Hz excitation winding, and a sense winding. All windings had 218 turns. The reversible permeability measurements versus applied bias fields are shown in Figure 10. It is obvious that continually applied fields decrease reversible permeability and, consequently, magnetic mode cable output. From these experiments we conclude that magnetizing a MILES cable enhances the stress mode output and not the magnetic mode output.

Laboratory Stress Mode Experiments

To investigate the stress mode sensitivity of cables we used one winding length (1.09 metres) of both round and flat* versions of the MILES cable and the tapping arrangement illustrated in Figure 11. A wooden drop weight (34.5 gms) was allowed to pivot so that it had a moment arm of 16.5 cm and was dropped from a height of 5 cm.

For a cable that had been demagnetized with an AC current, the cable output was not above noise level for either cable. A momentary one ampere magnetization current was then applied to the sense windings. The output due to the wooden drop weight rose to 2.7 volts peak-to-peak for the round cable as shown in Figure 12a. After several drops (less than 10) the output was reduced to noise level. Repeated application of the momentary current always brought the output up to significant values. This phenomenon was observed with both cable types. To decrease the ambient noise pickup, we repeated the experiment using a short (15 cm) length of flat core material which was wrapped with 100 sensing turns. The output of this short section after similar magnetization is shown in Figure 12b. After ten drops, the output was reduced to .18 volts peak-to-peak as shown in Figure 12c. The section was then bent back and forth many times over its entire length, straightened and retested. The output appears in Figure 12d. The signal produced by the first drop was rather large, but subsequent signals were on the order of those shown in Figure 12c. The section was then remagnetized and the high output was once again restored as can be seen in Figure 12e.

*Commercial version of MILES designed and built by Honeywell, Inc.

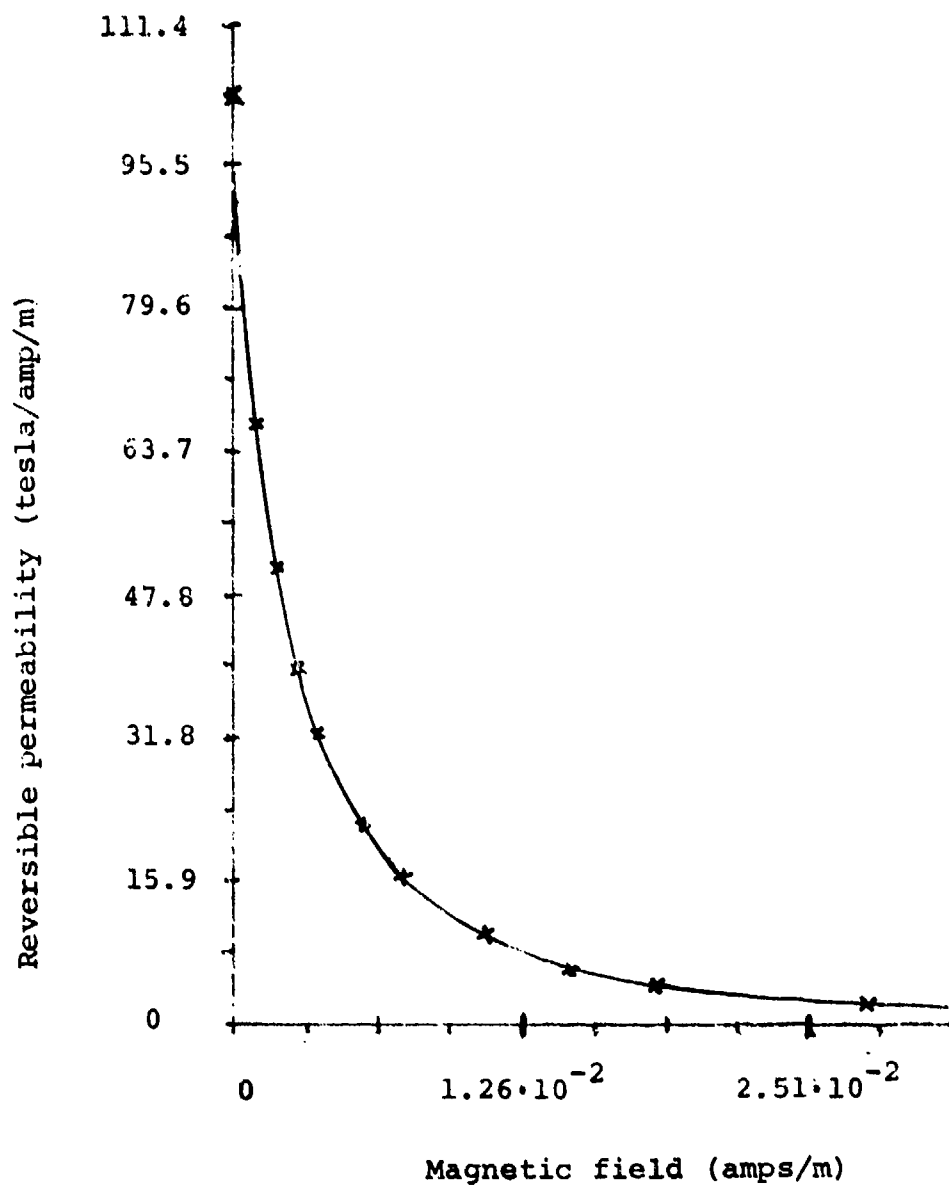


Figure 10. Reversible permeability versus applied bias field.

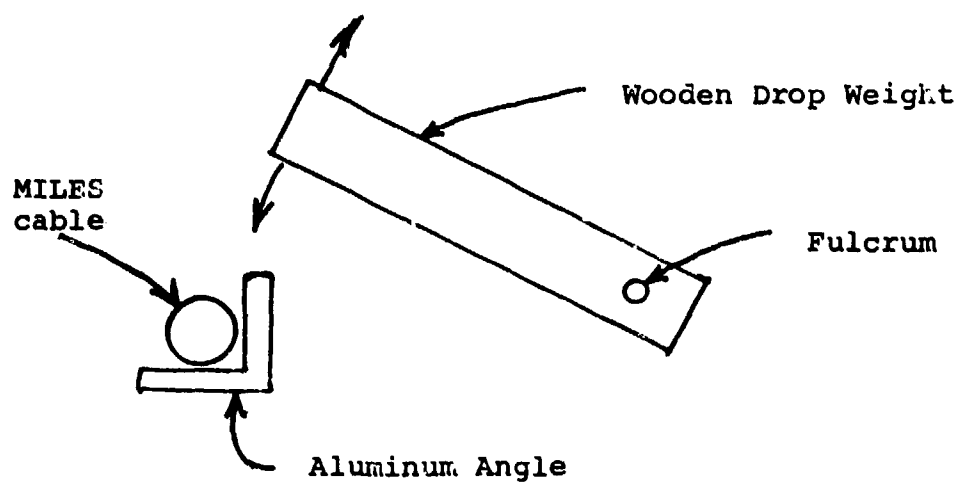
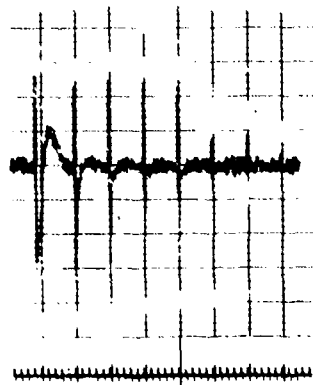
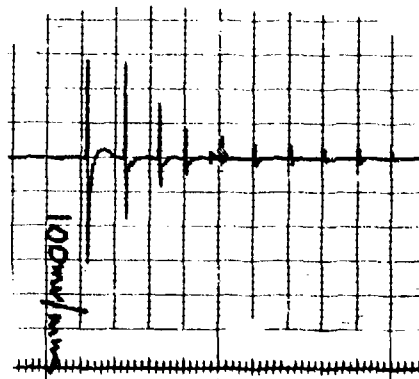


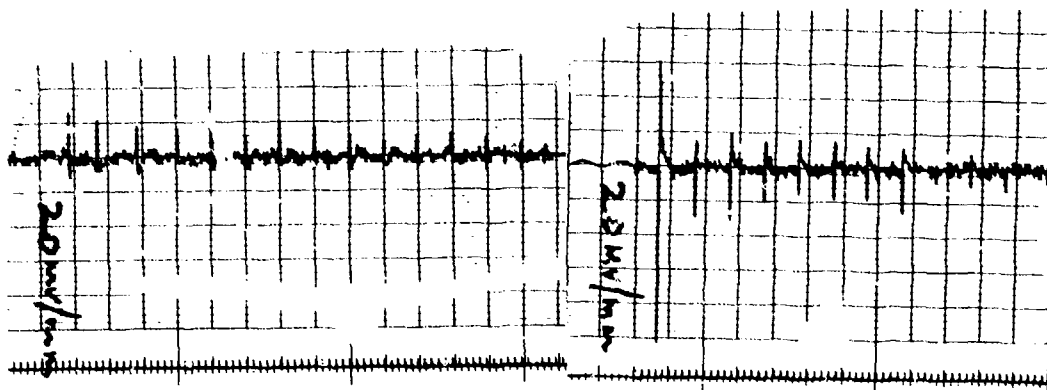
Figure 11. Tapping arrangement used to apply stress wave to cable.



a. 100 mV/mm
MILES cable

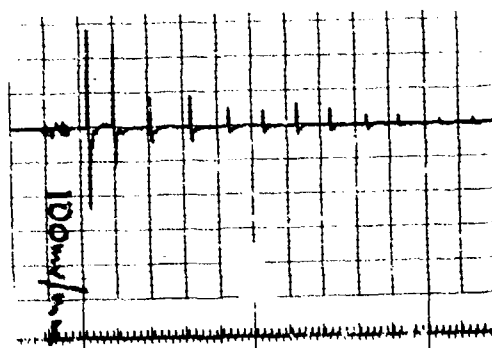


b. 100 mV/mm
Short Section



c. 20 mV/mm
Short Section

d. 20 mV/mm
Short Section



e. 100 mV/mm
Short Section

Figure 12. MAID output signals for cable and short section used in laboratory experiments.

STRESS AND MAGNETIC MEASUREMENTS ON BURIED CABLES

In testing buried MILES cables, it was found that the signal from a person walking over the cable varied so much from one crossing to the next as to obscure differences of the order of 50 per cent. The fact that the walker does not step in the same place and in the same way each time creates these differences. In order to obtain a consistent stress signal, a plastic pipe loaded with sand to obtain an acceptable signal was dropped from a tripod. For tests on cables buried in soil, the pipe weighed 4.7 kg. The end of the pipe was covered with a cap and some foam rubber. The purpose of the rubber was to produce a uniform impact and minimum soil disturbance. The effectiveness of the rubber was demonstrated by the fact that the signal from the first drop varied only a few percent from the following ones for a cable which had not been magnetized. This method produced a signal which was repeatable in both amplitude and waveshape (Figure 13). As an indication of the repeatability of the test, for this series of drops, the average value was 3.27 V, the maximum was 3.64 V, the minimum was 2.64 V, and the percentage standard deviation for 17 drops was 7.3%. This cable had not been magnetized, so signal did not decrease as in laboratory results discussed above. This effect is discussed in more detail below for cables in the field.

For the test discussed here, a standard round MILES cable was used, and the output signals were obtained with a MAID processor which had been modified to provide an analog output signal.

The magnetic sensitivity was measured with a battery powered oscillator driving an air core coil. The oscillator frequency (3 Hz) was chosen to be within the MAID bandwidth. No attempt was made to calibrate the coil and oscillator to provide a known magnetic field at the cable, but this could be done. Instead, a constant amplitude was used and measurements relative to other sections of the same cable were compared. The output of the oscillator was adjusted to give a reasonable output from the MAID/MILES and then left at that setting.

The coil and oscillator are useful to determine the location of transpositions in the cable--when the axis of the coil is oriented parallel to the cable, a null in cable output occurs when the coil is adjacent to a transposition. The null is sharp and the transposition can be easily located within a few centimetres (Figure 14). The coil and oscillator can also be used to locate the cable.

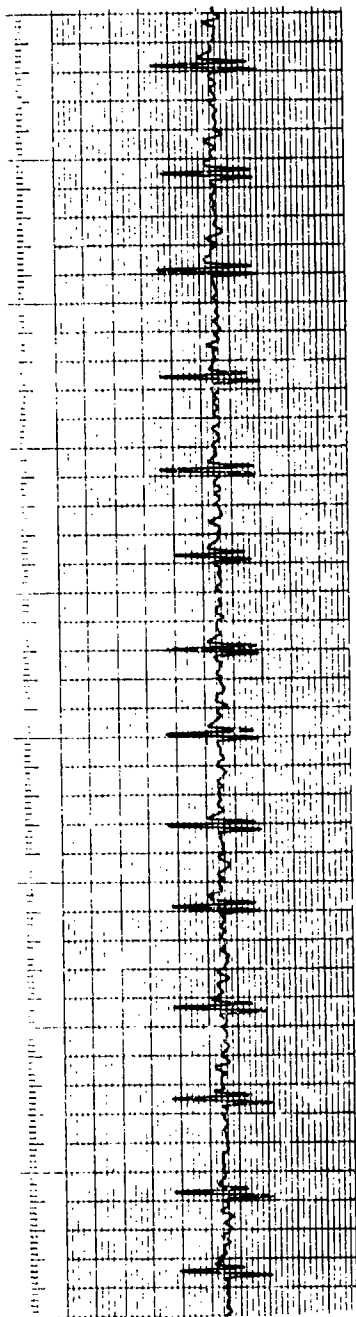


Figure 13. Typical pipe drop signal
Scale: 200 mv/mm vertical, time, 5mm/sec.

174

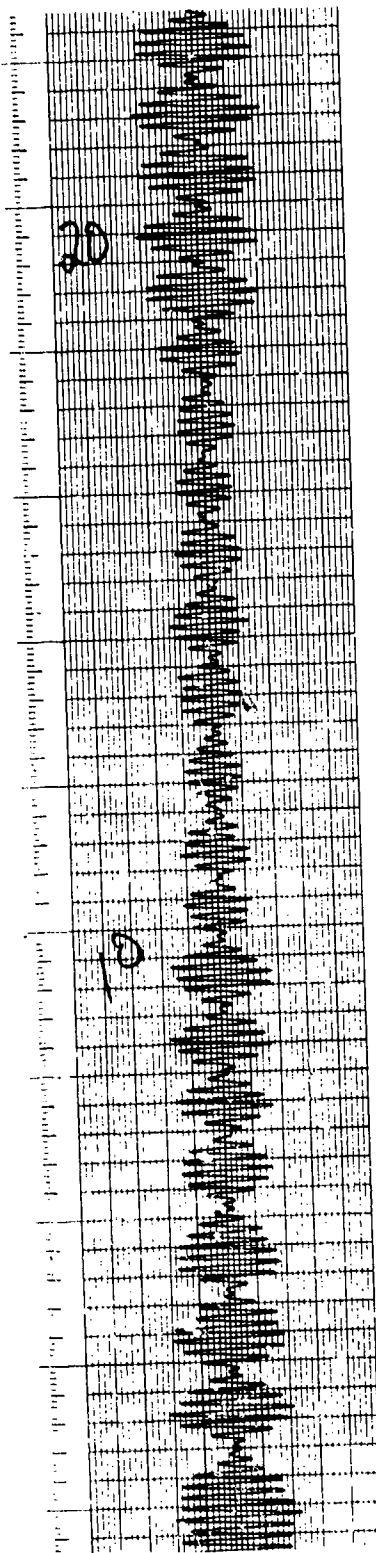


Figure 14. MAID/MILES output when excited by coil and oscillator moving at a uniform rate above buried cable.
Scale: 200 mv/mm vertical, time 5 mm/sec.

Data was taken performing the drop tests on the center of a given winding and then performing the magnetic sensitivity test on the same winding. The drop test was performed 10-20 times at each test point on the cable and the peak-to-peak readings averaged for the final result for that point. Data was taken at 11 random points along a 100 metre cable. The results are shown in Figure 15. The correlation coefficient correlating stress and magnetic sensitivity for this data was 0.46.

A similar test was performed on a cable set in a concrete pad. This cable was only six windings long. The data for these six windings are shown in Figure 16. It can be seen that the magnetic response was essentially constant, while the stress response varied by a factor of two. The correlation coefficient calculated for this data was -0.13.

In order to determine if results from some of the laboratory experiments could be duplicated in the field, experiments similar to those performed in the laboratory were performed on the cables, one in concrete and one in soil. The pipe drop test, using a 7.6 kg weight, was used to produce stress signals in the buried cable. The cable was either magnetized using a large coil with DC voltage applied to it or demagnetized (according to sequence shown below) using the same coil with an AC voltage applied to it. For the cable in concrete, the following series of results were obtained:

Magnetic Condition	Peak-to-Peak Drop Test Signals
No magnetization or demagnetization previously performed	1.4 volts
Magnetized once	3.1 volts
Magnetized again	3.8 volts
Magnetized again	5.2 volts
Demagnetized	0.6 volts

On all but one of the tests on the cable in concrete, following magnetization of the cable, the signal decreased after the first drop; the signal for the first drop was from 13% to 35% larger than the average for the series; for one series the first drop produced a signal that was equal to the average. This corroborates the laboratory results that showed that after magnetization the sensitivity decreased rapidly after a few pipe drops. However, for a cable either in concrete or in soil the decrease was only 35% or less, compared to the large decrease in the laboratory results. This small effect would not degrade an operational sensor. Also, after

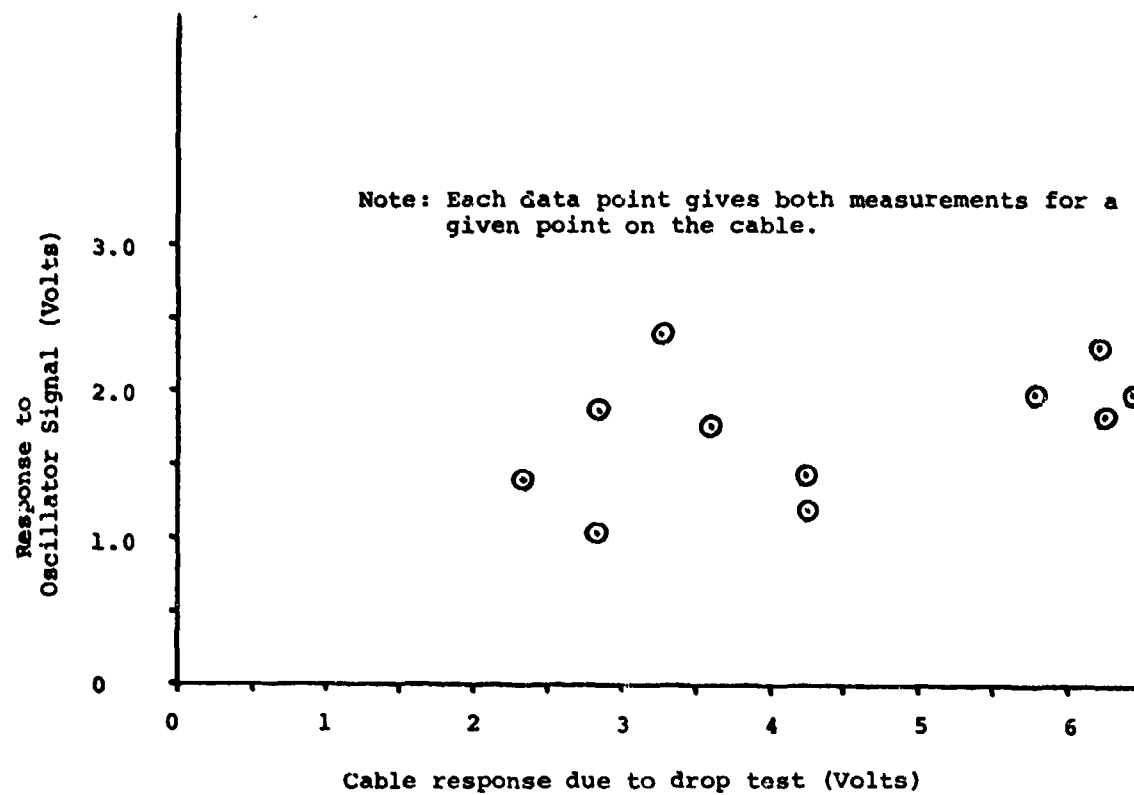


Figure 15. Magnetic and seismic signals for 11 positions along cable buried in soil.

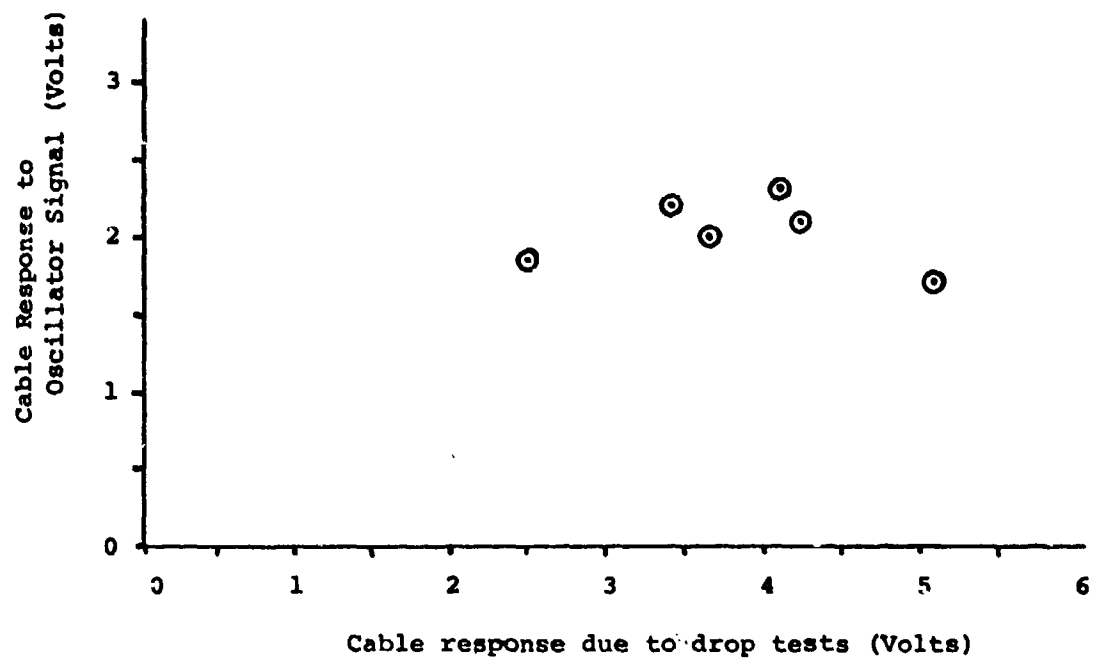


Figure 16. Magnetic and seismic signals for 6 positions along cable buried in concrete.

the decrease had occurred, the sensor was still considerably more sensitive than before magnetization.

SUMMARY

This paper has presented the results of laboratory and field measurements of magnetic and stress properties of MILES cables. It has been shown that the application of a large DC magnetic field has little effect on the magnetic mode sensitivity while it generally increases the stress mode sensitivity. After magnetization this improvement decreases when stressed a few times, but this effect was much greater in the laboratory work than in the field results. The small effect would not degrade an operational sensor, and, even after the decrease, the sensor was more sensitive than before magnetization. The sequence of magnetizing and demagnetizing can be repeated many times with no change in the results observed. Although the laboratory work hints that all cables can be improved by magnetization, some cables in the field are not improved, and it is not known why. Although magnetic properties such as reversible permeability and coercivity are drastically affected by mechanical cold working, the stress mode response does not appear to be as strongly affected. Finally, correlation between stress and magnetic sensitivity is apparently very poor. One as yet unanswered question which could not be addressed in this work is the long-term effects of magnetization. The work reported here was performed in order to better understand the operation of the MILES cable. In those few operational cases where its sensitivity is not adequate, the DC magnetization technique can be used to improve its sensitivity.

Acknowledgement

The authors acknowledge the assistance of E. White, Jr., F. V. Thome, and W. S. Olsen in the work described.

References

1. Starr, J. B., "Status Report for Period 1 July 1976 to 1 August 1976, MILES Signal Enhancement." Honeywell Report W3821-PR3, 9 August 1976.
2. Rome Air Development Center, "Solid Core Round MILES (Feasibility Trade-Off Study)," Honeywell, Inc., RADC-TR-77-46, January 1977.

ACTIVE ULTRASONIC TAPE PERIMETER SECURITY SYSTEM

by

G. Kirby Miller
Security Systems Department
GTE Sylvania Incorporated
Mountain View, CA 94042

Introduction

The Security Systems Department at GTE Sylvania, having been active in the security systems area for over fourteen years, has been aware of the need for reliable perimeter intrusion detection systems for both government and commercial applications. In the past, our main emphasis has been placed on permanent installations using electret coaxial cable transducers.^{1,2} More recently a need for a perimeter system capable of rapid deployment and suitable for temporary or short term security installations has been identified. One concept intended to meet this need is discussed in the following paragraphs. The remainder of the paper is devoted to a presentation of our initial results from the theoretical and experimental investigation of the special tape transducer and electronics required by the system.

The Concept

Figure 1 shows sketches illustrating the concept. The idea is to electrically drive a long multilayered tape transducer at an ultrasonic frequency so that it radiates a narrow beam of ultrasound all along its length (a sonic fence). An object moving into this insonified region reflects some of the energy back to the tape transducer. Some of the reflected energy is sensed by the transducer acting as a microphone and the received signal is separated from the driving signal by a special hybrid electronic package that utilizes the Doppler shift associated with the motion of the reflecting object. A special processor then operates on the signal to generate the appropriate alarm.

Advantages and Applications

Such an intrusion detector has a number of distinct advantages.

1. Because of its mechanical flexibility, it can be fastened to irregular surfaces and go around corners.
2. It can be manufactured with an adhesive on the non-radiating side so that it can be installed very quickly on reasonably smooth walls or ceilings.

3. Since it does not require burial or special supports (such as a fence), it can be quickly rolled into place around a nearly arbitrary perimeter to be protected.
4. Being active, it can be used even in very noisy environments where passive devices would be inoperable.
5. The very low volume of material per unit length coupled with current techniques for automatically making uniform laminated tapes in great lengths allow the likely cost for the transducer to be well below that for any other continuous line perimeter system.
6. Unlike most other perimeter protection systems, the ultrasonic electret tape system would not have stringent alignment or installation requirements.
7. Being acoustic, its operation does not provide an electromagnetic signal that could be used for terminal guidance of a hostile missile. Nor will it produce radiation that could interfere with the operation of SIGINT or ELINT collection equipment.

These attributes make the electret tape system an attractive candidate for a wide range of indoor as well as outdoor perimeter protection applications. Because of its ease of installation, this system has many applications in the area of mobile vehicles that are unattended for extended periods of time. One of the more obvious is for the protection of parked aircraft.

Military aircraft are, at times parked in areas where guards are not available. This system could be carried on the aircraft and be used to provide protection when the aircraft is unattended. Figure 2 shows a C5-A being protected. Immediately after parking, the tape could be quickly unrolled in a large circle surrounding the aircraft. Its upward-pointing beam would then be used to detect any intruder crossing the perimeter. This system would be very reliable and use relatively few personnel to achieve the desired security. Just prior to the plane's departure, the tape could be rerolled for storage on the aircraft. Also, aircraft on the ready-line require intrusion detection that does not hamper the rapid take-off required during an alert. The system would provide the required protection and not hamper the take-off procedure because the aircraft could taxi over the line without harming it.

In addition to vehicle protection where the rapidly deployable capability is important, other applications are of more permanent nature. For example, storage areas of valuable or dangerous materials would be obvious candidates -- oil, fuel, high explosives are specific examples.

Indoor installation of ultrasonic electret tape systems are also expected to be very useful. The tape can be either temporarily or permanently installed on the walls or ceilings of long hallways to provide uniform protection. It can also provide coverage of open doorways and windows into sensitive areas.

Clearly the realization of these advantages and applications hinges on the successful development of the tape transducer. Although electrets have been used in numerous microphone designs and in small-surface-area acoustic radiator design, no elongated tape design has been published nor has any design using an electret transducer both actively and passively.³ The following sections summarize the progress made so far in developing the electret tape transducer. Considerably more detailed treatments are available to the interested reader.^{4,8}

Theoretical Analysis

In order to understand the effects of the numerous design parameters on the performance of the proposed tape transducer and thus aid in its design, a mathematical model believed to simulate its steady-state small-signal operation in all important respects was derived from basic principles using the lumped-element electromechanical analysis of F. V. Hunt.⁵ A set of coupled algebraic equations in the phasor surface charge density and the phasor diaphragm displacement with complex constants derivable from fourteen transducer parameters was derived and solved to allow forming the important measures of transducer performance.

Basic Model and Assumptions

Consider the multilayered tape shown in Figure 3. This is the simplest electret transducer configuration. The driving amplifier is modeled by an ideal sinusoidal voltage source (E_s) in series with a complex source impedance (Z_s). The inactive capacitance, C_i , is made up of any connecting capacitance between the amplifier and the transducer and the capacitance of the shielding layers (not shown) located beneath the inner conductor. The conducting shielding layer is electrically connected to the outer conductor. The incident steady-state acoustic pressure field, p , is assumed uniform over the tape's surface. The outer-most layer is a protective insulating plastic jacket. This is rigidly bonded to the outer conductor which is likely to be of aluminum for lightness. Only these two outer layers are assumed to move (either due to the incident pressure or to the electric current from the driving amplifier). The charge stored in the electret is assumed to be equivalent to a uniform surface charge density, σ_e and the electret is assumed to be bonded rigidly to the inner conductor layer. If C_e is the capacitance per unit area of the electret and "a" is the thickness of the air gap/adhesive layer between the electret and the outer (moving) conductor, the first-order non-linear differential equation relating surface charge

density, σ , on the outer conductor to the applied voltage and air gap is:

$$\dot{\sigma} Z_s \left(S + \frac{C_i}{C_e} \right) + \dot{\sigma} a \frac{Z_s C_i}{\epsilon_a} + \dot{a} \sigma \frac{Z_s C_i}{\epsilon_a} + \frac{\sigma_a}{\epsilon_a} + \frac{\sigma}{C_e} = E_s - \frac{\sigma_e}{C_e} \quad (1)$$

where S is the total surface area of the sample,
 $S = w l$ and ϵ_a is the effective permittivity of
the air gap/adhesive layer

Note that only E_s , σ , and a are functions of time in this equation.

Now consider the mechanical aspects of the transducer. We wish to write an equation expressing the equilibrium of forces per unit area acting on the diaphragm. Aside from the incident acoustic pressure field, p , mentioned before, we have an electrostatic pressure on the outer conductor equal to $\sigma^2/2\epsilon_a$. The reaction pressure due to the acceleration of the moving layers is MX , where M is the total moving mass/unit area. The reaction pressure due to internal friction and heat loss is assumed to be proportional to the velocity of the moving layers with D , the constant of proportionality (damping constant per unit area).

Another reaction pressure proportional to the velocity is that of the radiation load presented by the surrounding medium. This pressure depends on the specific acoustic radiation impedance of the tape, Z_A . The remaining reaction pressure, Kx , is due to the stiffness of the trapped air in the air gap. $K(=\gamma P_0/a$ for air at audio and ultrasonic frequencies) is the effective spring constant/unit area of the air/adhesive layer ($\gamma=1.4$ for air and P_0 =atmospheric pressure). Taking the displacement, x , to be positive in the outward direction, we can write the equilibrium pressure equation as

$$MX + D\dot{x} + Kx + Z_A \dot{x} + \frac{\sigma^2}{2\epsilon_a} + p = 0 \quad (2)$$

Equations (1) and (2) form a mildly non-linear set in σ and x . We can linearize these equations by expanding the time varying quantities in the first few terms of a Fourier series and collecting terms of the same order in ω .

The resulting zero frequency or steady state equations can be solved simultaneously for x_0 , the static displacement of the diaphragm caused by the electret, and σ_0 , the static surface charge density the electret induces on the conductor.

The first order terms, those having harmonic time dependence at the driving radian frequency, ω , can be collected to form

$$\left. \begin{aligned} \sigma Z_e + x T_1 &= E \\ \sigma T + x Z_m &= -p \end{aligned} \right\} \quad (3)$$

where

$$Z_e \equiv \frac{1}{C_0} + j\omega S Z_s \left(1 + \frac{C_i}{S C_0} \right)$$

C_0 is the static capacitance/unit area of the electret device (with $p = E = 0$)

$T \equiv \sigma_0/\epsilon_a$ is the transduction coefficient

$$Z_m \equiv -\omega^2 M - \omega X_A + K + j(D + R_A) = R_m + jX_m$$

$$T_i \equiv T(1 + j\omega Z_s C_i)$$

The simultaneous solution of (3) for the phasors x and σ yields

$$\left. \begin{aligned} \sigma &= \frac{pT_i + EZ_m}{Z_e Z_m - TT_i} & (C/m^2) \\ x &= \frac{-pZ_e - ET}{Z_e Z_m - TT_i} & (m) \end{aligned} \right\} \quad (4)$$

When the transducer is used as a receiver, $E = 0$, and when it is used as a radiator, $p = 0$.

Using the same procedure we may solve for the second order solution x_2 and σ_2 :

$$\left. \begin{aligned} \sigma_2 &= \frac{GZ_m(2\omega) - HT_i(2\omega)}{Z_e(2\omega)Z_m(2\omega) - TT_i(2\omega)} \\ x_2 &= \frac{HZ_e(2\omega) - GT}{Z_e(2\omega)Z_m(2\omega) - TT_i(2\omega)} \end{aligned} \right\} \quad (5)$$

where

$$G \equiv -\frac{\sigma x}{2\epsilon_a} (1 + j2\omega Z_s C_i)$$

and
$$H \equiv \frac{\gamma P_0}{a_0^2} \left(1 - 4.5 \frac{x_0}{a_0} \right) x^2 - \frac{\sigma^2}{4\epsilon_a}$$

a_0 = air gap thickness when the pressure in the air gap is P_0 , the ambient pressure.

Performance Characteristics

From these basic solutions can be derived most of the important performance characteristics of the tape transducers. One of the more critical performance characteristics is the radiation efficiency defined as

$$\eta = \frac{\text{Acoustic Power Radiated}}{\text{Total Electrical Power Required}}$$

This takes on the simple form

$$\eta = \frac{1}{(1 + \frac{R_s}{R_{in}})(1 + \frac{D}{R_A})} \quad (6)$$

where $R_{in} = \chi_m T^2 / (\omega S |Z_m|^2)$ is the real part of the input impedance of the active portion of the transducer. Equation (6) shows clearly that for greatest radiation efficiency the source resistance should be made small with respect to the input resistance of the transducer and that the internal damping should be kept below the real part of the acoustic radiation impedance.

The open circuit receiving sensitivity is another important measure of performance. If S_p is the area of tape exposed to the incident acoustic pressure p , the voltage v , developed across the load impedance Z_s , (corresponding to the source impedance with the ideal voltage source shorted) is $j\omega Z_s$; so using (4) and letting $Z_s \rightarrow \infty$

$$|\frac{v}{p}| = \frac{\omega T S_p}{|Z_e Z_m - T^2|} |Z_s| = \frac{T \ell_p}{|Z_m| \ell} (V/Pa) \quad (7)$$

where ℓ_p is the exposed length and ℓ is the total length.

This result indicates an advantage for minimizing the magnitude of the mechanical impedance while maximizing the transduction coefficient. It also shows that there will probably be a practical limit for increasing the total length, ℓ , while maintaining a fixed length of tape exposed to the pressure p . Since the minimum mechanical impedance occurs very near to mechanical resonance it indicates the desirability of working in that frequency region.

The above performance characteristics treat the radiating and receiving functions individually, but the design treated here is intended to both radiate and receive simultaneously. Hence, a performance characteristic was needed that reflects both radiating and receiving performance. This main performance characteristic, which was used to evaluate the effects of the various parameters on the transducer design, is called the system sensitivity, SS. This quantity is defined as the ratio of the voltage across the inductor due to the target-reflected energy to the total electrical power out of the driving amplifier. The greater this quantity, the less power is required to achieve a given S/N on receiving a target-reflected signal with a given doppler shift.

Implementation and Some Results

A Fortran IV code was written for SSD's Nova computer implementing the relevant mathematical expressions in the previous section (along with many others). The code was designed to provide a user with a flexible and convenient tool for examining the effects of numerous tape-associated variables on the transducer's performance. Most of the program is straightforward. An exception is the calculation of the radiation impedance of the infinite strip. It is believed that the code for this complex quantity is unique to the current program. This is shown and discussed in Appendix C of reference 4.

The basic procedure for using the model to study the effects of the various model parameters was to choose a standard set of parameters and to examine the above performance parameters while varying the parameters being studied one at a time over their likely ranges. This usually led to a logical choice for a new "improved" standard set of parameters.

Some of the general design conclusions based on this computer analysis follow:

1. Use the lowest frequency possible (20 kHz for an ultrasonic system).
2. Use a moving mass that places the mechanical resonance slightly above the driving frequency.
3. Use a series inductance such that its reactance at the driving frequency precisely matches the magnitude of the reactance of the tape load. This is very important for achieving reasonable operation.
4. Use an inductor that has a high Q. Once this Q is chosen the dielectric thickness, air gap thickness, and electret surface potential are chosen on the basis of Figure 4.

Figure 5 shows how the main performance parameters are affected by choice of driving impedance Q when a 3m long tape is driven at 20 kHz by a 1V source, the internal mechanical damping is assumed to be 20 Pa-s/mm, the active width is 20 mm, and FEP teflon is the electret material (the proper parameter values from Figure 4 are also assumed).

In theory this figure shows that it is desirable to maximize the Q of the driving circuit. In practice this is expected to be limited by the increasing effect of short term drift as the Q is increased. In other words, the hybrid may be extremely sensitive to tiny sources of phase deviation if the Q is too high. The Q must not be made so high that the hybrids null balance is adversely affected by normal vibration, air currents or light precipitation.

The performance predicted by Figure 5 is quite encouraging. Assuming that a Q of only 80 is found to be economically practical, the model predicts that a single watt of power will be sufficient to produce a 39 mV received signal (assuming a standard reflector at 1m and a tape length of 3m. For a 30m long tape one watt will produce a receiver output of 390 μ V if all other conditions are unchanged.) To achieve this SS we require a source current of only about 70 mA and expect a diaphragm displacement of 30 nm. Under these conditions and the required 1100 V electret surface potential, the second harmonic is negligible and the radiation efficiency is nearly 0.5%. The ratio of transmitted to received voltage components across the series inductor is 87 dB. This means that in order to separate the transmitted and doppler shifted received signals the hybrid and associated electronics will need at least 96 dB of rejection of the fundamental.

Experimental Investigation

To actually show feasibility it is necessary to design, fabricate and test real transducers. This required a method of charging and measuring electrets, procedures for properly constructing a multilayered design, and testing facilities capable of being used to measure the relevant performance characteristics.

Electret Charging and Measuring

Although there is no reason why a standard electrostatic transducer could not be used, it was decided to use an electret rather than an external bias supply, mainly for the sake of simplicity. However, since electret material is not commercially available we were forced to find a method for charging potential electret materials. Fortunately a number of methods have been published. The liquid contact method was chosen as being suitable for making long thin electret strips in a fairly simple manner in the laboratory.⁷ The film to be charged (FEP Teflon) is slowly pulled over a flat conducting surface just beneath the edge of a fluid-saturated sponge that extends across the desired width. The fluid

(a mixture of ethyl and isopropyl alcohol) is held at the desired high potential (1-2 kV) with respect to the conducting substrate. When the liquid evaporates (a few seconds), the film is charged to the value of the applied voltage and decays at a rate of about 1 dB/time-doubling after the first ten days. This is shown in Figure 6 where each point is the average of nine samples and the solid curve represents 1dB/time-doubling. The thinner films (51 μm) seemed to achieve more stable surface charge and higher density than the thicker films tried (508 μm). It should be mentioned that to compile these data it was required to have a standard means of determining electret strength. This was done by using a special probe-equipped electro-static voltmeter (Monroe 144S-4) to measure the average surface potential and then converting this to equivalent surface charge density.

Transducer Fabrication

The basic practical transducer configuration consists of multiple parallel layers as shown in cross-section in Figure 3 but with the addition of three more layers beneath the inner conducting layer shown. In spatial order from the inner conducting layer these three are: an insulating layer, a shielding conducting layer connected electrically to the outer conducting layer of the figure, and an external insulating protective layer. Of the seven material layers required for this simple configuration some adjacent layers may be purchased already bonded or fused together, e.g., the Mylar-coated aluminum expected to be used for the moving (outer two) layers.

Each layer has some constraints placed on it or has some properties that it should exhibit. Starting from the bottom, the outer protective insulating layer should be tough and abrasion resistant and may be fairly thick ~1 mm but still quite flexible (to allow rolling up of the tape). The shield conductor should be just thick enough to provide a low electrical resistance over the length of the tape (100 μm is adequate). It is bent around the tape sides to join the moving conducting layer to assure complete shielding. The insulating layer between the shield layer and the center conducting layer should be as thick as possible and have the minimum dielectric constant. These requirements reduce the inactive capacitance. A foamed vinyl, about a millimeter thick, seems to be a good choice. The center conducting layer must be much more massive than the moving layer (by at least a factor of 20) and should have lower electrical resistance than the other conducting layers in parallel. The electret layer must of course be able to store charges for many years and should be easy to charge reliably up to 1200 V surface potential. Its thickness should be about 75 μm and it must be rigidly bonded to the conducting layer below it over the entire area of contact with no air traps. The average air gap thickness between the electret and moving conductor should be maintained at about 50 μm and should be rather uniform over the entire active surface of the tape. The moving

conducting layer must be thick enough to be a reasonable conductor (6 μm is adequate) but light enough so that, together with the outer moving insulating layer to which it is bonded, the moving mass density is about 125 g/m^2 .

The most critical bond is that between the electret and inner conducting layers. The reason for this stems from the fact that the electrostatic forces produced in the active mode occur between layers enclosing the air gap. These forces push downward on the electret (and its supporting layers) just as hard as they push up on the moving conductor. Since we wish to maximize the radiation and hence the motion of the outer layers, we need to design the mechanical impedance for the outer layers to be much smaller than that for the electret and its support layers. This is done by making the electret stiff and massive relative to the stiffness and inertia of the moving layers. This goal is made less constraining on the electret if it is rigidly bonded to the inner conducting layer. Since copper is at least four times as dense as Teflon, it does not take a very thick layer of copper to provide a substantial inertia relative to that of the moving layer.

However, any tiny air pockets remaining at the interface will allow the electret layer to move with relative ease and will absorb some of the energy that would otherwise have been usefully radiated by the outer layers. To avoid this potential problem, later transducer models were fabricated using an electret layer that was purchased fuse-bonded to a copper layer.

So far some fifteen samples ranging from .05 to 9 m in length have been constructed. The earlier samples were quite short and were intended to be easy to make, handle, and evaluate rather than optimal in performance. Figure 7 is a photograph of several of the samples made so far.

The biggest problem encountered in fabricating these transducers is in establishing and maintaining a uniform air gap. A number of different approaches to this problem have been tried. Using a center conductor layer that is bowed up in the middle (like an upside down metal measuring tape) allows edge tension on the moving layer to supply normal forces holding the moving conductor against a thin, acoustically transparent, spacing layer (such as an open weave or mesh fabric). However, this promising approach is considered too problematic for potential manufacturers. Other approaches include using a roughened or embossed moving conducting layer, using a thin spacing mesh, and in either case applying a slight vacuum to assure air gap uniformity. The question has not yet been resolved, but the next section indicates the performance levels achieved so far.

Tests and Results

Most acoustic measurements were made in a small anechoic chamber which has at least 99% absorption down to 250 Hz.

Sensitivity. Sensitivity was measured as a function of frequency by monitoring the standard sound pressure at a given position for both the tape transducer and a standard microphone (B&K 4133 and 4135 were used). The standard source was the JBL 075-105 super tweeter and it was driven by a Crown DC-300 being fed by a variable frequency signal generator. Figure 8 shows the rather flat amplitude versus frequency response of a small circular sample in the 10 kHz to 24 kHz range. At 20 kHz the measured sensitivity into a high impedance load is 3.3 mV/Pa or about -49.6 dB re 1 V/Pa. This is in amazingly good agreement with the results of the model. Even the gradual roll off above 18 kHz is in excellent agreement with the theory and reinforces the value, $(20 \text{ kPa} - \text{s/m})$ assumed for the mechanical damping in the model.⁷

Radiation Efficiency. Radiation efficiency is the ratio of the total acoustic power radiated by the tape to the total electrical power supplied by the power amplifier. This is calculated from measurements of the monitoring microphone's output, the amplifier's driving voltage, and the amplitude and relative phase of the current out of the amplifier, and from an estimate of the directivity factor based on measurements of the radiation at various off-axis angles.

The directivity factor was measured by rotating the sample about its long axis while driving it electrically and monitoring its acoustic output one-half meter away at a stationary microphone location. Figure 9 shows the results of this procedure plotted in dB relative to the maximum received signal as a function of angle from the axis. The pattern shows a large major lobe centered about 10° off axis with half-power points separated by about 36° . This implies that the effective radiating width is less than half of the active width. This and the lack of axial symmetry are believed to be evidence of nonuniformity in the air gap layer.

For the sample whose directivity is shown in Figure 9 we took data at frequencies ranging from 15 to 35 kHz. The calculated efficiencies fell in the range 0.001 to 0.012%. These are less than one-fiftieth the values expected from the model assuming that the source impedance matched the conjugate of the input impedance of the transducer. In practice that meant using a series inductance to nearly cancel the capacitive part of the impedance of the transducer. However, inductances are far from ideal and have both capacitance and resistance which may become important (as in the present case where large circulating currents between the inductor and the transducer capacitance were found to dissipate appreciable power when compared with the acoustic power). The suspected

nonuniformity of both air gap layer and electret surface charge density are also likely contributors to the low radiation efficiencies.

Using 8 to 30 V from the driving amplifier, the transducer drew only .2 to 1.3 mA from it (<40 mW) to radiate up to nearly a half microwatt of acoustic power. If the same power-to-transducer-area ratio were to hold for long lengths, then ~ 80 W would be required for a 100 m length to produce the same acoustic intensity. It is believed that considerable improvement in radiation efficiency will be achieved as development continues.

Concept Demonstration

So far radiation efficiency and receiving sensitivity have been considered separately. However, the detection concept depends on the use of both and preferably simultaneously.

Hybrid and Signal Extraction. To utilize the transducer simultaneously as both transmitter and receiver of acoustical energy, we used the setup shown in Figure 10. We designed and constructed a hybrid circuit. This consists of two matched high-Q inductors, one of which is tuned to series resonate with the tape sample and the other with a lumped element dummy tape. Pickoff windings of each inductor are connected differentially so that the driving frequency voltage is nearly cancelled (~47 dB of rejection). The error signal is then summed with an out-of-phase adjusted version of the reference to obtain another 37 dB of fundamental rejection. The remaining signal is then applied to a multiplier along with an attenuated version of the reference so that when their product is fed to a lowpass filter only the doppler components remain (another 40 dB of rejection is obtained).

When this instrumentation was used with several samples up to 3 m in length, the motion of insonified objects could clearly be correlated with variation on the display scope. Our first (and only) effort at driving a 90 m sample (Figure 11) with this arrangement has not provided satisfactory detection sensitivity. Apparently the system sensitivity does indeed degrade with the square of the length (as predicted by the model). In addition, the noise level (a quantity not included in the computer model) increases at least proportionately with the tape length so that difficulties compound rapidly with increased length. We expect to establish the maximum usable length in a continuing effort.

Dual Tape Concept. Although there is still some doubt about the feasibility of reducing a long single tape system to practice, this is not the case for a dual tape system. In this case two separate tapes are layed down side-by-side (possibly on the same substrate) but mutually shielded so that one may be driven while the other is used as a

receiver. This concept has the advantages of considerably greater simplicity in the electronics. It requires only the multiplier and filter portion of the block diagram in Figure 10. It has also been demonstrated on tapes as long as 9m. Because it can be manufactured on the same base and in much the same manner as the single tape, it is still expected to be small, rollable and inexpensive. Another advantage is that each tape can be designed to optimally perform a single function (radiation or receiving) rather than designed as a compromise to do both as well as this constraint allows.

Conclusions

The feasibility study has been primarily aimed at investigating the transducer portion of a new active ultrasonic line intrusion detection system concept. The following are conclusions resulting from this effort:

1. The ultrasonic doppler detection concept appears to be sound and the electret tape developed appears to be an adequate source and receiver for such a system. However, for long runs a dual tape transducer may be necessary.
2. Construction techniques are available for fabricating tape transducers (up to 9m so far) that have open circuit sensitivities of at least -50 dB re 1 V/Pa and radiation efficiencies of at least 0.01%. It is felt that significant improvements will be made in subsequent samples.
3. A computer-implemented model of the transducer has been developed for use in assessing its performance as a radiator, receiver and in a detection system. Agreement between the predictions of the model and the measurements in the laboratory are good with discrepancies believed due to imperfections in the construction and measurement techniques.
4. This model has been used to determine optimum single tape designs that depend on the Q of the source impedance.
5. A simple but effective liquid contact charging technique has been developed that produces effective surface charge densities on 50 μm FEP of at least 0.1 mC/m² even after four months. The typical decay rate is observed to be about 1 dB/time doubling after the first ten days. The electret surface potential achieved can be accurately controlled.

6. The internal mechanical damping is very large in the current transducers (50 to 70 times the characteristic impedance of air). This makes for lower efficiency but allows for fairly broad band operation so that the detection system can be operated over a frequency range of at least half an octave.

Acknowledgements

This work was sponsored by Rome Air Development Center, Contract Numbers F30602-75-C-0075 and F30602-76-C-0375, and by GTE Sylvania's Internal Research and Development program.

References

1. G.K. Miller, "Development of Electret Transducer Line Sensors," Proceedings 1974 Carnahan and International Crime Countermeasures Conference, J.S. Jackson, Editor, University of Kentucky, Lexington, Kentucky, pp. 22-25, August 1974.
2. K.M. Duvall, R.W. Scott, "Development of a Perimeter Sensor Using a Buried Electret Cable," Proceedings, 1975 Carnahan Conference on Crime Countermeasures, J.S. Jackson, Editor, University of Kentucky, Lexington, Kentucky, pp. 98-103, May 1975.
3. G.M. Sessler, J.E. West, "Electret Transducer: A Review," J. Acoust. Soc. Am. 53, pp. 1589-1600, June 1973.
4. G.K. Miller, Electret Tape Transducer Final Report, GTE Sylvania for RADC Contract No. F30602-75-C-0075, 26 November 1975.
5. F.V. Hunt, Electroacoustics, Harvard Monographs in Applied Science, No. 5, Harvard Univ. Press, Cambridge, Mass., 1954
6. P.W. Chudleigh, et al, "Stability of Liquid Charged Electrets," App. Phys. Lett., 23, No. 5, p. 211, September 1973.
7. W.M. Wright, "High-Frequency Electrostatic Transducers for Use in Gases," Technical Memorandum No. 47, for ONR Contract Number ONR-1866(24) at Harvard University, Cambridge, Mass., April 1962.
8. G.K. Miller, Electret Tape Intrusion Detection Final Report, GTE Sylvania for RADC Contract No. F30602-76-C-0375, June 1977.

SYSTEM CONCEPT

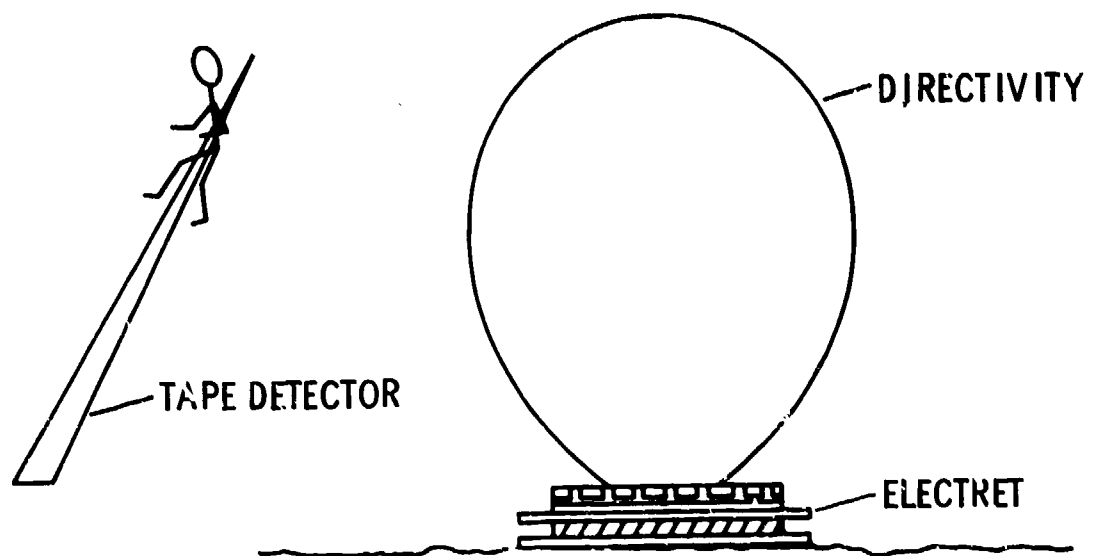


Figure 1 Active Ultrasonic Electret Tape Concept

PARKED AIRCRAFT PROTECTION

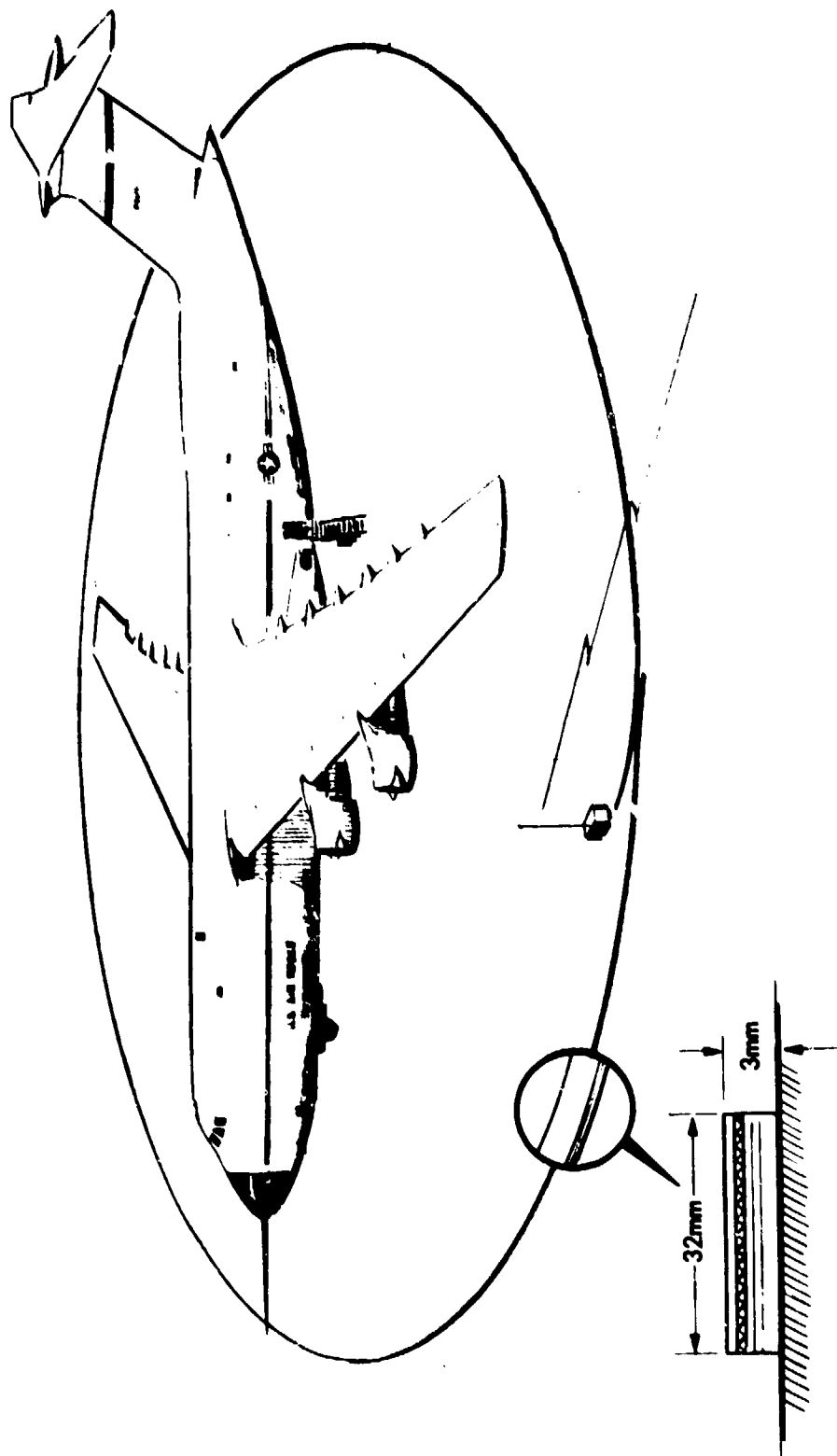


Figure 2 Parked Aircraft Protection

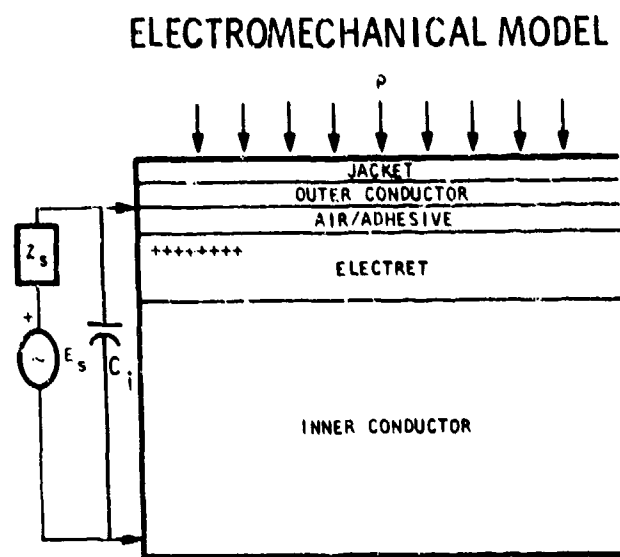


Figure 3 Configuration of Transducer and External Energy Sources Modeled

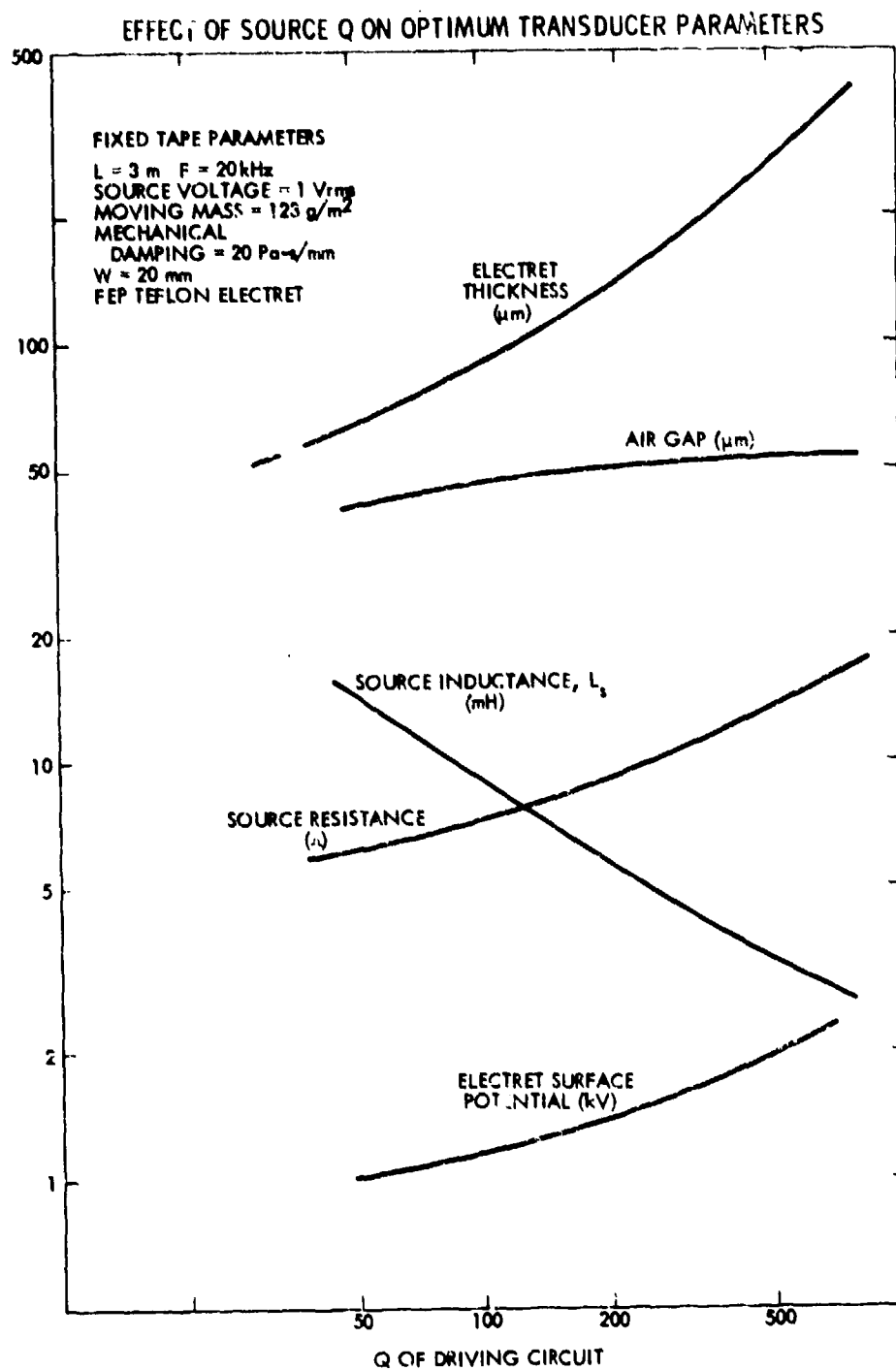


Figure 4 Computed Design Parameters for Optimum Single Electret Tape Transducer

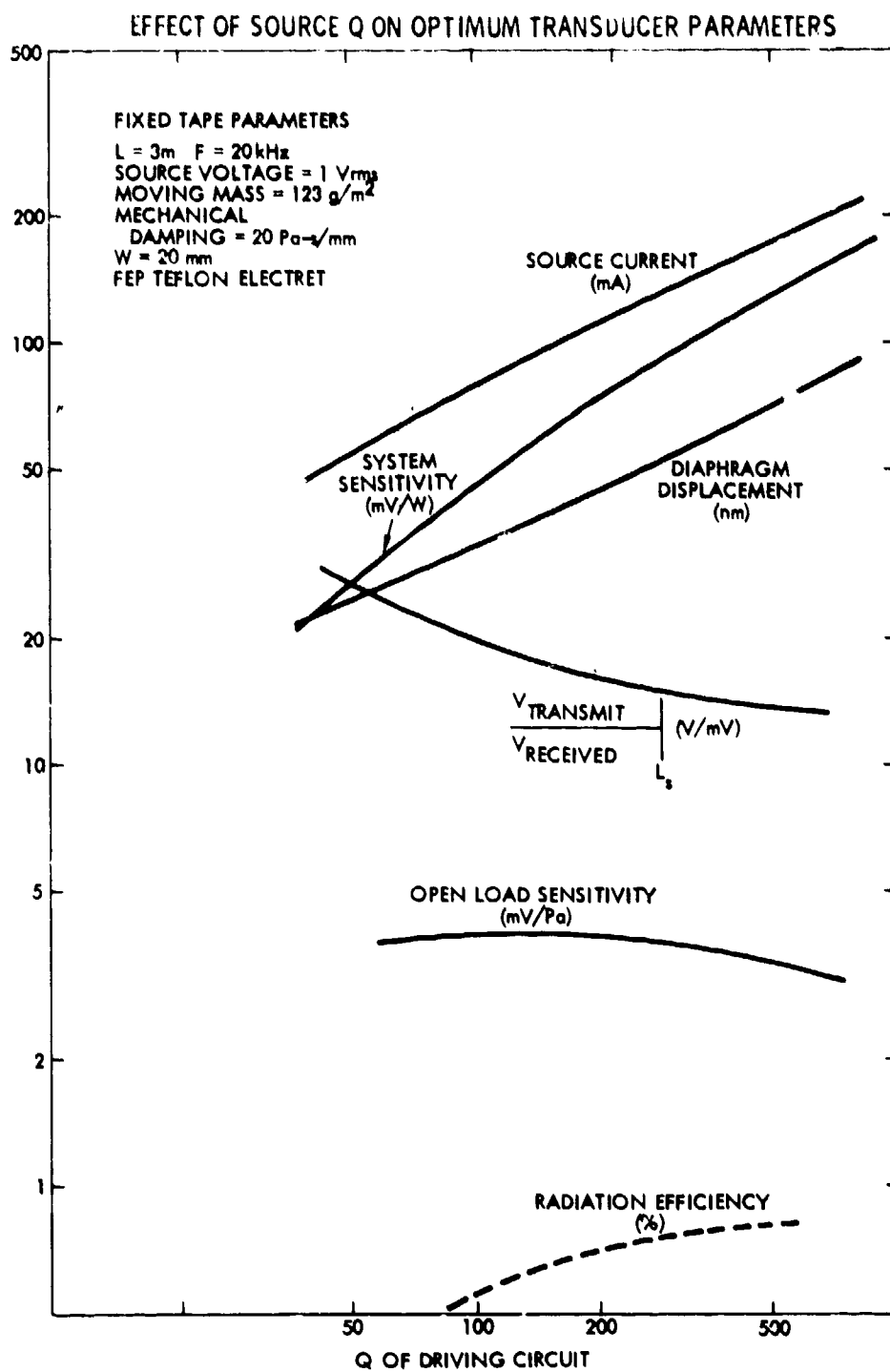


Figure 5 Computed Performance of Optimum Single Electret Tape Transducer

ELECTRET CHARGE DECAY

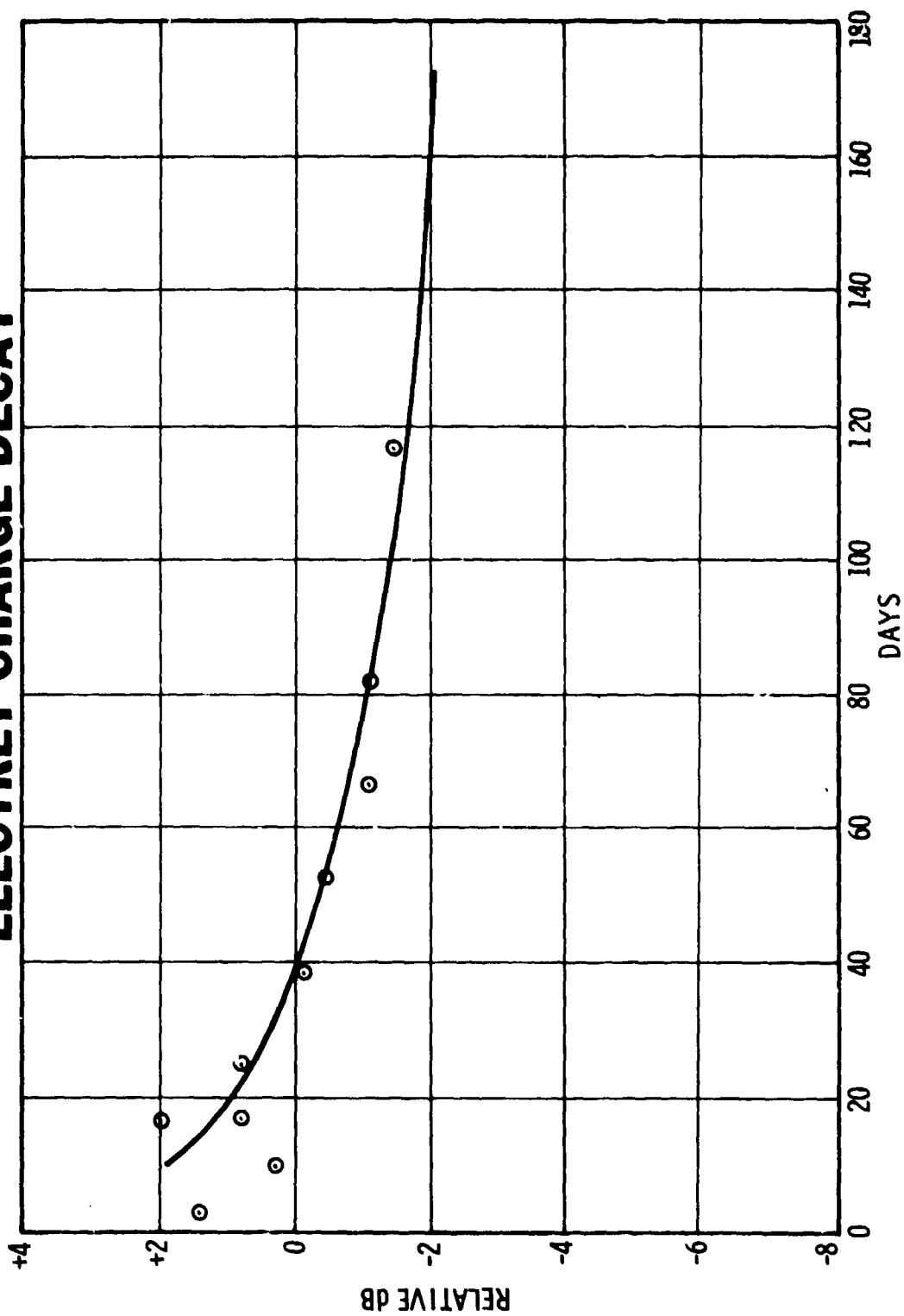


Figure 6 Measured Electret Charge Decay

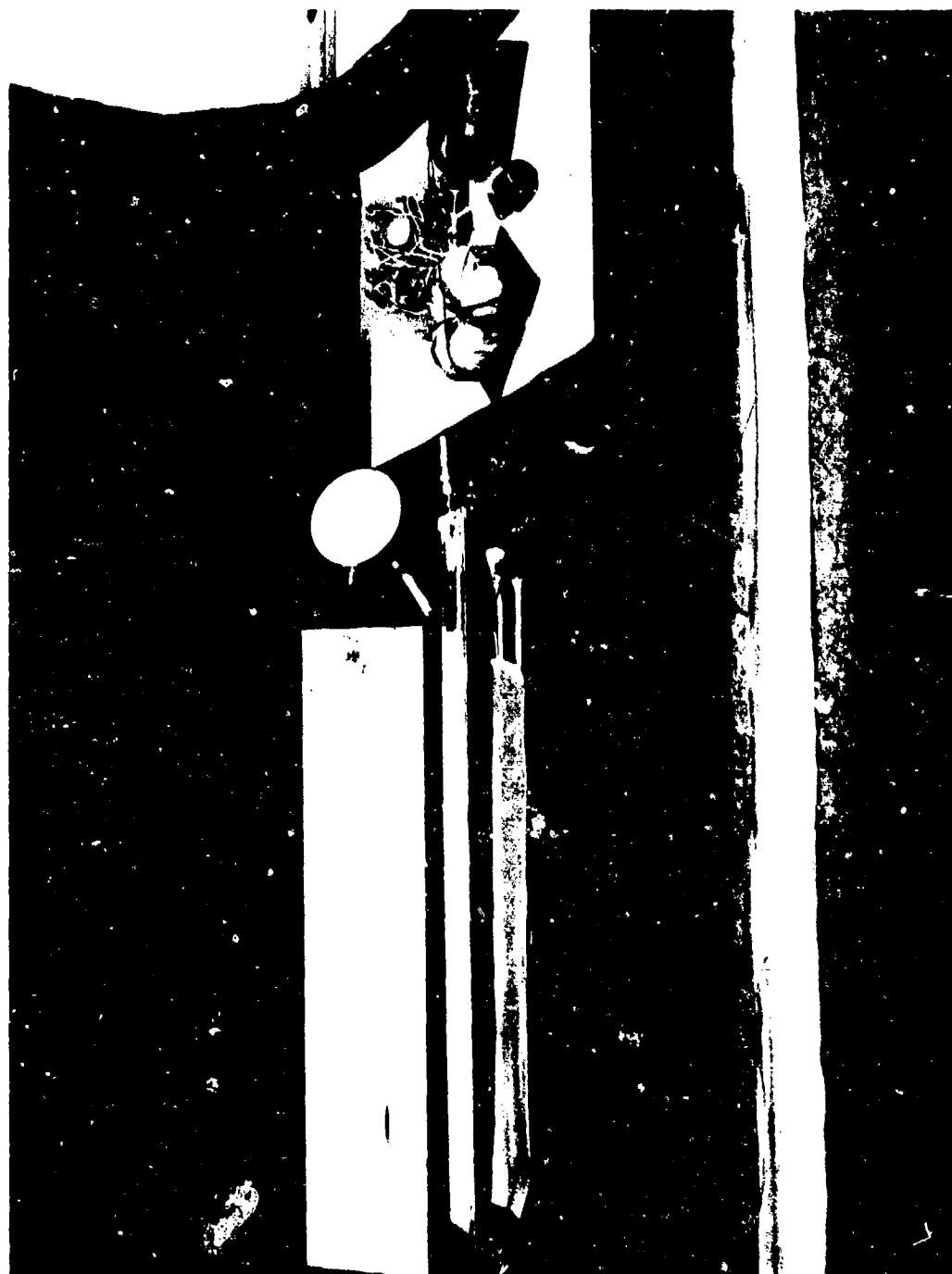


Figure 7 Several Different Electret Transducer Configurations

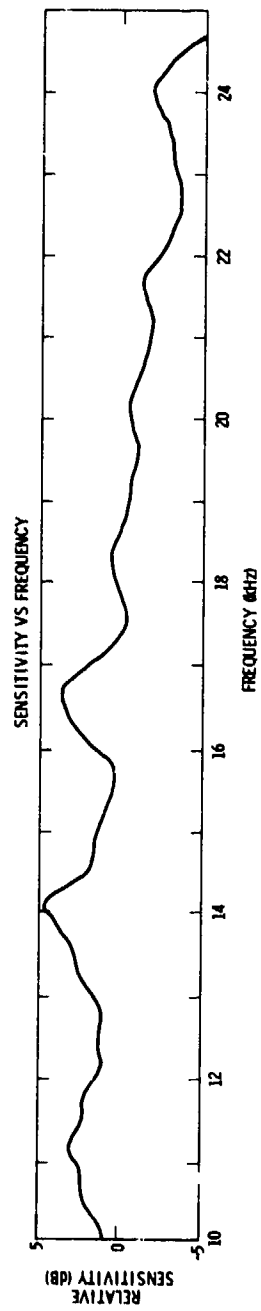


Figure 8 Typical Measured Amplitude versus Frequency Characteristic for Constant Incident Pressure

Figure 8

MEASURED DIRECTIVITY PATTERNS

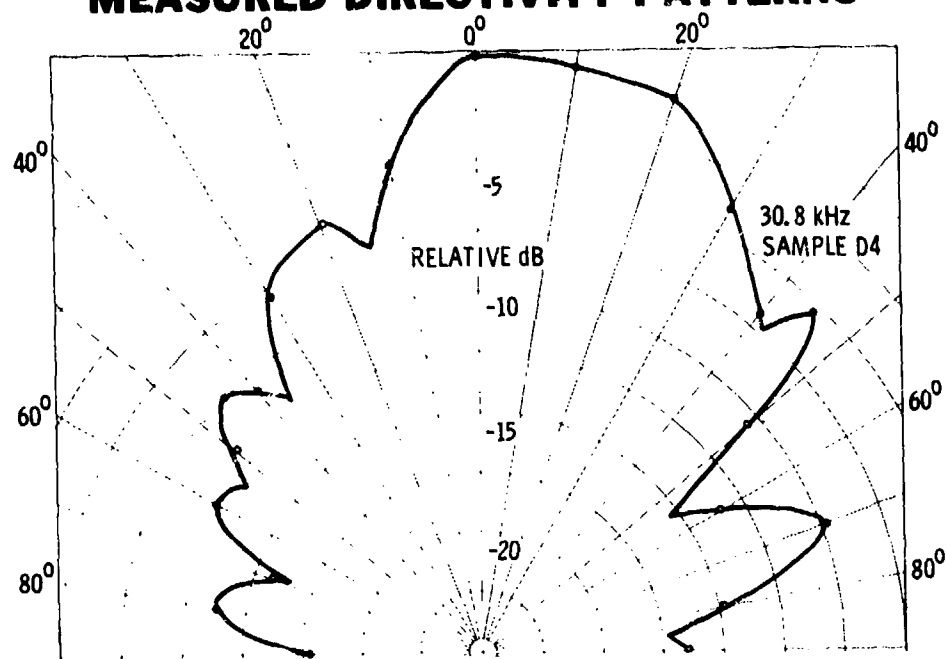


Figure 9 Measured Directivity of Short Sample

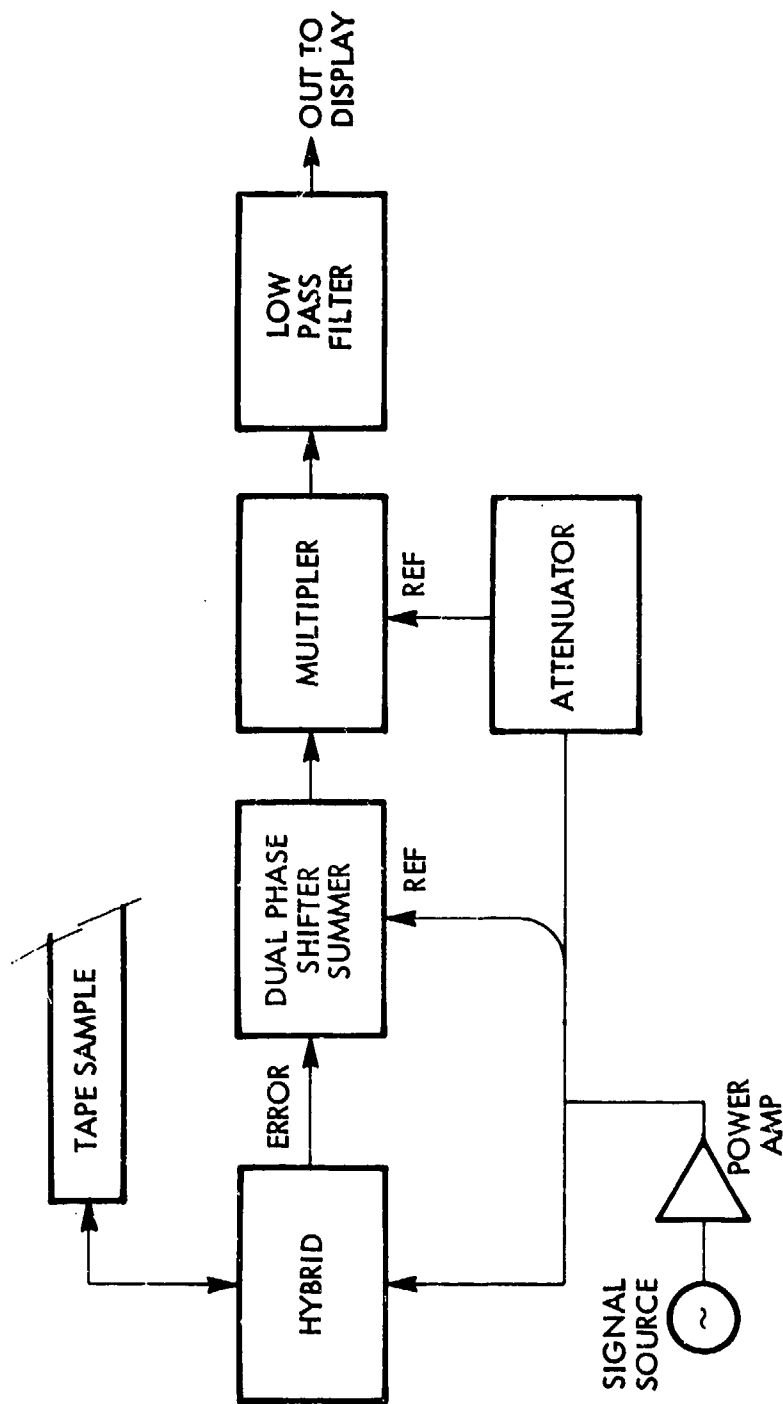


Figure 10 Block Diagram of Signal Extracting Setup

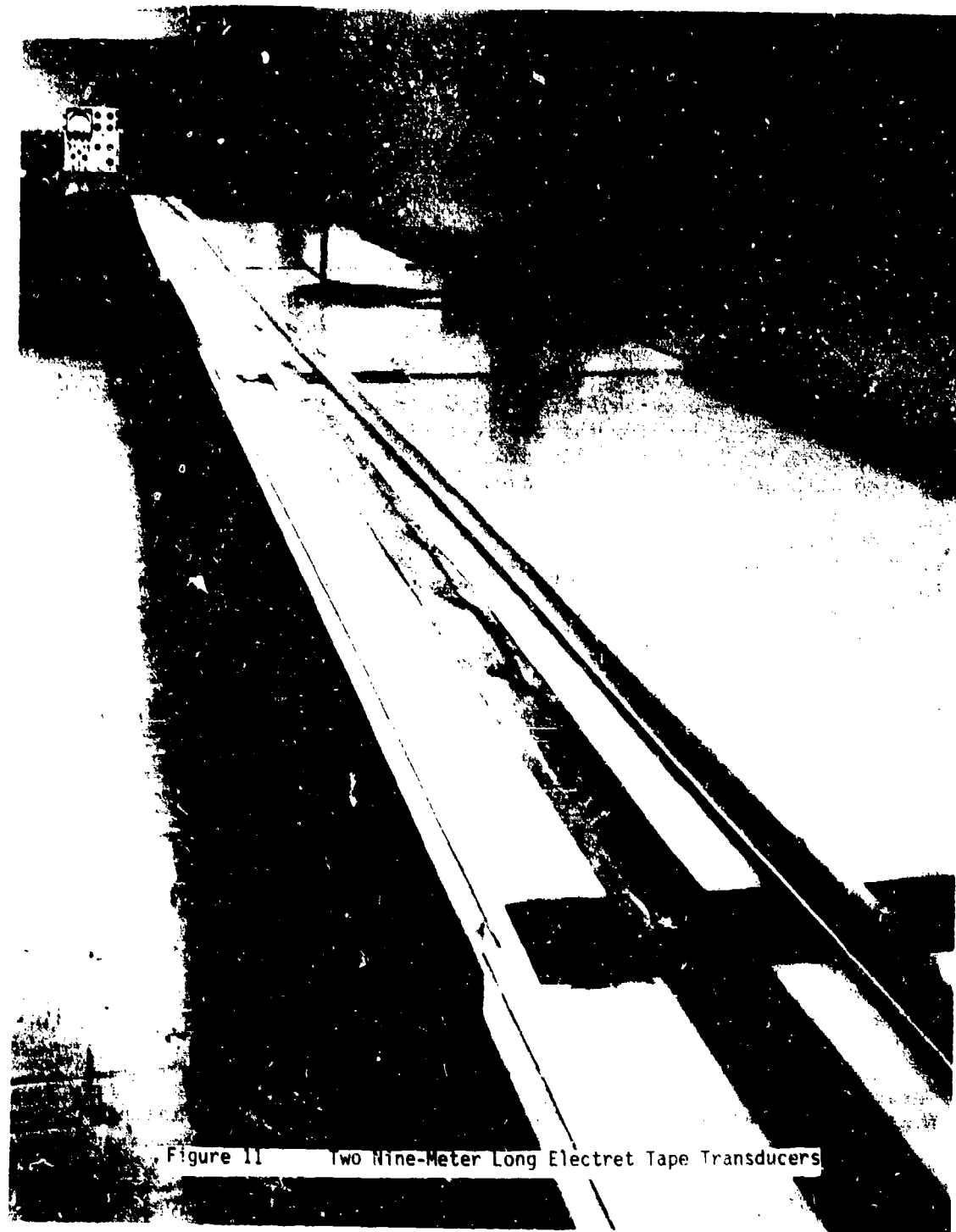


Figure 11 Two Nine-Meter Long Electret Tape Transducers

PIEZOELECTRIC AND PYROELECTRIC POLYMER SENSORS

Seymour Edelman
National Bureau of Standards
Washington, D.C. 20234

Abstract

The polymer poly(vinylidene fluoride) (PVDF) can be used as the active element of piezoelectric and pyroelectric sensors and has properties which make it useful in military applications.

The purpose of this talk is to summarize a number of applications of piezoelectric and pyroelectric polymer sensors. This compilation is meant to give a feeling for the versatility of the material and some idea of the kind of application for which a polymer sensor can be used with advantage over a conventional sensor.

As a piezoelectric material it has good response to dynamic stress or strain over a wide range of frequencies, is not likely to be harmed by the usual ambient conditions, salt water, soaps, common organic solvents, nearby explosions, or other mechanical shocks. It is readily available in relatively cheap, thin, light, flexible sheets of large area and is easily shaped for a particular application.

Many of the same characteristics hold for its use as a pyroelectric material. It has good sensitivity to temperature changes caused by radiation of a wide range of wavelengths from infrared to ultraviolet.

Piezoelectric polymer instruments can be used as microphones and sound sources in air, as hydrophones in water over the frequency range from a few hertz to many megahertz, as detectors of stress or strain in the soil, for a number of biomedical applications, as detectors of acoustic emission on a wide variety of materials and structures, as vibration detectors, to monitor the acoustic signature of components of machinery as a means of detecting incipient failure, and for intrusion detection.

Pyroelectric polymer instruments can be used for intrusion detection, for infrared imaging, to detect incipient fires, and to monitor temperature changes in operating machinery from a distance.

PIEZOELECTRIC AND PYROELECTRIC POLYMER SENSORS

The purpose of this talk is to summarize a number of applications of piezoelectric and pyroelectric polymer sensors. This compilation is meant to give a feeling for the versatility of the material and some idea of the kind of application for which a polymer sensor can be used with advantage over a conventional sensor.

Conventional piezoelectric materials are typically crystalline or polycrystalline, hard, stiff, brittle, and dense. It is difficult to machine them into thin layers or to obtain them in sheets of large area and they are expensive. Polymers are compliant, flexible, tough, and light. They are available commercially in layers as thin as six micrometers (.00025") they are available in 1000 meter rolls over one meter wide; and they are relatively cheap.

Measuring instruments using conventional piezoelectric materials usually have metal bases and housings and require threaded holes or specially ground flat surfaces of appreciable area for mounting. Polymer instruments [1,2] typically consist only of the active material and a lead of evaporated metal on the same polymer. The active material can be cut to any shape that is suitable for a particular use and can be attached to a surface whose only preparation is cleaning. Rubber cement, cyanoacrylate, epoxy, or other cements can be used. A polymer gage can be attached to curved, twisted, or compliant surfaces.

Conventional instruments tend to have many high-Q resonances both because of their internal spring-mass systems and because of the effect of the mass of the instrument on the elastic compliance of the mounting surface. The responses of polymer instruments are flat with frequency over wide ranges, typically into the megahertz range, their resonances are low-Q, and their mass is so low that they do not resonate with the mounting surface. The piezoelectric modulus, g , measures the usefulness of a material as a sensor. Its value for the usual piezoelectric polymer, poly(vinylidene fluoride) (PVDF), is about six times as large as for a typical lead zirconate titanate ceramic. On the other hand, the value of the d modulus, which measures the usefulness of the material as a generator of motion or as a sound source, is larger for the ceramic by a factor of about 21.

There are some cases of considerable importance where polymer instruments are uniquely suited. Usually the advantages of polymer instruments show up in dynamic measurements. A typical case is measuring the level of vibration at a point on a thin metal sheet. Such a panel might be part of a helicopter structure or a propeller

blade. A conventional accelerometer mass loads the object to which it is attached and significantly increases the surface density. The vibration pattern of the sheet will rearrange itself so that the motion at that point is minimized and the measurement is unrepresentative. On the other hand, cementing a small piece of polymer film to the metal sheet need not change the surface density significantly and a meaningful measurement can be made. The amplitude of vibration and the variation of vibration level with frequency measured by the polymer are more nearly representative of what the level at the point would be with no instrument attached. Conversely, both the vibration amplitude and the spectrum of resonances measured by an accelerometer would be affected by the presence of the instrument. Thus, it is practicable to distribute a number of polymer vibration gages over the surface of a panel and to infer from their reading the mode of vibration of the panel under various conditions. This kind of study cannot be performed effectively with conventional vibration measuring instruments.

Polymers have somewhat similar advantages for studying the noise signatures of bearings, gears, and transmission systems. The mass of a conventional instrument acting on the compliance of the mounting surface introduces a set of resonances which combine with the noise spectrum being studied and which may hide the changes of the spectrum which indicate the first signs of deterioration. Also, the size of conventional instruments and their need for a threaded mounting hole may dictate their location at some distance from the origin of the noise. A polymer gage, almost always, can be mounted directly to the noise source with a much better chance of picking up an uncluttered spectrum. This makes it possible to monitor the condition of operating machinery continuously or at short intervals and to give the operator adequate warning before catastrophic failure occurs.

Polymer gages are handy for acoustic emission studies on helicopters, tanks, and other vehicles. They can be bonded to irregularly shaped surfaces and provide good coupling. Their high internal damping minimizes the effects of ringing. They have a wide useful frequency range extending well into the megahertz region. Their sensitivity is adequate for most work and can be increased by stacking and by the use of bias, if necessary. It is cheap and convenient to use gages in sufficient numbers so that noise sources such as growing cracks can be located by triangulation in time to prevent serious damage.

With the addition of lead foil as a seismic mass, polymer gages can be used as flexible accelerometers with an unusually wide frequency range but rather low sensitivity.

The detailed mechanism of piezoelectric activity in a polymer is complicated and controversial. The composition of the polymer, its division into amorphous and crystalline parts, the crystal structure, the presence of surface and space charges and of ionic impurities have all played parts in different explanations. We get useful guidance in preparing material for use in measuring instruments if we consider the polymer to consist of long chains of identical units called monomers. In the case of PVDF, the commonly used piezoelectric polymer, the chains consist of linked carbon atoms and each monomer consists of two carbons, one joined to two hydrogen atoms and the other joined to two fluorine atoms. Each monomer has a strong dipole moment. As the material is received the dipoles are oriented randomly. The material is heated, a strong electric field applied, and the material returned to room temperature with the field applied. We can consider that this process results in the alignment of a significant number of dipoles normal to the plane of the sheet. The dipoles can be considered to be stiffer than the bonds between dipoles in adjacent chains so that any stimulus that changes the thickness of the sheet will change the surface density of charge on each surface. A compensatory flow of charges through the circuit connecting the electrodes forms a signal. More detailed analyses have been published [3].

As strain gages, polymer gages have about the sensitivity of semiconductor gages but they can be used without the need for bias voltage or bridge balancing. Also, they are not brittle and can be used where mechanical shock occurs and on curved surfaces. However, they differ from the usual type of strain gage in several ways and these differences can be useful or annoying, depending on the circumstances. Our polymer gages respond with equal sensitivity to strain in any direction in the plane of the sheet. It is possible to make strain gages of stretched material whose response is greater in the stretch direction than perpendicular to it by a factor of about seven. If charge or short-circuit current is measured, the sensitivity is proportional to the area of the gage. If open-circuit voltage is measured, the sensitivity is proportional to the thickness of the gage.

A potentially important use of polymer strain gages is to detect and measure the strains accompanying stress waves in the soil. Such gages might be used to detect and follow tunnelling operations, to detect vehicle movements, to calculate the effect of explosions on buried structures, etc. The gages used for soil motion are in the form of long thin ribbons. The length of the ribbon determines the range of frequency or wavelength for which it is suitable. If the ribbon is too long for a particular wavelength, much of its output will come from flexure caused by shorter wavelengths rather than strain and if it is too short it will not experience enough strain to give a good signal-to-noise ratio. Within its frequency range such a ribbon works very well. It is easily placed in the ground and quickly becomes a part of the soil, moving exactly as the surrounding soil moves. Calculation of all of the components of strain at a point is simplified if six such ribbons are arranged along the edges of the corner of a cube. Three gages of equal length extend along the positive x, y, and z axes from the origin and three more join the outer ends of the gages along the axes, x to y, y to z, and z to x. This geometry separates the components of shear from longitudinal motion quite easily and thus gives a complete representation of the movement of the ground at that point. A modification of such gages might be used to detect disturbed ground and buried mines.

Similar gages supplemented by acoustic emission sensors attached to bedrock can be used to detect and locate mining operations, progress of a tunnel, sudden movements in earth dams, incipient avalanches in snow fields, etc.

Piezoelectric polymers have been used in hydrophones for sonar use [4,5]. Similar units can be made up as arrays and used for finding fish or for underwater geophysical exploration.

The flexibility, light weight, and freedom from fatigue of polymer gages and their leads make them suitable for measuring deflections and stresses in tires. Their pyroelectric properties, to be discussed later, make them suitable for determining heating in tires as well.

Voice communication in combat vehicles is difficult because of the noisy environment. Piezoelectric polymers can improve communication over conventional instruments. A stack of polymer sheets can conform to boney surfaces and provide sound to the ear by bone conduction without the discomfort imposed by conventional bone-conduction sound sources. The flexibility and light weight of the polymer make it feasible to line the inside of an earphone with the polymer providing a higher sound level with greater fidelity than can be achieved by the small conventional speakers usually used. If another sheet of polymer is used to coat the outside of the earphone and its signal is fed back to the speaker inside the shell it is possible to adjust the signals so that the ambient noise is mostly cancelled and the speech is maximized, optimizing intelligibility.

The thinness of the polymer sheet allows it to be used as the active material in a noise-cancelling microphone which responds very well to a nearby source such as a speaker's lips while minimizing the effect of ambient noise. Such a microphone can be lighter than one using conventional materials.

The thinness and flexibility of polymer gages make them feel and act mechanically very much like skin. This characteristic is used in automobile crash studies. A pattern of polymer stress gages are put on the head and chest of anthropomorphic dummies to detect the areas of contact and the time history of the impact. Since the gages behave very much like skin, they do not disturb the anthropomorphic behavior of the dummy and, since they are flexible they are not likely to be damaged in the crash. Conventional pressure gages form concentrated masses whose behavior during a crash would be much different from the behavior of the rest of the skin of the dummy and they are likely to be damaged during a crash. Their impact is also likely to damage parts of the automobile in ways that are not characteristic of real crashes.

Similar gages could be used to measure the dynamic stresses exerted by vehicle seats, seat belts, harnesses, helmets, etc. under battlefield conditions allowing redesign to minimize fatigue.

The similarity of polymer gages to body tissues has other potential uses. We have developed gages to be inserted into monkey brains to determine how much of an impact to the outside of the head is felt as a pressure pulse in the brain. The polymer gage is used here because its density is close to that of the brain material. If a conventional pressure gage were used, inertial effects would produce more signal than the pressure change.

Polymer gages can be applied like bandaids to monitor heart sounds and pulse rates of patients during exercise. Conventional instruments can be used but their size and mass make the patient conscious of their presence and his behavior is not entirely normal. He is much more likely to forget polymer gages. Similar considerations hold for monitoring during combat. Arrays of such gages can be used for acoustical holography and provide better coupling to flesh than the transducer usually used.

A different kind of application depends on the fact that poling a polymer stores about one and a half times as much energy per unit volume as is stored in piezoelectric ceramic under similar conditions. One example we have worked on is development of detonators for ordnance where polymer sheet is preferable to ceramic because it is lighter for a given energy storage, can be connected to provide a desired electrical output impedance more readily, and can be used to line enough of a shell to provide detonation for any angle of incidence.

A typical sensor consists of a sandwich of two polymer sheets. Each sheet has evaporated metal electrodes on both faces and the sheets are cemented together so that charges of the same polarity appear on the inner faces. The center conductor of a coaxial cable is connected to the electrodes on these inner faces and the shield of the cable is connected to the electrodes on the outer faces. In this way all exposed surfaces are at ground potential and the signal inside the sensor is well shielded. Usually, the active area of the gage is connected to the coaxial cable by a long thin strip of metal evaporated onto an inactive portion of the same polymer sheet that contains the active part of the gage. In this way, the masses of the connectors and cables are kept from affecting the measurement. The active portion of the gage can be cut to any reasonable size and shape needed for the measurement.

PVDF is pyroelectric as well as piezoelectric [6]. If we consider the picture of a poled polymer as containing a large number of electrical dipoles aligned normal to the plane of the sheet, we can see that lowering the temperature will make the sheet thinner, just as pressure will. In either case, the effect is to change the surface density of charge on the surfaces, giving a signal. Since a signal due to pressure comes from the same phenomenon as a signal due to temperature, there is no way to separate the two effects if they occur at the same frequency. Fortunately, many of our measurements are made at constant temperature except possibly for the effect of adiabatic heating which can be taken into account in the calibration process. In many other cases, the temperature changes slowly compared to the rate of pressure change so that the effect of temperature can be filtered out. Nevertheless, it must be realized that the polymer gages have a very large pyroelectric effect and also that the sensitivity of the pressure gage varies with temperature. A change of one degree celsius gives an output of about three volts for a typical thickness of 25 μm .

In those cases where the temperature changes at the same frequency as the pressure or where the ambient temperature changes drastically, we have evaporated a bismuth-antimony thermocouple right onto the polymer surface. This polymer thermocouple is an interesting instrument in itself since the metal is only a few hundred angstroms thick giving a very fast response. It is not subject to fatigue and has many of the other advantages of polymer instrumentation. In this application, the thermocouple signal is proportional to temperature but not to pressure. The pressure gage signal is a function of both temperature and pressure. A little arithmetic gives the effect of pressure alone.

As the active material in pyroelectric measuring instruments, PVDF is not quite as sensitive as some crystalline materials but it is much cheaper, can be obtained in thinner sheets of large area providing a fast response, and it is less subject to damage or spurious readings because of ambient conditions.

We have made a number of sensors for the Air Force which could detect an increase of heat behind a metal wall prior to spontaneous combustion. They could also detect changes in the operating temperature of machinery from a distance, providing a warning for either heating or cooling outside of an acceptable range.

We have made detectors capable of responding to the flame of a paper match at four meters or the body heat of a man at 15 meters.

These numerous applications demonstrate the versatility of polymer sheet for dynamic measurements. This makes it possible to design the measuring instrument to be suitable for the conditions under which the measurement is made rather than to try to adapt the conditions of measurement to suit the needs of a conventional instrument designed to have general utility.

References

- [1] S. Edelman, S. C. Roth, and J. F. Mayo-Wells, U. S. Patent 3,970,862, July 20, 1976.
- [2] S. Edelman, L. R. Grisham, S. C. Roth, and J. Cohen, J. Acoust. Soc. Am. 48, Part 1, 1040 (1970).
- [3] F. I. Mopsik and M. G. Broadhurst, J. Appl. Phys., 46, 4204 (1975).
- [4] S. Edelman, Nat. Bur. Stand. (U.S.) Interagency Rep. 75-760, pp.210-217 (1975).
- [5] J. M. Powers and T. D. Sullivan, J. Acoust. Soc. Am., 60, Suppl. No. 1, 547, Fall (1976).
- [6] J. Cohen, S. Edelman, and C. F. Vezzetti, Nature Physical Science, 233, No. 36, 12, (1971).

DISCUSSION OF SELECTED NEW
SENSOR TRANSDUCER TECHNOLOGY
by Herbert Reich

In development of line sensors several principles dominate design objectives: a sensor must demonstrate a high probability of detection, a low false alarm rate, and the ability to discriminate between targets. Ease of installation is another consideration but is often subordinated to achieve better performance.

Three sensor phenomena which help fulfill the above objectives have been favored by MERADCOM in the past 2 years. These have been strain, magnetic and radiation.

A. The Strain Sensitive Cable Sensor.

The Strain Sensitive Cable Sensor affords the user an effective strain sensor with simple installation. The following properties of this sensor make it attractive:

1. Inverse R^5 signal drop-off affords immunity to urban noise.
2. Responsiveness to cautious intruders.
3. Single trench installation.
4. Signal generated is amenable to target classification.

Description:

The SSCS operates on the tribo-electric principle wherein the outer shield and the inner conductor of a selected coaxial cable behave as plates of a capacitor (See Figures 1 and 2). Minute strain movement of any section of the coaxial cable results in generation of a charge which can be bled off and amplified by either a voltage or current type amplifier. A voltage type amplifier can be used with short cable lengths; however, where longer cable lengths are used, a current type amplifier must be used to prevent the added shunt capacity from having an adverse effect on the signal.

Background and Current Application:

Work on the SSCS was started at MERDC in 1970. Work was initiated by Mr. Art Tiemann. The first effort was directed toward finding the best possible transducer. Sixty-two different cables were tested to obtain best signal output. The cable which MERDC found to make the best transducer was the Microdot equivalent of the RG188.

FIGURE 1 - Strain Sensitive Cable Sensor (SSCS) Transducer

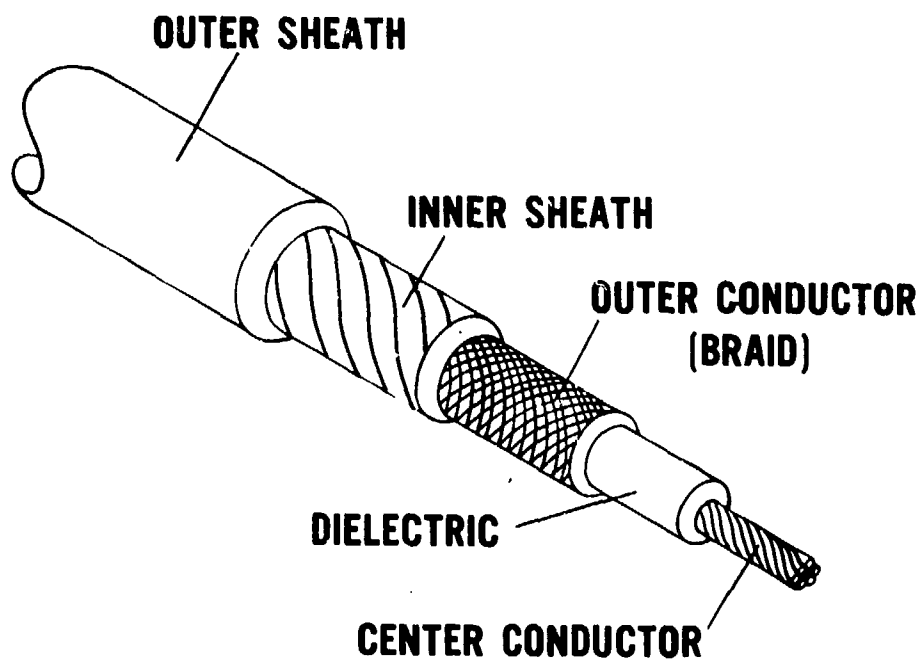
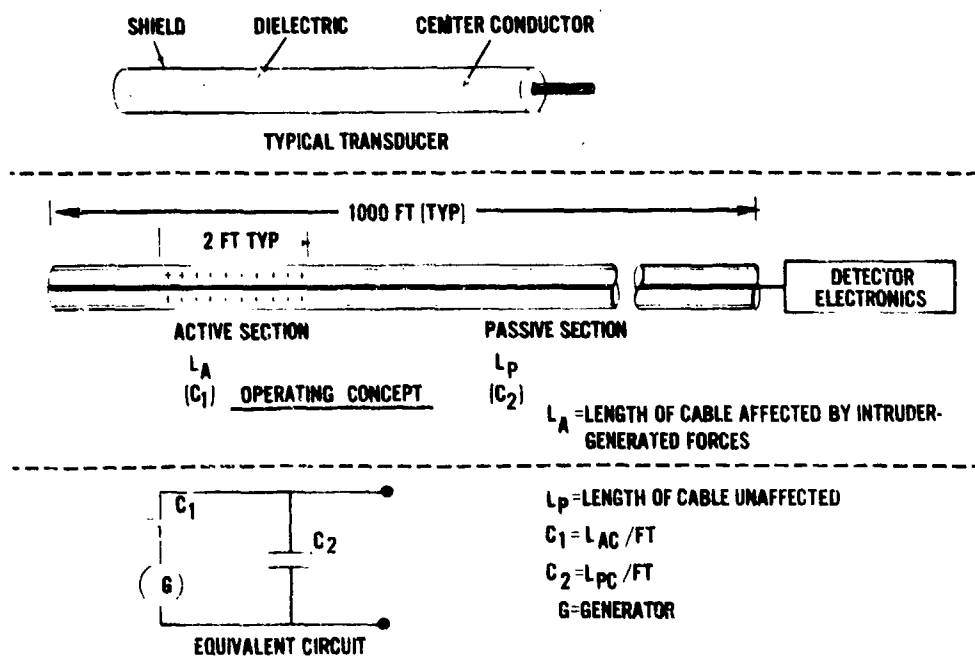


FIGURE 2 - SSCS, Principle of Operation



The most successful application of the SSCS has been its use as a Wheel Base Classifier (See Figures 3, 4 and 5). Using frequency discrimination technique as shown in the accompanying diagram over 80% success has been achieved in discriminating between tracked and wheeled vehicles, and personnel. Detection probability is virtually 100% in normal soil environments. There are presently about 30 of these classifiers deployed in the Sinai demilitarized zone.

Variants of the SSCS:

The Strain Sensitive Cable Sensor with Spring Outer Conductor (SSCS-SOC); the Westinghouse Wire in Tube (WIT). These variations of the SSCS were developed with the intent of improving sensitivity and securing more uniformity of sensitivity along the line.

1. SSCS-SOC: When the outer braid of the SSCS is replaced by a lightly wound spring sensitivity is improved considerably. Measured under controlled conditions in the laboratory, the SSCS-SOC exhibited a 10 dB improvement in strain sensitivity. Results in field tests validated an improvement in sensitivity. Further testing in a frozen ground environment should determine if the SSCS-SOC will overcome a deficiency of the SSCS: insensitivity in frozen ground.

2. Wire-in-Tube (WIT): The Westinghouse WIT is simply an insulated wire emplaced in a copper tube. Apparently minute movement of the wire in a tube, by rubbing action, induces a charge differential between the copper tube and inner conductor. This charge is bled off and amplified as in the SSCS.

One significant difference between the signals generated by the WIT and the SSCS is the detection-zone width (See Figure 6). Note the wider detection zone exhibited by the WIT. This is a result of a wider frequency response for the transducer.

B. Mechanical Self-Adjusting Pressure Switch.

Another strain type sensor which has been conceived and developed at MERADCOM is the Mechanical Self-Adjusting Pressure Switch. It was originally designed to detect the presence of intruders climbing over a fence. The MSPS is a sealed cylindrical unit containing a normally closed set of contacts. One of the contacts is rigidly fixed to one end of the cylinder. The moveable contact is held against the first by a spring pushing against the other end of the cylinder. The movement of this contact is viscously damped using a liquid filled piston-sleeve arrangement (See Figure 7).

If the cylinder is compressed and released, the contacts are held

FIGURE 3 - Wheel-Base Classifier with MINISID Radio Transmitter

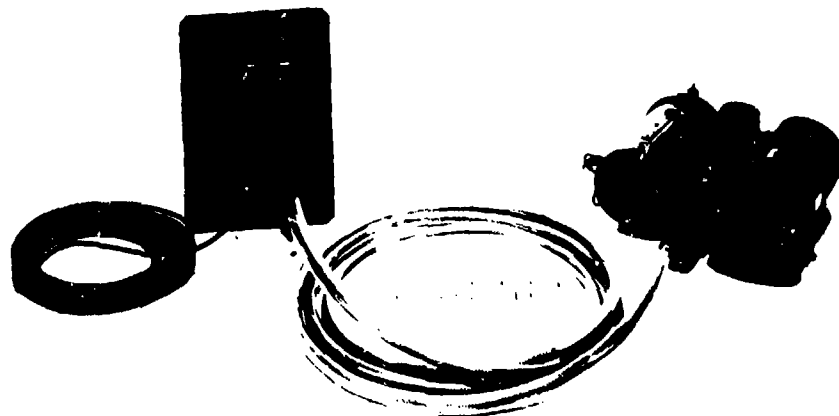


FIGURE 4 - Intrusion Characteristics Utilized by Classifier

BIPED CROSSING LINE IN STEALTH

- VERY LOW AMPLITUDE SIGNAL
- VERY LOW RISE TIME (LOW FREQUENCY)
- VERY FEW IMPULSES OVER RISE (TYP 1 TO 2)
- EARTH CHARACTERISTICS CRITICAL

VEHICLE, WHEELED

- HIGH AMPLITUDE SIGNAL
- FAST RISE TIME
- MULTIPLE IMPULSES (2 MIN, 4 MAX FOR 2 AXLES)
- EARTH CHARACTERISTICS RELATIVELY IMPORTANT

BIPED CROSSING LINE IN NORMAL WALK

- LOW AMPLITUDE SIGNAL
- MEDIUM RISE TIME
- FEW IMPULSES OVER RISE (TYP 2 TO 7)
- EARTH CHARACTERISTICS IMPORTANT

VEHICLE, TRACKED

- HIGH AMPLITUDE SIGNAL
- FAST RISE TIME
- ONE MAJOR, MULTIPLE MAIN IMPULSES
- EARTH CHARACTERISTICS RELATIVELY IMPORTANT

FIGURE 5 - Filter System of Classifier

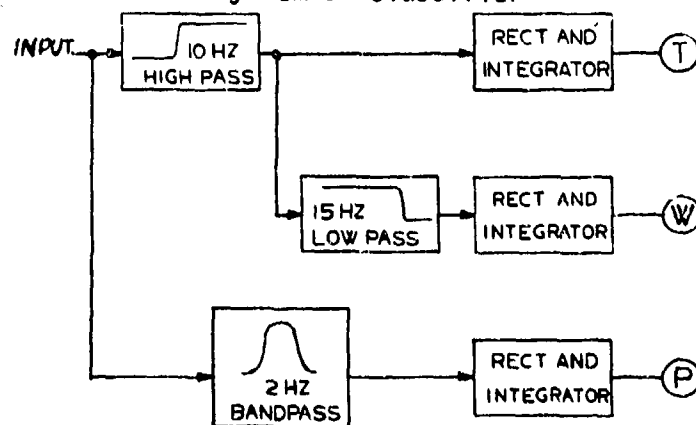


FIGURE 6 - Detection Zones: SSCS vs WIT

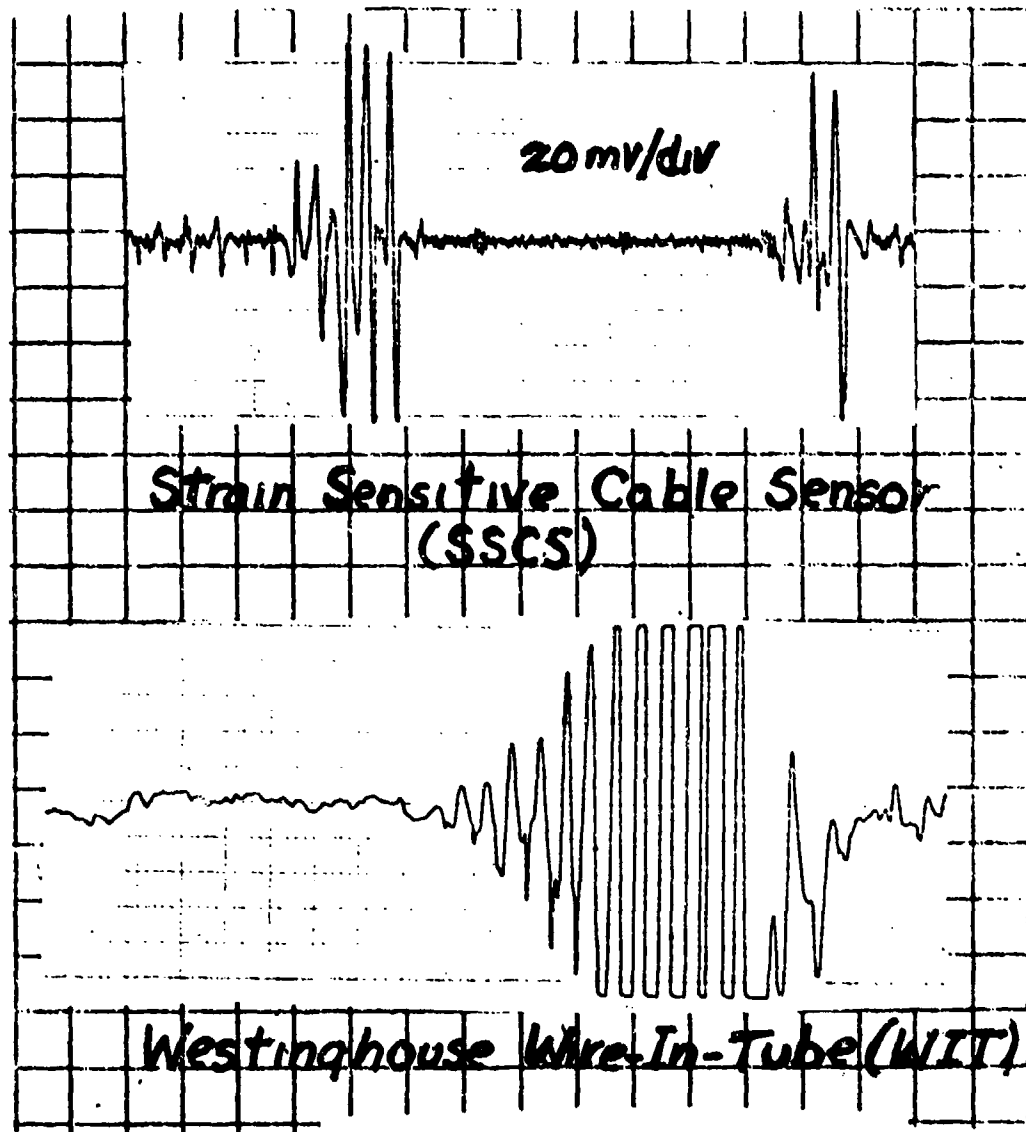
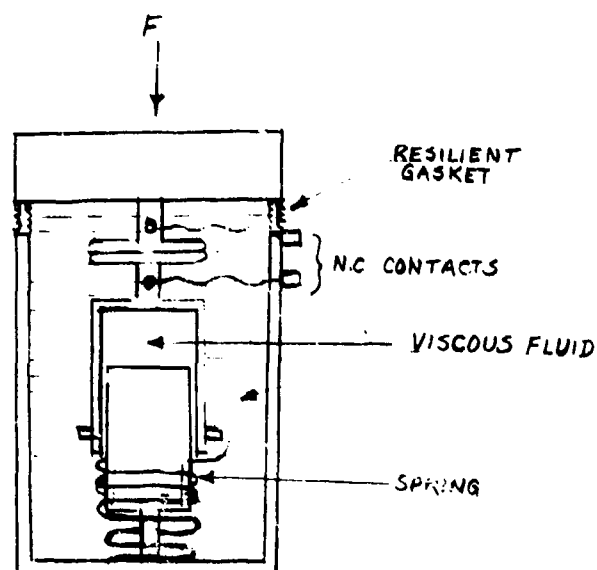
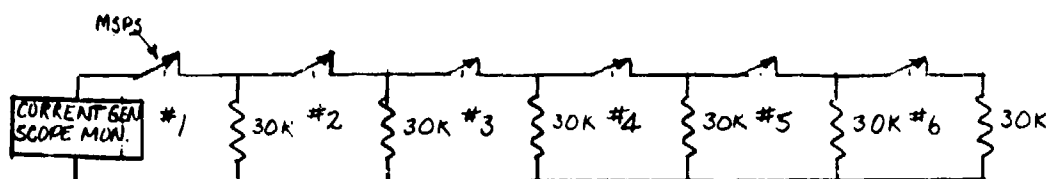


FIGURE 7 - Mechanical Self-Adjusting Pressure Switch and Typical Application



MECHANICAL SELF-ADJUSTING PRESSURE SWITCH (MSPS)



POSSIBLE METHOD OF DEPLOYMENT	
ZONE VIOLATION	RESISTANCE
1	∞
2	30K
3	15K
4	10K
5	7½K
6	6K
NONE	5K

open for a short period of time by the damping system. Since the damping force is constant and the spring force essentially linear, the pulse width, i.e., the time that the contacts stay open, is linearly proportional to the pressure applied to compress the cylinder. The minimum amount of pressure needed to open the contacts is approximately 2 1/2 oz. This corresponds to a cylinder deformation on the order of a few millionths of an inch. The cylinder, as designed for a fence sensor, is 6 1/2 inches in height and 1 1/2 inches in diameter.

The reliability of the MSPS should be excellent because it is a sealed unit. The contacts are protected from the effects of the environment.

Application:

As designed, the MSPS is used to sense the very slight amount of bend induced in rigid structures such as fence posts when an intruder is climbing the fence. A few possible applications of this type of sensor to interior security situations are protection of:

1. Desk drawers
2. Safes
3. Cabinets.
4. Locked doors - sensor would alarm at motion between door and door frame due to application of crow bar attack or if door opened.
5. Staircases - the sensor would react to the vibration caused by footsteps on staircase.
6. Windows.

C. Experimental Multi-turn Passive Magnetic Sensor.

Description:

The most successful passive magnetic sensor to date has been the Multi-purpose Concealed Intrusion Detector (MCID), a single passive loop transposed at intervals to reject far-field geomagnetic excitation. Several disadvantages and deficiencies in this transducer include:

1. Requirement for cross-trenches for transposition.
2. Vulnerability to moisture and rodent attack, and interdiction.
3. Vulnerability to some man-made and geomagnetic electrical

disturbances.

4. Insufficient sensitivity and dynamic range.

The experimental Multi-turn Magnetic Sensor overcomes these difficulties and deficiencies in the following ways:

1. A single cross-over is used and a loop balancing potentiometer is used to cancel far-field effects. This was formerly achieved by multi-loop transpositions.

2. The loops are enclosed in copper tubing to avert moisture and rodent attacks and interdiction.

3. The copper tubing is shorted to attenuate higher frequencies which may cause false alarms when they operate in a non-linear mode. Also, electrostatic common mode and ground-current gradients are eliminated.

4. The 4-turn loops theoretically enhance signal/transducer noise by 6 dB (4:1) thereby increasing sensitivity. The rejection of higher frequencies, with then subsequent lower frequency generation across non-linear components, enhances dynamic range. FM processing also contributes to improving dynamic range.

Figure 8 compares the configuration of the Multi-turn Sensor with that of the MCID and the Non-Transposed Loop Sensor (NTLS).

D. Gamma Ray Intrusion Detector (GRID). (Figure 9)

A gamma ray beam-breaker radiation sensor affords a unique method for detecting and discriminating intruders. A low-level Krypton 85 source was employed in tests conducted by Battelle Columbus Labs. Figure 9 shows the layout for these tests.

The following characteristics were demonstrated by these tests:

1. Ability to function with a low gamma source strength: 118 Curie Krypton 85.
2. Intrusion detection better than 99%.
3. Discrimination possible between various mass interceptions: persons, dogs, simulated birds, snowfall.
4. Detection of speed and direction of intrusion possible.
5. Ability to function in a high noise field.

FIGURE 3 - Comparison Between Passive Magnetic Sensors

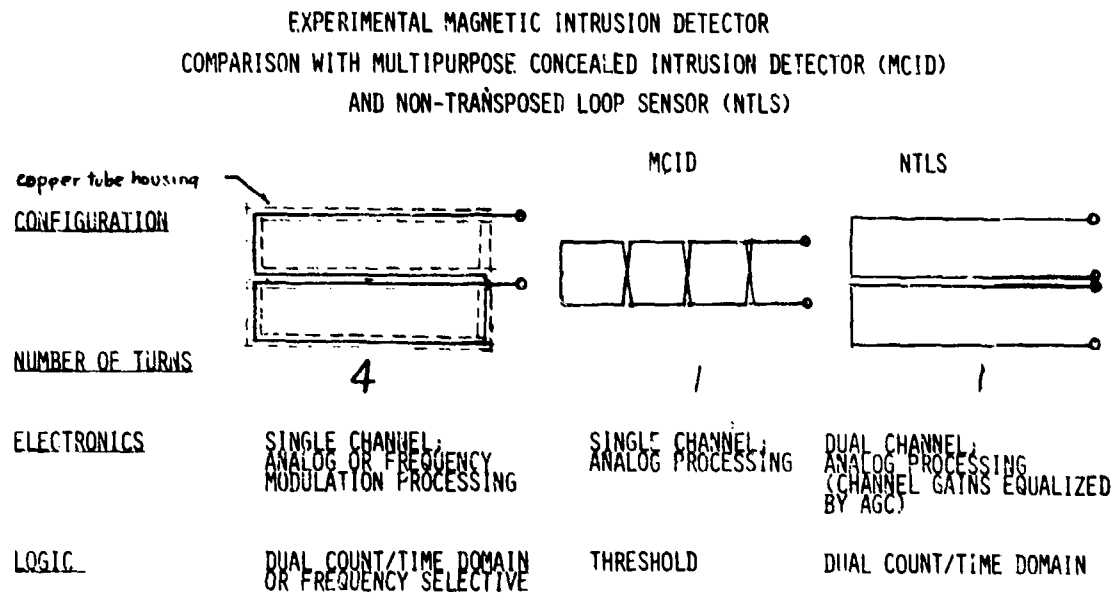
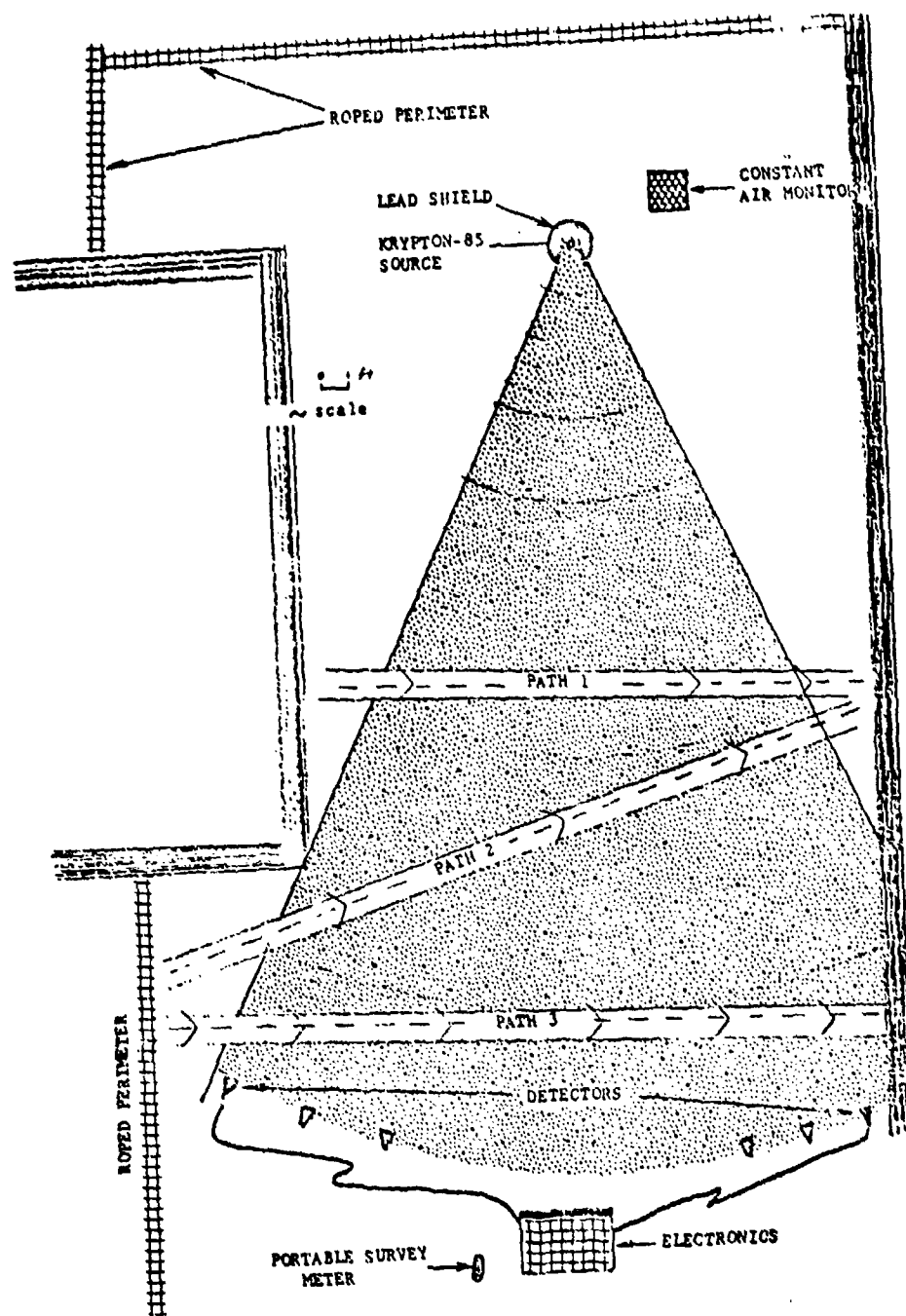


FIGURE 9 - Test Layout of Gamma Ray Intrusion Detector (GRID)



The GRID is a rapidly deployable detector which can be used in both tactical and strategical scenarios. It is immune from most cultural (man-made) noise. Although it cannot be concealed as effectively as other line sensors, its flexibility in application make it an important element in any safeguard system.

All of the preceding sensors have undergone feasibility studies at MERADCOM. In all cases feasibility has been demonstrated and further investigatory effort is justified.

SELECTIVE DIGITAL FILTERING

Glenn Elliott
Sandia Laboratories
Digital Systems Division - 1734

Abstract

The Base and Installation Security Systems Program is funding a project at Sandia Labs to develop the application of adaptive digital filtering to improve sensor analog signal-to-noise ratio. Adaptive digital filtering algorithms have been developed and implemented on laboratory computers as well as on a small microprocessor for real time use. Application of the technique to field recorded sensor data has shown significant improvement of sensor analog signal-to-noise ratio.

SELECTIVE DIGITAL FILTERING

Glenn Elliott
Sandia Laboratories
Digital Systems Division - 1734

This is a report on the progress of a development program to improve the performance of certain type sensors by using state of the art signal processing techniques. This development program at Sandia Laboratories is funded by the Base and Installation Security Systems (BISS) Program. The objective is to have hardware utilizing these new techniques available for integration into the overall BISS program in the early 1980's.

The program, as presently defined, has been divided into three phases: (1) Improvement in signal-to-noise characteristics of sensor analog signals; (2) Development of methods of detecting an intruder by processing the filtered signal; and (3) Demonstration of the feasibility of applying these techniques on small fieldable processors in a cost-effective manner.

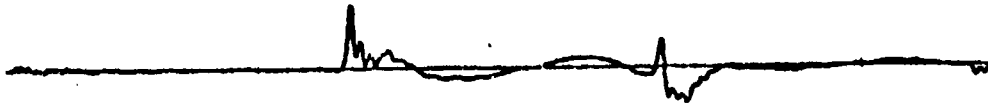
Much of Sandia's effort to date has been directed toward the first phase, improvement of signal-to-noise, which is the main subject of this paper. It must be emphasized that the project as presently defined is highly developmental and does not yet include the deployment of hardware.

Improvement in Signal-to-Noise by Selective Filtering

Ideally, a technique to improve signal-to-noise ratio (SNR) should remove all noise regardless of its source or the characteristics of the noise signal without degrading the signal created by the intruder regardless of its characteristics. Practically, a technique of this capability is not possible; however, intelligent compromises can result in practical approaches yielding effective performance as will be shown. Another property required for improvement in SNR is a wide bandwidth frequency response. This becomes apparent from the difference in frequency content of footstep signals from a seismic sensor with different types of intruders. Figures 1A and 1B show time and frequency information for four different types of intruders. Here, the light-weight running intruder produces a footstep signature entirely different from a heavy, careful walker with a significant quantity of magnetic material in his boots.

Typical noise sources vary widely in their effect on sensors. Alternating current power sources and distribution systems produce narrow-band, generally continuous signals. Distant seismic sources produce very low frequency, narrow-band signals, while nearby seismic disturbances produce broad-band signals in the middle frequency ranges. Figure 2 shows idealized frequency characteristics of some typical noise sources. Each curve

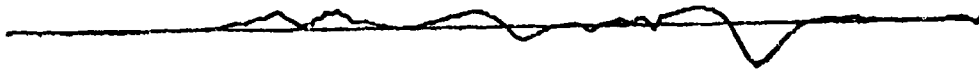
Adult walking, nonmagnetic



Child Running, nonmagnetic



Adult walking, magnetic



Dog Running, nonmagnetic



1 second

Figure 1A Analog Signals From Seismic Sensor

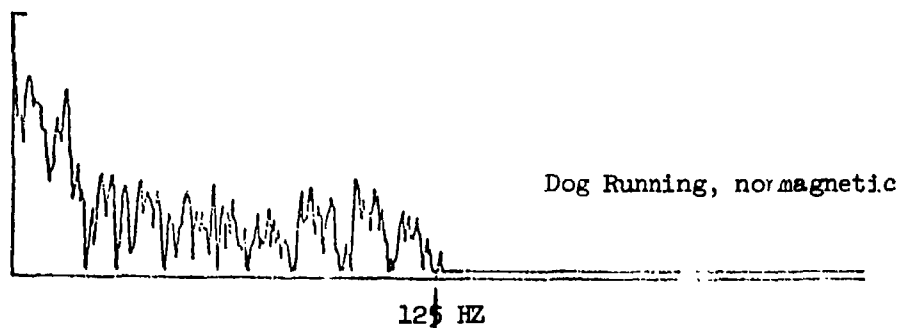
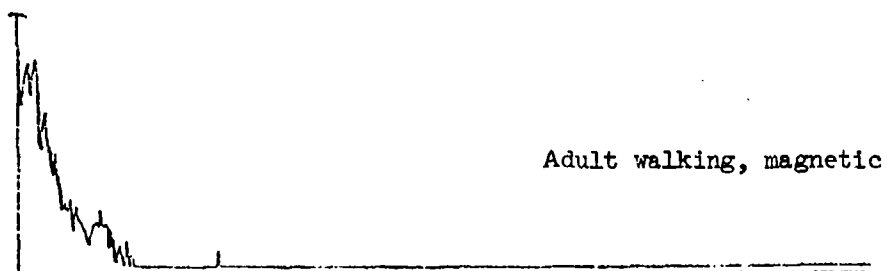
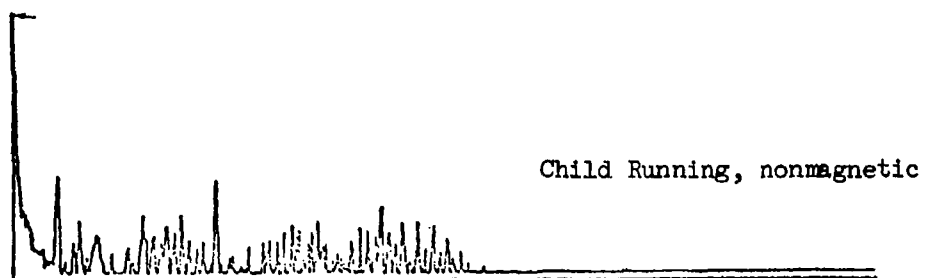
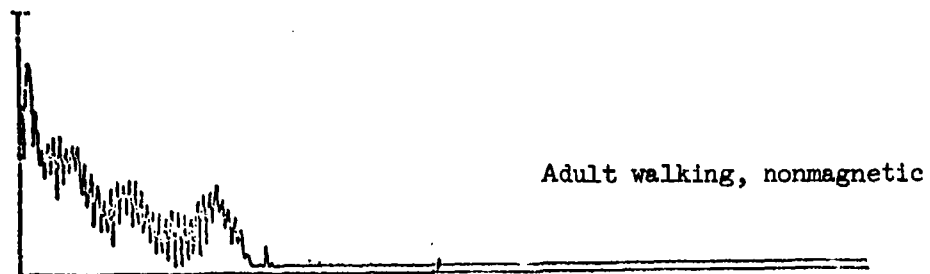


Figure 1B Power Density Spectral Plots of Data
in Figure 1A

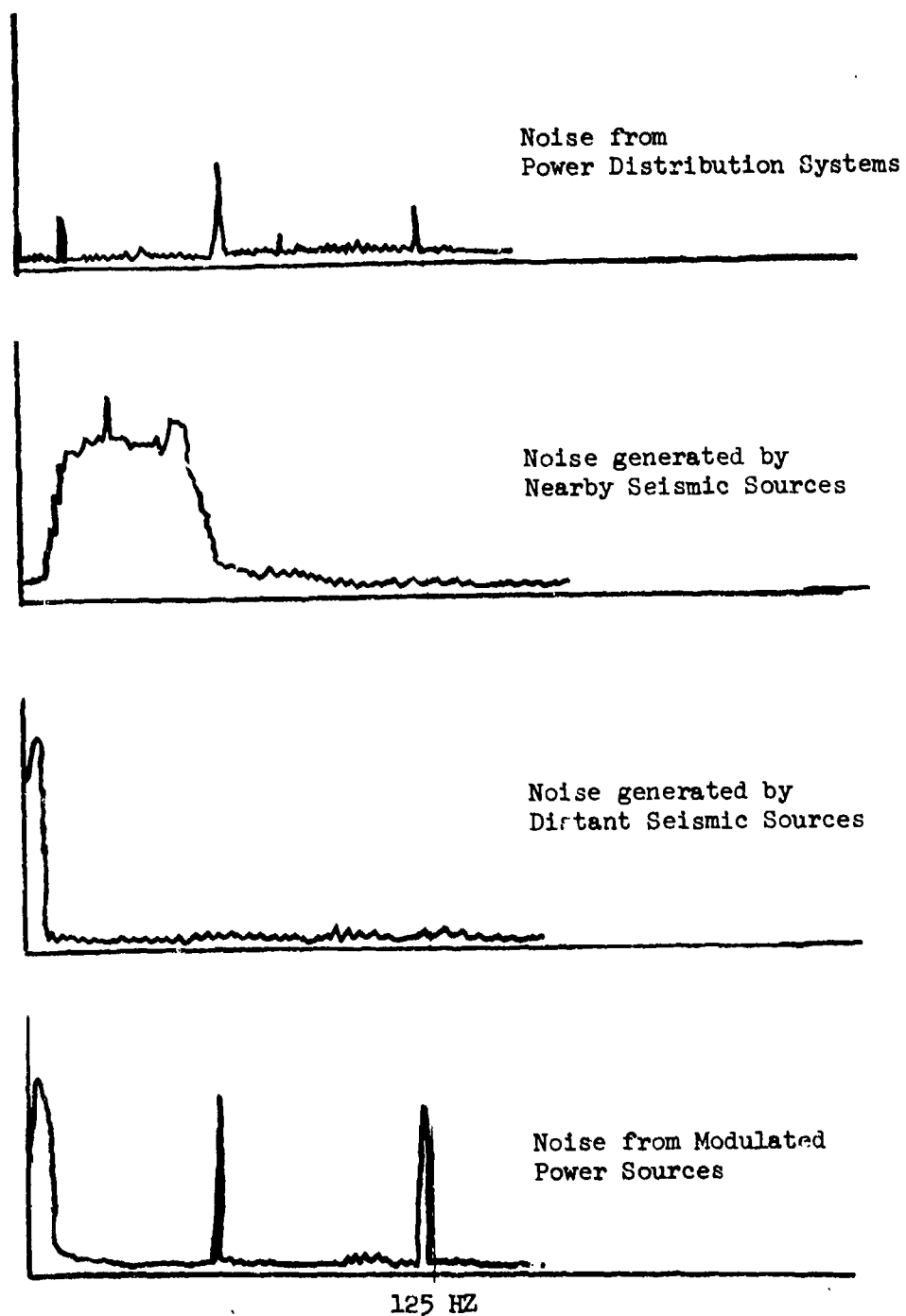


Figure 2 Power Density Spectral Representations
of Typical Noise Sources

is a composite of results from a number of different tests at several locations. However, as more testing is done, it is almost certain that other noise sources will be found with characteristics which deviate from those depicted here.

The only unique difference between the noise and intruder signal is that the noise signals tend to be continuous while the intruder signals tend to be transient in nature. The statistical term generally applied to signals like sensor noise which either vary not at all or slowly over a period of time, is "stationary." It is upon this feature that Sandia's selective filtering technique is based. If the long-term and most of the short-term noise can be removed, then the task of detecting the intruder in the cleaner signal should become much easier. One would also expect the false alarm rate to be substantially reduced. Of course, one would like to eliminate all the noise, short-term as well; but, limits of practicality dictate that some unusual noise signals will be passed. An example of long-term stationary noise signals are those generated by a power line, while short-term noise signals would come from passing vehicle traffic on a nearby road.

A process which would dynamically change to handle the varying noise environment is called an adaptive process. Specifically, Sandia's approach to selective filtering is a process called "Adaptive Digital Filtering" (ADF). ADF technology, while in theory several decades old, has only been used on any significant scale in the last five years with the advent of the small, cheap digital processors. The basic ADF function is depicted in the block diagram of Figure 3A. Appropriate processing of the output signal forces the coefficients of the digital filtering section to form an output which, when subtracted from the input at the summing junction, reduces the noise content of the output. One can see that the filtering section becomes somewhat of an anticipator of the incoming signal.

Basically, the method used for dynamically adjusting the coefficients of the filter section is a familiar technique first developed by Norbert Wiener and frequently called "Wiener Filtering." The algorithms used are developed from Wiener's theory that the stationary signal content of the output will be minimized if the expected power is also minimized. While the mathematics of arriving at the algorithms used by Sandia, as one would expect, are intricate and will not be presented here, the algorithms are easily implemented on minicomputers and some microprocessors in real time. For more complete discussions of the math, the reader is referred to the works of Widrow (1, 2), Stearns (3), and Ahmed (4).

Examples of Sensor Signal Processing

Over the past 16 months, Sandia has acquired considerable field data from seismic sensors and a modest library now exists of time domain and frequency domain data. More recently, data has been obtained using a

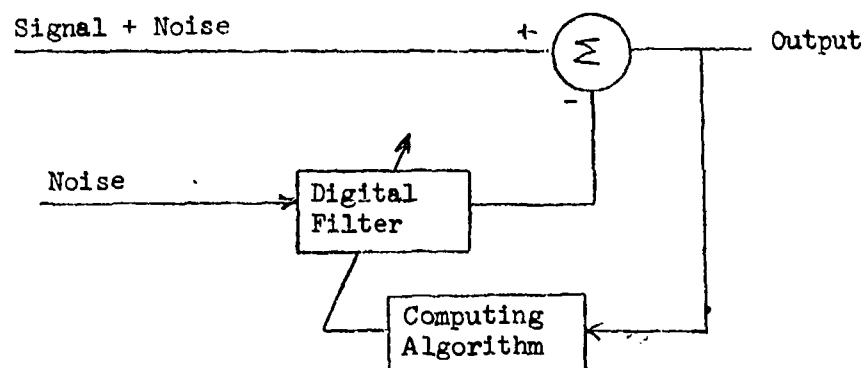


Figure 3A Basic Adaptive Digital Filter

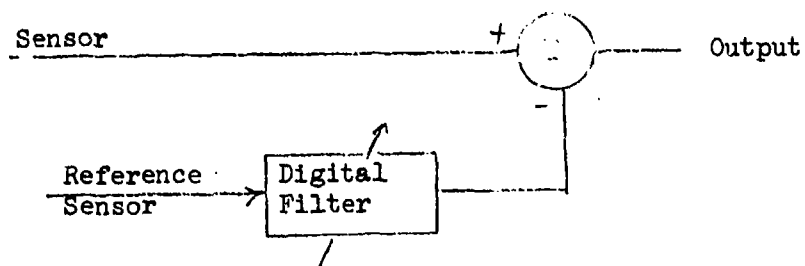


Figure 3B Filter Mode

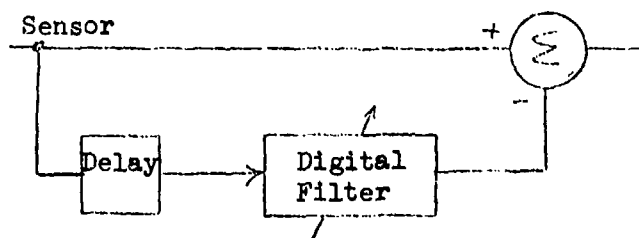


Figure 3C Predictor Mode

specially-designed portable data acquisition system which is exceptionally noise-free and very versatile. This wide-band system uses several techniques, including optical isolation and direct digital recording for noise reduction. It was designed and built at Sandia especially for obtaining improved sensor data for the BISS program.

We have processed a number of these data using various versions of the ADF algorithm on a laboratory computer system dedicated to BISS projects as well as a small microprocessor. This system now has a very complete library of signal processing programs; see Jacklin (5).

Figures 4 through 6 show three examples of processing using the ADF algorithm. In each figure, the upper curve is the raw data directly from the sensor, and the lower curve is the processed data from the output of the ADF. Vertical scales for raw data and ADF output are the same for each figure. Predictor mode, Figure 3C, was used in all cases. The data in Figure 4 comes from a seismic sensor which is buried near the power line

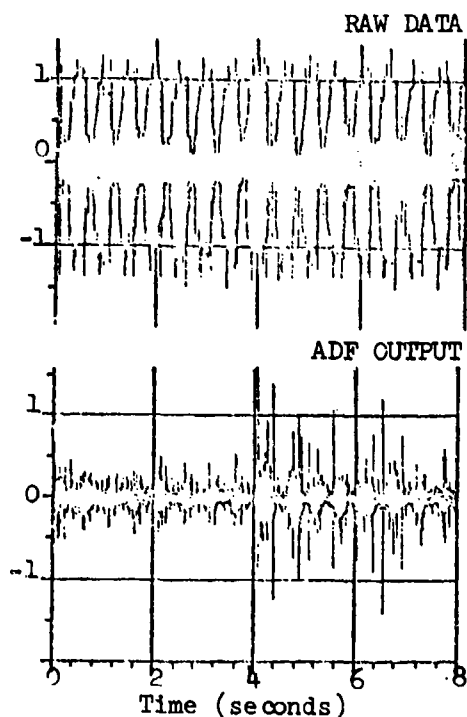


Figure 4 Strobe Light Interference
Vertical Scales Identical

for the runway strobe lights. For this record, a walker approached the cable reaching it about four seconds into the record and then walking along it. The improvement in SNR is approximately 14 db. Figure 5 shows data from a sensor which is responding to a distant seismic disturbance, in this case, a train about 3 km away; considerable power line interference

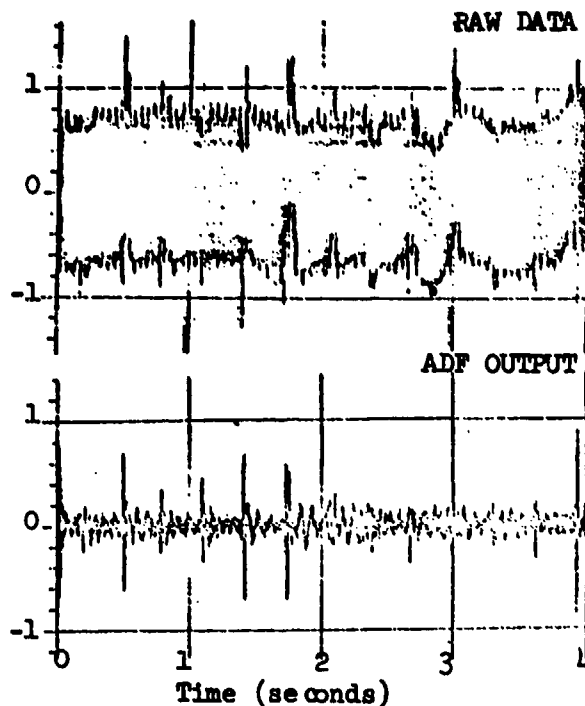


Figure 5 Distant Seismic
Disturbance
Vertical Scales Identical

is also present. A walker is present for the entire record. Again, there is an improvement of 12 to 14 db in SNR. The data from Figures 4 and 5 were processed on the laboratory computer using the same algorithm with no change in constants. Figure 6 is also data from a distant train with a walker crossing the sensor at about a 45° angle. In this case, the ADF was run in real time on the microprocessor system discussed in the next section. Footstep signals are very apparent as the walker approaches the cable and crosses about two seconds into the record. Improvement in SNR is approximately 12 db.

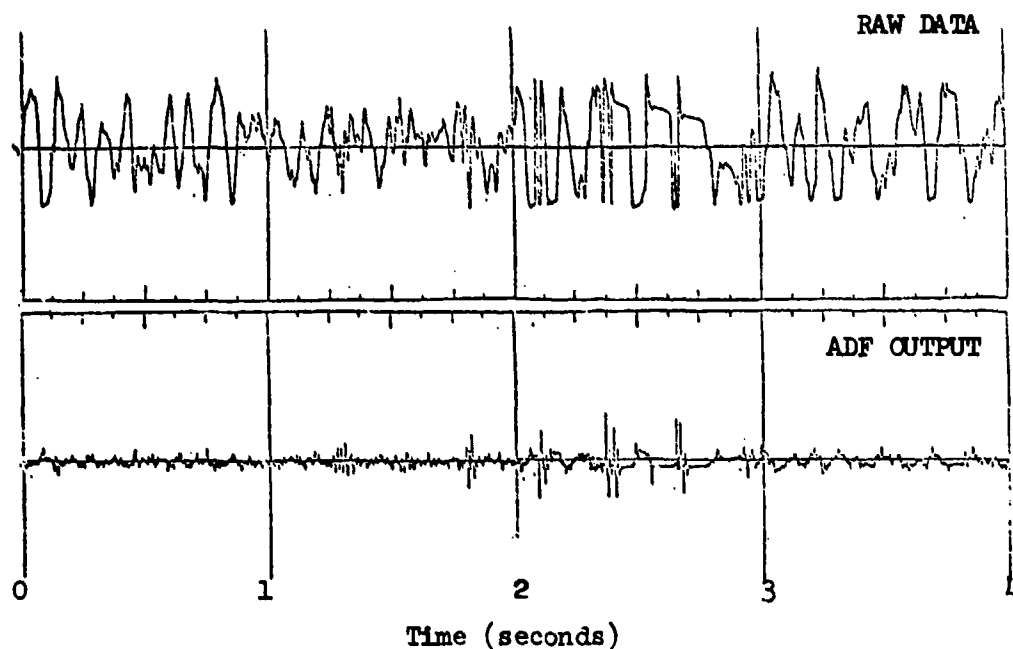


Figure 6 Distant Seismic Disturbance
Vertical Scales Identical

Development Models for Hardware Implementation

The ADF algorithms have been implemented on two different small processors at Sandia. One, a portable system based upon the LSI-11 microcomputer, is being used for checkout of algorithms when operating in real time. This system is portable and versatile and is especially suited to investigation of the performance of the algorithms at different locations.

The second system is based upon a microprocessor, the IM6100. This processor uses CMOS technology and takes advantage of the low-power, high-noise immunity characteristics inherent in CMOS devices. The objective of this effort is to determine the feasibility of using fieldable microprocessor systems for sensor signal processing. The device has been operated with the ADF algorithms in the laboratory in real time, and a model is being fabricated now for field trials. Figure 7 is a representation of the field unit along with a portable test and programming device. This unit, unofficially termed the "Sensor Signal Processor Development Unit" (SSPDU), is scheduled for preliminary field trials in July 1977.

Summary

In summary, from the work done to date, it appears that Adaptive Digital Filtering algorithms have the potential for providing a major improvement

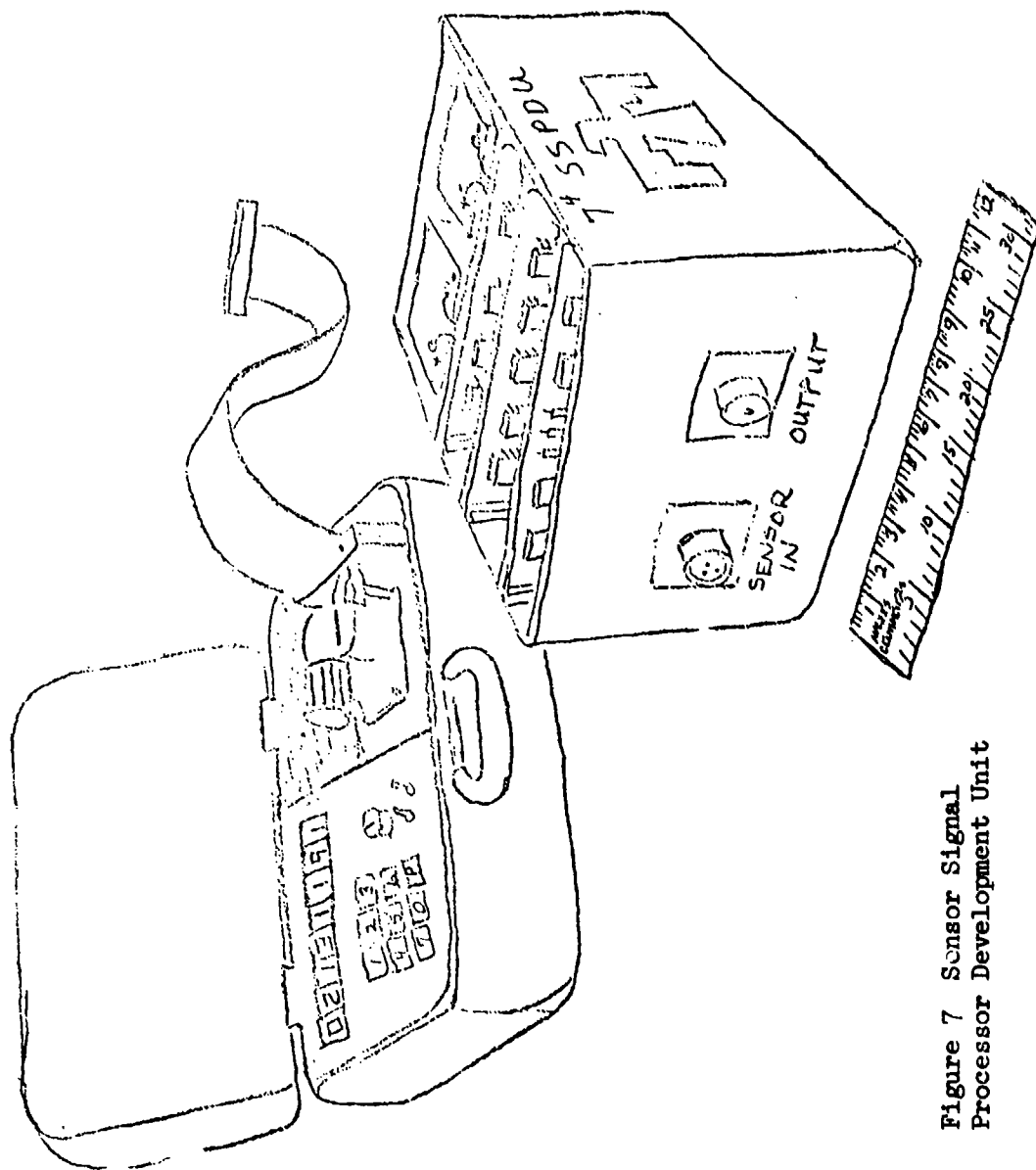


Figure 7 Sensor Signal
Processor Development Unit

in the signal-to-noise ratio of intrusion detection sensors. It also appears that these algorithms can be effectively implemented to run in real time on small digital processors. Future work in this project, while continuing to optimize the algorithms, will emphasize the development of functional hardware for field implementation of this signal processing technology.

BIBLIOGRAPHY

1. B. Widrow, et al, "Adaptive Noise Cancelling, Principles and Application" Proceedings of the IEEE, Vol. 63, December 1975.
2. B. Widrow, et al, "Stationary and Nonstationary Learning Characteristics of the LMS Adaptive Filter" Proceedings of the IEEE, Vol. 64, August 1976.
3. G. Elliott, W. Jacklin, S. Stearns, "The Adaptive Digital Filter" Sandia Laboratory Development Report 76-0360, August 1976.
4. N. Ahmed, "A Study of Adaptive Digital Filters" Sandia Laboratories Development Report 77-0102.
5. W. L. Jacklin, "Digital Signal Processing Algorithms for the PDP11" Sandia Laboratories Development Report 77-0803.

RADAR VIDEO PROCESSING WITH CHARGE COUPLED DEVICES *

by

W.H. Bailey, W.L. Eversole, L.R. Hite
Texas Instruments Incorporated
Dallas, Texas

and

J.A. McCray
USAECOM
Ft. Monmouth, New Jersey

I. INTRODUCTION

During the past decade dramatic improvements in radar video signal processing have become possible due to the increased sophistication of integrated circuit technology. Digital integrated circuits provided the initial impetus for these developments. The advent of the charge coupled device (CCD) has offered unique possibilities for implementation of such functions in the analog domain offering lower power and higher density than conventional digital processing. Of particular importance is the use of CCD transversal filter techniques in performing convolution operations.

CCD technology has matured relatively slowly since its inception in 1970¹ due to the radical departure of its basis from the mainstream of integrated circuit technology. Additional complications arising from the integration of analog interface and peripheral circuitry functions using MOS related techniques alongside the CCD's have also slowed progress. Integration of these auxiliary functions has required the development of MOS analog circuitry.

Radar video processing is an area where significant improvements in radar performance may be achieved by exploiting recent technology advances. The general radar video processing problem is outlined in Figure 1 which shows returns from the k th range bin which include an aircraft, wind driven precipitation, and ground returns. The spectrum of the returns for the k th range bin between DC and the PRF is also shown in this figure. These typical spectral characteristics indicate the desirability of some form of target classification based upon spectral characteristics rather than upon amplitude alone.

The two most common approaches to this problem are the Moving Target Indicator (MTI) and transform processing. The MTI is a sampled data filter which differences successive samples from the same range

* This effort has been supported by ECOM Contract DAAB07-76-C-0912

bin creating a bandpass filter characteristic which has nulls at DC and the PRF. The degree of sophistication of such filters ranges from a single delay feed-forward canceller having a $\sin x$ frequency response characteristic to multi-pole recursive approaches having classical filter characteristics (e.g., Butterworth, Chebyshev). Factors which often become significant in the design of an MTI are stability, feedback coefficient precision, circuit complexity, and phase response.

Transform processing is a second approach to video processing which has received widespread attention. This technique has conventionally utilized digital implementations of the Fast Fourier Transform (FFT). While this approach to video processing is more powerful than MTI processing, it is also more complex. Conventional digital implementations utilize a large "corner-turning" memory in conjunction with a high speed FFT processor through which data from all range bins are multiplexed. The size, power, weight, and cost for such processors frequently become prohibitive.

Transform processing may also be realized in analog form by utilizing CCD's in an implementation of the Chirp Z Transform (CZT) algorithm. The advantages of this technique are derived from the powerful computational equivalency of CCD transversal filters utilized to perform the convolution required in the CZT. The use of CCD transversal filters alongside integrated analog peripheral circuitry provides a very attractive means of video spectral analysis. An alternative approach utilizes an analog CCD "corner-turning" memory in conjunction with a high speed CZT which may be implemented using CCD or Surface Acoustic Wave (SAW) technologies.

II. MTI PROCESSING

One of the most important applications for CCD's in radar signal processing is the delay line canceller or MTI.^{2,3,4} In radar systems, the returns from the stationary or slowly moving targets are frequently larger than the returns from moving targets, therefore a moving target indicator, MTI, is needed to either enhance the signals from the moving targets or suppress stationary target returns. Since clutter or stationary targets are characterized by zero doppler shift, their returns are periodic spectra at DC and multiples of the PRF, while moving targets have returns shifted by their doppler frequencies. Figure 1 shows the relation between clutter and a typical moving target. Because this filtering must be performed on up to a few thousand range bins simultaneously, recursive filtering is attractive. This recursive filter can be realized using digital approaches but the cost and complexity of analog-to-digital conversion may be prohibitive. Acoustic delay lines can be used to implement the delay stages in the recursive filter transfer function but controlling the delay time accurately is a problem. Charge coupled device (CCD) signal processing eliminates

these problems of the digital and acoustic delay line approaches to recursive filters. CCD's take advantage of the precise timing of digital processing techniques without the requirement for analog-to-digital conversion. The stability of the CCD filter characteristics is determined by precise delay times which are achieved by synchronously clocking the CCD from signals derived from the radar's master clock.

Since the more sophisticated MTI's are recursive filters having internal storage, the transfer function for such an N^{th} order filter is

$$H(z) = \frac{\sum_{i=0}^N a_i z^{-i}}{\sum_{i=0}^N b_i z^{-i}}$$

CCD's may be utilized to implement the delay terms Z^{-i} in the above equation in analog form. The number of samples, N , which can be stored in a CCD delay line, the clock frequency, f_c , and the time delay, T_d , of a signal passing through a continuously clocked delay line are interrelated by

$$T_d = N/f_c$$

The CCD clock frequency constrains the range resolution achievable with the MTI while a total delay of a sample for a given range bin must be the reciprocal of the radar's PRF in order to maintain range bin registration at the weighting junctions. These requirements often lead to an additional storage time, ΔT , such that

$$\text{PRF} = \frac{1}{T_d + \Delta T}$$

The most significant CCD performance limitation, with regard to the MTI, is the dispersive effect of incomplete charge transfer which has the effect of incomplete cancellation of the residues from stationary targets.² This effect may be minimized by use of a multiplexed configuration such as indicated in Figure 2. This configuration permits the division of a very large number of range bins into smaller segments which can be adequately handled with achievable values of charge transfer efficiency.

Thermal leakage current provides a minor limitation to MTI performance.⁶ Leakage current accumulates in the potential wells in which signal charge also resides. Since leakage current is a function of

temperature, a trade-off between maximum storage time and highest operating temperature is necessary for a given leakage current rate.

The precision with which the filter corner frequencies are determined is primarily determined by the feedback coefficient precision, while the cancellation ratio is determined by feed-forward coefficient precision. Adequate results have been achieved using precision resistor networks which control operational amplifier gains for implementation of weighting coefficients.

The stability criterion for a CCD recursive filter requires that all poles lie inside the unit circle of the Z-plane. The ease of achieving this stability is related to the relative separation between filter cutoff frequency and the PRF.

A four pole, five pulse MTI canceller has been developed using 150 stage, 2 phase N-channel CCD delay lines having the design parameters listed in Table I. The MTI filter sections shown in Figure 2 are recursive sections and have a transfer function given by

$$H(z) = \frac{(1-z^{-1})^4}{(1-\alpha_{11}z^{-1} - \alpha_{21}z^{-2})(1-\alpha_{12}z^{-1} - \alpha_{22}z^{-2})}$$

The feedback coefficients are calculated to provide the filter with a Butterworth response. The feed-forward and feedback coefficients are implemented with variable gain operational amplifiers. The filter also have electronically selectable cutoff frequencies implemented with analog switches and resistors. A photograph of the frequency responses is shown in Figure 3. The responses at zero frequency are due to the zero frequency marker in the spectrum analyzer. The response of the MTI filter to two different frequencies is shown in Figure 4. The upper photograph of Figure 4 shows the spectrum of the input to the MTI filter. There are two frequencies present, one in the passband of the filter, the other one at the PRF. The lower photograph shows the output of the MTI filters with the frequency in the passband still present while the frequency at the PRF has been cancelled.

III. CCD TRANSFORM PROCESSING

A. CZT Implementations

CCD's may be utilized in two slightly different implementations of the CZT. The exact mathematical equivalent of the Discrete Fourier Transform (DFT) may be implemented utilizing CCD's.⁷ Implementation of an N point transform requires at least N-1 zeros be inserted between sets of N samples creating a nominal 50% duty cycle operating condition. These N signal samples are multiplied by N samples of a linear FM

waveform that sweeps from $-f_c/2$ to $f_c/2$ in a time NT_c where $T_c=1/f_c$ is the period of the CCD clock. The CCD transversal filter is required to have $2N-1$ stages and a linear FM impulse response which sweeps from f_c to $-f_c$. This implementation calculates the exact DFT including the proper transformed phase characteristics. However, the 50% duty cycle operation and the requirement for filters having a length $2N-1$ for an N point transform are relatively inefficient.

The sliding CZT is a more efficient implementation scheme which requires filters of length N to perform an N point transform. Input data blanking is not required since a spectral component is calculated as new data samples are entered using the new sample and $N-1$ of the old samples. The sliding transform improves implementation efficiency at the expense of phase information, however, in many cases the power spectrum is the quantity of interest and phase information becomes unimportant making the sliding transform highly desirable for such applications.

B. Configuration Trade-Offs

Two general approaches may be taken to the use of the CZT in radar video processing. A CCD implementation of an analog "corner-turning" memory may be used in conjunction with a high speed CZT, which is often implemented using surface acoustic wave device (SAW) technology in order to realize the transform processing speed required for the multiplexed data from all range bins.^{8,9} This architecture, shown in Figure 5, appears very straightforward and capable of high density implementation. Its disadvantages are high speed CCD operation, low bandwidth SAW filtering operations, and inefficient memory utilization due to load/unload incompatibilities. Up conversion of the reformatted video may also be a concern due to incomplete local oscillator cancellation.

The second CZT approach, shown in Figure 6, utilizes a filter bank configuration in which a set of CCD filters is dedicated to each range bin being processed.^{10,11} The initial chirp multiplication may be performed on the raw radar video prior to range sorting. Following range sorting, the samples are stored in the CCD transversal filter which performs both storage and convolution functions. Either the sliding or the true CZT may be implemented using this approach, but the sliding transform is the more efficient approach providing the retention of phase information is unimportant. The advantages of this configuration are the low CCD operating speeds (i.e., the PRF) along with the corresponding low power dissipation and the simplicity of the control circuitry. The disadvantages of the configuration are the requirement for integration of peripheral circuitry functions on the CCD chip and the requirement for several chips to implement systems with large numbers of range bins.

C. Processor Chip Development

Implementation of this latter configuration has been pursued in the development of a processor whose design parameters are listed in Table II, which will be compatible with the AN/PPS-5 battlefield surveillance radar. The processor chip is configured to perform the functions indicated in Figure 7 for 5 range bins. An 80 point transform length is used which yields an unambiguous 40 point resolution with the AN/PPS-5 since quadrature video is not available. Since the AN/PPS-5 has a 4 kHz PRF, the achievable doppler resolution for this processor is 50 Hz.

While the use of the powerful computational equivalency of the CCD transversal filter is a key factor in this approach, the use of external circuitry to perform the required peripheral functions indicated in Figure 7 would be prohibitive from the standpoint of cost and size. As a result, the design effort associated with the development of the processor chip has concentrated on the integration of the peripheral functions using analog MOS circuitry. Due to the difficulty of implementing analog functions with MOS relative to bipolar technology, very little data base exists for the design of such circuitry. Much effort has been expended in device characterization and circuit modeling using the SPICE computer analysis program.

D. Results to Date

Results achieved with an earlier processor design which contains 32 point CZT processing for 5 range bins is indicated in Figure 8. The upper photograph indicates two doppler frequencies located in different range bins. The lower photograph indicates the two doppler frequencies within the same range bin with the input amplitude of the higher frequency component reduced by a factor of 2.

REFERENCES

1. W.S. Boyle and G.E. Smith, "Charge Coupled Semiconductor Devices", Bell System Technical Journal, Vol. 49, pp 587-593, April 1970.
2. J.E. Bounden, R. Eames, and J.B.G. Roberts, "MTI Filtering for Radar with Charge Transfer Devices", Proc. CCD Technology and Applications Conf., pp 206-213, Edinburgh, September 1974.
3. W.J. Butler, W.E. Engeler, H.S. Goldberg, C.M. Puckette, IV., and H. Logenstein, "Charge-Transfer Analog Memories for Radar and ECM Systems", IEEE S. Solid-State Circuits, SC-11, -p 93-100, February 1976.
4. J.E. Bounden and M.J. Tomlinson, "CCD Chebyshev Filter for Radar MTI Applications", Electronics Letters, 10, pp 89-90, April 1974.
5. L.R. Rabiner and B. Gold, Theory and Application of Digital Signal Processing, Prentice-Hall, 1975.
6. A.F. Tasch, Jr., R.W. Broderson, D.D. Buss, and R.I. Bate, "Dark-Current and Storage-Time Considerations in Charge-Coupled Devices", Proc. CCD Applications Conf., pp 179-187, San Diego, September 1973.
7. R.W. Broderson, C.R. Hewes, and D.D. Buss, "A 500-Stage CCD Transversal Filter for Spectral Analysis", IEEE J. Solid State Circuits, Vol. SC-11, pp 75-84, February 1976.
8. J.B.G. Roberts, R. Eames, R.F. Simons, "A CCD-SAW Processor for Pulse Doppler Radar Signals", in Proc. CCD Applications Conf., San Diego, CA., pp 295-300, October 1975.
9. J.B.G. Roberts, R. Eames, D.V. McCaughan, and R.F. Simons, "A Processor for Pulse-Doppler Radar", IEEE J. Solid State Circuits, Vol. SC-11, pp 100-104, February 1976.
10. W.H. Bailey, M.W. Whatley, R.W. Broderson, D.D. Buss, W.L. Eversole, L.R. Hite, and R.H. Sproat, "CCD's for Radar Pulse Doppler Processing using the Chirp Z Transform", in GOMAC Digest of Papers, Boulder, Co., pp 76-77, June 1974.
11. W.H. Bailey, D.D. Buss, L.R. Hite, and M.W. Whatley, "Radar Video Processing using the CCD Chirp Z Transform", in Proc. CCD Applications Conf., San Diego, CA., pp 283-290, October 1975.

Cancellation Ratio	> 40 dB
Response Characteristics	Butterworth
Selectable Cutoff Frequencies	2
Roll-off Rate	24 dB/Octave

Table I - Design Parameters for MTI Processor

Doppler Resolution	50 Hz
Sidelobe Suppression	45 dB
Dynamic Range	40 dB
Transform Length	80
Range Sampling Rate	3.75 MHz
PRF	4 kHz
Processing Range	10 Km
Range Resolution	40 m

Table II - Design Parameters for AN/PPS-5 Processor

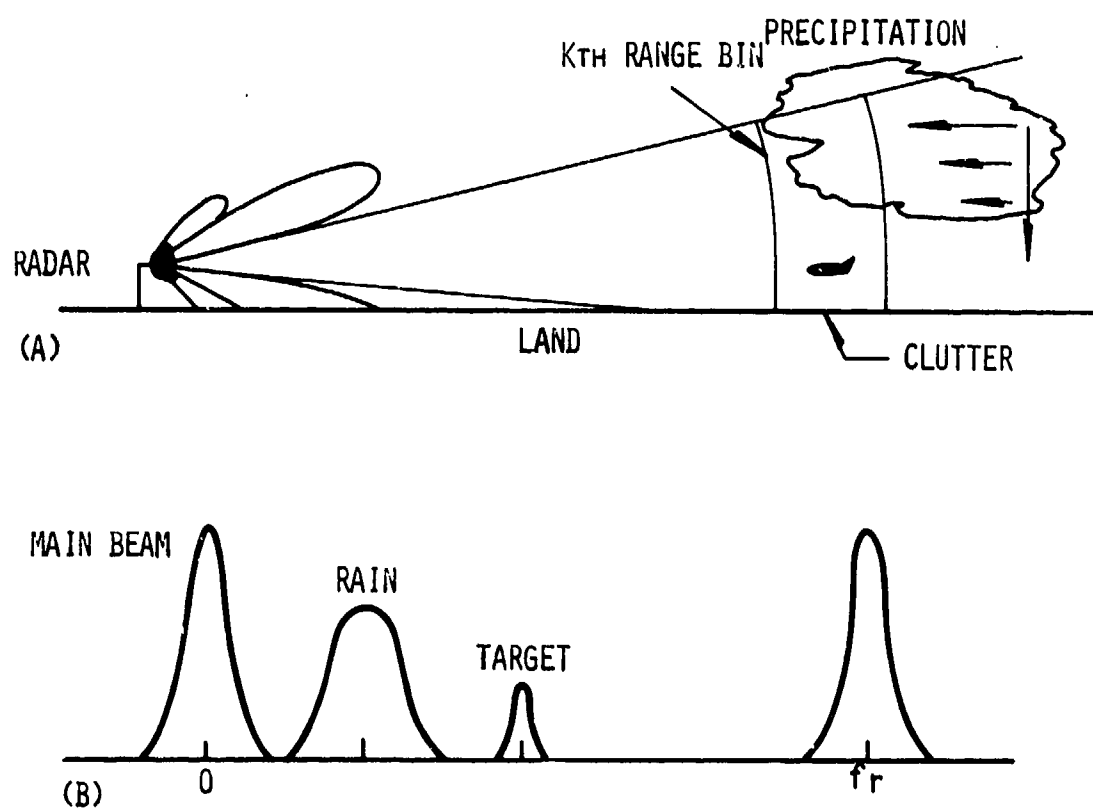


FIGURE 1. RELATIONSHIP BETWEEN (A) RADAR
OPERATING ENVIRONMENT AND (B)
SPECTRAL CHARACTERISTICS

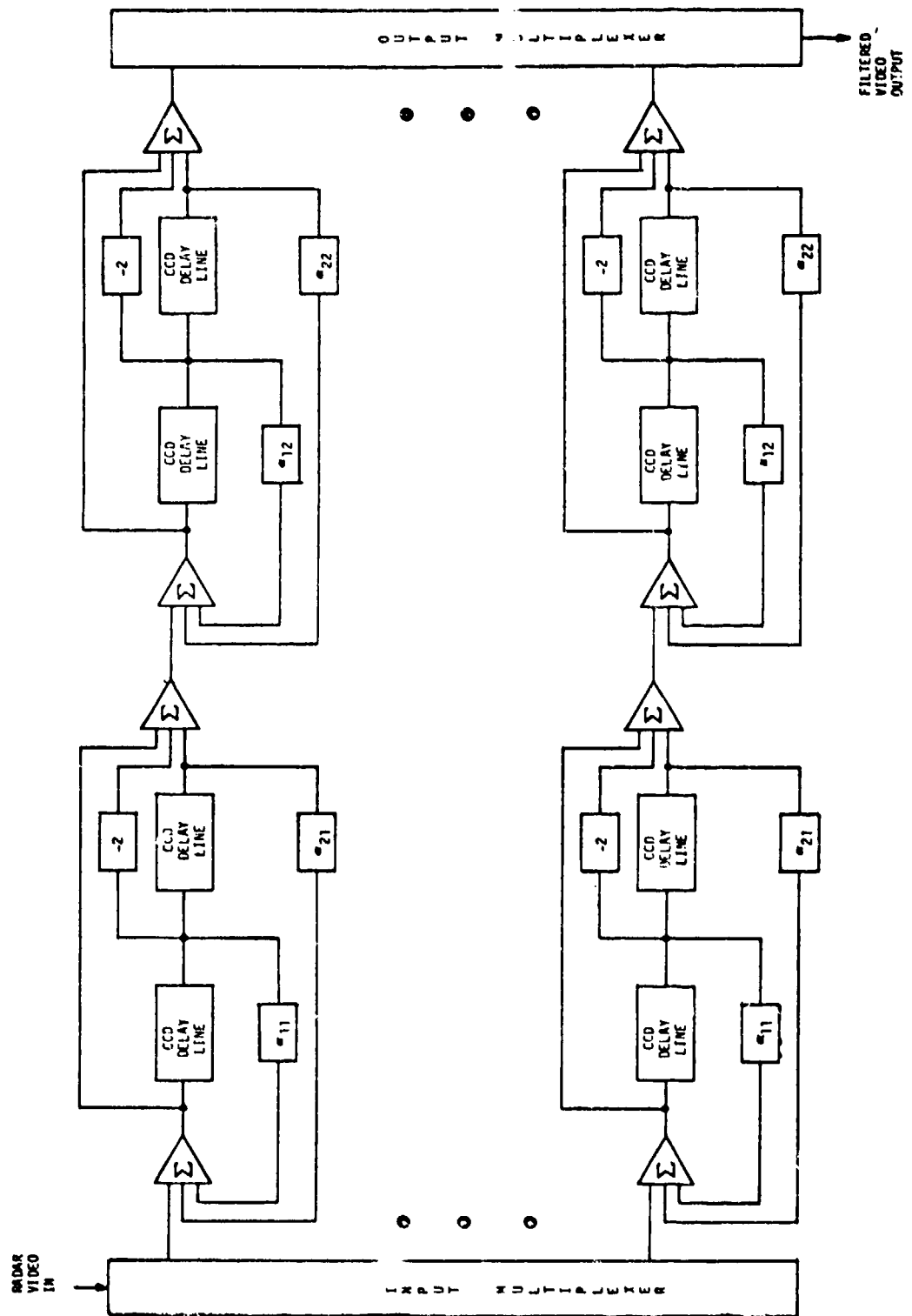


Figure 2. Multiplexed CCD MTI

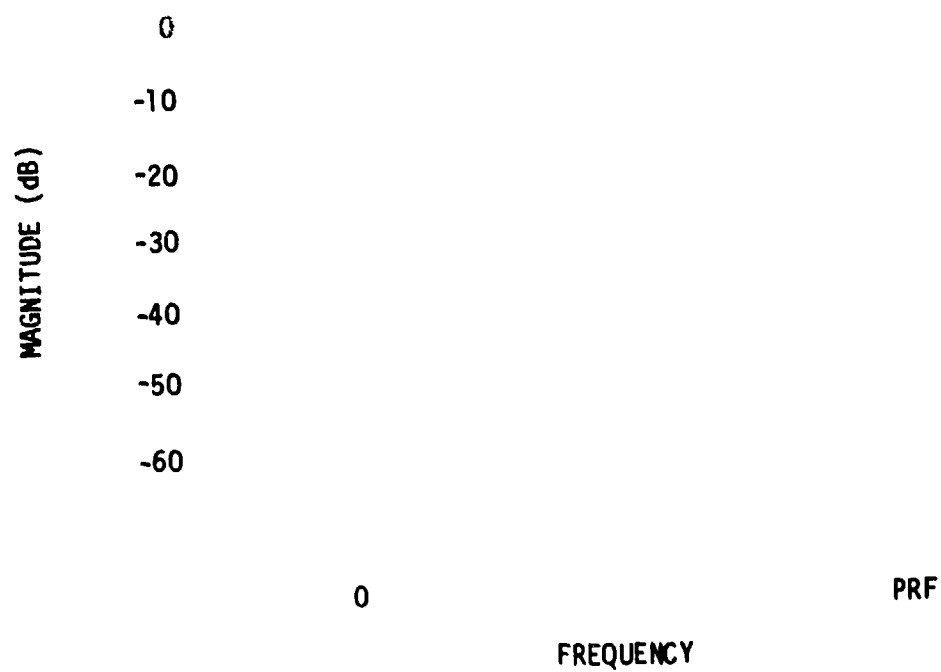


Figure 3. MTI Transfer Function Responses

MAGNITUDE (dB)
0
- 10
- 20
- 30
- 40
- 50

INPUT

DC

PRF/2

PRF

FREQUENCY

MAGNITUDE (dB)
0
- 10
- 20
- 30
- 40
- 50
- 60

OUTPUT

DC

PRF/2

PRF

FREQUENCY

FIGURE 4. PHOTOGRAPHS SHOWING SPECTRA
OF (A) INPUT AND (B) OUTPUT
OF SIGNALS FROM THE MTI.

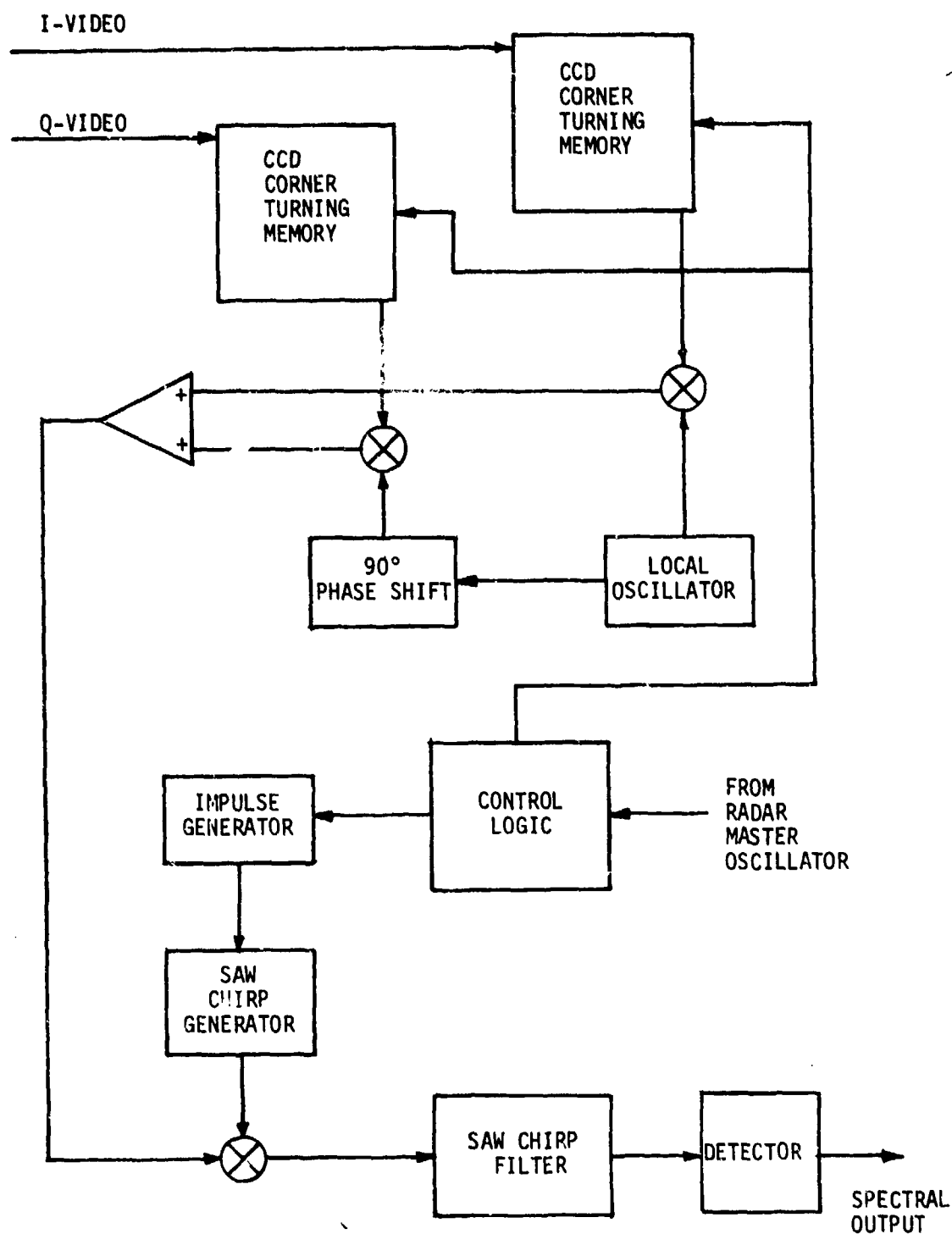


Figure 5. Doppler Processor Utilizing CCD Memory and SAW CZT.

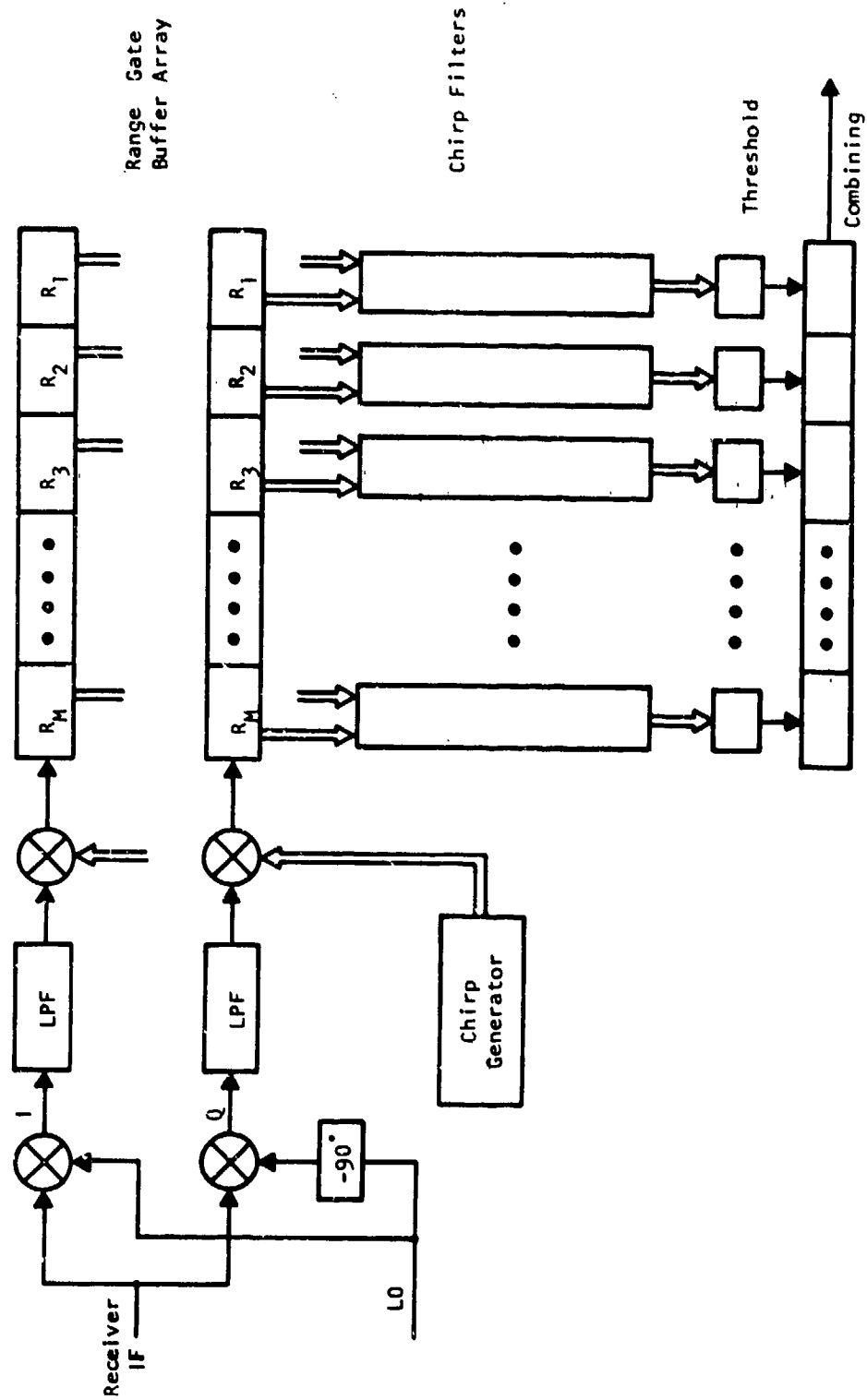


Figure 6. Doppler Processor Utilizing Range Gated CCD CZT's

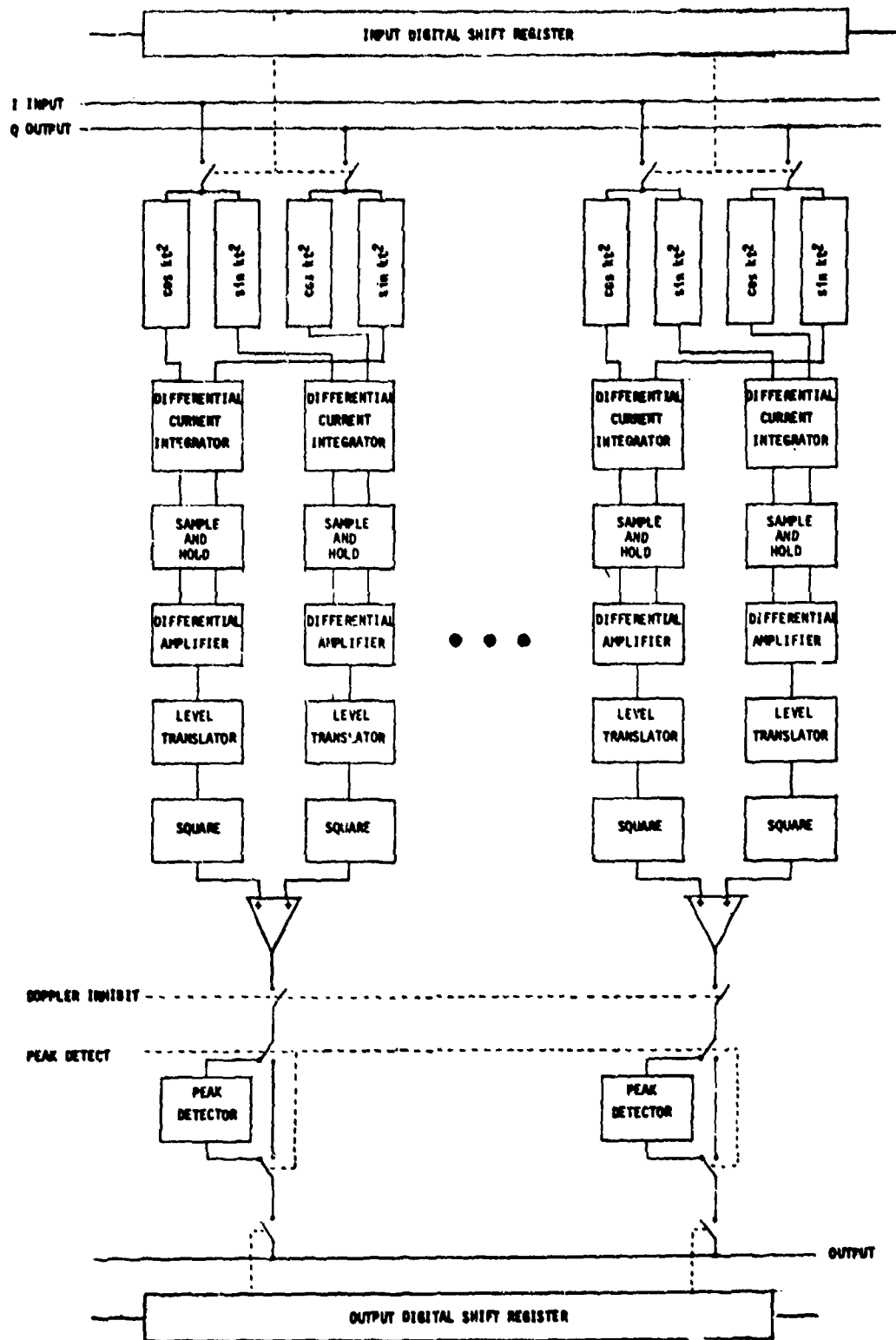


Figure 7. CZT Processor Block Diagram

RANGE BIN OUTPUT

$F_D = 62.5 \text{ Hz}$

RANGE BIN OUTPUT

$F_D = 250 \text{ Hz}$

0 250 500 750 1000

F_D

RANGE BIN OUTPUT

$F_D = 62.5 \text{ Hz}$

$F_D = 250 \text{ Hz}$

0 250 500 750 1000

F_D

FIGURE 8. FIVE RANGE BIN, 32 POINT CZT RESULTS FOR DIFFERENT DOPPLER FREQUENCIES (A) IN DIFFERENT RANGE BINS AND (B) IN THE SAME RANGE BIN.

PAR DETECTION LOGIC FOR LINE SENSORS

Mr. Raymond J. D'Amore
Dr. Robert J. Dick
Dr. Donald H. Foley
Dr. Om P. Gupta

Pattern Analysis & Recognition Corporation
228 Liberty Plaza
Rome, New York 13440

1. INTRODUCTION

This paper presents the detection logic developed by the Pattern Analysis and Recognition (PAR) Corporation for the MILES family of buried line transducers, buried nine inches in the ground. These transducers consist of a magnetic core surrounded by a coil and have been observed to produce an output voltage whenever there is a change in the neighboring magnetic field or when a seismic disturbance occurs in the vicinity of the transducer. The detection logic was developed for two versions of the MILES transducers.

The MILES 42 Round transducer consists of 19 strands of super-permalloy center core covered with an insulation layer and a single wound layer of copper wire over its 100-meter length. The copper wire winding is transposed every 42 inches in order to minimize the effects of far-field or broad area disturbances. It has a polyvinyl outer jacket.

The MILES 42 Flat transducer is an advanced development model consisting of a center ribbon core of super-permalloy metal approximately 10/32 inches by 1/32 inch covered with a layer of insulation and then wound with copper wire transposed every 42 inches. It has a stainless steel outer covering.

Every effort was made to keep the logic the same for both the flat and round transducers. The purpose of the logic is to detect human crossings (intrusions) and vehicle crossings. The design goals were to detect intruders weighing over 75 pounds and crossing at 0.2 meters/second. Range containment is to be 5 meters. The probability of detection is to be greater than 0.9. The system is to give few alarms due to weather activity, outside the range containment, or for animals weighing under 25 pounds.

The detection logics reported herein have been based upon the analysis of a vast amount of data collected over two years from three different sites (Site-2D at RADC Griffiss AFB, Fort Drum Watertown, NY, and Barksdale AFB, LA). The data base consisted of more than 1,000 intrusions and many hours of false alarm data for a variety of scenarios. The features used in the logic are directly related to the characteristics observed repeatedly in the signals.

By having an extensive data base and features related to signal characteristics, we hope to have avoided "statistical traps" - the problem of getting high (but non-repeatable) performance on a limited data base.[1] In addition to these precautions the transducer signals are processed digitally. The digital logic has been implemented on an LSI-11 microprocessor for real time operation in field tests. This microprocessor implementation maintains a flexibility in design not afforded by a dedicated hardware implementation. While it is expensive to make changes dictated by some unforeseen field conditions in a dedicated hardware logic, these changes can be easily implemented in the microprocessor through reprogramming.

Altogether three logics, namely A, B, and C were developed. Two of them, logic A and logic B, have been implemented in an LSI-11 microprocessor for real time operation in the field and are being tested at RADC Site-2D, Griffiss AFB. Logic A has better probability of detection (POD) but the logic B has better F106 afterburner alarms and thunder and lightning rejection capability. A recommended logic C combines the features of both the logics A and B, thus retaining better POD, and features that can reject thunder and lightning and F106 afterburner alarms. However, logic C needs more computing power (a faster CPU) than that which can be provided by the LSI-11 microprocessor.

2. FEATURES

The MILES transducers are currently deployed with simple analog threshold detection electronics known as MAID. The bandwidth of the MAID electronics is only 0-4 Hz. A previous study conducted by PAR [2] indicated that better POD and FAR (False Alarm Rate) statistics can be obtained by utilizing information outside the above bandwidth. The bandwidth of the signal processed by the PAR detection logic is 0.1-55 Hz. This logic is sometimes also known as a "wideband" system for this reason.

The response of the sensor is not uniform over the entire length of the sensor. There are some "dead spots" where the signal may be lower by as much as 20 dB. Another 20 dB variation may be expected due to seasonal variation from unfrozen to frozen ground conditions. Therefore, in defining features in the sensor output signals, every effort was made to avoid features that depended upon the absolute voltage levels. Most of the features used are the ratio of energies in two different time intervals or two different frequency bands. In this way the logic is independent of any human interaction requiring day-to-day system gain changes. The exact structure of the signals in the time domain is not the same for all the events in a class. The detection logic presented here does not use any time domain structural details (e.g., rise time, fall time, number of peaks, etc.) for detection.

A valid intrusion creates impulsive activity in the time domain. Wind and jets also give rise to impulsive activity. Therefore, any simple logic to detect only impulsive activity in the wideband channel is liable to give quite a large number of false alarms. Fortunately, wind and jet energies rarely lie only in the band where footsteps have their energy. This allows distinguishing valid intrusions by searching for impulsive activity in different frequency bands.

3. FEATURE ALGORITHMS

The features used to date in the MILES-PAR logic are:

1. Sliding window ratios in three frequency bands.
2. Rate of zero crossings.
3. Saturation feature.
4. Ratio of background energy levels in two frequency bands.

The removal of dc from the data is necessary before computing any feature for the logics described here. It may be noted that the zero crossing feature in particular is extremely sensitive to any dc offset.

4. PERFORMANCE STATISTICS

Both logics A and B as well as the proposed logic C are combinations of the features presented above. The following Tables 1 and 2 provide the performance statistics based on the analysis of the digital data base.

Conclusions:

The intruder detection logics developed by PAR for MILES family of buried line transducers have been presented. Two of these logics, namely logic A and logic B, have been implemented on LSI-11 for real time operation and are undergoing extensive field tests at Site 2-D, RADC, Griffiss AFB, NY. The initial field test results are very encouraging. One important observation to be made here is the advantage of digital simulation of the logic.

Either of these two logics can be run on the same hardware by simply loading appropriate software from a papertape through a teletype. It is our experience that a data base, however comprehensive it may be, is never all inclusive and field operation is the best test of any logic. A digital logic avoids the huge investment in special-purpose hardware development before any significant field tests.

TABLE 1
PERFORMANCE OF LOGICS A AND B FOR FLAT TRANSDUCERS

Intrusions	Logic A	Logic B
Human crossing over frozen ground	POD > 85%	POD > 75%
Human crossing with quiet background	POD > 90%	POD > 80%
Human crossing in high wind	POD > 90%	POD > 80%
Human crossing during aircraft noise	POD > 90%	POD > 80%
Human crossing during land vehicle noise	POD > 90%	POD > 80%
Vehicle crossing	POD ≈ 100%	POD ≈ 100%

Nuisances	Logic A	Logic B
Lightning stroke nearby	No rejection	90% rejection
Gale force wind (30 mph +)	FAR 2 1/2/hr*	FAR 5/hr*
F106 takeoff nearby	No rejection Total	Total rejection**
Railroad train 1/2 mile away	rejection	Total rejection

* Site unattended for data for these statistics; animals, not wind, may have caused these alarms.

** Data base is small for this statistic.

TABLE 2

PERFORMANCE OF LOGICS A AND B FOR ROUND TRANSDUCERS

<u>Intrusions</u>	<u>Logic A</u>	<u>Logic B</u>
Human crossing over frozen ground	POD >90%	POD 85%
Human crossing with quiet background	POD >95%	POD 95%
Human crossing in high wind	POD >90%	POD 85%
Human crossing during aircraft noise	POD >95%	POD 75%
Human crossing during land vehicle noise	POD >90%	POD 75%
Vehicle crossing	POD 100%	POD 100%

<u>Nuisances</u>	<u>Logic A</u>	<u>Logic B</u>
Lightning stroke nearby	No rejection	95% rejection
Gale force wind (30 mph +)	FAR 1 1/2/hr*	FAR 1/hr*
F106 takeoff nearby	No rejection Total	Total rejection
Railroad train 1/2 mile away	rejection	Total rejection

* Site unattended for data for these statistics; animals, not wind, may have caused these alarms.

** Data base is small for this statistic.

Acknowledgements:

The authors thank the following individuals for their contributions in making this effort a success: Joseph Caralyus (PAR) for digitizing data and operating the electronics; Frederick Budelman for analyzing the data on GCOS 6180 system; Arthur Desens (RADC) project engineer; Lt. Michael Lavelle (RADC) and John Yermas (PAR) for developing hardware for this program; RADC personnel for building some of the hardware; and Raymond Allen, RADC, BISS program manager, for his overall direction and cooperation throughout the duration of the contract. This work was sponsored by the BISS Project Office, Electronic Systems Division, Hanscom Field, AFB, MA through the Rome Air Development Center, Griffiss, AFB, NY.

REFERENCES

1. Foley, D.H., "Considerations of Sample and Feature Size," IEEE Transactions on Information Theory, Vol. 27-18, No. 5, September 1972.
2. D'Amore, R.; Yermas, J.P. and Foley, D.H., "Analysis of Line Sensor Data," RADC-TR-76-8, September 1975, Vol. I, January 1976, (Confidential), XGDS-3 (ADC005249L).
3. Dick, R.J.; Yermas, J.P.; Gupta, O.P. and Foley, D.H., "Analog Signal Analysis Logic Design," RADC-TR-77-127, April 1977.

DETECTION OF MECHANICAL WAVES
GENERATED BY CONCEALED PERSONS

FRANCIS J. COOK

ENSCO, INC.

ABSTRACT

The feasibility of reliably detecting the presence of persons concealed in vehicles by externally sensing the low frequency mechanical waves generated by such persons has been established. The approach was to detect the heartbeat of a concealed person in a motorized vehicle in a high ambient noise environment by contacting the vibrating surface of the vehicle with a low frequency geophone. The feasibility of the approach was demonstrated by applying special signal processing techniques that recognize the heartbeat signal buried in interfering vibration noise produced by wind, adjacent traffic, engine operation and ground motion. The reliability of the approach was determined by applying the method to port-of-entry data collected at San Ysidro, California. Analysis of these data demonstrated the detection was performed to a high degree of reliability, and that an economical reliable hand-held portable sensor system for real time vehicle checking is feasible.

INTRODUCTION

With as many as 200,000 vehicles passing through 128 manned border ports-of-entry in one day, there is a need for a rapid and reliable means of checking vehicles for concealed people. We have investigated the mechanical waves transmitted from a human in a vehicle, coupled to the frame of the vehicle, and then detectable at the surface of the vehicle. The approach to the problem has been to concentrate on a special class of mechanical waves generated by humans, namely to detect on the vibrating surface of the vehicle the heartbeat of the concealed person. The heartbeat causes the vehicle surface to vibrate with an amplitude less than one millionth of an inch at a frequency corresponding to the basic human heart rate, i.e., about one and one half cycles/second. Such vibrations can easily be measured using contact geophones. The problem is to isolate the heartbeat vibrations from those due to wind, adjacent traffic, running engine, ground motion and a host of other interfering sources.

The key elements of the solution have been to develop a seismometer detection system using very low frequency geophones; the application of signal processing techniques for frequency domain filtering the signal

of interest; spectrum analysis for heartbeat structure; and phase detection analysis to exploit the coherent relationship between the fundamental and harmonically related heartbeat waveforms. Out of this work, we have formulated definitions of pattern classification variables. For passenger vehicles, we have shown that when represented in this classification space, our data indeed clusters into two groups: one predominantly representing empty vehicles and the other representing vehicles containing a concealed person. A summary of the methods and results follows.

METHODS

The signal from a L-4C Mark Products 1.0 Hz geophone was fed into a Sprengnether AS-110 high gain amplifier and recorded on an FM multi-channel analog instrumentation tape recorder. The output of a wind meter was also recorded so that our results could be correlated with local wind conditions. The geophone is the device that contacts the vibrating surface under consideration.

For the purpose of identifying heartbeat spectral features, the mechanical vibrations at a person's chest were first studied. With the subject reclining on his back and the geophone placed on his chest, time series and power spectra such as those of Figure 1 were obtained.

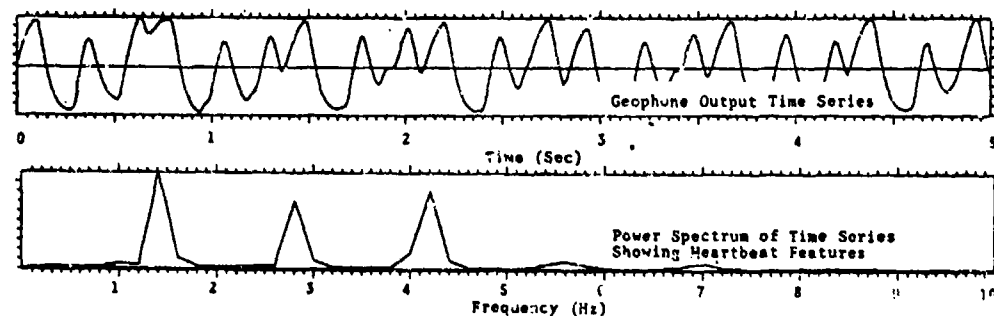


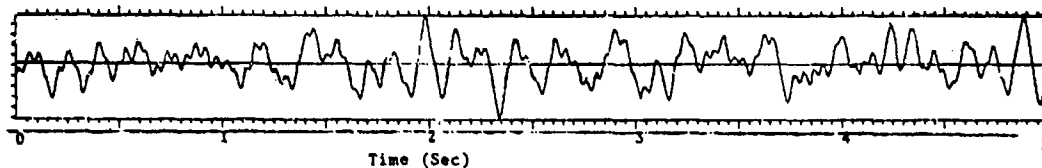
Figure 1. Mechanical Vibrations of Subject's Chest

In this typical example, at least three strong power spectrum peaks located at 1.4 Hz, 2.8 Hz and 4.2 Hz are clearly present. The first spectral line at 1.4 Hz corresponds to this subject's basic heart rate of 84 pulses/minute. All the remaining spectral lines are integer multiples of this fundamental and correspond to harmonics of the heartbeat waveform.

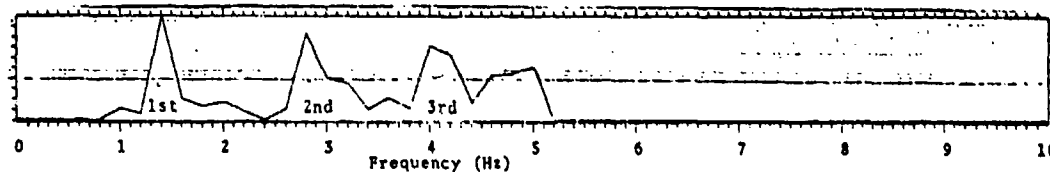
These spectral lines constitute the heartbeat features that are exploited to effect a detection.

This data collection system was used to record 220 minutes of mechanical vibration data on 160 vehicles crossing the San Ysidro, California port-of-entry. The vehicles included passenger cars from sub-compact to stationwagons, and including vans, buses, campers, motor homes, pickup trucks, intermediate trucks, and tractor-trailors. The vehicle conditions were combinations of engine on/off, vehicle with/without driver and/or passengers, and with/without one person concealed in the vehicle. Figure 2 shows an example of the detection under real port-of-entry conditions for one person concealed in the trunk of a passenger vehicle. Although the harmonic features are clearly noticeable

- San Ysidro, California
- Heavy Local Traffic
- Person Concealed in Trunk
- Extreme Ground Vibrations
- 10-15 mph Winds Present
- 1966 Mustang, Engine On



Measured Time Series of Mechanical Vibrations of Car Roof



Power Spectrum Showing 1st, 2nd and 3rd Heartbeat Harmonic Features

Figure 2. Detection Under Real Port-of-Entry Conditions

in this example, sufficient interfering vibration lines are usually present such that a detection method that only looks for spectral lines associated with the heartbeat will not be very reliable. We have developed a robust method to lock-in on the coherent properties of the heartbeat waveform, namely the stable relative phase differences between regularly spaced harmonically related phasor components of the heartbeat signal. This relative phase detector algorithm outputs a vector sum whose amplitude is a measure of the harmonic content in the signal. The interfering noise present in the signal produced by wind, adjacent traffic, engine operation and ground motion is relatively free of temporally stable harmonic structure in the 1 to 5 Hz band. Figure 3 shows

the results of applying the harmonic detector to simulated heart data and to real car roof vibration data. The strong peak in this amplitude

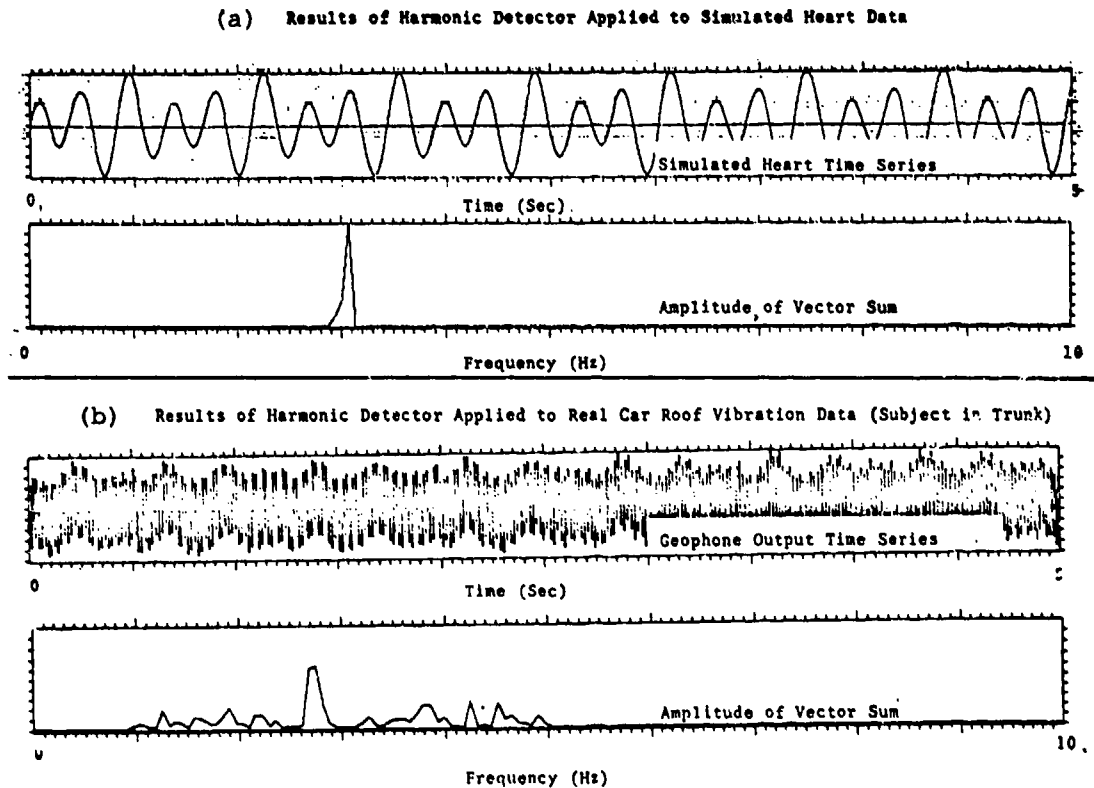


Figure 3. Relative Phase Harmonic Detector Results

plot indicates a successful detection. In addition to this amplitude information, the harmonic detector extracts from the data at least 15 other variables that can be used as inputs to an automatic pattern recognition classifier.

PERFORMANCE

An example of the pattern classification obtained for about 70 passenger vehicles, half of which were empty while the remaining contained a person concealed in the trunk is shown in Figure 4. Twenty-five percent of the vehicles had the engine on. The two classification variables labeled X and Y were built out of the harmonic detection algorithm. The classifier can distinguish empty vehicles from those containing a concealed person. The sloping lines on this scatter plot represent detector

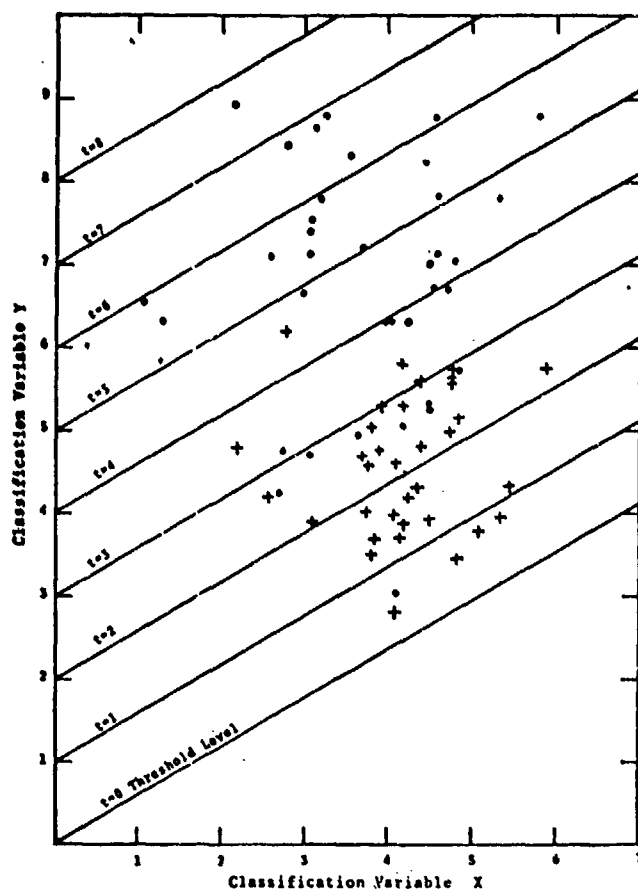


Figure 4. Harmonic Detector Classification of Empty Passenger Vehicles (+) and Those With a Person Concealed in the Trunk (•). San Ysidro, CA., Port-of-Entry Data

threshold levels. When the detector is activated such that the incoming signal combines to produce a classification point (X,Y) lying above a preset threshold level, an alarm can be made to sound.

The data we have collected allow certain performance probabilities to be experimentally determined without knowing how many vehicles crossing the port-of-entry actually contain a concealed person. Two such probabilities are:

- $P_{CP}(s>t)$: The probability that the alarm will sound given that there is a concealed person in the trunk.

- $P_E(s>t)$: The probability that the alarm will sound given that the vehicle is empty.

Using the data of Figure 4, these two probabilities are represented in the receiver-operating-characteristic curve shown in Figure 5. The diagonal line gives the expected results for a completely random detection method. We see that our results are decidedly outside the possibility of random detection and indicate a good performance capability.

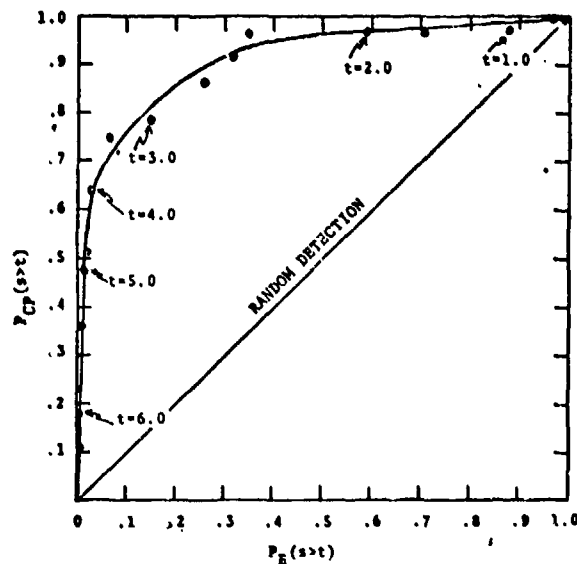


Figure 5. Receiver-Operating-Characteristic Curve Showing the Detection Probability, $P_{CP}(s>t)$, and the False Alarm Probability, $P_E(s>t)$, for the Harmonic Detector Using Passenger Vehicle Data Collected at San Ysidro, CA.

To illustrate the dependence of reliability on threshold level let us make an assumption about the fraction of vehicles crossing the port-of-entry that actually contain a concealed person. Suppose that 10000 passenger cars are tested ($N_T=10000$) and we assume that 100 of these cars have a person concealed in the trunk ($N_{CP}=100$). How many of these 100 persons will be apprehended and how many of the 10000 vehicles need be searched to realize that apprehension rate? Using the San Ysidro data of Figure 4, we obtain the reliability results of Table 1. These results tell us for example, that with a threshold level of 3.0, the alarm will sound for 17 percent of the vehicles tested and that 85 percent of the total number of concealed persons will be found in those vehicles for which the alarm has sounded.

Table 1
DETECTOR RELIABILITY FOR PASSENGER CARS AT SAN YSIDRO, CA.

$N_T=10,000$ $N_{CP}=100$

DETECTOR THRESHOLD	VEHICLES FLAGGED	VEHICLES WITH CP
t	$N_{s>t}$	$N_{s>t}(CP)$
1.0	8800	99
2.0	5700	96
3.0	1700	85
4.0	380	64
5.0	110	43

NOTE: N_T = Number of Vehicles Tested with the Detector
 N_{CP} = Number of Vehicles with a Person Concealed in the Trunk
 $N_{s>t}$ = Number of Vehicles for which the Detector Alarm Sounds
 $N_{s>t}(CP)$ = Number of Vehicles Containing a Concealed Person and for which the Detector Alarm Sounded

CONCLUSIONS

The results obtained in this work establish the feasibility of detecting the heartbeat of a person concealed in a passenger vehicle. The method also works for other large vehicles such as vans, buses, campers, motor homes, pickup trucks, intermediate trucks, and tractor-trailors. The reliability results presented were obtained using a first generation detection algorithm and no specialized fine tuning. Our continuing work to increase the detection rate will include modifications to incorporate multiple harmonic detection, account for residual heart feature instability caused by heart rate drift and optimize the choice and use of available classifier variables. An improved single and multiple sensor approach is under development to extend the application to railroad cars, aircraft, ships, and buildings as well as to locate and count concealed personnel. A single sensor engineering model of a portable hardware detector for real time vehicle checking is also being implemented.

ACKNOWLEDGEMENTS

The work was supported by the Department of Justice, Immigration and Naturalization Service under Contract CO-3-76. The author was aided by the diligent interest of INS Chief of Research and Development, Harry Frankel.

The author would like to recognize Dr. Richard Sebastian of ENSCO, Inc. for his role in the development of the harmonic detector.

ON-SITE DATA COMMUNICATION IN SECURITY SYSTEMS

Robert J. Carpenter
Computer Systems Engineering Division
Institute for Computer Sciences and Technology
National Bureau of Standards
Washington, D.C. 20234

Security systems for a single site, be it an office building or a weapons storage facility, require substantial communication from sensors to a central station and from that central station back to actuators. Even the simplest burglar alarm system has solved many of the same problems which face the designer of modern site security systems; just the level of performance is very different.

Elements of a Communication Link

Each on-site communication link must be designed to meet certain basic requirements. These are-

- a) data rate,
- b) reliability,
- c) distance,
- d) error control,
- e) security against intentional substitution of data,
- f) security against eavesdropping,
- g) ability to detect eavesdropping,
- h) environmental considerations,
- i) cost.

Each class of application calls for a different mix of these requirements. The term "line supervision" is often used to lump together (d) through (g). A good design requires that these important characteristics be considered separately.

The digital wave sweeping the communications industry has reached the site security field, for example the Facilities Intrusion Detection System (FIDS). Why would one choose to go to digital communication? The most obvious reason is that the data to transmit is digital (yes-no data). Digital transmission also allows the most flexibility in obtaining an optimum mix of the various factors in line supervision. Digital error control methods using check bits are well understood and can give nearly any desired level of assurance against erroneous data transmission. Data encryption can be used for security against substitution of data, and to make eavesdropped data less useful to the interceptor. Digital data encryption can be done to any desired degree of complexity, often with relatively inexpensive integrated circuit elements. While digital data can be communicated in a bit-parallel manner using multiple tones, the bit-serial technique is almost universally

used. This provides a better match to available circuit components.

Some on-site communication, such as voice and video will be by analog means for many years to come.

Communications Media

The practical techniques for communication are electrical and optical. Each has its advantages and drawbacks. Electrical communication will be divided into baseband (directly at the bit rate) and carrier (modulated radio-frequency carrier). Radio-frequency signals may be either transmitted in a wire or through the atmosphere. Likewise, optical signals may be transmitted directly or guided in an optical fiber.

Optical communication

Optical communication is getting increasing attention, usually when guided by glass fibers. Optical communication components are in a state of development comparable to electrical communication components sixty years ago. Optical sources (transmitters) are low-power and generally not coherent, or are very expensive and short-lived. Modulated optical power above a few milliwatts is hard and expensive to generate. Receivers directly detect the received power; the optical superheterodyne is a laboratory curiosity. For these reasons the spread between maximum practical transmitter output and minimum signal required at the optical detector is relatively small. This allows little margin for propagation attenuation or splitting of power among many users in a multidrop system. In a system with a 10 kilobit per second data rate, common optical detectors require at least -30 dBmW signal power for acceptable performance. For comparison an electrical receiver optimized for a 10 kilobit per second transmission rate will perform with an input signal power of -100 dBmW. The optical receiver requires ten million times as much received signal power. Optical fiber presently costing \$12 per meter is compared with coaxial cable costing \$3 per meter in Table 1.

While one may recall the nationwide semaphore signaling system in Napoleonic France, optical transmission through the atmosphere would seem to be a last resort in most cases. The path can be interrupted too easily by smoke, fog, dirt, and man-made obstructions.

Optical fiber transmission is a rapidly advancing field. The cost of low-attenuation cables is rapidly falling. Now at about \$12 per meter, we should see a price of under \$1 per meter in just a year or so. The connector problem remains severe, but will doubtless be solved in time. The simultaneous transmission of data and multiple TV signals on a single optical fiber is not yet practical in low-cost systems.

All of this is not necessarily bad for a site security system. The fact that optical detectors require substantial signal power to operate means that eavesdropping from an optical fiber is very difficult in a well-

designed system; though eavesdropping can be relatively easy near the sending end of long runs where the optical signal level is high, since direct leakage from the fiber could be enough to allow signal recovery. In most cases the intending interceptor would have to break the cable and insert a power splitter quickly to avoid being detected. With the present difficulty in making optical fiber connections, this seems extremely difficult. The cable would probably have to be broken in order to insert false data. For these reasons, the only coding or encryption of data required on most fiber optic links would be for verification of the sender.

Optical communication is essentially unaffected by severe electromagnetic interference such as EMP. However if power supply to repeaters is carried in wires along with the optical fiber, the voltage induced by lightning or EMP may be large enough to destroy the repeater unless it is protected as a wire-line repeater would be.

Electrical Communication

Electrical communication is a mature art, though certainly still dynamic in its application.

Radio frequency propagation through the atmosphere should not be used for on-site data communication for a number of reasons. Very sharp antenna beams are impossible because of the long carrier wavelengths, making eavesdropping from off-site very easy. Likewise off-site jamming would be relatively easy to create.

As already mentioned, electrical receivers require very little signal power, allowing multidrop systems. The choice between a baseband or carrier system may be dictated by other possible uses of the connecting wire. The combination of television and digital signals on a single coaxial cable is done in plant security systems. Carrier transmission is required when using cable-TV components such as booster amplifiers using power transmitted down the same cable as the signals. With electrical communication confined to a cable, the choice between baseband and carrier transmission is a trade-off. Cable leakage is higher at carrier frequencies, allowing easier eavesdropping from quite a few feet distant. As mentioned, cable-TV booster amplifiers require carrier transmission. Cable attenuation is rather high at the tens and hundreds of megahertz employed in cable-TV systems. Carrier transmission is much less susceptible to electrical interference from poor power line grounds and lightning.

Electrical communication is susceptible to interference induced by nearby lightning or EMP. This may cause data errors or even damage to the equipment. Protective circuitry can prevent damage except in cases of a very close lightning strike.

The pros and cons of optical and electrical techniques are summarized in Table 2.

Communication Networks

When there are more than two points of communication, the choice of best means for routing the signals and handling contention for the communication resources becomes significant. We all take the telephone switching system for granted. It is a fine example of a star network as shown in Figure 1a. The addition of local exchanges creates a system of interconnected stars as shown in Figure 1b. In the 19th century, before electronic amplification, these were the only practical choices for a network.

Of course, the rural multiparty line (multidrop) was required where cable costs were significant, as shown in Figure 1c. When not heavily loaded it was a tolerable solution, though eavesdropping left little data security. Modern communication techniques overcome most of the disadvantages of the multidrop system. This system is also termed "broadcast", since all stations can hear each other. A central control station is not needed in some applications.

The third major network configuration is the ring or loop, as shown in Figure 1d. It is receiving wide attention in the computer data communication industry. When used for digital communication, an active device such as a flip-flop stage is placed in the loop at each node. There seem to be real reliability problems with this approach in large systems. The network will fail if any station on it fails or has its power interrupted, unless a successful automatic bypass scheme can be developed.

Physical vs. Logical Network Organization

One should not overlook that the logical organization of a network may be quite different than the physical routing of the communication medium. A physical star configuration can be used as a multidrop network if all outgoing lines are driven from a single data output port and all incoming lines are combined into a single input port. Approaches of this sort may allow us to achieve the best features of two techniques. Even though optical fibers are limited to perhaps a 6-way power division, a physical star network of a number of such 6-way multidrop cables can be logically used as a multidrop network. Here we have the security of optical transmission and the reliability advantages of small subnets each with its own driver, and the broadcast (multidrop) network advantage of a single port on the central station computer for communication with all secondary stations. Thus no central switching system is required.

Methods of Digital Communication

Digital communication networks for site security systems are characterized by having one central station and many secondary stations at remote sensors or actuators. Thus the system design must be such that secondary stations are inexpensive. The central station must have means to establish a connection with each secondary station individually, and data must be sent back to the central station. In a star network, this is straightforward: merely connect to the private line of the station in question.

If concentrators are used, the concentrator must accomplish the line selection, which may be done in a hierarchical manner in the central station as well.

In multidrop and loop networks there must be some form of address signalling to establish communication with the desired secondary station.

In most cases, modern digital communication is accomplished by short messages called "packets". Each packet usually contains the following:

- 1) synchronizing field
- 2) address(es)
- 3) a control field; which contains packet sequence number(s)
- 4) data (may be optional in control packets)
- 5) error control field

A sample packet is shown in Figure 2.

The packet designer assigns sizes to each of these fields to suit his requirements. The address field need only contain the address of the secondary station if communication is always to and from a single central station. Systems allowing full interconnectibility usually require both source and destination address fields.

There must be a control field, in which packet type and sequence numbering is placed. One of the strengths of the packet concept is that each data packet is serially numbered, so that it may be retransmitted until successfully acknowledged by the intended receiver. A sending station presumes that a packet has been lost and repeats it unless an acknowledgement is received in a reasonable time. The sequence numbers allow both parties to the communication to keep track of which packets have been successfully communicated. The acknowledgement is generally accomplished in the control field.

The data field may either be optional in all packets or may require a special DATA packet type. In some systems, with highly formalized communication protocols, the data field may be of fixed length and may contain a complete message. Security communication may fit in this class. The more flexible situation is to have a variable-length data field.

Either a character-count or an end-of-data flag must be sent.

The error control field at the end of the packet contains a parity check or cyclic redundancy code check. Each packet received must be checked for errors by means of this field. Damaged packets are discarded and not acknowledged. The sending station will retransmit unacknowledged packets.

Polling vs. Random Contention by Remote Stations

The loop and multidrop networks allow time sharing of a wideband medium among many users. The system design must provide some means for handling the contention of the users for the medium. The designer must also decide whether the data flow in his system will be relatively uniform or have large peaks (bursts) and valleys. If there will be peaks, how many stations will have peak data requirements at the same time? If all stations may have their peak requirement at the same time, there can be no economizing based on statistical demand assumptions. The situation of simultaneous peaks from all remote stations may be conceivable in a security system, such as when the building is struck by a crashing plane; but usually these catastrophes render correct functioning of the network unimportant. The network need only give timely results for conditions which can be reasonably countered by the response facilities available. One should design for a graceful degradation of performance upon overloads and for automatic recovery upon removal of the overload.

Network Examples

Contention for the communication medium may be handled two ways. There may be a central controller which specifically grants time on the cable or fiber to each secondary station, or control may be distributed so each station contends for the medium when it has data to transmit. In most contention systems more than one station will transmit at the same time, resulting in destructive interference and a need to retransmit the lost data. Centrally controlled networks usually use some form of polling so that the control station can determine the actions required by the secondary stations. In networks with separate channels to and from the central station, only the central station uses the outbound channel so that there is no contention problem on that channel.

A Polled Network

This network is based on the assumption that all remote stations must be polled continually and that data will be reported in a fixed format on each reply. This network employs one data path from the central station to all remote stations and another path used for all return messages. They may be two frequency bands on a bidirectional cable-TV system.

Polling of secondary stations is implied in the following way. For example assume that the status of the remote station is reported by an

eight-bit word. This is the basic word length of the entire communication system.[1] Eight-bit cypher feedback encryption may be used if required. The central station sends fill characters of this standard word length on the outgoing channel if it has no commands to issue to the remote stations. Both the central and all remote stations keep word counters, incremented after each received word. Each remote station sends its one-word status message when its word counter equals its own address. Thus the polling is implied. The trick is to keep the counters at all stations synchronized. This is accomplished by a special synchronizing sequence from the central station that commands all stations to reset their counters to zero. The remote stations continuously monitor the command stream from the central station which contains messages in a conventional packet format, each message starting with a flag character followed by the address of the intended receiving station.

Advantages: Since the design eliminates all contention for resources, the results are very predictable. There is nearly perfect utilization of the cable bandwidth in the inbound link since there is no contention or overhead. This design is well suited to an installation in which all raw sensor data is reported back to a central decision-making system. The variable response commands from the central station can be flexibly addressed as required. Since all the sensor data is always reported to the central station, no peak loads exist.

Disadvantages: Since all the remote stations use a common reply line, they must place their data on this line so as to avoid overlaps. Unless delay adjustments are made at installation and repair times, this limits the length of cable to one which has a round-trip delay time of a small fraction of one bit duration. With 100 stations each sending an 24-bit status report twice a second, the round-trip delay is one-tenth of a bit duration with a cable length of about 2 km. These values result in about 4800 baud transmission. A cable of perhaps 20 to 30 km would be practical with careful delay adjustment at each remote station.

A Random-Contention System

In systems where considerable preprocessing is accomplished at the sensors, only exception data need be transmitted from the remotes to the central station. Much less data is transmitted, but it comes in bursts. Each remote station must contend for use of the communication link. Data must be composed into formal packets with all the overhead of addresses, control fields, etc., thus reducing the effective utilization of the cable bandwidth. Most designs of this type allow nearly unlimited cable delays. The central station and remote stations must keep up frequent traffic and require replies in order to verify the continued proper operation of the communication system.

There are a number of protocols suitable for this application. The ALOHA system, developed at the University of Hawaii [2]; and the Xerox ETHERNET [3] system are both very suitable. The ETHERNET provides for

entirely coequal stations and full connectability - which is not required in the security application - and results in more complex remote terminals. It will produce somewhat better utilization of the cable bandwidth. Despite these advantages, at least a variant of the ALOHA protocol seems better matched to the security application.

Assume an ALOHA system in which any station is free to transmit any time it has sufficient data. Destructive interference will occur if two stations send at the same time. Complete packets are sent since the sending station does detect collisions while sending. If the packet is received without damage, it is acknowledged. Unless acknowledgement is received in a reasonable time, the packet is retransmitted. A randomized wait before retry is required to avoid all parties to a collision from retrying at the same time. The theoretical maximum throughput of such a system is $1/2e$ of the cable bit rate (about 18%). [2] If the cable used to transmit to the central station were first examined to be sure it was not in use before transmissions were initiated, the theoretical maximum utilization of cable bandwidth is $1/e$ (about 36%). [4]

If a means is also added to sense for interference continuously during each transmission, and if transmissions are terminated immediately when "collisions" are detected, much better efficiency is predicted. These are the principles of the ETHERNET. Bandwidth utilization of up to almost 100% is predicted, depending on packet size. [3]

These numbers do not include the overhead of address, synchronizing, error control, etc., or acknowledgement packets. The useful bandwidth is thus likely to be only 2 or 3% of the cable bit rate for packets containing only 8 data bits. The efficiency becomes much higher for larger packets since the overhead is not a function of the number of data bits in the packet.

Advantages: The cable bandwidth is shared among the various stations on the basis of momentary need. Acknowledgement of good packets or retransmission of lost packets are automatic.

Disadvantages: These systems are based on random demands for service and will overload if all stations simultaneously require service. The utilization of cable bandwidth is very poor with short packet lengths. Secondary stations are more complex than in some polled systems. In ETHERNET, the bit rate is limited such that packets must last twice as long as the longest cable delay.

Network Failure Estimates

All man-made equipment is prone to failure, and communication networks are no exception. The various basic configurations will be analyzed to provide an estimate of their reliability.

Types of failure

Major types of failure include:

- a) Power supply failure,
- b) Continuous sending (chattering),
- c) Improper forwarding of data,
- d) Loss of synchronization,
- e) Component failure,
- f) Station shorting the cable,
- g) Cable breakage.

The remote stations should be designed to minimize the number of possible failures that disable the whole network. One would always choose to have a remote station fail such that it alone was disabled.

Star networks

To the extent that a separate data path exists to each remote station, failure of the remote station or its data path will not impact the rest of the network. For reasons of economy, a complex switching system is generally provided at the central station, which may fail catastrophically. An even more likely economy measure, to save the cost of separate communication paths from the central station to each secondary station, is to install remote concentrator stations serving a cluster of secondary stations. Each concentrator would have only one or two links to the central station. The reliability of such a system is substantially poorer than a one-level star network since the concentrators are remotely located and have many of the same failure modes and consequences mentioned below in loop networks. Fortunately the failure of a single concentrator may result in loss of communication to only one segment of the network. Breakage of the cable itself will generally affect only those secondary stations served by the defective cable.

Multidrop Networks

Each station is bridged across a single data path. If a station disconnects from the path when it fails, the rest of the network is undisturbed. If a station is limited to a certain duty cycle, a simple circuit can be built to disconnect it from the network should this duty cycle be exceeded. This overcomes almost all network station failure modes. Breakage of the cable itself will probably disable the entire subnet it serves, even those stations between the break and the central station, due to electrical reflections from the broken end.

Loop Networks

A single data path reaches from station to station. Data passes through each station. In most designs the station must synchronize to the incoming data and provide a place to store incoming data which arrives while the station is itself sending. Thus each station must correctly receive store and retransmit all the data on the network. The failure of

any station brings down the network. Likewise breakage of the cable itself will disable the entire loop. These problems are so severe that practical systems of this type employ reversible loops, dual loops, or other means to allow operation with at least one broken station. Automatic bypass means can be provided to cut broken stations out of the loop-- however the station must be able to tell that it is broken. This is a problem since duty cycle alone cannot be used; the data itself must be examined for errors.

The most likely failure impacts for the various types of networks are given in Table 3. In large installations using loop or multidrop networks, the installation should be broken into separate geographical regions with a separate network in each to avoid a single component from shutting down the whole system.

Failure Rate Predictions

Typical failure rates for multidrop and loop networks will now be calculated. Assume that a multidrop station fails so as to jam the network only half as often as a loop station. This seems plausible since fewer failure modes cause net failure. A net-jamming failure rate of 0.11 per thousand hours on the loop station and 0.05 per thousand hours on the multidrop station is assumed. In both cases the overall network reliability would be unacceptable. The failure rate of an automatic isolation unit for a multidrop network has been calculated to be 0.0005 per thousand hours. This unit has only 11 electronic components - 5 resistors, 2 diodes, two linear integrated circuits and one relay. This calculation is very conservative since most component failures would unnecessarily disconnect the station rather than disable the network. Since a design for an automatic bypass unit for a loop station was not at hand, the prediction of its failure rate cannot be as accurate, but it is assumed that such a unit would have many more active parts. An assumed failure rate of 0.005 per thousand hours is used. The tabulated data is given in Table 4. Cable failure rather than station failure would seem to be a more frequent cause of network failure if station-failure amelioration techniques are employed.

Conclusions

There are so many variables in data communication, that an overall best approach cannot be recommended for all on-site security systems. There seem to be separate situations which require at least two generic approaches.

Where television signals must be transported nearly everywhere, a carrier system using a polled multidrop approach on a TV cable would seem to offer the best solution. A large system of this type should be cheaper than a star network and more reliable than a loop. Dual separately-routed cables should be used if increased reliability is re-

quired.

If TV information is not required, an optical fiber star network should be considered. Power division and cable lengths should be chosen so that repeaters are not required, or power to the repeaters should be carried on wires in the cable. The network should logically be used as a multidrop network if more than a few secondary stations are involved.

Economical means for combining TV and data on a multidrop optical fiber system should be investigated.

References

- 1] Introduction to Autopoll, Interactive Systems, Inc., Ann Arbor, Michigan, 1976.
- 2] N. Abramson and F. F. Kuo, Computer-Communications Networks, Prentice-Hall, 1975, pp. 501-517.
- 3] R. M. Metcalfe and D. R. Boggs, Ethernet: Distributed Packet Switching for Local Computer Networks, Comm ACM, Vol 19, No. 7, July 1976.
- 4] L. G. Roberts, Capture Effects on Aloha Channels, Proceedings of Sixth Hawaii Conference on Systems Sciences, Jan. 1973.

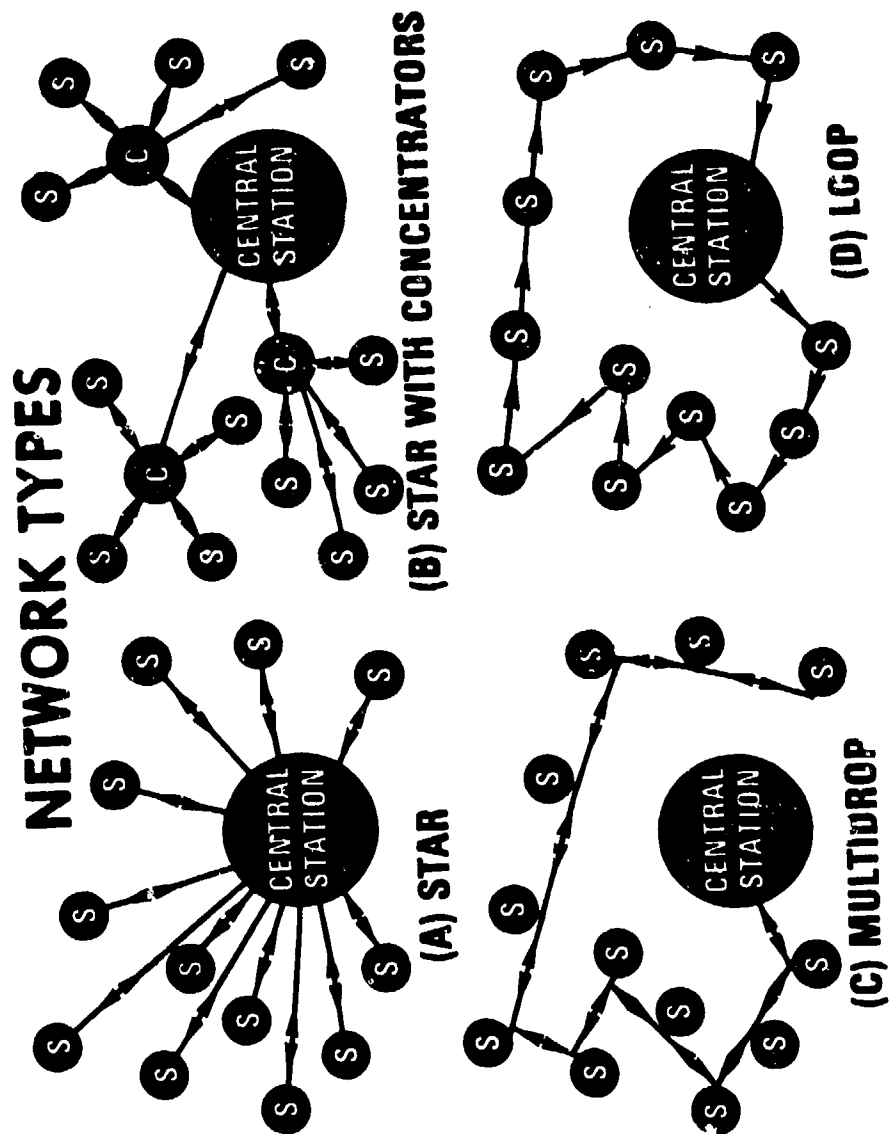


FIGURE 1

FIGURE 2
SAMPLE PACKET

Start				End
Sync	Address contains one or two addresses	Control Field contains one or two seq- uence numbers	Data Field may also contain byte count of data if variable length	Error Check

TABLE 1
ATTENUATION OF TRANSMISSION MEDIA

	1 cm Diameter Coaxial Cable			Optical
Frequency	<1 MHz	10 MHz	100 MHz	Fiber
Loss/kilometer	4 dB	12 dB	30 dB	10 dB
Percent loss	60%	94.5%	99.9%	90%

TABLE 2

COMPARISON OF OPTICAL AND ELECTRICAL COMMUNICATION

Characteristic	Optical		Electrical	
	Atmospheric	Guided	Atmospheric	Guided
Data Rate	Very high	Very High	Moderate	High
Ease of Eavesdropping				
a) From On-Site	Easy	Very Difficult	Very Easy	Easy
b) From Off-Site	Possible	Impossible	Very Easy	Very Difficult
Ease of Substitution of Data:				
a) From On-Site	Fairly Easy	Very difficult	Very Easy	Difficult
b) From Off-Site	Moderate	Impossible	Very Easy	Nearly Impossible
Environmental Effects				
a) Snow, fog, etc.	Serious	None	Very Small	None
b) Man-made Obstruction	Serious	None	Very Small	None
c) EMP Data Errors	Not Likely	Not Likely	Serious	Very Serious
d) EMP Damage*	Not Likely	Not Likely	Not Likely	Likely
Ease of Intentional Damage or Jamming	Possible	Difficult with Buried Cable	Very Easy	Moderate with Buried Cable
Distance Without Repeaters				
a) No Splitters, Taps	1 km	1 - 2 km	5 - 30 km	2 - 5 km
b) With 6 Nodes	Impossible	100-200 meters	5 - 30 km	2 - 5 km
c) With 50 Nodes	Impossible	Impossible	5 - 30 km	1 - 3 km
Cost				
Transmitter, Receivers Cable, etc.	Wideband \$600 Telescopes, \$500 each	Wideband \$600 \$10 per meter, soon \$1-2	Radios \$1000 Antennas, \$100 No distance	About \$250 \$3 per meter
Installation	Mounting	\$10 per meter Burial	Mounting	\$10 per meter Burial

*Damage likelihood can be reduced through application of protective measures.

TABLE 3

NETWORK IMPACTS OF FAILURES AT SECONDARY STATIONS

Failure Type	Star	Concentrators	Multidrop	Loop
Power Failure		X		X
Continuous Sending		?	X	X
Improper Forwarding		X		X
Loss of Sync		X		X
Component Failure	X	X	X	X
Shorting Cable		X	X	X
Central Switch	X	X		

TABLE 4

MEAN TIME TO NETWORK FAILURE CAUSED BY STATION FAILURE (HOURS)

Number of Stations	Loop Network		Multidrop Network	
	No Bypass	With Bypass	No Anti- Chatter	With Anti- Chatter
10	909	20 000	2 000	200 000 (22.8 years)
20	454	10 000	1 000	100 000 (11.4 years)
50	182	4 000	400	40 000 (4.5 years)
100	91	2 000	200	20 000
200	45	1 000	100	10 000
500	1.8	400	40	4 000

DATA ENCRYPTION

S. Jeffery and D. K. Branstad
National Bureau of Standards
Washington, D.C. 20234

SUMMARY

Encryption can be an effective process for protecting data during transmission within computer systems and networks. The degree of protection provided by encryption depends on the encryption algorithm employed, the implementation of the algorithm and the administrative procedures regulating its use. Additional security requirements of user identification, access authorization and auditing may be satisfied by combining encryption technology with a network access control machine in a network security center. This paper presents an encryption algorithm for use in computer data communications, and discusses the security requirements that are satisfied by proper use of the algorithm.

INTRODUCTION

The desire to decentralize computer systems, data bases and computer terminals has led to an increasing use of computer data communications. This decentralization has provided more readily available access to the authorized users of computers and data but has also created more opportunities for unauthorized individuals to gain access. Computer systems and networks which are storing, processing and communicating sensitive or valuable information require protection against such unauthorized access.

The need for protection of the computer data as it is being transmitted between terminals and computers, or among computers, requires that the communication facilities be physically protected, or that the data be protected against unauthorized disclosure and undetected modification through the process of encryption. The word "encryption" has been derived from the word "cryptography" (Greek for "hidden writing") and means to transform data into a hidden, or unintelligible form, called cipher. Decryption is the inverse process and restores the cipher to its original form.

Encryption may be achieved either through the use of a secret process or through a generalized process which depends on a secret parameter. In order to allow compatibility of encryption processes among all potential network components, the latter method is preferred. The encryption process may be uniquely and unambiguously specified in an algorithm and the parameter which is supplied to the algorithm is called the key. In this paper, an

encryption algorithm which has recently been adopted as a Federal Information Processing Standard is described.

SECURITY ENVIRONMENTS

The security of computer networks will depend on many variables in the environment in which it operates. Some of these variables are measurable while others must be estimated. The number of users, terminals and computers potentially comprising the network may be estimated, but the actual number will vary because of different time zones and working hours, equipment needing maintenance and security violations pending investigation. The potential data paths within the network may be computed and charted, resulting in an estimate of the scope of vulnerability of the data. The potential number of unauthorized users seeking access to the network or other types of network security vulnerabilities cannot be counted or estimated accurately. Nevertheless, such factors must be considered in the design of a secure network.

Some assumptions regarding the network environment must be made in order to incorporate data encryption in an effective security design. One set of assumptions regarding the security environment may be stated as follows:

1. Both authorized and unauthorized users have knowledge of the operation of the network.
2. The internal mechanism (logic, memory, electrical connections, etc.) of a terminal is physically protected from unauthorized access.
3. Physical access to the external controls (keyboard, control buttons, identification input device) of a terminal is available to all potential users.
4. There exist individuals with the desire and technical capability of copying or modifying computer data as it is transmitted within the network.
5. There exist individuals with the desire to gain unauthorized access to the network through authorized terminals.
6. Administrators of the network desire to prevent the activities in assumptions 4 and 5.

BASIC ENCRYPTION METHODS

Encryption is a transformation of data from its original form to an encrypted form. Two basic transformations may be used--permutation and substitution. Permutation changes the order of the symbols of the text or data. In substitution, the symbols of the text or data are replaced by other letters, symbols or numbers. In ciphers which depend on permutation, the characters retain their identities but lose their positions. In substitution, the characters retain their positions but lose their identities. The basic transformations of permutation and substitution can be combined to form a complex transformation. Since the symbols used for computer data are groups of one or more binary digits ("1"s and "0"s), encryption of computer data consists of rearranging the order of the bits, or substituting one group of bits for another. The substituted group of bits may be smaller, the same size or larger than the group replaced.

When the encryption transformations involve substitution, encoding is usually distinguished from enciphering. A code is a replacement symbol for each symbol of plain text; a replacement symbol may consist of a letter, a syllable, a word, a phrase or a special symbol. A code book is a listing of all possible symbols or elements of plain text and the equivalent code word or code group, and encoding consists of finding every element of plain text in the code book and substituting its code group for it in the message to be transmitted. Decoding consists of finding the received code group in the code book and substituting the equivalent plain text for it, thus reconstructing the original message.

The basic unit of a code is a word or phrase while the basic unit of a cipher is a letter or a fixed-size group of letters. There is no clear-cut method of distinguishing codes from ciphers in many cases, but ciphers may be thought of as operating on units of fixed length while codes operate on units of variable length. Another useful distinction is that code typically operates on linguistic entities while cipher operates on syntactic entities. In most computer applications, bits or groups of bits are used in encryption algorithms without regard to their linguistic content. Therefore, the term enciphering is generally used for computer encryption methods based on substitution.

CHARACTERISTICS OF THE ENCRYPTION ALGORITHM

The algorithm which has been adopted as a Federal Information Processing Standard is a block cipher (electronic code book) of block size 64 bits, which uses an encryption key of

length 56 bits plus 8 bits for parity. The algorithm is based on several permutations and a set of substitution tables specifying the substitution transformation. Encryption proceeds by generating a binary pattern with one half of the input data and adding it (Modulo 2) to the other half; the two halves of the data are then swapped and this operation is repeated sixteen times. The cipher produced by the algorithm has several characteristics that are cryptographically desirable and advantageous for implementation in computer networks.

An important characteristic of this algorithm is its flexibility for implementation and use in various data processing applications. Each cipher block is independent of all others, allowing decryption of a single block in an encrypted message or data structure. Independent transmission of data blocks and random access to encrypted data is therefore possible. Neither time nor position synchronization of data encryption/decryption operations is necessary.

The format of a data block may be defined for each application. The entire block of 64 bits need not be entirely filled with data. It may be necessary or desirable to include other information in each block along with a smaller quantity of data. The only requirement for correct operation between the transmitter and the receiver of encrypted data is that a common interpretation of the subfields of the block be made. Subfields of each block may be defined to include one or more of the following: a block sequence number; a random number for ensuring that identical data fields result in different cipher blocks; error detecting information for preventing undetected modifications, either accidental or intentional, of the cipher; handshaking information to prevent adding or deleting of data blocks in an interactive communication; user, terminal or message identification; etc. Handshaking in this context means to include a portion of the last received message in a block being enciphered for transmission. The recipient must temporarily store transmitted blocks in order to check the handshaking field for accuracy. This operation prevents the recording of a message and the subsequent retransmitting of it to the same intended receiver by an unauthorized recipient of the cipher.

The security of the algorithm is based entirely on the secrecy of the key used for a particular operation. A key must be generated and then distributed to all authorized recipients of a particular set of data. Each group of users will independently generate a key or set of keys for its own use. Administrative procedures must be established to ensure that only authorized users have access to the keys and that the same key is available to encipher

and decipher a data message. Even though the encryption algorithm is public, an unauthorized recipient of encrypted data, possessing matching input data, is not aided in decrypting the entire message if the key is not known. With matched plain and cipher blocks, hundreds of years of computation would be needed on the fastest computers of today to obtain by systematic testing the correct key.

The algorithm produces cipher text in which every bit is a function of all of the data bits. A difference of only one bit in the data or key results in an equal probability for change in each of the cipher bits. Conversely, any error in transmission of cipher results in equally likely changes in the plain text after decryption. Thus an error in a single bit in a cipher block results in a radically different data block when it is deciphered. The algorithm specifies both the encryption operation and the decryption operation, which are similar, but not identical.

SUMMARY OF THE ENCRYPTION ALGORITHM

The algorithm is designed to encipher and decipher blocks of data consisting of 64 bits. Deciphering must be accomplished by using the same key as for enciphering, but with the schedule of addressing the key bits reversed so that the deciphering process is the inverse of the enciphering process. A block to be enciphered or deciphered is subjected to an initial permutation IP, then to a recirculating block product cipher process, and finally to a permutation which is the inverse of the initial permutation IP^{-1} . The operations of the algorithm are diagrammed in Figure 1. These operations are outlined below.

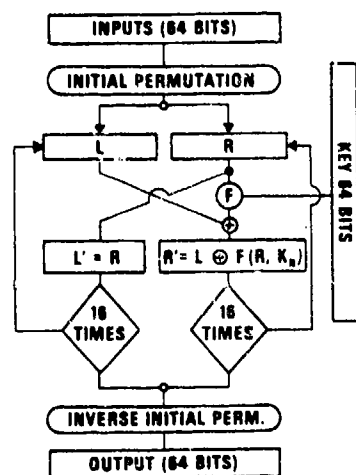
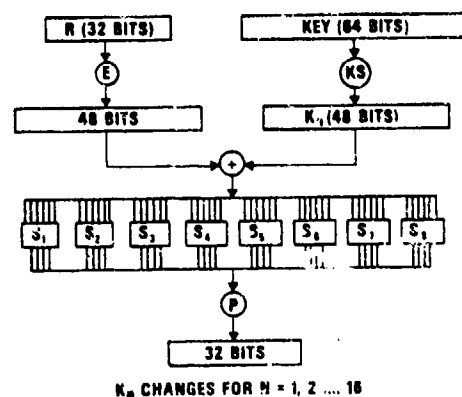


Fig. 1. Encryption Algorithm

Each input block, either of data or cipher, is subjected to the following transformation:

1. An initial permutation, or "shuffling," of all 64 input bits to evenly distribute the bits of each 8-bit byte of the input into two data vectors (L and R) or 32 bits each.
2. For $n=1,2,\dots,16$ perform the following operations:
 - a) Add (Modulo 2) the left data vector (L) to the result of combining the right data vector (R) and a subset of the encryption key (K_n) using an enciphering function F. Set $T = L + F(R, K_n), \text{ Mod. } 2$.
 - b) Set $L = R$.
 - c) Set $R = T$.
3. A final permutation of L and R into an output block which is ready for transmission (after enciphering) or use (after deciphering).

The security of the algorithm is provided by the effectiveness of the enciphering function F in combining the data and the key. The function F used in this algorithm uses the basic encryption transformations of permutation and substitution in order to change both the position and content of the input. The details of this function are depicted in Figure 2.

Fig. 2. Combining Function $F(R, K_*)$

E is an expansion operation which duplicates selected bits of R and results in a 48-bit data vector. KS is a KEY SCHEDULE function which iteratively selects a 48-bit subset K_n of KEY. S_1, S_2, \dots, S_8 are eight substitution tables which are used to replace 6-bit bytes with corresponding 4-bit bytes. P is a 32-bit permutation which shuffles the bits resulting from the eight separate substitution operations and results in $F(R, KEY)$.

The same algorithm is used to decipher data except that K_n are used in reverse order, i.e., $n = 16, 15, \dots, 1$. Of course, the identical KEY must be used to decipher the data as was used to encipher it. Since a large number of KEYS are possible for the algorithm and a large number of cipher blocks can result for the set of possible input blocks, the algorithm offers a high degree of security for computer data.

PRIMARY ALGORITHM IMPLEMENTATION

The data encryption algorithm specifies only the transformation of 64 bits of data into 64 bits of cipher. The algorithm is completely specified as to the results of the transformation but no specifications are given for its implementation. Variations in implementing and using the algorithm provide flexibility as to the application of the basic algorithm, how the input block is formatted and how the encryption key is generated and distributed.

Implementation of the algorithm is most efficiently and securely done in special purpose electronic devices. Overall security is based on two primary requirements: secrecy of the key and reliable functioning of the algorithm. Implementation of the basic encryption algorithm in dedicated electronic devices provides the following economic and security benefits:

1. Efficiency of algorithm performance is much higher in specialized electronic devices.
2. Standardized primary implementations of the algorithm will result in cost savings through high volume production.
3. The device may be functionally tested and certified outside the security environment.
4. The encryption key may be stored within the primary device and thus be protected from disclosure.
5. The security interface between the device and its environment may be completely and easily specified and hence is amenable to security monitoring.

6. Unauthorized and undetected modification of the algorithm is very difficult to achieve.

7. Redundant devices may independently perform the algorithm and a simple test of their output before transmission will yield a very high level of reliability and security.

8. Control of the primary encryption device as well as the interfaces necessary for the particular application or implementation may be contained in a secondary implementation device.

In addition to these economic and security benefits, implementation in certifiable electronic devices may be required to satisfy Government procurement requirements and export controls.

SECONDARY ALGORITHM IMPLEMENTATION

The primary encryption device performing the basic data encryption algorithm must be contained in a secondary device performing other services. These services interface the primary device to the network component (terminal or computer) and the data communication channel; e.g., data must be collected and entered into the primary device, various types of buffering methods may be needed, the encryption process must be initiated when the data has been entered, the status lines of the primary device must be monitored to detect completion of the encryption process or an error in the primary device, encrypted data must be accepted from the device and then properly entered into the data communication channel according to the required protocol. In some cases, e.g., asynchronous ASCII data communications, certain characters are reserved for control, and if enciphered data contains these characters the communication protocol will be violated. Procedures which circumvent problems associated with such occurrences must be performed by the secondary device.

When cipher is received at its destination in a computer network, the secondary device must be able to collect it, enter it into the primary encryption device, initiate the deciphering process, accept the plain text output and transmit it to the receiving device. These tasks may range from trivial to very difficult, depending on the communicating devices and the communications protocol.

Other security provision based on encryption techniques may be performed by the secondary device. An identification code for the network component and an authentication code for one device itself may be permanently embedded in the device. The identification code

would be transmitted whenever the device required identification, and the authentication code would be used as an encryption key to transmit an authentication message. IC will be used to mean the identification code of a terminal, a person or a computer; the IC may be commonly known and is only a claimed identity. AC will be used to mean the authentication code of a terminal, a person or a computer; the AC is an encryption key and must be protected. The key itself would never be transmitted through the network. The remote device requiring or performing the authentication operation must "know" the AC of the device. This would be entered into the encryption device at the remote site and if the authentication message is correctly enciphered, the device is authenticated.

A similar scheme may be used for the identification and authentication of the user of the device. An identification entry device must be available to the user to enter the user's IC and AC. The bank cash dispenser of today typically requires a magnetic striped card containing the user's IC and related information, while the AC (called the Personal Identification Number or PIN) is entered via a push-button keyboard. The user's IC is used for data file indexing while the PIN, which the user has been instructed to memorize and keep secret, is used for authentication.

CIPHER FEEDBACK

Most computer data that is to be transmitted or stored is coded in either 6-bit or 8-bit codes; the latter is more common today. An 8-bit code is chosen so that 256 possible data characters or control characters may be represented: ASCII and EBCDIC are examples. Most recently constructed terminals use one of these codes, and magnetic tape units are usually designed to handle either 6-bit or 8-bit bytes, which are written on one frame of the magnetic tape. In many communications disciplines, data is transmitted in bit mode or in character mode rather than block mode. The requirement of transmitting 64 bits of output of the algorithm when a full 64 bits of input are not available may put an undue burden on the communications system or on the storage system. Thus an alternate mode of using the algorithm was needed. The cipher feedback mode is defined to satisfy this requirement for using the data encryption algorithm in applications where the block mode cannot be used efficiently. The method allows generation of encrypted data of arbitrary block size from one to 64 bits.

The cipher feedback mode of operation is shown in Figure 3. The input to the Data Encryption Standard algorithm is not the data itself, but rather a string of the output that was previously generated by the transmitter of

the data. In the cipher feedback mode both the transmitter and the receiver of communicated data must be using the encryption function only.

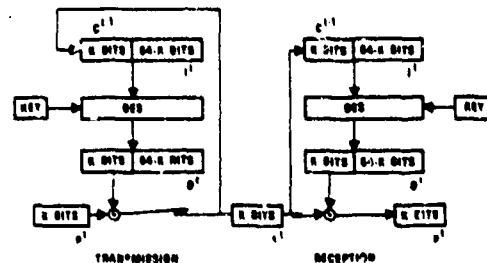


Fig. 3. Cipher Feedback

The transmitting and receiving encryption devices, when operating in the encryption mode with the same key and the same input, will produce an identical string of random bits in the output register. K-bits of this string are Modulo 2 added to K-bits of the data string, resulting in a K-bit encrypted word. This K-bit encrypted word is then shifted into input registers of both the transmitting and receiving devices. Therefore, after 64 bits of data, both devices are synchronized and the random string appearing at the receiver is exactly the same as that being generated at the transmitter. The Modulo 2 addition of this string to the encrypted data produces clear text. As one can see, the system is self-synchronizing but does require framing. A one-bit error in transmission will cause a 64 bit error at the receiving end but the devices then resynchronize automatically.

SUMMARY

The need for protecting messages and knowing the identity of the source and destination of those messages has been apparent for thousands of years. The need for protecting information in computer systems and the need for restricting access to it has recently become very real and apparent.

The implementation of security measures in a computer network will be based on several technical and administrative issues.

The procedures and costs of implementing security in a general computer network are not currently known. Several studies of network security have been conducted and the results are soon to be available from the National Bureau

of Standards. Network security will be based on the use of the new Data Encryption Standard.

REFERENCES

1. Branstad, Dennis K., "Encryption Protection in Computer Data Communications," Fourth Data Communications Symposium, October 7-9, 1975.
2. Branstad, D., "Security Aspects of Computer Networks," AIAA Conference Proceedings, Huntsville, Alabama, April, 1973.
3. Feistel, H., "Cryptography and Computer Privacy," Scientific American, May, 1973, pp. 15-23.
4. Branstad, M., D. Branstad and S. Jeffery, "Terminals: Out of Sight But Under Control," Digest of Papers (presented at COMPCON 74, February 26-28, 1974), IEEE Computer Society, 1974, 3 p.
5. Jeffery, S., "NBS Data Encryption Standard," presented at American Bankers Association, Bank Card Security Seminar, Louisville, Kentucky, October 13, 1975.
6. National Bureau of Standards, "Data Encryption Standard," Federal Information Processing Standards Publication 46, January 15, 1977.

CROSS CORRELATION VEHICLE CLASSIFICATION

RICHARD L. SEBASTIAN

ENSCO, INC.

INTRODUCTION

The cross correlation approach to automatic vehicle classification was the earliest implementation of a successful high speed algorithm. At its inception in 1971, the algorithm was designed to classify vehicles by specific type in rapid succession, possibly in a convoy situation. A first field implementation enclosed in a van and named VACIDS included such hardware items as two back-to-back minicomputers, an array processor, and a high speed digital filter. Today a fully minaturized version of the cross correlation classifier can be built.

The original design goals for the cross correlation classifier (CCC) called for single sensor classifications of passing vehicles at the rate of one every two seconds. The classifier was to use acoustic, seismic, or magnetic signals, or all three. For any of these signal types, isolating individual vehicles for classification without the use of directional sensors requires classification at the closest point of approach or point of maximum received power. Unfortunately, this is the point of maximum instability of the source signature. Extensive field work by the Army and ENSCO showed that differing terrain and weather conditions caused further variations. Thus, as originally developed, the CCC had to contend with very brief (0.5 seconds) signal segments which varied greatly within each classification category.

THE CROSS CORRELATION PROCESS

The cross correlation classifier is diagramed schematically in Figure 1. The preprocessing consists of the transformation of the power spectrum to a logarithmic frequency base and the calculation of the logarithm of the amplitude. The logarithmic frequency based spectrum effectively models the variation of spectral features with vehicle speed. This processed spectrum, termed the characteristic series, is then cross correlated with a set of references derived from the data base, resulting in a set of cross correlation functions. By a procedure to be described later, a set of vectors of correlation coefficients is derived from these correlation functions. The dimensionality of these vectors is equal to the number of classification categories, which represents a substantial reduction from the original 256-point power spectrum.

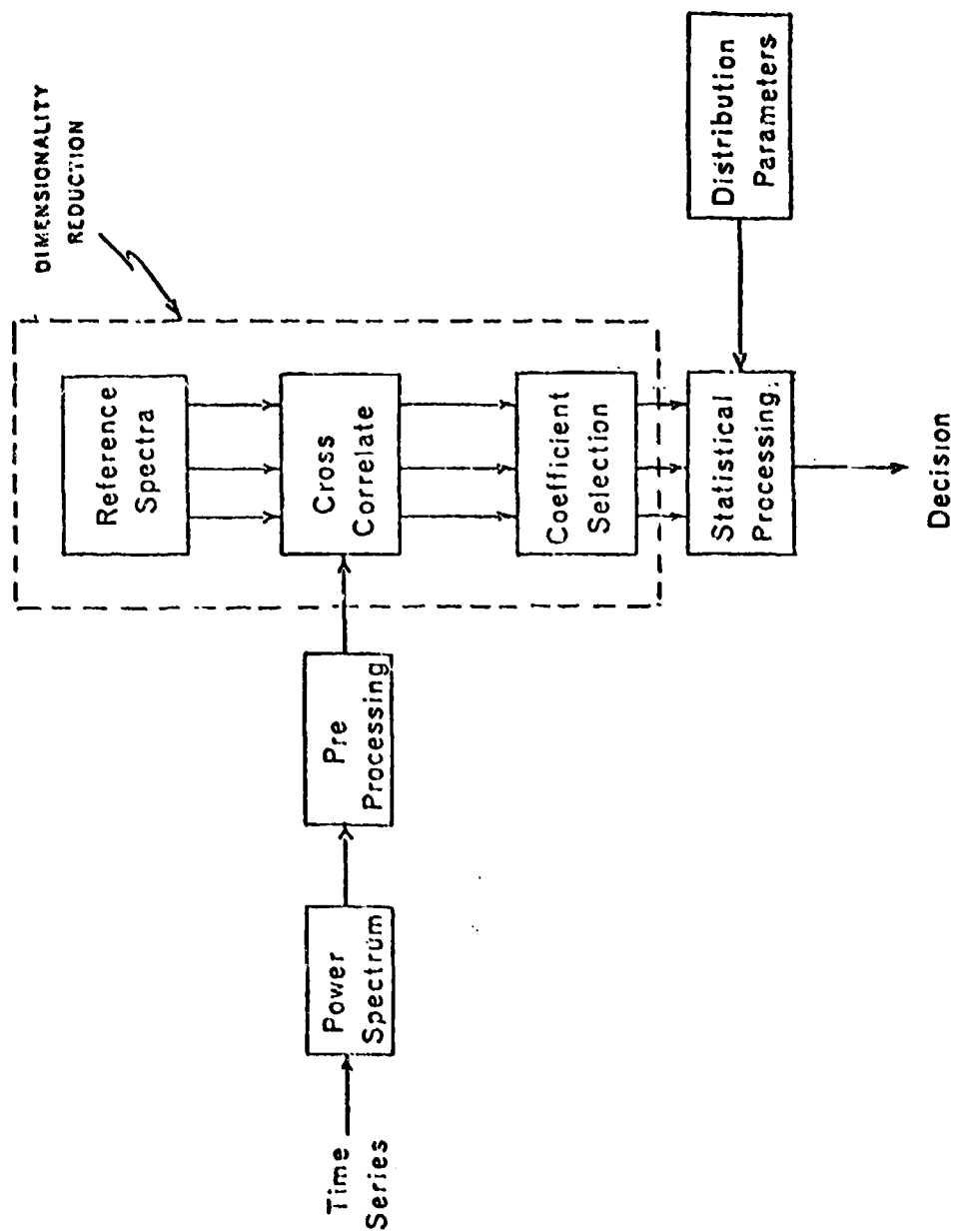


Figure 1. Cross Correlation Classifier

The correlation vectors derived from this preprocessing turn out to be separable by a maximum posterior probability calculation based on a normal density approximation. The parameters of the distributions used in this decision procedure are computed from the samples in the known data base. The following sections describe each step in the process in some detail.

The basic processing applied is identical for seismic, acoustic, and, when used, magnetic sensors.

The first step in the preprocessing is the calculation of the power spectrum of the input via the FFT. This power spectrum is then resampled at logarithmically spaced frequencies. The final step in the preprocessing sequence is the computation of the log amplitude of the spectrum samples.

The preprocessed spectrum vector is cross correlated with a set of reference vectors which have been selected from the data base as being representative of the classes of interest, and preprocessed in the same way as the input vectors. The resulting cross correlation functions are expressed as functions of the relative shift between the spectra on the log-frequency scale, which is equivalent to expressing them as functions of spectrum expansion factor on a linear frequency scale. Thus, the correlation of the input vector with shifted versions of a reference vector can be interpreted as correlating the input vector with a reference vector which has been adjusted for speed variations.

The spectral characteristics of a single vehicle vary so widely over the entire range of vehicle operating conditions that, even with log-frequency speed compensation, it turns out to be unrealistic to represent a single vehicle type by only one reference vector. This difficulty is alleviated by using an ensemble of three or four references to represent each category.

Since each spectrum is composed of components which vary with different operating features, it is clear that the correlation function between the unknown vector and a reference vector taken from the same vehicle type under similar operating conditions may have more than one peak value at different relative shifts. In addition, correlation of the unknown with references from other vehicle types may also produce peaks for relative shifts which cause one or more spectral lines to line up. Since most of the emanating energy lies in narrow lines, these spurious correlation peaks can have significant values. These problems are approached by the following procedure.

We have from the cross correlation calculations a set of cross correlation functions, one for each reference spectrum. If there are N categories of classification and an ensemble of M references for each

category, then there are $N \times M$ correlation functions. From each function six coefficients are selected by choosing the maximum value of the function in a set of six windows. Each window is symmetrical about the zero shift position, and is unity over an equal positive and negative range of shift values. It is zero elsewhere. The "zero-shift" window has a width of only one shift value, and hence selects the correlation coefficient for zero relative shift. The remaining five windows are successively wider, with the widest encompassing about one-half of the correlation function. A diagram of the idea is shown in Figure 2 for four windows, including the zero-shift window. From the $6 \times M$ coefficients derived from each ensemble of references a single six element array of coefficients is determined by finding the average of the coefficients in each window. These $6 \times N$ resulting coefficients are arranged as a set of six N element correlation vectors, and are the output of the correlation and coefficient selection procedure.

In the subsequent processing, we view these six vectors as somewhat independent, reduced dimensionality transformations of the raw data input. Any one of the six can be used independently for classification. In the application of the decision rule, each is treated separately up to the last step as described below. The cross correlation and coefficient selection procedure is summarized in Figure 3.

Consider the correlation vector from a single window. For different samples of vehicles of a specific type, this vector will be distributed in N -dimensional space according to some probability distribution which is unknown. For samples of vehicles of another type, it will be distributed according to a different, also unknown distribution. The success of the cross correlation classification technique rests on the experimental observation that these distributions separate for different vehicle types sufficiently to allow classification with satisfactory success rates. Although the actual forms of the distributions are unknown, they are approximated in the computational procedure by multivariate normal distributions with independent elements.

For each window correlation vector $C^k = C_1^k, C_2^k, \dots, C_N^k$, where k is the window index, a likelihood is computed that the vector was drawn from class (vehicle type) i . The parameters for the likelihood calculation are computed off-line from the data base for each window and are pre-stored for use in the decision rule.

A likelihood is computed from each class, and then these likelihoods are normalized by their sum to give posterior probabilities P_i^k .

$$P_i^k = L_i^k / \sum_i L_i^k.$$

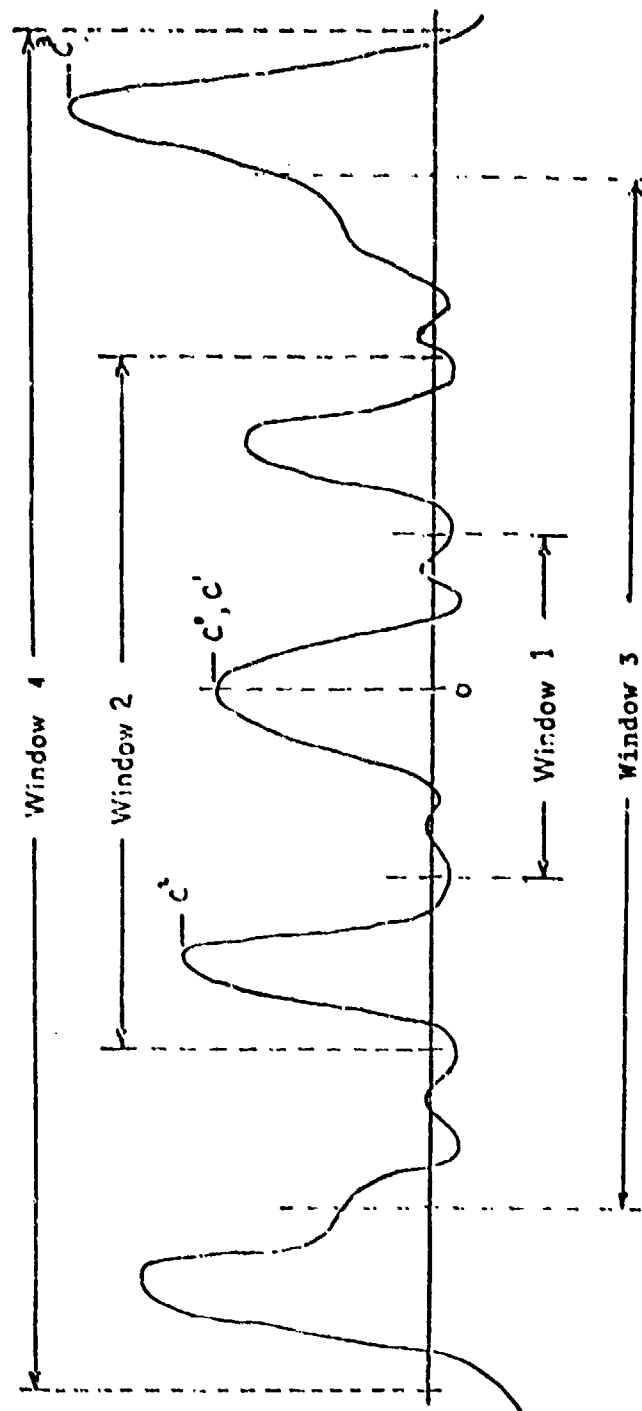


Figure 2. Correlation Windows

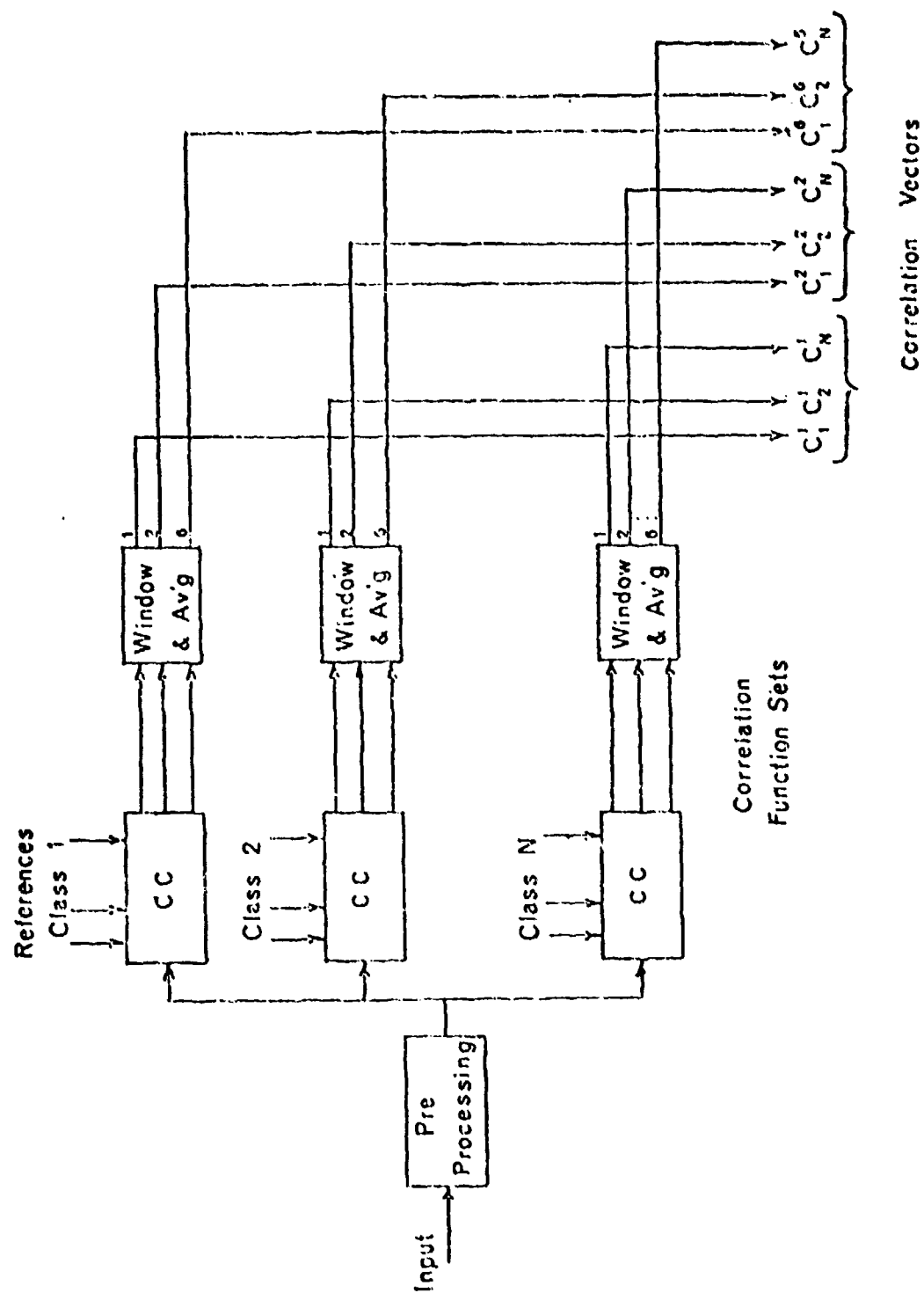


Figure 3. Correlation and Coefficients Selection

With an assumption of equal prior probabilities of occurrence of the different vehicle types, a decision could be made for each window vector by choosing the class for which P_i^k is maximum. Then a voting procedure could be used to arrive at a final decision. Instead of taking this approach, however, we average the probabilities of each class over the set of windows. This gives a single probability P_i for each class, where

$$P_i = \frac{1}{6} \sum_{k=1}^6 P_i^k.$$

The decision is then made by choosing the class for which P_i is maximum.

This procedure is essentially an application of the maximum likelihood decision rule. Use of this rule depends upon the representation of the probability densities involved by computationally convenient forms, in this case, the normal form. Clearly, alternate approaches to the decision rule can be envisioned. Well known examples are the nearest neighbor decision rule, and the use of potential functions to synthesize a more accurate representation of the true probability densities. The development of the cross correlation approach had as an overriding requirement the need for computational simplicity. The use of normal approximations and the maximum likelihood decision rule fulfills this requirement.

TEST RESULTS

The cross correlation process described above was implemented as a general purpose programmable classifier called VACIDS. In this section we summarize the performance of the basic VACIDS system. The results presented are taken from a series of tests conducted on a wide variety of data. The data consist of recordings of actual vehicle and aircraft passes made at a number of different sites. The system was tested in various operating modes with a number of different classification breakdowns.

The data base used for the test was recorded at five different sites -- Aberdeen Proving Grounds (APG), Fort Belvoir (EPG), Fort Bragg (FB), Grayling, Michigan (GR) and Yuma, Arizona over a period of about 18 months. A total of 1,084 vehicle passes were used, each "pass" consisting of a half second of data taken at CPA. Sensor spacing varied from 35 feet to 100 feet from the track. The vehicles used for the tests comprised two kind of tanks, several APC's and various heavy trucks, light trucks and jeeps. At Grayling and Yuma, data were taken from both fixed and rotary-wing aircraft. Success rates for wheel-track classification are given in Table 1.

TABLE 1
SUCCESS RATES: WHEEL-TRACK CLASSIFICATION

<u>Source</u>	<u>Wheel</u>	<u>Track</u>	<u>Average</u>
Aberdeen	100	91	96
Fort Brag	75	97	88
Fort Belvoir	99	77	88
Grayling	70	82	76
Yuma	38	97	67

The results for a four-class vehicle-aircraft classification as shown in Table 2.

TABLE 2
SUCCESS RATES: FOUR-CLASS VEHICLE-AIRCRAFT CLASSIFICATION

<u>Fixed-Wing</u>	<u>Helicopter</u>	<u>Wheeled</u>	<u>Tracked</u>
95%	100%	70%	91%

MINATURIZATION

Minaturization of the cross correlation classifier has been possible since the arrival of LSI technology. The degree of minaturization which can be accomplished is a function of the amount of specialized componentry which development cost limitations will bear.

The heaviest computation during the classification process occurs in the fourier transform computation. There are $MN+2$ fourier transformations for each classification, where N is the number of vehicle classes and M is the number of ensemble states within a class. This total arises as follows.

1. One transformation to obtain power spectrum
intervening step: (log interpolation)
2. One transformation to obtain complex fourier transform of the log frequency base power spectrum
intervening step: (complex multiply conjugate transform of reference spectrum)
3. Inverse transform of cross spectrum to obtain a correlation function
(one transform for each of the NM reference spectra)

Single chips soon will be available for performing the necessary transforms. For example, the T₁ Micro Vector Processor chip will be available in 1978. It is based upon high density, low power microprocessor/semiconductor technology integrated injection-current logic (I²L). The chip measures 0.25" x 0.25" and will be able to perform a 500 point transform in under one msec. Allowing for 300 percent overhead computation time this will allow a completed four-class classification in with six ensemble states for each class in approximately 0.2 second. This is five times faster than real time, thus continuous classification is possible (0.5 second vehicle spacing). This speed is also 15 times as fast as the current VACIDS field capability for performing the cross correlation classification.

ENVIRONMENTAL ADAPTABILITY

The principal problem with all automatic vehicle classifiers has been performance degradation accompanying changes in terrain or weather conditions. Field tests with the CCC have shown that adjustments to the final statistics stage without altering the reference spectra could be used to obtain high classification success rates after environmental changes occurred. These changes can be estimated from a few passes of known vehicle types. There is reason to believe that background noise or noise from unknown vehicle types could be used to accomplish the environmental adaptation. The important result is that the environmental adaptation can be accomplished at a final stage in the classification computation. This stage can be separated from the deployed sensor and requires an information input of vastly reduced bandwidth from the original acoustic, seismic, or magnetic signal.

SUMMARY

This paper has described the operating principles and procedures used in cross correlation vehicle classification. The algorithm was related to a methodology outline used in most approaches to pattern recognition. The novel processing features which make the algorithm successful are connected with the "feature extraction" phase of the processing, and are specifically intended to compensate systematically for some of the more obvious sources of signal variation within classes.

The approach was developed to meet the objective of classifying vehicles into narrowly-defined categories. It has subsequently been found that the same approach is also successful in classifying into broadly defined classes such as wheeled and tracked. It should be observed that success in narrow classification does not necessarily imply success for the same technique in broad classification. Principal features of the cross correlation classifier are: 1) only one-half second

of data is required; 2) it is computationally efficient, with the simulation producing results in live tests in less than 1.5 seconds; 3) it is adaptable in that new class definition can be easily introduced and the statistical distributions can be updated and modified to allow for a wide range of operating conditions; and 4) new digital hardware developments, particularly single chip fourier transforms, make the prospect of a minaturized cross correlation classifier quite promising. We also note that after the correlation coefficients have been extracted, the CCC is working with only a few numbers. It is possible to transmit these numbers and complete the classification process outside of the sensor, thus avoiding the need for duplication of this logic in each sensor. This procedure also allows the capability of adapting the classification to match the environment.

COMPARISON OF AVAILABLE TARGET CLASSIFICATION TECHNIQUES

by

Donald W. Keehan
US Army Mobility Equipment Research and Development Command

A capability to selectively classify military targets on the battlefield has been much sought after, with our current methods, however deficient, derived through many successive iterations of logics originally designed to reject the "non-target." For in developing a capability to reject undesirables, we needed to know more about how they were different from valid targets. Having perfected the capability to "reject," we therefore inferred an ability to "classify."

Our capability to classify targets was for many years constrained by our inability to develop sufficient hardware, which was field worthy, power efficient and inexpensive. We have in the past years minimized this problem especially with the advent of low cost microprocessor technology. With the microprocessor came more powerful methods or algorithms to assist in more finely separating or resolving target classes.

Classifying sensors today are configured in all forms from the simple threshold level identifier to the highly sophisticated cross correlation processor capable of actually learning on site. Level of complexity tends to track the degree to which a user attempts to identify specific classes of targets; but not always. These exceptions to the rule are the most interesting to study because they seem to contradict the theorem that more complex designs will ensure better performance.

During the course of this discussion we will compare many of the most prominent classification techniques in use today, attempting to highlight their strengths, weaknesses, and commonalities. We will also discuss our expectations for future hardware developments considering several months of recent testing against a variety of vehicles and sites. We hope to show that, in general, technology is no longer the pacing item in building classifier hardware.

Time Domain Processing Techniques

Time domain feature extraction techniques generally operate on an analog signal derived from a transducer (seismic, magnetic, acoustic, etc), properly conditioned and gain controlled. The features of a class of targets are relatively few in the time domain and generally tend to be related to physically observable phenomena, i.e., the footfall rate of walking personnel, the quite noticeable blade slap rate of a helicopter,

the characteristic whine of a jet aircraft or the engine noise of a wheeled or tracked vehicle. Integration or differentiation of these analog signals generally show respectively short or long term variations on these analog signals and, therefore, more fully describe the analog signal. This type of processor performs best against a small category of targets because of its inherent inability to resolve many features and the similarity that exists between some target classes, i.e., light and heavy wheeled vehicles.

Many of the feature extraction classifiers rely also on gross power spectral data to determine the presence and relative magnitude of energy in low and high portions of the transducer spectrum. The classification decision is further impacted by this information.

Figure 1 shows a typical block diagram of a feature extraction classifier with some of the features utilized to make a class decision. It holds the unique distinction of being the most tested, of all the techniques to follow. We have investigated its performance over 2000 target runs in the past 6 months and have generated a large base of information on its capabilities.

Power Spectrum Classification

The power spectral techniques used in target classification were motivated by a need to more finely resolve and more precisely define targets on the battlefield. To this end, a voluminous data base of military targets were recorded to provide users with descriptive data from which they might find target identifiers. In power spectral classification, the energy spectra of a target was resolved in the frequency domain into many energy bins, the number and size of which were motivated more or less, by the features inherent in the data base. Frequency domain resolution brought many new features to better light, especially those related to engine and cylinder firing rates, track pad rates, ancillary machinery noises, etc (Figures 2 and 3). In highlighting the features more fully, the new technique also showed the features to be functions of many variables some of which are uncontrolled.

Recognizing Spectral Energy Variations In Battlefield Targets

Attempts were made to classify using comparative energies and their associated frequency spectrums (Figure 4). These techniques were significant because they were the forerunner for present day implementation of complex hardware in a fieldable configuration. In a comparatively few field trials, the power spectral classifier appeared to be a feasible approach to identifying targets.

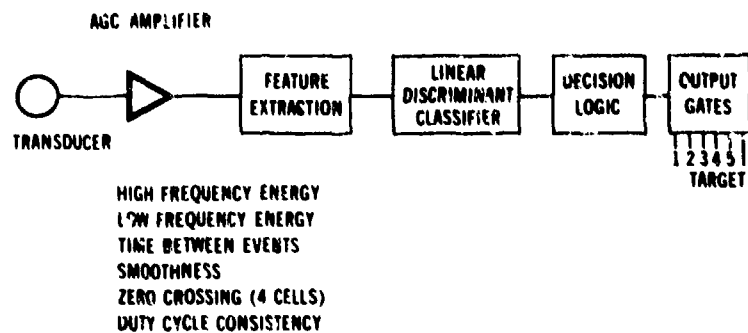


Figure 1. Block Diagram -- Feature Extraction Classifier



Figure 2. Acoustic Energy Spectrum of a Tank's Tread Line and Vehicle Exhaust System

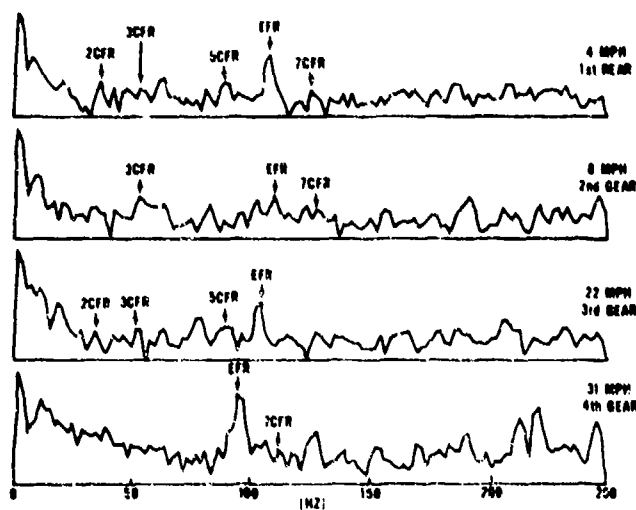


Figure 3. Spectra of Engine and Cylinder Firings for a Typical Vehicle

FEATURE	FREQ	RANGE	
1	20	25.2	ACOUSTIC
2	25.2	31.7	ACOUSTIC
3	31.7	40	ACOUSTIC
4	40	50.4	ACOUSTIC
5	50.4	63.5	ACOUSTIC
6	63.5	80	ACOUSTIC
7	80	100.8	ACOUSTIC
8	100.8	127	ACOUSTIC
9	127	180	ACOUSTIC
10	180	201.8	ACOUSTIC
11	201.8	254	ACOUSTIC
12	254	320	ACOUSTIC
13	1ST MOMENT OF ACOUSTIC SPECTRUM		
14	1ST MOMENT OF SEISMIC SPECTRUM		
15	28	85	SEISMIC
16	20	250	SEISMIC

Figure 4. Typical Feature Set for a Seismic Acoustic Target Classifier

Cross Correlation Classification (Figure 5)

Another level of hardware complexity resulted when feature "pictures" were stored in memory and were later compared with live targets in the field. The cross correlation technique provided extremely fine resolution of spectral lines and attempted to compensate for frequency and amplitude variations due to vehicle engine speed, etc. After features were selected for each type of vehicle, they were stored in memory to be later recalled and compared with a real time target vehicle passing the sensor.

The cross correlation classifier approach was unique in that the references stored in memory could be changed as desired to represent vehicles not already present or to represent vehicles at sites not already present in memory. A developer could then, for example, investigate the performance of the classifier at Fort Belvoir and use statistics from Fort Hood, Fort Bragg or both and then determine the variance or invariance of the classifier decision as functions of site or vehicle.

Many of the processing techniques currently being explored in sensor classification were approaches which achieved some measure of success in other related fields. Power spectral techniques were successful at identifying specific aircraft. Cross correlation processors have successfully been employed in target location roles in an underwater scenario. Perhaps the greatest difference in our sensor classification mission from those approaches mentioned is the extreme variability of our targets, environment and propagation media. We expect to find our limits in performance being more related to these variables than to our lack of processing capability. In fact, when a new design is proven successful in software, its credibility must remain questionable until the software is tested on many of the variables to be seen in field measurements.

In comparing the three most prominent approaches to target classification, we can say that none of the three have so far totally demonstrated the overall capability essential to meet a world-wide usage scenario. With "good" seismic and acoustic coupling and transmission and with solid targets, all perform well but in those less than "good" situations all can be found lacking somewhere. The reasons may be so obvious that we are missing their significance.

Let us examine the total problem, Figure 6. Our target source emits some energy form which can be sensed. Its emission is dependent on the sources (seismic, acoustic, magnetic, etc. signature) which must be coupled to the transmission medium. The source characteristics are subject to change, within limits by its nature (speed, weight, etc). The signals from the source arrive at the transducer through a medium

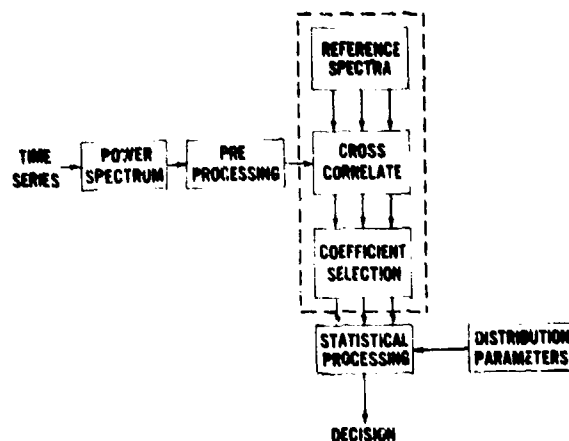


Figure 5. Block Diagram -- Cross Correlation Classifier

THE TOTAL SEISMIC DETECTION PROBLEM

TARGET SOURCE	TRANSMISSION MEDIUM	SENSOR
1. ENERGY COUPLING		
2. SURFACE MODULATION		
3. SPEED vs RPM OF ENGINE	1. LOW PASS FILTER RESPONSE ••• HIGH FREQUENCY ATTENUATION	1. TRANSDUCER COUPLING
4. VEHICLE VARIABILITY	2. MULTIPATH	2. DYNAMIC RANGE
	3. SOIL STRUCTURE	3. FIXED REFERENCES
	4. DISCONTINUITIES	a. SITE(S)
	5. BACKGROUND MODULATION	n. VEHICLE(S)
	a. RAIN	c. VARIATIONS IN SITE AND VEHICLE
	b. WIND	
	c. THUNDER	
	d. ETC.	

Figure 6. Variability as Related to Target Source at Mission Media and Sensor Interface

which generally imposes a low pass filter response on the signal. At the same time, other cultural and background noises are mixed with the signal source. The composite contaminated and filtered signal undergoes one more attenuation at the transducer due to coupling and finally enters the conditioning electronics and processors.

When a designer starts out, he first must select features from the target that are unique, exhibit some consistency and tend to propagate well through the medium. He then tries to find out how these features change as the medium changes. (This requires considerable data from many sites.) Having determined his features and their range of variability, he then defines the equation to represent the feature. All he needs to do then is to be sure no other target looks like the one he just finished defining.

It is our feeling that site variability will be the limiting factor and will therefore determine our ultimate ability to classify. In fact, comparative invariance of signal transmission medium is probably an important factor in the success of the spectral and cross correlation approaches in underwater tracking and aircraft identification. Hardware capability is no longer the pacing item as it was five years ago.

While some theoretical investigations have been conducted to determine the effects of the transmission medium on sensor performance, very little has been done to verify these theories and even less to implement techniques that might reduce site to site variations in existing classifier designs. Contractors have attempted adaptive processing in an attempt to stabilize a sensor in many environments but so far the adaptation has been found lacking.

After we have totally investigated the medium and know as much about it as we do our processors, we will be in a position to bound our performance. We will then be able to say that we are now extracting the maximum performance from our sensors and classifiers. We will no longer be quoting performance specifications that are as good or bad as the sites we tested at to derive our specifications.

In conclusion, let us restate we feel strongly that electronic processing exists to perform our classification mission and in most aspects we can afford it. We should now look to the medium between our target and classifier for complete definition and develop the techniques to adapt our processing capabilities over as many environments as possible. All sensors have limitations and the sooner we learn our real limits, the faster we can assist a user in developing application scenarios.

MIXED AND MULTITARGET CLASSIFICATION FEASIBILITY STUDY*

By

Dr. Marvin P. Pastel, Technology Advisor

US Army Training and Doctrine Command

1. INTRODUCTION.

In the fall of 1975, PM REMBASS recognizing the need for a fresh but knowledgeable review of the application of technology to the development of future REMBASS systems formed the REMBASS Scientific Panel. Especially, the Panel was to address the technical question of unattended ground sensor classification of targets in a multi and mixed target environment.

The Panel consisted of four members:

Dr. Marvin P. Pastel, Chairman
Technology Advisor
US Army Training and Doctrine Command

Mr. Howard Briscoe
Senior Technical Staff
Boit, Beranek and Newman

Dr. John Staudhammer
Professor of Electrical Engineering
North Carolina State University

Dr. Stewart A. Hoering
Professor of Electrical Engineering
University of Arizona

2. REMBASS MULTITARGET SYSTEMS.

The Panel recognized the hand implant "leave behind" and the artillery or air delivered "throw ahead" as two basic REMBASS Sensor classes each operating in different modes, with technical requirements and admitting to different types of technology.

The hand-implanted can generally be larger, more complicated in operation, and require critical placement and orientation for maximum utility. Because of the human selection of the site for these devices, local natural and cultural features can be used to reduce device detectability. The devices would include imaging sensor, IR beams, and road emplaced pressure cables.

*Scientific Advisory Panel Report, March 1976, PM-REMBASS, Ft Monmouth, New Jersey.

The "throw ahead" sensor, on the other hand, can only be located with any certainty, within 100-meters of the desired location and the ability to orient the devices is very limited. Because acoustical and seismic energy from a vehicle is generally omni-directional and of sufficient intensity to accommodate for the sensor locate variances the "throw ahead" sensor would, in most probability, be of the seismic and acoustic sensing types. This means of implanting would require that they be smaller and more rugged than the hand-implanted.

The Panel felt that the "throw ahead" class as offering a wider range of application and presenting the more difficult problem expended most of their effort in that area.

While the Panel recognized the system aspects of REMBASS, which may offer greater flexibility for system integration, the study generally addressed a single sensor operation rather than REMBASS as total system.

The block diagram, figure 1, illustrates the Panel's concept of a generic REMBASS Sensor classification unit. Each block represents a fundamental function or element required in the target identification process in a multi-target environment from target energy detection and final classification.

In a throw ahead application, the sensor unit appears to be generally limited to combinations of geophones and microphones. The subsequent discussion, while emphasizing acoustics, with differing specific problems apply equally to seismic detection.

In any given instrument design, the actual physical parts may not be neatly discernible as a given block. Thus, as well, the elements may be combined in different ways or even split as to location where the function or parts of a function are performed. This is especially the situation for the energy separation function. Hence, an understanding of the fundamental limitations of the various approaches of each is a basic requirement for development of a multitarget classification sensor system.

In a specific case, the functions need not be performed at a particular site. Distribution between sensor sites and at the central base, possibly with the aid of an operator, may be advantageous.

The block diagram of a single target classification sensor system would only omit the energy separation function. This assumes that energy separation is not necessary because only one target is within the field of the sensor or the energy from one target strongly predominates the others. Hence, the key to target identification in a multi and mixed

target environment is the separation of the energy from each target in such a way that subsequent functions of feature computation and ultimate classification can be accomplished on each target individually.

The Science Panel identified the following approaches to energy separation as having possible application to REMBASS:

- (a) Closest point of approach.
- (b) Sensor antenna.
- (c) Bigradient sensor.
- (d) Long base line array.
- (e) Short base line array.
- (f) Single sensor array.
- (g) Frequency and mode.

Other approaches may exist. However, those are the techniques which were brought to the attention of the Science Panel or were devised by the Panel. Except for the last scheme, each of these involves spatial separation and gives some degree of target location. If multitarget classification is developed, target location should be re-evaluated as a REMBASS objective.

Each of these techniques will be briefly discussed:

(a) The Closest Point of Approach attempts to give dominance to a single target by making a measurement when the time variation of energy at the sensor is a maximum. This assumes that there is sufficient spacing between vehicles for one target to dominate. Close spacing or a mix of high and low energy level targets will limit the usefulness of this straight forward and comparatively simple approach.

(b) The Acoustic Antenna array achieves multi-target energy separation by acoustical beam focusing similar to a directional radio antenna. The difficulty of this is the length of array required to provide reasonable gain and directivity at low acoustic frequencies. However, an array of 13.5 meters length will give some directivity and appreciable gain at 12 HZ. Such a length of array, however, to be delivered by artillery or aircraft and then to self-erect, poses interesting mechanical problems which may be amiable to space derived technology. With the target energy function performed in the sensor portion of the unit, the subsequent steps leading to classification essentially reverts to that of a single target device. In a throw ahead application, the orientation of the

However, preliminary calculations indicate that, in general, the phase and Doppler shift are not of sufficient magnitude to make the technique practical. Also, subject to question, is the assumption that the targets maintain essentially constant operating conditions over the period of time required for the measurements. However, the feasibility of performing multitargets classification by single sample warrants the approach be given some further consideration.

(g) By fine frequency separation using all available energy mode may, in principle, enable energy separation either by small variations between vehicle characteristics or varying conditions of operation. Indeed, a strong correlation for separating tread and engine signals appears to be a combination of acoustic and seismic energy. Moreover, this technique may be as useful as supplemental to the previous approaches.

The amplifier places basic limitations on the collection of target energy within the field sensor taking measurements in a multi and mixed target environment. The amplifier dynamic range and broad band target noise may limit the variation of signal strength to about 30db. For multitargets radiating a similar energy level, this is not a problem; however, weak acoustic targets in proximity to strong targets, but at greater range, may not be even detected, yet classified.

The target energy separation, feature selection and classification functions in multitarget REMBASS sensors will require the packaging of large electronic computational and storage capability within a small volume and using a minimum power.

Fortunately, the past few years has seen great strides made in solid state electronic circuitry in this very area. Large scale integrated electronic in the form of microprocessors have been developed by most major integrated electronics manufacturers and at very low prices. These together with 4K bit chip memories are available at very low cost per chip. The CMOS technology offer the low power consumption required for REMBASS application.

Useful large-coupled-devices (employing CMOS technology) with 16,000 bit memory chip units became available last year with increased access speed. CCD's also have an analog storage capability for fast Fourier transform applications.

The interconnection of microprocessors, memories, linear amplifiers and A/D and D/A converters on a closely packaged single substrate using thin film techniques, are the next logical sequence in electronic packaging. This, in effect, produce a microcomputer, which in a few years, should be well suited to meet REMBASS size, power and RAM requirements.

array would be random and some phasing of the array would be necessary to insure the beam would intercept the target paths within the sensor surveillance area.

(c) The bigradient sensor for multitarget classification is a logical extension of the work already underway at Naval Weapons Research Laboratory. However, faster techniques than phase lock loops would be necessary. Most probably, a Fast Fourier Transform would be required, followed by sufficient data storage and computational capability to sort out the energy from each target by direction of target energy source, since the energy separation function requires a fine grain frequency measurement. Classification techniques utilizing frequency spectrum such as power spectrum cross-correlation can be employed resulting, hopefully, in improved classification. A third bigradient phase may be required to eliminate readings in the pull of the phone reducing the noise level and insuring sufficient angular resolution.

(d) The long base line array would consist of three sensors positioned within a few hundred meters of each other and with the capability of two of the units to communicate to a master unit. Using correlation techniques distances between sensor and targets should be determinable. With this information, cross correlation procedures could be employed to pull specific target signatures out of a cluttered multitarget background. For this technique to be successful, target position relative to sensors must be measured to distance considerably less than that of the separation between targets. The array itself would initially be located by tracking a known target path; i.e., an aircraft. In a typical tactical situation, this would be sufficient accuracy for indirect/fire.

(e) The short base line array is a three sensor array forming a triangle about a meter on the side. Phase measurement difference between the sensors permits determination of target direction and in principle separation of acoustic energy from multiple targets that may be present. Actual processing and classification would be similar to the bigradient sensor.

(f) The single sensor array employs a single sensor to take multiple measurements. Each measurement is processed to determine the received signal frequency spectrum, most probably by performing an F.F.T. The frequency spectrums are stored and compared. Because the targets are moving, the phase and doppler shift of the frequency spectrum from each target will vary for subsequent measurements. But the changes in frequency, due to doppler, and the phase shift because of changes in distance, will be related for the frequency of a given target. In principle, target energy could be accordingly separated.

However, preliminary calculations indicate that, in general, the phase and doppler shift are not of sufficient magnitude to make the technique practical. Also, subject to question, is the assumption that the targets maintain essentially constant operating conditions during the period of time required for the measurements. However, the attractiveness of permitting multitargets classification by single simple sensor warrants that the approach be given some further consideration.

(g) By fine frequency separation using all available energy mode may, in principle, enable energy separation either by small variations between vehicle characteristics or varying conditions of operation. Indeed, a strong criterion for separating tread and engine signals appears to be a comparison of acoustic and seismic energy. Moreover, this technique may be useful as supplemental to the previous approaches.

The amplifier places basic limitations on the collection of target energy within the field sensor taking measurements in a multi and mixed target environment. The amplifier dynamic range and broad band target noise may limit the variations of signal strength to about 30db. For multitargets radiating a similar energy level, this is not a problem; however, weak acoustic targets in proximity to strong targets, but at greater range, may not be even detected, yet classified.

The target energy separation, feature selection and classification functions in multitarget REMBASS sensors will require the packaging of large electronic computational and storage capability within a small volume and using a minimum of power.

Fortunately, the past few years has seen great strides made in solid state electronic circuitry in this very area. Large scale integrated electronics in the form of microprocessors have been developed by most major integrated electronics manufacturers and at very low prices. These together with 4K bit chip memories are available at very low cost per chip. The C MOS technology offer the low power consumption required for REMBASS application.

Useful charge-coupled-devices (employing C MOS technology) with 16,000 bit memory chip units became available last year with increased access speeds. CCD's also have an analog storage capability for fast fourier transform applications.

The interconnection of microprocessors, memories, linear amplifiers and A/D, D/A converters on a closely packaged single substrate using thin film techniques, are the next logical sequence in electronic packaging. This will, in effect, produce a microcomputer, which in a few years, should be well suited to meet REMBASS size, power and RAM requirements.

3. DEVELOPMENT PLAN.

The study suggested a program for development of a basic seismic/acoustic system for a multitarget environment. The program consists of modeling, testing, setting of requirements and system implementation, all in context with the state-of-art. The interaction of these elements in the program is shown in figure 2.

Development of a new sensor system is always based on physical concept of the system operation. This concept may range from an implicit "seat-of-the-pants" understanding of the problem to an extensive explicit mathematical model of the system from the energy generation mechanism through the energy propagation and sensors to the signal processing algorithms and classification procedure. However, a multisensor approach to a mixed and multitarget detection and classification problem is sufficiently complex that an orderly efficient development program must be based on an explicit description of the physical phenomena that influence the system operation.

In this approach, the operational requirements for the system are used to define the range of phenomena that must be accounted for in the system model. As the model is developed and it is experimentally tested, it, in turn, can be used to evaluate the ability of any system design configuration to meet the operational requirements. The operational requirements can then be refined, based on basic theoretical limitations and costs.

4. CONCLUSIONS.

The study made the following conclusions:

A. The panel felt that with some limitation in terms of range, number, and classes of targets, mixed and multitarget classifying by unattended "throw ahead" sensors is possible. The extent of these limitations cannot be specified without a detail analysis beyond the scope of the study; however, the panel did not feel that the restrictions will seriously reduce the operational utility of the sensor for the majority of tactical situations.

B. The Panel felt that the 1980 state-of-art will support the packaging of mixed and multitarget classifying into "throw ahead sensor" within effectiveness and cost constraints.

C. The bigradient sensor, sensor antenna and long base line array appear to offer the greatest potential approach for future mixed and multitarget energy separation techniques.

D. Although target location was not explicitly investigated by the panel, it appears that multitarget classification and target location techniques are closely related.

SYSTEM COMPONENTS

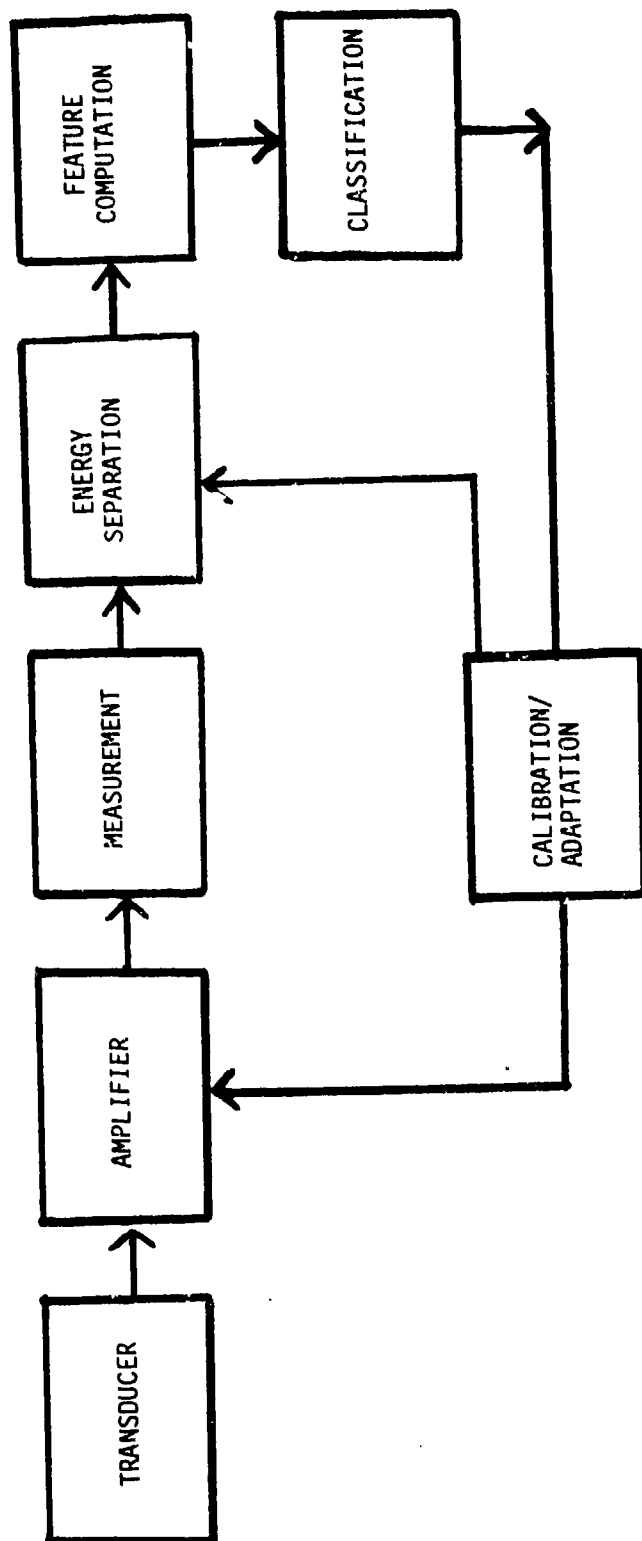


FIGURE 1

DEVELOPMENT PLAN

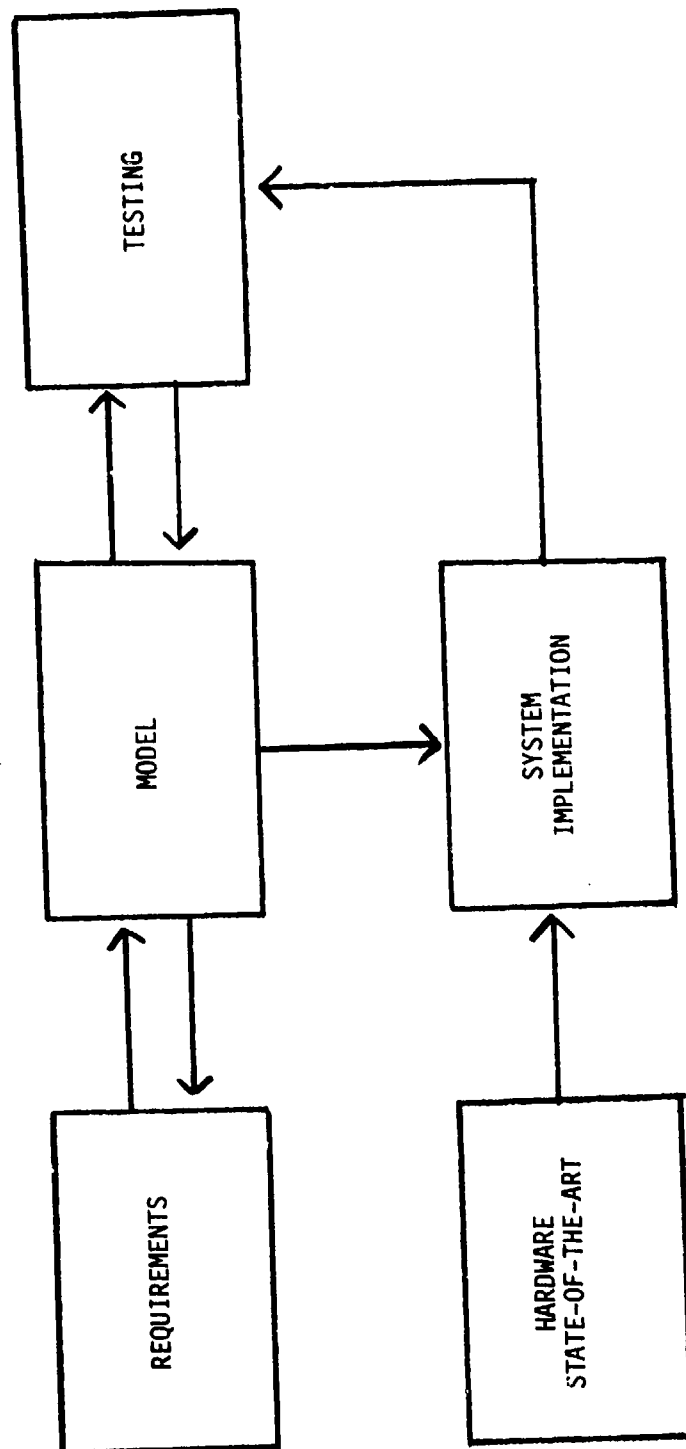


FIGURE 2

IMPROVED TECHNIQUES FOR SEISMIC
AND SEISMIC-ACOUSTIC PASSIVE RANGING
FROM A SINGLE SENSOR

Roger L. Barron
ADAPTRONICS, INC.
McLean, Virginia

June 1977

Paper Presented at
Technical Seminar on Sensor Technology for
Battlefield and Physical Security Applications

Submitted to:
U. S. ARMY MOBILITY EQUIPMENT RESEARCH
AND DEVELOPMENT COMMAND
Attention: DRDME-XS (Mr. Benjamin C. Barker)
Fort Belvoir, Virginia 22060

Submitted by:
ADAPTRONICS, INC.
Westgate Research Park
7700 Old Springhouse Road
McLean, Virginia 22101
703/893-5450

INTRODUCTION

It is considered highly desirable that a passive sensor system be developed that is capable of single-sensor range measurements for certain classes of surface targets. Such a system would eliminate the need for active ranging or cumbersome passive techniques based upon triangulation, etc. It would reduce system complexity, eliminate sensor-to-sensor communications, and facilitate operational deployment of mines and other devices that require ranging capability.

It has been long known that the seismic and acoustic signatures of targets such as tanks, trucks, personnel, and taxiing aircraft vary as a function of target range from the sensor. This is because ground and air propagation mediums attenuate some frequencies differently than others, thereby affecting the spectral content of the seismic and acoustic waves. What has been missing in previous investigations of the ranging problem is the ability to exploit this frequency-selective attenuation in design of passive equipment that extracts range information from seismic and/or seismic/acoustic waveforms.

This paper outlines several alternative approaches to solution of the passive, single-sensor range measurement problem. One of these approaches is examined in sufficient depth to establish, at least preliminarily, its feasibility for range measurements of in-motion tracked vehicles. It is shown that good range measurement accuracies are obtained for ranges from zero to at least 100 meters in simulation evaluations using field data representing a variety of geographical sites, tracked-vehicle types, and vehicle speeds. Substantial use is made of nonlinear signal processing functions realized via the Adaptive Learning Network (ALN) methodology discussed in the Appendix and the References.

The sensor of a single-sensor passive range measurement system could be implemented with equipment similar to that investigated for the U.S. Army REMBASS project. The range sensor could include target classification capabilities if desired.

BASIC PRINCIPLES

The accuracies of conventional target classifiers are sensitive to target range. These classifiers generally must be tuned for a stipulated nominal band of target ranges and exhibit degraded performance for targets outside of that band. However, it has been demonstrated (References 1, 3) that the accuracy of nonlinear ALN classifiers can be made insensitive to target range throughout the detection envelope of a seismic transducer. This indicates that the influence of range on at least the seismic signal can be successfully filtered out by appropriate transformations, even though conventional classifiers generally do not compensate fully for the effects of varying range. In summary, range information is present in the seismic and acoustic signals; it has been anticipated that this information could be extracted from at least the seismic channel by using a processor similar to the ALN previously used to eliminate range sensitivity for target classification purposes.

The physical basis for passive, single-sensor seismic range measurement is that the frequency content of a target-induced seismic signal depends on the distance the original seismic signal^{1/} has propagated through the ground, as well as on the type of target, the terrain, etc. Generally, the high frequencies are attenuated more than low frequencies. As range increases, the ratio of high frequency content to low-frequency content in the

^{1/}Not the seismically-coupled acoustic wave.

seismic signal decreases. The seismic propagation paths can also be frequency dispersive: coherent energy tends to spread into an ever-widening band of frequencies as range increases.

The Earth acts as a filter for seismic waves. If the class of a target is known (or established via a target classifier), the approximate spectrum of seismic disturbances generated by that target is known implicitly. Thus, the frequency content of the received seismic signal can be used in an ALN that estimates target range, knowing the actual or probable class and the received target spectrum.

In fact, the range-measurement ALN may not have to be told the identity of the target in explicit terms. However, since the lethal ranges of mines vary with the type of target, explicit class information is very useful for mine detonation logic. The greatest range-measurement accuracy is potentially achieved by use of explicit class information from a target classifier to "point" to an ALN that has been synthesized for the same class of targets.

Some information as to range is, presumably, conveyed by mean amplitude of the seismic signal, but this parameter is untrustworthy for ranging (and for classification), because sensor calibration factors, soil conditions, and target weight, speed, and heading all influence the mean signal amplitude in unpredictable ways. Amplitude, however, may be used to indicate whether there is a potential target in the environment, and thus may be used a turn-on logic for the processor unit.

The frequency content of seismic signals is subject to alteration by soil characteristics and target properties. But the information in the seismic signal can be augmented by that available through the acoustic channel. For acoustic propagation, the atmosphere also acts as a low-pass filter, with high-frequency components of the sound wave being attenuated increasingly with increasing range. (There is, additionally, some dependence of the filtering characteristics on air temperature, humidity, and wind velocity, but this is not pronounced.) But the atmospheric characteristics are more predictable than those of the seismic medium; in particular, the acoustic velocity in the atmosphere is much more nearly constant than are the seismic velocities.

Using the seismic and acoustic signals simultaneously, their phase (time of arrival) differences may be computed, provided certain questions of solution uniqueness are resolved. If ALN's can deal with the uniqueness problem and if they may also be used to estimate the seismic velocities, a two-part measurement of range may be possible as an alternative approach.

Finally, it has been found that certain cepstral features of the seismic signatures from prototypical target vehicles are potential partial indicators of vehicular range. These cepstral features measure the difference in arrival times of the seismic and seismically-coupled acoustic waves.

ALTERNATIVE APPROACHES

Figure 1 illustrates alternative approaches for passive range measurements from a single sensor. As shown in the figure, the input seismic waveform and (if used) acoustic waveform are preprocessed to extract numerical values of the relevant signal

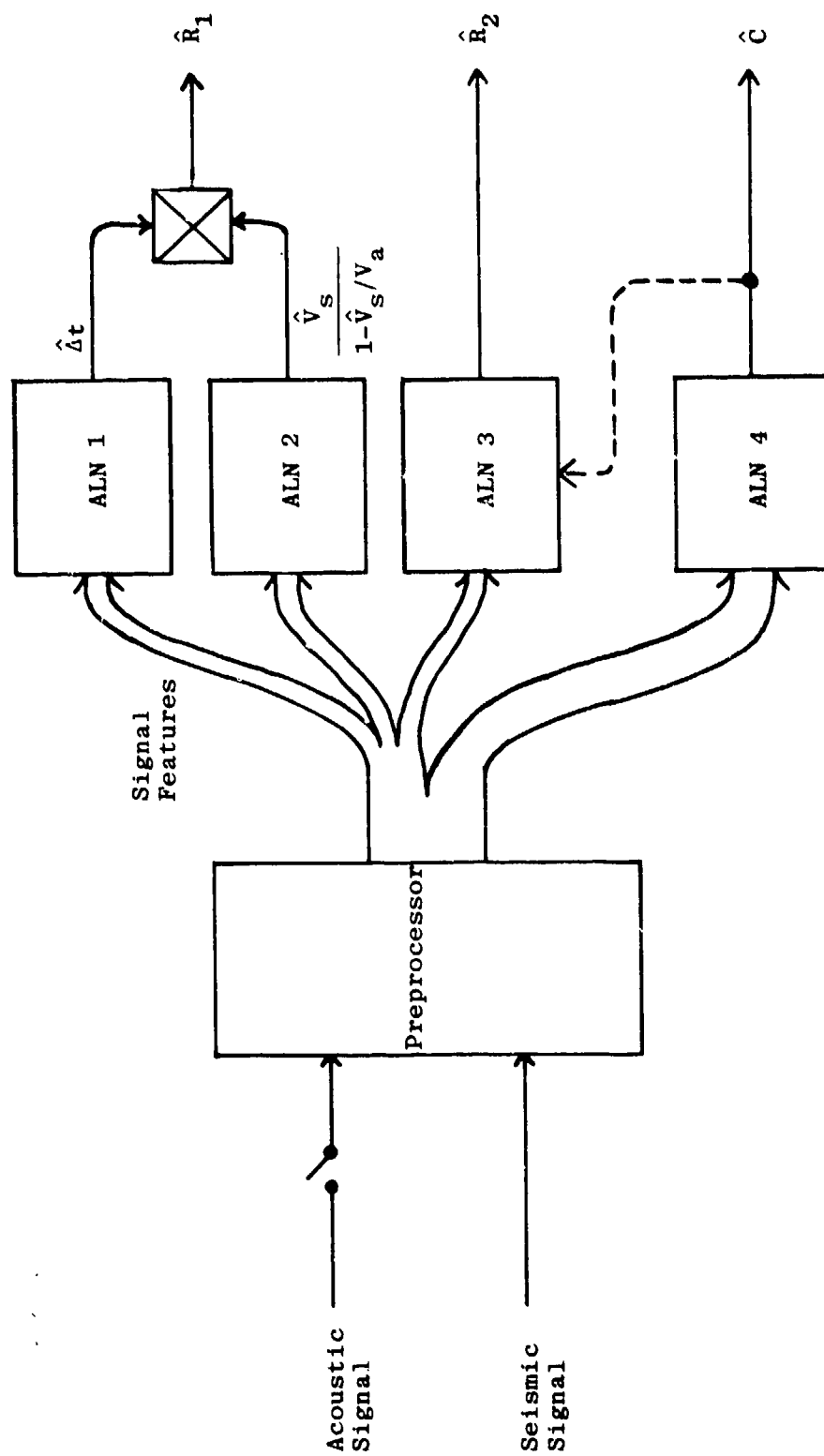


FIGURE 1. ILLUSTRATION OF ALTERNATIVE APPROACHES FOR PASSIVE, SINGLE-SENSOR RANGE MEASUREMENT

features. (As discussed in the Appendix, these features are selected during design of the sensor by means of the ALN methodology.)

A first approach is to compute an estimate (\hat{R}_1) for target range using the relationship^{1/}

$$\hat{R}_1 = \frac{\hat{V}_s \Delta t}{1 - \hat{V}_s/V_a}$$

in which:

Δt = time delay between acoustic and seismic wave fronts

V_a = acoustic propagation velocity

V_s = seismic propagation velocity

($\hat{}$) = estimated quantity

In the first approach, ALN 1 could transform its input features into an estimate ($\hat{\Delta t}$) of the time delay between the received acoustic and seismic wavefronts. Several potential values of Δt could be found in a cross correlation of the two signals, and the smallest Δt 's would correspond, generally, to correlations between

^{1/}Obtained by solving for R_1 in the following system of physical equations:

$$R_1 = V_a(t_a - t_d)$$

$$R_1 = V_s(t_s - t_d)$$

$$t_s - t_d = t_a - t_d + \Delta t$$

where t_a is the time of arrival of the acoustic wave front, t_d is the time the disturbance originated, and t_s is the time of arrival of the seismic wave front.

the acoustic wave and various seismically-coupled acoustic waves. A somewhat larger Δt would correspond to the correlation between the primary seismic wave front and the acoustic wave front; this is the time delay of principal interest for ranging. Compression (longitudinal) waves travel faster (by a factor of approximately two) than do shear waves, so the primary seismic wave front reaches the sensor after being propagated chiefly in the longitudinal mode. Additional time-delay solutions, involving Δt 's larger than for the primary seismic wave, could be expected to result from seismic propagation via longer paths and/or slower modes. It follows that correlation techniques cannot generally produce unique solutions for Δt , inasmuch as a plurality of correlations usually exist for different values of the delay time. However, ALN 1 could work with more information than is involved in a classical correlation process and therefore have a better chance of finding the proper Δt .

As previously noted, it would also be possible to measure the time difference between arrival of the first seismically-coupled acoustic wave (which has been propagated most of the unknown distance R at acoustic velocity) and the primary seismic wave. Cepstral analyses have been shown to be helpful in measurement of this time delay; however, uniqueness problems arise much as in the seismic-acoustic correlations, so ALN techniques again ought to be valuable in achieving Δt uniqueness.

Using the first approach, one would estimate V_s , now understood to be the velocity of the seismic compression wave, and use this information with $\hat{\Delta t}$ to obtain \hat{R}_1 . Knowledge about the value of V_s must be obtained from the input waveforms, because of substantial site-to-site variations in this velocity. It is believed to be

feasible to estimate V_s by means of ALN techniques, as indicated in Figure 1. In the figure, ALN 2 produces the quantity

$$\frac{\hat{V}_s}{1 - \hat{V}_s/V_a}$$

which then multiplies $\hat{\Delta t}$ from ALN 1, yielding \hat{R}_1 . However, estimation of \hat{V}_s or the above ratio has not yet been attempted with an ALN, because a waveform data base for ALN synthesis has not been available in which the true values of V_s are annotated.

The second approach is to estimate range (viz., \hat{R}_2) directly in a single network, ALN 3, as shown in the figure. Use of direct estimation in ALN 3 eliminates the problem of uniqueness of $\hat{\Delta t}$ and \hat{V}_s solutions. It also avoids the compounding of errors from separate estimates of Δt and V_s , and it allows the ALN methodology to discover the best form of the range inference transformation. Just as important, the second approach is realizable using existing data bases, and it has been shown to be workable in a preliminary simulation experiment (described in this paper).

Figure 1 shows a dashed line leading from the output of ALN 4, the target classifier, to ALN 3. (\hat{C} is the estimated target class.) This is drawn to indicate that the designer can employ a different \hat{R}_2 network for each target class. It has not yet been established if this is necessary.

SIMULATION EXPERIMENT

During work on target classification as part of the REMBASS project, the question of range sensitivity of signals present in the seismic and acoustic channels was investigated. (References

1, 3, and 4). This study had the limited objective of determining if target signature sensitivity to range is quantitatively important; if so, a conventional classifier (and, most particularly, a linear classifier) could not be expected to function equally well for all ranges of interest. This investigation very clearly showed a dependence of the seismic signature on target range (Reference 1). Further research has showed that this dependence is sufficient for range measurements by an ALN sensor, as reported for the first time below.

Before proceeding, the limitations of the data base will be mentioned. These data had been originally recorded for work in classification -- not ranging. Absolute amplitudes were not recorded, since these are not critical in classification. For each 10-second epoch of the data, the records had been hand-annotated by field personnel to show the approximate range of the target during that epoch. Some error in visual range estimation and in timekeeping was unavoidable. Visual range estimates were recorded to the nearest five meters (16.4 feet) at approximately the middle of each epoch. Because some targets were moving as rapidly as 30 miles per hour toward or away from the geophone and thus moved 440 feet in a single 10-second epoch, any small discrepancies in timekeeping (perhaps of the order of one second) constituted a significant loss in accuracy of the recorded range.

All of the seismic records pertaining to tracked vehicles within approximately 100 meters were assembled from those in the REMBASS digitized seismic data file. These records were sorted to remove those that involved multiple tracked vehicles. The data base was then partitioned into fitting, selection, and evaluation subsets, taking care to include examples of each available site (Hood, Yuma, and Hill) and a balanced distribution of ranges in each subset. The average range of all target epochs in the special data base was 54 meters (177 feet), the minimum range was zero, and the maximum

was 95 meters (312 feet). A total of 45 tank epochs were available -- most from M-60 runs but some from M-48 runs. Additionally, several APC epochs were available.

Sixty-one candidate features were computed for each epoch (Reference 1). An adaptive learning network (Figure 2 and Table 1) was then synthesized. The performance of this network proved that the frequency content of the seismic signature is highly indicative of tracked vehicle range. A nonlinear ALN transformation was found to be necessary. It was also established that seismic reverberations having periodicities out to four and perhaps six seconds are highly informative to the range-inference processor.

The computing elements in the network of Figure 2 are six-term polynomial functions, as discussed in the Appendix. The output of the network is scaled as the logarithm of range so as to enhance accuracy for small ranges.

RESULTS

Figures 3 and 4 present typical evaluation results obtained with the passive, seismic range-inference network. These figures are plots of tank runs, shown as distance from the closest point of approach (CPA) versus time. Solid curves represent the recorded range data, while broken curves denote the estimated ranges. The CPA was nearly zero for all runs, which mostly proceeded along straight paths directly by the geophone. An exception was Run 2 at Hood, in which the tank ran at nearly constant range (about 47 meters -- 154 feet) for two epochs (20 seconds) before turning onto a radial heading passing by the sensor.

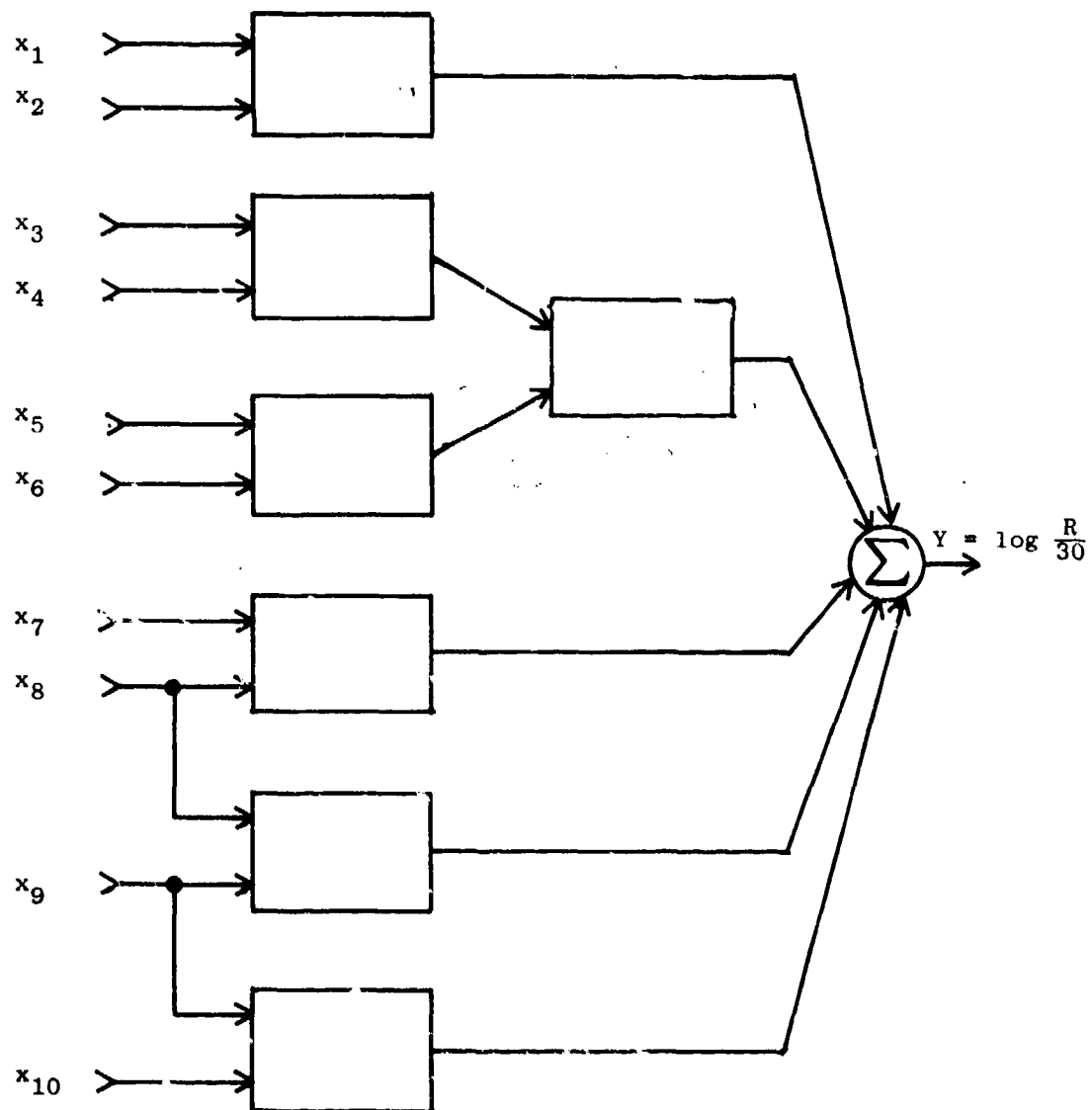


FIGURE 2: ALN FOR PASSIVE INFERENCE OF RANGE OF MOVING TANK VIA SINGLE GEOPHONE

TABLE 1

INPUT FEATURES USED IN ALN FOR PASSIVE INFERENCE
OF RANGES OF MOVING TANKS VIA SINGLE GEOPHONE

<u>Feature</u>	<u>Description</u>
x_1	Maximum of Time Waveform
x_2	Shape Factor* S_1 of Auto-Correlation Function
x_3	Shape Factor* S_2 of Cepstrum
x_4	Shape Factor* S_5 of Cepstrum
x_5	Area in 4.096 - 6.144 Sec. Band of Auto-Correlation Function
x_6	Maximum Value in 0 - 2.048 Sec. Window of Cepstrum
x_7	Energy in 62.5 - 125 Hz Band of Power Spectrum
x_8	Shape Factor* S_1 of Cepstrum
x_9	Maximum Value in 0 - 4.096 Sec. Window of Cepstrum
x_{10}	Minimum of Time Waveform

* Shape Factor

$$S_1 \equiv \int_0^E x(\xi) d\xi$$

$$S_2 \equiv \frac{\int_0^E x(\xi) \tau d\xi}{S_1}$$

$$S_5 \equiv \frac{\int_0^E x(\xi) \tau^4 d\xi}{\left[\int_0^E x(\xi) \tau^2 d\xi \right]^2}$$

where $\tau \equiv \xi/E$.

NOMINAL SPEED: ① 30 MPH
 ② 7 MPH

Field records shown by solid lines, ALM inferences by broken lines.

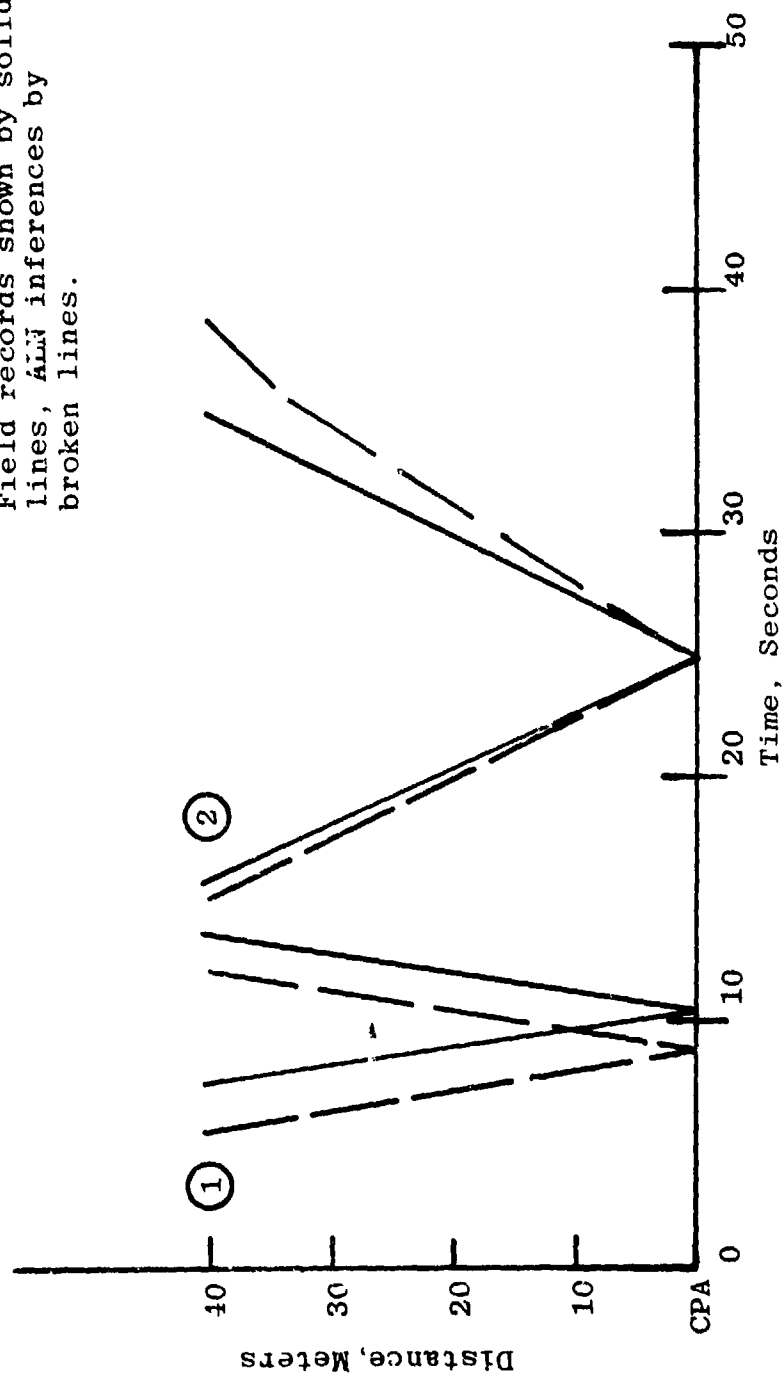


FIGURE 3: RESULTS OBTAINED WITH PRELIMINARY NETWORK FOR M-48 TANK RUNS AT A. P. HILL

NOMINAL SPEED: ① 23 MPH
 ② 2.5 MPH

Field records shown by solid lines, ALN inferences by broken lines.

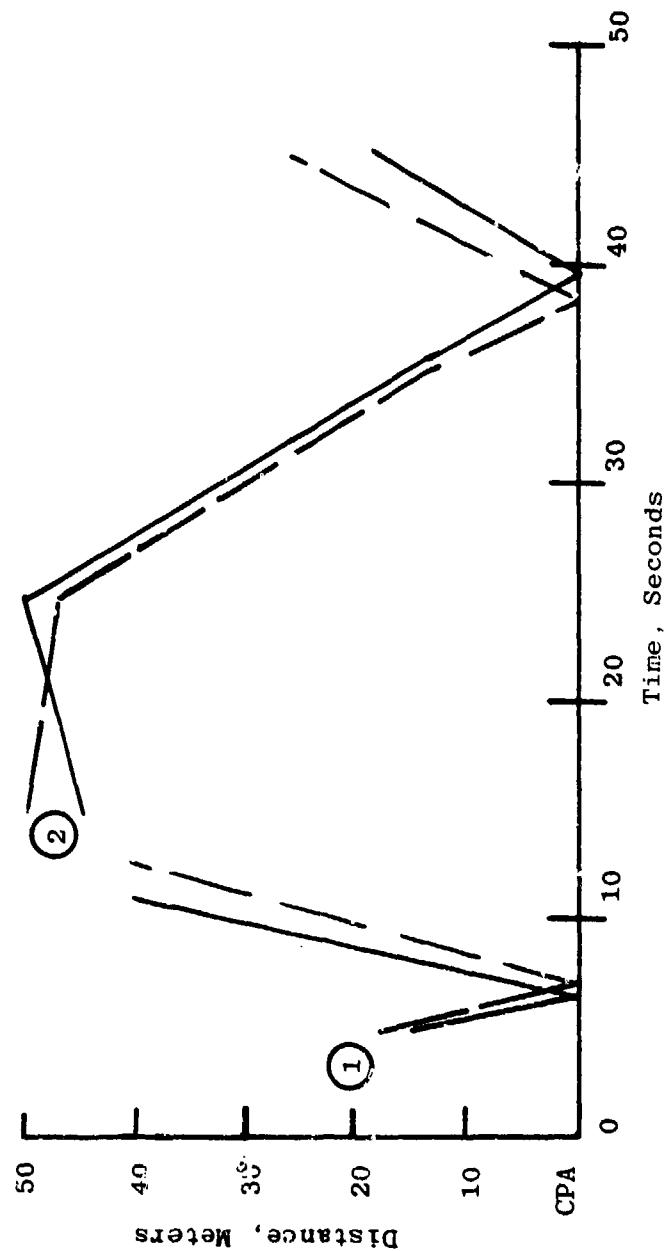


FIGURE 4: RESULTS OBTAINED WITH PRELIMINARY NETWORK FOR M-60 TANK RUNS AT HOOD

It is emphasized that a single network (Figure 2), using one set of numerical coefficients, was employed for all of the inferences of tank range -- independently of field site, tank type, and speed and heading of the tank.

Inspection of Figures 3 and 4 reveals that:

- (1) The slopes, i.e., estimated speeds, are quite close to the actual slopes (speeds) for each tank run.
- (2) The separations between the curves for estimated range and for actual range are generally quite small in both time and range.
- (3) There is no obvious dependence of range accuracy on range, site, speed, or type of tank.

Concerning each of the above three points in turn:

- (1) The accurate recognition of speed (viz. $\Delta R/\Delta t$, the change in estimated range from one epoch to the next) is very encouraging, particularly for logic that must compute CPA's for vehicle paths not passing directly over the geophone. For these paths it is desirable to detect relative closing speeds very accurately to avoid errors in determining when the CPA occurs.
- (2) The separations between actual and estimated range curves are approximately equal to the temporal and spatial errors believed to have been present in the manually-recorded time and range values in the data base. The mean time separation of the apparent actual curves and the estimated curves is 1.05 seconds (the average estimate was early by this amount). The mean absolute separation viewed in terms of range was 8.96 meters (29.4 feet). It is felt that these numbers are close to the best that can be done with this particular data set.
- (3) To help bear out the "universality" of the ALM, it was further tested in simulation (without retraining) on data for APC's running at both Hood and Yuma. The results were comparable to those just cited for tanks.

CONCLUSIONS AND RECOMMENDATIONS

Seismic disturbances produced by surface targets have waveform characteristics that vary with the range to a sensing geophone. If the type of target is known (or can be estimated via a signal classifier), this range can be inferred by suitable processing of the received signature. Additionally, information in the acoustic channel can be employed to enhance performance of the processor.

This paper presents two approaches for improved measurement of target range from a single passive sensor. The first approach would obtain explicit time-delay (Δt) and seismic velocity (V_s) information from either (i) the acoustic and seismic waveforms or (ii) the seismically-coupled acoustic and seismic waveforms. Estimates of Δt and V_s would then be combined in the formula

$$R = \frac{V_s \Delta t}{1 - V_s/V_a}$$

to estimate range. The second approach uses parameters of the seismic waveform (and, optionally, of the acoustic waveform) for direct estimation of the range.

Both approaches require nonlinear transformations to obtain correct results. The method of adaptive learning networks is well suited to this requirement and has been applied to synthesis of an ALN transformation based on the second approach. In this, a range-inference ALN has been created using recorded tracked-vehicle seismic data from the REMBASS project.

The range-inference ALN has an accuracy that is comparable to the accuracy of range information in the data base, i.e., about nine meters in distance and one second in CPA. This ALN also gives

very close estimates of vehicle speed. Performance of the ALN is found to be uniform over the three sites (Hood, Yuma, Hill), three vehicle types (M-60, M-48, and APC) different ranges (0 - 95 meters), different speeds (2.5 - 30 MPH), and different directions of motion of the tracked vehicles represented in the data base.

The range-inference processor could be used very effectively in conjunction with the USA REMBASS seismic or seismic-acoustic classifiers, as a component in the USAF ERAM sensor, or in other remote monitoring and mine systems.

Further work is recommended to synthesize range-inference ALN's for wheeled vehicles and for personnel. The multiple-target case should also be investigated. Development of integrated classification/ranging hardware is suggested.

REFERENCES

1. Whalen, M. F. and A. N. Mucciardi, Synthesis of Nonlinear Adaptive Learning Network Seismic Target Classifier, Adaptronics, Inc. Interim Report to U.S.A. MERDC, Contract DAAK02-74-C-0322, March 1975.
2. Barron, R. L., "Learning Networks Improve Computer-Aided Prediction and Control," Computer Design, August 1975, pp. 65-70.
3. Whalen, M. F., J. D. Sanders, and A. N. Mucciardi, Performance Evaluation of Nine Candidate REMBASS Single-Target Classifiers, Adaptronics, Inc. Final Technical Report to U.S.A. MERDC, Contract DAAK02-74-C-0322, February 1976.
4. Adaptronics, Inc., "Empirical Design of Sensor Logic," Paper presented at Second Symposium on Design, Testing, and Deployment of Unattended Ground Sensors, Waterways Experiment Station, Vicksburg, MS, May 11-12, 1976. (in publication)
5. Barron, R. L., M. F. Whalen, et. al., REMBASS Classifier Design Approach: Volume I (Methods, Design Approach, Simulation Results, and Recommendations), Adaptronics, Inc. Final Technical Report to RCA Corporation, Purchase Order 989454-0001-66, November 1976.
6. M. F. Whalen, R. Shankar, and R. L. Barron, Seismic and Seismic-Acoustic REMBASS Target Classifier Design Modifications for Improved Tracked-Wheeled Discrimination, Adaptronics, Inc. Final Technical Report to RCA Corporation, Purchase Order 901750-8466-66-C24, April 1977.
7. Naval Surface Weapons Center, Multiple Target Classification and Location, Final Report, July 1976.

APPENDIX

ADAPTIVE LEARNING NETWORK SYNTHESIS METHODOLOGY

Adaptive learning network (ALN) training involves operations with data that are obtained as a result of "observing" a physical process. The classical approach to design of signal processing functions has been to determine explicitly all the relevant characteristics, deterministic and/or statistical, of the process being observed, and to use these measurements (and assumptions) in design synthesis. Very often the mathematical structure of the processor is assumed and its design consists of calculating the values of the coefficients in this structure.

However, in many applications the inputs (observables) are difficult to describe analytically, and the best or even an acceptable structure for the processor cannot be determined a priori. In this case, it is desirable to have a structure that is found from a representative data base. That is, the structure is learned as well as the coefficients.

To achieve trainability in structure, similar elementary building blocks may be used in a network having interconnections that are learned from the data base.

Thus, it is desired to implement a general (usually nonlinear) function of certain input variables which we can call observables. Since little may be known about the characteristics of the observables, the parameters of the network are not known a priori. The network will have to be trained with representative inputs. The questions are now:

- What should the structure of the elements of the network be?
- How should the element parameters be adjusted?
- How should the elements be interconnected and what should their complexity (i.e., number) be?

To make the ideas clear, suppose that the input consists of N observables, x_1, x_2, \dots, x_N . Also suppose that the output is a scalar whose value may be considered as the estimate of some property of the input process. In general, y will be some non-linear function of the x_i 's as follows:

$$y = f(x_1, x_2, \dots, x_N) \quad (1)$$

Extraction of Parameters From a Time Waveform

In the passive range sensor problem, it is envisioned that the inputs to a range measurement processor would be analog time waveforms coming from acoustic and seismic sensors. Learning networks require as their inputs a set of parameters or features, x . Therefore, the range inference system requires an intermediate transformation between the analog time signals and the parameter inputs to the network. This intermediate computational unit is referred to as the preprocessor. In one computational burst, the preprocessor operates on an epoch, approximately 0.1 - 1.0 s, of data from each of the transducers and determines features that characterize the seismic and acoustic waveforms for that epoch.

Typically, important features or parameters to be extracted from the waveforms are such things as average amplitude of the waveform during the epoch, power of the waveform in certain frequency bands, shape factors, number of zero crossings, peak values, and

cepstral analyses. In all, the preprocessor of the passive range sensor computes a total of approximately ten to twenty parameters from the seismic and acoustic waveforms.

The remainder of this brief outline of ALN methodology deals with the functional synthesis of networks which operate on the parameters or features of the analog time waveforms.

Polynomial (Multinomial) Approximation

Under fairly general conditions, a function of N variables may be expressed in an N -dimensional series as follows:

$$y = a_0 + \sum_{i=1} a_i x_i + \sum_{i=1} \sum_{j=1} a_{ij} x_i x_j + \sum_{i=1} \sum_{j=1} \sum_{k=1} a_{ijk} x_i x_j x_k + \dots \quad (2)$$

In the most general case, the coefficients, a_0, a_1, \dots , are functions of time, but for many cases of interest, the underlying characteristics of the x 's do not depend on time and consequently the coefficients are constants.

Two questions which arise in the use of Equations 1 and 2 are:

- What should the observables or features x_i be?
- How many terms in Equation 2 will provide an acceptable approximation to the desired function?

The answer to the first question is: Those features that the designer believes could have a significant role in the application are evaluated initially. The relevant features are selected by the learning algorithm, and the ones which its trials show to be of little or no use are discarded. The second question is answered by using a nonlinear ALN whose complexity determines the number of terms in Equation 2. This network consists of interconnected elements, each implementing a simple nonlinear function of two inputs. The total network can be trained to provide an acceptable approximation to Equation 2.

The basic element of the learning network is a two-input single-output device that implements the following function of its inputs x_1, x_2 :

$$y = w_0 + w_1x_1 + w_2x_2 + w_3x_1x_2 + w_4x_1^2 + w_5x_2^2 \quad (3)$$

Networks of the Basic Element

In a network of two layers of the basic elements (see figure), each second-layer output can contain pairwise products up to the fourth degree. Note that the first layer can provide all possible pairs of three inputs x_1, x_2, x_3 . To implement a fully general multinomial (polynomial in many variables), the number of elements in each layer would have to grow as one proceeds deeper into the network. However, it is found empirically that acceptable approximations are obtained without this growth; in fact, the number of elements in successive layers can decrease (usually two or three layers), until only one or at most a few are left as inputs to the final adder.

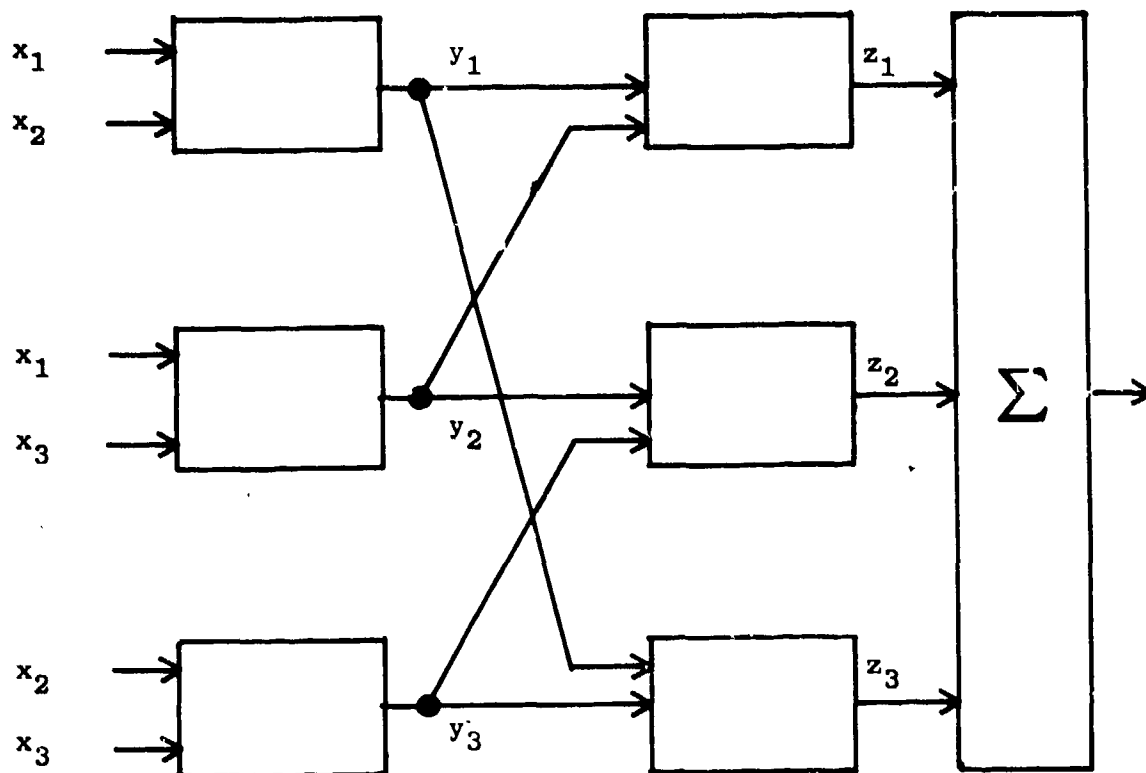


FIGURE A-1: TWO-LAYERED NETWORK OF BASIC ELEMENTS

Now we turn to the matter of determining the number and inter-connections of the elements in the ALN and the coefficients within these elements. These tasks are accomplished with a "known" data base; that is, a data base for which the values of the dependent variable (range) are known. The principal steps involved are:

- (1) Optimizing the coefficients in each element of the first layer.
- (2) Selection of those elements whose output is acceptable while rejecting poor performers.
- (3) Repetition of steps (1) and (2) for each layer.
- (4) Global optimization of all coefficients in all layers based upon network output.

The known data base is divided into three independent but statistically similar subsets:

1. Fitting subset
2. Selection subset
3. Evaluation subset

The fitting subset is used to determine the coefficients of the elements. The selection subset is used to reject the poor performers. The fitting and selection subsets are also used for the global optimization. The evaluation subset is used to estimate the overall performance. Since the evaluation subset is not used for network synthesis, the performance of this subset is an accurate estimate of the ability of the network to generalize to new, previously unseen data.

Training the Network

Network structure and element coefficient determinations are based upon a numerical fit to a desired output, whereby the

elements are first adjusted by a matrix algebraic procedure and then by a recursive search or optimization procedure.

Fitting and selection subsets are used alternately in training each layer. First, N specific observables that are the inputs to each element are chosen, more or less arbitrarily, and arranged into $N(N - 1)/2$ pairs, feeding a like number of trainable elements. Then the fitting subset of the known data base is applied to establish the coefficients, using a recursive search procedure. The procedure is repeated for each of the $N(N - 1)/2$ elements.

Not all pairwise combinations are significant in extracting the desired information. The selection process, using the selection subset, eliminates those elements whose performance is not acceptable, as gauged by the error criterion. There are now, say, R elements that survive.

The process is repeated for the second layer, which initially contains $R(R - 1)/2$ elements, involving all pairs of the surviving elements in the first layer - which now is again fed by the fitting subset. Coefficients of each element in the second layer are determined as in the first. Then the selection subset is fed a second time into the first layer and the unacceptable pairs eliminated from the second layer.

The process is repeated with succeeding layers until the error rate on the selection subset reaches a minimum. Although further reductions in error rate on the fitting subset could be made by incorporating additional layers, to do so would produce overfitting of the fitting data. When the appropriate number of layers has been found, the last layer will -- in general -- comprise a

plurality of elements, each capable of producing an estimate of the dependent variable (range). These estimates may be numerically weighted and summed, or the single element that produces the lowest error rate vis-a-vis the selection subset may be retained, while the other output-layer elements (and all other parts of the network not needed to feed the surviving output element) are discarded.

A final step in the training process is a vernier adjustment, or fine tuning, of the coefficients. This may be desirable because the coefficients of each element have been adjusted in the absence of interactions with other elements following them in the network; optimum coefficient values may be different when these interactions are present. Fitting and selection subsets are also used for this final adjustment process. The vernier adjustment - a global search - may use a random technique to obtain final values of the coefficients, as well as for subsequent network adaptation. After final adjustment of coefficients, the evaluation subset is used to estimate performance of the entire network.

Avoidance of overfitting is a key aspect in the training of learning networks. Good functional approximations to the fitting data subset must be obtained that also closely approximate the data in the separate selection subset - that is, the network must be taught to generalize properly on its experience in fitting the points in the first subset, so that error rates in later uses will be low. If overfitting is not avoided, the network may produce deceptively small errors in approximating its first set of data and then do poorly on subsequent new data. By using three independent subsets of the available data - taking care that each is statistically representative of the whole data base, the problem of overfitting is virtually eliminated and good advance estimates of operational error rates on similar data are obtained.

PASSIVE INFRARED MOTION SENSOR (PIMS)

Robert A. Brubaker

MERADCOM

ABSTRACT

The Passive Infrared Motion Sensor is a low cost, high performance intrusion detection device which utilizes intruder body heat to determine presence in a protected area. This paper considers the design and producibility of both the PIMS reflective, non-imaging optical system and low noise electronic signal processing circuitry. The anticipated performance of the sensor preamplifier in high background turbulence is discussed.

I. INTRODUCTION

Indoor Physical Security is generally accomplished through the utilization of physical barriers (i.e., locked doors, barred windows, etc.) and intrusion detection equipment. Intrusion devices may be classed into three categories: penetration, point and motion.

Briefly, the penetration sensors determine whether a physical barrier has been, or is being, breached and they allow maximum security force response time. Point sensors can be configured to respond only when sensitive items are being compromised, allowing access to the general vicinity of the protected areas. Motion sensors, in addition to providing detection of intruder's movement, provide a unique backup to both point and penetration sensor, since movement is involved in most aspects of intrusion.

Ultrasonic doppler and microwave techniques have provided a solution to most motion detection requirements. Some situations exist, however, where their operation is less than desirable. With improved performance and declining detector costs, passive infrared sensors are filling a useful requirement for detecting motion in a volumetric area.

This paper describes a Passive Infrared Motion Sensor (PIMS) under development for the JSIIDS/FIDS program. The sensor operates with up to six infrared receivers connected to a single processor with a total power consumption of less than 150 milliwatts. Intruder motion between 0.1 to 15 feet per second generates analog signals within the bandpass of the Infrared Processor. The IR detector is designed so that natural thermal changes will have minimal effect on the operation of the unit.

The PIMS has an optical configuration that detects motion in any area of 20 x 30 feet by optically dividing the area into 15 fields of view (FOV). While the actual area of coverage at normal room temperatures is

much larger than this, (40 x 60 feet), the PIMS continues to provide the 20' x 30' coverage at temperatures between 90° - 100°F. Most Passive Infrared devices are severely degraded within this temperature range. A point of limited useful contrast is reached as the background temperature increases to that of a human. Useful detection also depends upon such parameters as emissivity, transmission loss and radiation perturbations. This maintains a useful detection range of 20 x 30 feet even at background temperature crossover.

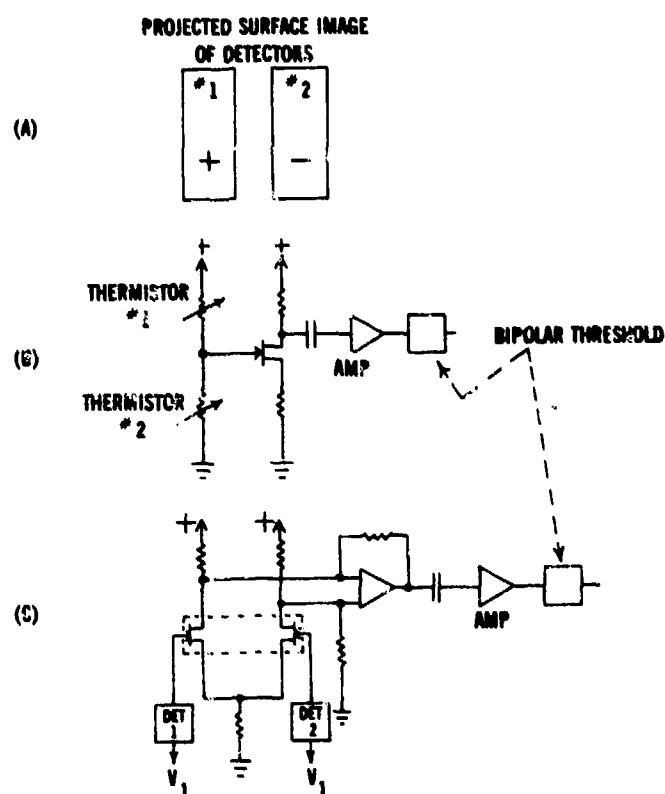


FIGURE 1

II. ELECTRONICS

In general, the PIMS utilizes conventional analog bandpass amplification in conjunction with simple bipolar threshold and logic alarm processing. Analog frequency distribution of signals as low as 0.01 Hz are of value. This appears as D.C. drift with higher frequency components superimposed on the waveform. Sensitivity and dynamic range are therefore improved by utilizing two independent amplifier channels in the processor. Each channel is further enhanced by incorporating a dual bandpass filter with separate threshold criteria. The frequency response has been optimized to allow low velocity target signatures to be processed against a minimum background noise level, protecting the system from defeat against the skilled slow moving intruder. Of particular importance to this system is the front end (preamplifier) electronics. At the extremely low frequencies involved in this circuit, any offset drift, in effect, becomes system noise. To minimize this effect, the PIMS incorporates a dual, matched FET in a differential configuration which drives a low drift operational amplifier. (Fig. 1) Power for the preamplifier requires three stages of voltage regulation in addition to the standard regulation for the processor electronics. The actual detector and its electronics are described subsequently.

III. TRANSDUCER

An infrared (thermal) to voltage converter assembly receives energy through germanium window material. The flat window is precision coated with multireflective layers causing the detector element to "see" and hence respond to variations in a limited spectral range (8 - 14 micron).

a. Detection Elements: Two detecting surfaces are placed adjacent to one another and at the optical focal point with their outputs having opposite polarity [Fig. 1 (a)]. They produce a low composite output if a signal of equal amplitude exists on both detecting surfaces, as would be expected with only background in the field of view. An intruder enters a single detector subbeam within a field of view, producing a substantial output since no opposite polarity cancellation takes place. Two detector types are being evaluated: variable resistance and voltage generating.

b. Variable Resistance Detector: The variable-resistance detector configuration [Fig. 1 (b)] consists of two thermistors mounted side by side which can be either square or rectangular depending on the desired beam dimension. Optimum signal to background noise performance is obtained when the acceptance field of view (beam) is completely filled by the intruder. The exact shape of the detectors is dependent on the ability of the system optics to accurately project a beam into

the protected area. The area of sensitivity projected by the optics will have the same shape as the detectors. The sensitive areas are side by side, and their outputs wired to subtract causing a cancellation of the effects of energy sources contained in both beams. The thermistors are connected to the amplifiers as shown. When there is an equal change in energy on both thermistors their resistive ratios remain the same. The voltage on the gate is constant and no change in current through R_g is produced. The charge at C_{out} remains constant and no signal is produced for the amplifier and threshold to act on. If, however, a single thermistor changes its resistance due to change in the IR energy seen by it, change is produced throughout the system, causing an alarm.

c. Voltage Generating Detector: For the voltage generating type of detector (thermopile, pyroelectric, etc.), the hookup is shown in Figure 1(c). In the figure, the output of the input amplifier is fed to a differential amplifier which only has an output when the voltages generated by Detectors 1 and 2 are different. The operation of this differential amplifier behaves essentially as the FET device above, producing the same effect at C_{out} as the amplifier and bipolar threshold device. Again the configuration is stable over wide ambient temperature ranges due to the cancellation of background effects.

IV. GENERAL OPTICAL SYSTEM

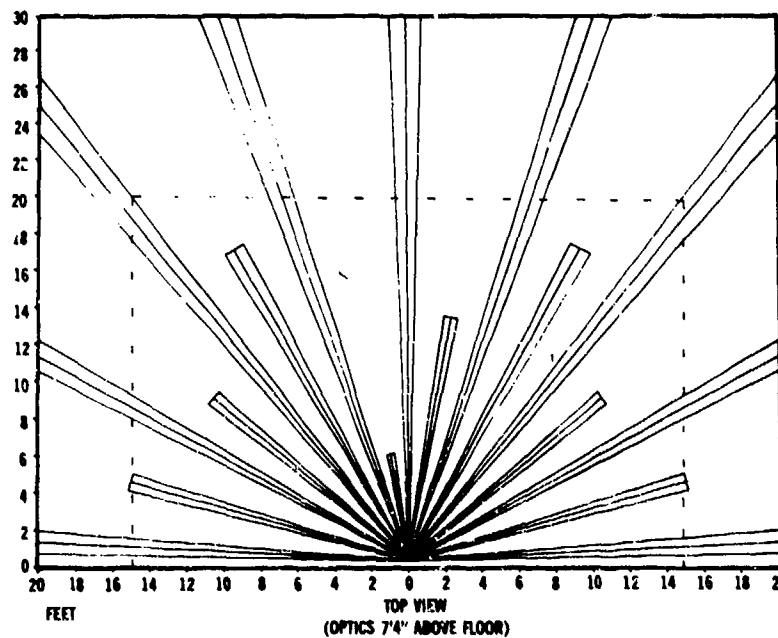
The capability of focusing infrared energy from selected portions of the protected area is perhaps the most critical and difficult task in the IR sensor design.

Providing solid unbroken coverage of the secure zone will result in severely reduced sensor sensitivity from two major factors.

Turbulent thermal clutter exists under many situations, especially if a forced ventilation, heating, or cooling system is used. This clutter energy will provide a clutter background signal far in excess of internally generated noise. An intruder entering near the range limits of a full coverage FOV optical configuration will replace only a limited portion of the background further reducing the signal to (background) noise ratio. In addition, any spectral frequency improvement to low velocity target waveforms generated by steep slope phenomena is practically negated, requiring signal extraction deeper into 1/F noise limitations.

An optimum sensitivity is obtainable when much of the target surface area fills the optical FOV at the same time it is completely replacing the energy received from the background. For diverging FOV sensors, the size and aspect ratio of the beam is configured to match the target at the greatest detection range. This configuration allows greatest

improvement in the optical system's ability to produce usable variations of energy on the detector, however, it limits detection to a single narrow beam. Image quality demands consideration, since signal detection is based upon both the magnitude and spectrum distribution of the a.c. signal response to a moving target. Ray trace and spot diagram computer techniques provide a method to determine the convolution of an edge of an extended image with respect to the detector. This results in the maximum usable steep slope waveform allowing an extremely slow moving target to be detected, utilizing a passband that is $1/F$ noise limited



PIMS SYSTEM COVERAGE AREA

FIGURE 2

In order to approach the advantageous operation of a single beam system while providing volumetric coverage, the PIMS utilizes a series of narrow beams that diverge in a complex, somewhat random manner into the protected area (see Figs. 2 and 3). This multisegmented field of view allows a relatively limited background area to be viewed. The unit's performance in effect approaches that of a single beam system, while insuring almost 100% probability of target/beam intersection.

MULTI-SEGMENTED ACCEPTANCE BEAM PROJECTION INTO PROTECTED AREA

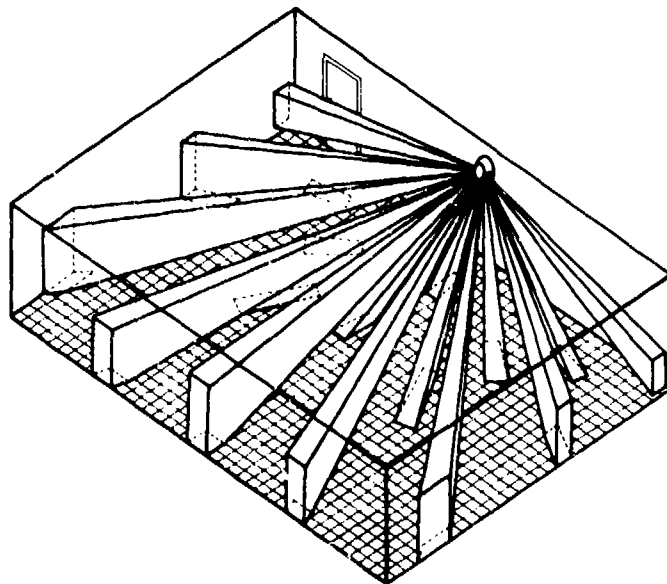


FIGURE 3

V. OPTICAL DESIGN AND MANUFACTURE CONSIDERATIONS

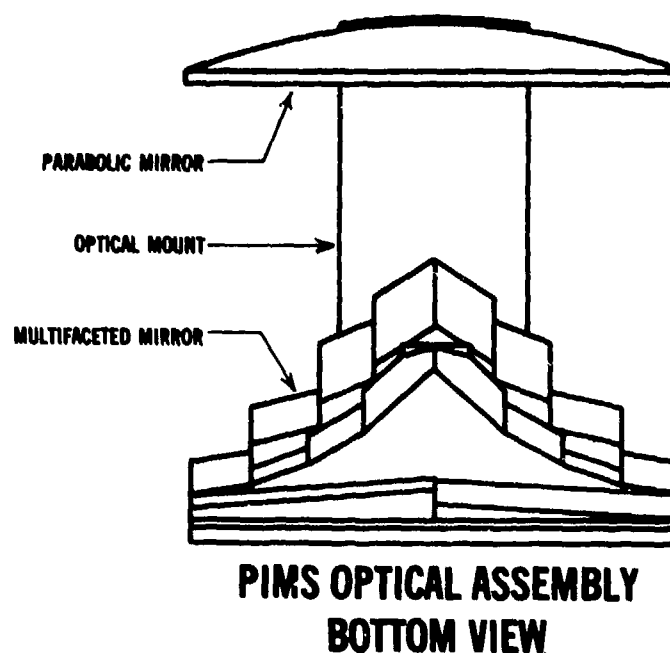


FIGURE 4

In order to meet necessary cost constraints, the PIMS was developed on the premise that a complex, plastic based, metal coated reflecting optical system (Figs. 4 and 5) could be made operational over a range of stringent environmental conditions. In addition to the need for steep slope detection, each beam consisted of two opposite polarity subbeams (see detectors). Any substantial system aberration would cause subbeam overlap with resultant target sensitivity cancellation.

PIMS REFLECTING OPTICAL ASSEMBLY

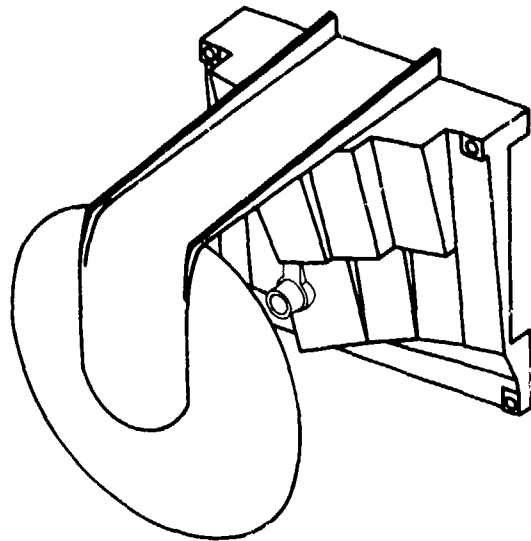


FIGURE 8

Various manufacturing tolerances therefore were considered in the optical system design.

- 1) Mirror facet angle error
- 2) Mirror facet surface figure
- 3) Collimating mirror surface figure
- 4) Misalignment between the axis of the collimating mirror and mirror facets.

The effect of thermal expansion on the geometry of the system was investigated in order to determine those manufacturing materials and techniques compatible with system performance requirements over wide temperature variations.

An error in the mirror facet angle causes two effects: The point in object space is imaged at the wrong position on the detector and the fan of rays entering the collimating mirror will intercept a slightly different portion of the mirror at potentially higher incidence angles with a resulting reduction in edge response. (Fig. 6) Edge responses contribute to a steep slope waveform which produces the necessary frequency components for detection of slow moving targets.

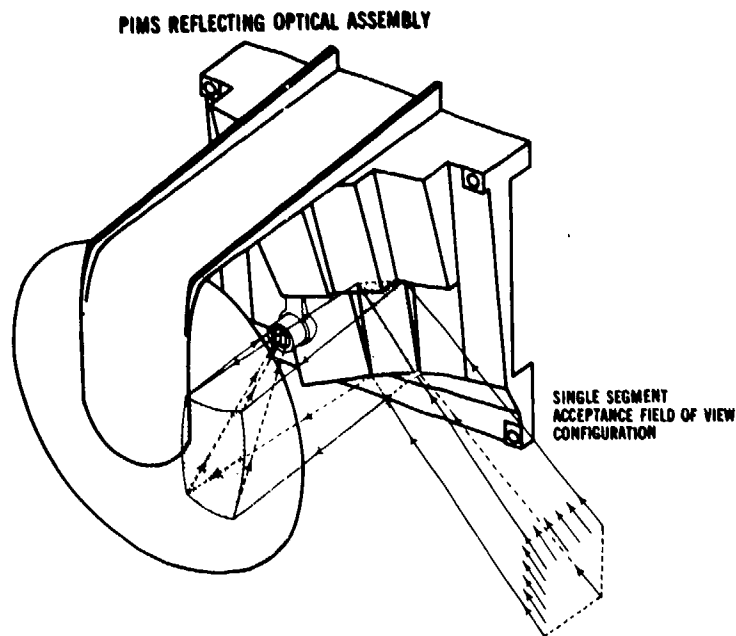


FIGURE 6

Mirror facet surface figure errors (i.e. flatness) in the various mirror segments have a worst case condition when unwanted curvature produces fringes. These fringes, if too excessive, can reduce the signal power of the system.

To assess the impact of the collimating mirror surface figure, consider the high incidence angles at the edge of the collimating mirror. The edge of the collimating mirror is deformed from a parabola, and results in reduced image quality. Some improvement is obtained by increasing the effective area of the collimating reflector with system size constraints acting as a limit to this approach.

Angular misalignment between mirrors is equivalent to the angular facet error described above and is negligible. Axial and lateral displacement are also small contributors to system performance, however, small variations in any direction can be tolerated.

Since the system has no refracting elements, the change of index with temperature has no effect on system performance and the coefficient of thermal expansion is the only parameter of interest. Assuming that the optical elements are heated uniformly and come to thermal equilibrium at a constant temperature over the full optical surface, the geometry of the element will simply scale up/down with increasing/ decreasing temperature.

A linear dimension, $L(t)$, changes with temperature in accordance with the expression:

$$L(t) = L + L \cdot \theta \cdot \Delta T$$

where L is the dimension of interest at room temperature (20°C), θ is the coefficient of thermal expansion and T is the change in temperature. Of primary interest is the change in focal length. The room temperature focal length is 78 mm. The change in focal length has been calculated for several materials of interest:

<u>Material</u>	<u>$\theta/^\circ\text{C}$</u>	<u>Change in Focal Length Per $^\circ\text{C}$ (mm)</u>
7740 Pyrex Glass	$.33 \times 10^5$.00026
Electroformed Nickle	1.2×10^5	.00098
Acrylic (Injection molded)	7×10^5	.00550
ABS (injection molded)	2×10^5	.00120
ABS, Glass filled 40% (inj. molded)	3×10^5	.00230
Epoxy (lay-up replication)	5×10^5	.00390

At a maximum T of 100°C , the increase in focal length is just tolerable for injection molded plastics. A secondary factor must also be considered. Expansion of the plastic substrate will be significantly greater than expansion of the reflecting surface material and grazing (hairline fractures) will occur if the strength of the reflecting material is poor or lacks malleability. For this reason, the best materials choice of plastic mirrors appears to be an ABS substrate with

an electroplated chrome surface. A gold surface was tested which had a somewhat improved infrared reflectance, however, an unacceptable level of grazing did occur.

The location of the spectral filter between the detector and the collimating mirror can have a significant effect upon signal levels. Considering the worst case angles of incidence of the system, it was determined that the reflectance of the filter is 36%. Since transmittance T is equal to the square of 1 minus the reflectance R , i.e.

$$T = (1-R)^2$$

the signal should not be reduced more than 41% of its possible value regardless of which mirror segment is utilized.

A similar experience for the optical cover window material can be shown. This window is fabricated from a durable form of polyethylene and has a transmittance of 92%.

Various manufacturing considerations are involved in the fabrication of reflecting optics. The most cost-effective method of producing mirrors is through the electroplating of injection molded substrates. Vacuum deposited coating cannot withstand the expansion and contraction associated with plastic substrates. Special electroplated coatings can withstand these thermally-induced stresses and provide good optical performance.

Three substrate materials (plastics) are suitable for electroplating applications: ABS, polysulfane, and polypropylene. Cost differences of the three plastics are of no significance. ABS has the best molding properties and a low distortion behavior in the surface plating cycle. It is being utilized as the substrate material for the optical assembly.

VI. SUMMARY

The Passive Infrared Motion Sensor, now in the production prototype stage, gives every indication of successfully meeting its original cost and performance goals. While a thermopile detector has shown a slight performance advantage, a thermistor configuration has operated quite acceptably and is being utilized for its reduced cost benefit. Pyroelectric materials are no longer being considered for the PIMS due to their limited response to slow infrared variations. The optical cover, as an assembly, still remains aloft from simple production tooling. This is due to limited field experience with the required strength versus transmission thickness of the window cover material. The availability of sufficient prototype units for thorough field testing will provide the final input for production tooling of this

sensor.

VII. ACKNOWLEDGEMENTS

The major portion of the PIMS production prototype design and development was due to the successful efforts of the prime contractor, Aerospace Research, Inc., Boston, MA. In addition, their subcontractor, Diverse Technology Inc., Covina, CA provided excellent support in the analysis, design and fabrication of the optical assembly.

SENSOR TEST SYSTEM FOR THE FIDS
By L. J. Nivert, J. E. Bender and A. R. Zushin
Intrusion Detection Division, MERADCOM

SYNOPSIS

The fundamental goal of any sensor system is the reliable detection and transmission of information concerning the occurrence of various types of stimuli. This goal is especially important when the sensor system is designed to provide physical security protection for items which may be prime targets of threats posed by organized criminal elements, insurgent organizations, or espionage or sabotage groups. Probably the best systematic approach to verifying the operational capability of any sensor system is to periodically provide an appropriate stimulus to each sensor in the system, and thus verify the proper operation of the sensor transducer, sensor signal processor and data processing and communication equipment. This presentation discusses the Army's Facility Intrusion Detection System (FIDS), an integrated physical security system, with an emphasis placed upon the remote test capabilities for the sensors within the FIDS.

INTRODUCTION

MERADCOM is currently developing an intrusion detection system (FIDS for Facility Intrusion Detection System) which is intended to fully satisfy the Army's needs for interior physical security over a worldwide range of installation environments. Figure 1 illustrates the components of the system.

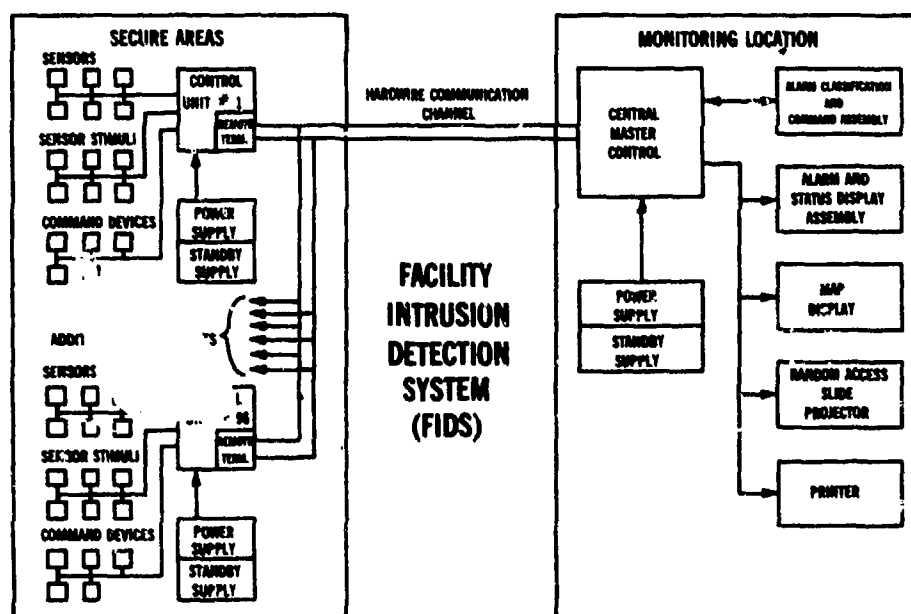


FIGURE 1

The FIDS is a microcomputer controlled system designed to monitor and display the status of up to 96 remotely located areas. Each remote area is protected by a Control Unit (CU) which monitors the Alarm/Non-Alarm status of up to six sensors and an entry control device. Sensor stimuli for each sensor are also present at the remote area, and it is possible to remotely test the proper operation of each sensor in a system by activating the appropriate sensor stimulus. Appropriate response and surveillance devices may also be activated at the CU when an alarm condition is received.

Communications between each remote area and the central monitoring location is achieved through a Remote Terminal (RT) which is installed inside the CU. The RT consists of three plug-in circuit boards: a transmitter, a receiver, and an FSK modem. Data transmission is asynchronous (interrogate-respond) half-duplex FSK. All alarm and status data transmitted by the RT is enciphered, and all command data to the RT is also enciphered. A Special Application Remote Terminal (SART) is also available to interface the FIDS with the Joint-Services Interior Intrusion Detection System (J-SIIDS) Control Unit.

At the central monitoring location, an integrated display and command system is utilized to present the system status to the operator and to enable appropriate operator response actions. The heart of the FIDS is a Central Master Control (CMC) at the monitoring location. The CMC contains microprocessors, input-output interface devices and FSK modems (for the RTs) to maintain communications with and control of the RTs and other peripheral devices in the system.

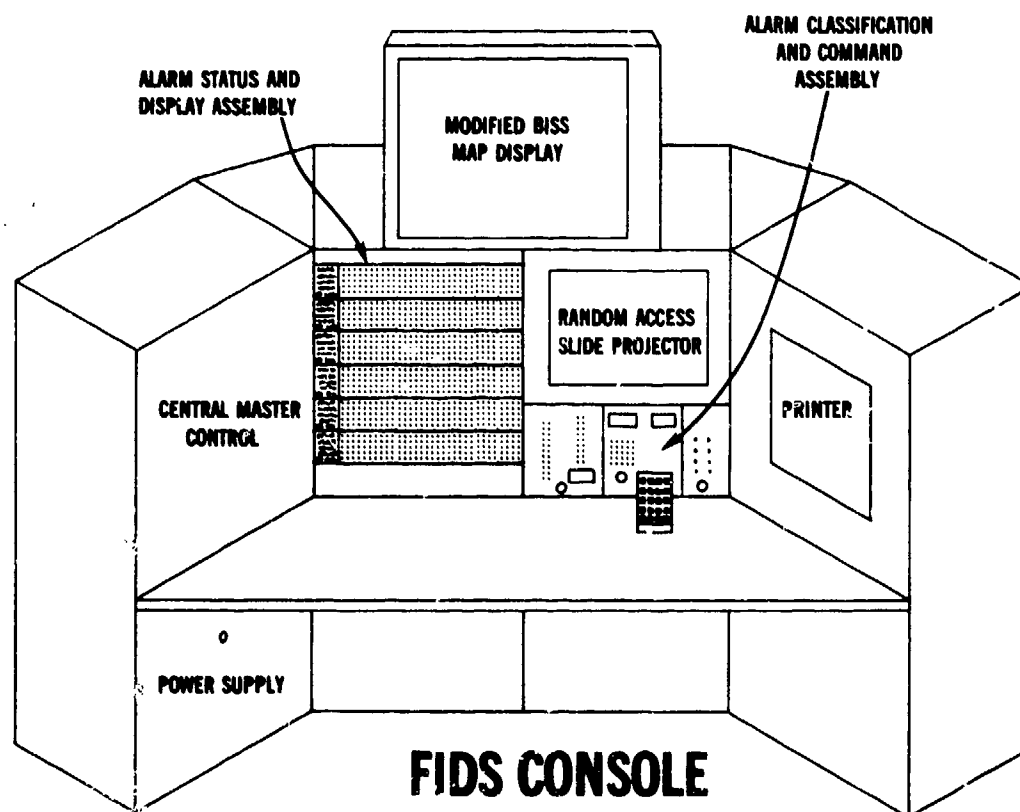


FIGURE 2

The current status of each remotely located area is presented to the system operator via light panels called the Alarm and Status Display Assemblies (ASDA) and a hardcopy Printer. A modified Base Installation Security System (BISS) Map Display is also available to rapidly display the exact location of an alarm condition.

The capability for the operator to classify any alarm and to command any CU in system is provided by the Alarm Classification and Command Assembly (ACCA). The ACCA is comprised of visual classification and command status indicators and a command keyboard by which the operator may select and command any CU.

A Random Access Slide Projector (RASP) is also available to display the physical characteristics or special instructions to the operator concerning each of the 96 remote locations. The RASP display is controlled via the keyboard of the ACCA.

All of the subassemblies in the monitoring location are physically configured into a console as depicted in Figure 2.

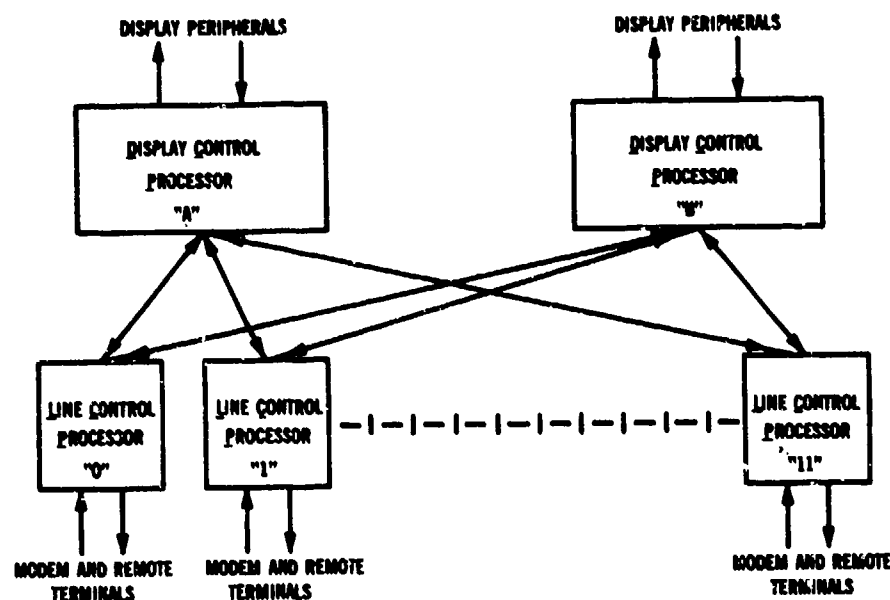
CENTRAL MASTER CONTROL (CMC)

The CMC is a microcomputer assembly which contains microprocessors, associated memory, I/O interface devices and modems to enable data processing and communications between the RTs and the control of the Alarm and Status Display Assemblies, Alarm Classification and Command Assembly, Printer, Random Access Slide Projector, and the Map Display.

The CMC utilizes a unique redundant/distributed design architecture to insure that a single component failure will not inhibit either the interrogation/response communications with, or the display of status conditions for, all of the 96 remote locations. This design concept (illustrated in Figure 3) incorporates two Display Control Processors (DCP) and up to twelve Line Control Processors (LCP). Each DCP or LCP is a stand-alone microcomputer, and each employs an Intel 8080A microprocessor as the central processing unit (CPU). Each DCP or LCP is also contained on a separate printed circuit card module or module group in the CMC.

Each LCP is capable of communicating with up to 16 Remote Terminals; although, in normal operation each LCP would only communicate with approximately 8 Remote Terminals. Consequently in a fully utilized FIDS, a single failure in an LCP would only disable communications with approximately one-twelfth of the RTs.

Each DCP can communicate with each of the LCPs over separate I/O channels. Each DCP may also, if required, control all the display



FIDS CENTRAL MASTER CONTROL (CMC)
FIGURE 3

devices in the monitor console. The control of the display devices may be simply allocated between the DCPs through individual miniature connectors located on the rear of the CMC chassis.

In normal operation, one DCP would control the Printer and Random Access Slide Projector, and the other DCP would control the Alarm and Status Display Assemblies and Map Display. Each DCP also monitors the keyboard of the Alarm Classification and Command Assembly and is capable of recognizing the command inputs from the keyboard. Once a DCP receives a command from the ACCA, the command information is provided to the proper LCP for enciphering and transmission to the RT. Because of this partitioning concept in the DCP duties, a single failure in any DCP, ASDA, ACCA, RASP, Map Display or Printer could not possibly inhibit the display of status for or the transmission of commands to any of the RTs.

The design of the CMC places an emphasis upon the maintainability of the CMC and the minimization of effective down time should a failure occur. The modularization of the DCPs and LCPs allows for a failed card module to be readily replaced without removing power to or inhibiting the operation of the other DCP or LCP card modules. Also, because each LCP is capable of communicating with 16 RTs and because each DCP is capable of controlling all display devices, full system operational capability could readily be restored simply by switching transmission lines or the display device connectors on the rear of the

CMC chassis should a failure occur and a replacement module is not available.

The DCPs and LCPs continually check their own random access memory (RAM) and programmable read only memory (PROM). Should an LCP or DCP discover faulty memory within itself, it will terminate execution of its program. Also, should catastrophic failure occur in a device, other than memory, in a DCP or LCP, information concerning the failure will be made available to the DCP which controls the Printer. In the event of either occurrence, failure information will be printed which should isolate the failed module within the CMC.

As far as MERADCOM is aware, no other physical security system, either commercially or governmentally developed, offers these unique maintainability and inherent test and troubleshooting characteristics of the FIDS CMC.

SECURE AREA EQUIPMENT

At each of the 96 remotely located areas a Control Unit, Remote Terminal, and various commandable devices, sensors and sensor stimuli are installed to provide for the detection of an intrusion and to enable a command response capability. A typical secure area installation is illustrated in Figure 4.

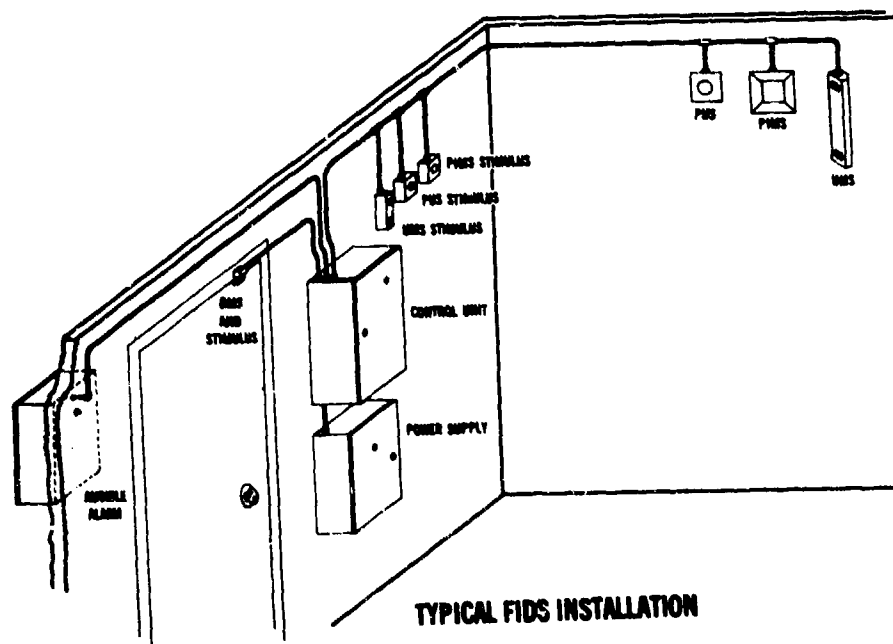


FIGURE 4

Each Control Unit provides the interface between the sensors, sensor stimuli, commandable devices and the Remote Terminal. The CU is capable of monitoring an intrusion alarm and a tamper alarm from each of six sensor signal processor printed circuit cards. These cards themselves simply plug into existing printed circuit card connectors in the CU.

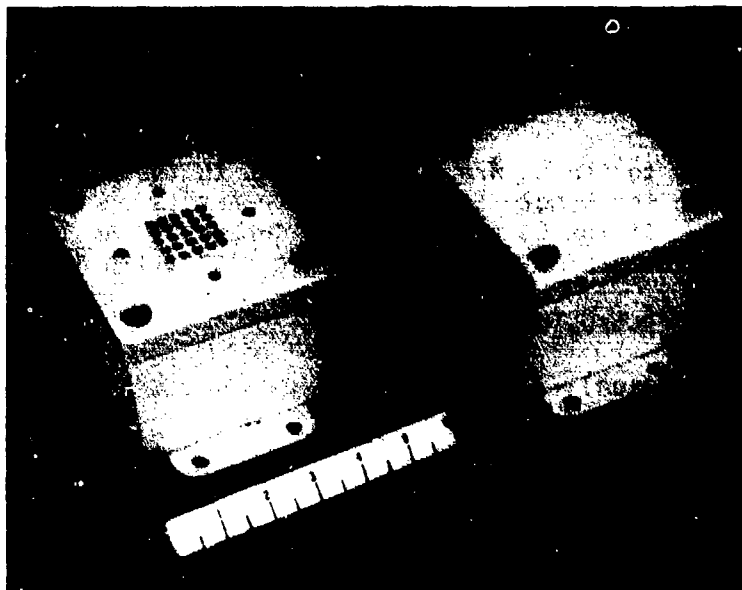
All alarm inputs to the CU are classified as to the type of alarm and are presented to the Remote Terminal for transmission to the Central Master Control. If the CU is monitoring sensors in an interior location, then the alarms will normally be classified as either:

- Penetration (Intrusion)
- Motion (Intrusion)
- Point (Intrusion)
- Duress (Intrusion)
- Other (Type to be specified)
- Contraband
- Entry Denial
- Tamper

If the CU is monitoring line or perimeter sensors for an exterior application, then these classifications may easily be changed, by removing a jumper in the CU, to provide the operator with the location of the specific sensor which reports an alarm condition.

The Remote Terminal is also contained in the CU, and mounted into plug-in card module slots. Each RT is comprised of a transmitter card, a receiver card and a modem card. The modem utilized in the RT is physically and electrically identical to the modems employed in the CMC. In addition to processing and transmitting the current CU status to the CMC, the RT also receives the various possible commands from the CMC and causes the CU to activate various commandable devices. Among these would be the sensor stimuli, an audio listening device, and devices, such as a Audible Alarm, which might inhibit or delay an intruder. A photograph of the audio listening device is shown in Figure 5.

A variety of sensors are available for use is the FIDS so that the sensor system may be tailored for optimum performance in each secure zone. Each sensor type would have a corresponding type signal



AUDIO LISTENING DEVICE

FIGURE 5

processor mounted inside the CU, and also, each sensor type would have a corresponding stimulus which produces an environmental change detectable by that type of sensor. At the present time, the following types of sensors are contemplated for the FIDS.

Balanced Magnetic Switch (BMS)

Grid Wire Sensor (GWS)

F Pressure Sensor (FDS)

Capacitance Proximity Sensor (CPS)

Vibration Sensor (VS)

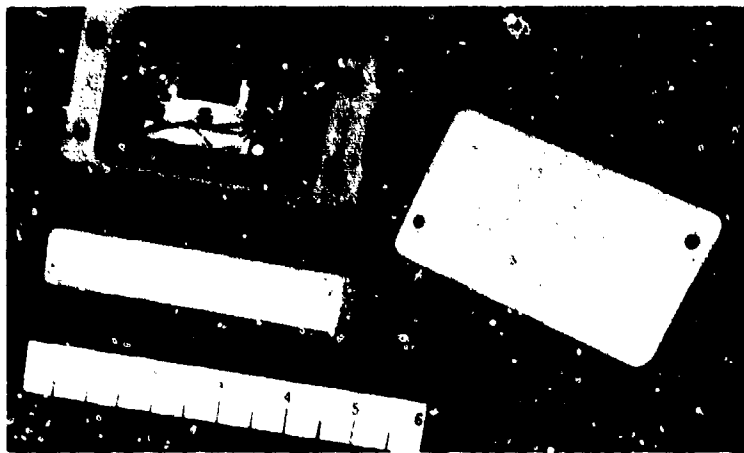
Passive Ultrasonic Sensor (PUS)

Ultrasonic Motion Sensor (UMS)

Passive Infrared Motion Sensor (PIMS)

Stimuli for each of these sensors, except the FDS, have been developed.

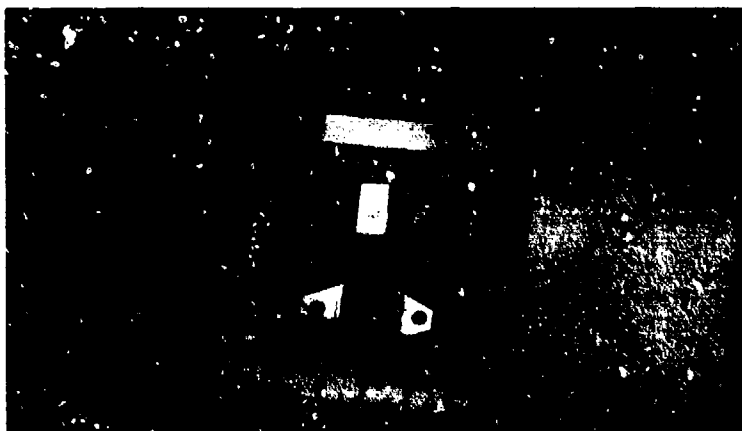
Figure 6 is a photograph of the BMS with the stimulus installed. The appropriate stimulus in this instance is simply an electromagnetic field which unbalances the magnetic field in the proximity of the BMS's Reed Switch and generates an alarm condition.



BALANCED MAGNETIC SWITCH AND STIMULUS

FIGURE 6

In Figure 7, the Vibration Sensor and its stimulus are illustrated. The stimulus simply consists of a 10 to 15 kHz oscillator which drives a transducer mounted to the VS detector mounting plate.

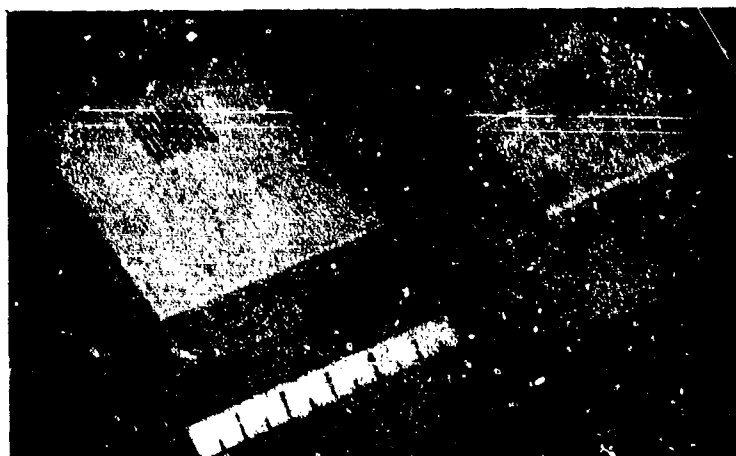


VIBRATION SENSOR AND STIMULUS

FIGURE 7

For both the BMS and VS, it is possible to locate the stimuli inside the case which houses the sensor transducer; however, in the case of the PUS, UMS and PIMS, this technique is not desirable. The PUS, UMS and PIMS are volumetric sensors which are designed to detect environmental disturbances which normally would be propagated in an air (or even a vacuum in the case of the PIMS) type of transmission medium. Consequently, if the stimuli for these sensors were placed inside or even adjacent to the actual sensor housings, it would be a relatively easy task to cover both the sensor and its stimulus with a temporary enclosure (e.g., a foil covered cardboard box) and thereby defeat not only one of the purposes of a remote test capability, but also - at least partially - defeat the sensor system itself. Therefore, the stimuli for the PUS, UMS and PIMS are contained in separate housings and may be mounted up to 25 to 30 feet from the actual sensors themselves.

Figures 8, 9, and 10 depict the stimuli for the PUS, UMS and PIMS respectively. The PUS stimulus generates an ultrasonic tone which sweeps from 18 to 24 kHz within the passband of the PUS receiver. In the case of the UMS stimulus, ultrasonic energy is generated only in one sideband around the UMS's transmitted signal to simulate a doppler shift caused by the motion of an individual. For the PIMS, the appropriate stimulus is an infrared source of energy which is detectable by the PIMS thermistor bolometer detector.



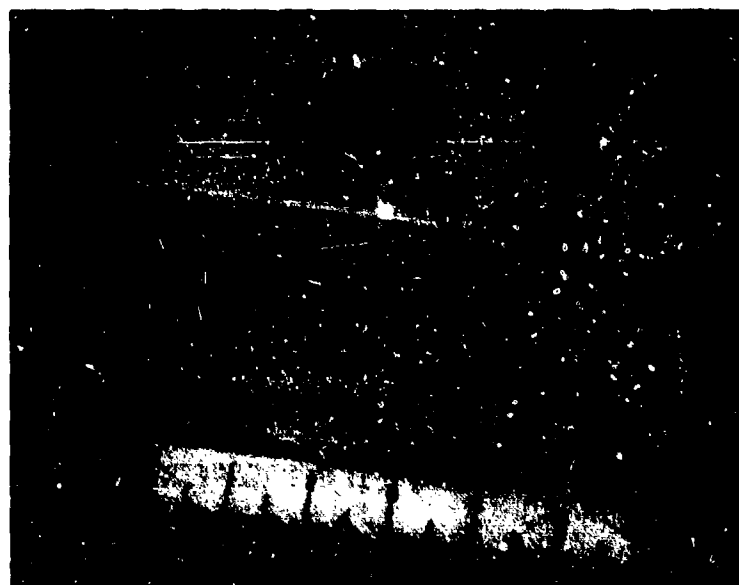
PASSIVE ULTRASONIC SENSOR AND STIMULUS

FIGURE 8



ULTRASONIC MOTION SENSOR AND STIMULUS

FIGURE 9



STIMULUS FOR THE PASSIVE INFRARED MOTION SENSOR

FIGURE 10

In all cases, an important feature of the stimuli for all FIDS sensors should be noted. Each specific stimulus has been tailored to produce an environmental change which simulates the actual change caused by an intruder at a specific sensor. Thus, when the test of a remotely located area is conducted, the entire sensor system - not merely the signal processing and communication electronics - is tested.

REMOTE TESTING

The most reliable method to verify the operational readiness of any system such as the FIDS is to actually "walk-test" the sensor system and verify that each sensor responds to the presence of a human stimulus. In systems which are comparable in size and complexity to the FIDS (both in terms of numerical sensor quantities or in terms of physical expanse), "walk-testing" may not be practicable on a routine or even on an extraordinary basis. In such cases, it becomes more critical to incorporate test capabilities into the system to allow remote testing of each of the secure zones.

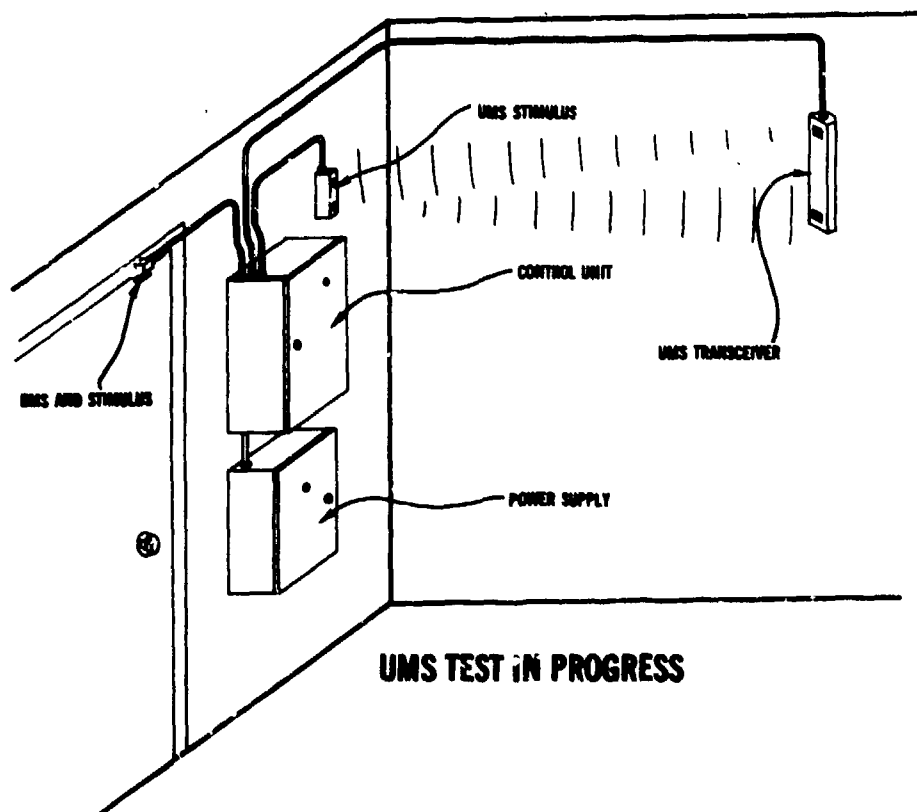


FIGURE 11

As previously described, each of the FIDS sensors has a corresponding stimulus which is designed to produce an environmental change which is detectable only by a specific sensor type. For example, as is illustrated in Figure 11, the UMS stimulus is generating an ultrasonic signal which is detected by the UMS transducer. If the UMS transducer, signal processor card, Control Unit and the Remote Terminal are all functioning properly, then a test alarm condition should be detected, processed and transmitted to the Central Master Control. In this manner, the operational readiness of all detecting and processing circuitry associated with a specific sensor will be verified. All FIDS sensor tests are accomplished in a manner similar to that illustrated in Figure 11 and as described above.

The remote testing of the FIDS sensors may be initiated in several possible ways. Periodically, the CMC will automatically initiate a "System Test" (i.e., a test of all sensors which are installed in the FIDS) by commanding a test at each secure zone. The time interval between these automatic "System Tests" is selectable through the ACCA keyboard and may be adjusted from a period of one hour to eight hours depending upon the operations requirements at a given installation. Also, whenever a specific remote area reports a change in status - from an ACCESS mode to a SECURE mode - the CMC will automatically initiate an "RT Test" (i.e., a test of the sensors in that area only) by commanding a test at that secure zone. If desired, both the "System Test" and "RT Test" may also be placed under the control of the system operator who can then enter these test commands through the ACCA keyboard. Finally, an "RT Test" may be initiated by maintenance personnel at the remote area by depressing a test switch which is located inside the CU.

Whenever a test of any zone is initiated either at the monitoring location or by depressing the test switch in the CU, the CMC will sequentially (by slot) transmit commands to the RT(s) to activate the sensor stimulus associated with a specific slot position. Assuming that no equipment failure has occurred, the RT(s) will shortly report alarm indications for that slot. Once a valid test alarm is reported for a specific slot, the CMC will transmit commands to the RT to deactivate that specific slot's stimulus and activate the stimulus for the next sensor slot position. The test will proceed in this manner until all six sensor positions have been tested. In the event that any particular sensor position fails to produce a test alarm, then the CMC will store this information in memory and continue to test the remaining sensors. It should be noted, that if an alarm condition is reported by any sensor, other than the one currently being stimulated, then the Control Unit will terminate the test, and a valid alarm condition will be reported to the CMC. This feature insures that the testing of the sensors will not inhibit the actual operation of the FIDS and allow the system to be compromised. Also, in actual operation

only approximately 30 to 40 seconds on the average, will be required to conduct any "System Test" or "RT Test" with the maximum test time not exceeding 90 seconds.

Once a "System Test" or "RT Test" has been initiated, then the CMC stores the test results as they are reported by the RT(s). At the conclusion of testing, all test results will be printed. For an "RT Test", these printed records will indicate the type of sensor installed in each CU slot, and pass/fail indications for each sensor; for a "System Test", the record will indicate pass/fail information for each zone. However, should any sensor fail during a "System Test" then an "RT Test" printout will be generated to pinpoint the specific failure. In addition to the Printer record of any test failures, the operator will be presented with visual and audible indications of failures via the ASDA and ACCA if test failures occur.

CONCLUSION

The full measure of any sensor system is to a great degree determined by the operational readiness of that sensor system to perform its intended mission. The fully integrated test capabilities which are inherent in the FIDS insure that the system will be capable of providing reliable and maintainable physical security protection in order to satisfy the Army's requirements in the 1980's.

ELECTRIC FIELD SENSOR STUDIES*

R. D. Griffith
S. Parks
Sandia Laboratories,
Albuquerque, N.M. 87115

INTRODUCTION

Sandia Laboratories has evaluated several models of electric-field intrusion sensors manufactured by Stellar Systems, Inc., of Santa Clara, CA. These models contain a field generator operating at about 10 kHz and a single channel receiver.

One example of an electric-field fence is the two-wire configuration shown in Fig. 1. The electric-field is generated by driving the top wire. A conductive body or a body with a high dielectric constant (such as the human body) in the vicinity of the wires will change the sense wire signal level. Thus, the sensor is a proximity detector with a range typically about 0.5-1 metre for a walking intruder.

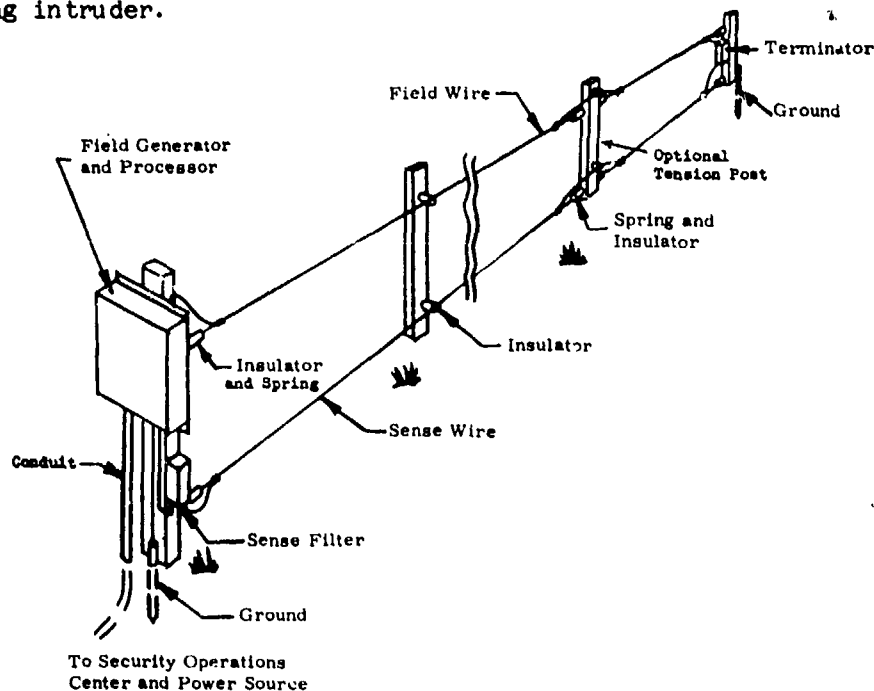


Fig. 1 Two-Wire Free-Standing Electric-Field Fence

* This work supported by the United States Energy Research and Development Administration

A more common installation consists of three wires with the center wire as the field wire and the outer wires connected in parallel as sense wires. The wires can be mounted on stand-offs on a chain-link fence to provide a proximity fence sensor, although this type of installation is susceptible to wind movement of the chain link ground plane. The electric-field sensors provide both volume detection and terrain following capability.

Evaluation of these sensors indicates a susceptibility to environmentally caused alarms, especially electromagnetic interference and animals. This paper summarizes development efforts on both above ground and buried wire systems to identify methods of improving performance.

ABOVE GROUND SENSORS

Equivalent Circuit

The field generator frequency should be much less than the quarter-wave resonant frequency of the wires to minimize electromagnetic radiation. For a 100 metre system wire resonance is about 600-700 kHz depending upon the wire height, therefore, operation below about 60 kHz is desirable.

Measurements have verified that at these low frequencies, although the wire capacitances are distributed, the coupling is equivalent to the simple lumped capacitive model shown in Fig. 2. The receiver input impedance requirements depend upon the field generator frequency and the value of the wire capacitances.

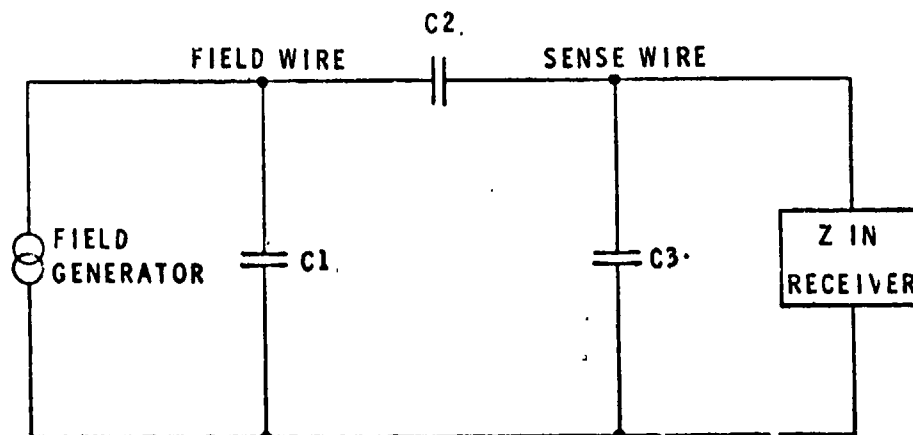


Fig. 2 Low Frequency Model of Fig. 1

The proximity of the earth or any other ground plane such as a chain-link fence affects the values of all three capacitances. For a fixed spacing between the field wire and the sense wire, the capacitance, C2, between them decreases as their distances to the ground plane decrease. Measurements on several 100 metre configurations indicate that typical values are 600-1000 pf for C1 and C3 and 20-120 pf for C2.

The capacitance of the wires to ground and the total capacitance between the wires (C2 in parallel with the series combination of C1 and C3) can be calculated using standard engineering handbook formulas. The calculation of the coupling capacitance C2, however, involves the small difference between two relatively large numbers, thus is not very accurate.

Field Generator Frequency

The intruder can cause either an increase or a decrease in signal depending upon the proximity of the intruder to ground. Measurements of the fractional intruder signal change indicate that it is independent of frequency for these short detection range configurations, and requires a receiver sensitivity of about 60 dB for a 100 metre system to detect the crawling intruder.

Since the intruder signal is independent of frequency, the small value of C2 and the wire resonance limitations indicate that operation anywhere in the 10-60 kHz range should be satisfactory for a 100 metre system. A longer sensor length will require a lower operating frequency plus greater receiver sensitivity and result in a lower signal-to-noise ratio.

Receiver Passband

The wires are maintained under spring tension to minimize wire movement in wind. From basic physics, the fundamental vibrational resonant frequency of the wire is related to the wire size, post spacing, and wire tension by:

$$f = \frac{1}{2L} \sqrt{\frac{T}{M}}$$

where L is the post spacing
 T is the wire tension
 M is the mass per unit length

A typical installation which consists of 6 metre (20 ft) post spacing, 0.81 mm (#20 AWG) stainless steel wire with 10 mil Tefzel insulation, and 22.7 kg (50 lb) wire tension provides a resonant frequency of about 15 Hz. The resonant frequency varies slightly with temperature, dependent upon the thermal expansion coefficient of the wire and the spring constant.

A small diameter wire is desirable not only to obtain a high resonant frequency but also to discourage the roosting of birds. At low operating frequencies where the field generator current is low, considerable wire resistance can be tolerated.

Slow intruder tests, including crawling and rolling, indicate that the slow intruder causes considerable signal change in the 0.01-0.1 Hz band. An 0.01 to 5 Hz receiver passband (and second order filtering) was selected for system tests in order to be at least one octave below the vibrational wire resonant frequency.

The 5 Hz upper frequency requires slowing the intruder, i.e., preventing running, jumping, etc. This can be accomplished by mounting the wires close to a barrier, such as a chain-link fence, or by using a multi-wire configuration. Tests have verified that parallel floating wires do not affect signal coupling. Wires which are grounded can be employed to shape the electric field.

Differential-Multiplier System

An electric-field sensor with improved tolerance to electromagnetic interference (EMI) and the capability of detecting the crawling or rolling intruder without alarming on animals such as rabbits, squirrels, and dogs is desired. Improved tolerance to EMI and field generator variations can be obtained using differential circuit techniques. The difference in physical size and mass between the human and the animal can provide a method of discrimination.

A system undergoing evaluation is shown in Figs. 3 and 4. Three sense wires A, B, and C are arranged as shown in Fig. 3. The receiver in Fig. 4 provides two differential signals, A-B and A-C, which are multiplied to produce $(A-B)(A-C)$.

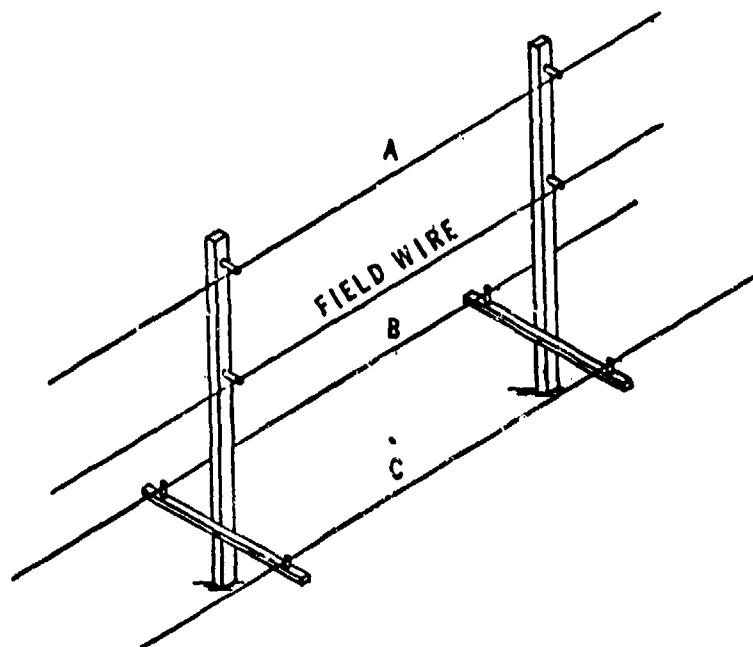


Fig. 3 Three Sense Wire Configuration

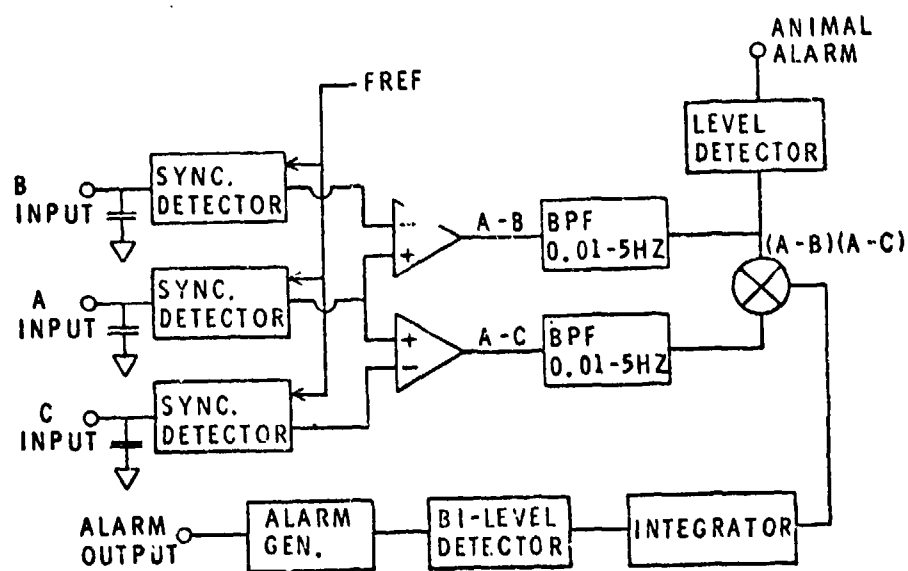


Fig. 4 Differential Multiplier System

The spacing between wires B and C is selected such that the animals, because of their smaller size and mass, tend to affect each differential channel sequentially as they go under the wires. The human whether walking, crawling, or rolling affects both differential channels simultaneously. The multiplied output is then greater for the human than for the animal. Large animals approaching the size of the human or multiple animals simultaneously under wires B and C can produce an alarm.

The multiplier output for a slow crawling intruder will have a lower amplitude but a longer duration than a walking intruder. The integrator provides approximately equal output amplitudes for the slow crawl and fast walking intrusions. The integrator output measurements indicate amplitude is a function of the size of the intruder.

For evaluation a 100 metre system was installed with wire A mounted 2.2 m (7.2 ft) high and wires B and C 25 cm (10 in) high. Tests on various spacings of wires B and C resulted in the selection of 60 cm (2 ft). The field generator operates at 20.45 kHz and at an amplitude of 55 volts RMS.

The thresholds for the bi-level detector were determined by using two trained dogs, a 13.2 kg (29 lb) dachshund and a 9.6 kg (21 lb) whippet. Tests consisted of walking, walking and stopping under each wire, running, jumping over wires B and C, and sitting up between wires B and C. These tests indicated the human intruder signals were three times greater than the $\bar{X}+3\sigma$ signals obtained with the dogs. Therefore, considerable range is available for setting the threshold levels.

For evaluation purposes, the animal activity is monitored by using the A-B differential channel to activate CCTV video recordings when animals are detected. To date, fourteen jackrabbits and one coyote have been observed going through the sensor with no output alarms occurring.

During this evaluation, winds up to 50 MPH have caused no effect on the A-B and A-C differential signals.

To obtain differential nulling, input gain adjustments are included in each synchronous detector (not shown in Fig. 4). With symmetrical spacing of the field wire, wire A has a much larger signal induced from the field wire. Approximately equal signals will be induced in all sense wires if the field wire height is the geometric mean of the heights of wires A and B.¹

Since wire A is higher above ground than wires B and C (Fig. 3), it is a better receiving antenna for EMI. The optimum location for the field wire (between the geometric mean and center) to obtain both signal and EMI nulling has not yet been determined.

Several other configurations are possible including (1) a multiplier-differential receiver to generate A^2-BC and (2) a four-sense wire configuration with the end view shown in Fig. 5 and a four-channel receiver to generate either $(AB)-(CD)$ or $(A-C)(B-D)$. The greater complexity of this latter concept may be warranted for severe EMI environments since all sense wires have the same height above ground.

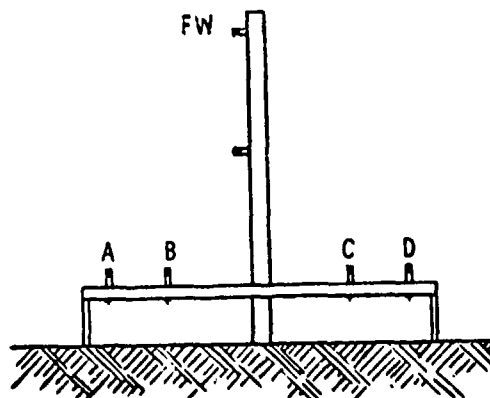


Fig. 5 Four-Wire Configuration

BURIED WIRE SENSOR

A series of feasibility studies were conducted from December 1975 through February 1976 on buried wire intrusion detection systems. Of the several configurations studied, a triangular system consisting of an overhead transmitter wire exciting two buried sensor wires appeared most promising for further development. The system to be described was completed in October 1976.

System Components

Figure 6 illustrates the experimental system setup employed.

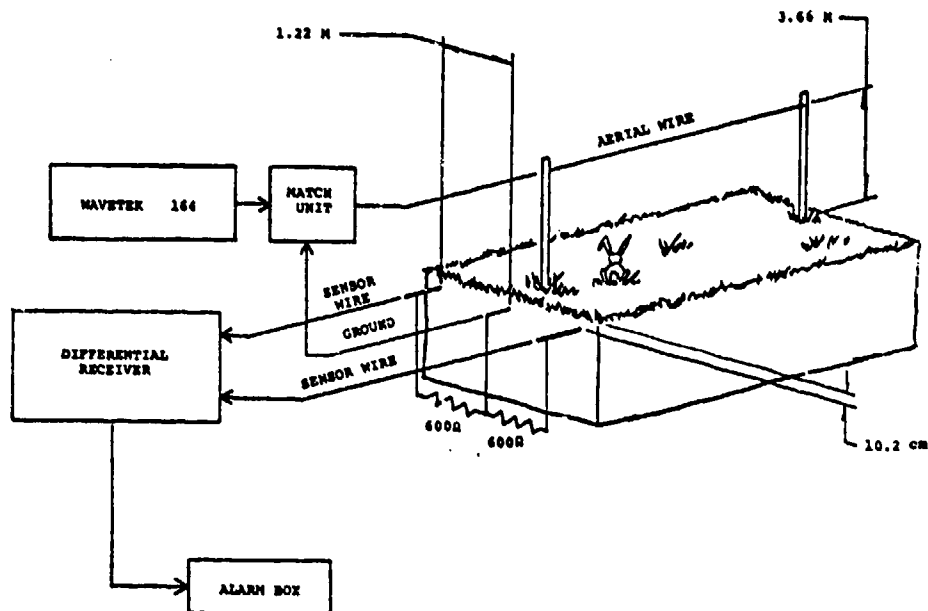


Fig. 6 Buried Line E-Field Configuration

The system consists of:

1. A 76 M long overhead insulated 14 AWG wire suspended some 4 M above ground by 5 guyed 2" x 4" posts.
2. One bare 1.63 mm (14 AWG) wire buried approximately 10 cm deep in the soil immediately below the overhead wire and 76 M in length. A ground reference is established via the buried bare wire for both transmitter and receiver.
3. Two insulated 14 AWG wires spaced 1.22 M on either side of the bare wire and buried 10 cm deep.
4. A resonant matching system to couple the transmitter to the overhead wire.
5. A differential receiver connected to the two buried sensor wires with output for analog oscilloscope recording.

6. A two-channel sonalert alarm output from the differential receiver.
7. A transmitter, which for convenience, consisted of a function generator.

System Operation

Seventy milliamps of overhead wire current at a frequency of 47.5 kHz result in approximately two volts induced into each of the buried sensor wires. A target object crossing either one of the sensor wires causes the voltage induced in that wire to change. This change unbalances the differential detector and the detection is signaled by the audio alarm.

An adult human crossing a sensor wire on foot causes a differential imbalance in the range of one part in 10^3 to one part in 10^4 (-60 to -80 dB). As the system is differential, it will sense the fact that an "intruder" is entering or leaving an installation depending on which buried wires are crossed.

A practical intrusion detection system would probably consist of a common transmitter feeding several contiguous 100-meter sections. Each of the 100 meter independent receiver sections would feed detection data to a central alarm board (or processor). A full perimeter system might consist of ten receivers and two transmitters per kilometer. Figure 7 illustrates this concept.

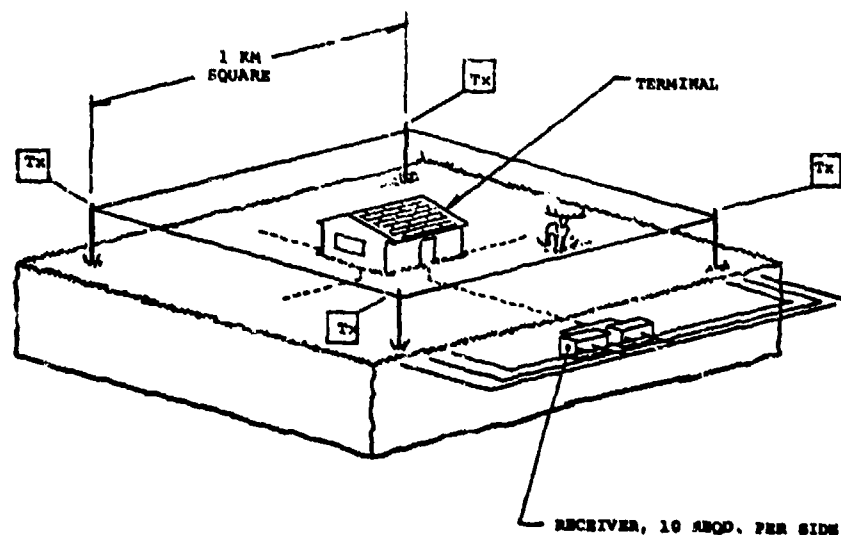


Fig. 7 Buried Wire Perimeter System

False alarm performance is of primary concern in any intrusion detection system. This parameter is arbitrarily fractioned into the following.

1. Equipment induced alarms.
2. Electromagnetic field induced alarms.
3. Alarms induced by non-threatening objects crossing the sensor whose dielectric characteristics fall within the detection sensitivity of the system.
4. Localized or general environmental disturbances, e.g., wind, ground disturbance, etc.
5. As a result of deliberate interference with the system, overt or covert.

Item 1 can be minimized by appropriate attention to component selection and circuit design supplemented by a reasonable level of automatic fault detection. An achievable level of equipment-induced false alarms is of the order of one per 1,000 hours per receiver. If sequential decision criteria are established for valid system detection, this would reduce alarms to approximately one per 10^6 hours; i.e., a bonafide intruder must cross both wires within some time limit and both receiver channels must unbalance within this time interval.

Based on experience to date, electromagnetic interference would probably be the major single receiver nuisance alarm contributor. The experimental equipment alarms on EMI about once per hour. This can probably be reduced to less than one per day by raising the transmitter power, lowering the receiver gain, and improving the common mode rejection. It is probable that an EMI pulse will be received by contiguous sections of a system (if not all sections) and that its time coincidence across sections, < 1 millisecond, will characterize it for exclusion processing. Thus, what appears as a problem for a single section (100 m) may well be no problem for several contiguous sections if rather crude processing is employed at the terminal.

Non-threatening objects of large enough cross-section will result in an intruder alarm without fail. Further study of the fine detail of disturbance waveforms may reveal some discriminants, however, this is pure conjecture.

Proper attention to overhead wire resonance may reduce wind induced false alarms to zero. The effects of rain, snow and ice are

unknown at this time. Localized ground disturbances that move any of the buried wires either transiently or permanently will result in an alarm. This phenomenon could well set the ultimate practical limit, site-to-site, for the system's false alarm performance. The phenomenon has been observed at the experimental installation but no meaningful data has been accumulated.

All attempts to tamper with the current installation have resulted in alarms and there is some evidence that attempts to jam or desensitize the system will also alarm it. More investigation is required to determine the jam-resistance of the system.

From the above discussion of false alarms in general, it appears mandatory that any further development work on the system should give the necessary emphasis to understanding and improving the system false alarm performance.

Sensor Performance

The experimental system was exercised intermittently during the period 9/1/76 to 9/30/76, and the following conclusions may be drawn:

1. Men moving on the ground in an upright position at speeds ranging from 2.5 cm/sec to 8 M/sec are invariably detected on both buried sensor wires.
2. A crawling man is detected on both wires but at reduced sensitivity.
3. A running broad jump clearing both wires results in 50% detection --- sometimes showing no effect, other times a solid detection (probably depends on whether a wire was disturbed).
4. Walking across the wires on .3 M pads taped to feet results in detection at reduced levels. Likewise for a plank supported .3 M above ground.
5. Any attempt to tamper with the system results in alarms.

Appendix 1 shows oscilloscope photographs of various intrusion efforts and should be referred to for relative quantitative data on intrusion tests.

As currently designed and configured, the experimental system has a detection threshold of -80 dB (one part in 10^4). A practical

limit appears to be in the order of -100 dB (one part on 10^5). This should be the goal for further circuit development. There is evidence in the Appendix 1 photos that a -100 dB system would be difficult to defeat.

In summary, the experimental installation has demonstrated the feasibility of a buried differential low frequency intrusion detection system. Its failure for the broad jump case indicates a requirement for increased differential sensitivity.

The Differential Receiver

A differential receiver is employed to detect the presence of an intruder in the field between the overhead transmitter wire and one of the buried sensor wires. The receiver operates by using the voltage induced in either wire as a reference and sensing the voltage difference in the other wire.

Referring to Figure 8, the receiver consists of two amplifier/rectifier/filter channels feeding a common differential detector. The output of the detector is then split into two equal gain filter channels terminating in the second differential detector. The output of the second detector is thresholded in a window comparator which in turn triggers the alarm circuit upon detection of a disturbance.

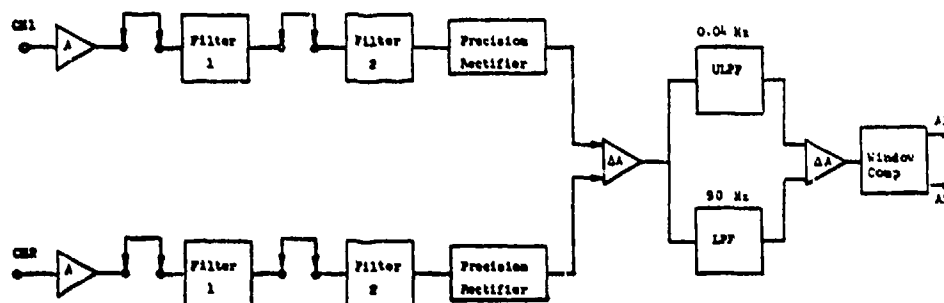


Fig. 8 Differential Receiver Block Diagram

The receiver has been designed to maximize the use of commercially available high performance operational amplifiers and linear LSI modules and there are no discrete transistor circuits employed.

The receiver pass-band has been arbitrarily selected as 0.04 to 90 Hz. This selection is based on target speeds of 75 seconds per metre to 95 km/h. The frequency determining capacitors are plug-in units so the pass-band can be rapidly changed as experiments continue.

Transmitter

The overhead wire is driven by a function generator via a 50-150 ohm transformer and a series variable inductor. The inductor, approximately 18.5 millihenries, is set to resonate the overhead wire at 47.5 kHz. At resonance the overhead wire voltage, referred to ground, is some 350 V RMS.

Current and Future Development

Field tests and evaluations of an advanced differential detector are now being conducted. This unit has some 20 dB better differential sensitivity and 40 dB common mode rejection improvement than the unit described above. This has been achieved by improved noise performance and better channel balance. Further details of the new unit would be premature at this time. At the conclusion of the current test series, a study will be undertaken to characterize applications for the system and evaluate its long-term performance in the field at a prepared instrumented test site at Sandia Laboratories. Tests will be performed to evaluate effects of soil moisture content, depth of burial, and wire configuration. Future development effort is dependent on the results of the test series and application studies.

SUMMARY

Based on the evaluation of commercial electric field sensors, a reduction in environmentally caused alarms is needed.

In the short term this improvement appears obtainable with above ground configurations. These preliminary results indicate the possibility of obtaining a greater tolerance to EMI and intruder size discrimination capability.

In the long term, these preliminary results on a buried wire sensor indicate that it has potential. Unknowns associated with the buried wires will require additional evaluation. Short sections, such as for gates, which would require less receiver sensitivity may be developed sooner.

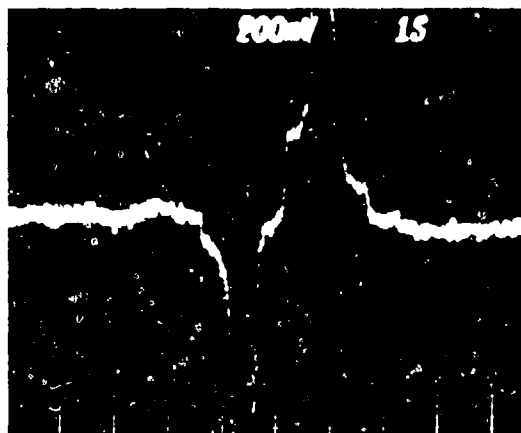
Development activity is continuing in an effort to identify the optimum mechanical and electrical configurations. If further evaluation indicates that production of one or more types of electric field sensors is warranted, a manufacturer(s) will be selected.

APPENDIX

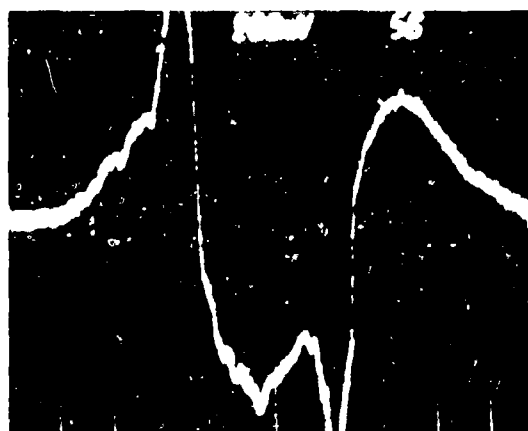
The following series of storage oscilloscope photographs were taken on the morning of 19/6/76. Each photo has a short description detailing the subject matter. For purposes of determining detection criteria, detection occurs at the 100 m/V level. All action photos are taken at 200 m/V CM.



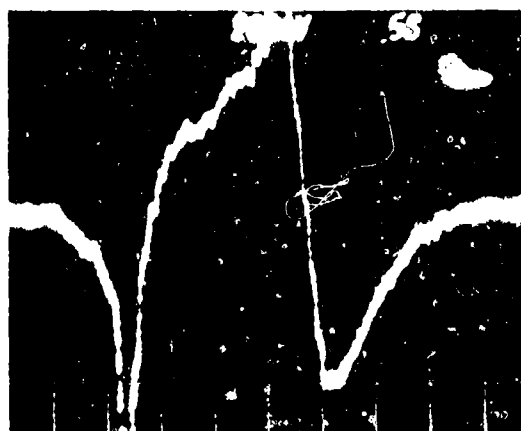
Man Walking N-S



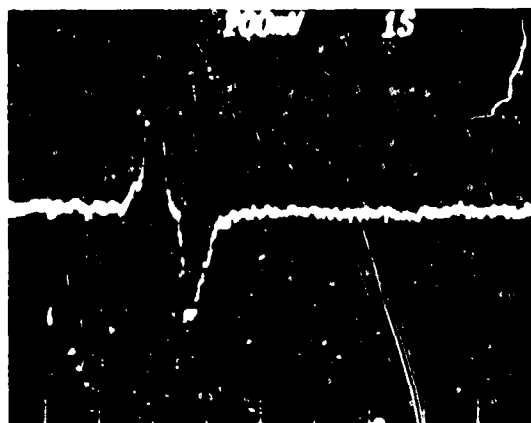
Man Walking S-N



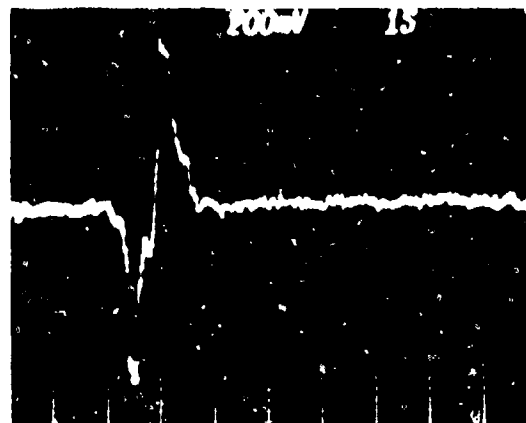
Man Stealthily Creeping N-S



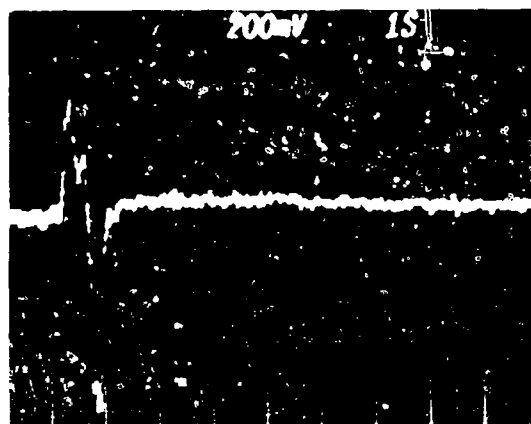
Man Stealthily Creeping S-N



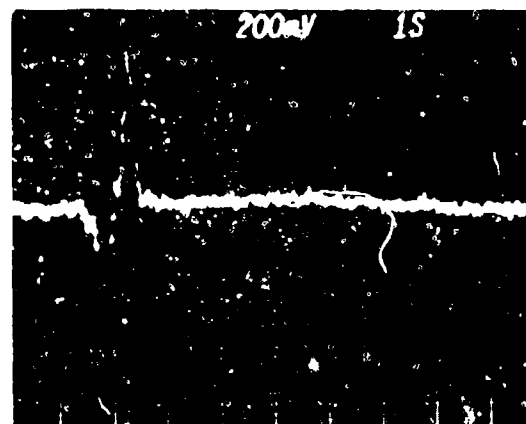
Man Jogging, 6 mph N-S



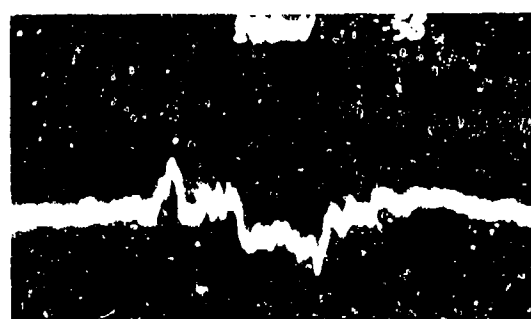
Man Jogging 6 mph S-N



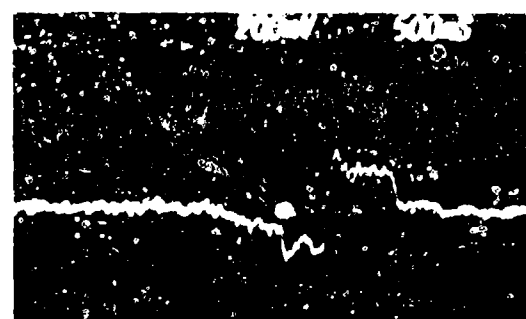
Man Sprinting 10 mph N-S



Man Sprinting 10 mph S-N



Man crawling over plastic sheet



Running broad jump

Footnotes

1. For a field wire having a height h above ground, the expression for the potential at any point in space surrounding the field wire, derived from basic field theory is:

$$V \propto \frac{\sqrt{(h+y)^2 + x^2}}{\sqrt{(h-y)^2 + x^2}}$$

This equation describes a family of circles, each being an equipotential line. If two sense wires of height A and B are located vertically above and below the field wire such that both wires are on the same equipotential line, then

$x = 0$, and $V_a = V_b$. Substituting the values into the expression above yields $\frac{(h+A)^2}{(h-A)^2} = \frac{(h+B)^2}{(h-B)^2}$. When this expression is

solved for h , the result is $h = \sqrt{AB}$

INSTALLATION SECURITY RADAR EMPLOYING MICROPROGRAMMED SIGNAL
PROCESSING AND THREAT ANALYSIS*

P. B. McCorison & C. E. Muehe
M.I.T. LINCOLN LABORATORY
Lexington, MA 02173

1. INTRODUCTION

Lincoln Laboratory and the Harry Diamond Laboratory have in the past cooperated in developing a personnel detection radar for field use. Several of these radars (the Camp Sentinel Radar) have also been used for security surveillance at large materiel storage areas.

Recent progress at Lincoln in the development of digital signal processing for enhancing radar signal continuity and rejecting clutter, applied initially to FAA aircraft surveillance radars slated for use in automated air traffic control systems, has direct application to the security radar problem. In addition, a programmable digital signal processor, the Parallel Microprogrammed Processor (PMP), initially developed for the improved FAA surveillance radar and capable of a wide range of digital processing tasks in addition to its primary function of enhancing the radar signal, could provide the basis for continuous, rapid, and "smart" security-threat analysis and action.

Combination of the technologies underlying the personnel detection radar and the PMP processor has led to the installation security radar described in this paper. The experimental model of this radar consists of a modified ground surveillance radar, the Camp Sentinel-III, with its original analog signal-processing electronics replaced by the PMP processor.

2. RADAR DESIGN

Radar design requirements call for security surveillance over a circular area of 3-km radius. Object velocities (radial) are expected to range from that of a person attempting covert penetration, less than 1/2 meter/sec. over an extended period, to that of motor vehicles, in excess of 30 meters/sec.

*This work was sponsored by Sandia Laboratories.

Parameters selected for the preliminary radar design are given in Table I. Figure 1 depicts the interconnection of the radar, the PMP and ancillary equipment.

TABLE I: INSTALLATION SECURITY RADAR CHARACTERISTICS

RF frequency	435 MHz
Antenna type	Circular array, step scanned
Pulse repetition frequency (total)	15 kHz (nominal)
Pulse width	120 nsec
Azimuth/range cell	14 degrees x 15 meters
No. of azimuths processed	32
No. of cells	1024

Antenna azimuth is stepped prior to each transmission so that one pulse is emitted in each azimuth before the beam returns to the first azimuth. The effective PRF in each azimuth is thus 1/32 of the total PRF. Several azimuth positions will, however, be skipped on each pulse. This will allow placing a low sidelobe of the antenna at each beam position during the time when range-ambiguous echoes might be received, thus further reducing the level of such returns. The radar's resolution cell is 14° by 15 meters. A total of 1024 such cells may be processed with the cells located arbitrarily in the coverage of the radar. The radar measures range, azimuth, and velocity of targets having radial velocity components between about $\pm 2/3$ m/sec and ± 40 m/sec. Targets up to ± 76 m/sec radial velocity are reported, even though their doppler is in error. Thus, the doppler velocity coverage is uninterrupted to 150 knots. Figure 2 is a block diagram of the signal processing operations which achieve this result.

Returns from several pulses are integrated coherently to obtain an effective PRF near 230 Hz. Sixteen of these samples are processed using a Discrete Fourier Transform with uniform weighting to obtain 15 doppler filters covering the velocity range between 2.5 m/s and 40 m/s in each direction. In addition, 22 of these same pulses are coherently summed to form a single data point for a second set of higher resolution, lower velocity filters. The next data point for these filters is composed of the similar sum from the above high-frequency data set commencing 16 data points later and so on.

To form the low frequency filter set, 16 data points are gathered to form a set of 4 transversal filters. These filters are formed by multiplying each complex data point by a suitable complex weight. The products are summed to produce a complex filter output. The magnitude of this vector is then used in the succeeding signal processing steps.

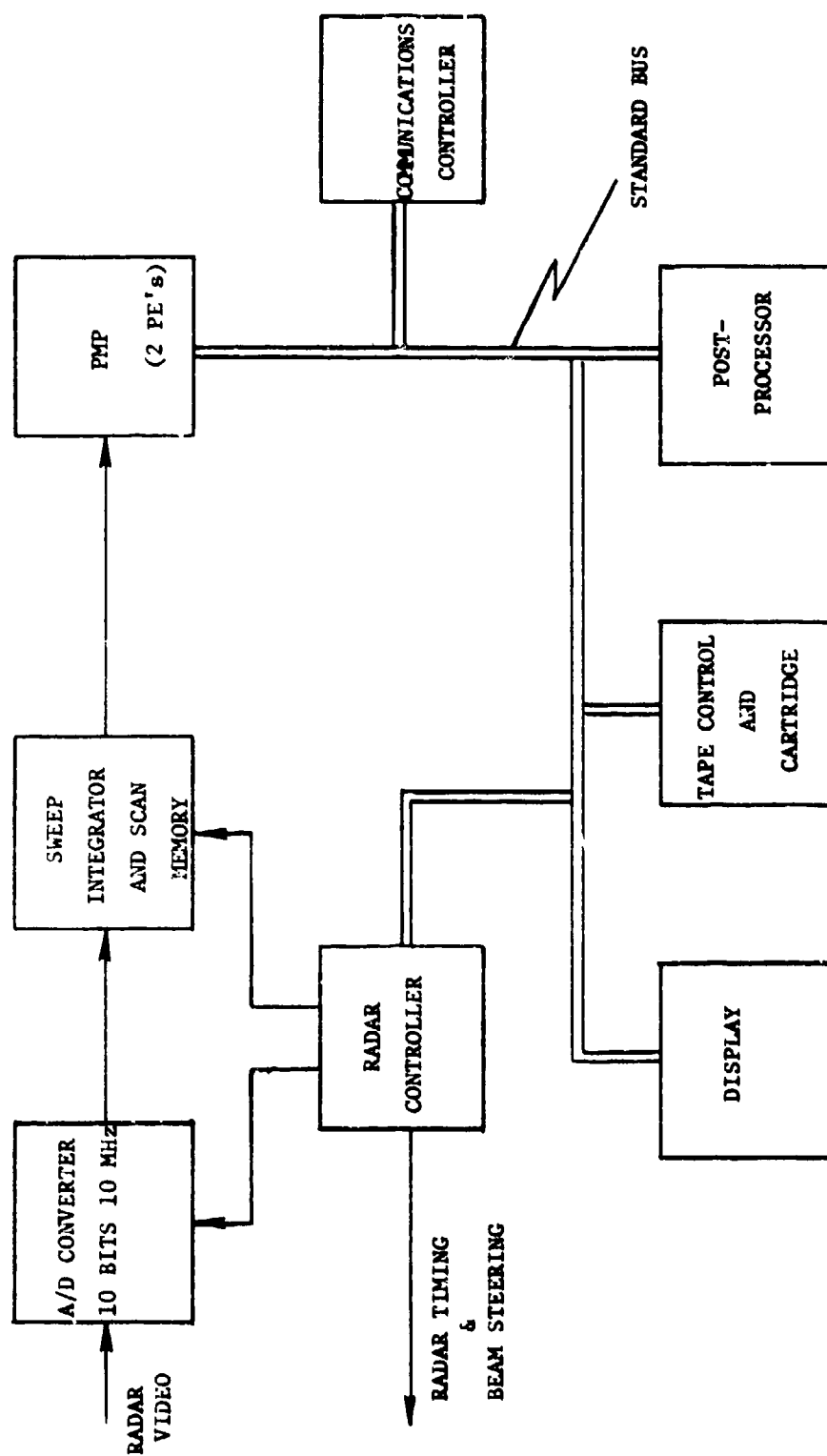
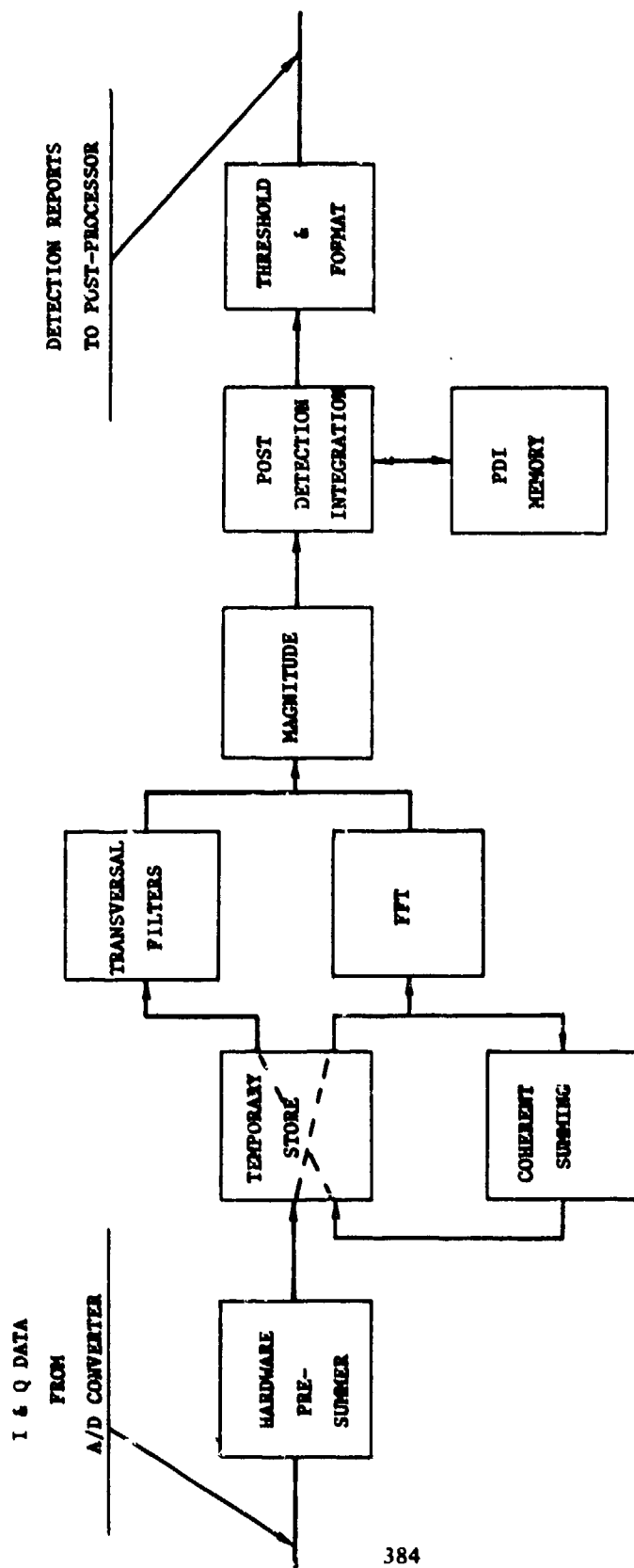


FIGURE 1 - ISR SIGNAL PROCESSOR CONFIGURATION



384

FIGURE 2 - ISR PROCESSING

The filter characteristics resulting from this system are given in Table II below.

TABLE II: FILTER PROPERTIES

Total PRF	15	kHz
No. azimuths processed	32	-
PRF per azimuth	468	Hz
No. returns pre-summed	2	-
Effective PRF per azimuth	234	Hz
No. pulses processed (high doppler filters)	16	-
Unambiguous doppler extent	± 40.8	m/s
	± 81.65	kts
Doppler resolution	± 2.55	m/s
Coherently summed returns	12	-
Effective PRF per azimuth (low doppler filters)	19.5	Hz
No. pulses processed	20	-
Unambiguous doppler extent	6.79	m/s
Doppler resolution	.339	m/s
	.678	kts

The effective PRF mentioned above results in a per beam repetition frequency of 486 Hz. This is higher than the required 230 Hz to provide an 80-m/sec ambiguity interval at 435 MHz carrier frequency. To maintain the maximum average power at each azimuth and still decrease the effective PRF, the successive returns from each range/azimuth cell are coherently summed after digitizing. The effect is to pass the data through a base-band filter of $(\sin x/x)$ frequency characteristic having a frequency separation between first nulls equal to the PRF divided by n . For this application $n = 2$.

The range of the target velocities of interest produces a wide range of time-on-target (t_{ot}). For the 15-meter range gate used, t_{ot} can vary from 25 seconds (corresponding to a radial velocity of 0.6 m/s) to 380 milliseconds (40 m/s velocity). Since this range exceeds the data-gathering time for a filter set in most cases, the filter magnitudes must be integrated to provide threshold decision data based upon the maximum available target energy. This is accomplished by passing the magnitude data through a single-pole recursive filter of the form.

$$Y_i = Y_{i-1} (1-k) + kD_i$$

Where Y_i is the filter output for the j^{th} data point D_i . The factor k is the recursion constant and is related to the inverse of the number data points contributing significantly to the filter output. Note that if k is taken to be an integral power of two less than minus one, the implementation $Y_i = Y_{i-1} - kY_{i-1} + kD_i$ is quite efficient.

A consequence of the use of post-detection integration is that a memory word must be provided for each filter output for each range gate processed. This requires 19 filters x 1024 range gates = 19,456 words of memory.

3. THRESHOLD GENERATION

The decision as to whether an object has been detected in a specific range/azimuth/doppler resolution cell is based on comparison of the output of the post-detection filter with a reference level or threshold. If the reference level is exceeded by a certain ratio, a detection is declared.

In the Installation Security Radar, the threshold is obtained in different ways for the high doppler filters and the low doppler filters. Since objects whose radial velocities lie in the high doppler filter-bank compete for detection only with receiver noise, a reference level based on that parameter can be used as a threshold for the high velocities.

Since the effective filters formed by an FFT all have a shape corresponding to the transform of the data weighting function, and since the receiver noise is spectrally uniform across the doppler band, a single value based upon the long time average of a filter output (or better, all the filters) is used to generate the threshold for all high doppler filters and all range gates. The ratio by which this threshold must be exceeded before a target is declared is a site adjustment and sets the false-alarm frequency of the filter-bank output.

In contrast, the method used to set the threshold for the low frequency doppler filters must deal with the fact that the output of these filters may be contaminated by returns from windblown foliage whose level varies and may be far above that of the desired signal. Since the foliage return spectrum is usually symmetrical with respect to zero-doppler (trees, on the average, don't go anywhere) and any threatening target is not, this distinction is used in forming the threshold. The output of a given doppler filter is compared with the output of an identically processed filter sensitive to doppler velocities of the opposite sense. If the ratio of the filter output being tested to that of its opposite number exceeds a fixed value (site adjustable), a detection is declared.

4. THREAT ANALYSIS

Analysis of radar detections to determine their impact on secure facility operation may be termed "threat analysis". Details of this post-processing function are a major topic of the second phase of the Installation Security Radar development. Threat analysis programs will be developed and tested using a commercial minicomputer connected to the standard bus (IEEE) output of the PMP.

A. Correlation & Interpolation

Since resolution cells overlap in all three dimensions of the radar's coverage, multiple responses to a single target may occur. This multiple report situation is aggravated by the multiple returns due to multipath from ground, buildings, and foliage. The first step in making use of the radar data is to combine these reports into a single one and to identify its most likely position in range, azimuth, and velocity. Field experience will be required to establish the most appropriate algorithms for this purpose. Initially, a criterion of geometric adjacency will be used to combine reports which may represent the same object. The most probable position is determined by relative response in adjacent resolution cells.

Provision for the use of "doppler signature" to distinguish among certain classes of targets is incorporated in this section of the processing.

B. Sequence Identification

Following detection, an attempt will be made to correlate the report with previous reports so that the progress of individual objects can be monitored. Reports will first be compared with the projected positions of previous reports; if this correlation fails, the new report will be projected in range and azimuth for comparison at a later time. In each case, projections are made based upon current velocity, past history, and signal strength. Correlation dimensions are selected commensurate with the notion that covert entry may imply accelerations comparable to the rates they effect. These high accelerations reduce the usefulness of conventional trackers in this application.

C. Target Reporting Criteria

When a "track" has been maintained on an object for a period of time, a decision as to whether to post the object in question on the display is required. This decision is based upon several criteria:

- Direction of motion (outgoing objects less threatening).
- Actual position (one is probably uninterested in vehicles on a nearby freeway).
- Deviations from straight-line motion (cows wander, attackers may come directly).
- Time of day (farmers work fields in the daytime, but not at night).
- Properties of the signal in track (one has low confidence in a track in which there is consistently poor agreement between doppler and range change).

These criteria and others will be refined in the field experimental phase of the development program to produce a system with maximum probability of intrusion detection, while maintaining a low level of "nuisance" reports.

5. DISPLAY

The security radar display will consist of a large CRT situation display, a keyboard for controlling radar and processor operation, and an audible alarm. The CRT display will provide a map of the installation showing enough detail to identify the significant features of the area. This map is stored on magnetic tape and entered directly into the display via the standard bus. Targets detected by the radar are posted on the CRT by the PMP using symbology controllable by the operator. The audible alarm is sounded upon decision that a target is threatening.

6. THE PARALLEL MICROPROGRAMMED PROCESSOR

A. Architecture

The PMP is a direct result of problems encountered with a special purpose hard-wired processor developed to improve the clutter rejection and continuous tracking performance of FAA airport surveillance radars. Signal processing requirements of the ISR and these FAA radars are in many respects very similar. Since the signals progressed in serial fashion through the logic blocks of the hard-wired processor, the entire radar stopped functioning properly if a fault occurred in any one block. This architecture also made it difficult to build in diagnostic mechanisms to quickly locate

faults. The hard-wired processor consisted of many diverse logic circuits, the detailed functioning of which had to be learned by technicians for proper servicing and the many diverse logic modules caused strain on the maintenance organization. In addition, processor improvements suggested by field experience were difficult to implement, often requiring rewiring.

The PMP overcomes all of the above objections to hard-wired processors. Its processing modules are in parallel so that a fault in one only partially degrades performance. It has self-diagnosing features which allows a spare processing module to be switched in automatically to replace a defective one. The number of different integrated circuit boards is small (four) so that maintenance and logistic functions are simplified. In addition, since the PMP is completely programmable, algorithm improvements in the field are easily implemented (by a simple replacement of the program memory card).

The Processing Modules (PM's) of the new PMP are in parallel and connected together by four buses (as shown in Figure 3). Each PM contains input memory and auxiliary memories appropriate to the radar processing job together with a Processing Element (PE) which performs all of the arithmetic functions. The PE is connected to the input and auxiliary memories via a local PM memory bus.

Functions performed within the PMP are divided into two types. The data handling and arithmetic functions are performed in the PM's and the program control functions are performed for all PM's within the controller.

B. Advantages

If the logic blocks of a special purpose processor are cascaded, each piece of hardware works only as fast as the signals are delivered to it. Thus, most of the hardware ends up working at about 1/10 the rate it is capable of achieving so that more hardware than necessary is included. The present approach has several sets of identical hardware, each set working near top speed, thus minimizing the amount and cost of the hardware. Since several modules are in parallel, if one fails the rest can still provide partial service. With the present approach, a diagnostic program could automatically be exercised to indicate a failing module. A spare module built into the equipment could then be automatically switched in when a failure is detected.

Maintenance procedures are facilitated by the parallelism of structure. The workings of only one processing element must be mastered by the technician. The automatic diagnosis routine even points to the failed module. Finally, needed logistic support is minimized since only one spare is required to cover all the parallel modules.

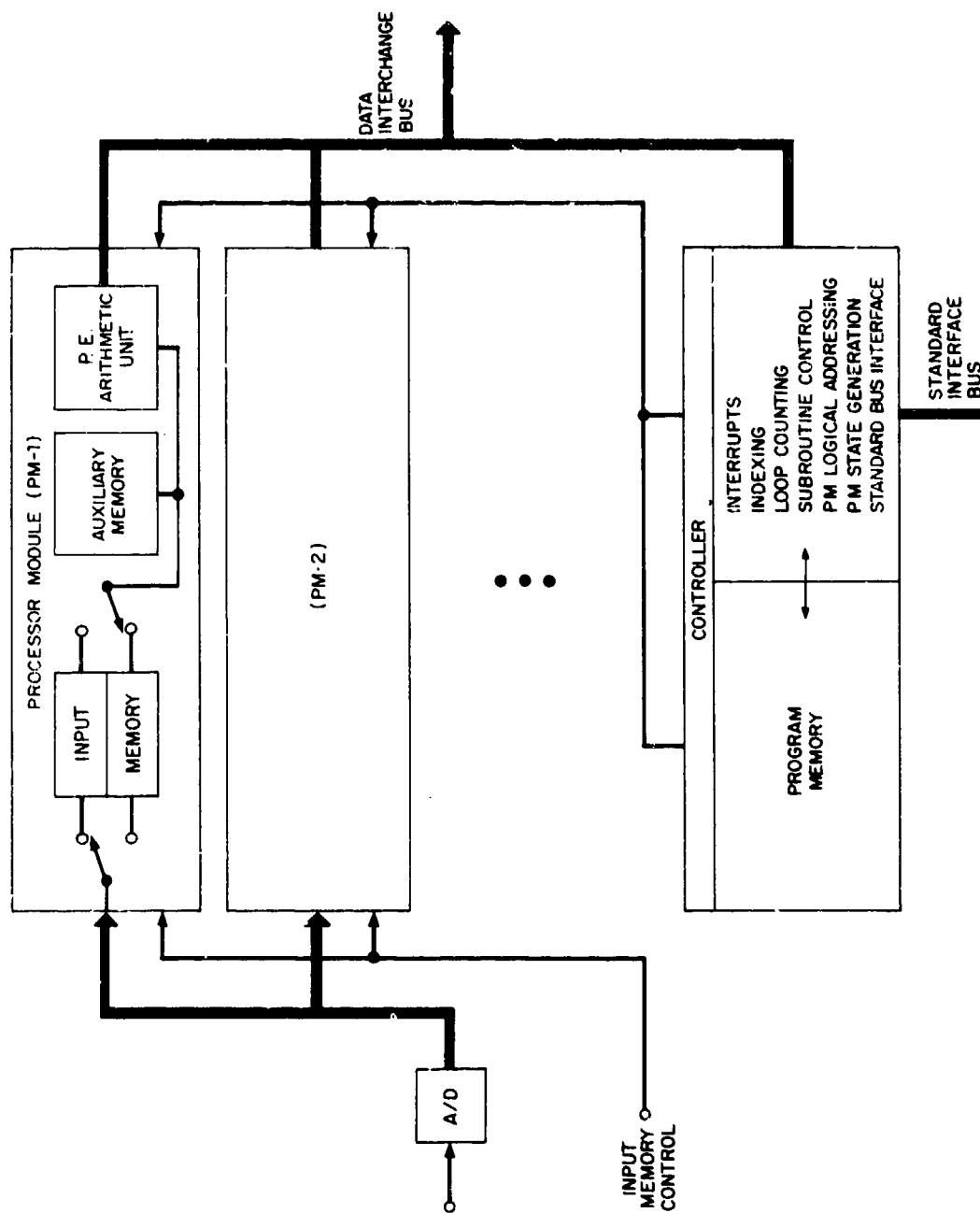


FIGURE 3 - PARALLEL MICROPROGRAMMED PROCESSOR (PNP)

In the design of the processing element itself, serial and microprocessor structures were examined and both found wanting. A serial structure would have the various major pieces (RAM, ALU, shifter) in a line separated by registers, the output of one providing the input of the next. This arrangement, while fast, is a programmer's headache since operations in the pipeline must be overlapped to attain speed. It also requires the designer to add a great deal of special hardware to perform special operations like fixed-to-floating point and magnituding of complex quantities. Also, a great deal of reading and writing of the RAM is required since there are no convenient holding registers outside the RAM.

The present PE structure finally evolved by drawing diagrams of the minimum hardware required to do each of the basic arithmetic functions (addition, multiplication, division, etc.) and combining all these into one module.

Because of the recent popularity of LSI microprocessors, these were examined carefully for possible inclusion in the PMP, particularly the PE. It was found that LSI microprocessors have two disadvantages as applied to the PMP. First, they are slower than MSI circuits chosen for the PE. This slowness is attributed to the instruction decoding performed in the microprocessor. The PE instructions are never decoded. Secondly, there appears to be no way of conveniently incorporating the PE shifting functions into presently available microprocessors. These shifters are required to perform very fast programmed multiplies. A careful examination of the PMP structure, however, shows several areas where LSI could be incorporated. For instance, each of the ALU's with its associated registers and shifters could be implemented using LSI.

For the cost involved, it was not deemed worthwhile to include a hard-wired (array) multiplier in the design of the PE. Practically all the multiplies are by fixed constants which can be programmed using shifts and adds. If both adds and subtracts are employed to reduce the programming steps, only $N/3$ steps are required on the average. Since most multiplies use 12-bit multipliers, two independent multiplies (one in each ALU) will take only four cycles exclusive of data fetch and storage. This is only 300 nsec. The present PE also multiplies very efficiently where the multiplier is either shorter or longer than that provided in the array multiplier.

C. Applicability

In summary the PMP is deemed to be eminently suited to the signal processing tasks of the Installation Security Radar application because

- Its architecture is tailored to tasks whose algorithms involve highly repetitive steps repeated in real time on a large data base.
- It has been designed to handle a large variety of radar signal processing tasks simultaneously and efficiently.

- It has been designed for minimum hardware despite large signal processing loads.
- It can readily diagnose its own faults, healing them by reassigning computing tasks among processing modules.
- Its circuit modules have been limited to only four types to reduce diagnostic, training, maintenance, and logistic problems.
- It is readily programmable - algorithms need not be finalized before hardware is made available. Initial design and test can be for one PM only with assurance that the performance can be expanded in a modular fashion. Field experience can be easily incorporated by simple program changes.
- It is readily expandable.

7. PROGRAM TO DEVELOP EXPERIMENTAL ISR

Lincoln Laboratory is presently proceeding to assemble a complete experimental security radar. This radar will be comprised of an existing Camp Sentinel Radar, a minimum version of the PMP, an available minicomputer and an adaptation of an existing display. Initial detection experiments are to be performed in the fall of this year and the system moved to a more suitable remote test site in early 1978. As field data becomes available Lincoln will participate with Sandia and the Harry Diamond Laboratories in the analyses necessary to optimize critical detection thresholds and to define threat declaration criteria. It is expected that final threat analysis algorithms and software will be developed at that time.

ACKNOWLEDGEMENT

We wish to thank Sandia Laboratories for their sponsorship of the work reported here and their constant encouragement. We also wish to acknowledge the assistance of Harry Diamond Laboratory personnel and the personnel from the ESD/BISS Office for their help in reviewing the ISR system concepts. We particularly want to acknowledge the help of D. Whitney who did the final editing and L. Wesley who prepared the manuscript.

PORTED COAXIAL CABLE SENSOR

by

R.K. Harman
Computing Devices Company
A Division of Control Data Canada
P.O. Box 8502, Ottawa, Ontario

and

N.A.M. Mackay
Department of Electrical Engineering
Queen's University, Kingston, Ontario

Abstract. An active line sensor using a ported coaxial cable transducer is being developed by Computing Devices Company, a division of Control Data Corporation under contract to the Canadian Government and the USAF. This sensor is based on GUIDAR (GUIded Intrusion Detection And Ranging) a sensor which was developed for the Canadian Penitentiary Service. An evaluation GUIDAR unit is currently installed and under evaluation by Queen's University at a medium security penitentiary. This paper describes the ported coaxial cable sensor development program as well as the GUIDAR unit and its on-going performance evaluation.

GUIDAR is an active line sensor designed for the all-weather surveillance of long perimeters. The sensor uses so-called ported (leaky) coaxial cables as a guiding structure for a low powered VHF radar processor. This has the inherent advantages of being independent of site topology and capable of detecting and locating simultaneous multiple targets. The processing is performed in a high speed microprocessor with an output presented in the form of an audible alarm and mimic board display.

The paper provides an overview of the sensor evaluation relating to the following factors: false alarm rate, probability of detection, target size, target velocity, dimensions of detection zone, variations in sensitivity along the transducer length, discrimination against nuisance alarms,

environmental effects, operational aspects of the transducer installation, effects of metallic fences and gates and operator reaction.

Two phases of the ported coaxial cable sensor development program have been completed. An Advanced Development Model (ADM) of a sensor specifically designed to meet the USAF Base Installation Security System (BISS) requirements has been built and is currently being tested by Computing Devices in Ottawa. This sensor will provide surveillance of perimeters up to 3200 meters long with the parallel transducer pair buried at a depth of up to 9 inches. A general description of the ADM and the total development program is presented.

INTRODUCTION

The ported coaxial cable sensor being developed by Computing Devices Company (ComDev) under contract to the Canadian Government and the USAF represents a totally new approach to the surveillance of long perimeters. The use of ported or so called leaky coaxial cables as a guided radar transducer is a new technology, developed at ComDev and Queen's University over the past six years.

In 1975-76 the company designed and built GUIDAR, an evaluation sensor employing the ported cable transducer for the Canadian Penitentiary Service (CPS). It was designed to process data from up to one mile of transducer buried at a depth of 3 to 4 inches. This unit was installed at a medium security Canadian Penitentiary in the fall of 1976 where it has been under evaluation by Queen's University and CPS. A portion of this paper is devoted to some of the results of this evaluation program.

As a result of this GUIDAR work, the USAF BISSPO became interested in this technology and its application to DOD requirements. In conjunction with CPS, the BISS supported a three month evaluation of GUIDAR at ComDev in the summer of 1976 prior to delivery of the unit to the penitentiary. In addition to testing the sensor performance, a preliminary design was formulated to more directly address the BISS requirement. Based on this work the Canadian Department of Industry Trade and Commerce (DOITC) together with the BISSPO supported a program for the design and fabrication of an Advanced Development Model (ADM) of the ported coaxial cable sensor. This ADM has been assembled and is currently under test at the company's site near Ottawa. It is designed to process data from 2 miles of cable transducer buried at a depth of up to 9 inches. This paper describes the ADM and gives some results of the testing program.

The results of the GUIDAR evaluation and ADM tests are most encouraging. This new sensor technology appears to provide reliable all-weather detection of humans. The transducer is easy to install in most terrains and is independent of site topology. As a result of this ADM testing a specification for a fully configured two mile system which meets the BISS development requirements has been developed. ComDev expects to enter a full scale development phase in the near future.

SYSTEM CONCEPT

The basic operational concept employed in GUIDAR and in the ported coaxial ADM sensor is illustrated in Figure 1. The transmitter initiates a pulse along one cable where it propagates at approximately 80% of free space velocity to be absorbed in a matched load.² As the transmit pulse propagates along some energy couples into the adjacent receive cable. Some of the energy coupled into the receive cable propagates in the same direction as the transmit pulse and this energy also is absorbed into a matched load. The most important energy in the receive cable propagates back to the receiver where it is demodulated. The demodulated waveform called the profile is digitized and stored in a microprocessor. When an intruder approaches the cable sensing pair the coupling is perturbed causing a change in the signal returning to the receiver. This minute change is detected in the microprocessor and the time delay between the onset of the transmit pulse and the reception of the change is proportional to the distance along the cable transducer, thereby enabling the microprocessor to turn on the appropriate LED on the mimic board display.

In order to better appreciate the evaluation program, it is important that a clear understanding of not only the system concept, but also of the method in which the various waveforms within the equipment are processed, be obtained. To this end, a generalized block diagram of the detection process is presented in Figure 1. The sensor is shown as two cables, terminating in radio frequency loads. One cable is connected to a transmitter which injects short bursts of RF energy into the sensor. The second cable is connected to the receiver where the return signal after demodulation appears typically as the upper solid waveform. This waveform essentially depicts the cumulative effect of reflections coupled from the transmit to the receive cable at every point along the sensor and is therefore a profile of return coupled power versus distance along the sensor. The advent of an intruder at some point along the sensor causes a change in coupled power at that point, thereby causing the received waveform to be modified according to the dashed line shown. This change in profile is detected by first digitizing the received waveform and dividing it into a number of range cells, each of which is related to a particular point along the sensor. A microprocessor continuously monitors the status of each range cell; any change in status that exceeds a pre-determined threshold is declared to be a target and the operator is alerted via a sonic alarm and light display.

GUIDAR DESCRIPTION

The electronics unit built for CPS is shown in Figure 2. This unit is completely self-contained requiring only the connection of two lengths of transducer pair as illustrated in Figure 3. The transducer pairs are designed in 1300 foot sections with 2600 feet on either side of the electronics unit. Line amplifiers will be included in both the transmit and receive cables between the two segments on each side and will be dc powered over the transducer cables.

The front of the electronics unit features a mimic board display and a number of operator controls. The mimic board depicts a plan view of the penitentiary with a sequence of light emitting diodes (LED) representing the location of the transducer cables between the perimeter fences. For simplicity of operation, only two major controls are provided to the operator. These are: ALARM OFF, LAMP OFF. Additional controls including ON-OFF, Manual Test, Lamp Test and Mask Keys are accessible behind a front panel.

The basic operational sequence is as follows:

- a) The sonic alarm beeps and an LED flashes; the LED defines the approximate location of a potential intrusion on the mimic board display.
- b) The ALARM OFF key is depressed causing the sonic alarm to stop and the LED to glow continuously.
- c) The operator verifies the alarm and takes appropriate action.
- d) The LAMP OFF key is depressed causing the LED to turn off.

The sensor can detect simultaneous or sequential targets at multiple locations. Each new alarm must be reset by means of the ALARM OFF key.

The leaky coaxial cable transducers were installed at the penitentiary in late August 1976. In this case the cables were simply buried in the existing gravel base between the fences as shown in Figure 3. The tolerances on burial depth and cable separation were not strictly controlled as the sensor inherently compensates for this type of variation. In those places where the transducer crosses entry walks and roadways the cables were pulled through plastic conduit buried in the concrete.

Some initial start up problems were encountered when the electronic unit was installed. One particular anomaly encountered was the difference in performance of the transducer buried in a gravel base as compared to

a similar transducer buried in sod at the Company's site. It was found that the coupled signal was larger and the cable attenuation lower than was predicted, thereby bringing the receivers close to saturation and severely limiting the dynamic range of the sensor. To overcome these problems, attenuators were inserted before each receiver and within each transducer.

GUIDAR EVALUATION

Parameters of Importance

The purpose of the evaluation program³ is to examine the performance of the GUIDAR system under operational and field conditions so as to determine the applicability of installing second-generation units, or closely related systems, in other Canadian penitentiaries. The performance factors of particular interest to this program are the following:

- a) Probability of Detection
- b) False Alarm Rate
- c) Sensitivity Profile
- d) Detection Zone
- e) Effect of Target Velocity
- f) Effect of Target Mass
- g) Multiple Target Behaviour
- h) Initialization Conditions
- i) Effect of Interference

Many of these factors are interdependent and therefore cannot be measured separately. The test program has been designed to isolate each parameter as much as possible in order to evaluate GUIDAR's suitability in other installations. The methods used to determine each parameter are based on those developed by the USAF Base and Installation Security System Program Office⁴ with modification for this study. Further tests to measure factors that are peculiar to GUIDAR are also carried out.

Measurement Equipment

In an evaluation program of this kind, in which one is interested in extrapolating the results obtained here to other installations, it is very important to obtain as much quantitative data as possible. For example, it is not sufficient to know that the GUIDAR unit does or does not function under certain environmental conditions. Rather, it is highly desirable to determine how well it functions, so that accurate predictions of its performance in other conditions or at other locations can be made. To this end, the performance of each step in the processing algorithm used by GUIDAR to detect a target is monitored where possible by the equipment shown schematically in Figure 4. An interface module is connected to the GUIDAR microprocessor. The particular feature to be monitored at any given time is selected via the "control" unit. External monitoring devices consist of a digital tape recorder, oscilloscope and chart recorder. Further analysis of the recorded data is performed on a PDP-15 computer located at Queen's University. An event recorder is also connected to the GUIDAR unit to separately monitor the status of all of the features which are normally controlled or observed by the operator. These include: status of each lamp, alarm condition, status of each button, power failure, etc.

Some typical data that is available either after further digital processing or via the chart recorder is shown in Figures 5 and 6. In Figure 5, a waveform similar to the digitized received waveform in Figure 1 is shown, indicating that a wide variation in received signal level from cell to cell can be expected. In Figure 6, the change in the signal received in one particular range cell is monitored as a human target moves along the sensor through the cell in question. Again, significant changes in sensitivity can be noted from cell to cell.

Measurement Procedure

Separate experiments are conducted to determine each of the parameters listed above under as many environmental and operational conditions as possible. Some tests are conducted on a daily basis by relatively untrained penitentiary personnel, some on a regular bi-weekly program and others at specific times when peculiar environmental conditions prevail. While details of these tests are too numerous to mention here, some general features of each can be noted:

(a) Probability of Detection (P_D):

Since GUIDAR not only detects the presence of an intruder but also defines his location, P_D is measured at all points along the sensor.

Tests are carried out to monitor the probability of detection of a human target crossing the sensor at a large number of random locations and also as a human target progresses continuously up and down the sensor.

(b) False Alarm Rate (FAR):

The FAR is measured both as a function of the overall detection process and on a cell-by-cell basis as well, so as to note any peculiarities in the detection algorithm.

(c) Sensitivity Profile:

This is a measure of the magnitude of the detected signal from an average human target at every point along the sensor. The final processed signal for each cell consisting of a number of waveforms (similar to that of Figure 6) is monitored as a target walks down the length of the sensor. This recording essentially provides a measure of the sensitivity of the system at each point along the sensor. By noting changes in this sensitivity profile over an entire year, and relating any changes to changes in ground and environmental conditions, it will be possible to predict potential changes in sensitivity for other installations of a similar nature.

(d) Detection Zone:

The detection zone of the GUIDAR system is contained within a volume extending several feet above the sensor and to within a few feet on either side of each cable. Tests which employ targets crossing the sensor at different heights are used to determine the zone. The experiments are repeated under different environmental conditions to observe any changes in the zone due to weather variations.

(e) Target Velocity:

Since GUIDAR essentially measures the change in a received signal, it is inherently dependent on target velocity. Tests to verify this factor use human targets traversing the sensor at a wide range of speeds, at different locations along the sensor and at different times of the year.

(f) Target Mass:

The size of the target has some influence on its detectability. Tests using humans of different heights and weights, in different postures are designed to measure this factor.

(g) Multiple Target Behaviour:

Since GUIDAR is intended to detect many targets at once, it is necessary to determine what effect a number of targets crossing the sensor at various locations will have on system detectability.

(h) Initialization Conditions:

Systems which depend on change to detect targets may inherently be themselves affected by drastic changes, such as a power failure. A monitor of FAR and P_D for an hour after each start-up is kept on a number of occasions during the program.

(i) Interference:

The anti-jamming features of GUIDAR are tested to determine the type of interfering signals to which the unit is most susceptible.

PRELIMINARY RESULTS

Although the results to date are still of a preliminary nature, it is possible to make some comments on a few of the parameters of importance. More information will be available at the time of presentation of this paper:

(a) Probability of Detection:

Out of approximately 500 crossings at random locations along the transducer length not one detection has been missed. In fact, it is likely that an adjustment of detection threshold is warranted to reduce the sensor sensitivity thereby further reducing the FAR and increase the discrimination of nuisance targets.

(b) False Alarm Rate:

The false alarm rate of the system has continually dropped as a number of construction features have been modified. Typically, the FAR is of the order of one alarm per several days.

(c) Detection Zone:

As might be expected, since the sensitivity of the system is higher than predicted, the detection zone appears to be larger as well. No quantitative figures are yet available for this feature.

(d) Target Mass:

The system appears not to be particularly sensitive to changes

in target mass of adult humans. However, further experiments will verify whether this is still the case when larger variations in target mass are considered.

(e) Initialization:

The system adjusts rapidly after start-up. There have so far been no false alarms related to this parameter.

(f) Nuisance Alarms:

It would appear that the increased sensitivity has caused some small animals to be detected, however further testing is required to verify this observation.

(g) Operator Reaction:

During the initial start-up problems the custodial staff were not very pleased with the high false alarm rate, thereby creating an early negative attitude towards the unit. Throughout the later months of evaluation this attitude has changed significantly and the guards seemed to accept the unit, and do respond to the alarms.

ADM DESCRIPTION

The ported coaxial cable sensor being developed for the USAF is based on GUIDAR⁵. The major differences are: an increase in transducer length from one to two miles, increased burial depth of up to 9 inches, an improved detection algorithm, improved transducer design, battery back-up and ruggedized construction to meet military specifications. Some of the performance goals for the ADM are:

- a) False Alarm Rate (FAR) < 1/24 hours (2 miles of transducer)
- b) Probability of Detection (P_D) > 99%
- c) Minimum Target Size 75 lbs.
- d) Target Velocities .02 - 10 meters/second

The ADM unit as shown in Figure 7 is effectively of "brassboard" construction. While this unit appears to meet its design performance goals it is not packaged to meet deployment requirements. In fact the construction is designed to facilitate the system development. For example, controls and interfaces are provided to interrogate the micro-processor during operation and to record selected data at various points in the algorithm. The output is a simplified LED mimic board which describes the installation at the company's test site.

The ADM is installed with two miles of cable transducer at the company's test site in Stittsville. The transducers cables are continuously graded (hole size increases with length) so that coupling is progressively increased with length to take account of cable attenuation in 1760 foot sections. Line amplifiers are installed between each of the three sections on either side of the electronics unit. For ease of testing, the two sides of the transducer are positioned roughly parallel to each other. Due to the ruggedness of the terrain; (swamp, rock, gravel, trees, etc) the cable routing is rather random with a number of abrupt corners as illustrated on the mimic board display. The installation includes cables made by Andrew Antenna and Cablewave with sections buried at different depths.

ADM TRANSDUCER

In the CPS GUIDAR sensor, the 1300 feet transducer sections are comprised of a sequence of the three commercially available Radiax cables made by Andrews Antenna. The small hole size RX4-1 was used at the start, RX4-2 in the middle and RX4-3 with its larger holes at the end. The increase in hole size with length was intended to account for the attenuation loss.

Experiments showed that this first design was "over graded"; that is it was more sensitive at the far end than at the beginning. This poor design was brought about by limited test data and inadequacy of the cable manufacturer's specifications.

In the USAF program the 1760 foot sections are continuously graded in a manner based on more detailed test data. Preliminary results indicate that this design is also "over graded" but is significantly better than the original CPS design. It would appear quite likely that future designs will continue to improve and should be capable of increased section length to 1/2 mile for frequencies below 60 MHz.

As part of the USAF contract, Queen's University has been developing a more suitable cable testing procedure to enable a more meaningful cable specification. A two-cable cavity test procedure is under evaluation. Basically, two short lengths of the test cable are mounted parallel to each other in a test cavity made up of large metallic plates with connectors for each of the cable ends. A swept frequency generator connected to one cable acts as a transmitter which excites the cavity. The signal received by the other cable is a function of the reflected coupled power, thereby providing a relationship between the cable pair sensitivity and frequency. The results of experiments on the known cable types correlate well with field sensitivity measurements. The cable cavity tests procedure could form a good economical means of comparing the performance of various cable designs for this application.

Detailed attenuation and sensitivity data is being collected on different cable types in various mounting configurations as part of the Phase 2 USAF contract. Tests have been performed over the winter and spring seasons on: cables mounted on posts, on sod surface, buried in gravel and buried in sod. Attenuation of cables on the surface and in the air is significantly more affected by the environment than those buried below the surface. In general sensitivity was highest above and on the surface and better in gravel than in sod. The quantitative results of these tests will be most useful in recommending transducer installation procedures.

The 1760 foot cable sections were buried at 3 and 9 inch depths for performance comparison. Surprisingly there was only a minor degradation with the increase of burial depth. Hence in future it may be desirable to go to greater depths.

ADM TESTING

Only limited test results were available at the time of writing this paper, however, some additional data will be included in the paper presentation. The tests to date include: signal response versus crossing velocity, weight and height above ground, sensitivity along the transducer length, profile shape and stability, the effects of line amplifiers and algorithm performance. Qualitative results based on the preliminary analysis of the test results are presented.

- a) Signal Response versus Crossing Velocity. Multiple crossings at one location along the transducer were conducted at a range of velocities from .02 to 8 meters per second. The relative output signal strength versus velocity is plotted in Figure 8.
- b) Signal Response versus Crossing Height. The giant saw horse shown in Figure 9 was used to have a human target cross at different heights above ground. The relative signal strength versus height above ground is plotted in Figure 10.
- c) Signal Response versus Weight. A number of human targets ranging in weight from 25 to 160 pounds crossed at one location on the transducer. The relative response versus weight is shown in Figure 11.
- d) Along Line Sensitivity. The maximum output signal was recorded at each instant of time as a man walked midway between the cable transducers for a complete mile (one half of the total length). This sensitivity plot is shown in Figure 12. The location of the line amplifiers is marked on the sensitivity dividing the curve into three sections. Each section can be seen to have an overall increase in sensitivity with length which is indicative of the "over grading" mentioned in the previous section.

- e) Profile Shape and Stability. The "fixed" return along one mile of transducer (same mile as in d) above) is plotted in Figure 13. This has been recorded during a variety of environmental conditions including two feet of snow cover, heavy frost, spring thaw, and rain. While these results have not been analyzed yet the general impression is that the profile is very stable under winter conditions and the rate of change during spring and summer is sufficiently slow to not cause the FAR to increase appreciably.
- f) Line Amplifiers. The line amplifiers located at 1760 feet intervals in each of the cable pairs are designed to account for the cable attenuation along the cable length. While some initial environmental difficulties were encountered these amplifiers do not present any major difficulty. The dc powering of the amplifier along the line has been very satisfactory.
- g) Algorithm Performance. The algorithm implemented in the ADM has a number of improvements over that used in GUIDAR. While the details of the algorithm and its operation are considered proprietary it is possible to state that it does include dynamic thresholding techniques to maximize Pd while minimizing FAR. Preliminary results indicate that the algorithm performs as designed.

FUTURE DEVELOPMENT

A fully configured ported coaxial cable sensor system will have similar performance to the ADM but will be designed to military specifications. This could include four hour battery backup, an interface with standard display, design for remote operation in a non-controlled environment, and the design for reliability and maintainability. Present plans are targeted at Service Evaluation Units available in mid-1979 and fully qualified units including logistic support items by mid-1980.

CONCLUSION

The success of the CPS GUIDAR unit in its evaluation program is most gratifying. While there are some areas of improvement which have been identified it has proved conclusively that the ported coaxial cable sensor technology does work and that it appears to work better than other sensors on the market.

The ADM development program is nearing completion. Significant improvements in cable design, electronic design and processing algorithm have been made. The feasibility and practicality of line amplifiers has been demonstrated for the first time. Queen's University have developed

a practical means of qualifying cable transducers for this application. Significant experimental data has been collected which will be very valuable in the subsequent development and deployment phases. The ADM unit as it is installed at the ComDev test site provides an excellent demonstration environment.

The ported coaxial cable sensor has numerous advantages over existing security sensors. Some of these advantages are:

- a) Works well in snow and frost conditions,
- b) Easily installed in all types of terrain,
- c) Not limited by site topology,
- d) Not appreciably affected by precipitation,
- e) Field is well contained (i.e. can be installed near roads, etc.),
- f) Can provide location accuracy of 50 meters or less,
- g) Can detect multiple targets,
- h) Performance characteristics are software controlled (i.e. Pd - FAR trade-off can easily be altered to suit the requirement),
- i) Virtually impossible to spoof (i.e. cannot make oneself look like a non-target),
- j) Interference is detected independently of target detection,
- k) Approximately 95% of sensor including the transducer and line amplifiers are under continuous self-test,
- l) Transducer cables are of rugged construction requiring no maintenance.

It is anticipated that this unique active line security sensor will find wide application to military requirements.

REFERENCES

1. R.K. Harman, N.A.M. Mackay, "GUIDAR: An Intrusion Detection System for Perimeter Protection", Proceedings of 1976 Carnahan Conference on Crime Countermeasures.
2. R. Patterson, N.A.M. Mackay, "Guided Radar for Obstacle Detection", to be published in June issue of IEEE Transaction on Instrumentation and Measurement.
3. R.K. Harman, N.A.M. Mackay, "GUIDAR Buried Line Sensor Evaluation" to be presented at the second International Conference on Crime Countermeasures, Oxford, England, 25-29 July 1977.
4. R.L. Allen, O. Chambers, A.W. Desens, J. Martin, "Buried Line Sensor Evaluation for BISS", Proceedings of 1974 Carnahan Conference on Crime Countermeasures.
5. Computing Devices Final Report (Draft), "Analysis and Feasibility of the Ported Coaxial Sensor System"(GUIDAR) #R799/101/FR submitted to the Canadian Commercial Corporation, Ottawa, Ontario in response to US Air Force solicitation no. F19628-76-R-0401 on 27 July, 1976.

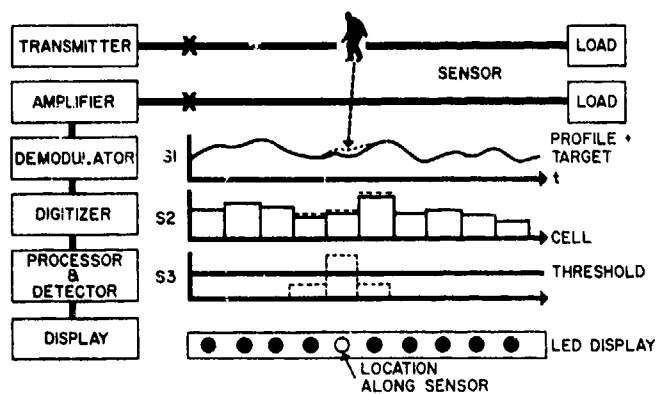


Figure 1
OPERATIONAL CONCEPT

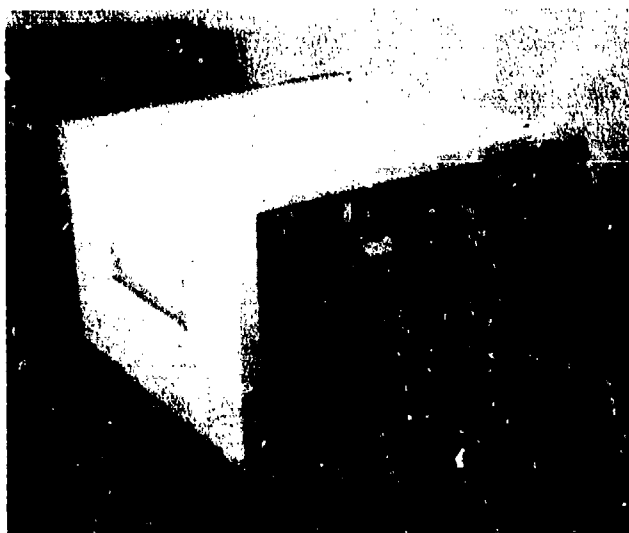


Figure 2
CPS GUIDAR EVALUATION UNIT

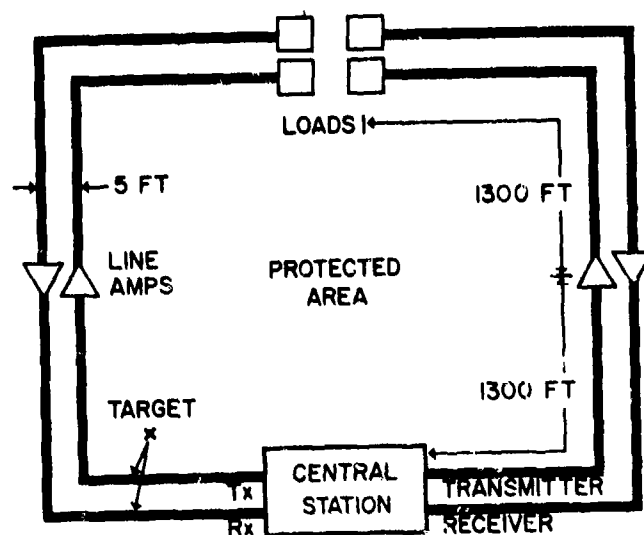


Figure 3
TYPICAL GUIDAR SENSOR LAYOUT

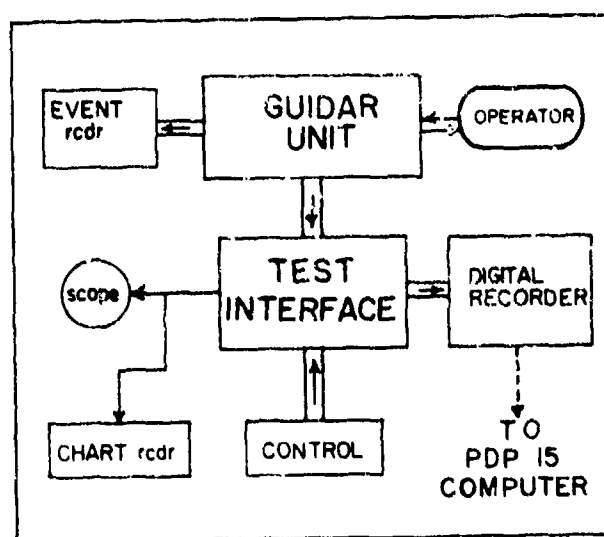


Figure 4
GUIDAR EVALUATION CONFIGURATION

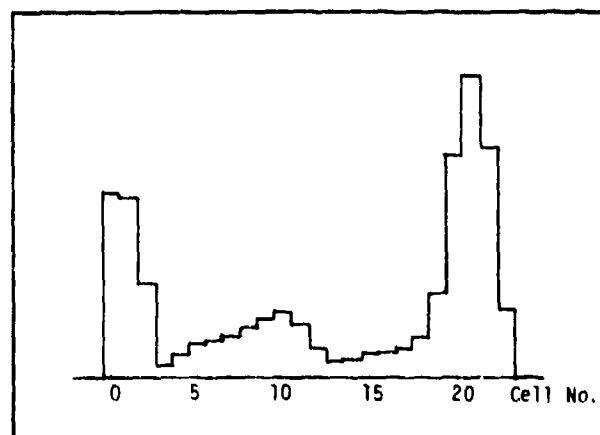


Figure 5
GUIDAR PROFILE

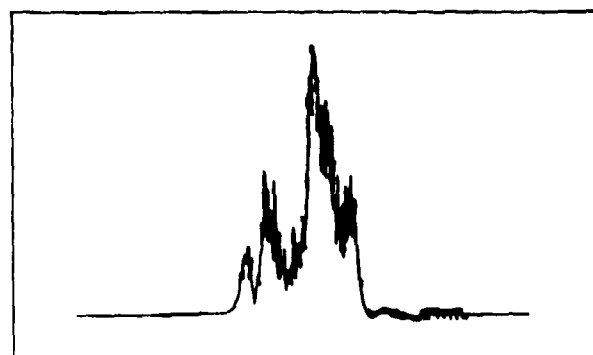


Figure 6
GUIDAR TARGET RESPONSE

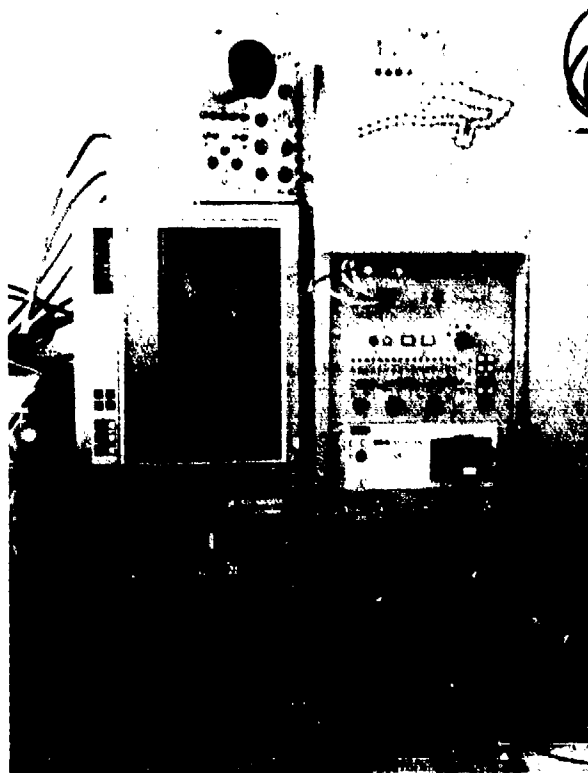


Figure 7
ADM PORTED COAX SENSOR

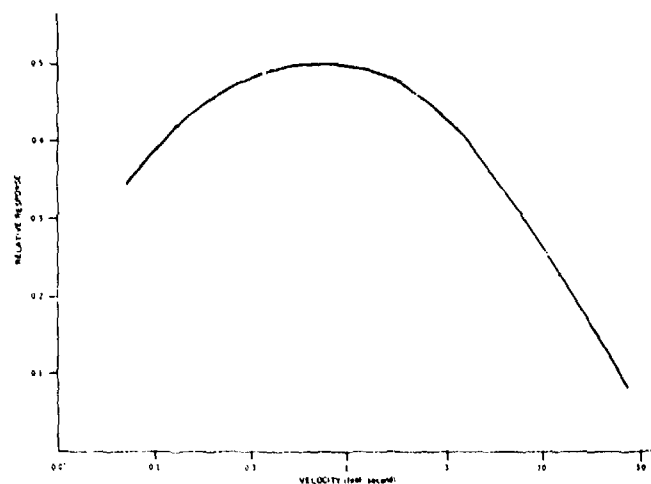


Figure 8
SIGNAL STRENGTH
VERSUS VELOCITY



Figure 9
GIANT SAW HORSE CROSSINGS

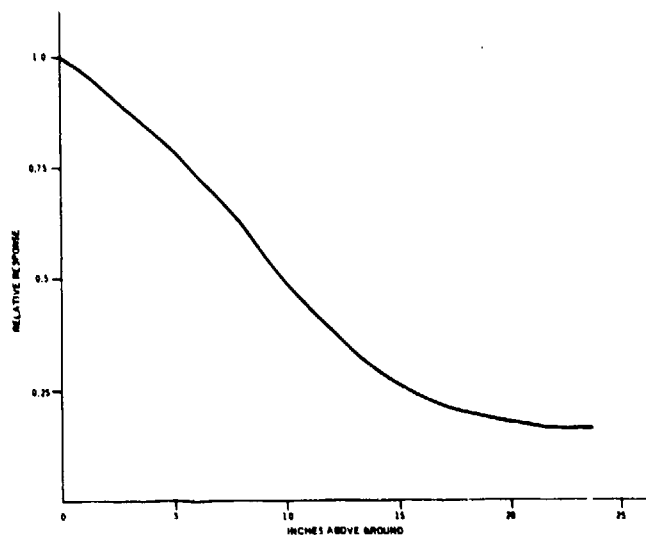


Figure 10
SIGNAL STRENGTH VERSUS HEIGHT

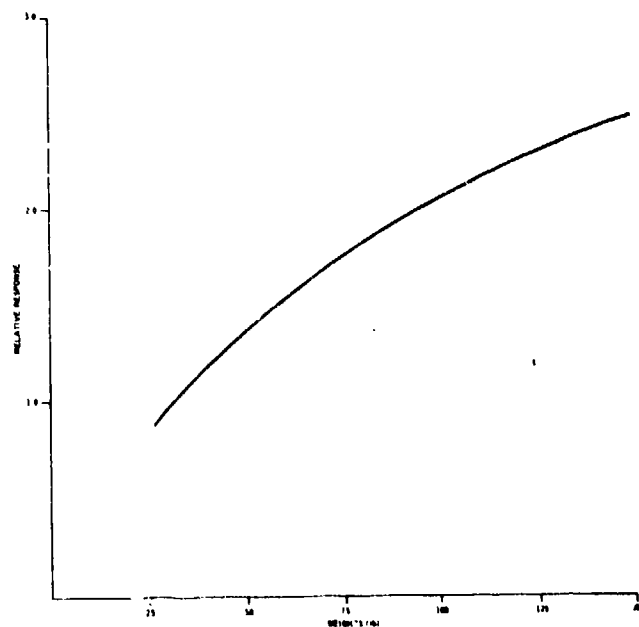


Figure 11
SIGNAL STRENGTH VERSUS WEIGHT

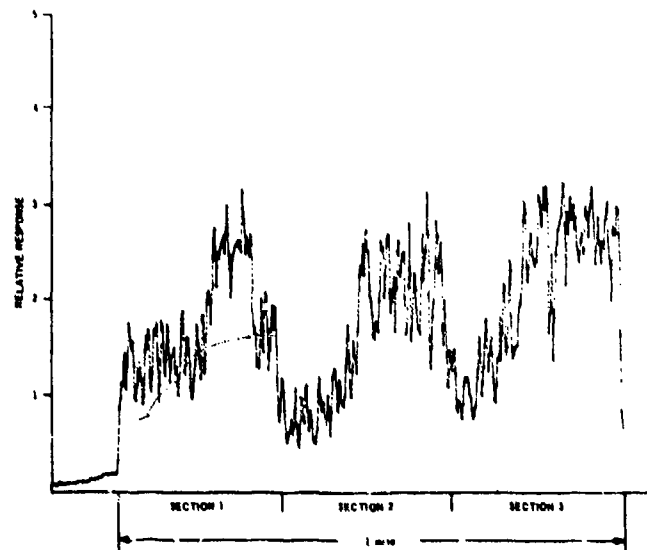


Figure 12
ONE MILE OF ADM
SENSOR SENSITIVITY

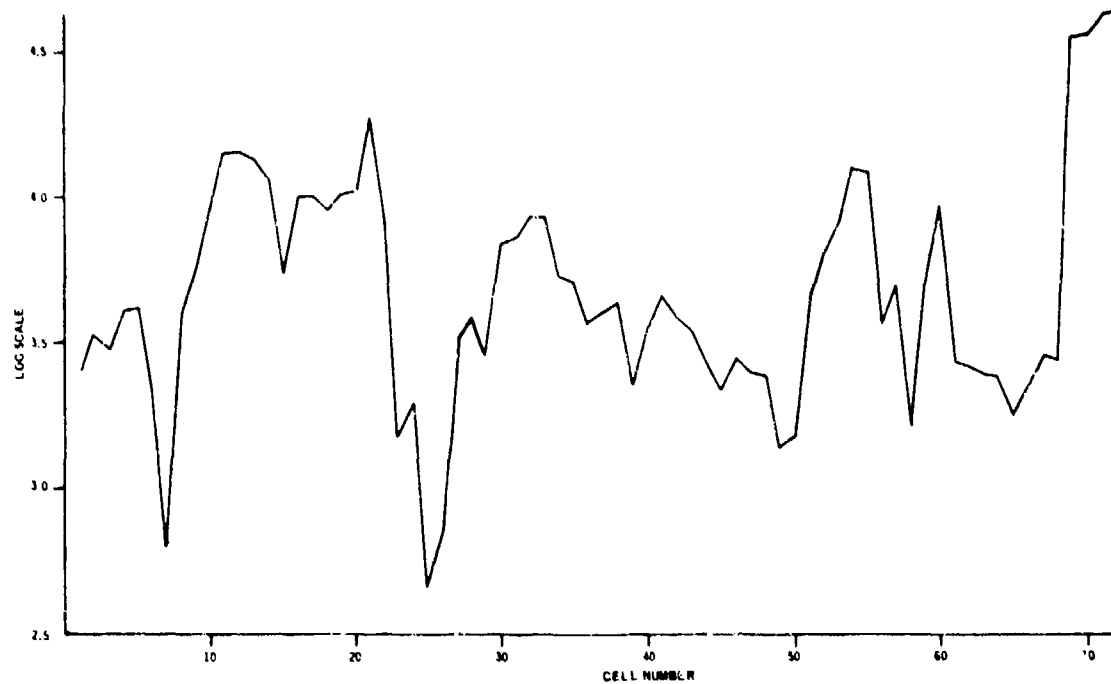


Figure 13
ONE MILE OF ADM
SENSOR PROFILE

PERSONAL ATTRIBUTES VERIFICATION

Dr. Mark R. Nelson
Mr. Raymond J. Staron, Jr.

Pattern Analysis & Recognition Corporation
228 Liberty Plaza
Rome, New York 13440

From the aboriginal native who covers his body with tribal and individual tattoos to the astronaut disembarking at a space station to register in a voice recognition booth in 2001, A Space Odyssey, man has sought, in fact or in fiction, the means to identify individual members of his race. Arthur Clark's vision of the future in 2001 is, like much of the better science fiction, based on fact. The technology necessary for automatic voice recognition has been pursued for some time and is currently the personal identity mechanism which is to be incorporated into the Air Force Base and Installation Security System (BISS). A speaker verification system has been developed by Texas Instruments which is able to meet the lowest level of BISS specifications, error rates near one per cent.

The Rome Air Development Center (RADC) has sponsored a considerable portion of the speaker verification work. Recently, however, this agency has begun to consider alternative means of identity verification and has, as a result, funded a modest investigation by Pattern Analysis and Recognition Corporation (PAR). This paper summarizes that effort and reports on the current status.

There are many reasons for pursuing alternate means of identity verification. First of all, the one per cent error rate is only the lowest level of BISS specifications. At the highest level of security, one would like to achieve error rates as low as one part in a million. It is by no means certain that voice recognition can attain this goal. One hope is that some new attribute might meet the more stringent specifications. Additionally, there is always the possibility that smaller error rates can be gained by combining speaker recognition with some other attribute, one perhaps to emerge from the PAR investigation. Another motive for seeking additional means of identity verification is that voice recognition may not always be the best technology for every application. It may sometimes be too costly, or too slow, or, perhaps, too difficult to use.

Let us digress for a moment to make more precise two ideas which we have so far been using interchangeably, "identification" and "verification." Identification is to label an unknown individual of a population, whereas verification is to ascertain whether a labeled individual of a population is correctly labeled. Identification is the domain of forensics. Verification is what is demanded in most security systems for

access control. Thus, an individual presenting himself for entry is assumed to cue the system by entering his name or code. The system simply verifies that the personal attribute being measured for that person agrees with the value already on file. The verification problem is obviously simpler, since any system which can perform identification can, a fortiori, perform verification.

A variety of means of identity verification alternatives to voice recognition are already under commercial development. Those known to the author include fingerlength measurement by Identimat Corp., fingerprint recognition by Calspan Corp., body vibration transfer function by Novar Electronics Corp., and face recognition by a variety of investigators. RADC deemed it appropriate, however, to fund a general investigation of personal attributes, with the exception that PAR was excluded from examining fingerprint or face recognition.

PAR undertook three tasks for RADC. First, we were to perform a general study of alternate means of identification. From a list of candidate personal attributes, we were to single out two especially promising techniques for in-depth investigation. For the two personal attributes selected under the first task, PAR was to collect data on 72 people at three sessions over a period of three months. The final task was to use this data to determine the error rates for each of the two attributes.

The attributes listed in Table 1 were selected by PAR for evaluation. Sources for these attributes included RADC suggestions, books on forensics, medical and physiological literature, and the imagination of the staff.

The various physical attributes were evaluated for utility in a verification system by assigning numerical ratings to them in six categories. The categories for evaluation are listed in Table 2. "Separability" means the error rate of the technique. For verification systems, the errors are labeled Type I, a "sin of omission," the probability that a legitimate applicant will be rejected by the system, and Type II, a "sin of commission," the probability that an illegitimate applicant will be accepted. The latter is assumed to be only a casual intruder and not a trained agent. To evaluate Type I and II errors theoretical formulas were derived which gave these errors as a function of standard deviations of the measured attributes for individuals and for the population at large. Acceptability was measured by circulating a questionnaire designed by PAR psychologists. The last four categories were evaluated by engineering investigations of verification systems based on the respective attributes. "Penetrability" was taken to mean ease of access by a determined intruder with knowledge of the detailed operation of the system.

Table 1 Personal Attributes Considered For Identification

1. Palm print (lines and/or ridges) and footprints
2. Finger folds
3. Finger lengths, hand area
4. Skin color, hair color, eye color
5. Vein pattern
6. Photoplethysmogram
7. Skin resistance
8. Total (body) resistance
9. Bone pattern (ultrasound)
10. Finger tremor pattern
11. IR radiation pattern
12. Eye scan path/dilation
13. Sonic characteristics of the teeth/skull
14. Bite patterns/fillings
15. Ear structure
16. Electroencephalograms
17. Visually evoked potentials of the brain
18. Visually evoked magnetic fields of the brain
19. Saliva
20. Blood composition
21. Odor/sweat
22. Height/weight
23. Gait
24. Electrocardiogram (ECG, DCG, Echocardiogram)
25. Ballistocardiogram
26. Verbal response pattern
27. Personal history
28. Typing style
29. Lip grooves
30. Polygraph
31. Implanted marks
32. Body vibration transfer function
33. Nail grooves

Table 2 Evaluation Criteria for Personal Attributes

1.	Separability	-	Type I and II Error performance
2.	Acceptability	-	User acceptance
3.	Feasibility	-	Technological risk
4.	Cost	-	Development, production and operating
5.	Speed	-	Time for user to gain access
6.	Penetrability	-	Ease of access by a trained agent

Table 3 Error Rates to Date for the Two Attributes in Detail

	<u>Handprint</u>	<u>C-Trace</u>
I	.014	.012
II	.0164	.0107

The six categories were weighted, separability and acceptability being most important, penetrability being the least, and the scores were combined to attain an overall ranking for each attribute. Some judgment was required since it was not always possible to assign numerical scores to the attributes.

Two attributes were selected for detailed investigation: first, flexion crease lines on the palm and fingers, and second, electrocardiograms. Crease lines on the palms, those lines used by chiromancers, are congenital flexure lines and are located where the outer layers of the skin are more firmly attached to the subcutaneous tissue. In choosing crease lines, we believed we would have an attribute as rich in detail as a fingerprint, as permanent as a fingerprint, but present on a larger scale. This latter point is a fundamental one for automatic recognition systems. It makes no matter how good an attribute is; the end result will depend just as strongly on how easily the attribute is transducible. The electrocardiogram (ECG) was selected because, although not unique at the same level as a finger or palmprint, theoretical estimates indicated that ECG's could meet BISS specifications. It was further believed that the ECG could be used to produce a low cost system. This is in contrast to palm or fingerprints which require optical input devices with consequent greater cost.

Palmprints were collected from 72 people by placing their hands on a photocopying machine. The copies were marked at a number of fiducial points such as crease lines in the fingers and width of the fingers halfway between each crease line. Major crease lines of the palm were extended to their intersection with the silhouette of the hand to gain further fiducial points. These fiducial points were then digitized with a graphics tablet. Interpoint distances were computed to form thirty-four measurements on each palmprint. These measurements formed a 34-dimensional "feature vector" in the jargon of pattern recognition.

The next step was to find those subjects whose hands looked most similar under this measurement. With one feature vector per subject, we had 72 points in a 34-dimensional space. The Euclidean distance between all pairs of prints was computed, and a set of 25 hands comprising "worst case" pairs and triplets was identified therefrom. For each person in the group of 25, a set of 10 handprints was collected, the subject replacing his hand on the machine for each copy. Additionally, two more prints were collected for all 72 subjects.

This data was placed into the On-Line Pattern Analysis and Recognition System developed by PAR and RADC [Sammon, 1970]. Using the measurement reduction routines in OLPARS, the 34 original measurements were reduced to nine which seemed to carry most of the distinctiveness between individuals. At this point, we were prepared to evaluate the Type I and II errors.

Let us denote the subjects by the symbols A, B, C, ..., and let us suppose that A is on the list of "worst case" hands. Thus thirteen handprints are available for A. Using ten of the thirteen prints, we designed a weighted nearest-mean vector logic [Sammon, 1970] with a reject boundary. All three sets of 72 hands are tested against this logic. The three prints of A are used to determine a Type I Error. They should be accepted by the logic. The 213 other palmprints representing intruders should be rejected by the logic and can be used to determine the Type II Error. This procedure is then repeated for the next subject on the "worst case" list until all 25 subjects have been completed. Then the Type I and II Errors are computed as an average over the errors for each individual. To date, no errors of either type have occurred. These results are presented in Table 3.

We now turn to a discussion of ECG data. It is envisioned that this access control device will consist of two electrodes to which the person desiring access will touch his hands. We therefore collected ECG's with electrodes attached to the two index fingers of the subjects. No ground electrode was used, nor was any electrode paste. The subjects were told to stand normally. Thus, the recorded waveform is a highly modified ECG and to avoid medical connotations we have called it a "C-trace." ECG's were collected on 72 subjects over three sessions. The waveforms were digitized and then entered into the PAR Waveform Processing System, WPS, for smoothing and automatic segmentation into individual beats. A ten-dimensional feature vector was extracted from the waveforms. The data was again manipulated in OLPARS in a fashion very similar to that described for the palmprints. The results at the time of this writing are shown in Table 3.

In conclusion, two promising attributes for personal identification have been studied. The handprint seems to possess a high degree of uniqueness. The feature extraction has, as of yet, been largely a manual process. It remains to be shown that automatic feature extraction software can do as good a job as a human. The electrocardiogram has a somewhat poorer performance, but all segmentation and feature extraction is being done in software. Thus, we are much nearer an automated system. Furthermore, we feel that improvements can be made in the ECG feature extraction process to enhance performance.

This work was performed under Contract #F30602-76-C-0377.

REFERENCES

1. Sammon, J.W., "Interactive Pattern Analysis and Recognition," IEEE Transactions on Computers, Vol. 19, July 1970.

WATERBORNE INTRUDER DETECTION SENSORS

Dr. Alan J. Stratton
DYNATREND INCORPORATED

Abstract

The Waterborne Intrusion Detection Segment (WIDS) of the Base and Installation Security System (BISS) is supporting the development of surface and subsurface sensors to detect and classify waterborne intruders. The classes of potential intruder threats include waders, swimmers, swimmer delivery vehicles, and a variety of surface craft. WIDS sensors will detect and classify such threats automatically, providing alarm signals to security personnel via BISS communications and display equipment. The equipment will be of modular design amenable to use in a variety of configurations with other BISS sensors to meet the specific security needs of individual sites. The WIDS sensors are currently in the Advanced Development phase and will complete Engineering Development in 1981. The primary surface threat sensor is a radar target detection unit which will perform automatic-alarm signal-processing functions and be compatible with a number of existing service-approved, small, low-cost radars. A low-frequency acoustic interferometric device is being developed for detection of waders. Two CW Doppler sonars, one monostatic upward-looking and the other bistatic horizontal-beam, are being developed for detection of swimmers. Arrangement of individual units of these last three devices side-by-side will provide a detection barrier-line capability.

Introduction

The four sensors discussed here are being developed within the Waterborne Intrusion Detection Segment (WIDS) of the Base and Installation Security System (BISS) Program. The WID Segment development efforts are funded by and receive overall direction from the BISSPO. The WIDS program is managed for the BISSPO by the Naval Coastal Systems Laboratory (NCSL), located in Panama City, Florida. DYNATREND INCORPORATED serves as the system engineering and integration contractor for WIDS and provides program management support to NCSL. Design and development of the waterborne intrusion detection sensors is being performed by the Engineering Experiment Station of the Georgia Institute of Technology in Atlanta, the National Bureau of Standards in Boulder, Colorado, and the Applied Research Laboratories of the University of Texas at Austin. Assistance provided by Mr. Nicholas C. Currie of EES/GIT and Dr. Hollis C. Boehme of ARL/UT in the preparation of this paper is gratefully acknowledged.

Background

The BIS Systems Program Office is chartered to develop external physical

security equipment and systems for protection of military bases and installations of all the services world-wide. Many of these bases and installations are located adjacent to bodies of water such as oceans, bays, lakes, and rivers which provide routes of access to important assets from the water-side. In recognition of this fact, and based upon the results of an assessment of the sensor technology then available for detection of waterborne intruders, the BISSPO initiated the WID Segment development efforts in 1975. The WIDS effort is presently in the Advanced Development phase. When their development is completed in 1981, the sensors will be added to the BISS equipment inventory and will complement the land-side sensors under development elsewhere in the BISS Program. In consonance with the BISS objective of minimizing demands placed on the security personnel who will use the sensor equipment, the requirements placed on WIDS sensors include automatic detection and classification of intruders in sufficient time to allow for security forces to carry out appropriate responses. The design and implementation of the signal processing functions necessary to discriminate actual intruder threats from both noise and non-threatening signal sources is perhaps the most challenging aspect of these sensor development efforts and will be discussed in more detail below. Each sensor, upon detection of a valid threat, will initiate an alarm signal to be transmitted and displayed to security personnel via BISS communications and display equipment.

The classes of potential intruder threats which these sensors must detect include personnel either wading or swimming, underwater vehicles used for delivery of swimmers, and a variety of surface craft. Both the operational and detectability characteristics of these threats have been investigated in the literature and by means of a series of target signature tests performed at NCSL and other locations. These characteristics have been documented and used to help define the sensor requirements.

In order to ensure the specification of realistic requirements for the sensors, a series of site surveys has been conducted. The conduct of these surveys has included visits to typical Air Force and Navy bases and other installations which have land-water boundaries, and an Army site will be visited in the near future. During these surveys, information has been gathered concerning the types and locations of important assets, existing security systems and policies, likely threat types, the physical characteristics of the land and water areas, and various environmental parameters which influence both threat and sensor performance. Analysis of the data acquired during these site surveys provides the means to verify or refine the technical performance requirements for the sensors, and aids in specifying the environmental qualification criteria which they must meet. It has been recognized since the inception of the BISS Program that a modular design approach would be necessary in order to provide different types of hardware usable in various combinations to meet the specific security needs of individual bases and installations. The site survey results provide a base of data which can be used in simulation

studies to examine the cost and performance parameters of various alternative combinations and configurations of sensor equipment.

In addition to the automatic-alarm and modularity design goals mentioned above, the WIDS sensors are being developed to be low in both procurement and ownership cost, and of minimum complexity consistent with the provision of automatic-alarm capability. Although a thorough system engineering program is being pursued to ensure that these goals are met, little more will be said of it here in view of the sensor technology focus of this conference.

Target Detection Unit

The primary sensor for detection of intruder threats on the water's surface is a radar target detection unit (TDU) under development by the Engineering Experiment Station of Georgia Institute of Technology. The TDU is a signal processing unit designed to operate with a number of different small, low-cost radars having certain common system characteristics; a representative set of system characteristics is given in Table 1. The initial design of the TDU has been largely completed, and fabrication of a prototype unit has been initiated. This prototype will provide flexibility in several areas to enable evaluation of alternate design options. The prototype will be tested, design options evaluated and performance deficiencies remedied. The result of these actions will be the conversion of the unit to an Advanced Development Model (ADM). The ADM will be tested to determine if the design it embodies meets the technical performance requirements which have been specified for the TDU.

For some operational situations, the problem which the TDU must solve is a difficult one. It must be able to discriminate at ranges of several kilometers between surface targets which constitute a threat to a protected asset and others which may be in the vicinity of the asset for a variety of legitimate reasons. Thus, in addition to distinguishing in a more or less conventional sense between targets and clutter or other types of noise, it must be able to make distinctions between radar targets which are threats to an asset and those which are not. An initial set of alarm criteria has been defined to address this latter problem.

The design features which will be implemented in the TDU include fixed target deletion, constant false alarm rate (CFAR) processing, scan-to-scan integration, and target track generation and prediction. Targets with large cross-sections will be processed separately from those with lower cross-sections. A simplified block diagram of the TDU is given as Figure 1. The shaded blocks in the figure will be included only in the prototype TDU, while the unshaded blocks represent the functional groups which will constitute the final version of the TDU when its development and testing are complete.

TABLE 1. ASSUMED RADAR PARAMETERS FOR TDU DEVELOPMENT

<u>Parameter</u>	<u>Value</u>
Peak Transmitted Power	25 KW
Beamwidth	1° (Azimuth)
Frequency	I-band
Pulse Width	100 ns
Scan Rate	20 RPM
Antenna Gain	30 dB
Receiver Noise Figure	8 dB
PRF	1 KHz (nominal)

The IF-video subsystem functions primarily to process the radar video into a format and data rate compatible with the PROC. It performs a LOG function and CFAR processing on the video, detects returns from high RCS targets through the use of an analog threshold, performs a three-bit A/D conversion on returns from low RCS targets, and performs bandwidth compression. In addition, the IF-video subsystem determines azimuth position, generates transmitter triggers, and monitors the transmitter status.

The processor which implements the PROC functions will identify, tag, and delete fixed targets, perform digital integration on low RCS targets, and accomplish centroid identification. The PROC will be microprogrammed which implies a well-defined control structure, or set of microinstructions, with each of the PROC operations taking place in one clock cycle (micro-cycle). Microinstructions are normally located in read-only memories; however, during the development of the TDU prototype they will be located in random-access-memories configured as a writeable control store. The writeable control store will be initialized by the display processor subsystem at power-on or whenever the microcode in the PROC requires changing.

In addition to providing overall control of the system, that is, functioning as the host processor, the decision processor subsystem accepts target information from the PROC, and accomplishes target verification and track generation functions. Specified tracking and alarm algorithms will be employed and targets which are determined to be threats will result in an alarm condition being transmitted to the BISS communications and display equipment.

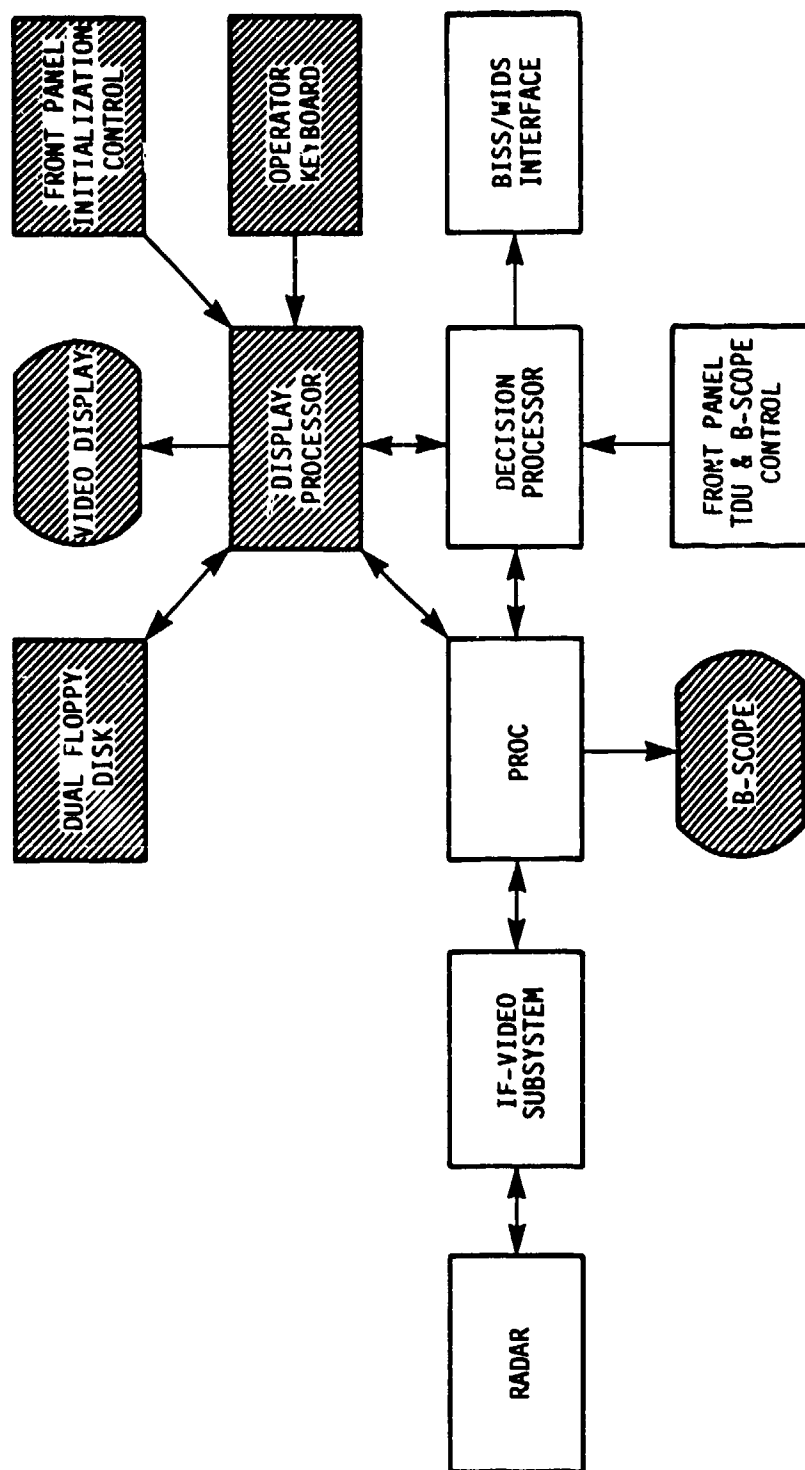


FIGURE 1. BLOCK DIAGRAM OF THE PROTOTYPE TARGET DETECTION UNIT FOR TESTING PURPOSES.

As shown on Figure 1, it has also been determined that during this current phase of development a fourth subsystem should be added to the prototype TDU. This is the display processor subsystem which will display target and tracking information during TDU test operations to aid in system evaluation, and provide an operator interface for the entry of site parameters and the adjustment of TDU parameters during operation. It will also provide mass storage for the system through the use of a floppy disk, and will perform the initialization of programs in the PROC and the decision processor at power-on and whenever algorithms are changed.

The PROC and decision processor functions are being simulated on two minicomputers as an aid in preliminary evaluation of design options and trade-offs prior to field testing. Present schedules call for formal testing of the prototype TDU at the Naval Coastal Systems Laboratory in November 1977, following a series of laboratory and preliminary field tests in the Atlanta area.

Acoustic Interferometer

The use of acoustic interferometry for intruder detection is based on the intruding surfaced or underwater threat interfering with an effectively stationary low-frequency sound pattern within a volume of water. Resulting modifications in the sound pattern can be reliably detected at limited ranges. This technique affords a high level of immunity from environmental problems and false target alarms as compared with high frequency, high resolution acoustic systems. Although not a doppler system, the acoustic interferometer shares a common feature with such systems in that neither yield direct measurements of target range; target location must be inferred from the geometry of reporting sensors.

This device is under development by the National Bureau of Standards, Boulder, Colorado. Early feasibility tests against swimmer targets showed potential for high detection probability at limited ranges using unsophisticated and therefore inexpensive equipment, and also demonstrated that small fish, floating debris, drifting weeds and intense water turbulence did not cause false target problems. Additional quantitative tests have explored effects of variations in carrier frequency, hydrophone and projector placement and target type to determine target strength data, signal spectra, and environmental noise characteristics.

An analytical model has been developed which describes the acoustical field generated and propagated for various test geometries, and provides the ability to assess the relative effectiveness of various system geometries and frequencies. Subsequent modifications to the computer model deal with the interaction of swimmers with the acoustical field and with effects of hydrophone and projector directivity.

The focus has recently been shifted to investigation of wader detection in ultra-shallow water, less than 1.5 meters deep. Results of initial tests were particularly promising. It appeared that the signals generated by waders resulted from the making and breaking of foot contact with the bottom rather than from motion through the water. On foot contact with the bottom, a broadband impulse occurs in the receiver output, with significant energy at much higher frequencies than is the case for swimmers. Signal processing based on temporal and spectral analysis of output signals offered promise of target classification as well as detection, with common system elements being usable for swimmers or waders. Field tests have supported these expectations, and yielded wader target signature data for quantitative analysis of spectral content.

The signal processing approach which has been implemented at present is as follows. After undergoing preprocessing functions, the receiver output enters a set of six bandpass filters. Four of the six outputs are combined to determine a measure of the slope of the spectrum. The slope measure is averaged with both long and short time constants and the results differenced to adaptively provide "noise" and "signal" outputs. A low, middle, and high frequency band is each separately averaged and differenced in the same fashion. The outputs of this process are then combined according to a set of decision rules to determine whether specified alarm criteria have been met. This scheme has been tested in the field recently, but results are not available as of this writing.

The anticipated application of the acoustic interferometer is in line or barrier configurations. As shown in Figure 2, a single projector will serve with several receivers. Present indications are that detection ranges (i.e., range from receiver) will be significantly less than previous sonar systems. In line configuration this rather small detection range converts to relatively good resolution for location. Thus, there are tradeoffs among detection range, location resolution and cost per meter of perimeter protected.

Upward-Looking Doppler Sonar and Bistatic Doppler Sonar

These two sensors, which are under development by the Applied Research Laboratories of the University of Texas at Austin, are discussed together due to the commonality of many of their features. Each of them is being designed for use in barrier line applications where the length of the line may be increased or decreased by adding or eliminating sensor units.

The upward-looking Doppler sonar is a bottom-mounted device intended for use in deeper water. Since the beam transmitted by this sonar is directed upwards from the bottom, the angle at which the acoustic energy insonifies the water tends to minimize the effects of vertical sound velocity gradients. Both the projector and receiver arrays are mounted on the same bracket. The projector is a potted, twelve ceramic stave,

curved face array designed to provide continuous transmission of sound at a frequency of a few hundred kHz. The 3dB beamwidth is approximately 60° in a plane parallel to the barrier line and approximately 10° in a plane perpendicular to the barrier line. The receiving array is identical in construction to the projector. A conceptual diagram of the coverage provided by two adjacent units is shown as Figure 3.

The bistatic Doppler sonar is a horizontal-beam device intended for use in shallower water. As implied by its name, its receiver and projector are physically independent and are separated by a selected distance. The bistatic configuration is particularly advantageous in regard to reducing the effects of surface reverberation since the transducers are spaced such that no surface area is insonified at a high grazing angle and short range is common to both the receiving and projecting arrays. As for the upward-looking sonar, the projector for the bistatic device provides continuous transmission of sound into the beam. The projector and receiving arrays in use at present are potted, 22 ceramic stave, curved face arrays designed to include about 48° of sector coverage. The vertical beamwidth is 6° for both the projector and receiver arrays. It is expected that the horizontal beamwidth will ultimately be substantially wider than at present in order to increase the volume of water common to both projector and receiver beams. However, the optimum choice is a function of noise parameters as well as coverage and will be determined by future trade-off studies. As a tool for use in such studies, a Doppler sonar surface reverberation model has been developed. Given the locations and orientations of the projector and receiver and their measured beam patterns, together with information on wind velocity and surface wave height, the model predicts the peak value, shift, and spread of Doppler noise and the relative strengths of contributions from the surface elements of interest. A conceptual diagram of the volume coverage afforded by a single unit of this device is shown in Figure 4.

Signal processing is accomplished in very similar ways in the two sonar sensors. Automatic gain control (AGC) voltage output is used for long-term background noise averaging, thus providing a measurement of environment that can be monitored. This voltage is also used internally to control the voltage-controlled gain amplifier input stage, thus dynamically providing an appropriate signal-to-noise ratio. The current Doppler sideband separator implementation generates the up-Doppler and down-Doppler information on separate channels. A scheme to offset the internal reference frequency is being considered, allowing both up-Doppler and down-Doppler information to be extracted in a single zero-referenced frequency spectrum output, using only one set of comb filters. Ten or more comb filters are used to break up the broad input spectrum prior to signal processing. By either time-sharing or equipment duplication, both sidebands are then processed.

Outputs from the processor to the alarm logic circuitry include the average

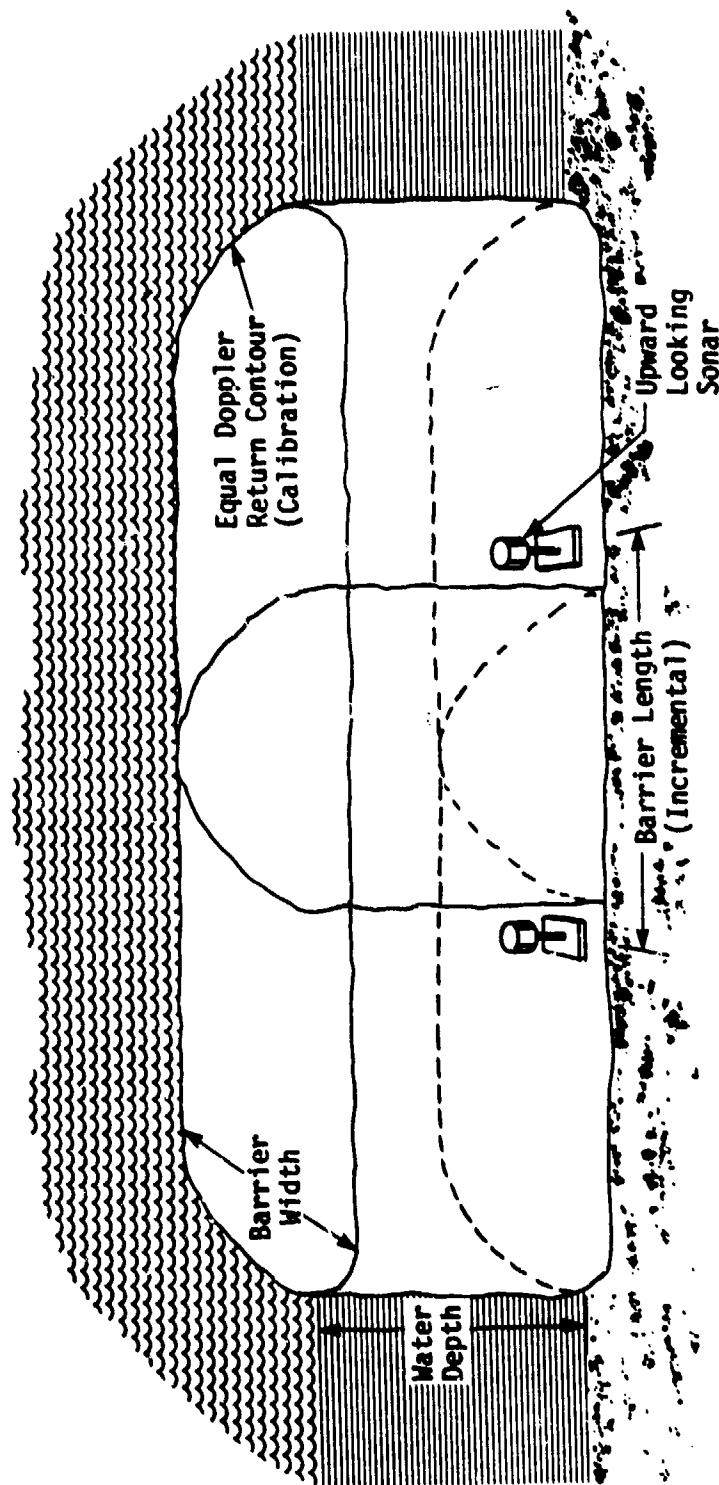


FIGURE 3. UPWARD-LOOKING DOPPLER SONAR VOLUME COVERAGE.

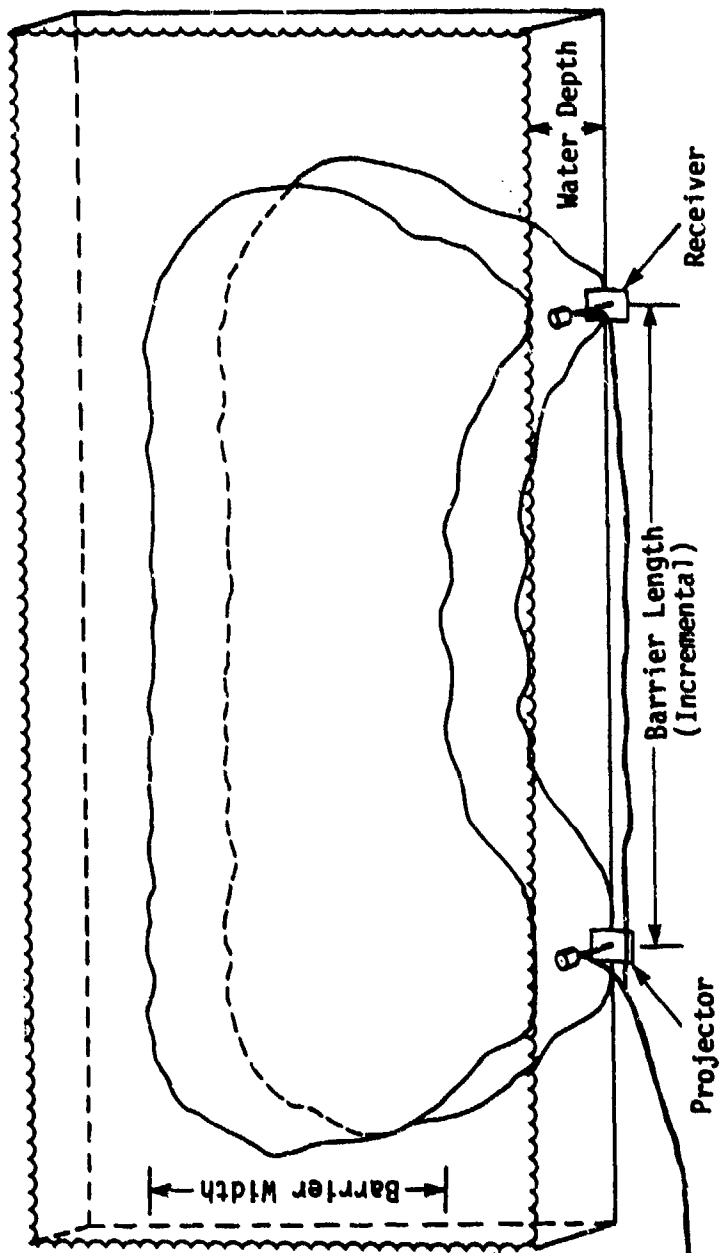


FIGURE 4. BISTATIC DOPPLER SONAR VOLUME COVERAGE.

AGC voltage over the entire input spectrum, and a difference of the long term and short term amplitudes and slopes for the frequency interval from each comb. Use of threshold, spectrum slope, or FM detection schemes in the logic trigger the detection alarm. Procedures developed by ADAPT Service Corporation for optimal data space transformations followed by application of techniques such as the Fisher discriminant are being evaluated for use in the alarm logic. The possibility of sending some non-stored data on for more elaborate alarm verification processing after an initial alarm is also being examined.

DETECTION OF TERRORIST EXPLOSIVES IN LUGGAGE AND MAIL
by J. ROLAND GONANO
US ARMY MOBILITY EQUIPMENT R&D COMMAND, FORT BELVOIR, VA 22060

Terrorists and disgruntled individuals have found that they can inflict damage, death and panic at little risk or cost to themselves by the use of explosives. For example, bombs can be mailed to an unsuspecting recipient or they can be concealed and carried by the bomber or an innocent victim (as luggage on aircraft or packages carried into a nuclear reactor). In this paper we consider detection systems which can be used at strategic check points to counter this type of threat. We attempt to identify and describe the most promising techniques now being developed. We do not consider weapons detection, identification of explosives for forensic purposes, search of building areas for bombs, or tagging to aid detection, each of which is a separate and complex subject.

The designer of detectors may identify three major scenarios: (1) Letters are small, composed mostly of paper and must often be handled in large numbers. In a letter bomb only plastic explosives can be used and these almost always are based on the compounds RDX or PETN or mixtures of them. The mass of explosive is comparable to the mass of innocent letters. (2) Luggage, such as that carried or checked on board aircraft, is fairly large and quite diverse. The present airport inspection systems are directed against weapons carried on the person or in carry-on luggage. They are relatively ineffective against explosives, and practically no inspection is provided for checked luggage. C-4 type plastic explosives, dynamite and sensitized ammonium nitrate mixtures constitute the major threat. In general, different techniques are required for pipe bombs. A bomb need not occupy a large part of the mass or volume of the luggage. Since the owner accompanies the luggage, deterrence value of detection is great and a certain number of false alarms may be tolerable since the owner can open suspect luggage for manual inspection. A closely related problem is the inspection of items carried by workers into sensitive areas such as nuclear reactors. (3) Parcel Post and air cargo include extremely inhomogeneous streams of packages, whose contents may interfere with detection or be damaged by a detector. Since items are separated from their owners, false alarms would cause major disruption. Any type of explosive can be used, but the major threats are the same as for luggage. The explosive may comprise a small fraction of the package. This group represents an extremely difficult problem.

In selecting and using a detection or deterrence technique, the following considerations must be addressed: Cost of an inspection system, both direct and indirect, must be justified by the level of perceived threat. The installation of some sort of system (whether or not effective) may be required by political pressure to "do something". System effectiveness may result as much from psychological deterrence as from objective ability

to detect bombs (as shown by the anti-hijacking effectiveness of the present airport weapon detection systems).

For any given detection technique, the tradeoff between detection probability (effectiveness) and false alarm rate (indirect cost) can be changed simply by adjusting the alarm threshold level. This is an important policy decision which should not be delegated to the operator or serviceman as appears to happen frequently.

Since no single technique provides perfect detection without false alarms, in a practical security system various detectors must be used together, and the way they are used determines their usefulness. In some cases, a single measurement is adequate for the primary detector. In other systems several measurements (individually not definitive) are made and the results are automatically compared to an alarm profile. In any case an alternate technique must be available to investigate the inevitable false alarms.

Detection techniques may be classified by whether they detect the presence of the explosive directly, the presence of vapor escaping from the explosive, or the presence of associated components (such as containment or detonator). In principle, direct detection is preferable since the other methods may produce false alarms or be defeated by a clever bomber. However detection of associated components (eg, metal) may be easier and faster, and detecting presence of escaping vapor may be more practical for large packages. This paper discusses the basic principles of some of the most promising techniques now being investigated for direct in situ detection and vapor detection of explosives. It does not discuss detection of associated components by methods such as metal detectors or X-ray imaging.

DETECTION OF EXPLOSIVE CONTENTS

The explosive contents of a bomb may be detected by techniques which recognize unusual atomic or molecular components. The false alarm rate is lowest for those techniques which respond to unique properties of explosive molecules.

Detection of means of Nuclear Resonance. Explosives can be detected by means of nuclear magnetic resonance (NMR) of their hydrogen content. This technique provides one of the most unique signatures for detecting explosives in situ. In the presence of a constant external magnetic field, the hydrogen nuclei present in all common explosives can resonantly absorb and re-emit pulses of radio frequency energy. The resonant frequency is proportional to the applied field; a common

operating condition is 600 Gauss and 2.5 MHz. The suspect item is exposed to a constant field, then exposed to pulsed rf energy at the corresponding resonance frequency. A small proportion of that energy is absorbed and reemitted by hydrogen atoms. The readiated signal is picked up in a coil and amplified, then analyzed to discriminate between signal due to explosive and that due to hydrogen contained in plastics, water and other innocent materials. This discrimination can be made very effectively for RDX and TNT within one second and for ammonium nitrate within about two seconds; detection of PETN requires ten to twenty seconds.

Experimental models of NMR mail bomb detectors, the most recent with an active volume of 1 X 6 X 6 inches, have been tested. About one ounce of plasticised RDX (C-4) can be reliably detected. Inspection for PETN is much less rapid since twenty seconds is required to detect three ounces. An experimental model of a luggage inspection system, with an opening 14 X 24 inches and active area about 12 inches long, has also been tested. In this volume reliable detection has been demonstrated for about one-and one-half pounds of C-4 (plasticised RDX), three pounds of dynamite or three pounds of ammonium nitrate water gel. Pipe bombs must be detected by other systems. In a test against fifty bags packed as if for travel and tested both with and without explosive simulants, the only incorrect indications arose from ten bags which contained certain unusual metal items which were excited to vibration by the radio frequency field. Presence of such effects is always detectable, and improved signal processing can overcome the difficulty in a large percentage of cases.

The magnetic fields required for NMR can sometimes erase information stored on magnetic tapes, but do not damage the tape itself. Studies have shown that the currents induced in electric blasting caps are very small and are quite safe.

In summary, NMR is an effective way to obtain a unique signal from most explosives. It has been shown that NMR can be used to detect letter bombs, but with marginal performance against PETN explosive. For inspecting checked aircraft luggage or items carried into a nuclear reactor area NMR detection is considered one of the leading candidate techniques, providing magnetic tapes can be removed from the stream. For inspecting parcel post or other small cargo items performance would be acceptable if the magnetic tapes could be removed. It is estimated that a hand-loaded mail bomb detector would cost about \$10,000 and a luggage inspection system with conveyor feed would cost about \$50,000.

Development has been performed by Southwest Research Institute, with technical support from MERADCOM and funding from FAA, Department of State and MERADCOM.

Detection by means of Dielectric Measurements. Explosive solids have unusually high dielectric constants at audio and low radio frequency. Therefore there is a significant increase in capacitance when a suspect item containing explosive is placed between two metal plates. A related technique (potentially more reliable but more difficult to implement) relies on the fact that the dielectric loss of a mixture depends much more strongly upon frequency than does the loss of its components separately. For commercial and military explosives a rapid change in loss with frequency occurs in the region 2 to 50 KHz.

A number of innocent items can also cause an increase in capacitance (or conceivably a frequency-dependent loss). These include moisture in paper or other absorbant material, large amounts of metal which reduce the effective gap between plates, and possibly large random arrangements of metal and dielectrics. Addition of a few pounds of explosive to a large suitcase may not affect the capacitance or loss more than random variations between suitcases. Therefore attention has been concentrated on detection of explosives in letters and large flat envelopes such as may contain books. Its effectiveness, along with its low cost and potential high inspection rate, make it the most attractive letter screening technique. However for optimum results capacitance should probably be coupled with other measurements as suggested below.

The following results were obtained in tests against 10,000 letters and flats coming in through the Georgetown University Post Office. With capacitance threshold set to detect about one ounce of C-4 or PETN sheet (a small letter bomb), 0.8% false alarms occurred. If alarm was based either on capacitance per unit weight or on capacitance plus metal content (as for a detonator), no false alarms occurred for the 10,000 letters. Two important attributes of this technique are its low cost and high speed. The capacitance measuring system alone could be produced commercially for a few thousand dollars, and the capacitance plus metal system for twice as much. This cost estimate does not include a mail transport system. Throughput could easily match the 500 piece per minute rate of automatic mail handling lines.

This techniques was developed by the Physics Department of Georgetown University with University funds and support from the State Department (via MERADCOM), Postal Service, and US Information Agency.

Gamma- or X - Ray and Neutron Transmission

The chemical makeup of explosives is rather different from that of common letter contents. Both hydrogen content and the average atomic number of explosives are lower than those of ordinary papers. The hydrogen content of explosives also is lower than that of most plastics. The hydrogen content may be measured by neutron transmission and the average atomic number may be determined from gamma- or X ray transmission at two different energies. These principles have been applied in a mail bomb detector designed to inspect 500 letters per minute, consistent with speeds of an automatic transport system.

Approximately 0.7% false alarms occurred in a test against approximately 10,000 first-class letters. When the suspect letters rejected the first time were passed again through the detector only 0.16% remained as false alarms. This difference is due to the fact that counting statistics are imperfect and there is some "noise" in the measurements. Bundles of photographs in an envelope were the only consistent cause of false alarms. In this test, the alarm criteria were adjusted so as to detect "almost all" letter bombs containing one ounce or more of explosive.

In analyzing these results, it appeared that useful discrimination was based only on the gamma-or X ray transmission at two energies. The neutron measurements did not affect the determination for any letters, although the neutron measurements account for much of the cost, weight, and complexity of the system.

This method has been demonstrated in working systems with integrated rapid mail transport systems. However it is expensive, complex, and requires license because of radioactive sources. Its false alarm rate is inconveniently high for large volumes of mail. The estimated cost in small commercial quantities is \$150,000; elimination of the neutron subsystem would reduce the price to one third of this without severely degrading performance.

The system was developed by the IRT Corporation with US Postal Service and Internal Revenue Service support. The tests cited above were performed at MERADCOM. Systems are presently installed at the California State Franchise Board and the US Department of State mail room.

Detection by Means of Escaping Vapor

Detection of vapors escaping from explosives has seemed a simple foolproof technique. It is most attractive to the user, because inspections can be made without damaging packages or harming people. Only recently have serious attempts been made to determine exactly which vapors are emitted, what concentrations are present outside packaging material, and what kinds and quantities of interfering vapors normally present. Although a significant amount of uncertainty and conflict exists in this field, some facts are becoming clear: Conventional nitroglycerine dynamites have relatively large amounts of unique vapors available from nitroglycerine (NG) and especially from ethylene glycol dinitrate (EGDN) (commercial NG usually contains a significant amount of EGDN). Equilibrium concentrations of EGDN over commercial dynamite are between thirty and one hundred molecules of EGDN per million molecules of air. Concentration of NG is less well established, but is approximately one-hundredth as great. These concentrations are greatly attenuated by packaging; the EGDN concentration outside a suitcase may range from far below one part per billion up to one part per million depending on details of containment. A suitcase may be exposed to reduced pressure, thus extracting some vapor from inside and increasing the vapor concentration inside the sample chamber by a factor of ten to one hundred, at significant cost in cycle time. It is suggested that a detection threshold of one part per billion EGDN would be useful in practice. These estimates overlap the limits of sensitivity of some detectors described below. However, most other explosives, such as sensitized ammonium nitrate water gels and military explosives, have much lower vapor pressures and their vapors are more strongly adsorbed on packaging materials. At the present or near-future state of the art, vapor detectors will in practice usually be dynamite detectors only. In itself dynamite detection is useful function, and it results in a significant psychological deterrent to all bombing. It appears that the importance of dynamite will rapidly decline over the next few years because of competition from the less expensive water gels.

False alarms are a severe problem with vapor detection under practical field conditions. Many vapors are present in crowded locations, and especially in airports, which resemble explosive vapors but are present in much higher concentrations. Therefore selectivity is needed in a detector, but this conflicts with the requirement for high sensitivity and rapid operation.

Vapor Detection by Means of Electron Capture Techniques. Vapors emitted from explosives generally contain highly polar molecules which capture free electrons. By trapping electrons, these vapors reduce current maintained between two electrodes. Since oxygen also traps electrons, electron-capture detectors cannot operate in the presence of atmospheric oxygen and two important methods have been used to separate explosive vapors from the atmosphere. Selective membranes, which are much more permeable to explosive vapors than to oxygen, can be installed in the inlet system and thus provide the required separation. However membranes also reduce the number of vapor molecules entering the detector. An alternative separation technique relies on the fact that vapors of interest selectively adsorb on noble metals such as Gold and Platinum. By exposing an adsorber to the atmosphere where it traps vapor, evacuating it to remove oxygen, and then heating it to drive off adsorbed vapors, the vapors can be separated from the atmosphere. This latter system has potentially great sensitivity but a slow cycle time. The adsorption also tends to concentrate explosive vapors relative to interferants.

Gas chromatography is an analytical technique often used with electron capture detectors to separate potential interferants from vapors of interest. Different vapors have different tendencies to adsorb and be released from surfaces. If a mixture of vapors is passed down a fine tube, especially a tube with properly treated walls, different vapors tend to be delayed for differing time intervals depending on this tendency to adsorb on the walls. If a sample of air is passed down a tube, the explosive vapors exit at a characteristic time different from that for various interferants. An electron capture detector can be made relatively specific by monitoring electron current at the proper time interval after introducing the sample into a gas chromatograph. However this introduces a delay, usually of several seconds, in response of the detector.

Most commercial vapor detectors available today use some combination of an electron capture detector with a membrane or adsorption system to separate the vapors of interest from atmospheric oxygen. Some use a gas chromatograph for additional specificity. For optimum performance, it is important to select the proper configuration for a given detection problem. A discussion of commercial detectors has been presented by Aerospace Corporation for LEAA¹ and by the Institute for Defense Analyses for FAA².

Vapor Detection by Means of Plasma Chromatography. Plasma chromatography is also called ion mobility spectroscopy. The vapors are ionized by various means. An electric field is suddenly applied to accelerate the ions toward a collector. The arrival time of a given type of ions depends on its average speed or mobility, which depends on mass, charge and other factors. The plasma chromatograph therefore can respond quite specifically to a vapor of interest in the presence of interferants.

Since it operates at atmospheric pressure, interface problems are reduced and sensitivity is probably greater than any other physicochemical method.

To date most study of the plasma chromatograph has been directed toward military explosives (especially TNT) rather than EGDN; design and operating conditions would have to be optimized differently for EGDN. The plasma chromatograph is presently a heavy expensive laboratory instrument which has not been adapted for field use. Much work remains to develop an optimized system. The techniques has been developed for explosives detection by Franklin GNO, now PCP Incorporated, with support and also in-house work by USAMERADCOM and USALWL. Army support has not been continued. Basic research has also been performed at several academic laboratories.

Vapor Detection by Means of Mass Spectrometry. Molecules can be identified quite specifically by means of mass spectrometry. Molecules are ionized, for example by capture of an electron from a hot filament or a radioactive source. They are then accelerated by an electric field and steered by electric and/or magnetic fields. Those having a specific ratio of charge-to-mass strike a collector, where the ion current (which is proportional to the concentration of ions of interest) is measured. Mass spectrometers are commercially available and widely used for analysis and detection of specific compounds. However only limited effort has been applied to optimizing mass spectrometer systems for explosives detection or to studying interferants.

It has been suggested that, if no unexpected problems arise, detection of one molecule in 10^{11} should be achievable. The cost is expected to be quite high, but is difficult to estimate since an optimum configuration is not yet defined. However the technique should be further investigated.

Vapor Detection by Means of Enzymes. Enzymes are complex organic chemicals which act to catalyze (or speed) chemical reactions. Each enzyme catalyzes a specific reaction, and so an enzyme can be used for analysis or detection of a particular compound in the presence of interferants.

An enzyme has been isolated which catalyzes breakdown of trinitrotoluence (TNT), and this TNT reaction has been coupled to a second reaction which results in emission of light. The presence of TNT results in a reduction of light output, which is detected by means of a photomultiplier system.

The reactions occur in a water solution, but TNT vapor can be transferred from air to solution by bubbling the air through the solution. The sensitivity to airborne vapors is estimated to be about one part in 10^{13} . To date only TNT has been detected but it appears that an enzyme could be isolated for detection of EGDN. This system should be (in theory) extremely specific to detection of the desired vapor, but all the subtle effects of interferants have not been explored. A major difficulty is

that the detection reaction presently requires at least ten seconds, and no major reduction is predicted.

This technique has been developed by Beckman Instruments with support from MERADCOM.

Summary

For inspection at a checkpoint (mail, checked airline luggage, and installation security) a detection system can find the explosive in situ, or by means of escaping vapors, or it can detect other suspicious items. At some risk of being proved wrong by subsequent developments, we try to identify most promising methods.

Several varieties of electron-capture vapor detectors have been receiving considerable public attention, since they are commercially well-developed. Under practical conditions these systems are most useful as dynamite (EGDN) detectors. However the importance of conventional dynamite is decreasing, and there is some question whether any vapor detection system in the foreseeable future can reliably detect other types of explosives under practical conditions. However vapor detectors are the only practical approach for large bulky cargo or sensitive items, or for detecting explosives on personnel.

For detecting explosives in situ, the nature of the target influences the choice of technique. For letters and flats where a limited range of contents is encountered the capacitance measuring system is most promising. It can be adapted to low cost low volume or higher cost (and better performance) high volume systems. For applications such as aircraft or nuclear reactor security (luggage and other hand-carried items) where a wider variety of items is encountered, nuclear magnetic resonance promises to be effective.

Detection of suspicious components appears least attractive in principle but is occasionally necessary. For example it appears that pipe bombs may reliably be detected by a two-energy X- or gamma-ray system. Although it is not well suited to identifying explosives, an X-ray viewer is quite useful for inspecting items which cause false alarms generated by other systems, and this method may be the only one applicable for inspecting certain targets.

Unfortunately development and evaluation is widely dispersed among different agencies, and communication is limited. There are no simple answers to this problem, and it is difficult for the outsider to gain full access to the information which is available. Summary reports such as those by Aerospace¹, by IDA² and this report have been prepared to help fill this void.

References

1. "Reassessment Survey Report on Explosives Detection and Identification Techniques" (ATR 77(7911-04)-1, Contract J-LEAA-025-73) The Aerospace Corporation, Washington, DC (1977)
2. "Protection of Airports against Explosives" (IDA Paper P-1057 Contract DOT-FA76WA-3813) Institute for Defense Analyses, Arlington, VA (1976).

HIGH-RESOLUTION SEISMIC DETECTION OF SHALLOW TUNNELS IN ROCK

by

T. E. Owen
G.T. Darilek
Southwest Research Institute
San Antonio, Texas

Supported by

U.S. Army Mobility Equipment
Research and Development Command
Contract DAAG53-76-C-0160

I. INTRODUCTION

An expedient series of field tests was recently conducted to evaluate surface seismic exploration techniques applicable to the problem of shallow tunnel detection in rock materials. These efforts were part of short-term activities undertaken by MERADCOM to achieve early detection of subversive man-made tunnels of military interest.

The seismic technology applied in these tests included specific equipment, field procedures, and data processing methods capable of yielding the highest possible target resolution attainable within conventional seismic exploration practice. That is, in support of the short-term requirement for early tunnel detection, only those techniques and equipment already developed and available from the seismic exploration industry were utilized. In this regard, the adapted methods emphasized the generation and detection of the highest practical seismic frequencies as the necessary requisite for observing the relatively small tunnel targets of interest. Field records were acquired using the unconventional seismic frequency range of 750-2,000 Hz, small explosive charge sources in the range of 1/3 to 5 ounces, and hydrophone seismic detectors emplaced in water-filled holes spaced 1.5 meters apart along the survey traverse. High-resolution digital field recordings were collected on magnetic tape using leased equipment currently available

from seismic instrumentation vendors. Small water-tamped explosive shots and multi-channel reflection records along survey traverses laid out over known underground tunnels provided the field data of interest. Seismic data processing consisting of digital filtering, spatial array filtering, and common depth point (CDP) cross-section displays were used for interpretation of results.

The results of the high-resolution seismic field experiments were sufficient to demonstrate successful detection of both natural caves and man-made tunnels in rock materials. In one case a narrow cave passage 150 feet (46 m) deep in limestone was detected and in another case a small mine adit 100 feet (30 m) deep in granite was detected.

The generally successful results of these tests using readily available seismic exploration equipment and data processing methods imply that similar techniques are potentially applicable to military tunnel detection requirements. In particular, tests utilizing the equipment system and field procedures evolved in the third field test of the recent series of experiments would be practical for military purposes in many field areas.

Also, in the course of conducting these state-of-the-art seismic experiments several innovations in field technique, equipment capabilities, and data processing were uncovered which warrant further investigation and development. These aspects of high-resolution seismic tunnel detection establish the technique more specifically as a long-term developmental method instead of a short-term method ready for operational use. For this reason, recommendations for continuing the investigation of high-resolution seismic surface exploration techniques for tunnel detection place emphasis on extension of the technology beyond the standard equipment and methods available in conventional seismic exploration practice.

II. TUNNEL DETECTION AND RESOLUTION

In contrast with oil-exploration targets, tunnels are essentially one-dimensional localized targets of relatively small size. As a result, tunnel targets have directional orientation aspects which can significantly influence their detectability, and they must be illuminated with short-wavelength seismic energy to produce practical reflections. To advantage, however, in comparison with the physical features which govern the seismic reflections from rock formations, tunnel voids always introduce a large seismic discontinuity in a rock medium. Hence, they produce strong seismic reflections provided that wavelengths comparable with the tunnel diameter are used. Thus, in order for tunnel detection by seismic reflection methods to be generally successful, the field survey must be directed along a traverse which crosses the directional orientation of the tunnel. In addition, the seismic source must be capable of illuminating the tunnel with sufficiently high frequency seismic waves, and the seismic system must be able to detect and record the resultant reflections. To the degree that this can be achieved, methodology developed for seismic reflection exploration for oil can be adapted and applied to the problem of tunnel search and detection.

The theoretical scattering of seismic waves by a circular cylindrical void in a solid medium was formulated by White⁽¹⁾ in connection with theoretical studies of elastic wave scattering and attenuation in polycrystalline materials. This analysis developed theoretical expressions for plane compressional and shear waves arbitrarily incident on an infinite cylindrical discontinuity in a nondissipative isotropic solid medium. The analysis also developed the scattering coefficients for elastic waves which undergo mode conversion whereby incident compressional or shear waves give rise to reflected waves of the opposite type. The results were expressed in terms of generalized scattering cross-sections for solid, fluid-filled, and empty cylindrical discontinuities.

Guided by the work of White, numerical evaluations of the elastic wave scattering cross-sections for cylindrical air cavities in a solid medium were computed by Lewis, Kraft, and Hom⁽²⁾ for several characteristic host materials. In these computed results, three types of normally-

(1) White, R.M., "Elastic Wave Scattering at a Cylindrical Discontinuity in a Solid," J. Acous.Soc.Am., 30:8, pp.771-785, August 1958.

(2) Lewis, T.H., Kraft, D.W., and Hom, N., "Scattering of Elastic Waves by a Cylindrical Cavity in a Solid," J. Appl. Phys., 47:5, pp. 1795-1798, May 1976.

incident waves were considered, viz, compressional waves, shear waves polarized normal to the cylinder axis, and shear waves polarized parallel to the cylinder axis. The results were expressed in terms of normalized scattering cross-sections versus the cylinder diameter expressed in wavelengths of the incident wave. Because of the importance of the scattering cross-section of a tunnel target in determining the seismic wave frequency spectrum required for its detection, selected results from the computations by Lewis, Kraft, and Hom are interpolated and summarized below.

The scattering cross-section of a cylindrical target is defined as the scattered power per unit length along the cylinder divided by the incident wave intensity. This cross-section may be further normalized by the cylinder diameter to yield the various possible seismic wave scattering cross-sections in the dimensionless forms

$$\begin{aligned}
 q_{cc} &= \frac{2}{ka} \left[|(A_0)_c|^2 + 2 \sum_{n=1}^{\infty} |(A_n)_c|^2 \right] \\
 q_{cs} &= \frac{2}{ka} \left[|(B_0)_c|^2 + 2 \sum_{n=1}^{\infty} |(B_n)_c|^2 \right] \\
 q_{sc} &= \frac{2}{ka} \left[|(A_0)_s|^2 + 2 \sum_{n=1}^{\infty} |(A_n)_s|^2 \right] \\
 q_{ss} &= \frac{2}{ka} \left[|(B_0)_s|^2 + 2 \sum_{n=1}^{\infty} |(B_n)_s|^2 \right] \\
 q_{ax} &= \frac{2}{ka} \left[|(C_0)_{ax}|^2 + 2 \sum_{n=1}^{\infty} |(C_n)_{ax}|^2 \right]
 \end{aligned} \tag{1}$$

where:

Subscripts (c,s) indicate the type of incident and reflected waves, respectively;

Subscript ax indicates shear waves polarized parallel to cylinder axis;

(A_n, B_n, C_n) are complex scattered wave coefficients for specific subscripted wave types;

$(k, \kappa) = \frac{2\pi}{\lambda_c}, \frac{2\pi}{\lambda_s}$ = Wave numbers of compressional and shear waves, respectively;

$a = \frac{D}{2}$ = Cylinder radius.

The boundary conditions for normal incidence reflections for the three types of incident waves on a cylindrical cavity are:

$$\begin{aligned} s_1 (A_n)_c - t_1 (B_n)_c &= \sigma_1 \\ s_2 (A_n)_c - t_2 (B_n)_c &= \sigma_2 \\ s_1 (A_n)_s + t_1 (B_n)_s &= \tau_1 \\ s_2 (A_n)_s + t_2 (B_n)_s &= \tau_2 \\ t_3 (C_n)_{sx} &= \tau_3 \end{aligned} \quad (2)$$

where:

$$s_1 = (ka)^2 \left[2 H_n''(ka) - \frac{\lambda}{\mu} H_n(ka) \right]$$

$$s_2 = 2n [ka H_n'(ka) - H_n(ka)]$$

$$t_1 = 2n [\kappa a H_n'(\kappa a) - H_n(\kappa a)]$$

$$t_2 = (\kappa a)^2 [2 H_n''(\kappa a) + H_n(\kappa a)]$$

$$t_3 = (\kappa a)^2 H_n'(\kappa a)$$

$$\sigma_1 = \text{Re}(s_1)$$

$$\sigma_2 = \text{Re}(s_2)$$

$$\tau_1 = \text{Re}(t_1)$$

$$\tau_2 = \text{Re}(t_2)$$

(λ, μ) = Lamé elastic constants;

$H_n(x) = J_n(x) + iN_n(x)$ = Hankel function;

(H'_n, H''_n) = First and second derivatives of Hankel functions, respectively.

For a typical hard-rock seismic medium, the Lamé elastic constants are approximately equal, leading to the descriptive host medium parameter

$$\frac{\kappa}{k} = \frac{v_c}{v_s} = \frac{\sqrt{\frac{\lambda + 2\mu}{\rho}}}{\sqrt{\frac{\mu}{\rho}}} = \sqrt{3} \quad (3)$$

The numerical results presented by Lewis, Kraft, and Hom have been approximately interpolated to obtain values of each of the normalized scattering cross-sections indicated in Equation (1) for a typical rock medium characterized by $\kappa/k = 1.732$. Figure 1 illustrates these cross-sections plotted versus the cylinder diameter expressed in units of incident seismic wavelength, λ_{inc} , applicable to either compressional or shear waves.

For values of $D/\lambda_{inc} \leq 0.16$, the scattering cross-sections are proportional to $(D/\lambda_{inc})^2$, corresponding to the well-known Rayleigh scattering law for small cylinders. For values of $(D/\lambda_{inc}) \leq 1$, the scattering cross-sections appear to reach individual asymptotic values which are essentially independent of frequency. The approximate high-frequency values of normalized scattering cross-section are, for $D/\lambda_{inc} = 1$:

$$\begin{aligned} q_{cc} &= 1.15 \\ q_{cs} &= 0.75 \\ q_{ss} &= 2.85 \\ q_{sc} &= 0.40 \\ q_{sx} &= 1.55 \end{aligned} \quad (4)$$

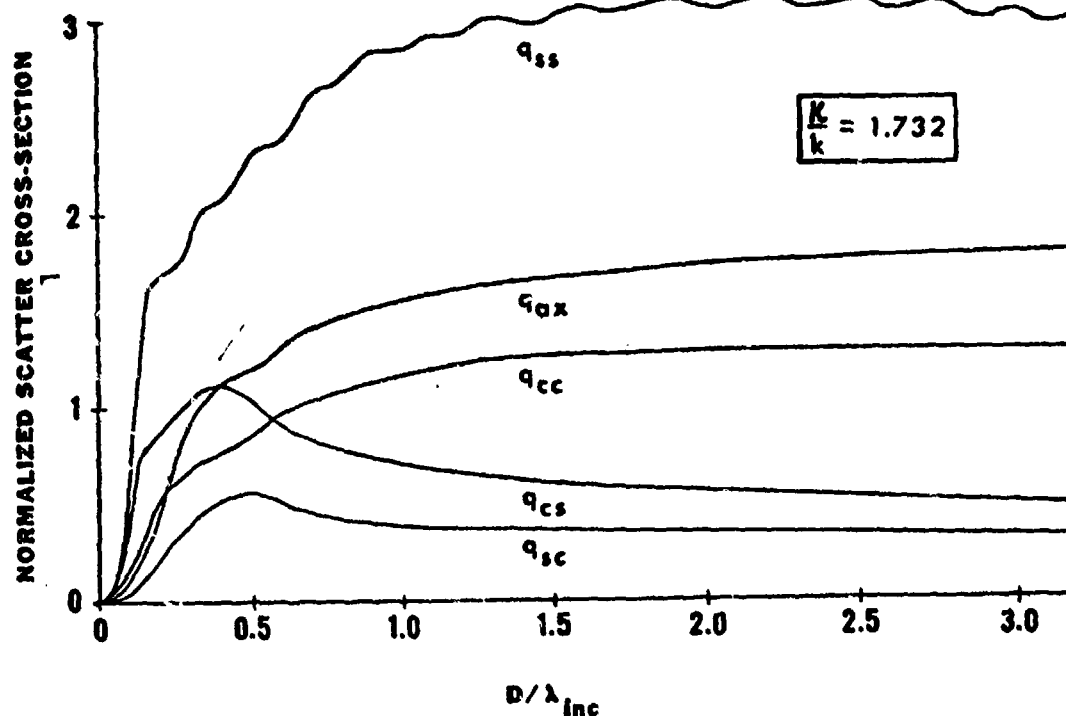


FIGURE 1. NORMALIZED SEISMIC SCATTERING CROSS-SECTIONS OF A CYLINDRICAL CAVITY IN A ROCK MEDIUM

As shown by the curves for q_{cs} and q_{sc} in Figure 1, peak-scattering effects occur at values of D/λ_{inc} of 0.38 and 0.48, respectively, possibly corresponding to some form of natural resonances of the cylindrical cavity target. No such peaks are evident in the non-mode-converting scattering cross-sections.

From the curves shown in Figure 1 and the values given in Equations(4), reliable reflections from a cylindrical target should be obtainable for $\lambda_{inc} \leq 2D$, with the non-mode-converting scattering cross-sections providing the strongest reflected signals. Practical considerations such as frequency-dependent propagation losses in the host rock medium and irregular shapes in the tunnel bore will influence the scattered energy partition finally received at the seismic detectors located at the surface. However, such effects are not estimated to have a

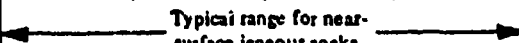
dominating influence on the scattering phenomena if the highest frequency content in the received seismic reflections is in the range corresponding with $D/\lambda_{inc} > 0.6$; that is $f > 0.6 v_{inc}/D$, as roughly interpreted from Figure 1.

From the results of this review of seismic wave scattering from cylindrical cavity targets, reliable reflections from such targets should be obtainable at frequencies given by

$$f_{min} > \frac{v_{inc}}{2D} \quad (5)$$

For typical rock media characterized by the condition $\lambda = \mu$ as stated in Equation (3), this minimum frequency of incident seismic wave energy can be explicitly defined. Table 1 summarizes the minimum seismic reflection frequency for a 2-m diameter tunnel in practical hard-rock formations having compressional wave velocities ranging from 2500 to 5000 m/sec.

TABLE 1. MINIMUM SEISMIC ILLUMINATING FREQUENCY FOR RELIABLE BACKSCATTER REFLECTIONS FROM A 2-METER DIAMETER TUNNEL TARGET

Incident Wave Type	Minimum Illuminating Frequency (Hz)					
	$v_c = 2500$ m/sec $v_s = 1443$ m/sec	3000 m/sec 1732 m/sec	3500 m/sec 2021 m/sec	4000 m/sec 2309 m/sec	4500 m/sec 2598 m/sec	5000 m/sec 3753 m/sec
Compressional	625	750	875	1000	1125	1250
Shear	361	433	505	577	650	738
<div style="text-align: center;">  Typical range for near-surface igneous rocks. </div>						

The minimum frequencies indicated in Table 1 are noted to be considerably higher than those used in conventional seismic exploration applications from the various standpoints of depth penetration, reflector resolution, and the seismic detectors and recording systems used to record the signals in the field. As a consequence, special considerations must be given to the field equipment applied to the tunnel-detection problem to assure that proper high-frequency response is achieved for detecting targets in the size range of 2-m diameter.

The highest frequency seismic signal content required for reliable tunnel detection is somewhat arbitrary since the elastic wave-scattering considerations dictate only that the target be illuminated with sufficiently high frequencies to produce useful reflections. In practice, however, the high-frequency content of the reflected signals should extend to at least twice the lowest reflecting frequency limit in order that the reflected seismic impulse source signals usually used in the seismic survey process will be reasonably bounded in time to facilitate good target depth and size interpretation; i.e., to reduce reflection signal ringing. At such high seismic frequencies, however, frequency-dependent absorption losses in the host rock medium will impose severe attenuation effects at high frequencies. In hard-rock materials, the "typical" attenuation loss which affects the high-frequency content of a propagating seismic signal can be expressed approximately in the form

$$\alpha = Kf^x \quad (6)$$

where:

α = attenuation factor in dB/m;

$K \approx 4 \times 10^{-4}$ for sedimentary rocks;
 1×10^{-4} for igneous rocks;

f = frequency in Hz; and

x = frequency exponent ($x \approx 1$ for both compressional and shear waves).

The associated two-way amplitude transmission and return loss assuming spherical wave propagation and perfect target scattering is expressed by

$$TL = 40 \log_{10} R + 2\alpha R \text{ dB} \quad (7)$$

where:

R = target depth, m.

From Equations (6) and (7), the spectral shading due to frequency-dependent absorption effects is

$$\frac{\Delta(TL)}{\Delta f} = 2KR, \quad (8)$$

hence, the frequency range over which an N-dB shading effect occurs is

$$\Delta f = f_{\text{high}} - f_{\text{low}} = \frac{N}{2KR} \quad (9)$$

Using this result, the upper frequency limit for $N = 20$ dB shading and a low-frequency limit of 500 Hz is, for hard-rock materials,

$$\begin{aligned} f_{\text{high}} &= f_{\text{low}} + \frac{N}{2KR} \\ &= 500 + \frac{1 \times 10^5}{R} \end{aligned} \quad (10)$$

Based on the 20-dB shading criterion, and the constraint that the high-frequency signal spectral content must be at least twice the lowest reflection frequency, the maximum target detection depth in hard rock will be limited to

$$\begin{aligned} R_{\text{max}} &= \frac{N}{2Kf_{\text{low}}} \\ &= \frac{1 \times 10^5}{f_{\text{low}}} \end{aligned} \quad (11)$$

For $f_{\text{low}} = 500$ Hz, the maximum detectable hard-rock tunnel depth is $R_{\text{max}} = 200$ m. For a 100-m deep tunnel in hard rock, the high-frequency signal spectrum limit will be, from Equation (10), $f_{\text{high}} = 1500$ Hz.

For the tunnel-detection application of interest, if the mid-band operating frequency is arbitrarily taken to be 1000 Hz, the approximate sensor spacing for a rock medium having a 3000 m/sec compressional wave velocity is

$$\left(\frac{\lambda_{\text{mid}}}{2} \right)_c = \frac{v_c}{2f_{\text{mid}}} = \frac{3000}{2(1000)} = 1.5 \text{ m (4.9 ft)} \quad (12)$$

If, for practical reasons, this spacing is selected as the minimum distance to be used in the field, it will, of course, be more than adequate if the rock velocity is higher than 3000 m/sec. and less than adequate for slower velocity media. Similar considerations for shear waves make use of the fact that incident shear waves impinging upon a given tunnel target produce useful reflections at somewhat lower seismic frequencies than compressional waves. For a rock medium having a compressional wave velocity of 3000 m/sec. and shear wave velocity of 1732 m/sec., the frequency information in Table 1 implies a mid-band shear wave signal frequency of about 600 Hz and, hence, the sensor spacing for shear wave reflections is

$$\left(\frac{\lambda_m}{2}\right)_c = \frac{1732}{2(600)} = 1.44 \text{ m (4.72 ft)}, \quad (13)$$

a value experimentally consistent with that derived for compressional waves.

Figure 2 illustrates the field layout requirements for the intended seismic reflection survey technique. This sketch shows an irregular surface terrain on which a straight line traverse in the plane of the figure is laid out containing a series of equally-spaced shallow vertical boreholes drilled a short distance into the top of the host rock medium. The shot point for each seismic sounding is offset from the nearest sensor by two or three hole spacings in order to prevent direct-signal overload of this sensor. The receiving sensors are located in consecutively spaced holes along the traverse. In operation, after each shot is fired, the nearest sensor is moved to the far end of the sensor spread, and the next shot is detonated in the next hole along the forward direction of the traverse. This procedure is repeated successively along the traverse whereby, in effect, the sensor array and the shot point with its fixed offset distance relative to the nearest sensor is moved at one-hole increments along the entire traverse length surveyed. A tunnel target oriented in a direction which passes under the traverse line will be detected when that portion of the field data collected along the traverse section lying above the tunnel is later processed and displayed for analysis.

Geodetic information describing the surface terrain and the actual seismic shot points and seismic sensor locations used in the survey is necessary in order to yield good spatial array signal processing. For the case where the survey traverse passes over the tunnel target, as will be required if distinctive target detection is to be achieved, the most important geodetic information is the elevation profile and nominal spacings of the shot point and sensors relative to some horizontal reference datum parallel to the traverse line. If the tolerances on the nominal shot and sensor hole spacings and the straightness of the traverse line comprised by the drilled holes is maintained within about ± 10 percent, the actual geodetic information in these parameters can be neglected. In any case, the geodetic survey accuracy need not exceed a value of about $\pm (1/10) (\lambda_m/2)_c$. For example, in a rock medium having a compressional wave velocity of 3000 m/sec., the geodetic survey accuracy requirement is ± 15 cm (± 6 in.).

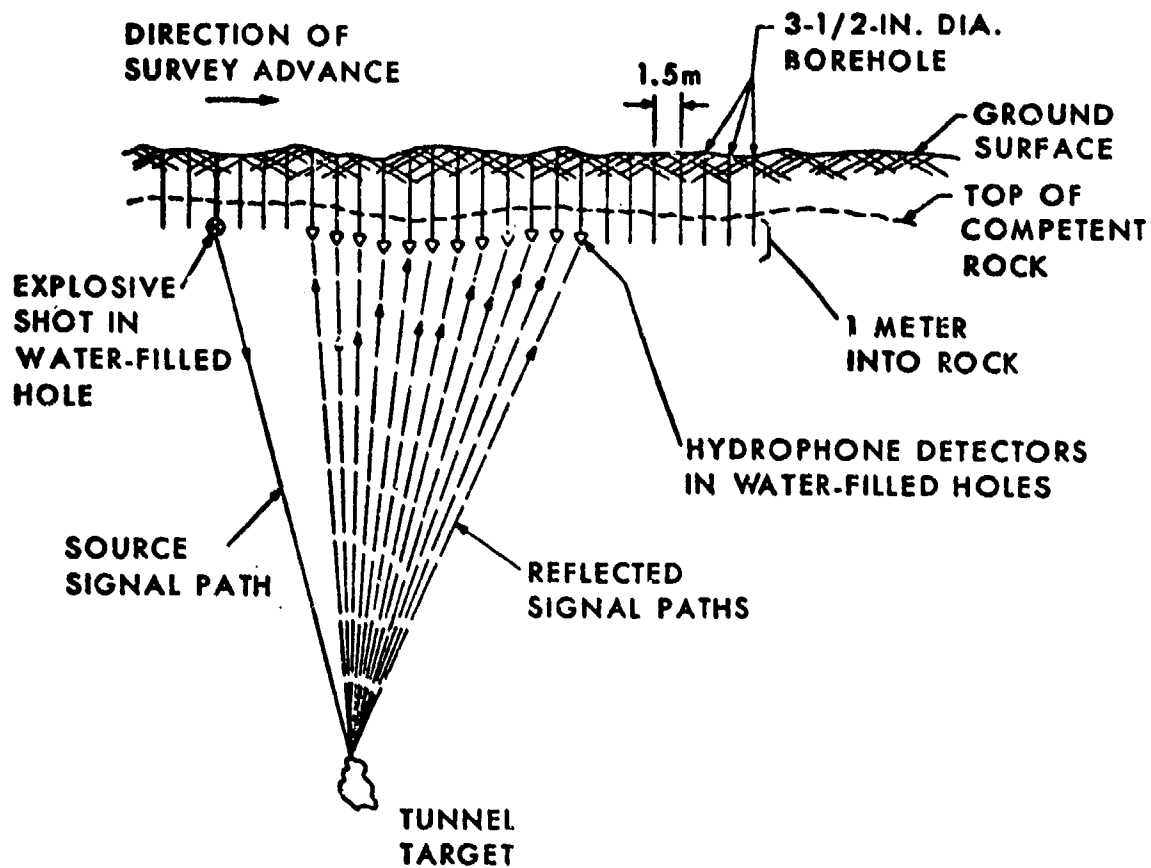


FIGURE 2. FIELD LAYOUT FOR HIGH-RESOLUTION SEISMIC REFLECTION SURVEY FOR TUNNEL DETECTION

III. SEISMIC DATA PROCESSING TECHNIQUES

The geometric shot point and seismic detector field layout illustrated in Figure 2 is a conventional configuration used in oil exploration seismic reflection surveys. Field data recorded with this layout is normally processed using the Common Depth Point (CDP) method of analysis and output display. The redundancy of subsurface reflection data resulting from the overlapping geometric shot-sensor layouts for each sounding yields a form of spatial filtering and synthetic array response when the CDP process is applied. Spatial filtering provided by CDP processing enhances the signal-to-noise ratio of reflections occurring at depth while discriminating against direct "ground roll" surface wave interference. The method operates by "gathering" and averaging all the shot-to-detector signals whose propagation paths are oriented symmetrically about selected vertical lines along which common depth reflections may occur. The assumed vertical line of symmetry between the incident and reflected seismic rays requires the corresponding assumption that the reflecting targets at any depth along the vertical are horizontally oriented strata. In processing oil exploration data, the CDP method emphasizes the response to planar geological structures. Knowledge of the formation velocity(s) can then yield the depth of the reflecting strata. Further, by processing and interpreting the results of more than one such reflection survey traverse over the same geological structures, the three-dimensional orientation of dipping formations can be derived.

In the tunnel-detection case, where reflections are produced by a localized one-dimensional target instead of a two-dimensional layer, the CDP method operates with equal effectiveness in discriminating against the unwanted ground roll signals but produces a non-layer-like target output display pattern and provides only a finite field of view with localized targets. The non-layer-like display pattern characterizing a localized target is an inherent result of the CDP-processing technique and is a hyperbolic curve whose vertex is centered on the surface traverse point located at the closest point of approach to the tunnel. The field-of-view limitation in detecting and displaying tunnel targets is caused by the intrinsic detection limits imposed by high-frequency seismic attenuation in the medium.

Figure 3 illustrates the manner in which the source and reflection rays are gathered for CDP processing. When the seismic detector spread consists of twelve sensors, there are six sensor signals which can be assumed to contain reflections from any common depth point directly below a sensor hole as a result of the source signals produced in the six symmetrically oriented shot holes. Also, from the same six shots, there are six sensor signals which can be assumed to contain reflections

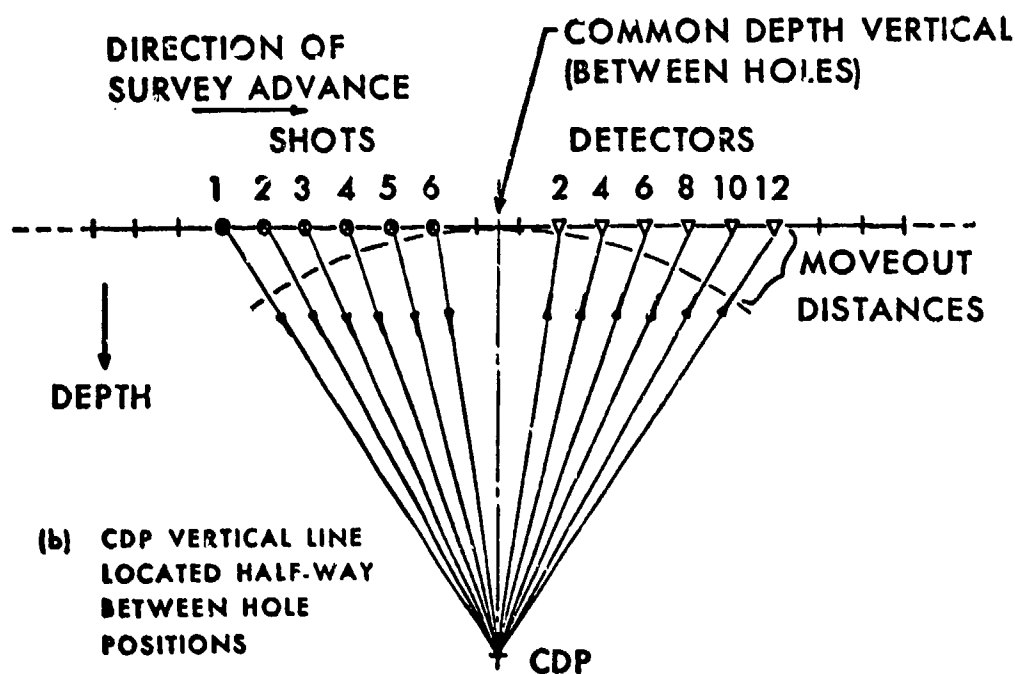
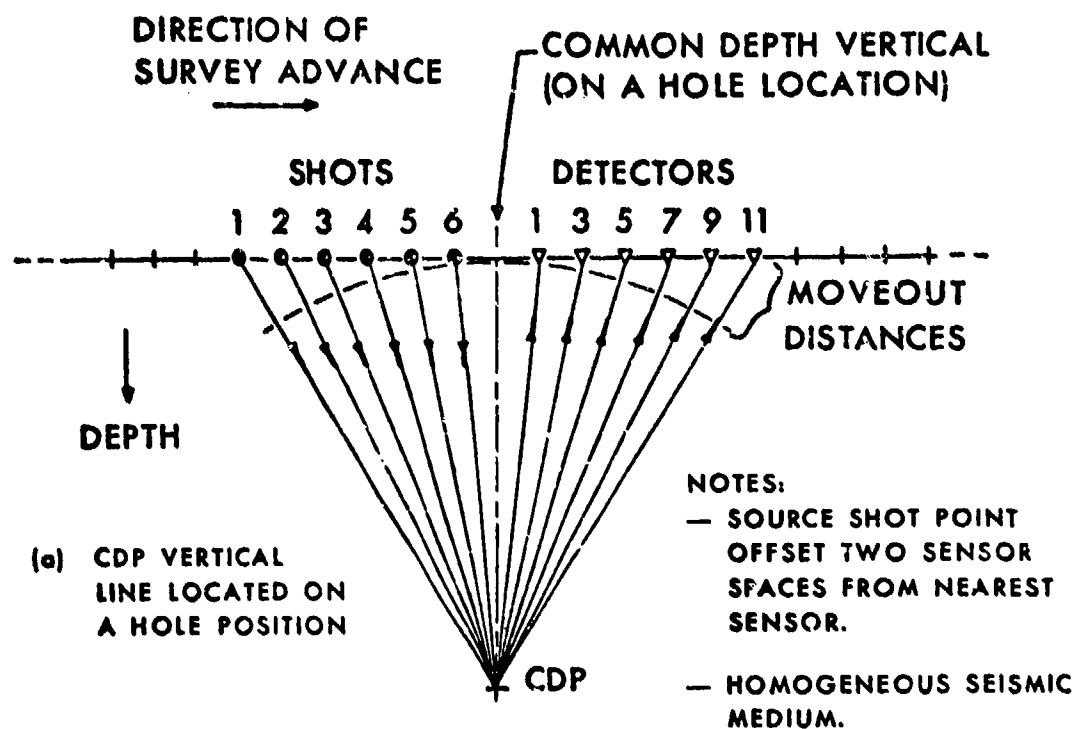


FIGURE 3. COMMON DEPTH POINT GATHERS FOR A 12-SENSOR DETECTION SPREAD AND SIX SUCCESSIVE SHOTS

from any common depth point directly below a location halfway between two sensor holes. Thus, the CDP process permits "six-fold" spatial averaging in a twelve-sensor detector spread along vertical trace lines located directly below the sensor hole locations and directly below locations halfway between the sensor holes. In the general case, CDP processing provides $M/2$ -fold spatial averaging for a detector spread containing M sensors.

Another feature of the CDP process to be noted from the shallow target illustrations of Figure 3 is that, because the up-going reflected rays arriving at the detectors always have a direction component in the forward direction of the survey advance (i.e., the detector array always "looks back" at the CDP), the strongest processed signals will occur after the CDP vertical line crosses a localized target.

The moveout distances shown in Figure 3 are compensated for in each of the six symmetrical source-reflection ray pairs by applying appropriate time shifts equal to the moveout distances divided by the seismic propagation velocity in each channel. These moveout distance corrections also take into account the actual geodetic information defining the spatial positions of the specific shot points and detectors involved. After applying the moveout time shifts (corresponding to the signal timing conditions for which the six gathered sensor records are equivalent to those that would be obtained if the shots and detectors had been located on a circular arc centered on the CDP), the six gathered traces are added to form a single trace segment associated with the response from the particular CDP being processed. Each common depth point on each common depth vertical line in the survey traverse is processed in this manner, resulting in composite CDP time records for each common depth vertical. The signal-to-noise ratio improvement for six-fold spatial averaging in a 12-sensor detector spread is $\sqrt{6}$, provided that the moveout corrections involving geodetic sensor layout data, formation velocity, and assumptions on the homogeneity of the medium are accurate.

The display technique used to present CDP-processed reflection data is one whereby each composite CDP time record trace is plotted rectilinearly with the survey traverse line representing the abscissa and subsurface reflection time (proportional to depth) representing the downward ordinate. Figure 4 illustrates a simplified portrayal of this type of display, including the trace-constructed image of a reflecting subsurface layer and the non-layer "diffraction" pattern typical of a localized target response. This display representation does not illustrate the interference produced by ground roll surface disturbances; however, such direct-arriving surface waves will always be present to some degree in the CDP-processed results and may endure in time long enough to interfere with shallow subsurface reflections of interest.

DIRECTION OF
SURVEY ADVANCE

POSITION OF LOCALIZED
TARGET ALONG TRAVERSE

SENSOR
SPACING

LOCALIZED
TARGET DEPTH
(NOTE STRONGER
RESPONSE TO THE
RIGHT OF TARGET
POSITION)

PLANAR
REFLECTING
TARGET

FIGURE 4. COMMON DEPTH POINT DISPLAY REPRESENTATION
FOR LOCALIZED AND PLANAR TARGETS

IV. TUNNEL DETECTION RESULTS

A. Valdina Farms Sinkhole Site - Field Test No. 1

Valdina Farms Sinkhole is a very narrow and relatively straight limestone solution cavity horizontally oriented at about 150 feet (46 m) deep in the Edwards Limestone near San Antonio, Texas. The surface terrain above this cave is flat and has a residual clay soil about 6 feet (2 m) thick overlying the fine-grained and homogeneous Edwards Limestone rock.

A 330-foot (100 m) seismic survey traverse was laid out crossing the cave at about 45 degrees. Shot and detector holes 4½ inches in diameter and about 8 feet (2.4 m) deep were drilled on 5-foot (1.5 m) centers along this traverse. Figure 5 illustrates this cave and seismic survey layout.

Twelve hydrophone seismic detectors having an emphasized high-frequency acoustic pressure response up to about 1500 Hz were placed in consecutive holes (Stations +150 through +95 as shown in Figure 5) and a 4-ounce charge of C-4 plastic explosive was detonated at a 20-foot (6 m) offset distance (Station +170). The seismic signals were recorded in the field using a Quantum Electronics, Inc. Model DAS-1 12-channel digital recording system having a frequency response of 250-1,000 Hz.

After digitally recording the seismic reflection signals on magnetic tape, the hydrophone at +150 was moved to +90, the second shot detonated at +165, and the reflection signals were recorded. This procedure was repeated, moving along the traverse at one-hole increments, until the entire traverse was surveyed.

The field records from over 30 shots along the traverse were digitally processed using conventional common depth point (CDP) seismic programs available at most seismic exploration firms. The result of this data analysis is shown in Figure 6 wherein the tunnel detection response appears as a hyperbolic "diffraction" pattern resulting from the fact that CDP processing assumes the origin of all reflections to be from horizontal planar subsurface layers.

The target response observed in Figure 6 is verified as a cave reflection corresponding to an incident shear wave which is reradiated and detected as a compressional wave. The experimentally determined compressional wave velocity in the Edwards Limestone is 11,300 ft./sec. (3,450 m/s) and the corresponding shear wave velocity is approximately 6530 ft./sec. (1,990 m/s).

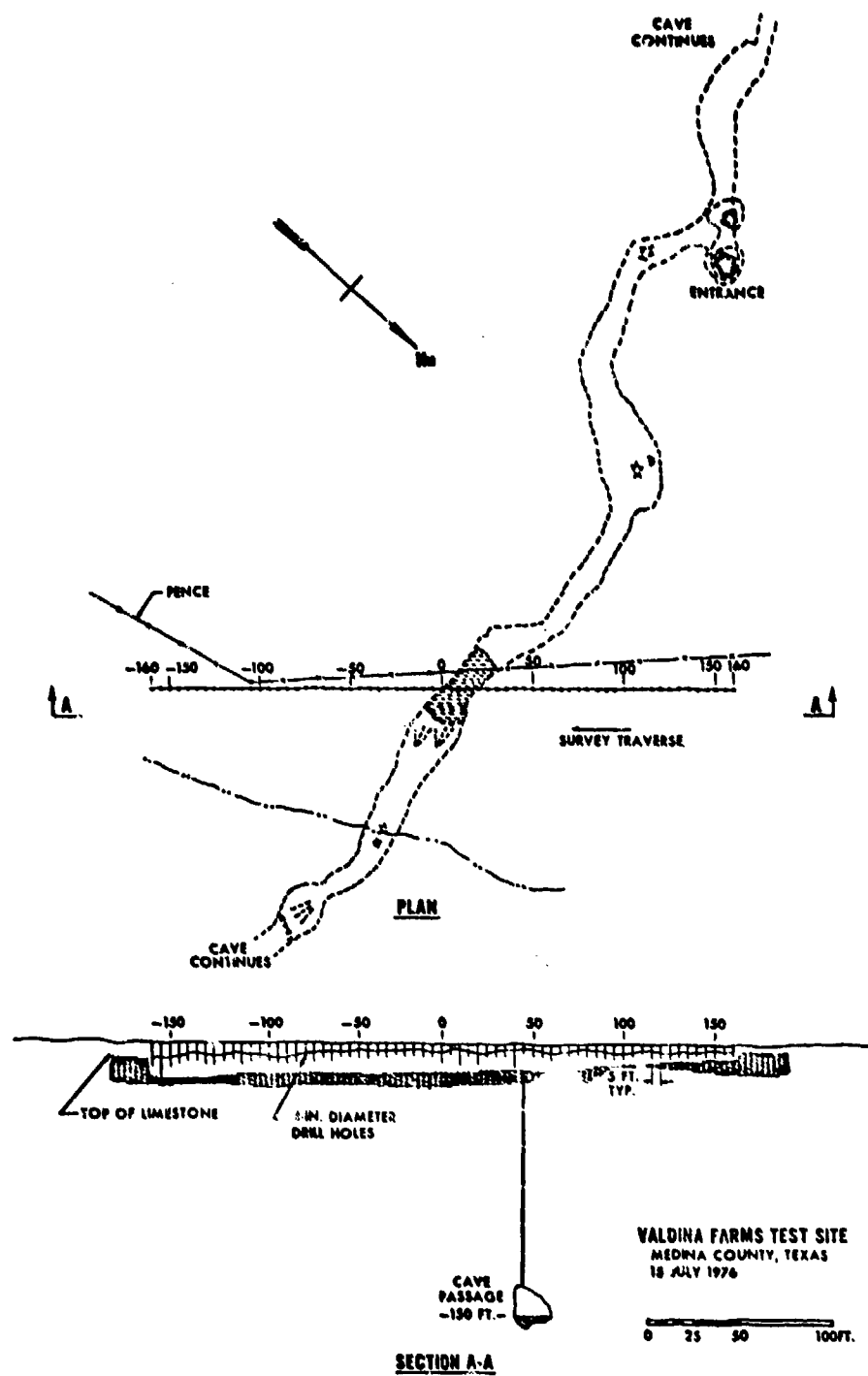


FIGURE 5. VALDINA FARMS TEST SITE

B. Hazel "A" Mine Site - Field Test No. 2

Hazel "A" Mine is an inactive gold mine whose adit is relatively straight and horizontally oriented in mountainous granite rock near Boulder, Colorado. The rock overburden above the adit varies because of the sloping mountain terrain; however, at a location where the mine depth is about 100 feet (30 m) deep, a reasonably flat traverse path exists which crosses the adit at approximately right angles.

A 200-foot (61 m) seismic survey traverse was laid out crossing the mine, and shot and detector boreholes $3\frac{1}{2}$ inches in diameter and about 5 feet (1.5 m) deep were drilled on 5-foot (1.5 m) centers. Figure 7 illustrates this mine and survey traverse layout.

Twelve hydrophone seismic detectors were emplaced in consecutive holes (Stations +70 through +15 as shown in Figure 7). The explosive source used in this survey was comprised of five separate charges installed first in +100 through +80 and weighted in the proportions 1:3:4:3:1 and detonated simultaneously. The unit charge weight used in this source array was $\frac{1}{3}$ ounce resulting in a total source size of 4 ounces. The purpose of the source array was to minimize the direct horizontally propagating interference waves arriving at the detectors by forming a downward source radiation pattern.

After detonating the first 5-element source array and recording the seismic reflection signals, the nearest hydrophone at +70 was moved to +10 and the source array was then loaded and detonated in Stations +95 through +75, representing a one-hole increment advance along the traverse. This procedure was repeated until the entire traverse was surveyed. The seismic signals were recorded on magnetic tape using the Quantum DAS-1 system having a frequency response of 250-1,000 Hz.

Records from 24 source array shots along the traverse were processed using CDP analysis resulting in the output display shown in Figure 8. The weakly evident hyperbolic tunnel reflection indicated in these records corresponds to a mode-converted shear wave reflection based on compressional and shear wave velocities of 9,030 ft./sec. (2,770 m/s) and 5,540 ft./sec. (1,690 m/s), respectively.

C. Hazel "A" Mine Site - Field Test No. 3

Because of the weak tunnel detection at the Hazel "A" Mine resulting largely from the limited high frequency response of the Quantum DAS-1 recording system, a repeat field test was conducted at this site. The repeat test utilized an Input/Output Model DHR-1632 8-channel digital recording system having a frequency response of 750-2,000 Hz operating with fixed gain rather than with automatic

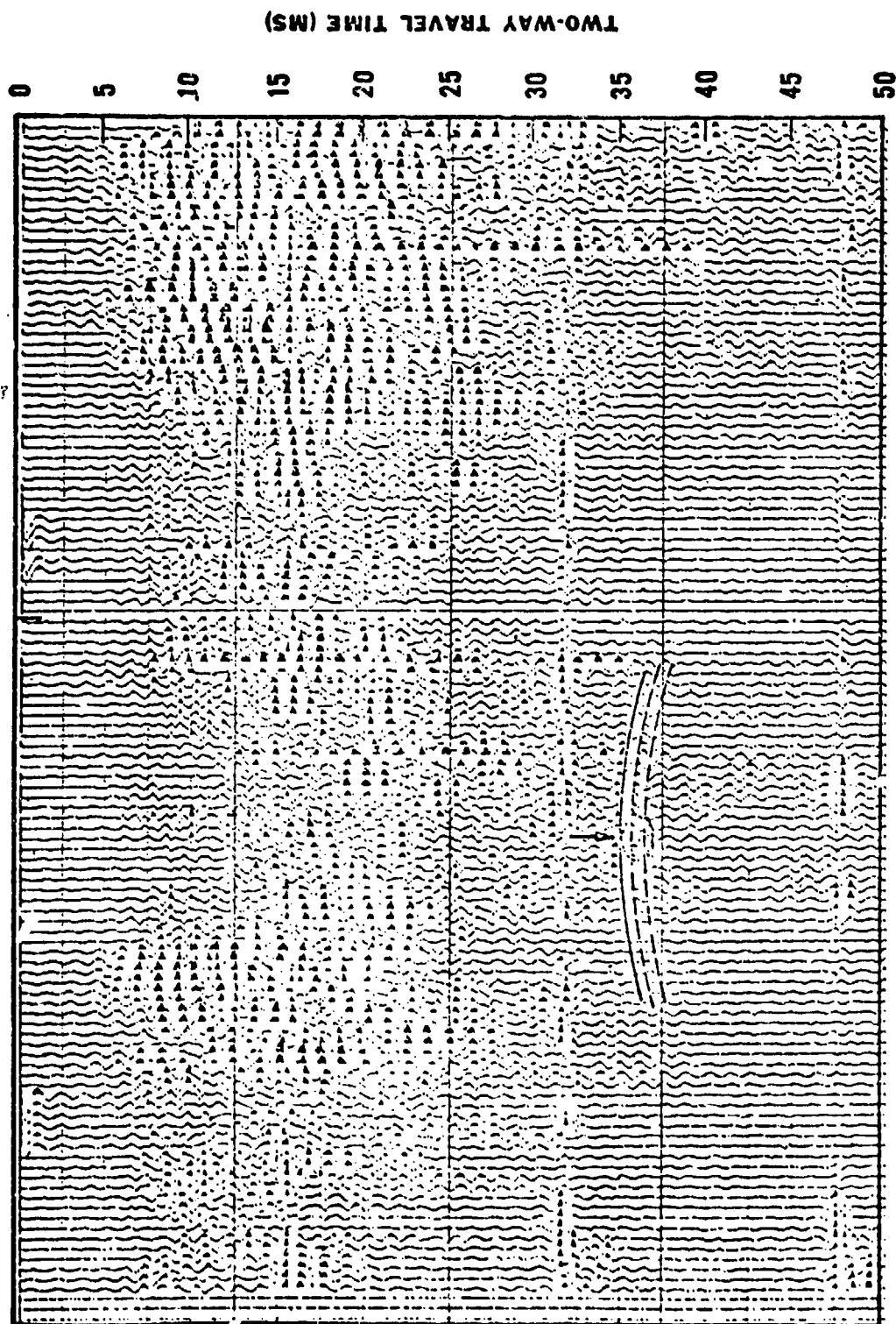
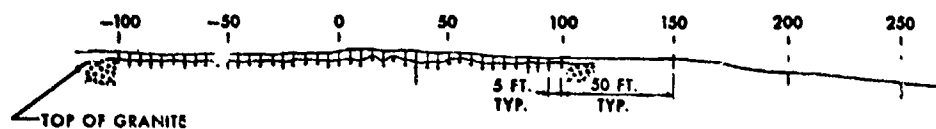
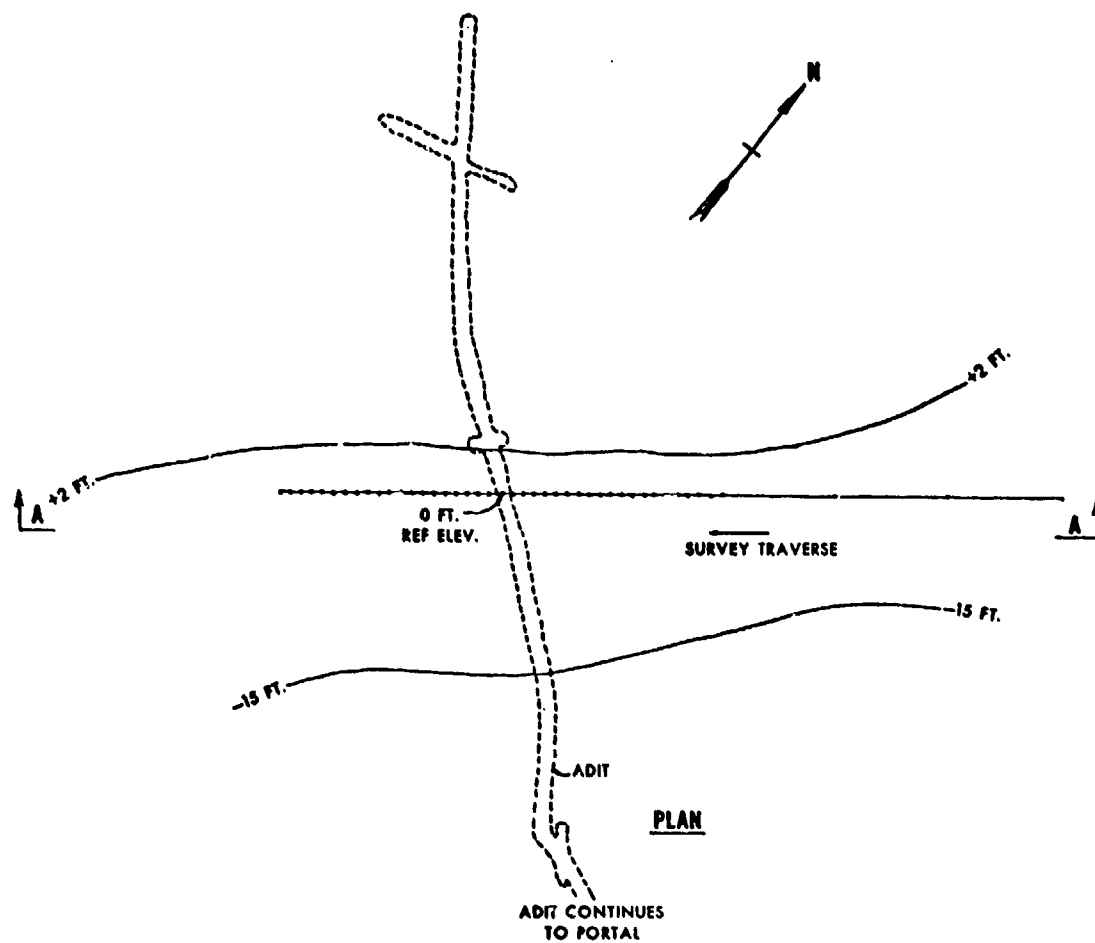


FIGURE 6 -
VALDINA FARMS TEST SITE RESULTS - FIELD TEST NO. 1



-105 FT. ADIT

SECTION A-A

HAZEL "A" MINE TEST SITE
BOULDER COUNTY, COLORADO
10 AUGUST 1976

0 25 50 100 FT.

FIGURE 7
HAZEL "A" MINE TEST SITE

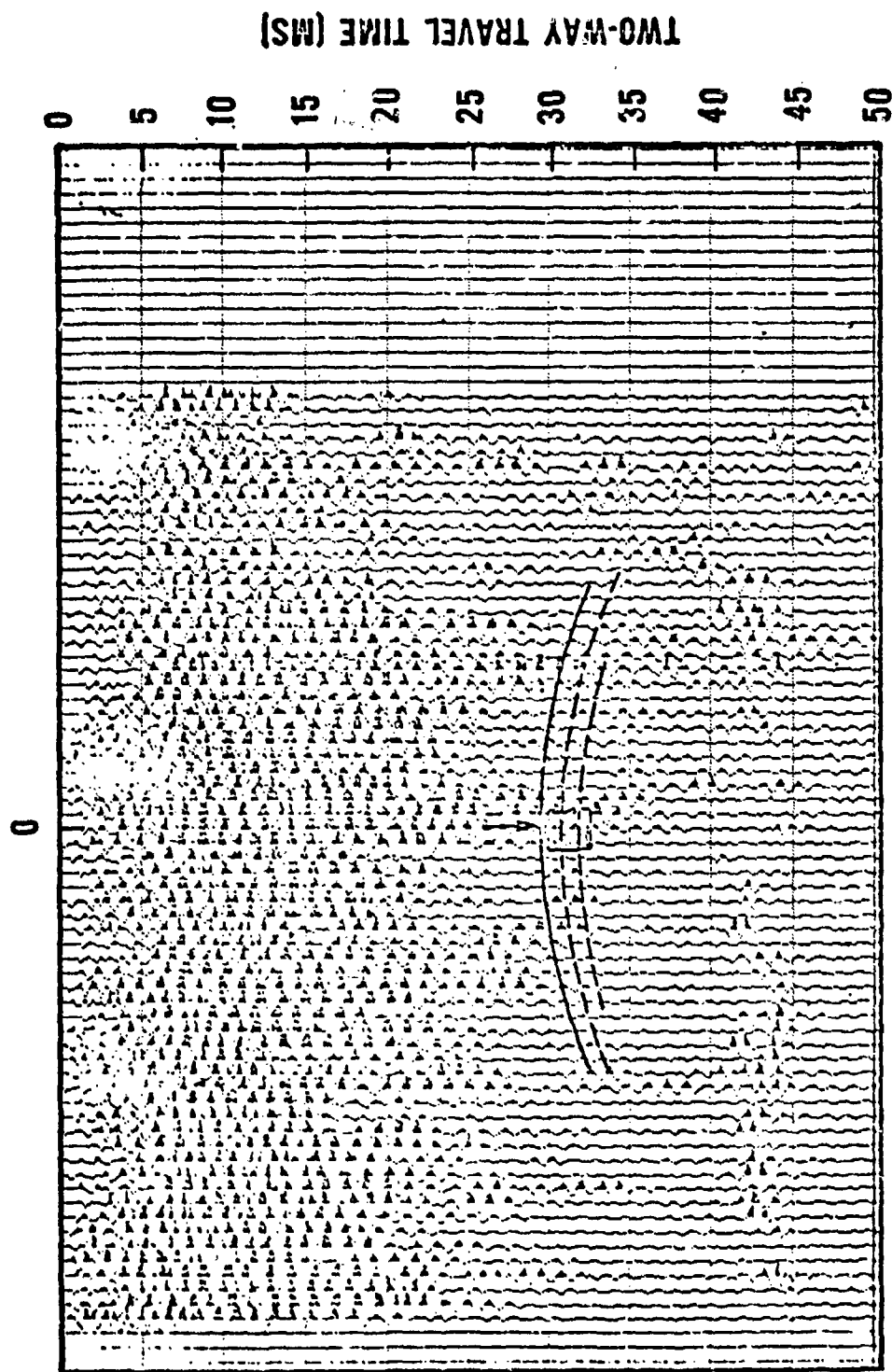


FIGURE 8
HAZEL "A" MINE TEST SITE RESULTS - FIELD TEST NO. 2

binary gain ranging. The Input/Output DHR-1632 system was found to have a particularly low system noise level in the high frequency range as well as other features advantageous to portable field operations in remote areas.

The seismic survey in this repeat test was performed along essentially the same traverse using new boreholes drilled at least 6 feet (2 m) deep. The traverse length, hole spacings and hole diameter were nominally the same as in the previous test. Because of borehole yielding problems and possible source waveform variability among shots encountered when shooting the 5-element source array, the repeat test was conducted using single-shot charges consisting of 1/3-pound commercial high explosive boosters fired at a 10-foot (3m) offset distance from the near-trace sensor. The first field record was obtained with the eight hydrophone sensors at Stations +90 through +55 as shown in Figure 7 with the shot detonated at Station +100. Over 30 records were obtained using the 8-channel survey system in traversing the 200-foot (61 m) test layout.

Figure 9 shows the CDP-processed test results obtained in the repeat survey of the Hazel "A" Mine. The tunnel target response indicated in this record section is somewhat clearer and is in agreement with that observed in the first survey. The improved clarity is attributed to the higher frequency response and lower system noise provided by the Input/Output DHR-1632 digital recording system. On the other hand, a somewhat offsetting disadvantage is the fact that the CDP data processing gain is less for the 8-channel system than for the 12-channel system used in the first test. The repeated survey appears to confirm the observed detection process as being one of incident shear waves converted to compressional waves upon reflection.

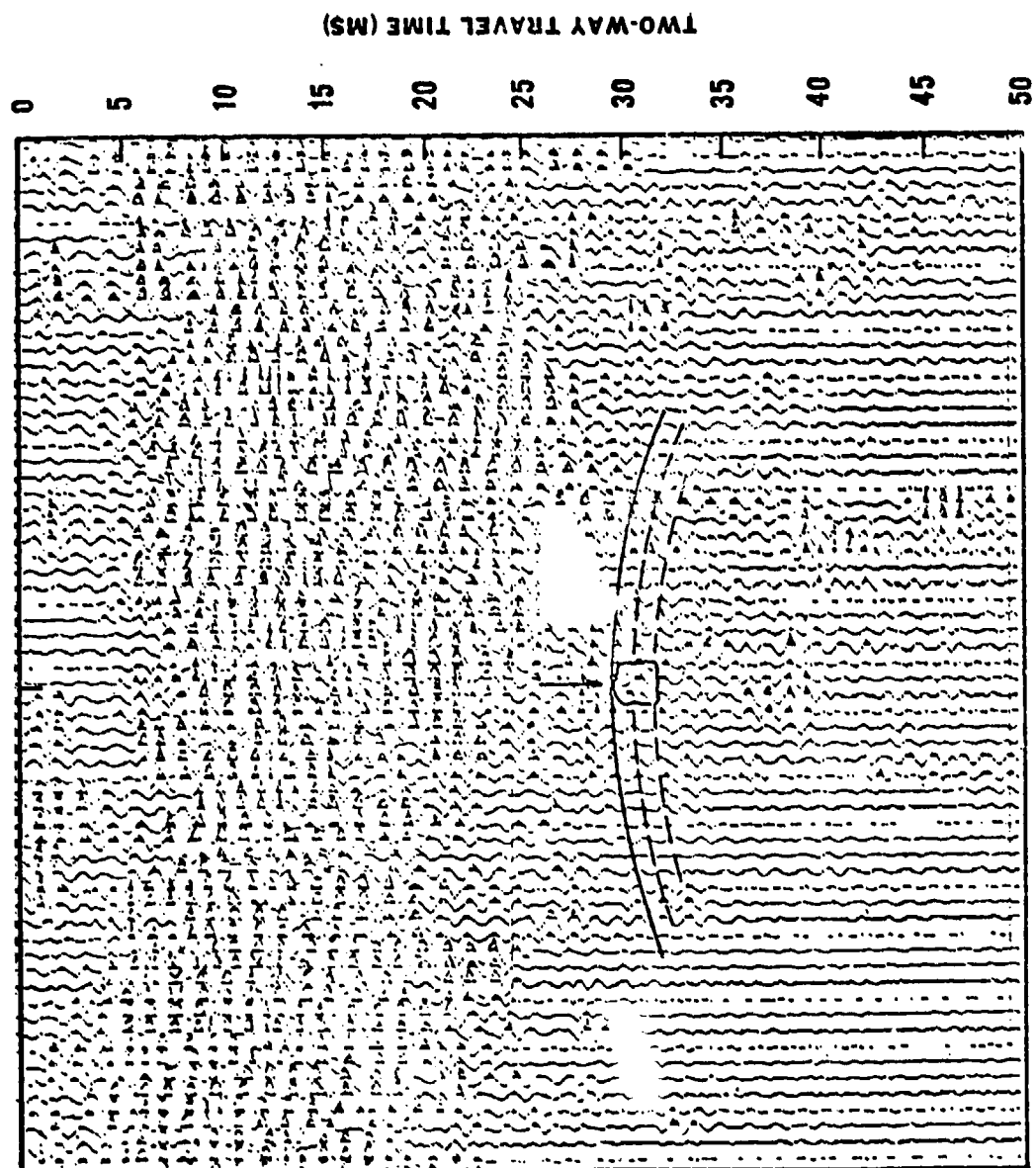


FIGURE 9
HAZEL "A" MINE TEST SITE RESULTS - FIELD TEST NO. 3

where

D - Target depth;

x - Distance along the traverse line relative to the position directly above the tunnel.

From the analytical constraints imposed by Equation (19), the hyperbolic curves of the target images are uniquely established by the seismic velocities, target depth, and survey traverse layout at each field site. Thus, any discrepancy between the fit of the calculated curves and the CDP-processed field records will indicate errors in either the seismic velocity or target depth. The curvature agreements in this respect are all noted to be reasonably good.

In further evaluating the high-resolution seismic survey experiments performed on this project, two additional comments are in order. The first is that, as with most seismic records, the general frequency content is predominantly in the lowest range of the recorded bandwidth. In this regard, even though the hydrophone detectors were obviously responsive to the high-frequency seismic waves of interest, their pre-emphasis of the high-frequency spectral components was inadequate to fully offset the absorptive losses suffered by the propagated seismic signals. Consequently, the adequacy of conventional geophysical hydrophones for use in high-resolution seismic surveys related to tunnel-detection applications is subject to question. Thus, while the hydrophone sensor and its accelerometer-like response is far superior to the land geophone in this application, there may be a more effective transducer adaptable to the need. Any advantages gained in this respect will accrue directly as improved tunnel reflection signal-to-noise ratio.

The experimental results of this project have successfully indicated the detectability of shallow tunnels and caves in rock materials using conventional seismic exploration methodology and equipment adapted for high resolution. The field tests in this respect were exploratory in that no previous studies of this type have been carried out for tunnel-detection purposes. The three field surveys resulted in valid evidence that the particular underground targets of interest produced detectable and interpretable seismic reflection signals, thereby establishing a general feasibility of the method.

The clarity of the tunnel-detection images obtained in the processed results was limited in all the seismic output displays, requiring careful evaluation and skilled interpretations to identify the targets. The reason for this limited target clarity was the relatively poor signal-to-noise ratio imposed by variations in seismic source and detector coupling with the host rock, limited seismic recording system bandwidth and high-frequency response, and insufficient pre-emphasis of the high-frequency spectral components of the tunnel-reflection signals by the seismic detectors.

V. EVALUATION OF RESULTS

The results of the three field tests presented in the preceding sections tend to confirm successful detection of the tunnel targets in each case. The clarity and sharpness of the hyperbolic target image are limited in each case, however, detracting from the conclusiveness of the detection interpretations. Signal-to-noise ratio limitations, caused by ground roll interference and variations in source and detector coupling in the boreholes, were observed in all the tests, but were more evident at the Hazel "A" Mine site. The shallow granite rock at this site appears to be fractured and jointed near the surface, giving rise to the observed variations in coupling and probable loss of high-frequency source energy.

Recording system bandwidth limitations (less than one-half octave with the Quantum DAS-1 system and about one octave with the Input/Output DHR-1632 system) also imposed fundamental constraints on the tunnel detection. In this regard, although no conclusive evaluation can be made without further test results, the apparent mode-converted shear wave reflection interpreted in each of the detections may be directly attributable to the absence of higher frequency signal content in the field records.

The validity and accuracy of the target detection results are well supported by their agreement with the surveyed field site conditions and target depths. In Field Test No. 1, the traverse line layout was erroneously centered at a location 12 m to the south of the cave, and this error was not detected until after the boreholes were drilled although it was resurveyed prior to conducting the seismic tests. The approximate 12-m offset at Hole 0 on the processed record of Figure 6 confirms this corrected field survey.

An additional indirect validation of the detected target interpretations is illustrated by the hyperbolic diffraction patterns sketched over the data printouts in Figures 6, 8, and 9. These sketched curves were calculated and plotted to the CDP display scale using the experimentally derived seismic velocities and associated target depths inferred from the apex of the hyperbolic curve. That is, for the mode-converted shear wave reflections used in the interpretations, the CDP two-way trace times to the hyperbolic curve is given to an accurate approximation by

$$\tau_{sc} = \frac{(v_s + v_c) \sqrt{D^2 + x^2}}{v_s v_c} \quad (19)$$

TERRAIN CONSIDERATIONS AND DATA BASE DEVELOPMENT
FOR SENSORS DESIGNED TO DETECT INTRUDER-INDUCED
GROUND MOTION

By

Daniel H. Cress
Physicist
Mobility and Environmental Systems Laboratory
U. S. Army Engineer Waterways Experiment Station
Vicksburg, Mississippi

The concern of management for the protection of military facilities and materiel has led to renewed emphasis on the development of security systems. Improvements in such security systems are controlled largely by the performance of the hardware used in them, particularly the sensors used to detect the presence of intruders. Such sensors must be capable of operating in a range of environmental conditions, have an acceptably low false or nuisance alarm rate, and have a long operational life with minimal maintenance. The Project Manager, Base and Installation Security System (BISS), as part of his responsibility for the development of integrated security systems has undertaken the task of developing new sensors and improving the deployment and operation of existing sensors.¹

Sensors being used, or developed, for intruder detection make use of seismic, acoustic, and electromagnetic energy forms. This presentation is concerned with the performance of seismic sensors. Sensors relying on seismic energy are generally of two types: point sensors and line sensors. Point sensors are being considered for use in detecting the presence of intruders in a small area having dimensions on the order of 50 m or less² (i.e. having a radius on the order of 25 m). Buried line sensors are being used for continuous perimeter protection for which the length of the perimeter may be as long as several kilometres. A buried line sensor referred to as the Maid-Miles³ has already proven itself to be a key element in the protection of Air Force installations in the U. S. and overseas.

Despite the successes of point and line sensors in detecting the presence of intruders, both types have been subject to false alarms due to background noise (both seismically and electromagnetically induced), to nuisance alarms (due to animals or other signal sources in the protection zone of the sensor), and to variation in intruder-detection performance in different environmental conditions.^{4,5,6} As a result of the sensitivity of sensor performance to environmental factors, the Project Manager, BISS, requested that work be done by the U. S. Army Engineer Waterways Experiment Station (WES) to provide information concerning the seismic signature characteristics of intruder-type targets in worldwide environments.

The purpose of the study was to develop a readily accessible body of information that defines the range of intruder signal characteristics within which seismic sensors must operate. Principal products from the study were to be:

- a. A data base of seismic signatures (recorded on magnetic tape) that is representative of the range of target types, travel modes, seismic environments, and background noise sources that can realistically be expected to occur for most base and installation environments occurring worldwide.
- b. Guidance to users of the data base that will support the needs of sensor designers and evaluators.

Description of Study

To address the purpose of the study, both a theoretical and an experimental approach were taken. The experimental approach consisted of collecting and analyzing the signatures of intruders and background noise sources in a wide range of terrain conditions. However, it was recognized that the range of conditions covered in the experimental data could not be expected to be fully representative of the range of terrain conditions that could be expected to occur worldwide. The theoretical approach consisted of applying mathematical models of the seismic signature generation and propagation phenomena so as to extend the data base of

experimental seismic signatures to include terrain conditions not represented in the data collection portion of the study.

This paper presents a portion of the overall study, namely a description of the data base of measured signatures and an analysis of selected portions of the measured personnel signature data. A WES technical report⁷ presents the results of the complete study. This paper is divided into sections covering the experimental approach: data collection, data analysis, and concluding comments.

Data Collection

The data-collection phase of the study consisted of the development of signature collection and site documentation plans, selection of data collection sites, and signature acquisition.

Signature collection plan

A signature collection plan that explicitly specified the targets, travel modes, travel paths, background noise sources, and sensor and sensor configuration was developed prior to the data collection. The rationale for the signature collection plan was based on the definition of the threat confronting Department of Defense assets and installations as outlined in the System Specification for Base and Installation Security,² past experience of WES personnel in analyzing the factors affecting the performance of devices designed to detect and classify intruder-type targets, and conversations with BISS and other Air Force personnel cognizant of the physical constraints and background noise common around high-value military assets. The plan specified individual targets, combinations of individual targets, target travel modes, and the test layout, i.e. sensor types, sensor orientations and spatial distribution, and target paths. The major considerations in developing the test layout are as follows:

- a. It was desired that vertical and horizontal components of the ground motion be measured to support design requirements of point sensors that employ vertical sensing geophones and line sensors that may be sensitive to the vertical component of the ground motion, the horizontal component, or both.

- b. Measurements of the spatial rate of change of signature properties were desired in the data to support sensor designs that make use of the spatial rate of change of signature to suppress background noise from distant sources.
- c. The direction of incidence of the seismic energy to the signature collection site should be recoverable from the collected data in anticipation of the development of techniques for spatial detection or classification algorithms.
- d. The acoustic energy component should be measured in anticipation of the development of techniques for removing acoustically induced seismic signature components from those induced by forces applied to the ground surface by ground-surface targets.
- e. During portions of the data collection, target-to-sensor distances should be less than 25 m to support point sensor deployment criteria, and should be 5 m or less to support line sensor deployment criteria.

Test layout. A triaxial geophone can be used to address consideration a. Considerations b and c can be addressed by using three or more sensors which are spatially separated in a nonlinear manner to form a polygonal array.⁸ Consideration d can be addressed by using a microphone. Consideration e can be addressed within the definition of the target paths. A typical test layout for the data collection is presented on Figure 1. The vertical and two horizontal components of target and background noise signatures were sensed by the triaxial geophone at G1. Vertical sensing geophones at G2 and G3 were used to complete the polygonal array. These sensors were placed 6 to 8 cm beneath the surface. A microphone was placed inside the triangular area defined by the three geophones. The spatial separation of G2 and G3 from G1 was two metres. The vehicle path was offset 8 m from G1. The personnel path is outlined by the control points A, B, C, and D. That portion of the path from C to A to D is perpendicular to the vehicle path. The semi-circular path defined by the path segment A to B to C, was used to provide data for

estimating the range in variation in the amplitude and frequency characteristics of personnel signatures with time for the individual(s) moving at a fixed target-to-sensor distance.

Major consideration in selecting targets, target mixes, and target travel modes included:

- a. Intruder-type targets used for data collection had to consist of personnel and ground vehicles as these are the major threats to the perimeter surveillance against which ground-motion sensing devices can be most effective. Particular emphasis was placed on wheeled and tracked vehicles. Aircraft signatures were collected, but they were regarded as background noise sources.
- b. Emphasis was placed on the intruder-type target and travel modes generally most difficult to detect. Among the ground targets considered, personnel were identified as most difficult to detect, particularly when engaged in a stealthy walk, or creep.

Test plan. The targets used for data collection were personnel and wheeled and tracked vehicles. The personnel travel modes creeping, crawling, walking, and running were emphasized in the test plan. To address the background noise requirements, tests were conducted in which several targets were moving simultaneously so that one target, referred to as the secondary target, generated background noise for the purpose of masking the signature of a primary target. During such multiple target tests it was necessary to specify the relative positions of the targets involved. A typical test plan for the BISS signature collection is presented in Table 1. The tests have been ordered so as to minimize the changes in gain settings on the instrumentation during the conduct of the tests. The target paths are keyed to the test layout (Figure 1).

Site documentation plan

The goal of site documentation was to measure the properties of the terrain that affect the generation and propagation of seismic signatures. Previous studies^{9, 10} have identified these properties as the bulk properties (compression- and shear-wave velocity, bulk density, soil

moisture, etc), ground-surface rigidity, and surface roughness. The measurements used for their description are summarized below:

<u>Measurement</u>
Compression wave velocity
Shear wave velocity
Bulk density
Soil moisture
Cone index
Plate load
Surface elevations

Selection of data collection sites

As stated earlier it was desired that sites having terrain properties that spanned a wide range of seismic response conditions be selected for use in the data collection program. Furthermore, such sites had to contain a reasonable range of ambient background noise sources. However, it was recognized that an attempt to define and collect background noise data that could be considered representative of those occurring worldwide would be impractical.

In order to estimate the range of seismic response conditions occurring worldwide, it was necessary to select a terrain measurement or measurements related to properties to which seismic signature generation and propagation mechanisms are sensitive and for which considerable data have been obtained in a variety of geographic locations. The compression wave velocity provided such a measurement. Seismic refraction data (obtained by measuring compression-wave velocities as a function of depth) have been collected by WES in the United States and selected foreign countries in support of WES sensor studies and subsurface investigations on construction sites. These data have been obtained at the locations indicated in Figure 2. Previous studies^{5,7,9} have indicated that many terrain conditions can be generalized as two-layer systems for purposes of estimating the seismic response using WES seismic propagation models. Figure 3 shows the distribution of top-layer compression wave velocities versus second-layer compression wave velocities for the measured terrain data discussed in the previous paragraph. It was

desired to select the data collection sites such that the top- and second-layer compression wave velocities were well distributed across the points represented in Figure 3.

The selection of sites for the collection of background noise field data was based on the following guidelines.

- a. The sites selected should be representative of background noise environments found in Army, Air Force, and Navy installations. Sites should be located near such military-related background noise sources as airports, housing areas, and training and cantonment areas.
- b. Some of the data collection sites should be located in or near highly developed nonmilitary cultural areas (urban and industrial) adjacent to military installations.
- c. Data should be collected in areas and environmental conditions where background noise is known to cause false alarms or masking of intruder signatures for presently deployed seismic sensors.
- d. Background noise data should be obtained in natural environments on or near military installations, especially at such times when rain, wind, and other sporadic meteorological conditions are contributing factors.

A preliminary list of installations was made to select sites in coordination with BISS personnel and supporting agencies. Based on geologic, topographic, soils and cultural data, and known background noise problems for deployed sensors, four installations were identified for selection of data collection sites: Barksdale AFB, Louisiana; Fort Hood, Texas; March AFB, California; and Seal Beach Naval Weapons Station, California. Compression wave velocities were measured at sites on these installations having different soils and topographic features. Two to four data collection sites were selected at each installation. The selected sites at each installation are identified in Table 2 along with the surface and near-surface site documentation data. The compression and shear wave velocities for the selected sites are presented in Table 3. The top-layer compression layer velocities are plotted against the second layer compression wave velocities for the selected sites in

Figure 4. Comparison of the compression wave velocities in Figure 4 with those of Figure 3 shows that the top-layer compression wave velocities for the selected sites spanned the range in variation occurring for the assembled terrain data. However, the second-layer compression wave velocities for the selected sites do not cover the higher velocities represented in the assembled data. These higher velocities occur in very rigid terrain conditions, often found in mountainous areas. Such areas present problems in deploying sensor systems and in collecting field data. The difficulty of selecting a set of test sites that encompasses the range of variation in worldwide conditions points out the importance of applying analytical procedures, such as simulation models, to extend the data base to conditions not represented in the data collection program.^{7,9}

Signature acquisition

The intruder signature data and background noise data were collected using Mark Product, L4-30 geophones and a Brüell and Kjaer type 4921 microphone. The data recording system consisted of a Lockheed Electronic Corporation Model 4170 7-channel tape recorder which can record in the direct and frequency modulated (FM) mode. All signatures were recorded on magnetic tape at tape speeds of 1 7/8 in./sec which, for the direct mode recorded reproducible frequencies between 100 Hz and 6000 Hz and, for the FM mode, recorded reproducible frequencies from 0 to 625 Hz. Since most seismic information is below 600 Hz because of the limits on geophone response and the large attenuation of the propagating seismic signal for frequencies in the hundreds of Hz, the FM recording of geophone signals was used. However, the acoustic signatures were recorded in both the FM and direct mode. Background noise signatures of aircraft were recorded in the direct mode because such acoustic signatures contain substantial energy with frequencies in the thousands of Hz.

Data Analysis

Selected signatures of personnel were analyzed as a function of the data collection variables: target-to-sensor distance, terrain condition,

and travel mode. This section is partitioned into discussions of the variance induced by these three data collection variables.

Plots of signature characteristics describing the frequency distribution and amplitude content of the signatures as a function of the data collection variables are presented in Figures 5, 6, 8, and 9. Each frequency domain plot contains three curves. The three curves in the figures denote maximum, mean, and minimum amplitudes derived in the following manner:

- a. Between six and twelve time segments of the signatures (depending on the availability of appropriate segments of the data), 0.68 sec in length, were selected for which the target was in the proper target-to-sensor distance (for example, 0-0.5 m and 0.5-2 m for Figures 5a and 5b, respectively).
- b. The time segments were digitized at a rate of 1500 samples per second and converted to the frequency domain by application of a Fourier transform so that each segment had an amplitude value for each frequency.
- c. The maxima, means, and minima were obtained using the amplitude values at each frequency (six to twelve of them, one for each time segment). The maxima, means, and minima for the appropriate target-to-sensor distances are presented in the top, middle, and lower curves, respectively, for each frequency-domain plot.

Target-to-sensor distance

Preliminary analysis of the data indicated that the variation induced by changes in target-to-sensor distance were most severe in the distance region of 0 to 2 m relative to the farther distance regions. Figure 5 illustrates the dependence of the signature characteristics on the target-to-sensor distance for the vertical component of a signature obtained from a man-creeping on a rigid (high compression and shear wave velocity) terrain condition, site 8a at Fort Hood, Texas. Both Figures 5a and 5b show the frequency domains for the vertical component of the particle velocity of the ground for man-creeping signatures within the distance regions indicated (0-0.5 m and 0.5-2 m, respectively). As can

be seen in the figure, the amplitudes for all frequencies are greater for the 0- to 0.5-m distance and the predominant frequencies of the signatures shift from less than 10 Hz for target-to-sensor distances less than 0.5 m to approximately 80 Hz for target-to-sensor distances exceeding 0.5 m. Based on the data collected in this program, this trend is not atypical for targets whose weight is equivalent to or exceeds that of a man, in general the signatures are dominated by low frequencies (less than 5 Hz) for target-to-sensor distances on the order of 0.5 m to 2.0 m (depending on terrain properties). For distances beyond some target-to-sensor distance on the order of 2 m, the predominant frequencies vary from greater than 10 Hz to 80 Hz or more, with the predominant frequencies being a function of the discontinuities in the layers of media and the layer depths. The predominant frequencies for distances exceeding several metres do not change near so rapidly with changes in target-to-sensor distance as they do very near to the target (i.e. less than 2 m). The dependence of the predominant frequencies on terrain condition are discussed in the next section.

Terrain condition

In view of the dichotomous nature of the frequency domain characteristics of target signatures with target-to-sensor distance, it is convenient to partition the discussion of terrain induced variation into the two signature types: those for which the low frequencies predominate (below 10 Hz) and those for which the higher frequencies predominate (above 10 Hz). Those for which the low frequencies predominate are referred to as near-distance signatures. Those for which the higher frequencies predominate are referred to as intermediate-distance signatures. For the analysis of the near-distance signatures, the man-creeping signatures will be discussed because their low amplitudes were more conducive to near-distance recording (without exceeding the dynamic range of the tape recorder) than were the other personnel travel modes. For the intermediate-distance signatures, the man-walking signatures will be discussed.

For purposes of characterizing signatures of intruders in different terrain conditions, data from five sites were selected. The sites (see Table 3) were Barksdale, site 1A; Fort Hood, sites 5A, 8A, and 9, and

Seal Beach, site 3. These sites were selected because they spanned the range of all terrain conditions used in the test program. It is convenient to organize the discussion of sites according to the increasing or decreasing top-layer shear wave velocities whichever seems most appropriate for the signature characteristics being discussed. For the five sites for which the signatures were analyzed, the order of increasing top layer shear wave velocities is Seal Beach (site 3), Barksdale (site 1A), Fort Hood (sites 9, 5A, and 8A).

For the near-distance signatures, Figure 6 presents the frequency-domain plots (maximum, mean, and minimum amplitudes) for the vertical component of the particle velocity for man-creeping signatures. The target-to-sensor distance for which the low frequencies predominate are 0- to 2-m for the three lower shear wave velocity sites: Seal Beach, Site 3, Barksdale, Site 1A, Fort Hood, Site 9. For Fort Hood, Site 5A, the minimum amplitude curve for the 0-2 m distances is very small (less than 1×10^{-5} m/sec) indicating that, at least for some of the signature segments used to derive the curve, the low frequencies do not dominate. For Fort Hood, site 8A, the low-frequency characteristic of the near-distance signatures did not dominate until the target-to-sensor distance was less than 0.5 m (Figures 5a, 5b, and 6a). In each instance presented in Figure 6, the maximum and mean frequency-domain curves have considerably higher amplitudes for the low frequencies than for the higher frequencies. The amplitudes tend to decrease as the shear wave velocity increases (i.e. the mean amplitudes for Seal Beach, Site 3 for the low frequencies are around 0.2×10^{-3} cm/sec, whereas they are on the order of 0.05×10^{-3} cm/sec for Fort Hood, Site 8A).

The average amplitudes of the vertical and horizontal components (in the direction from the target to the sensor) of man-creeping signatures can be compared in Figures 7a and 7b. Average amplitudes for both unfiltered and filtered signatures are presented. Filter cut-offs were 5 Hz and 10 Hz with filter roll-off of 24 db per octave. The sites have been placed in the order of decreasing top-layer shear wave velocity. For both the vertical and horizontal components, the amplitudes tend to increase as the shear wave velocity decreases with the exception of the

horizontal component for Barksdale AFB, site 1A, and Fort Hood, site 9. It should be noted that the top layer shear wave velocities at site 1A at Barksdale AFB, and site 9 at Fort Hood are very similar, being 120 m/sec and 122 m/sec, respectively. Therefore, such sites could be expected to have overlapping signature amplitudes, which is, in fact, what is noticed when comparing Figures 7a and 7b. The amplitudes of the vertical component tend to exceed those of the horizontal component, particularly for the sites having the higher shear wave velocities (Fort Hood, sites 5A and H-8A).

The change in amplitude with target-to-sensor distance for the vertical and horizontal components of the man-creeping signatures were estimated by dividing the unfiltered average amplitudes for the footfall 0.5 m from the sensor by the average amplitudes for the footfall at the sensor. The resulting ratios are presented in Figure 7c. In each instance, ratios for the vertical component exceed those for the horizontal component, indicating that the rate of change in amplitude with distance for the horizontal component generally exceeds that for the vertical component for the near-distance signatures. The rate of change in amplitude with distance is greater for the more rigid sites (as indicated by smaller ratios for sites 5A and 8A) than for the less rigid sites.

For the intermediate-distance signatures, the frequency domain plots for man-walking signatures, Figures 8a-8e, are discussed. The predominant frequencies for man-walking signatures and for a target-to-sensor distance of 6 m vary from around 12 Hz (Seal Beach, site 3) to 80 Hz (Fort Hood, site 9). Although the predominant frequencies appear to increase with increasing shear wave velocity, one should be careful in making this interpretation without considering layering effects as well. The three Fort Hood sites, 5A, 8A, and 9, represent terrain conditions having large discontinuities in the shear wave velocities of the layered media. It is the relative discontinuity of a slow, shear-wave velocity medium over a faster, second-layer velocity medium, rather than the absolute values of the shear wave velocities of both media, that leads to the selective coupling of frequencies of the target stresses on the surface so as to favor the higher frequencies.⁷

Travel modes

Personnel travel modes consisted of creeping, crawling, walking, and running. The near-distance signatures for man-creeping were discussed previously. Figure 9 presents the frequency domain characteristics for man-creeping, -crawling, -walking, and -running for the denoted distances for Fort Hood, site 8A. The predominant frequencies for each travel mode are between 60 and 100 Hz. The site conditions affect the coupling and transfer of the frequencies of the stresses impacted to the surface so severely that frequency differences in the stresses for creeping, crawling, walking, and running are filtered out to the extent that the predominant frequencies are very similar for each travel mode. The amplitudes differ, as could be expected. The peaks of the mean amplitude curves for the man-crawling, -walking, and -running modes vary from 0.01×10^{-3} cm/sec for man-crawling signatures to 0.03×10^{-3} cm/sec for man-running signatures. The man-creeping signatures are plotted for only the 0.5-2 m distance because signal amplitudes were not sufficient for recording at the 6 m distance.

Concluding Comments

A set of seismic signatures of ground targets and background noise has been collected for a range of seismic terrain conditions that spans a wide range of near-surface (top-layer) conditions. However, the variation found in measured compression wave velocities greatly exceeded that in the data collection program (Figure 3) and points out the importance of applying analytical procedures such as simulation models, to extend the data base to terrain conditions not represented in the measured data collection program.

For measurements near the surface, the frequency-domain characteristics of target signatures are very sensitive to the target-to-sensor distances, particularly the distances between 0.5 and 2 m (Figure 5). For intruder distances of less than 2 m, the low frequency components (less than 10 Hz) predominate (Figure 6); but for distances beyond 2 m, the frequency domain is dominated by higher frequency (10 to 100 Hz) characteristics (Figure 8).

Most present line sensors rely on low-frequency characteristics of the signatures for detection. For higher shear wave velocity sites, such as Fort Hood sites 5A and 8A, it may be necessary to use parallel deployment of line sensors to attain detection zones having satisfactory widths. Another alternative is to develop detection algorithms that incorporate the higher frequencies of the signatures as well as the low-frequency components. Such algorithms could emphasize the identification of the higher frequencies of the impulses that would be generated outside the near-distance region, particularly by a man trying to jump across the low-frequency response zone surrounding the sensor.

For near-distance sources, the spatial rate of change of the horizontal component of the ground motion near the surface is greater than that of the vertical component (Figure 7) so that for target-to-sensor distances on the order of 0.5 m, the vertical component of the ground motion is greater than the horizontal component. Because of this, the vertical component should be preferable from the point of view of maintaining the largest detection zone for a given sensor.

The predominant frequency characteristics of the intermediate-distance signatures are dominated by the local site conditions to the extent that the signatures for all personnel travel modes have essentially the same predominant frequencies at a given site (Figure 9). For the data analyzed, the predominant frequency characteristics of the signatures vary from 10 Hz to 80 Hz, depending on site conditions.

Literature Cited

1. Base and Installation Security System Program Management Plan, July 1972, Air Force Systems Command, EDS, Hanscom Air Force Base, Massachusetts.
2. System Specification For Base and Installation Security System (BISS), BISS-PO, Air Force Systems Command, ESD, Seps. No. A63714-64715 BISS, Code Identification 50464, 1 November 1973. Hanscom Air Force Base, Massachusetts.
3. The referenced document is not for public release, and, therefore, cannot be referenced in this paper.
4. Cress, D. H., "A Comparative Analysis of Selected Seismic and Acoustic Target Classifiers," Technical Report M-76-7, June 1976, U. S. Army Engineer Waterways Experiment Station, CE, Vicksburg, Mississippi.
5. Lundien, J. R., "Terrain Constraints on the Design, Testing, and Development of the Gator Mine," ADTC-TR-75-15 (AFATL-TR-75-57), March 1975, Munitions System Program Office, Deputy for Armament Systems, Armament Development and Test Center, U. S. Air Force Systems Command, Eglin Air Force Base, Florida; prepared by the U. S. Army Engineer Waterways Experiment Station, CE, Vicksburg, Mississippi.
6. Safe Programs Equipment Siting Criteria, 5 March 1976, BISS Program Office, Hanscom Air Force Base, Massachusetts.
7. Cress, D. H., "Terrain Considerations and Data Base Development for the Design and Testing of Devices to Detect Intruder-induced Ground Motion," (in preparation) U. S. Army Engineer Waterways Experiment Station, CE, Vicksburg, Mississippi.
8. Cress, D. H., "Seismic Methods of Locating Military Ground Targets," Technical Report M-76-13, June 1976, U. S. Army Engineer Waterways Experiment Station, CE, Vicksburg, Mississippi.
9. Lundien, J. R. and Nikodem, H., "A Mathematical Model for Predicting Microseismic Signals in Terrain Materials," Technical Report M-73-4, June 1973, U. S. Army Waterways Experiment Station, CE, Vicksburg, Mississippi.
10. Lundien, J. R. and Benn, B. O., "Generation and Propagation of Microseismic Signals from Footsteps," Miscellaneous Paper M-73-12, September 1973, U. S. Army Waterways Experiment Station, CE, Vicksburg, Mississippi.

Table 1
Typical Test Plan for BISS Signature Collection

Test No.	Target		Travel Mode		Target Paths
	Primary (number)	Secondary (number)	Primary	Secondary	
1	personnel (1)/NA		walking/NA		1
2	personnel (1)/NA		walking/NA		1
3	personnel (3)/NA		walking/NA		1 (personnel two metres apart)
4	personnel (1)/NA		crawling/NA		1
5	personnel (1)/NA		crawling/NA		1
6	personnel (3)/NA		crawling/NA		1 (personnel two metres apart)
7	personnel (1)/NA		running/NA		1
8	personnel (1)/NA		running/NA		1
9	personnel (3)/NA		running/NA		1 (personnel two metres apart)
10	personnel (1)/NA		creeping		1
11	personnel (1)/NA		creeping		1
12	personnel (3)/NA		creeping/NA		1 (personnel two metres apart)
13	1/4-ton vehicle (1)/NA		8 kph/NA		2
14	1/4-ton vehicle (1)/NA		32 kph/NA		2
15	1/4-ton vehicle (1)/personnel (1)		32 kph/walking		3
16	1/4-ton vehicle (1)/personnel (1)		32 kph/creeping		4
17	2-1/2-ton vehicle (1)/NA		8 kph/NA		2
18	2-1/2-ton vehicle (1)/NA		32 kph/NA		2
19	2-1/2-ton vehicle (1)/personnel (1)		32 kph/walking		3
20	2-1/2-ton vehicle (1)/personnel (1)		32 kph/creeping		4
21	M113 APC (1)/NA		8 kph/NA		2
22	M113 APC (1)/NA		32 kph/NA		2
23	M60 tank (1)/NA		8 kph/NA		2
24	M60 tank (1)/NA		32 kph/NA		2

* Target paths (see Figure 1): (1) Start at A, move around semicircle past B to C, then move out to D; (2) Start vehicle at E and proceed to F; (3) Personnel intruder starts at A when vehicle is at the closest point of approach to the sensors, proceeds around the semicircle past B to C; test stops when personnel intruder reaches C; (4) Personnel intruder starts at C when vehicle is at closest point of approach to sensors; test stops when personnel intruder crosses semicircle (at A).

Table 2
Summary of Surface and Near-Surface Measurements for the Selected Data Collection Sites

Area	Site	$K_{s,c}$ (n.m ²)	Z_{max} (m)	Depth, cm		Density, g/cm ³		Moisture Content, %	Cone Index
				From	To	Wet	Dry		
Barkdale AFB, LA	1A	1.01×10^8	0.0045	0.0	7.5	1.85	1.57	18.0	280
				15.0	22.5	1.88	1.57	19.6	240
				30.0	37.5	1.91	1.59	20.1	220
	5	6.2×10^7	0.0056	0.0	7.5	1.71	1.45	17.9	345
				15.0	22.5	1.85	1.53	21.4	362
				30.0	37.5	1.86	1.53	20.2	308
	7	3.1×10^7	0.0090	0.0	7.5	1.81	1.55	17.0	335
				15.0	22.5	1.95	1.67	17.4	344
				30.0	37.5	1.89	1.58	20.3	317
Fort Hood, TX	5A	1.76×10^7	0.0045	0.0	7.5	1.61	1.47	9.7	1125
				15.0	22.5	Rock	Rock	14.4	-
				30.0	37.5	Rock	Rock	14.1	-
	8A	1.53×10^7	0.0110	0.0	7.5	Rock	Rock	14.1	831
				15.0	22.5	Rock	Rock	5.0	-
				30.0	37.5	Rock	Rock	-	-
	9	1.67×10^7	0.0130	0.0	7.5	1.69	1.45	17.1	414
				15.0	22.5	1.76	1.44	22.3	458
				30.0	37.5	1.60	1.46	22.8	394
March AFB, Riverside, CA	1			0.0	7.5	1.92	1.81	6.2	430
				15.0	22.5	1.99	1.86	6.6	340
				30.0	37.5	1.81	1.58	7.4	750
	2			0.0	7.5	1.85	1.76	5.4	-
				15.0	22.5	2.17	2.07	7.5	-
				30.0	37.5	Rock	Rock	6.5	-
Naval Weapons Station Seal Beach, CA	1			0.0	7.5	1.69	1.52	11.5	454
				15.0	22.5	2.07	1.78	14.2	750
				30.0	37.5	2.01	1.70	18.2	-
	2			0.0	7.5	1.58	1.32	19.4	71
				15.0	22.5	1.83	1.54	19.2	204
				30.0	37.5	1.81	1.48	23.4	257
	3	1.08×10^6	0.102	0.0	7.5	1.84	1.34	37.9	51
				15.0	22.5	1.75	1.20	44.8	47
				30.0	37.5	1.26	0.78	60.8	39
	4			0.0	7.5	1.82	1.59	14.5	345
				15.0	22.5	1.75	1.50	16.8	417
				30.0	37.5	1.73	1.47	17.6	389

* $K_{s,c}$ and Z_{max} are the surface spring constant and the asymptotic value of the rutting depth for compaction-type soil conditions,⁷ respectively. Values are obtained from plate load tests. Such tests were not taken at March AFB or Seal Beach Naval Weapons Station. Values were estimated for Seal Beach, site 3 on the basis of rutting depth for a walking man.

Table 3

Seismic Compression and Shear Wave Velocities for Selected Sites

Area	Site No.	Compression Wave			Shear Wave		
		Layer No.	Layer Depth, m	Velocity m/sec	Layer No.	Layer Depth, m	Velocity m/sec
Barksdale AFB	1A	1	0.0-4.4	353	1	4	120
		2	4.4+	1700	2	4+	170
	5	1	0.0-1.2	367	1	3.8	125
		2	1.2+	533	2	3.8+	150
	7	1	0.0-1.5	357	1	4.6	115
		2	1.5+	593	2	4.6+	280
Fort Hood	5A	1	0.0-2.0	780	1	0.0-1.8	203
		2	2.0+	1950	2	1.8+	381
	8A	1	0.0-1.9	1410	1	0.0-2.1	253
		2	1.9+	2825	2	2.1+	427
	9	1	0.0-3.1	300	1	0.0-3.8	122
		2	3.1+	1675	2	3.8+	203
March AFB	1	1	0.0-0.9	270	1	0.0-3.1	210
		2	0.9	695	2	3.1+	260
	2	1	0.0-1.0	390	1	0.0-6.25	280
		2	1.0+	1030	2	6.25+	450
Seal Beach NWS	1	1	0.0-1.3	220	1	10.0+	93
		2	1.3+	1400	-	-	-
	2	1	0.0-3.5	300	1	0.0-2.2	75
		2	3.5+	1200	2	2.2+	145
	3	1	0.0-1.1	165	1	0.0-3.0	75
		2	1.1-3.0	497	-	3.0+	125
		3	3.0+	965	-	-	-
	4	1	0.0-0.4	260	1	10.0+	125
		2	0.4-2.5	265	-	-	-
		3	2.5+	600	-	-	-

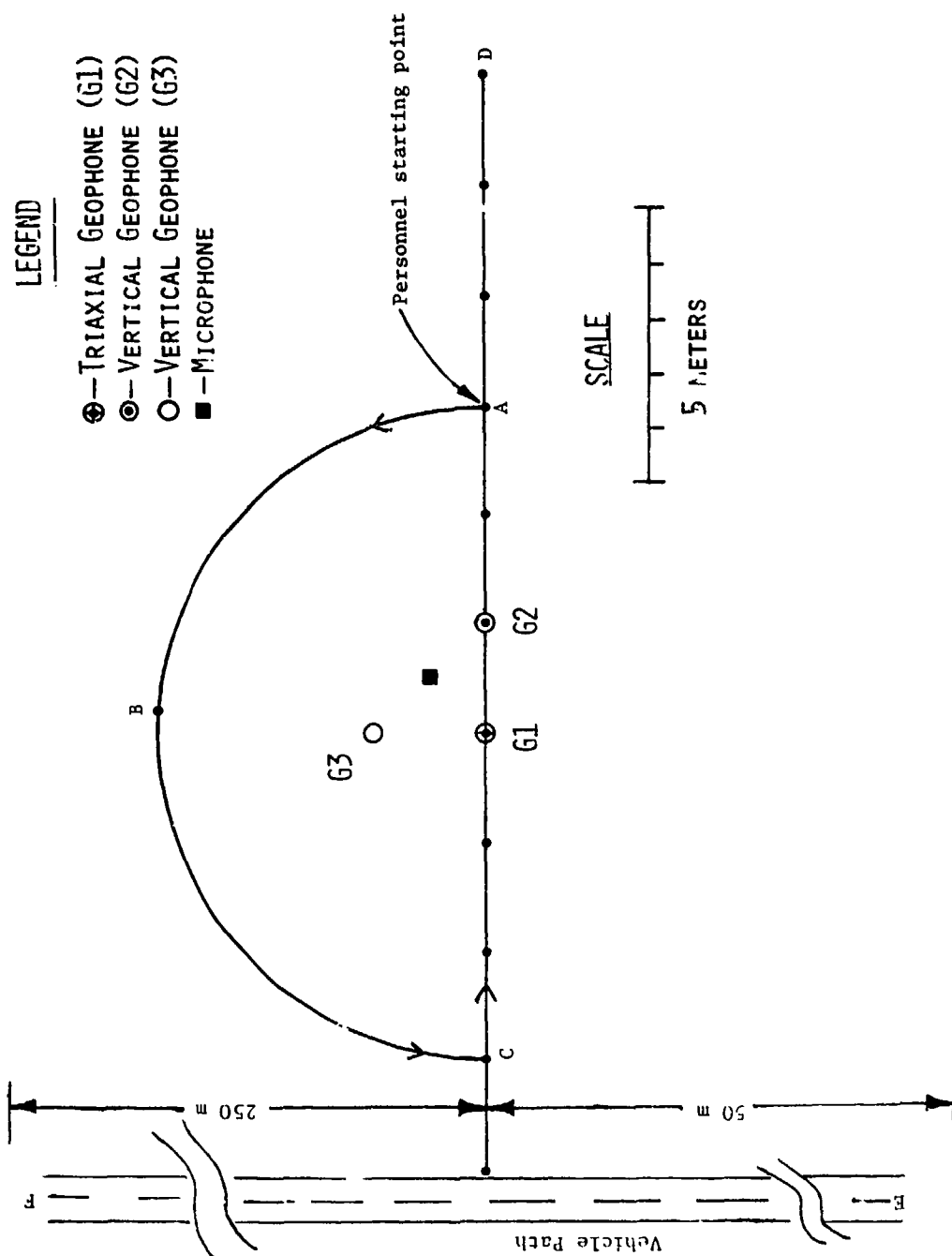


Figure 1. Typical test layout for BISS data collection

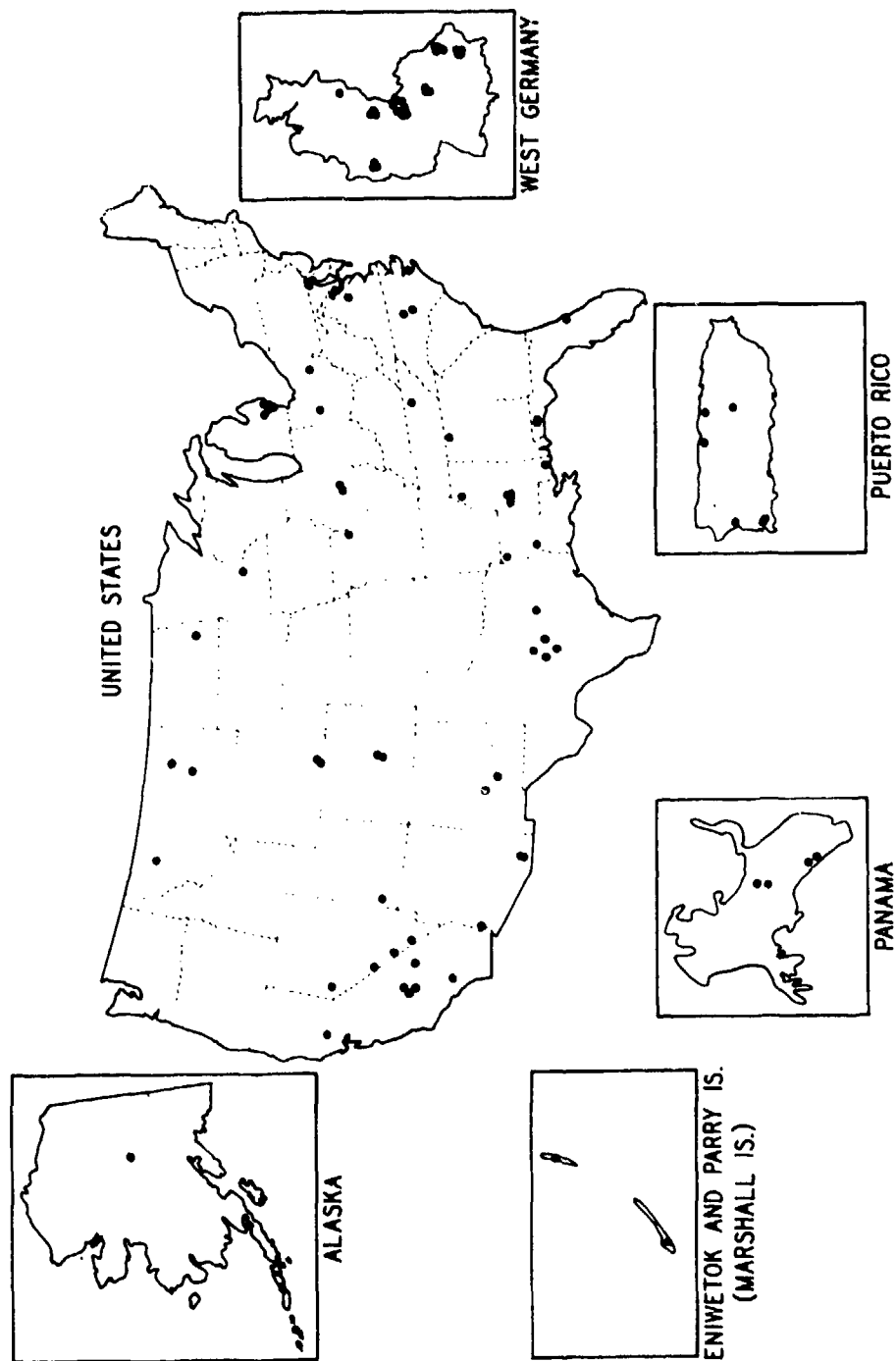


Figure 2. Locations of seismic refraction measurements

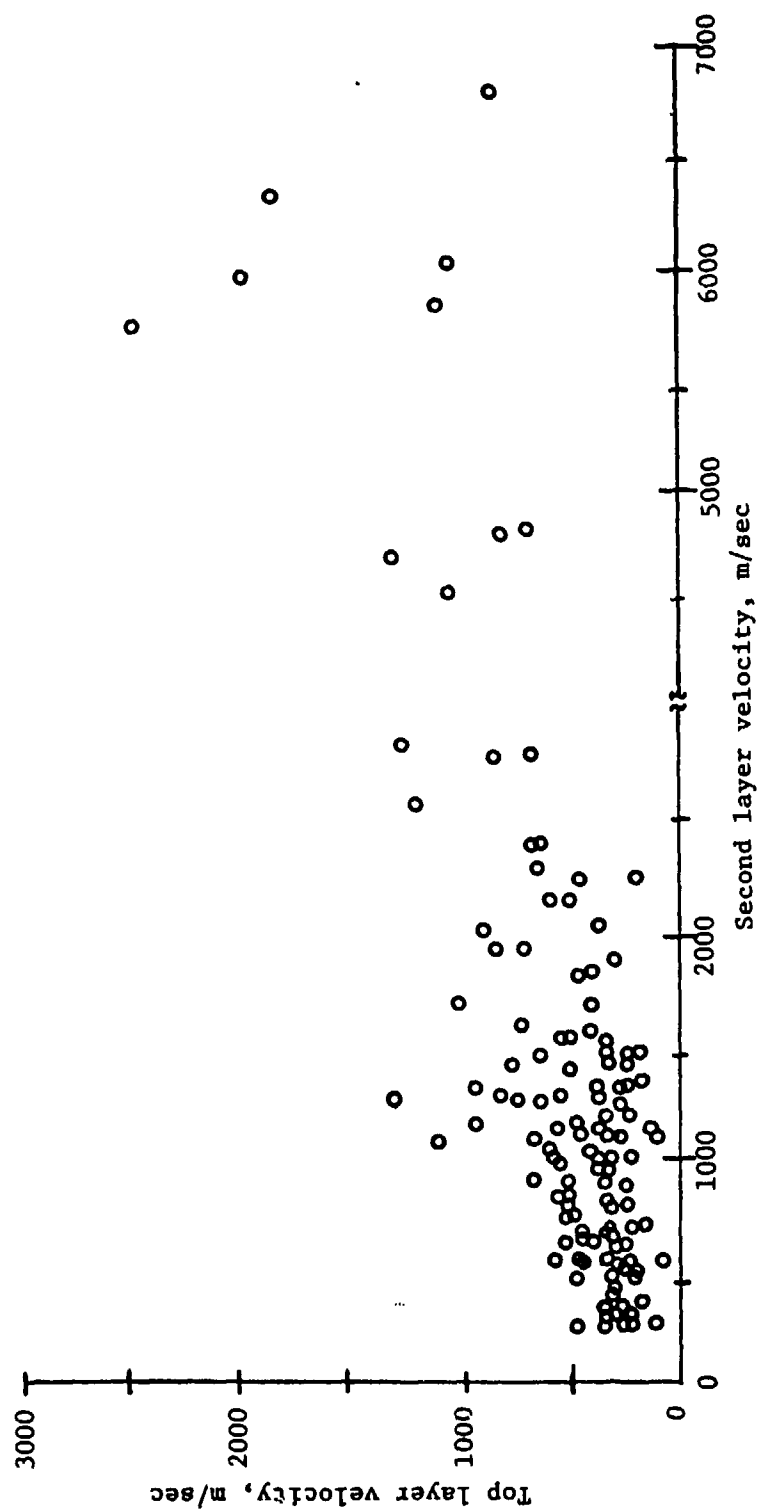


Figure 3. Top- and second-layer compression wave velocities for terrain data

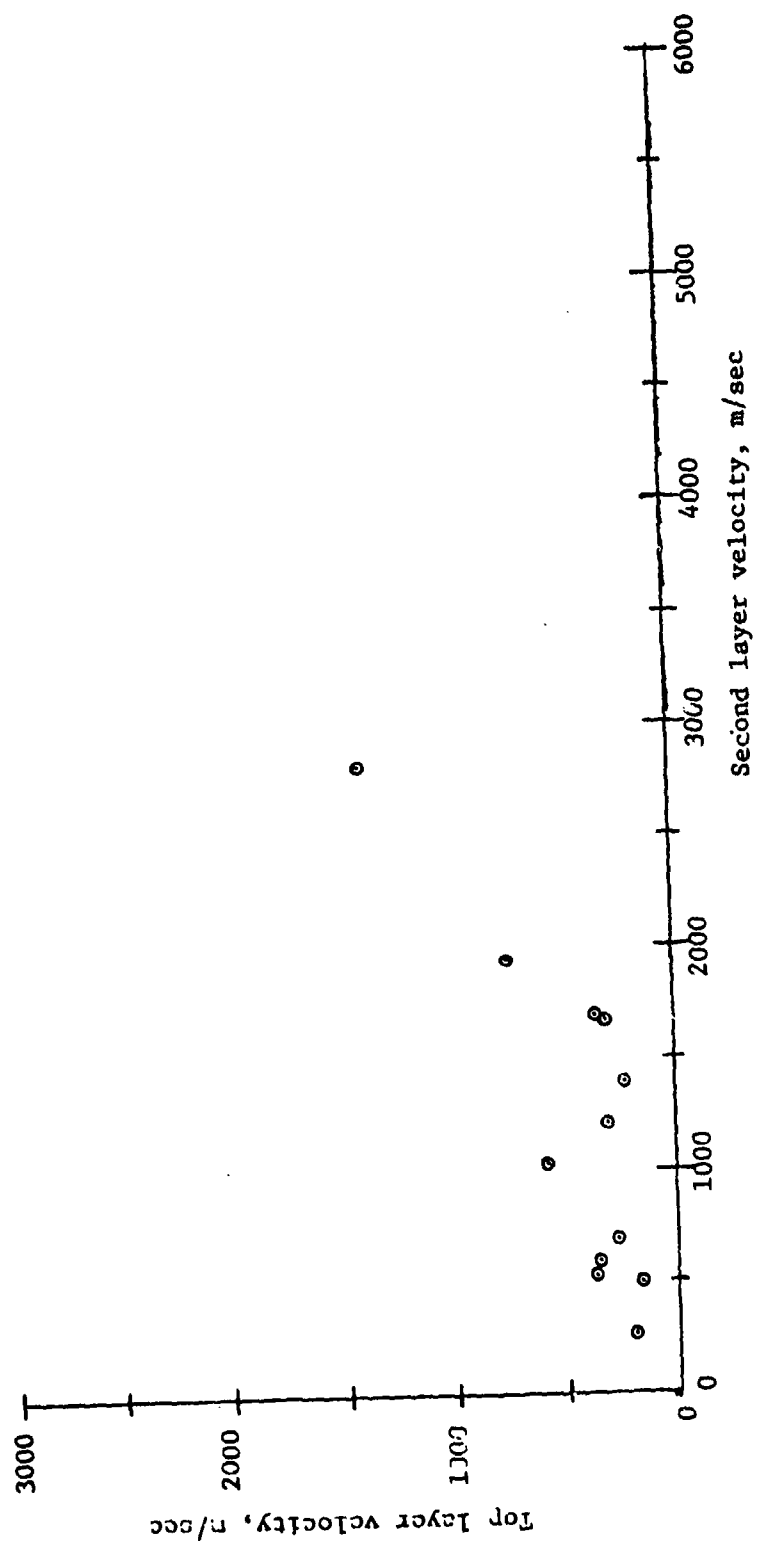


Figure 4. Top- and second-layer compression wave velocities for selected sites

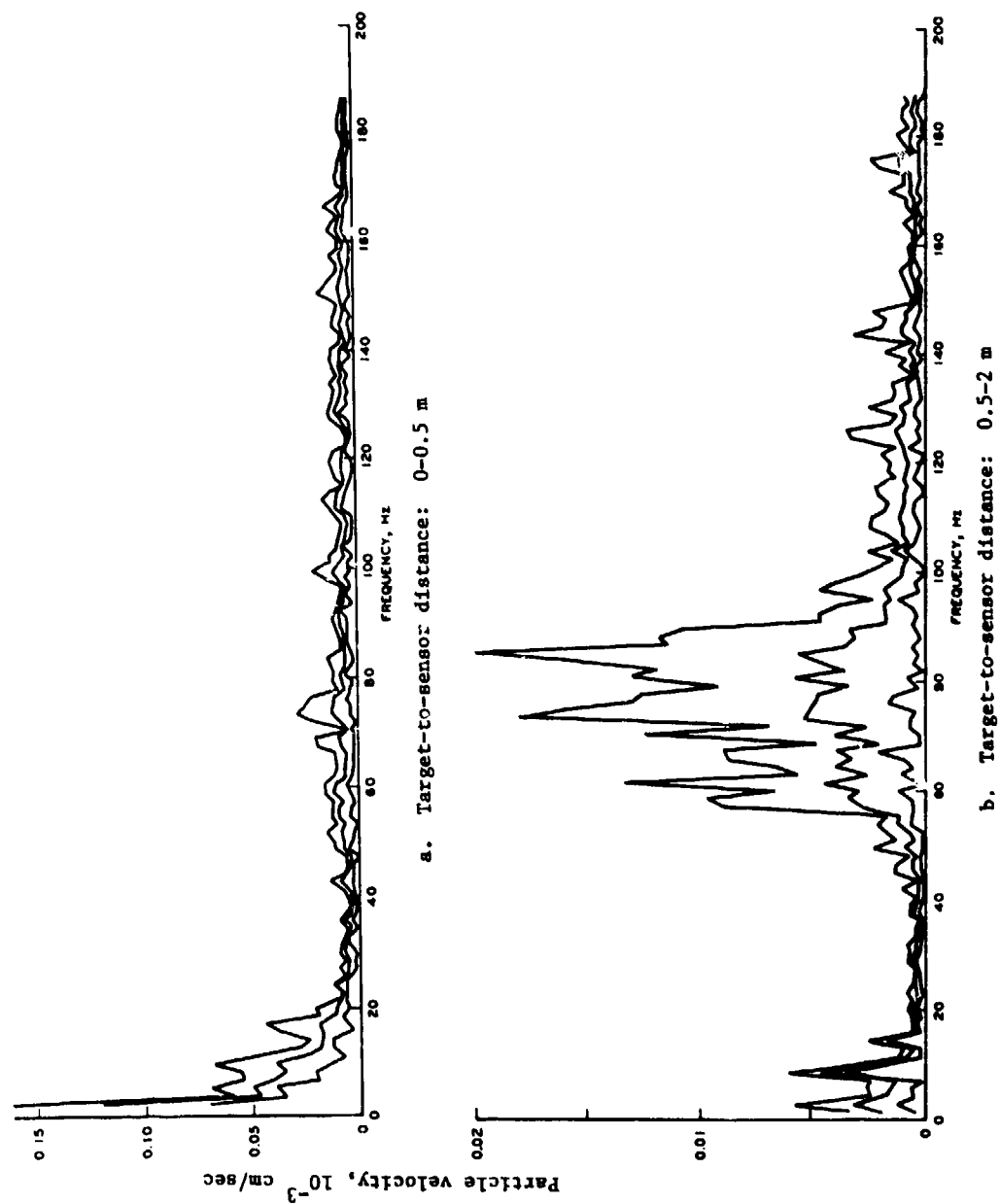


Figure 5. Example of the change in the frequency domain characteristics with target-to-sensor distance for man-creeping signatures (Fort Hood, site 8A)

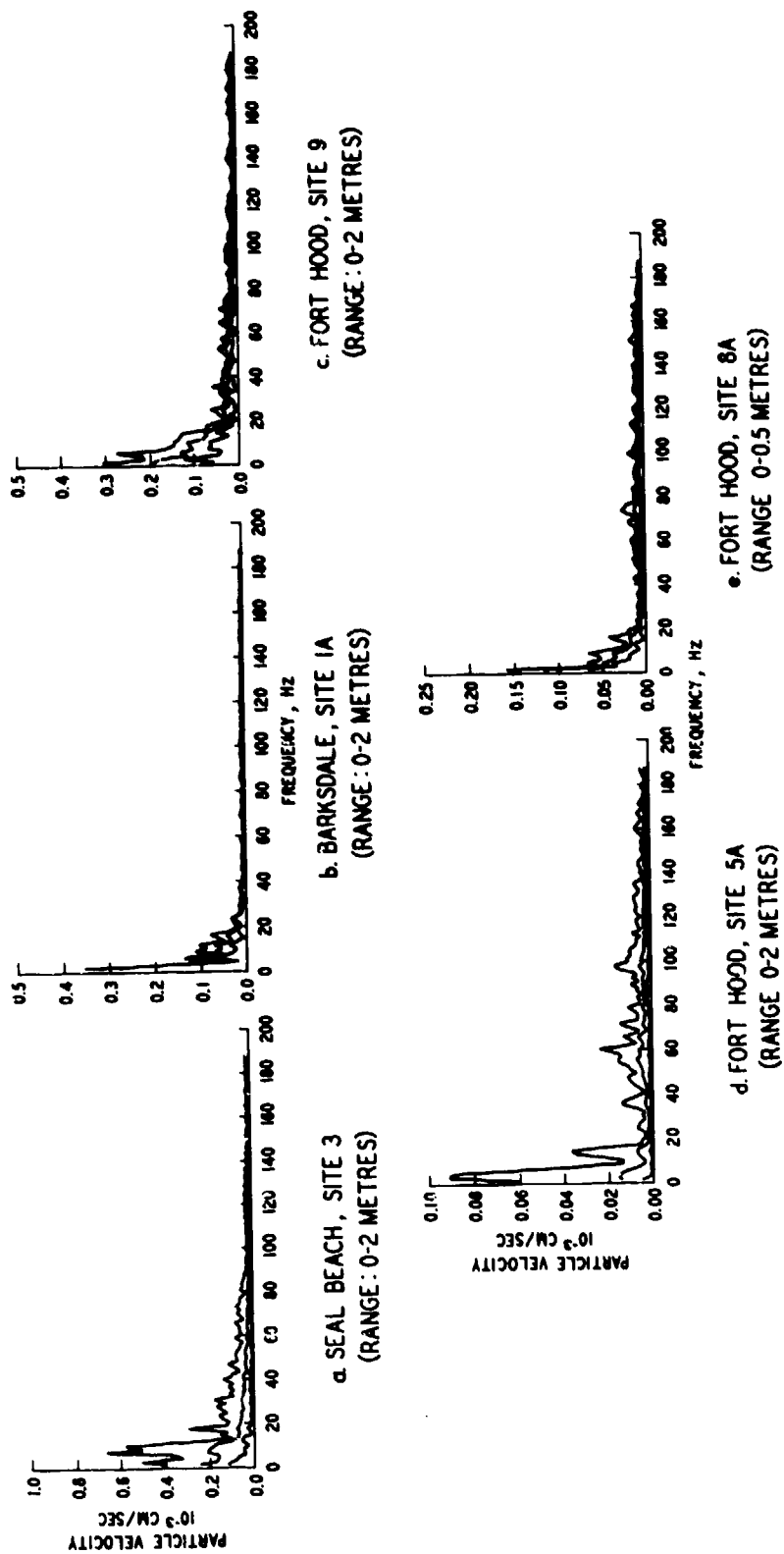
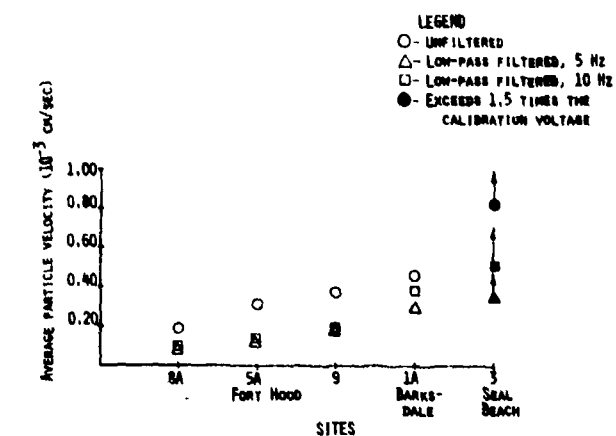
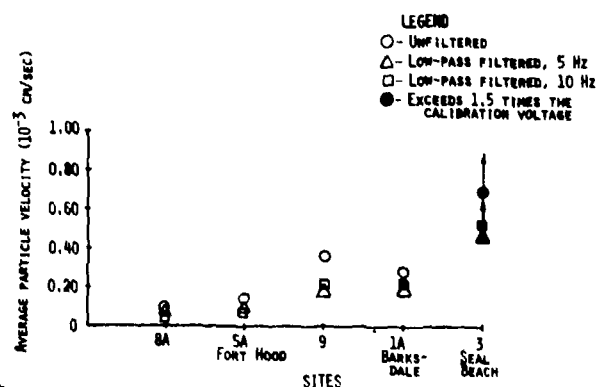


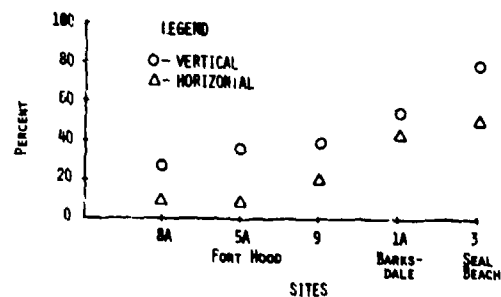
Figure 6. Frequency domain characteristics for man-creeping signatures



a. AVERAGE PEAK PARTICLE VELOCITY FOR VERTICAL COMPONENT OF MAN-CREEPING SIGNATURES FOR FOOTFALL 0.5 M REMOVED FROM SENSOR LOCATION



b. AVERAGE PEAK PARTICLE VELOCITY FOR HORIZONTAL COMPONENT OF MAN-CREEPING SIGNATURES FOR FOOTFALL 0.5 M REMOVED FROM SENSOR LOCATION



c. RATIO OF AVERAGE PEAK AMPLITUDE FOR FOOTFALL 0.5 M FROM SENSOR TO THE AVERAGE PEAK AMPLITUDE FOR FOOTFALL AT THE SENSOR

Figure 7. Average amplitude and amplitude ratios for near-distance, man-creeping signatures

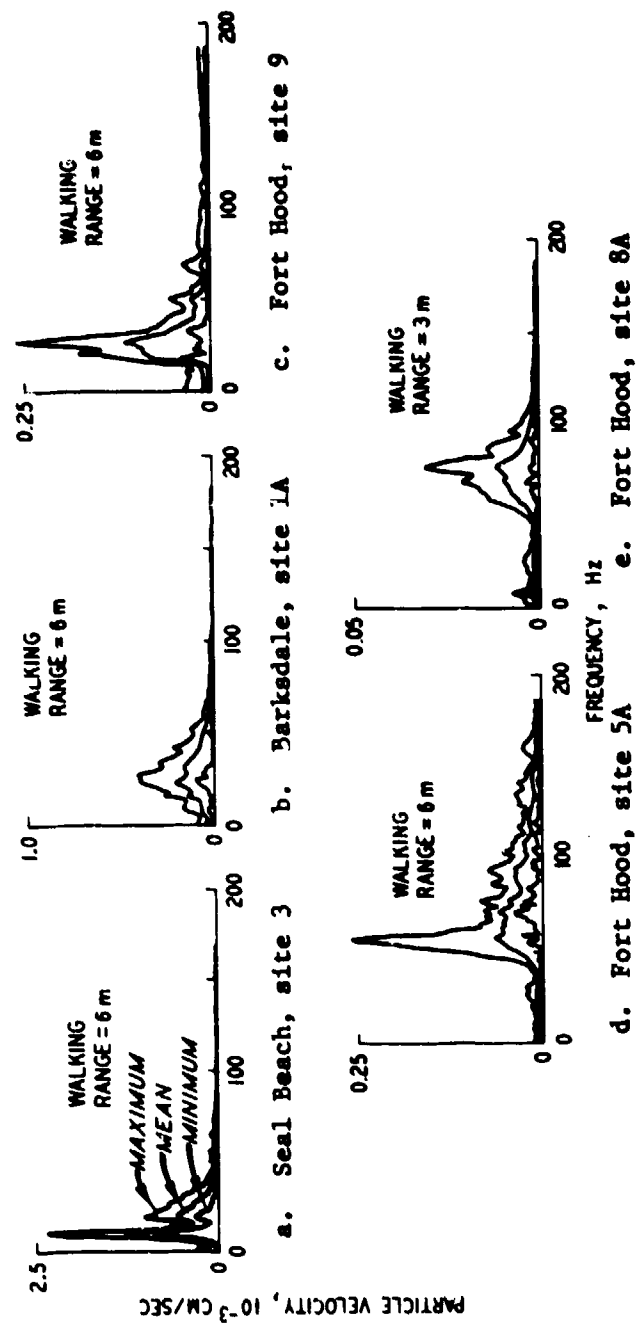
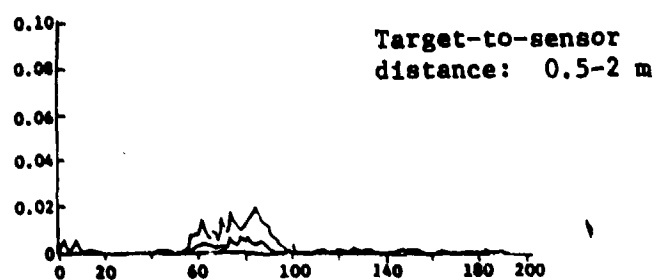
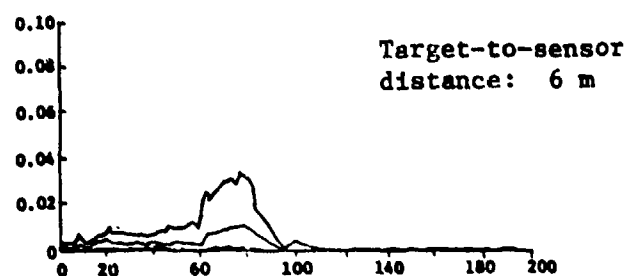


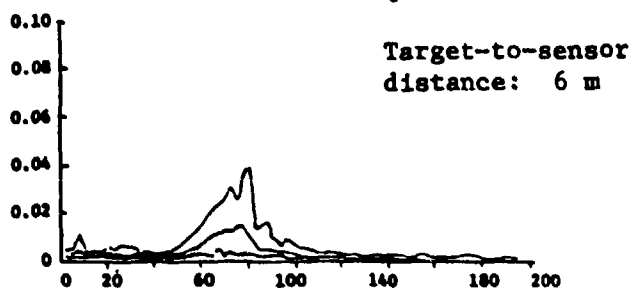
Figure 8. Frequency-domains of man-walking signatures (target-to-sensor distance = 6 m)



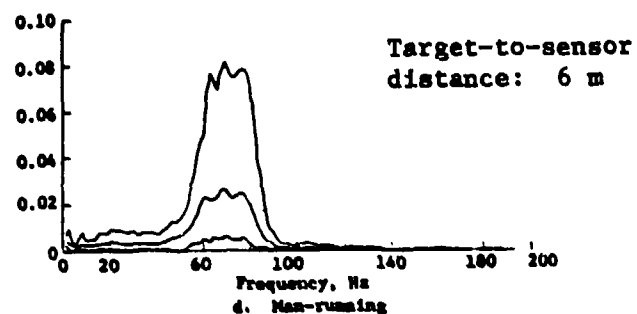
a. Man-crawling



b. Man-crawling



c. Man-walking



d. Man-running

Figure 9. Frequency-domains of personnel signatures for Fort Hood, site 8A

THE EFFECTS OF ARTIFICIAL LIGHTING
ON
CCTV PERIMETER ALARM ASSESSMENT SYSTEM

By

B. B. Jancowskis and D. K. Bellinger

Naval Avionics Facility
Indianapolis, Indiana

INTRODUCTION

BISS Advance Development Imaging Subsystem tests were conducted at BISS Test Site, Eglin Air Force Base, Florida. The objective of the tests was to demonstrate the accomplishments of initial development objectives as identified in the Program Management Directive, to assess the imaging subsystem performance, to provide test data with which to evaluate trade-offs and from which specifications and requirements could be prepared.

The test site installation consisted of an intrusion detection and alarm assessment systems. The intrusion detection system consisted of perimeter fence and fence disturbance sensors (FDS) on the fence, MAID/MILES 20 feet outside the fence, sensor communications (Small Permanent Communications and Display Segment (SPCDS)), and the Master Control Tower (MSCF) where the sentry was located. The advance development imaging subsystem integrated with the intrusion detection system consisted of silicon vidicon cameras, associated baseband and multiplex video communications, video switching and selection equipment, and a selection of potential artificial lighting configurations for around-the-clock alarm assessment capability. Although there were many objectives in the test program, this paper presents the alarm assessment results under the selected lighting configurations.

The role of the imaging subsystem is to provide an efficient around-the-clock intrusion sensor alarm assessment capability for high asset areas. The characteristics of current day intrusion sensors are excessive nuisance or false alarms which are generated as a result of system noise, natural phenomena and wild life. Thus in an operational scenario, the imaging subsystem role will predominantly require assessment of absence of an intruder and ascertain the cause of that alarm, which is a formidable task. In order for the imaging subsystem to be cost-effective it needs to establish the MSCF operator's confidence through efficient and reliable performance under a variety of environmental conditions. Prior to the test, the role of artificial lighting appeared to be straightforward. The test results indicate that the type of lighting,

its uniformity, and its location to the perimeter fence all contribute significantly to an effective imaging system.

LIGHTING CONFIGURATIONS EVALUATED

Two basic lighting configurations were evaluated: (1) IES Roadway (overhead street lighting), and (2) flood lighting (or frontal lighting). In the overhead configuration three separate variations were evaluated: (1) General Electric M250A luminaire (150 watt bulb) placed directly over the fence at a spacing of 105 feet, (2) General Electric M250A luminaire (150 watt bulb) placed over the inside fence of a double fence installation at a spacing of 85 feet, and (3) General Electric M400A luminaire (250 watt bulb) placed two feet inside the fence at spacing of 107 feet. In all of the overhead configurations the luminaires were at a height of 24 feet and used the high pressure sodium vapor bulbs. The flood luminaires (twin 250 watt bulbs) were 15 feet inside the fence at a height of 15 feet and a spacing of 115 feet. Photographs No. 1 through 4 show the respective lighting configurations.

LIGHTING CONFIGURATIONS EVALUATION METHOD

To evaluate the various artificial lighting configurations and the affect they have on the imaging subsystem, intrusion scenarios were prepared and intrusion tests were conducted. All cameras used in the intrusion scenarios provided the same field-of-view, thus, the intruders represented the same number of television lines. The intrusion corridors were at distances at which the intruders occupied 26, 39 and 52 television lines. The intrusion scenarios conducted required that the Air Force TAWC/TEHL operator make the assessment within 25-30 seconds. The objective of the intruders was to reach the fence and stay at the fence for 25-30 seconds, during which time the assessments were made. Table 1 shows the test results under the various lighting configurations.

SUMMARY

Table 1 summarizes the test results obtained during the imaging tests under the various artificial lighting configurations. The test results indicate significant performance differences exist under the various lighting configurations.

The best results were obtained in the most uniform overhead lighting (photographs 1 and 2). This lighting configuration presented no fence shadows or significant hot/cold spots.

The next best performance results were obtained with lighting which contained significant non-uniformity and fence blooming, but which created minimum fence shadows as shown in photograph 4.

The poorest performance results were obtained with overhead lighting which exhibited non-uniformity, fence blooming and fence shadows. The greatest contribution to the poor performance was the fence shadowing as shown in photograph 3.

CONCLUSION

Based on test results, the optimum lighting configuration for a silicon vidicon imaging alarm assessment system is the overhead IES using the General Electric M250A luminaires with the 150 watt high pressure sodium vapor lamps. This configuration is capable of providing uniform lighting with minimum fence glare.

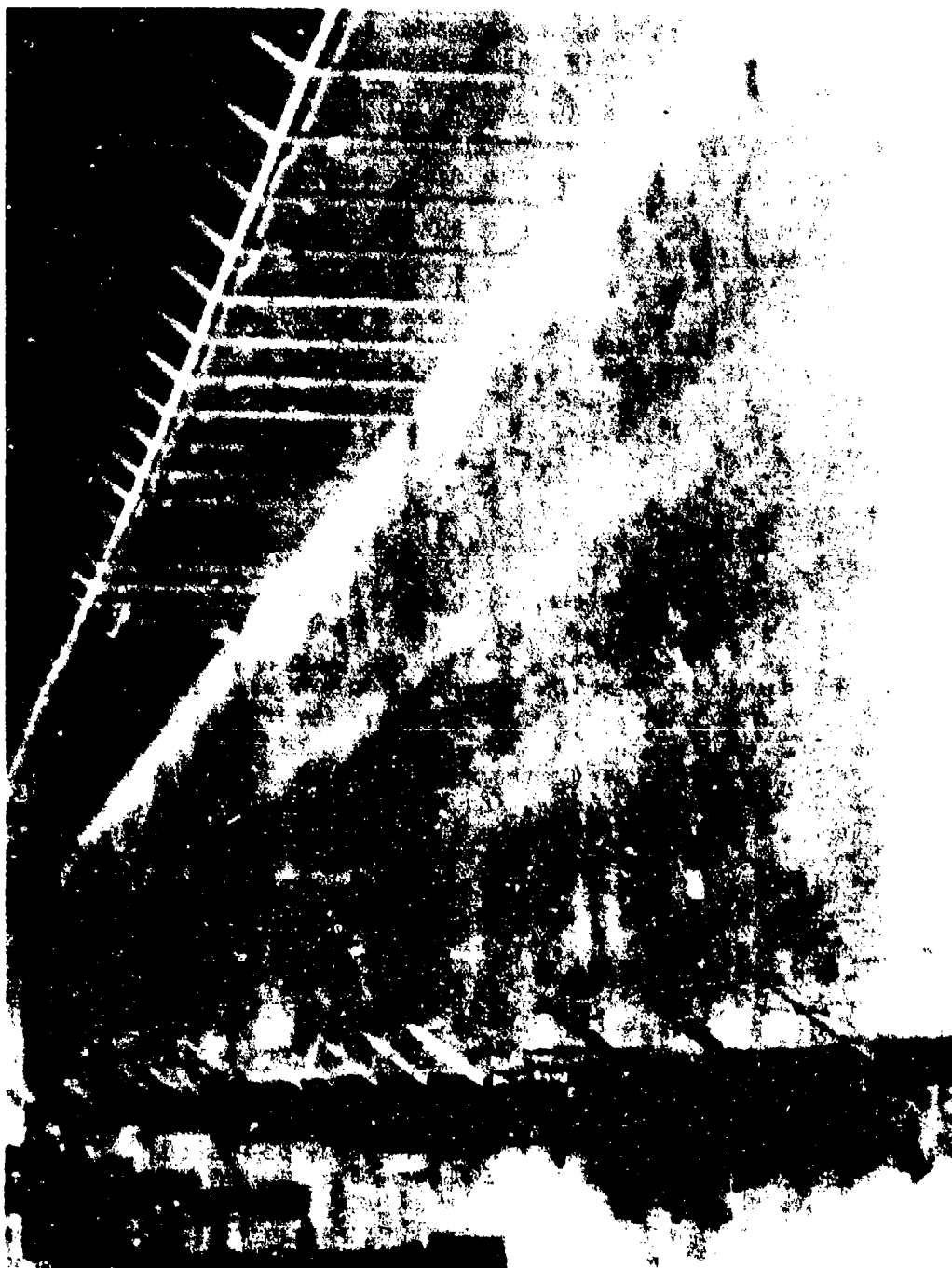
Table 1. Lighting Configuration Test Results

	IES Roadway Over Fence Photographs 1 & 2			IES Roadway Inside Fence Photograph 3			Flood Lighting Photograph 4		
Intruder Distance (ft)	320	215	160	320	215	160	320	215	160
No. of TV Lines	26	39	52	26	39	52	26	39	52
Probability of Correct Assess.	100%	100%	100%	32%	74%	100%	38%	86%	100%
Average Time to Assess	4.778	8.060	-	9.847	15.44	9.12	12.14	10.993	-
False Alarm Average Time to Assess									10.73

Photograph #1. IES Roadway, G.E. M250A
Directly Over The Fence



Photograph #2. IES Roadway, G.E. M250A
Double Fence Installation



Photograph #3. IES Roadway, G.E. M400A
Inside The Fence



Photograph #4. Flood Lighting



AN/GSS-20
BY
GERALD J. ZDYP
U.S. AIR FORCE ELECTRONIC SYSTEMS DIVISION
L. G. HANSCOM FIELD
BEDFORD, MASS. 01731

Introduction

General Purpose

(U) The Restricted Area, Anti-Intrusion Alarm Set, AN/GSS-20 hereafter known as the AN/GSS-20 is designed to provide warning of unauthorized entry into critical indoor areas such as warehouses, hangars, weapon storage structures, etc. A complete system consists of one console plus alarm set groups with associated control-power supplies for up to fortyzone . Each alarm set group and control-power supply combination is capable of guarding a specific indoor zone and reporting back to its own alarm module at the console. For covering large zones several groups can be connected to report to a single alarm module. Provision is made for authorized entry into protected areas by means of switch-locks and a two-wire multiplexing scheme allows placement of detection groups over a wide area such as a military base. Presently, the Air Force is procuring production quantities of the alarm set graphs to operate with the SPCDS (Small Permanent and Display Segment).

Functional Description of System

(U) A block diagram of the alarm system appears in figure 1 to 20 reporting control-power supplies may be placed across each twisted pair data link. Additional control-power supplies may be connected in tandem. Only one typical combination is shown.

(U) The console functions as a central alarm monitoring point for up to 40 detection zones. The console interrogates each master in turn and indicates its status on a separate alarm module. Provision is made to send a "self test" instruction to any zone as desired, which should result in an "alarm" for that zone. It is noted that interrogation scheme is fail-safe in that failure of any alarm set group in a zone to respond results in "no alarm" indication for that zone.

(U) Actual intruder detection is performed by the alarm set group which sends an alarm to the control-power supply, which in turn alerts the console via the twisted pair data link. Operating mode of the detection group is set by the switch-lock. Two modes are provided: "secure" which gives an alarm if an intruder moves within the protected area and "access" which allows authorized entry without an alarm.

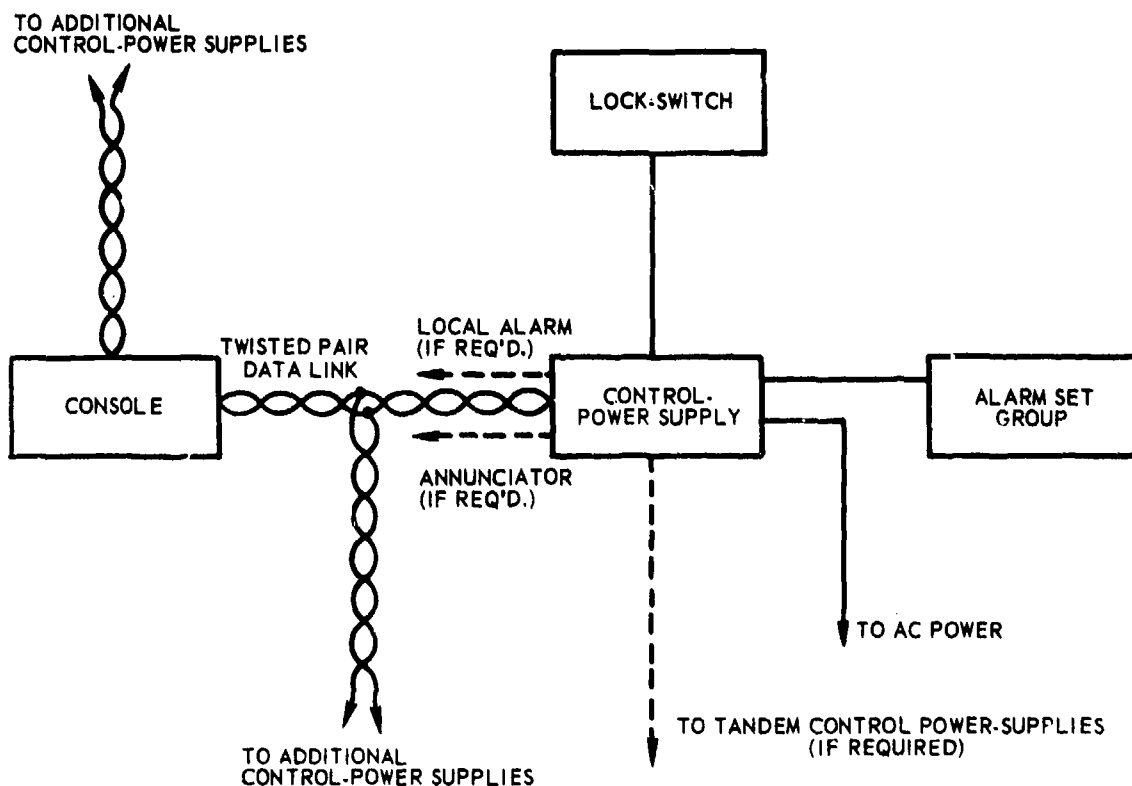


Figure 1 . Indoor Security Equipment Block Diagram

Principle of Intruder Detection

Actual detection of an intruder is carried out by means of a typical alarm set group. Briefly, the group transmits energy of a fixed frequency into its zonal environment while simultaneously receiving energy reflected back from that environment. As long as no moving intruder is within range of the group, transmitted and received frequencies are identical and no alarm is given. However, a moving intruder produces a Doppler shift between transmitted and received frequencies which is immediately detected by the group and interpreted as an alarm.

An important feature of the AN/GSS-20 is that each alarm set group employs two types of energy and derives two separate Doppler intrusion channels. An alarm is sent only when an intruder affects both channels simultaneously, thereby greatly reducing the probability of false alarms. The two types of energy employed are microwave (915+13 MEGA HZ) and ultrasonic (23KHZ), which have opposing trends with regard to false alarm susceptibility. Other features of the alarm set group include fail-safe tamper/performance monitoring and self-test circuits which can simulate an intruder.

Data Transmission and Monitoring

In many detection equipments operation of up to forty detection groups in conjunction with one console would require forty wire-pairs running back to the console. The AN/GSS-20 design reduces this to two wire-pairs by multiplexing up to twenty detection groups on a single pair. The multiplexing is time-division in that the console sends an interrogation code to each zone in turn and waits for a proper response before indicating a "secure or alarm" condition. The system is fail-safe in that lack of response from a given zone gives an "alarm" indication for that zone. Provision is also made for an "access" indication at the console when the switch-lock for a particular zone has been set to allow authorized entry. The console is equipped with rechargeable batteries to assure continued operation during a power failure.

Multiplexing at the alarm set group end of the circuit is accomplished in a control-power supply unit associated with each group. This unit also contains power supplies and rechargeable batteries for continued operation during a power failure. Provision is made for connecting several detection groups in tandem when large areas such as hangars, etc., are to be protected. The overall information transmission scheme also provides for radio and/or annunciator links.

Operation

Once the system is put into operation, the operator's functions are monitoring for alarms, acknowledging authorized access to the protected areas, and performing periodic system self-tests.

In the event of an alarm, the operator would set the RESET/ACK switch on the alarming module to acknowledge (ACK) to terminate the audible alarm. If there was prior knowledge of an authorized entry or exit from the area, the operator would reset the visual alarm indicator and note the change in the secure and access indicators. In situations where the cause for alarm is not known to be the result of an authorized entry or exit, the operator would notify the proper security forces, reset the alarm, monitor to see if the alarm situation persists, and keep the security forces advised.

The operator would also perform system self-tests at intervals defined by the cognizant security agency. This would require that the test switch on each alarm module be momentarily set to the system position and that each module be monitored for an alarm condition. An alarm condition under these circumstances informs the operator that the control-power supply, alarm set group equipment, the multiplexer link, and the console circuits associated with each alarm module are in an operating condition. At the end of these checks each alarm module would be reset to put the system back into the normal alarm monitoring status.

Characteristics and Arrangements

With reference to figure 2, the ISE consists of four parts-Alarm Set Group OA-8704/G, Control-Power Supply C-9173/G, Switch-Lock SA-1891/G and Console, and Anti-Intrusion Alarm Set OJ-279/G. The first three items are installed at the area to be secured and perform the functions of intruder detection and alarm data transmission. The Alarm Set Console is located remotely and serves to monitor the status of the various secured areas. It will be frequently referred to herein as the Central Monitoring Facility (CMF).

Alarm Set Group

The purpose of the alarm set group is to perform the actual intruder detection. A photograph of the alarm set group is shown in figure 3. In general, the units of the alarm set group consisting of one detector and two transducers are mounted approximately nine feet above the floor in the manner of light fixtures. Standard electrical conduit is employed throughout the installation. The group is protected by circuitry which sends an alarm if a tamper attempt is made. The detector dimensions are 13.125 inches by 13.125 inches by 2.5 inches and weighs 13 pounds, 8 ounces. Each of the two transducers is 5.5 inches by 5.5 inches by 2.5 inches and weighs 1 pound, 10 ounces.

Many variations of alarm set group installation are possible. For example, a small room may require only the detector. Large areas such as hangars will require a multiplicity of detectors and transducers. In such a case, alarm set groups must be operated in acoustic lock to avoid crosstalk within the ultrasonic portion of the system. Usually the units will be operated in tandem.

A block diagram of a typical alarm set group appears in figure 4. As mentioned previously, the group employs two types of energy for sensing intruders. Hence, the radar sensor block represents a complete microwave Doppler system, while the acoustic sensor block represents a complete ultrasonic Doppler system. Alarm outputs from these two sensors are fed to the combining logic, which sends an alarm to the control-power supply only when the radar and acoustic sensors alarm simultaneously.

This intruder simulation is made by applying a 28-Hz self-test voltage to the radar and acoustic sensors. This voltage is switched on temporarily when the "system self-test" switch is pressed at the console. The 28-Hz signals simulate Doppler from an intruder at both sensors, thereby bringing the system into alarm to indicate proper functioning.

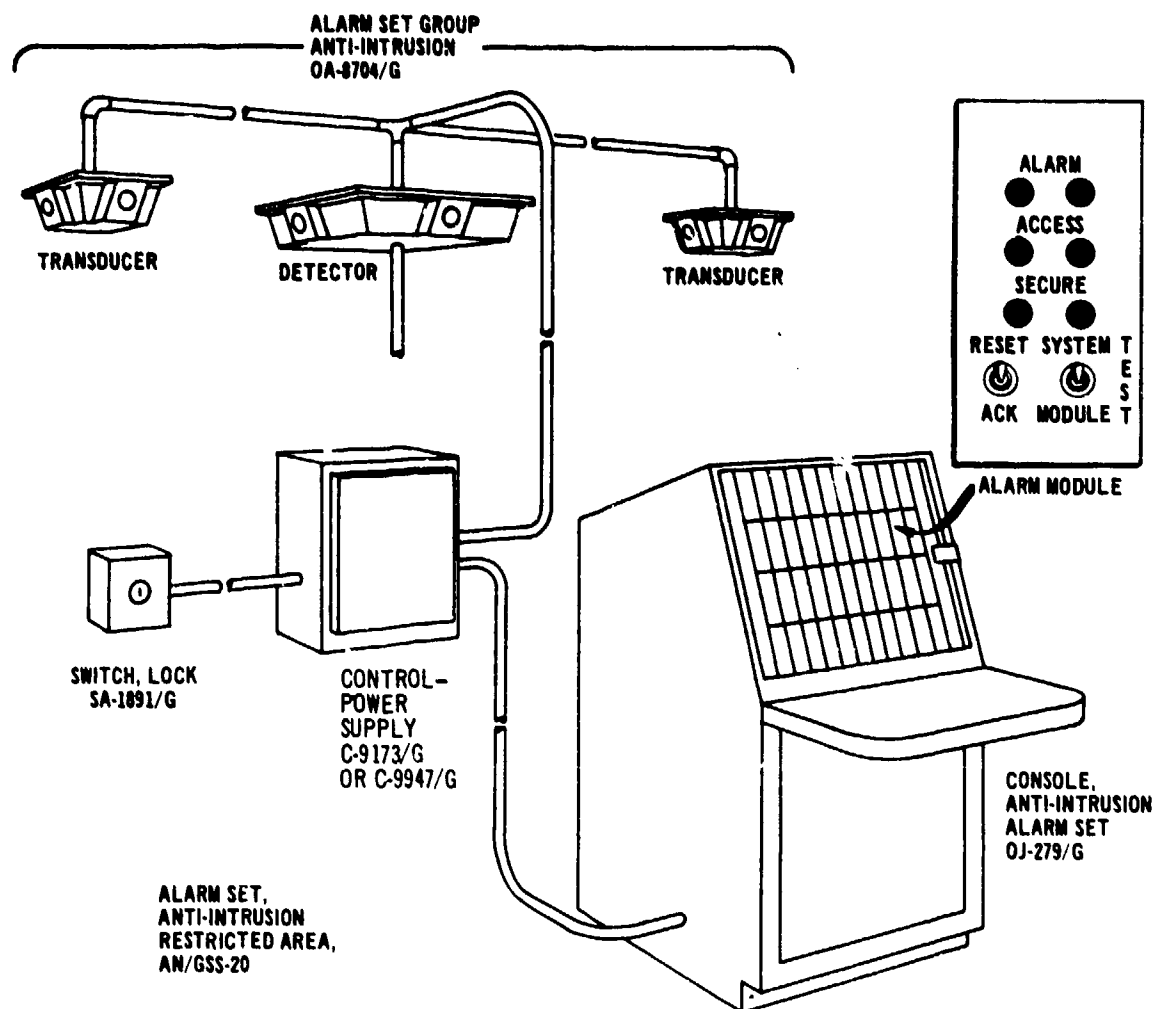


Figure 2 . Typical Detection Group Installation



Figure 3 . Alarm Set Group

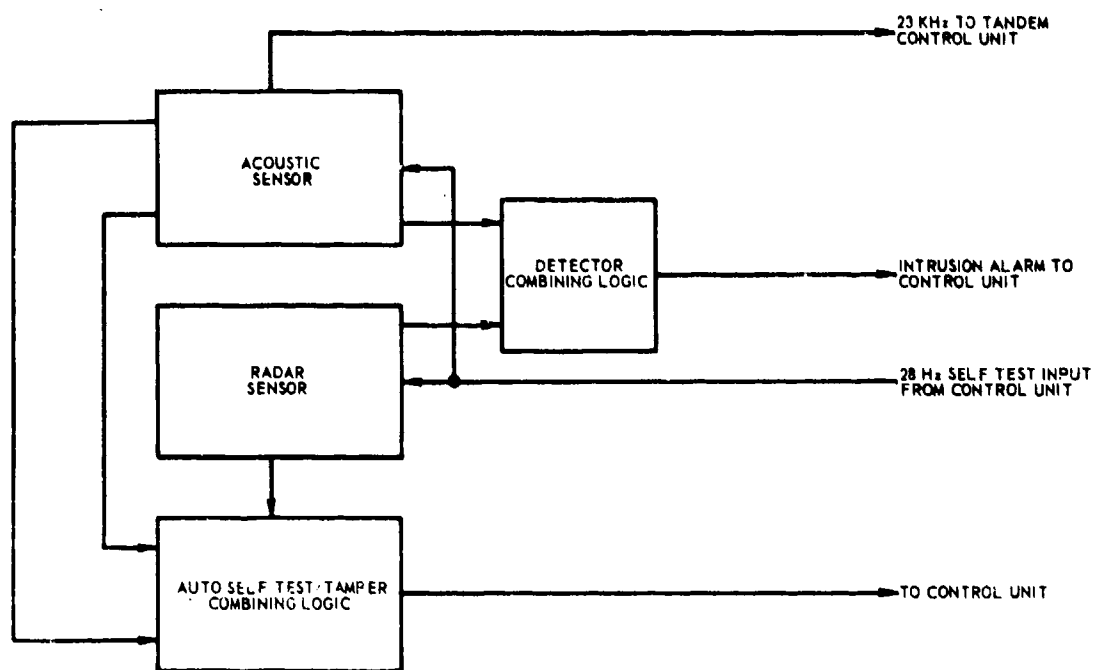


Figure 4 . Alarm Set Group Block Diagram

The block diagram of the radar sensor is shown in figure 5. A transistorized microstrip oscillator feeds microwave power through a special balanced mixer to a transmit/receive antenna extending from the underside of the detector. The mixer is capable of operating monostatically, i.e., it uses a single antenna for transmit/receive functions simultaneously. The mixer heterodynes the transmitted and received frequencies to derive the Doppler signal present when there is motion and applies this signal to a high gain Doppler amplifier. This amplifier consists of a filter-preamplifier driving a filter-postamplifier.

Assuming a Doppler signal has been detected and amplified, it is applied to the rectifier-integrator circuit. If the Doppler signal is of sufficient amplitude and duration, the rectifier-integrator builds up a dc level sufficient to trigger the alarm level detector and initiate an alarm output from the radar sensor. It is important to note that the integrator is an RC type which resets on its time constant, as contrasted with a C-type integrator which must be reset periodically by the logic.

A block diagram of the acoustic sensor appears in figure 6. This sensor differs basically from the radar unit in that the transmission and reception functions are carried out by separate sets of ultrasonic transducer elements, whereas a single transmit/receive antenna is employed in the radar sensor. Also, individual ultrasonic transducer elements are somewhat directive, as contrasted with omnidirectional azimuth coverage by the microwave antenna.

With regard to physical location of the various transducer elements, the four receiving sensor elements are aimed through apertures on the sides of the detector so that each sensor element covers a 90° azimuth segment. A single transmitting element (actually the ultrasonic frequency stabilizing element) is aimed through an aperture on the bottom surface of the detector. Power from this device enables the sensor to operate without the transducer units if only a small room is to be covered.

When more ultrasonic power is required, the transducer units must be used in conjunction with the detector unit. Each transducer unit employs four individual transmitting transducer elements with each covering a 90° azimuth segment. It is important to note that the transducer units and detectors may be rotated on the supporting conduit. For, example, one detector and one transducer might be aimed directly toward a high value resource for additional sensitivity in that region. Conversely, transducers might be aimed away from noise sources such as space heaters, etc.

Returning to the diagram of figure 6, outputs from the four receiving sensor elements in the detector unit are added in an RL combiner and applied to the 23-kHz filter-preamplifier. This circuit serves to restrict out-of-band noise and to amplify the desired signal. The amplified signal is next fed to a balanced mixer which derives any Doppler output present and applies it to the Doppler filter-amplifier. The rapid low end roll-off discriminates against the "wind noise" present in ultrasonic Doppler systems. Output from the Doppler filter-amplifier again drives a rectifier-integrator-level sensor chain, as described previously, relative to operation of the radar sensor.

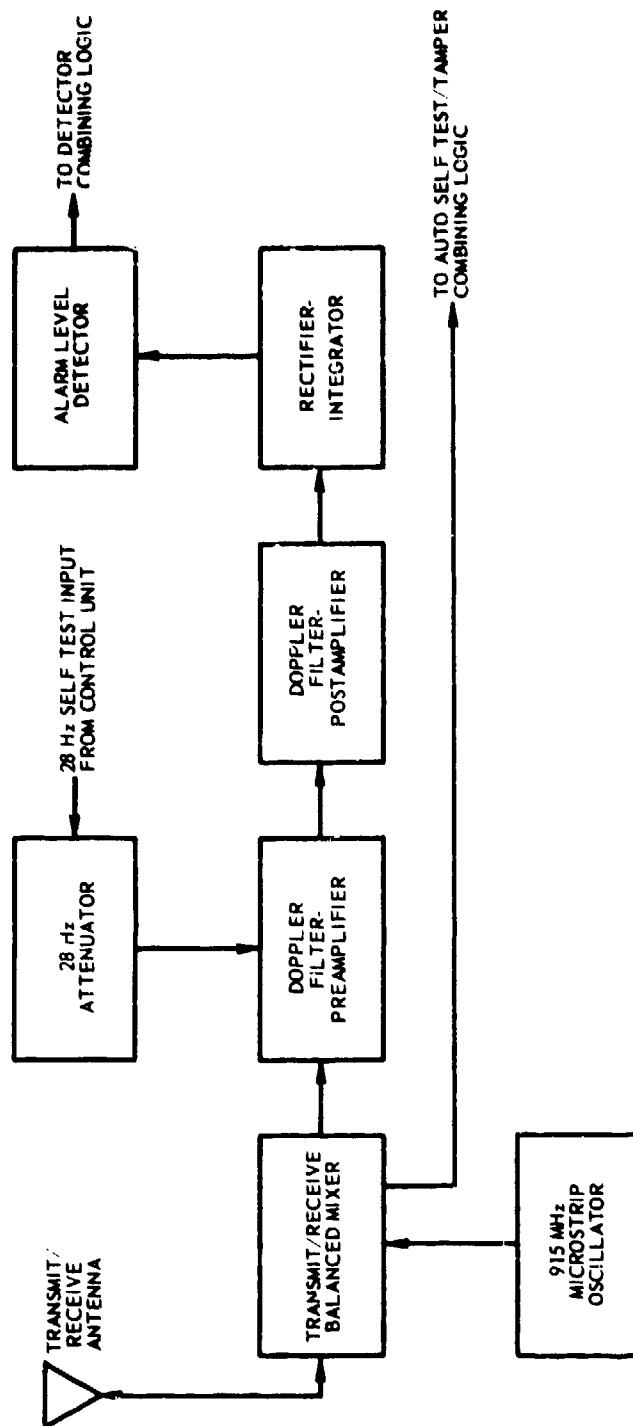


Figure 5 . Radar Sensor Block Diagram

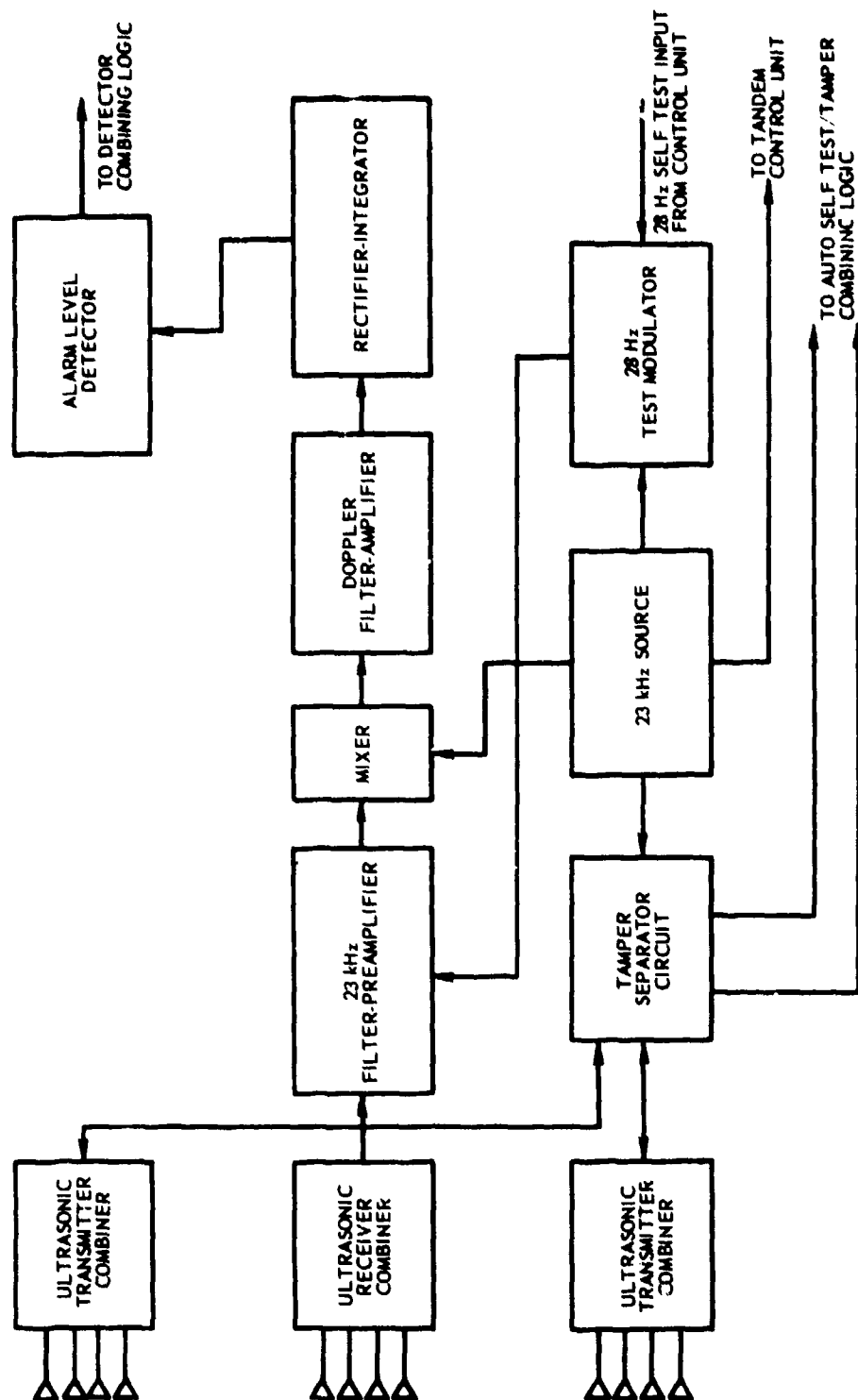


Figure 6: Acoustic Sensor Block Diagram

The acoustic sensor must be provided with means for injecting the 28-Hz self-test signal. While the sensor could be alarmed by coupling a 28-Hz voltage directly into the Doppler filter-amplifier, the 23-kHz filter-preamplifier and balanced mixer would not be tested by this procedure. This is circumvented by using the 28-Hz test modulator to amplitude modulate a sample of the 23-kHz operating power at 28 Hz. This modulated power is coupled into the 23-kHz filter-preamplifier, thereby the entire acoustic chain.

Ultrasonic operation power for the acoustic sensor is provided by the 23-kHz source. It is seen that this source drives the transducer units (via a tamper separator circuit), the receiving mixer, and the 28-Hz test modulator. A fourth connection is available for tandem arrangements. One important feature of the 23-kHz source is that the operating frequency is stabilized by the downward-pointing transducer element in the detector unit. Some 23-kHz voltage is developed across this stabilizing element, hence it transmits some ultrasonic power, as noted previously.

Figure 7 is a block diagram of the detector processor. The detector processor assembly contains the operational circuits which provide alarm outputs to the control-power supply when injected with the proper Doppler frequency and dc inputs.

Two channels which are identical except for biasing are provided for processing Doppler frequency inputs. Each channel consists of an active full wave rectifier, an active integrator and a dc level sensitive switch. The rectifier circuit accepts a Doppler input and converts it to a plus level at the output which varies in direct proportion to the input ac swing. The integrator circuit integrates the dc level at the rectifier output with respect to time. The integrator output swings negative for a positive input and is a function of the input signal level and duration. The switch circuit is biased from a zener regulated source, such that its output is more negative than the switch bias point. When the integrator output swings more negative than the switch bias point, the switch changes state and its output goes to a level more positive than -1 Vdc. The two Doppler processing channel outputs are connected to a diode AND gate. The AND gate output remains negative when either or both inputs are negative. When both inputs are positive the AND gate output goes positive. This output is supplied to the control unit as an intrusion alarm.

Control-Power Supply

The control-power supply provides the interface between the alarm set console and the remote alarm set group intrusion sensors. As an interface unit, its alarm logic processes intrusion and tamper alarms and secure/access status information, and its transmission link logic controls the transmission of the status information to the monitoring alarm set console. In addition, it supplies power to the alarm set group and to its own internal logic circuits.

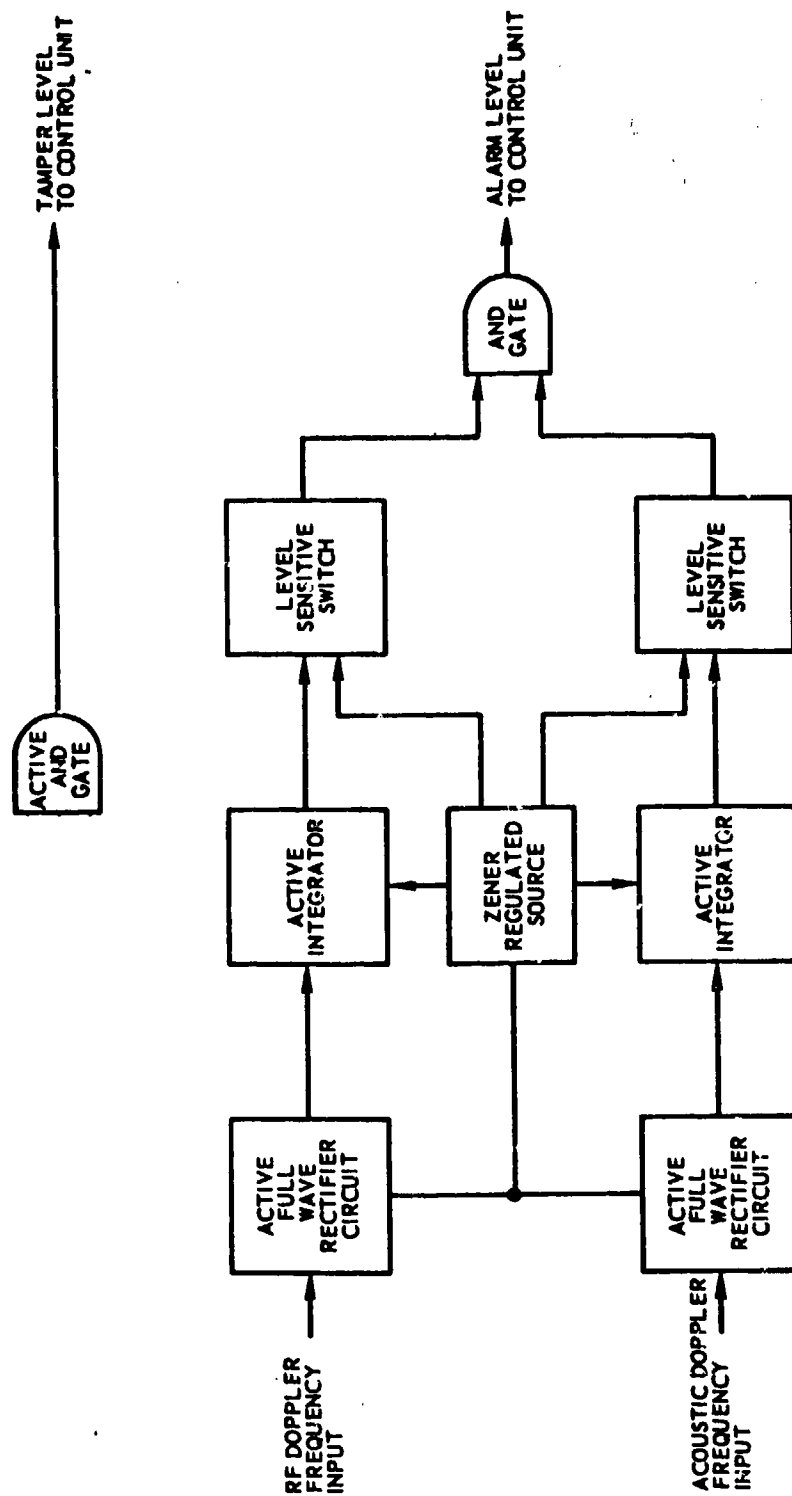


Figure 7 Detector Processor Block Diagram

The Control-Power Supplies (CPS) C-9173/G and C-9947/G are functionally identical in their application with other units of the AN/GSS-20 Alarm Set System. The C-9173/G unit contains additional interface circuits which permit alternate security system configurations to be formed by employing DSPG sensors and radio transmission equipments.

The two models of the CPS unit, shown in figures 8 and 9, are housed in aluminum boxes having the following features. Flanges are provided for convenience in mounting the units onto the wall. The hinged front covers are fitted with Ace-type locks. An interlock, tamper switch, is also provided so that a warning (in the form of an alarm) is given when the covers are opened. This tamper switch can be manually reset to terminate the warning alarm while performing maintenance on the CPS unit.

The dimensions and weights of the CPS units are as follows: The C-9173/G unit is 12 inches wide, 16 inches long, and 8.5 inches high. The unit's weight including batteries is 43 pounds. The C-9947/G unit is 14 inches wide, 16 inches long, and 6 inches high. The unit's weight including batteries is 38 pounds. The C-9947/G unit is presently being procured by the AF.

The CPS was designed for operation over the temperature range of -20°F to $+150^{\circ}\text{F}$, and for storage over the temperature range of -80°F to $+160^{\circ}\text{F}$.

The CPS will operate from any ac source of 120 volts $\pm 10\%$ at 2 amperes, at a nominal frequency between 50 Hz and 400 Hz. An indicator lamp is provided on the top of the CPS unit to indicate when the ac power is on. The ac input passes through an RFI filter, located inside of the CPS, before going to the power supply. In case of a power failure, the CPS was designed to operate for periods up to 24 hours from 4 self-contained batteries.

Switch-Lock

The switch-lock, shown in figure 10, is contained in a box 3.75 inches square and 2.5 inches deep. The unit weighs 1 pound, 4 ounces. It contains an interlock, tamper switch, which gives a warning if the cover is loosened or removed. It also contains an Ace-type switch which operates an off/on switch as it is rotated from the SECURE to ACCESS position. The switch-lock being procured under the present AF contract will allow only key removal in the secure mode.

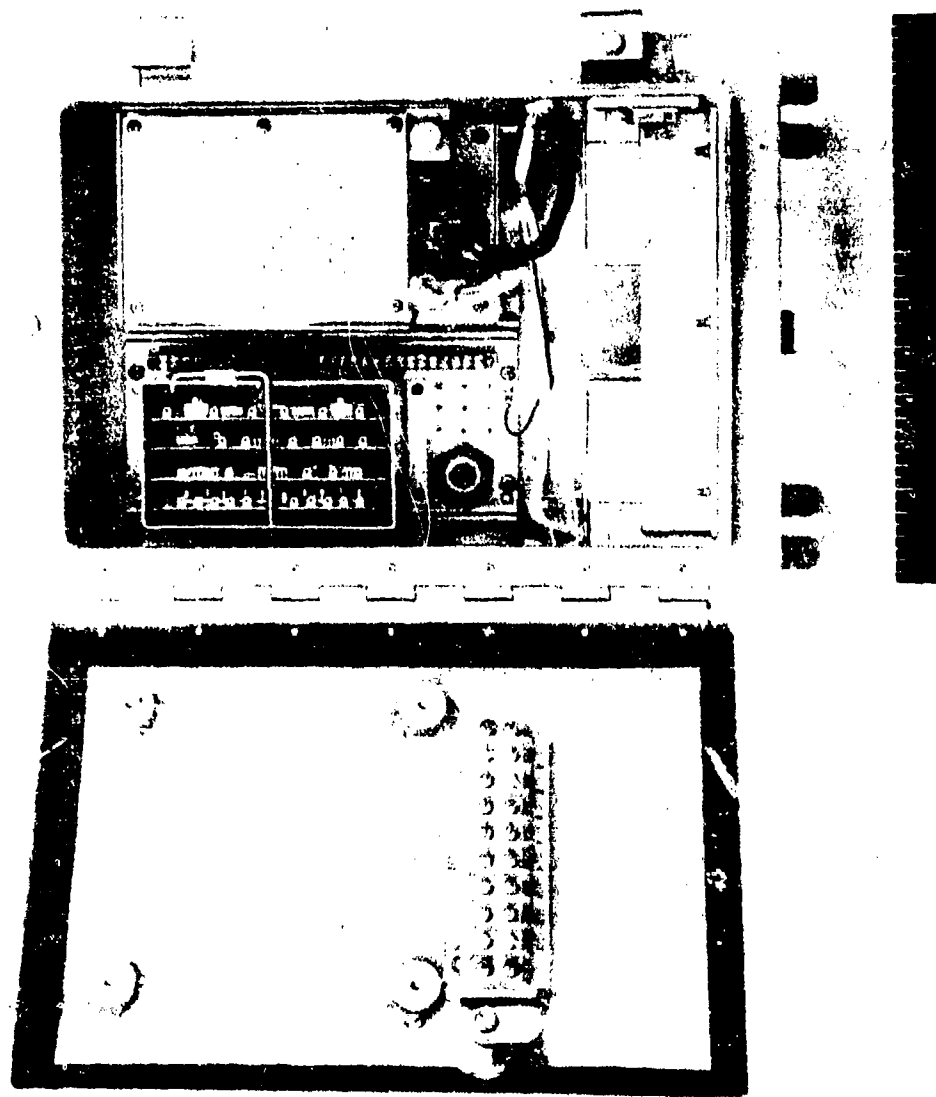


Figure 8 . Control-Power Supply, C-9173/G

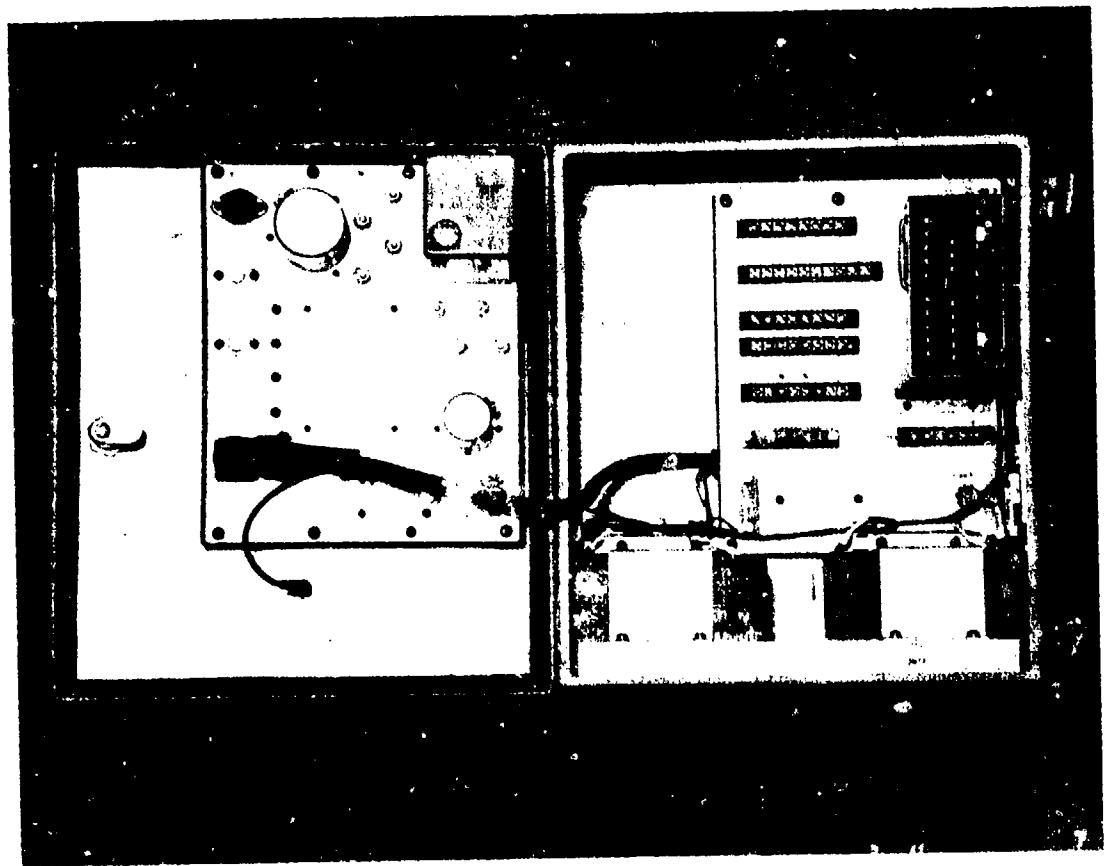


Figure 9 . Control-Power Supply, C-9947/G



Figure 10 . Switch-Lock

Console, Anti-Intrusion Alarm Set

The console, anti-intrusion alarm set serves as the Central Monitoring Facility (CMF) when the appropriate number of alarm modules are installed. It is housed in a commercial-type rack enclosure as shown in figure 11. The lower portion of the enclosure contains the batteries and power supply, all of which are mounted on the base of the enclosure. Mounted in a module tray at the top of the lower compartment are the control switches and the control logic circuit boards. A door, on the lower compartment, has a writing surface on the top providing the operator with a work surface approximately 27 inches by 13 inches.

The upper portion of the enclosure contains 4 card trays that permit the use of up to 40 alarm modules. The modules plugged into their respective positions from the front are held firm by a door constructed like a grid which can be locked when operating the CMF.

The rack for the CMF measures 27.5 inches wide, 25.5 inches deep, and 52 inches high, not including the writing surface mounted on the door of the lower compartment. The CMF weight is approximately 300 pounds without the batteries.

The CMF will operate from any ac source of 120 volts \pm 10% at 5 amperes, and a frequency of 50 Hz to 400 Hz. The ac passes through an RFI line filter located inside the CMF rack before going to the power supply. In case of a power failure, the CMF was designed to operate for periods up to 24 hours from 4 self-contained batteries.

The CMF was designed for operation without batteries over a temperature range of -20°F to +150°F, and for storage over a temperature range of -80°F to +160°F.

Provisions have been made to permit a console to also operate as a remote monitor unit. When used in this manner the CMF controls interrogation of the CPS's and the remote monitor also observes the replies.

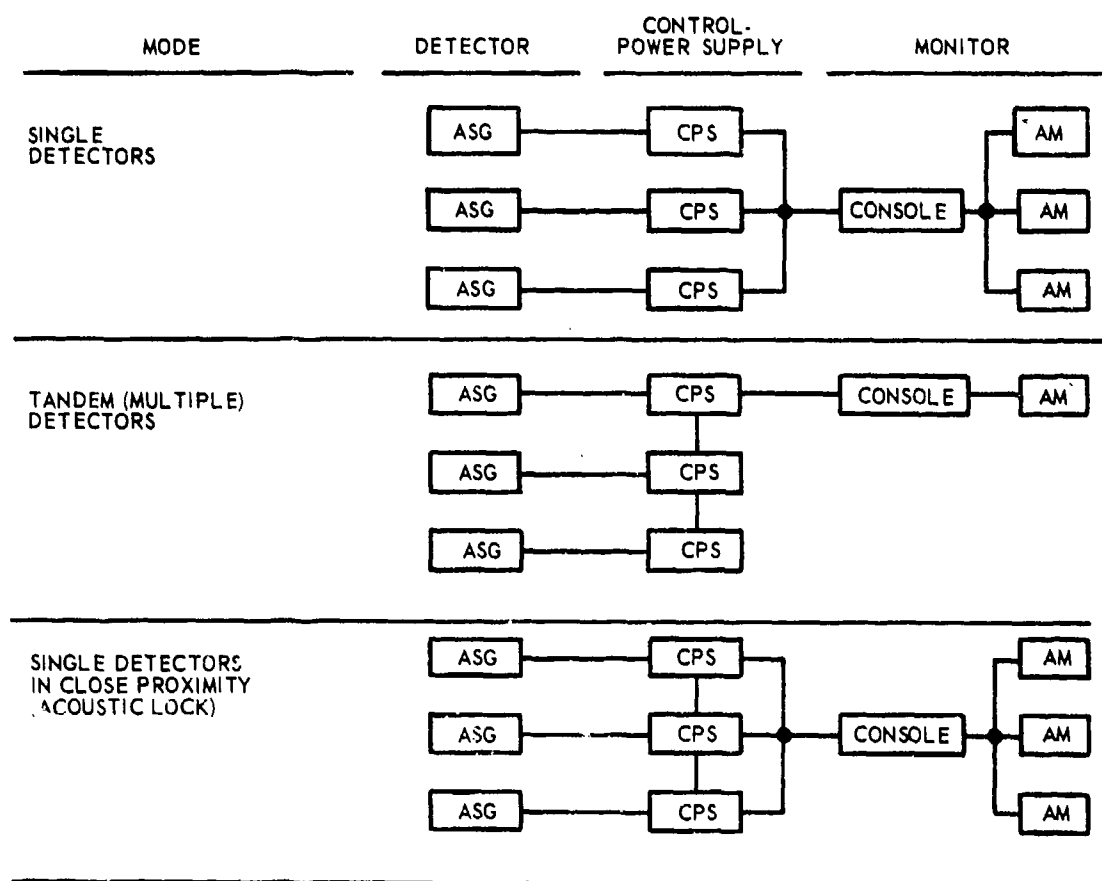
Modes of Operation

The AN/GSS-20 system is designed to operate in one of several modes as shown in figure 12. These modes are obtained through appropriate interconnections between and within the CPS units.

Alternate security system configurations can be formed using components of the AN/GSS-20 Alarm Set in conjunction with DSPG specified security devices. Certain of these alternate configurations are, however, obtainable only with the C-9173/G CPS unit.



Figure 11 . Console



*ALARM MODULE

Figure 12. AN/GSS-20 System Modes

AN/GSS-20 System Modes

The two basic AN/GSS-20 system modes of operation are: (1) the single detector mode, (2) the tandem(multiple) detector mode. In addition it is possible to operate single detectors in acoustic lock when close proximity could provide mutual interference.

In the single detector mode of operation, the status of each alarm set group (ASG) is presented on a separate alarm module at the monitoring console. This mode is normally used when the area to be protected is small enough to be covered by a single alarm set group and the security requirements warrant separate monitoring of the area's status. It is also applicable in large areas covered by multiple alarm set groups where the security requirements warrant independent monitoring of the specific sectors covered.

In the tandem (multiple) detector mode of operation, the status of two or more alarm set groups are consolidated for presentation on a single alarm module at the monitoring console. This mode would be used to cover a large area such as aircraft hangars or a group of isolated areas such as secured areas in the same building. In the tandem mode, the outputs of the multiple alarm set groups are transferred via their respective control-power supplies and mixed in one CPS for transfer to a single alarm module in the monitoring console.

In acoustic lock operation, the acoustic oscillators of adjacent alarm set groups are locked to the same acoustic frequency to prevent interaction of the acoustic systems of the two alarm sets. Acoustic lock is therefore used whenever there is insufficient acoustic isolation between adjacent alarm set groups. This condition may exist when alarm set groups are operated in either the single or tandem detection modes.

Alternate Security Configurations

Alternate security system configurations can be obtained by substituting various detectors and/or monitoring equipments.

Sensors designed to DSPG specifications can be used with the CPS C-9173/G in place of the alarm set groups in either the normal or tandem modes of operation as shown in figure 12. Acoustic lock operation would not apply to this sensor.

Similarly, the DSPG specified Status Transmitter/Line Supervisor (ST/LS) equipment can be used with the CPS C-9173/G as monitors in place of the CMF console.

Local Audible Alarm Sets and the ID-1631/AGSQ Annunciator can be used in conjunction with either model of the CPS.

TEST RESULTS

Following environmental qualification at the contractor's plant and at an independent testing facility, which verified that all design requirements had been met, the equipment was sent to the Armament Development and Test Center (ADTC), Eglin AFB, Florida. Much of the data and observations which follow are extracted from an ATCD Technical

Report which was prepared by Mr. W. Garrett of the 3246th Test Wing. The last paragraph addresses a separate evaluation of the AN/GSS-20 against weapons storage safety requirements, with emphasis on nuclear weapons.

The AN/GSS-20 sensors were installed at Eglin AFB, Fla., in five warehouse type building of a variety of construction material including wood, concrete block, and metal. Tests were conducted with and without programmed stimuli under various conditions. All intrusion attempts at all buildings were detected. Statistically, (there were 620 programmed intrusions) this works out to a probability of detection of 0.95 or greater at the 90- per cent confidence level. Intrusion speed was approximately 1 foot per second. False alarm testing was conducted for 1,246.6 detector hours. During this period twenty-four alarms occurred. Seventeen of these were correlated (by monitors keeping each detector under constant visual surveillance) to known sources, leaving a total of seven false alarms. Twenty vehicle passes were made along the exterior walls of each building. These vehicle passes generated no false alarms. The system operated with up to 5.1 miles of telephone cable (26 AWG) between a protected area and the central monitoring facility. Under extreme temperature and humidity conditions (-20°F to +150°F at 95% humidity) some variations in the detection range (adjusted at 70°F) were noted. Operationally, however, the sensitivity could be adjusted to give the designed detection range at these environmental extremes. Generally, motion was not detected when objects opaque to the transmitted energy (such as stacked oil drums) prevented a clear line-of-sight between detector and the intruder.

Building were selected at Eglin AFB were actually in use by various base activities. Three of these were specifically selected to provide certain "worst case" operating conditions. One (bldg 606) was a large (40X200X20 ft) metal building of "Quonset Hut" type construction. This building expanded and contracted with the weather and had large suspended sliding doors which were susceptible to movement from wind. Another (bldg 609) was a large (40X200X12 ft) wooden warehouse with numerous holes in the walls and exhaust fans in the roof. A third was also of wooden construction. The other building selected were more "normal" and included a concrete block warehouse and a metal laboratory building.

The building 609 installation was a "worst case" effort, but results are representative, so these are presented. This building was primarily used to store furniture, including: desks, chairs, dressers, and mattresses in large stacks. All of this material was in a constant state of flux, so at any one time different areas of the building would be "shaded" by the stored material.

Intrusions were made at three speeds: walk at 3 to 5 feet per second (normal), walk at 1 foot per second, and crawl on hands and knees at 1 foot per second. All movements were made as fluid as possible. Hands and arms were held firmly down by the sides of the intruders and footsteps were as slow as possible while maintaining the required speeds. The movements were executed in this manner to prevent a rapid foot or arm movement from generating an alarm. All intrusions were detected.

False alarm test time for building 609 was 50.8 hours. Since there were ten detectors, this represents a total detector time of 508 hours. During this period one false alarm was reported. The telephone line length between building 609 and the CMF was 2.9 miles.

The system in building 609 was also run with the AC power disconnected. It operated normally for three days on internal batteries before the voltage dropped low enough to cause constant alarms.

Twenty vehicle passes by a 3/4 ton pickup truck, within between 2 and 3 feet of the building, caused no false alarms. The microwave channel was detecting the truck through the wooden walls, but the ultrasonic was not, and hence no alarm.

On several occasions, the ceiling exhaust fans were turned on. Specific, tabulated intrusions were not run, but each channel was examined to see how it reacted. The ultrasonic channel showed a slight increase in sensitivity, but did not false alarm. The microwave channel was not affected. The detector housing forms the ground plane for the microwave antenna. The detectors were approximately 8 feet above the floor. The fans were another 10 to 12 feet above the detectors. For this reason there was no appreciable microwave energy at the fans, and hence their motion was not detected.

Weapons Storage Criteria: An operational AN/GSS-20 system was installed in two, empty special weapons storage facilities and evaluated jointly by the Air Force Weapons Laboratory (with inputs from the Defense Nuclear Agency) and the RISS Program Office. Particular attention was given to a fail-safe analysis (there is no failure mode in which the microwave power-out can increase) and radiation field strength. Allowable field strength, at the frequencies in question, is 18 volts per meter for all weapons, and 200 volts per meter for personnel. The AN/GSS-20 created field strengths which ranged from 0.0081 to 0.630 volts per meter.

Additional analysis was conducted on the radio link relay, which is the only moving part in the system. The cognizant Air Force Office for weapons storage safety is AFSC/IGF. On 16 July 1974, AFSC/IGF issued authorization for the use of the AN/GSS-20 in both conventional and nuclear storage facilities.

However, Provisions of AFM 127-100 (C5) must be strictly met. Based on calculations for the worst-case failure mode, the minimum distance between the AN/GSS-20 antenna and containerized FED's having leads (shorted) is 0.78 ft. For containerized leadless EED's the minimum distance is 6.0 ft per AFM 127-100(C5). The above assume a minimum "No Fire" sensitivity of 50 milliwatts. The AN/GSS-20 should not be installed in structures used for EED storage if the above minimum separation distances cannot be met by the Base munitions maintenance agency. In class 1, division 1 hazard areas and in any area where flammable dusts, gases or vapors may be generated the AN/GSS-20 should not be used.

PRACTICAL TESTING AND CALIBRATION
OF
ELECTRODYNAMIC SEISMOMETERS (GEOPHONES)

by
Louis Lechenger

Louis Lechenger is a 1942 graduate of the University of Texas College of Engineering with a B.S. degree in Mechanical Engineering. Upon graduation, Mr. Lechenger served in the United States Navy as an aeronautical engineering officer in overseas service units and with the maintainance division of the Bureau of Aeronautics. Mr. Lechenger served in the fields of business management, aeronautical radio, and electrical calibration prior to joining Geo Space Corporation in 1966. He currently holds the position of Staff Engineer in the Sensor Division with Geo Space, and is in charge of the development and test of geophones, hydrophones, and other sensor related products.

DESCRIPTION AND GENERAL CHARACTERISTICS

Geophones, seismometers, or velocity sensors of the electrodynamic transducer family may be tested and calibrated by many methods. Some are simple, and some are more complex. Some methods require only a good oscillator, a few resistors, a good oscilloscope, and a few other items usually found in any small plant that has basic test equipment. Other methods of investigation require complex real time analyzers, automatic tracking vibration systems, and complex analysis programs.

Geophysical seismometers, currently manufactured, range in weight and size from 19 gm and 1.68 cm diameter to 1680 gm and 11.1 cm dia. Construction is generally cylindrical with a central magnetic structure surrounded by a moving coil suspended on dual spider springs and a cylindrical outer pole which sometimes serves as the outer case of the seismometer. A sketch of a typical small single coil unit and a hum balanced dual coil unit is shown in Fig. 1. A typical large seismometer with provision for frequency adjustment, a separate calibration coil, and a double wound hum canceling moving coil is shown in Fig. 2. When properly attached or coupled to the ground, or any other vibration transmitting medium such as a building structure, a vehicle, or even the water, the outer case of the seismometers will follow the particle motion of the medium and a voltage will be generated in proportion to the relative motion between the inertial element (the moving coil) and the magnetic structure (the case and magnet). Typical frequency response curves of this large seismometer are shown in Fig. 3. Fig. 4 shows typical phase response curves of this type of sensor.

A. Factors affecting the amplitude and phase of the generated voltage are:

1. Amplitude and frequency of the wave particle velocity.
2. Ratio of the excitation frequency to the natural frequency of the seismometer.
3. Intrinsic sensitivity of the seismometer.
4. Damping of the seismometer.
5. Ability to properly couple the seismometer to the driving media.

- B. Factors affecting performance and reliability are the effects of heat, cold, humidity, shock, and vibration on the life and calibration of the seismometer.
- C. Other factors are operational limits such as tilt position, minimum and maximum signal amplitude limits for noise distortion, and linearity.

The parameters most commonly sought are intrinsic sensitivity, power-to-weight ratio, natural frequency, open circuit damping, damping characteristics under loaded conditions, and coil D.C. resistance. Other parameters of importance in the analysis of signals processed by the transducer are spurious responses within the useful frequency band, locked coil inductance, electrical balance of the coils in dual coil units, cross-axis response, harmonic distortion generated by the transducer, and amplitude linearity.

In addition, environmental tests are often required to determine the changes in geophone characteristics with temperature, tilt, aging, and mechanical shock.

TESTS FOR NATURAL FREQUENCY

The "natural frequency" of a geophone is generally accepted as being the un-damped frequency of the spring mass system. This measurement is most easily carried out by a phase resonance method utilizing a calibrated oscillator, a series resistance of around ten times the geophone coil resistance, and an oscilloscope with horizontal and vertical amplifiers having identical phase characteristics. For extremely accurate determination of the natural frequency, phase comparators may be substituted for the oscilloscope and a frequency counter can be used to accurately measure the frequency where the phase resonance occurs. The simple circuit shown in Fig. 5 is commonly used for this test.

TESTS FOR DAMPING

Measurements of damping are generally made using the circuit of Fig. 6. A small current is used to displace the seismometer moving coil from its equilibrium position, and when the current circuit is broken, the coil is accelerated and the ratio of the amplitudes of succeeding damped oscillations are measured. The method of measurement can be either the traces on an oscilloscope screen or peak sample and hold voltmeter readings electronically compared as to amplitude

ratios. These ratios may be electronically converted to fraction of critical damping or the fraction of critical damping may be calculated. A picture of an electronic damping measurement instrument is shown in Fig. 7.

The damping of a geophone is usually electromagnetic, and is the result of the current generated in the metallic coil bobbin by the magnetic field. Since most springs used in geophones have a limited linear displacement range, care must be taken to stay well below this range when measuring damping or natural frequency. Spring non-linearity is found by increasing the electrical drive to the geophone and noting the point at which a change in drive level will cause a shift in natural frequency. When measuring damping, the overswing ratio should be exactly the same when the initial displacement of the coil is made in one direction and then in the opposite direction (i.e., polarity of displacing current reversed). Failure to get identical values of damping by displacing the coil in either direction indicates excessive displacement into the region of spring non-linearity and an erroneous measurement.

TESTS FOR INTRINSIC SENSITIVITY A. SENSITIVITY BY MECHANICAL EXCITATION

Intrinsic sensitivity is the transduction response of the geophone measured well above the natural frequency on the linear portion of the response curve. This sensitivity is usually stated in volts per unit of particle velocity, that is volts per inch per second or volts per cm/sec. The measurement of intrinsic sensitivity lends itself to several different methods which may be used to cross check each other. The easiest method, which also involves the most expensive equipment, utilizes a calibration-type shaker table which can be set to an accurately-known velocity by means of a previously calibrated standard sensor. This sensor can be an internal velocity coil, a standard seismometer, or a standard accelerometer. An optical method for calibrating a shaker table equipped with an internal calibration coil is illustrated in Fig. 8. The basic parameters measured for this calibration are the peak-to-peak displacement of the table, the operating frequency of the system, and the voltage output of the calibration coil. From the frequency and displacement the velocity or acceleration is calculated and the calibration coil voltage output per unit of velocity or acceleration is then determined. Having determined the transduction constant of the calibration coil by the above method, the velocity of the shaker table system can be conveniently set

to a value required for testing. The sensitivity of the seismometer being tested can then be determined from the known table velocity and the output voltage of the seismometer. The accuracy of this method is determined by the accuracy of the calibrated standard, the accuracy of the measuring voltmeters, or voltage ratio comparator. Accuracy is also influenced by the method of mounting the seismometers in relation to the standard sensor, distortion of the waveforms of the seismometer, the standard sensor, or the shaker table. Causes of distortion could be over-driving any of the units or distortion in the shaker system power amplifier. Care must be taken to account for any loading of the outputs of the seismometer or standard sensor by the measuring instruments. The shaker table system is especially convenient when used to match similar seismometers for phase response and sensitivity. A suggested method of mounting the seismometers is shown in Fig. 9. This type of mounting aligns the operating axis of both sensors with each other and with the operating axis of the shaker and reduces the effects of shaker lateral motion and wobble on the accuracy of the test. With care, sensitivities of seismometers may be compared to within less than 1% of each other. For the measurement of absolute sensitivity, accuracies of within 2% are obtainable, assuming that the standard sensor has a known accuracy better than 1%.

B. SENSITIVITY BY DAMPED RESPONSE

A simple, inexpensive but time-consuming method of determining intrinsic sensitivity along with almost every other important seismometer characteristic is illustrated by the calibration sheet shown in Fig. 10. This method arrives at sensitivity by measuring all parameters necessary to solve the sensitivity equation shown here. Intrinsic Voltage

$$\text{Sensitivity (G) volts/inch/second} = \frac{\sqrt{4\pi(F_n)(M)(R+r)(B_t-B_0)}}{10^{-7} \times 2.54}$$
 This procedure utilizes the simple equipment necessary to measure natural frequency, coil resistance, weight of the moving mass, and the damping of the seismometer under varying resistive loads.

The calibration sheet illustrates an orderly method of establishing the damping constant (C_D) of the seismometer. This damping constant is equal to the product of the coil current damping (b_t-b_0) and the sum of the coil resistance and the damping load resistance ($r + R$). All of these values are measured as carefully as possible, using the basic procedures for measuring damping and D.C. resistance.

The largest source of error, using calibration sheets of this type, is in the measurement of damping by the overswing method using an oscilloscope. The instrument shown in Fig. 7, which utilizes sample and hold techniques to measure the overswing ratio, is the most accurate means of measuring damping. Correlation of the sensitivity determined by this method and sensitivity determined by the shaker table is usually within 2% to 6%, depending on the care with which the tests are run.

There are still other methods of increasing the accuracy of this sensitivity-damping measurement. One such method statistically determines the open circuit damping and the damping constant by the method of linear regression. The plot of total damping versus $\frac{1}{(r + R)}$ shown in Fig. 11 is theoretically a straight line which intercepts the damping ordinate at $\frac{1}{r + R} = 0$. This plot or the linear regression calculation gives a check of the accuracy of the damping constant measurements and a check of the accuracy of the open circuit damping measurement. Increasing the number of measurements of the damping constant also increases the accuracy of the sensitivity measurement within practical limits. A typical set of measurements and the linear regression test check results are shown in Fig. 12.

SENSITIVITY BY MOTIONAL IMPEDANCE

The measurement of motional impedance at the natural frequency by the simple method of resistance substitution as shown in Fig. 13 is yet another method of arriving at the damping constant and determining the geophone sensitivity. Fig. 14 shows the relationship between the sensitivity, the damping constant, the open circuit damping, and the motional impedance. It can be concluded that this is another partially independent method of checking the damping constant. Again, the ability to measure open circuit damping limits the accuracy of this method.

SENSITIVITY BY CALIBRATED IMPULSE RESPONSE

There is yet another method that is convenient for the calibration of large HS-10 type seismometers. This method involves removal of a known static force from the moving mass of the seismometer and determining the intrinsic sensitivity, the open circuit damping, and other parameters from the resulting response of the damped mass spring system. A one or two gram balance weight conveniently supplies a steady cali-

brated force under the influence of gravity.

The undamped natural frequency of the spring mass system is carefully measured using the phase resonance method. During the assembly of all HS-10's the weight of the moving mass is carefully measured and recorded. The open circuit damping is measured by measuring the overswing ratio using the methods previously described or by using the weight lift to initially pulse the seismometer. The main coil output pulse resulting from removing (lifting) the 1 or 2 gram mass is measured and recorded using a calibrated oscilloscope or a sample and hold type peak reading voltmeter. If the HS-10-1 has a calibration coil, the calibration coil motor constant can be adjusted to apply the same force to the main spring mass system as a one or 2 gram mass, with a known direct current applied to the calibration coil. This is a very convenient feature for remote calibration and functional checking the HS-10-1B seismometer. This is illustrated in Fig. 15.

Using the above test procedures, the following parameters are measured or calculated:

- f_n - Natural Frequency (Hz) - Measured
- b_o - Open Circuit Damping (fraction of critical)
Measured
- V_p - Main Coil Response (O-P volts) - from a 1 or 2 gram force - Measured
- W - Weight of Moving Mass (gms) - Measured
- K - Spring Rate (gms/cm) - Calculated ($K = W_n^2 W/g$)
- X_o - Displacement (cm) - Calculated ($1/K \times$ weight lift mass (1 or 2 gms))
- w_n - Natural Angular Frequency (rad/sec) - Calculated at f_n
- w_d - Natural damped angular frequency (rad/sec) calculated $w_d = w_n \sqrt{1 - (b_o)^2}$
- t_o - Initial condition with 1 gm force applied ($t = 0$)

Equations of motion for damped free vibrations:

$$\text{Displacement } X = e^{-bw_n t} (A \cos w_d t + B \sin w_d t)$$

at t_0 , $X = A$

$$\text{Velocity } X' = -bw_n e^{-bw_n t} (A \cos w_d t + B \sin w_d t) + w_d e^{-bw_n t} (-A \sin w_d t + B \cos w_d t)$$

at t_0 , $X' = 0$, $B = 0$

Using calculated and measured values for the seismometer in the velocity equation the peak velocity may be determined at $t = \pi/2$ and the ratio of the measured peak output voltage to the calculated peak velocity is the sensitivity in volts per cm per second.

Example:

Calibration of HS-10-1B

S/N 100679

- f_n = Natural Frequency = 1.0 Hz (measured)
- b_o = Open Circuit Damping = .267 (measured)
- R = Main Coil Resistance = 4040 ohms (measured)
- R_{cal} = Cal coil resistance = 200 ohms (measured)
- M = Main moving mass = 957.6 gms (measured)
- F_m = Forcing mass (1 cm scale weight with lifting thread attached)
- V_p = Main coil O-P voltage pulse = .37 volt (measured)
- Cal Coil Adjustment - gives .37 volt O-P pulse from main coil when circuit carrying .015 ampere to cal coil is opened (equivalent of 1 gm force removal)
- w_n = Undamped natural angular frequency = 6.2832 rad/sec (calculated)
- w_d = Damped angular frequency = 6.0551 rad/sec (calculated)
- K = Spring rate = 38.5487 gms/cm (calculated)
- X_o = Mass displacement = .02594 (calculated)
- A = Initial condition amplitude constant = X_o = .02594 cm
- B = Initial condition quadrature amplitude constant = 0

Solving the velocity equation gives a velocity of .1135
cm/sec @ t = .215 sec

$$\frac{.37 \text{ volts O-P}}{.1135 \text{ cm/sec}} = 3.26 \text{ volts/cm/sec} = 8.28 \text{ volts/in/sec}$$

Calibration coil motor constant .015 amp gives the equivalent of 1 gm force therefore:

$$\frac{1 \text{ gm}}{.015 \text{ amp}} \times .009807 \text{ newtons per gm} = .6538 \text{ newtons per ampere}$$

TOTAL HARMONIC DISTORTION

Total harmonic distortion of a seismometer is defined in a familiar manner. It is a percentage ratio of the spurious harmonic products generated to the fundamental signal output when the seismometer is excited at a given amplitude and frequency. The most commonly accepted test conditions for small geophysical seismometers are that the test should be made at the natural frequency of the seismometer, and the amplitude of excitation should be set at 0.7 in per second peak-to-peak velocity. For other purposes, a test frequency different from the natural frequency could be used and the amplitude could be specified in terms of displacement, or acceleration rather than velocity. It is quite likely that displacement, which is the limiting factor in spring linearity, could be a more meaningful amplitude specification for distortion tests.

Distortion testing equipment at Geo Space, shown in Fig. 16, utilizes a low distortion oscillator as a constant current source to drive the geophone electrically. An HP 332 distortion analyzer is used to measure and display the total harmonic distortion products of the geophone. When driven at the natural frequency, the motional impedance of the geophone is resistive and the computations of the proper drive level to simulate a given velocity amplitude are greatly simplified. The test set-up for motional impedance measurements is illustrated in Fig. 13. An excellent explanation of the equivalency of the electrical drive to mechanical excitation is given in Dr. Badger's paper on the Geophone Analog. Typical values of total harmonic distortion for small high quality geophones are 0.2% to 0.5% for .7 inch per second drive amplitude at the natural frequency.

COMPARISON OF SEISMOMETER PERFORMANCE BY USE OF NORMALIZED PARAMETERS

Geophones come in an almost infinite variety of sizes, shapes, natural frequencies, weights, coil resistances, and damping characteristics. Therefore some logical methods of comparing various parameters should be established. For comparing intrinsic voltage sensitivity the most obvious normalization would be to eliminate the coil resistance factor. Normalized sensitivity would then be stated as $\text{Sensitivity} = G_n \sqrt{R_c}^*$ volts per unit of velocity and G_n would be the unit of com-

parison. To compare open circuit damping characteristics of two geophones with slightly different natural frequencies, the normalized open circuit damping could be used. It is the product of f_n and b_o . This product would be the unit of comparison regardless of variations in the natural frequency between sensors.

In order to compare the shunt load damping characteristic a normalized damping constant is used. This is usually stated as damping constant = $K \times R_c / f_n$ where K would be the unit of comparison regardless of natural frequency or coil resistance. Other normalized parameters which are frequently used for comparison are power per unit weight and normalized voltage sensitivity per unit weight.

TESTS FOR SPURIOUS RESPONSE

Many methods are used to determine the various spurious responses of seismometers, and many friendly arguments result over the application of these methods and the validity of the results. Some typical response modes are shown in Fig. 17.

The more we strike, vibrate, jolt, and tickle seismometers the more reinforcement we get for the opinion that each different form of excitation elicits a different response. How human this is. However, rather than start an argument here because of my opinions on the subject, I will merely furnish an overview of various methods used to excite and detect spurious responses. The simplest method is merely to strike the geophone normal to its operating axis and observe any ringing with an oscilloscope. Some seismometers excite just this easily. A further refinement is to observe the response on a FFT real time analyzer. Still better is the ability, available in some analyzers, to analyze the signal from a force gage attached to the excitation source and remove this excitation spectrum from the total response of the geophone, thus normalizing the response of the geophone for comparison with other geophones tested the same way.

The average shaker table system is not very satisfactory when used to excite a seismometer normal to its operating axis because of the inherent lateral motion, wobble, and other

*Note coil resistance is used as an indication of the number of turns and the generator source resistance. (See page 10)

spurious responses of the shaker. Certain hydrophone test facilities have been used for specialized response testing of geophones used in sonabouy applications. Electrical excitation of the geophone is sometimes used to try and detect spurious responses or anomalies in the frequency response plot.

Tests involving transient shocks applied normal to the seismometer's operating axis will reveal the following important information:

- A. Relative amplitude of the resonances
- B. Frequencies of resonant modes
- C. "Q" or damping of the resonances.

These tests are mainly comparative in nature because of the difficulty of applying excitation which is absolutely uniform as to amplitude, and point of impact. It is also difficult to select the proper point of impact relative to the center of gravity of the geophone.

ENVIRONMENTAL AND RELIABILITY TESTS

Among geophysical seismometer manufacturers, the most widely used method of reliability testing has been the rotating tumble barrel. This device consists of a six-sided hardwood drum with internal paddles, which lift and drop the geophone as the barrel rotates slowly. This machine gives a reasonable test of the mechanical ruggedness of most geophones, but should not be considered to have any absolute correlation to field life of the instruments. Other tests are destructive vibration at known resonance points, swept vibration tests according to various military specifications, shock tests in various orientations, humidity tests, water penetration tests, thermal testing, common mode voltage breakdown tests, and tests for resistance to corrosives or nuclear radiation, where applicable.

FUTURE TEST EQUIPMENT AND METHODS

Future test equipment will probably feature portability, complexity, and automation as the history of technology follows its usual course. One example of a now and future method is the Geophone Quality Meter, shown in Fig. 18, which is portable, and tests either an individual seismometer or a string of seismometers for activity and distortion. The activity test is very useful for matching individual seis-

mometers, determining if all units in a seismometer string are operative, and assessing the general quality and uniformity of similar seismometers. The distortion measuring function is useful in determining the distortion of individual seismometers and remotely indicating whether all units in the string were properly planted.

Another small instrument, intended for field use, is the geophone string tester, Fig. 19, which checks the response of a planted string of seismometers. An unmistakable auditory alarm results if the string voltage output is out of tolerance for any reason. A repeating click at 1.4 second intervals indicates that the voltage output is within tolerance, a continuous tone indicates low output, and an alternating tone indicates high output.

In the realm of automation, Figs. 20 and 21 illustrate an automatic seismometer production test system. Fifty-unit batches are tested sequentially for natural frequency, distortion, coil resistance, operation when tilted, coil centering (drive test) common mode isolation (electrical leakage between case and coil), and damping. This device can selectively print out all parameters of each seismometer or just those parameters which are out of the specified tolerance.

This brief paper can not possibly cover all facets of seismometer testing, but hopefully will remove most of the mystery from the use and testing of these very useful sensors.

In conclusion, I wish to express my appreciation to my audience and to those fellow technologists whose contributions to the art and science of calibrating and testing sensors have formed an important part of this presentation.

Example:

Calibration of HS-10-1B

S/N 100679

f_n = Natural Frequency = 1.0 Hz (measured)
 b_o = Open Circuit Damping = .267 (measured)
 R = Main Coil Resistance = 4040 ohms (measured)
 R_{cal} = Cal coil resistance = 200 ohms (measured)
 M = Main moving mass = 957.6 gms (measured)
 F_m = Forcing mass (1 gm scale weight with lifting thread attached)
 V_p = Main coil O-P voltage pulse = .37 volt (measured)
Cal Coil Adjustment - gives .37 volt O-P pulse from main coil when circuit carrying .015 ampere to cal coil is opened (equivalent of 1 gm force removal)
 w_n = Undamped natural angular frequency = 6.2832 rad/sec (calculated)
 w_d = Damped angular frequency = 6.0551 rad/sec (calculated)
 K = Spring rate = 38.5487 gms/cm (calculated)
 X_o = Mass displacement = .02594 cm (calculated)
 A = Initial condition amplitude constant = X_o = .02594 cm
 B = Initial condition quadrature amplitude constant = 0

Solving the velocity equation gives a velocity of .1135 cm/sec @ $t = .215$ sec

$$\frac{.37 \text{ volts O-P}}{.1135 \text{ cm/sec}} = 3.26 \text{ volts/cm/sec} = 8.28 \text{ volts/in/sec}$$

Calibration coil motor constant .015 amp gives the equivalent of 1 gm force therefore:

$$\frac{1 \text{ gm}}{.015 \text{ amp}} \times .009807 \text{ newtons per gm} = .6538 \text{ newtons per ampere}$$

GENERAL REFERENCE INDEX

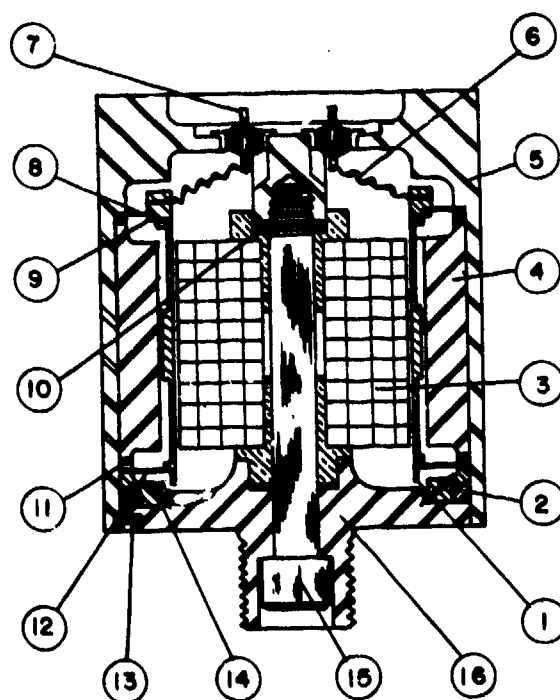
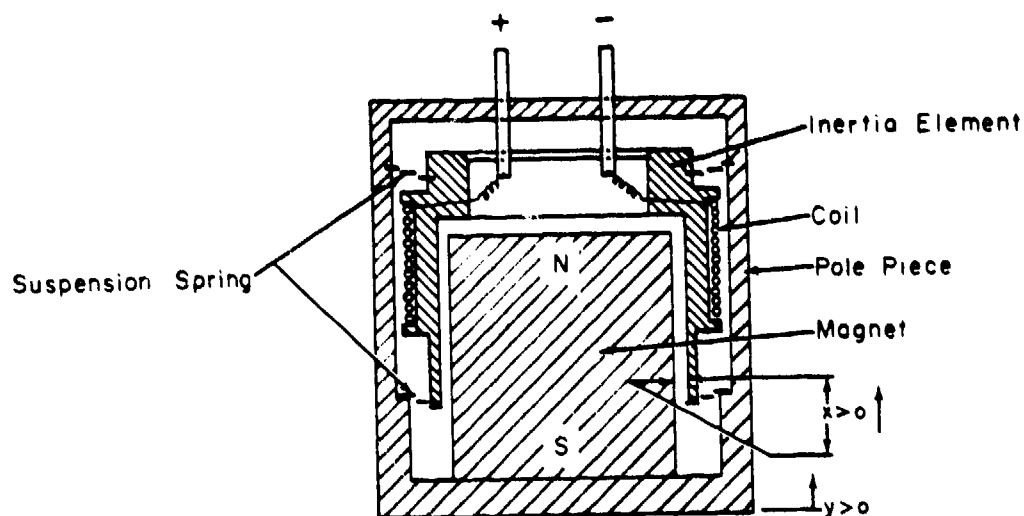
Heiland C.A., 1968, Geophysical Exploration: New York,
Hafner Publishing Co.

Jakosky J.J., 1957, Exploration Geophysics: Newport Beach,
Trija Publishing Co.

Von Kármán T. and Biot M.A., 1940 Mathematical Methods in
Engineering: New York, McGraw-Hill Book Co., Inc.

Badger A.S., 1967, The Geophone Equivalent Circuit in
the Dynamic Analogy: 37th Annual International Meeting
of the S.E.G.

G.S.C. Staff, 1965, Geophone Response Equations and Their
Application: Houston, Geo Space Corporation



ITEM	DESCRIPTION
1	COIL FORM
2	"O" RING
3	MAGNET ASSEMBLY
4	POLE PIECE
5	CASE
6	PIGTAIL
7	SEAL
8	TOP SPRING
9	SNAP RING
10	"O" RING
11	SPACER RING
12	BOTTOM SPRING
13	PIN, NO. 00- 1/8
14	SEAL RING
15	SCREW
16	CASE BOTTOM

Figure 1. Basic Geophones

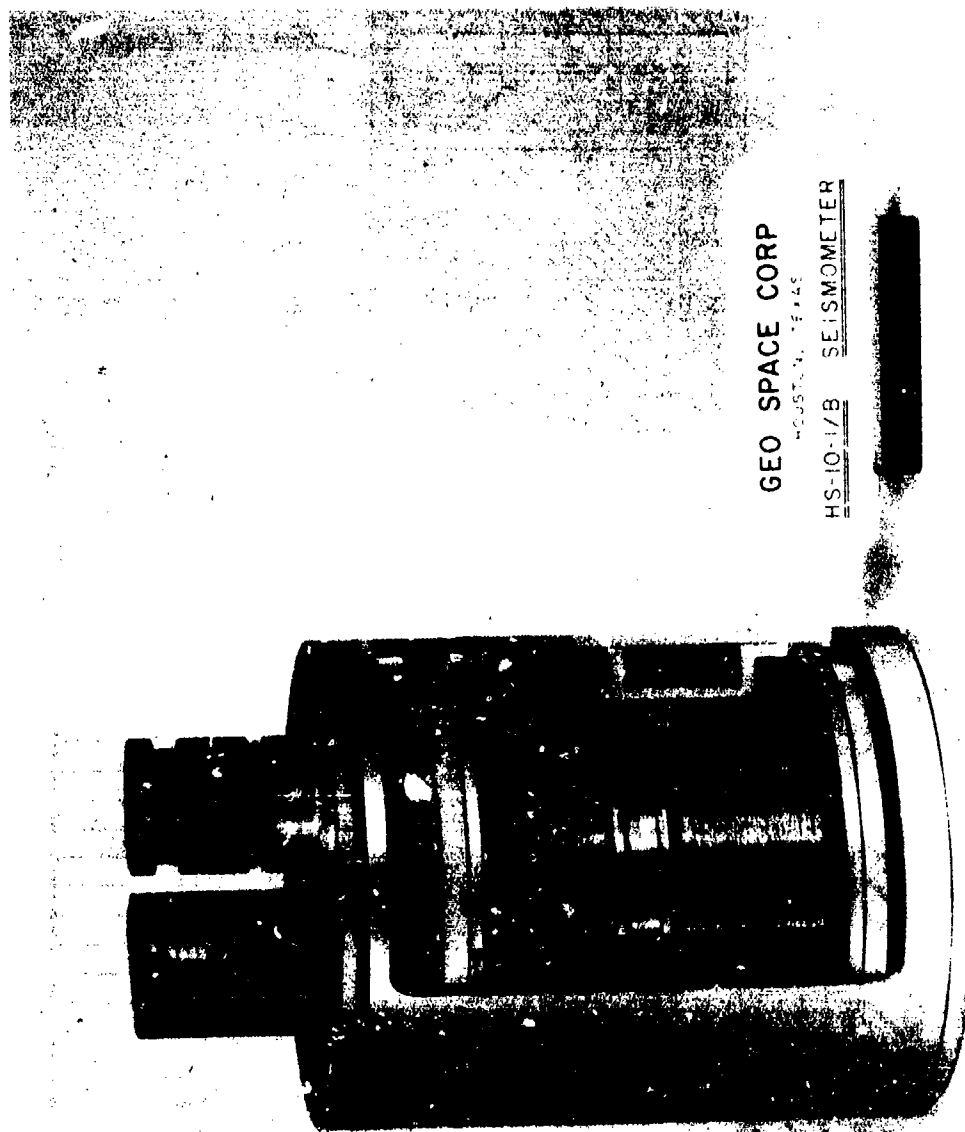


Figure 2. HS-10-1/B Seismometer

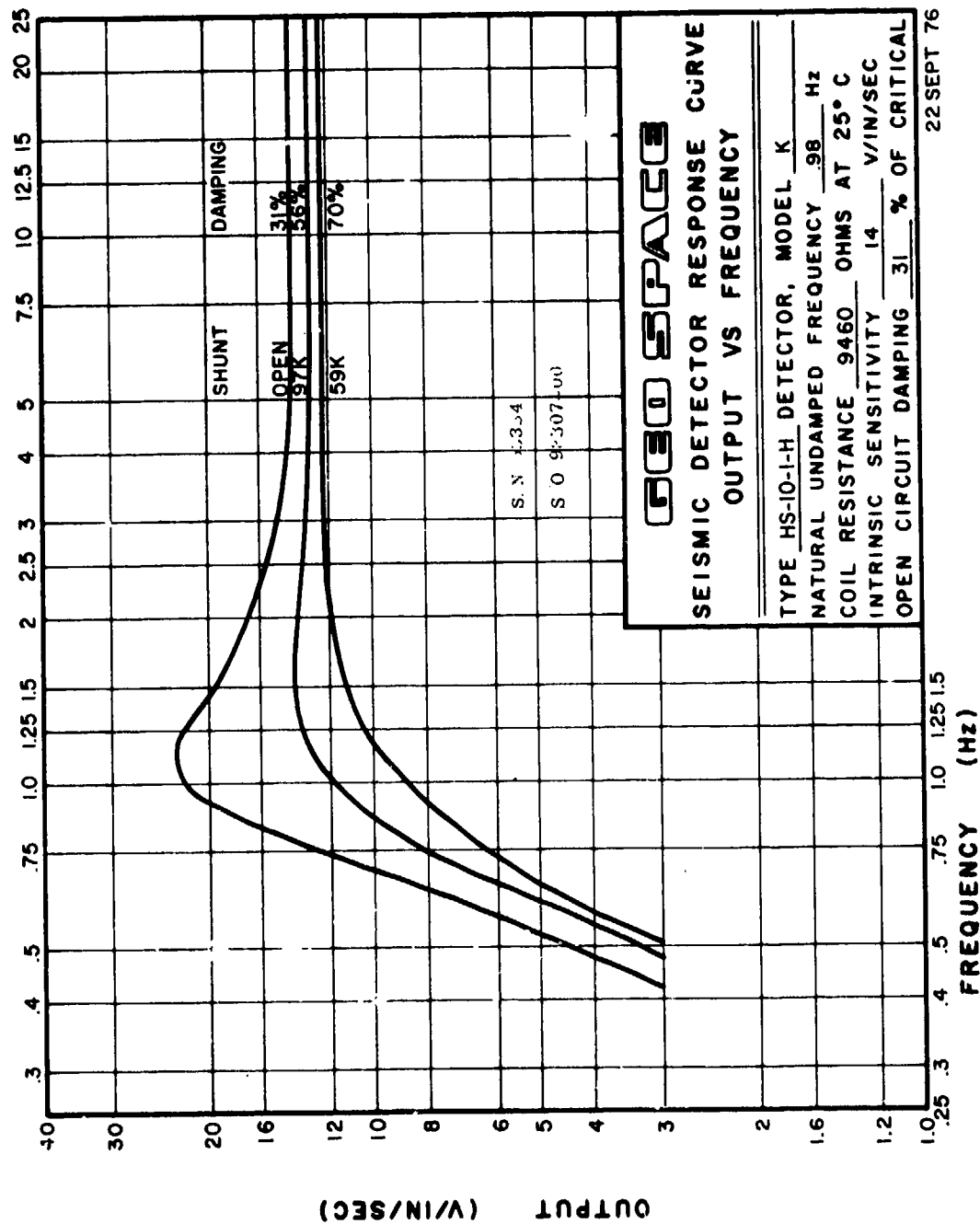


Figure 3. HS-10-1/B Frequency Response

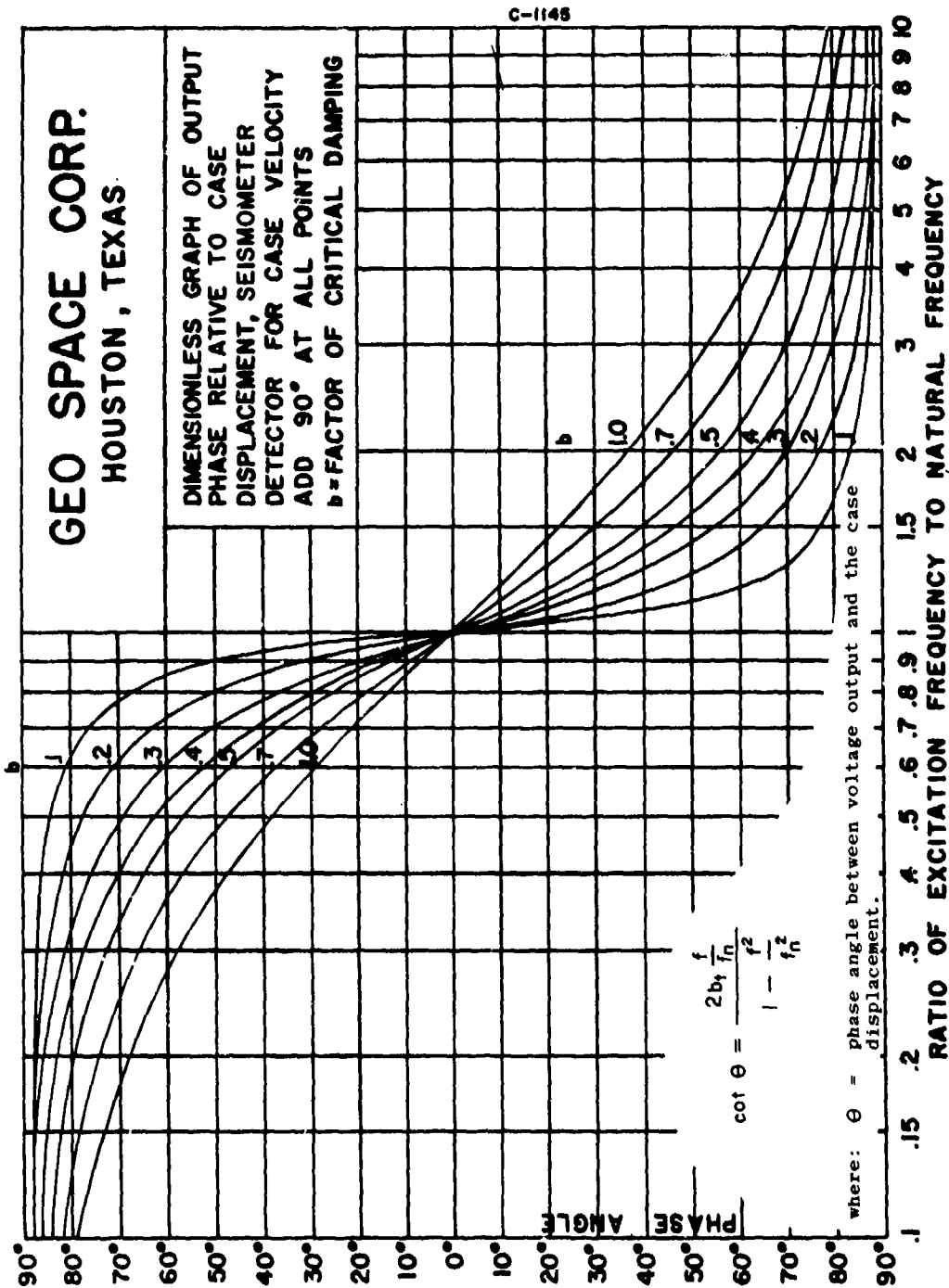


Figure 4. Seismometer Phase Response (Normalized)

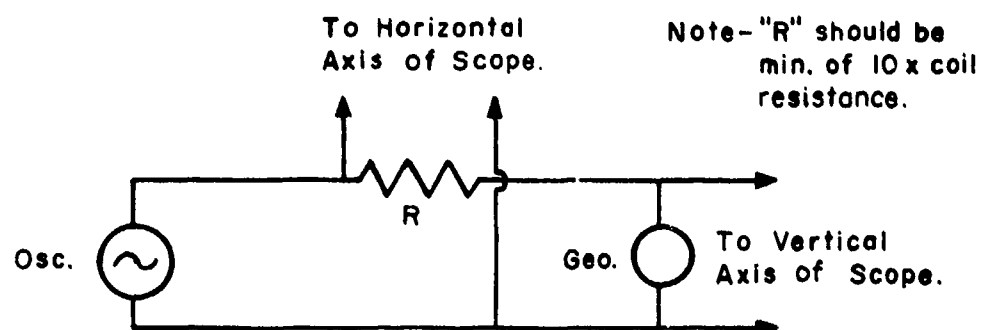


Figure 5. Basic Phase Resonance Circuit (Also 5A)

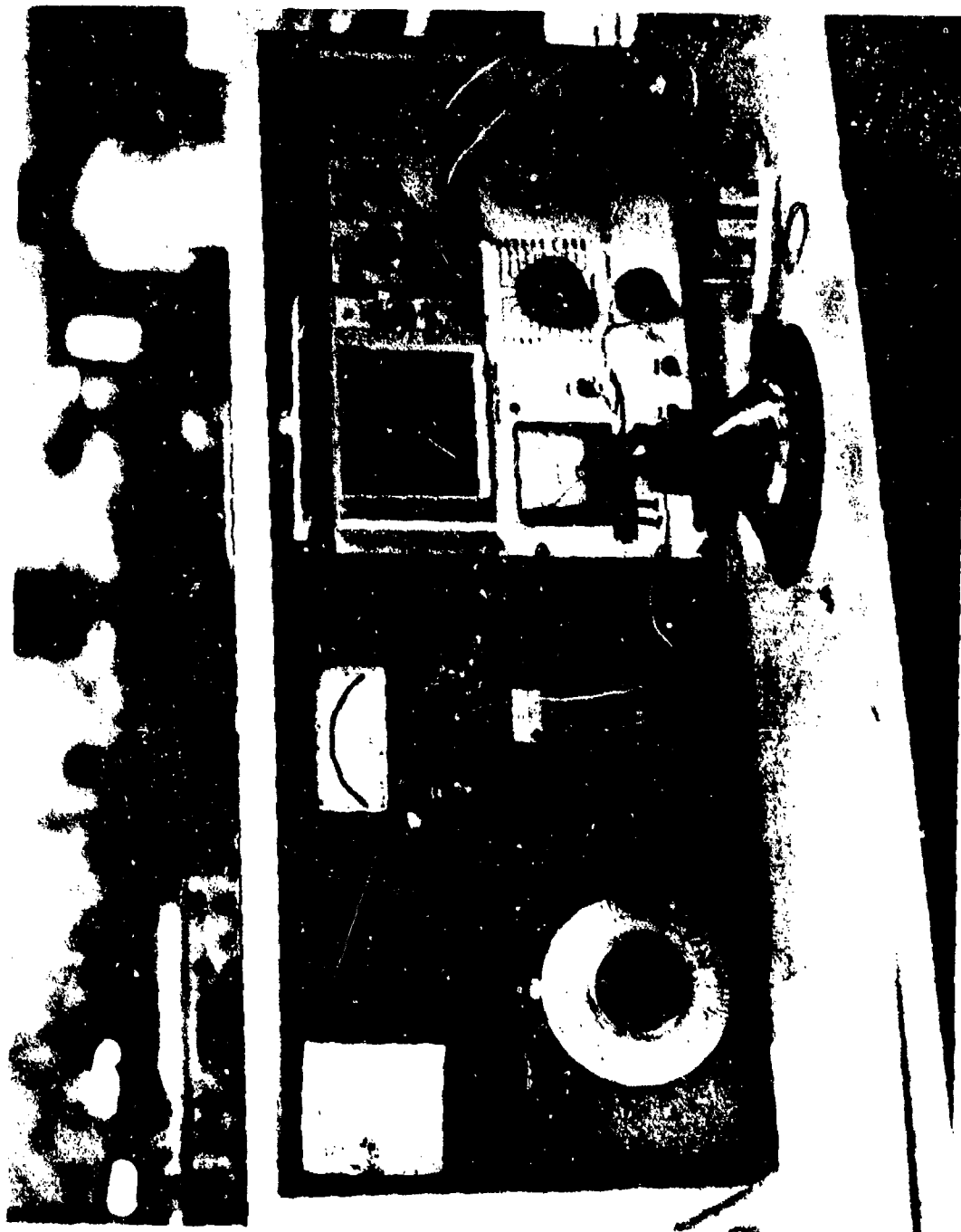
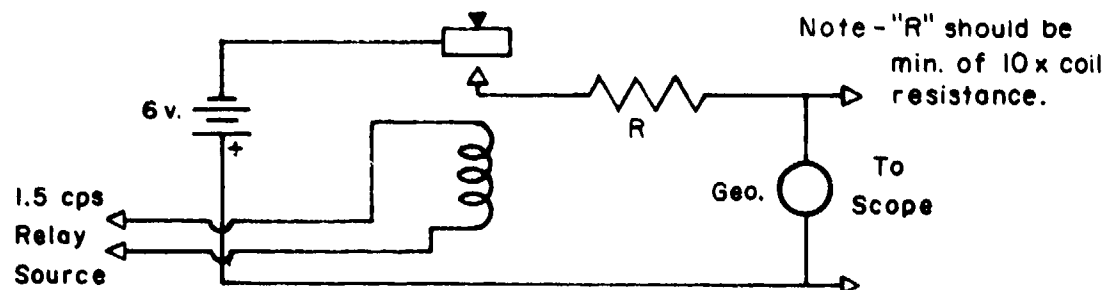


Fig. 5A



$$b_f = \frac{\log_e \frac{A_1}{A_2}}{\sqrt{\pi^2 + \left(\log_e \frac{A_1}{A_2}\right)^2}}$$

where: $\frac{A_1}{A_2}$ = the overswing ratio

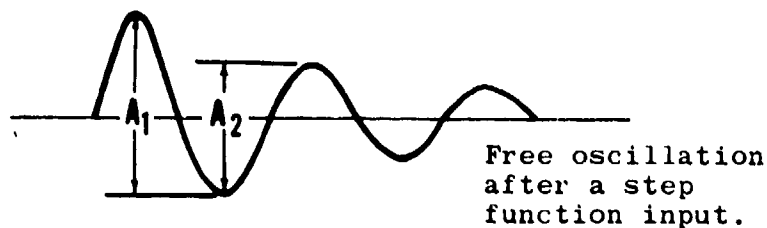


Figure 6. Basic Damping Testing Circuit

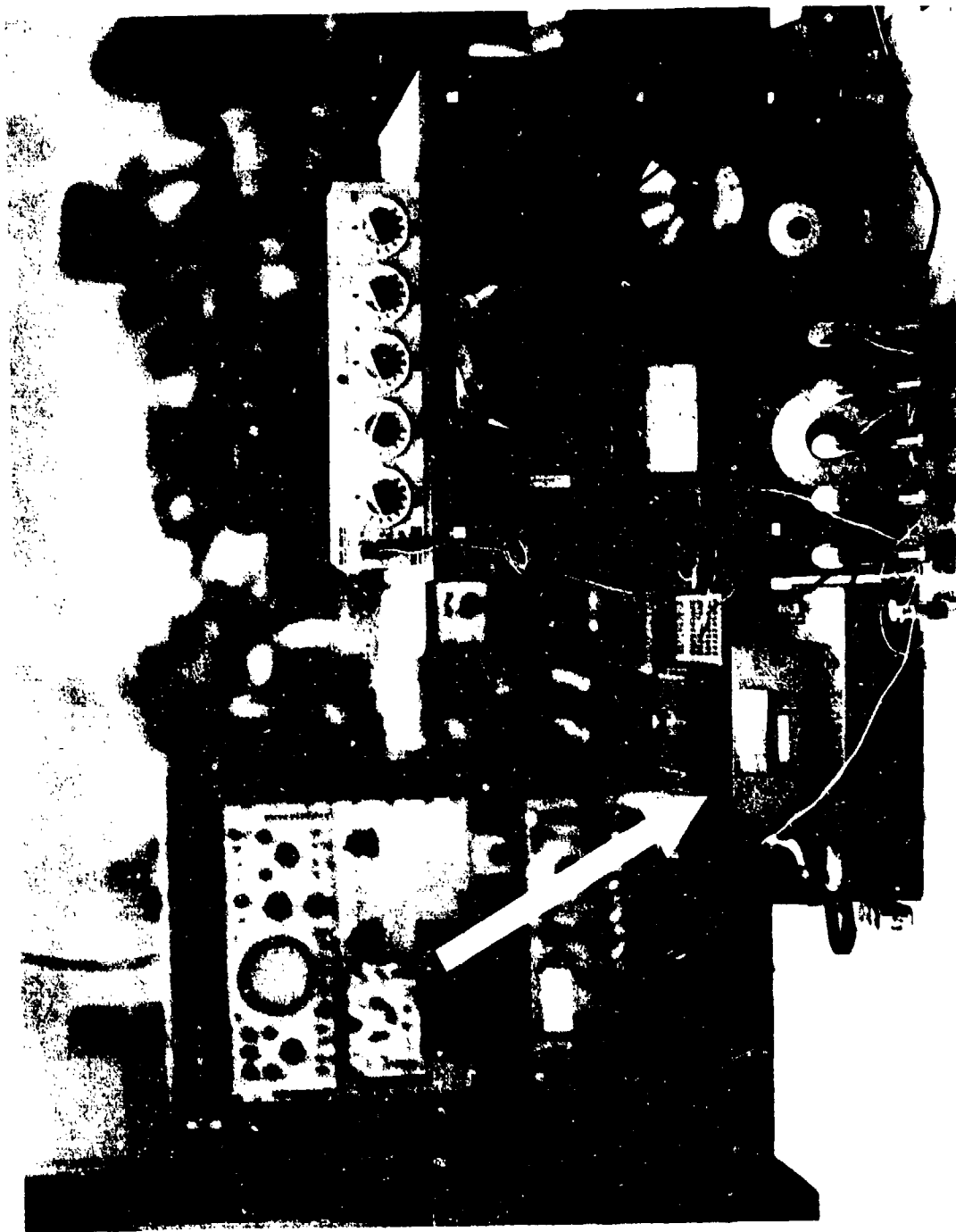


Figure 7. Picture of Electronic Overswing Ratio Instrument

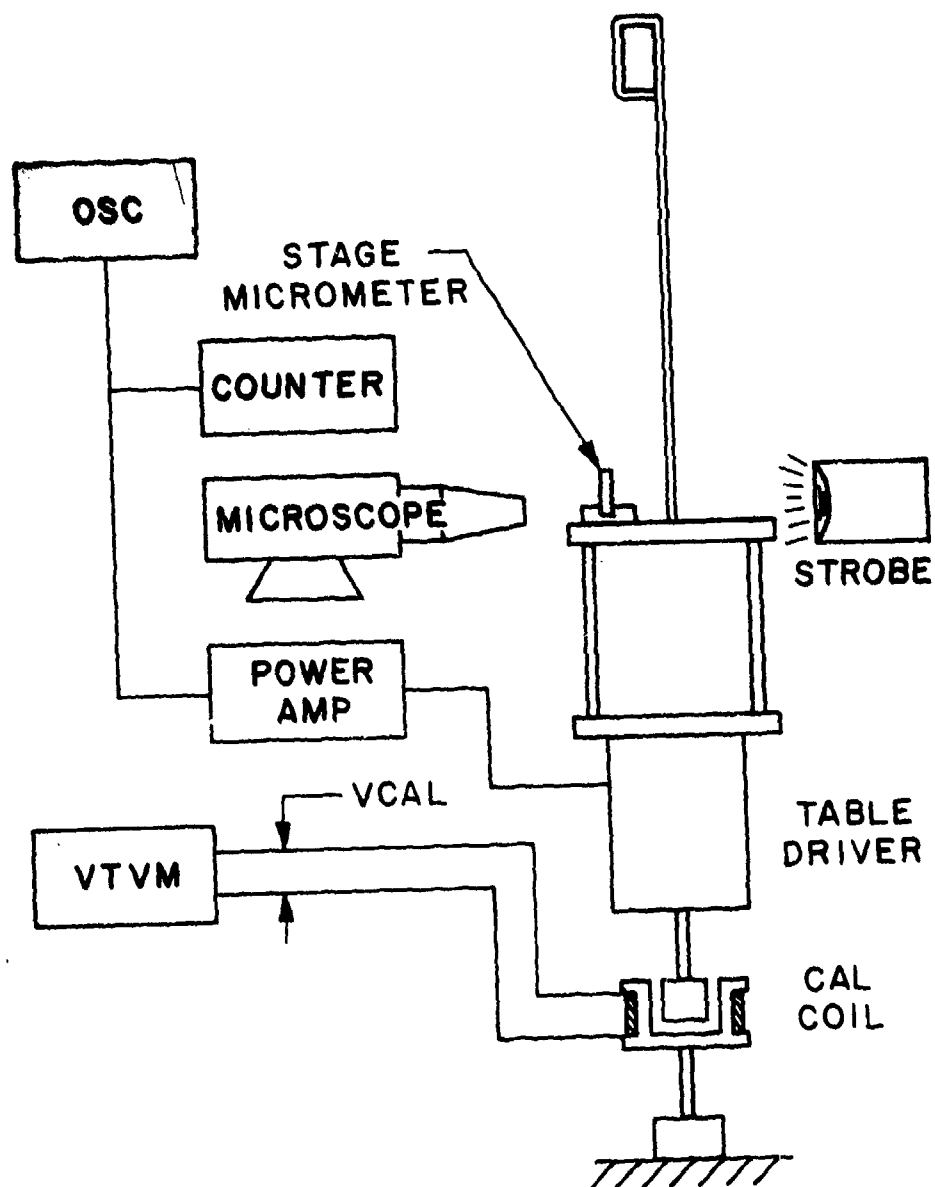
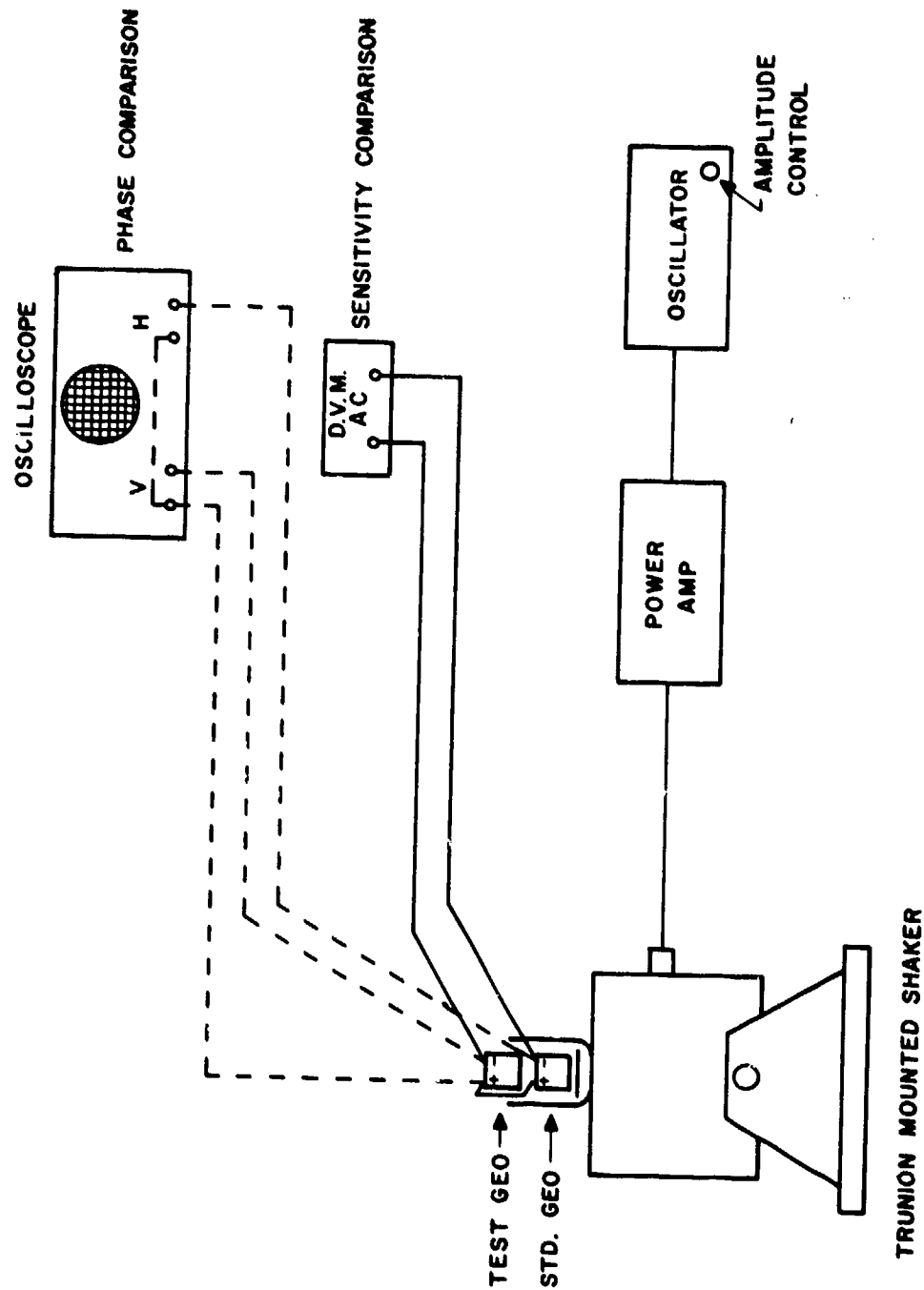


Figure 8. Optical Method for Shaker Table Calibration



GEOPHONE MATCHING SYSTEM

Figure 9. Co-axial Mounting of Geophones for Comparison

Model No. _____ Serial No. _____ S. O. No. _____
 Natural Undamped Frequency (F_n) _____ cps. Resistance (r) _____ ohms.
 Open Circuit Damping (B_0) _____ % of critical. Mass (M) _____ grams.
 Data taken by _____ on _____

R	$\frac{A_1}{A_2}$	B_1	$(B_1 - B_0)$	$(R + r)$	$(R + r) (B_1 - B_0)$
TOTAL					
AVERAGE					

$$\text{from G} \quad \sqrt{4 \pi (F_n) (M) (R + r) (B_t - B_o) \times 10^{-7} \times 2.34}$$

where $(R + r)(B_t - B_0)$ from above data,

Output (E_0), at any frequency (f) in v. in. sec. with μ for μ_0),

$$(1) \quad E_0 = \sqrt{\left[1 - \frac{2}{F^2}\right]^2 + 4\left[\frac{P}{F^2} + \frac{R}{F^2}\right]^2} \times \frac{R}{F^2}$$

To Compute Damping (B_x) resulting from a load condition (R_x)

$$(2) \quad B_x = \frac{B_0}{(R_x + r)} + B_0$$

To Determine Load (R_x) required to produce a damping condition (ζ)

$$(3) \quad R_x = \frac{B_t - B_0}{B_t - B_0} = 1$$

M - 1043 (Rev. Feb. 1966)

SENSOR DIVISION



GEO SPACE CORPORATION

5803 GLENMONT DRIVE • HOUSTON, TEXAS 77036

TELEPHONE: AREA CODE 713-MO 6-1611 • CABLE ADDRESS: GEOSPA

Figure 10. M-1043 Geophone Calibration Data Sheet

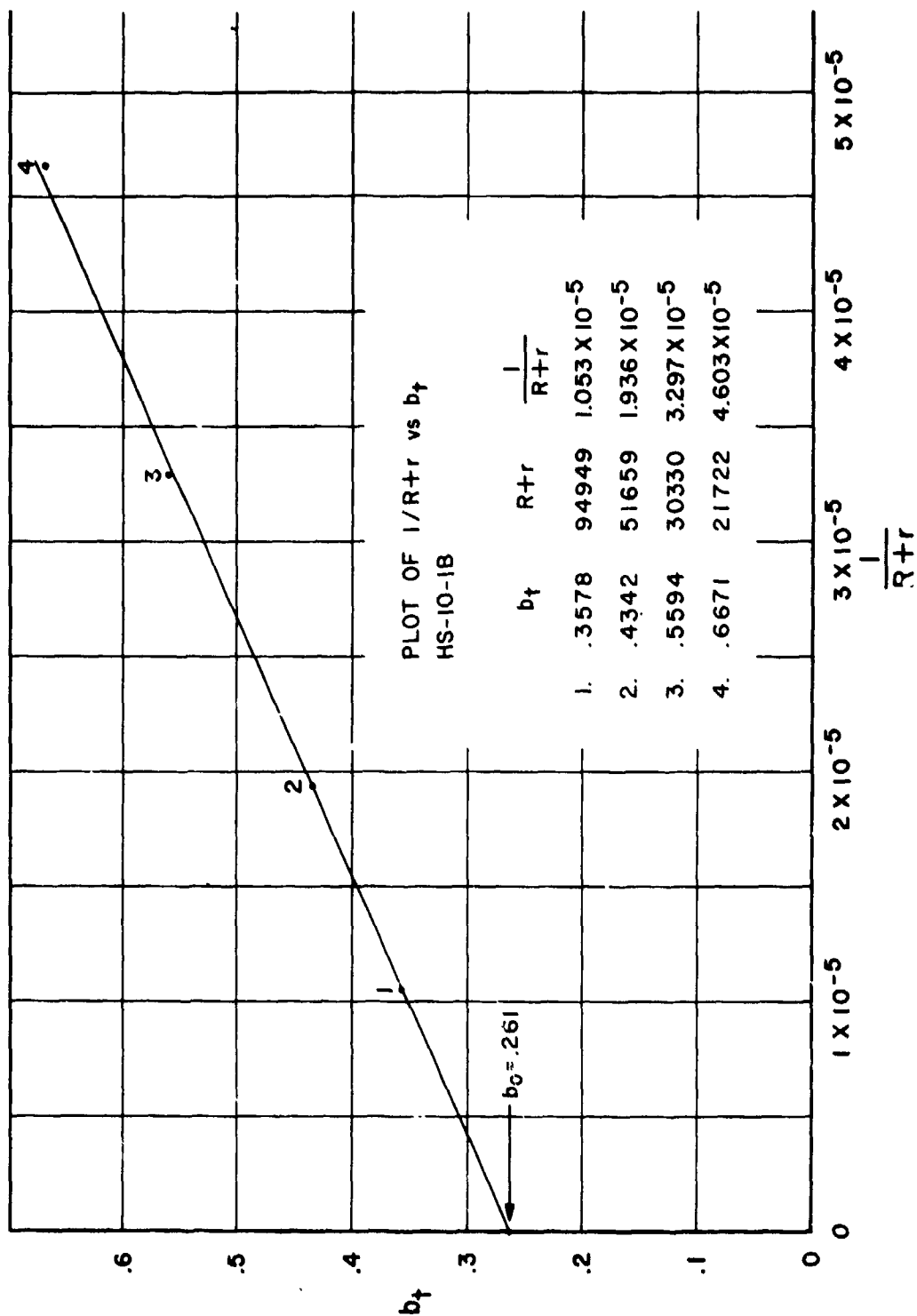


Figure 11. Plot of Total damping vs. $1/(r + R)$

GEOPHONE CALIBRATION DATA SHEET FOR

Model No. HS-10 1/B Serial No. 100679 S. O. No. 99358
 Natural Undamped Frequency (F_n) 1.00 cps. Resistance (r) 4040 ohms.
 Open Circuit Damping (B_0) .2670 $\frac{\text{Weight}}{\text{Mass (M)}}$ of critical. 957.6 grams.
 Data taken by L.L. on 5-31-77

R	$\frac{A}{AF}$	B_t	$(B_t - B_0)$	$(R + r)$	$(R + r)(B_t - B_0)$
90909	10/3.0	.5578	.0908	94949	8621.37
47619	10/2.2	.4342	.1672	51659	8637.38
26290	10/1.2	.5594	.2924	30330	8868.49
7682	10/0.6	.6671	.4001	21722	8697.97
Linear Regression Calculation ($y = a_1 x + a_0$) ($x = 1/(R+r)$)					TOTAL 34818.21
a_0 .2670					AVERAGE 8704.55

a_1 8736 ($G=8.24$ vis), τ^2 .9997
 Intrinsic Voltage Sensivity (G) 8.22 volts/inch/second
 from $G = \sqrt{4\pi(F_n)(M)(R+r)(B_t - B_0)} \times 10^{-7} \times 2.54$

where $(R + r)(B_t - B_0) = \underline{8705}$ from above data.

Equations for Customer Use:

Output (E_0), at any frequency (f) in v./in./sec./ with a load (R),

$$(1) \quad E_0 = \frac{8.22 \times R}{\sqrt{\left[1 - \frac{1}{F^2}\right]^2 + 4 \left[.267 + \frac{8705}{R + 4040}\right]^2} \times \frac{1}{F^2}}$$

To Compute Damping (B_x) resulting from a load condition (R_x),

$$(2) \quad B_x = \frac{8705}{(R_x + r)} + B_0$$

To Determine Load (R_x) required to produce a damping condition (B_x)

$$(3) \quad R_x = \frac{8705}{(B_t - B_0)} - r$$

M - 1043 (Rev. Feb. 1966)

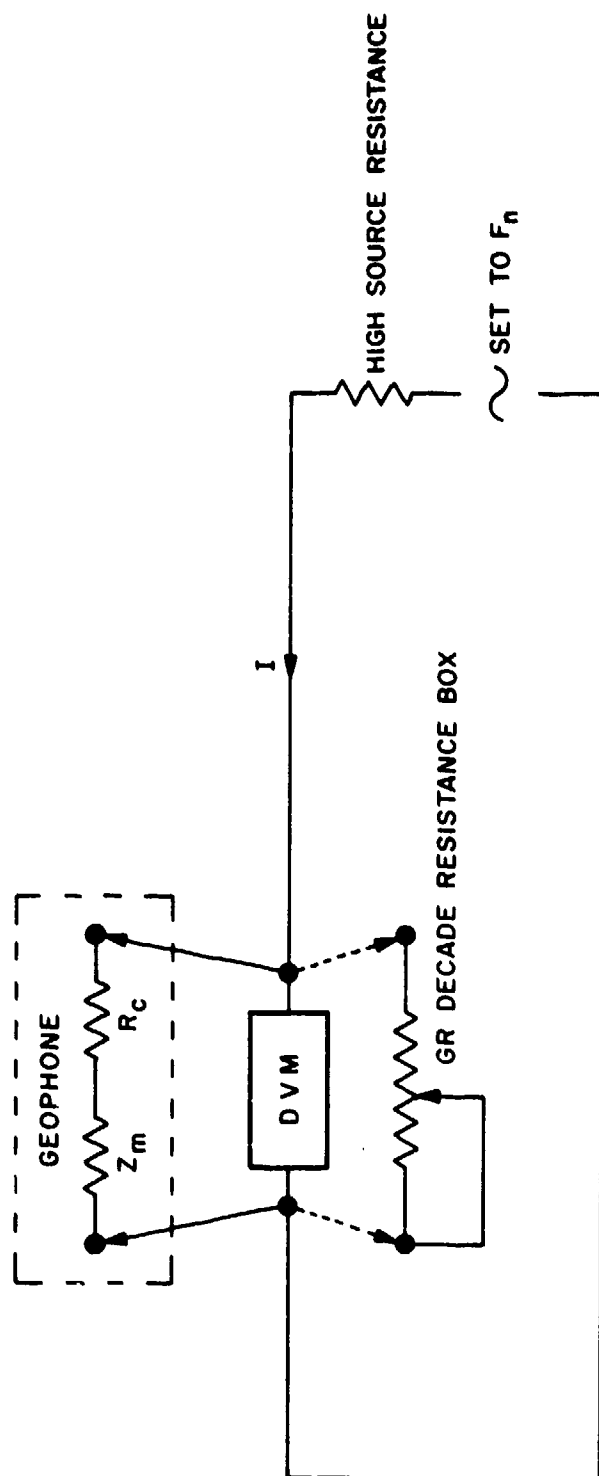
SENSOR DIVISION



GEO SPACE CORPORATION

5803 GLENMONT DRIVE • HOUSTON, TEXAS 77036
 TELEPHONE: AREA CODE 713-MO 8-1811 • CABLE ADDRESS: GEOSPA

Figure 12. Example of Seismometer Calibration Data



SET DECADE TO GIVE SAME VOLTAGE AS VOLTAGE MEASURED ACROSS GEOPHONE
 READING OF DECADE IS Z_T (TOTAL IMPEDANCE)
 Z_m (MOTIONAL IMPEDANCE) = $Z_T - R_c$ (SEIS COIL RESISTANCE)

Figure 13. Motional Impedance Circuit

MOTIONAL IMPEDANCE USED IN SENSITIVITY CALCULATION

1. $R_{eq} = Z_m @ f_n \quad (1)$
2. $R_{eq} = G^2 \times 10^7 \times \frac{1}{B} \quad (1)$
3. $(B = 2 b_o W_n \bar{M} \times 980.7)$
4. $\therefore G^2 = \frac{2 W_n R_{eq} b_o \bar{M} 980.7 \times 10^{-7}}{\text{Also}}$
5. $G^2 = 2 W_n \bar{M} \times 980.7 (R+r)(b_t - b_o) \quad (2)$
6. $\therefore R_{eq} b_o = (R+r)(b_t - b_o)$

Where:

- G = sensitivity (volts/cm/sec)
- W_n = $2\pi f_n$ (radians/sec)
- F_n = natural resonant frequency (Hz)
- R = shunt load damping resistance (ohms)
- r = geophone coil resistance (ohms)
- R_{eq} = motional impedance at f_n (ohms)
- B = linear damping coefficient ($\frac{\text{Dyne-sec}}{\text{cm}}$ or $\frac{\text{gm-sec}}{\text{cm}}$ x 980.7)
- \bar{M} = mass of moving element (gms = weight/980.7)
- b_o = open circuit damping factor in fraction of critical damping
- b_t = shunt loaded damping factor in fraction of critical damping

- (1) Badger A.S., The Geophone Equivalent Circuit in the Dynamic Analogy, P-7
- (2) Geophone Response Equations and Their Application, P-9, Eq 9

Figure 14. Motional Impedance used in Sensitivity Calculation

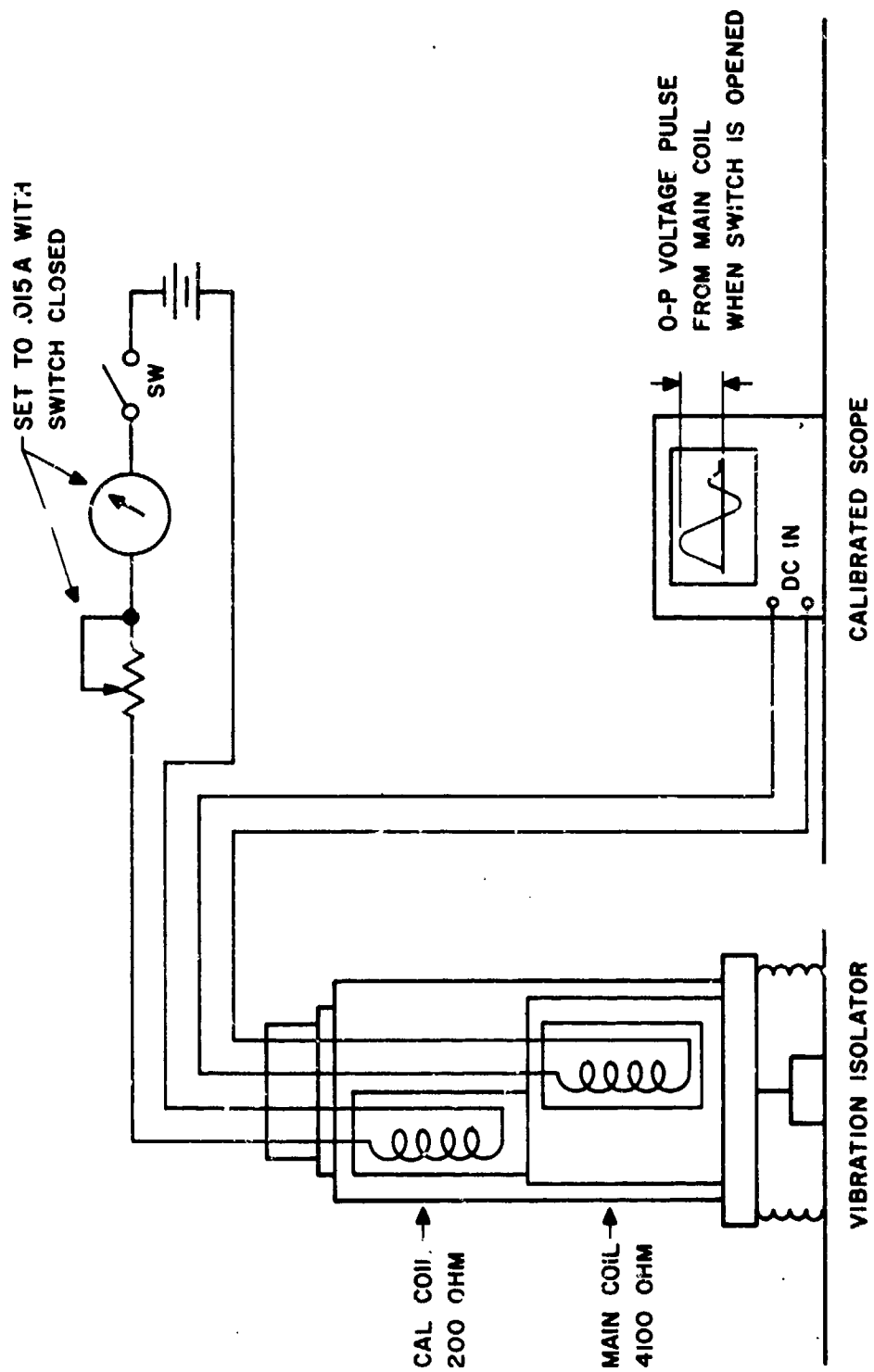
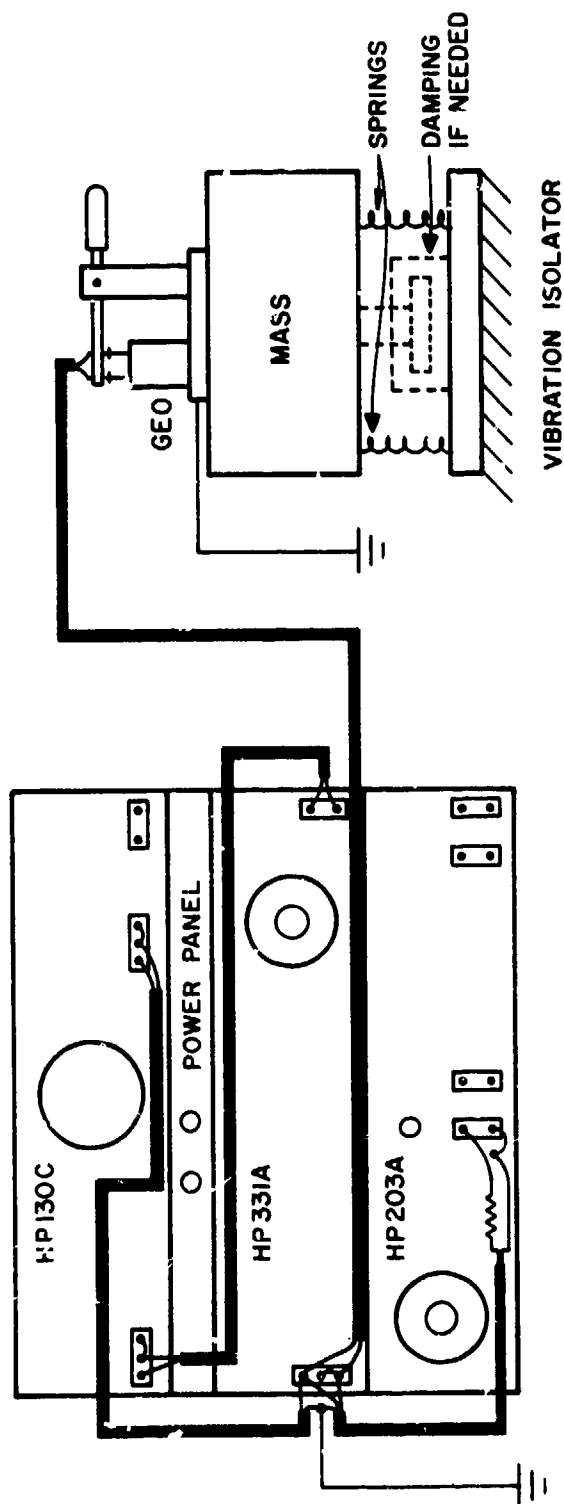
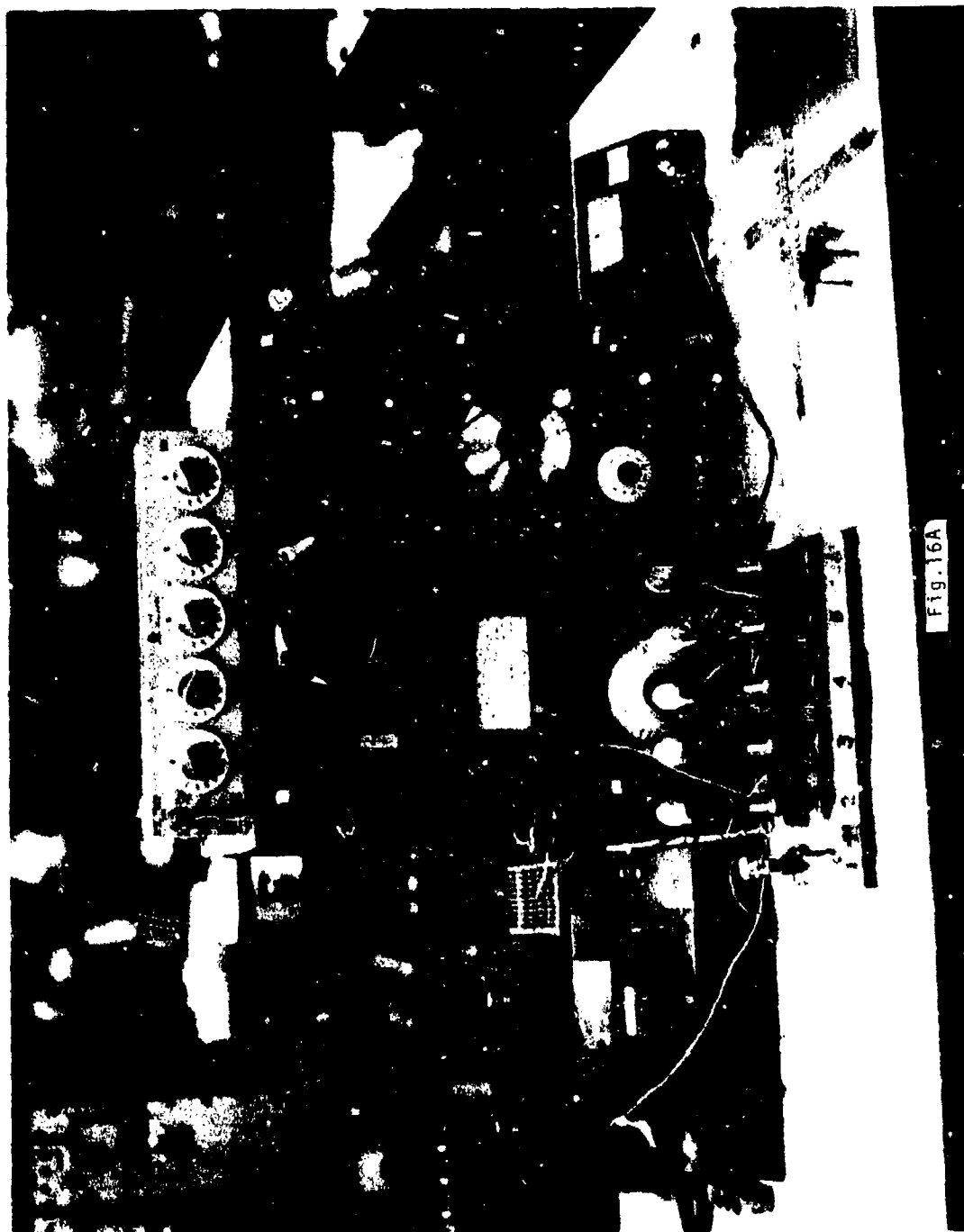


Figure 15. Calibration Coil Motor Constant Adjustment



DISTORTION STATION

Figure 16. Harmonic Distortion Test Equipment (also 16A)



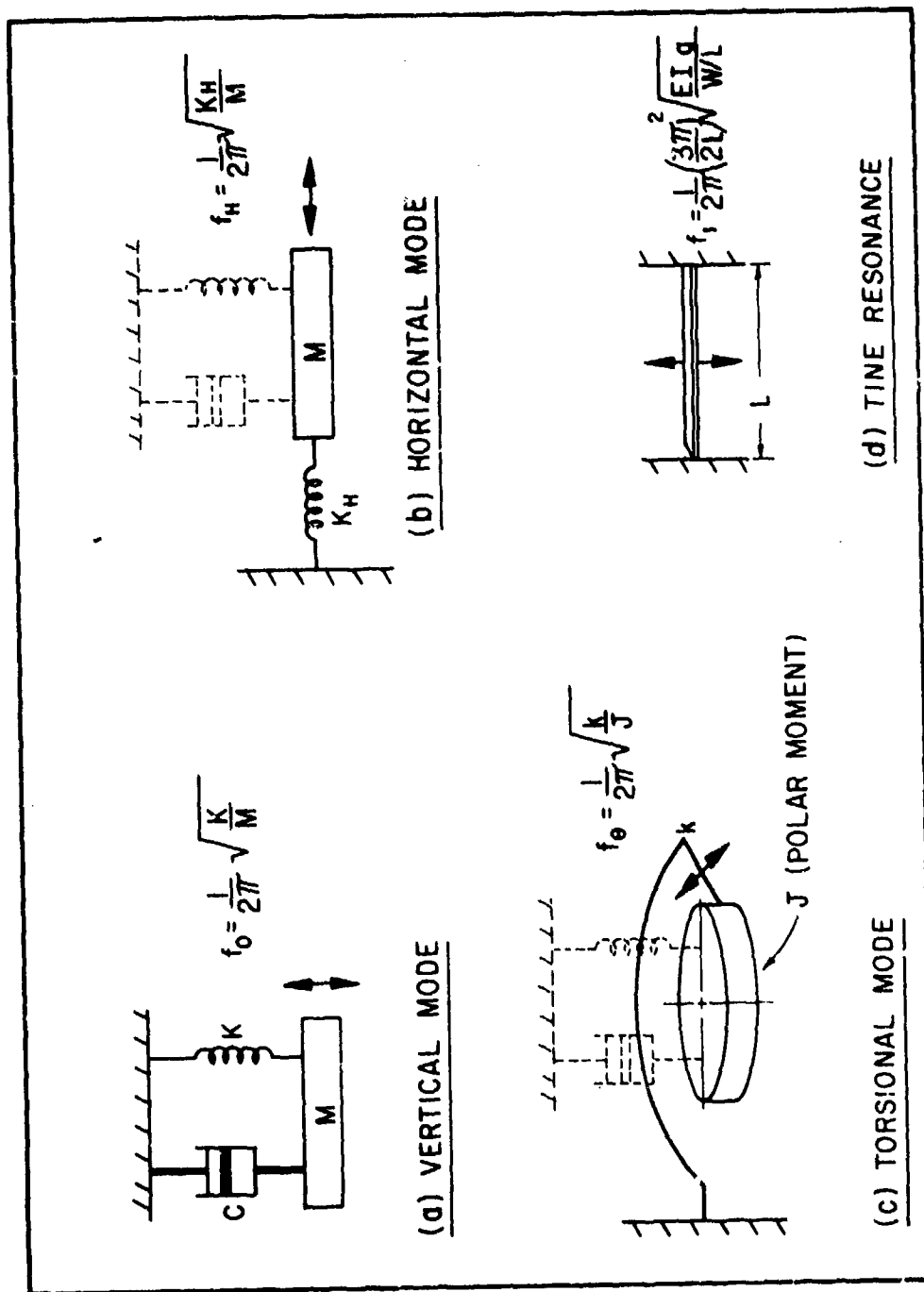


Figure 17. Spurious Response Modes

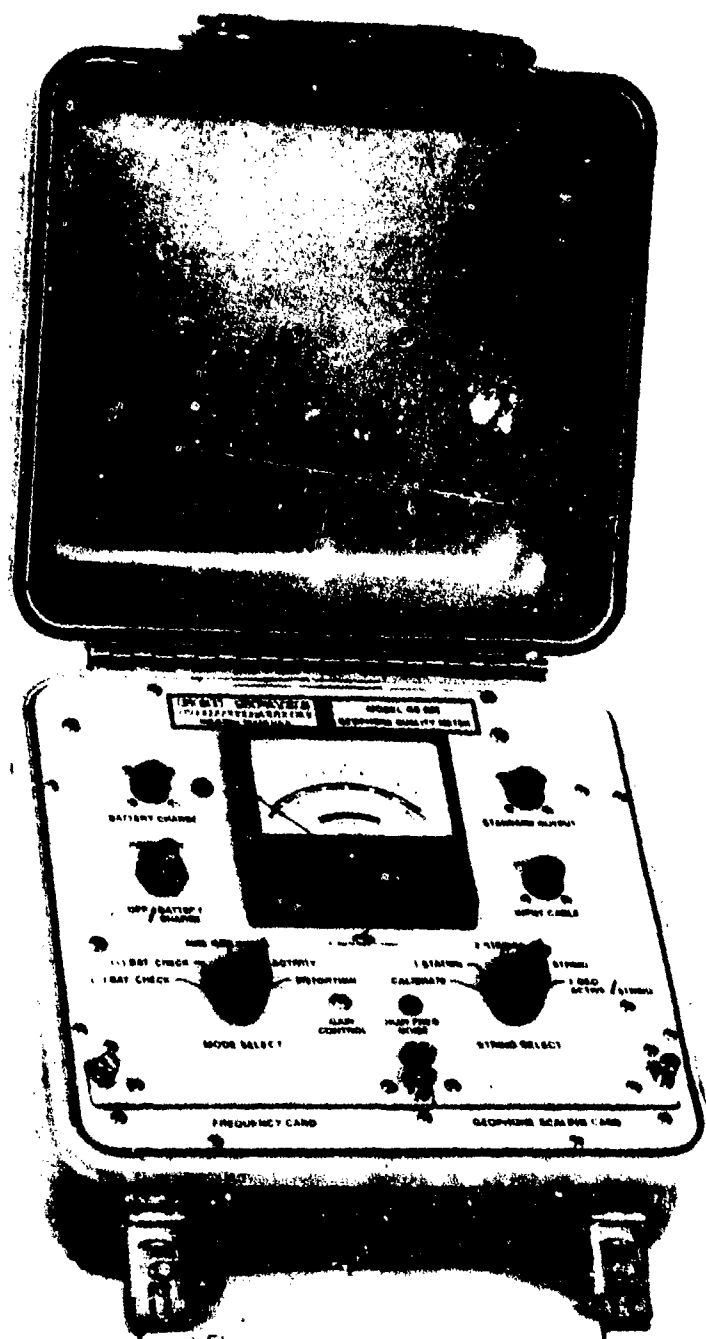


Figure 18. Geophone Quality Meter



Figure 19. Geophone String Tester

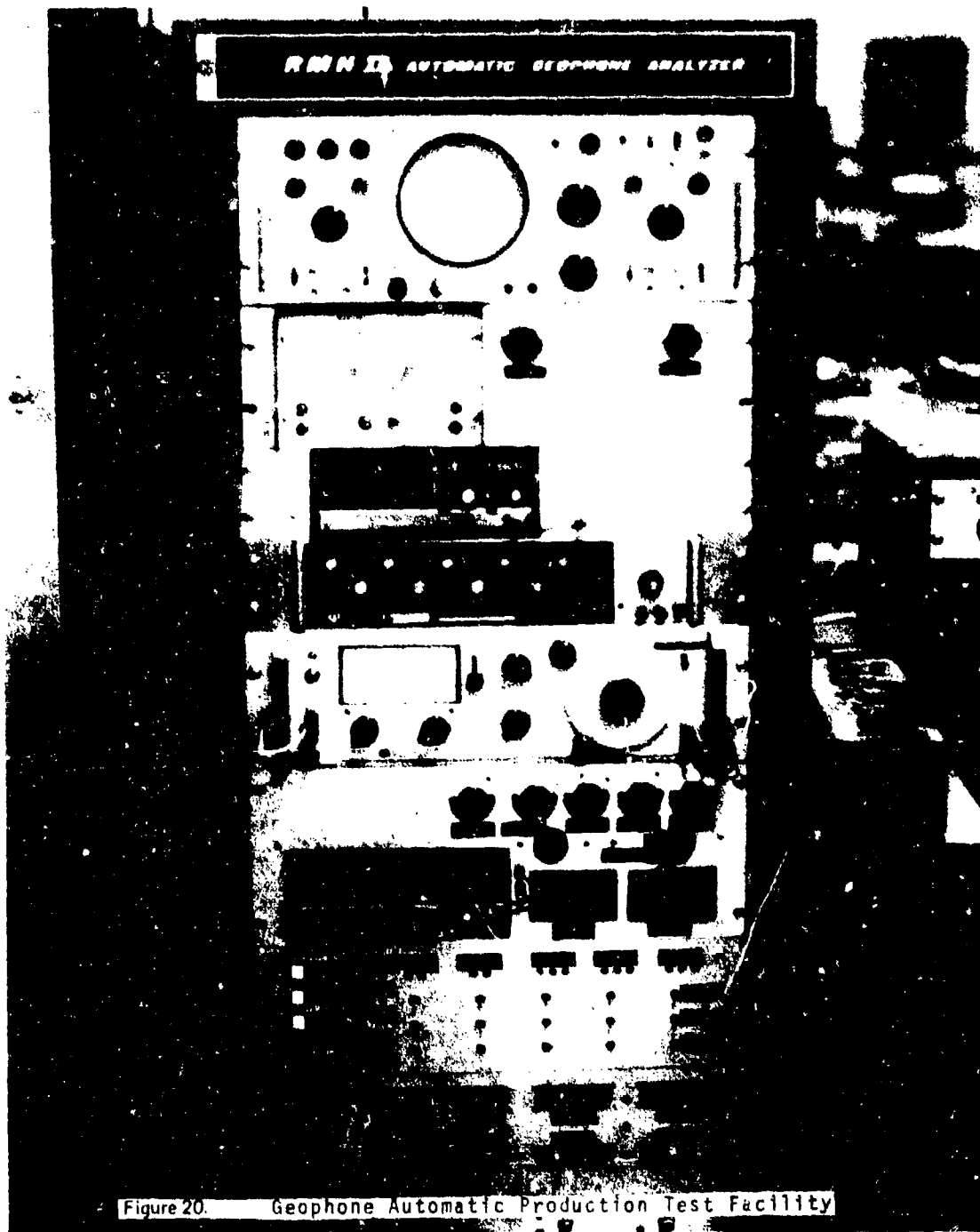


Figure 20. Geophone Automatic Production Test Facility

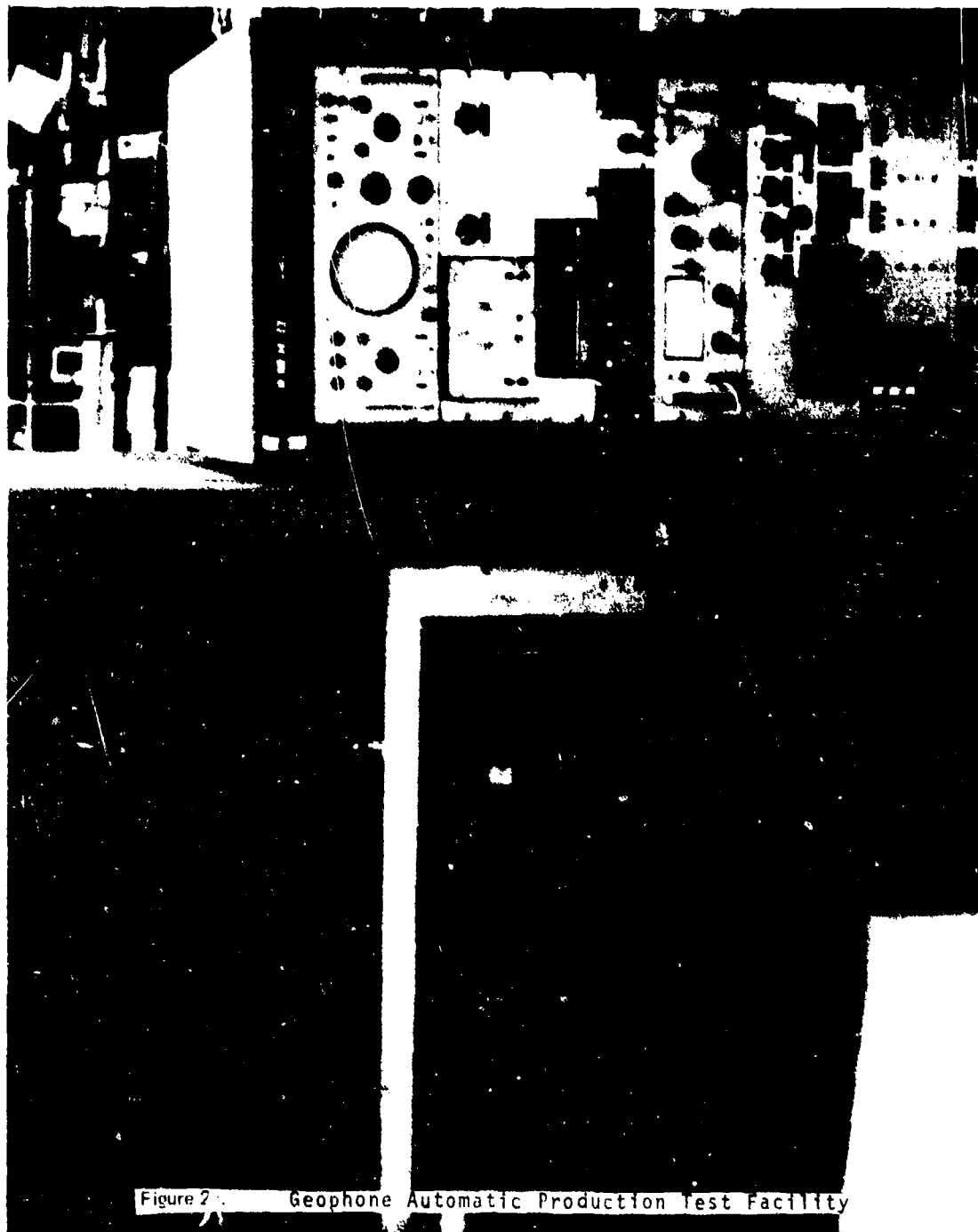


Figure 2. Geophone Automatic Production Test Facility